Ugandan crater lakes: limnology, palaeolimnology and palaeoenvironmental history

Ugandan Crater Lakes

Limnology, Palaeolimnology and Palaeoenvironmental history

by

Keely Mills

A Doctoral thesis

Submitted in partial fulfilment of the requirements

for the award of

Doctor of Philosophy of Loughborough University

January 2009

Abstract

This thesis presents the results of contemporary limnological and palaeolimnological investigations of a series of crater lakes in order to reconstruct the palaeoenvironmental history of western Uganda, East Africa. The research examines questions of spatial and temporal heterogeneity of climate changes in the context of growing human impacts on the landscape over the last millennium.

Sediment records from two lakes, Nyamogusingiri and Kyasanduka within the Queen Elizabeth National Park (QENP) were investigated to look at the long term records of climate and environmental change (spanning the last *c*. 1000 years). Five shorter cores across a land-use gradient were retrieved to assess the impact of human activity on the palaeoenvironmental record over the last ~150 years.

High-resolution (sub-decadal), multiproxy analyses of lake sediment cores based on diatoms, bulk geochemistry (C/N and $\delta^{13}C$) and sedimentary variables (loss-on-ignition, magnetic properties and physical properties) provide independent lines of evidence that allow the reconstruction of past climate and environmental changes. This multiproxy approach provides a powerful means to reconstruct past environments, whilst the multi-lake approach assists in the identification and separation of local (e.g. catchment-scale modifications and groundwater influences) and regional effects (e.g. climatic changes).

The results of a modern limnological survey of 24 lakes were used in conjunction with diatom surface sediment samples (and corresponding water chemistry) from 64 lakes across a natural conductivity gradient in western Uganda (reflecting a regional climatic gradient of effective moisture) to explore factors controlling diatom distribution. The relationships between water chemistry and diatom distributions were explored using canonical correspondence analysis (CCA) and partial CCA. Variance partitioning indicated that conductivity accounted for a significant and independent portion of this variation. A transfer function was developed for conductivity (r^2_{jack} = 0.74). Prediction errors, estimated using jack-knifing, are low for the conductivity model (0.256 log units). The final model was applied to the core sediment data.This study highlights the potential for diatom-based quantitative palaeoenvironmental reconstructions from the crater lakes in western Uganda.

Sedimentary archives from the Ugandan crater lakes can provide high-resolution, annual to sub-decadal records of environmental change. Whilst all of the lakes studied here demonstrate an individualistic response to external (e.g. climatic) drivers, the broad patterns observed in Uganda and across East Africa suggest that the crater lakes are indeed sensitive to climatic perturbations such as a dry Mediaeval Warm Period (MWP; AD 1000-1200) and a relatively drier climate during the main phase of the Little Ice Age (LIA; *c*. AD 1500-1800); though lake levels in western Uganda do fluctuate, with a high stand *c*. AD 1575-1600). The general trends support the hypothesis of an east to west (wet to dry) gradient across East Africa during the LIA, however, the relationship breaks down and is more complex towards the end of the LIA (*c*. AD 1700-1750) when the inferred changes in lake levels at Nyamogusingiri and Kyasanduka are synchronous with changes observed at Lakes Naivasha (Kenya) and Victoria and diverge from 'local' lake level records (from Edward, Kasenda and Wandakara).

Significant changes in the lake ecosystems have occurred over the last 50-75 years, with major shifts in diatom assemblages to benthic-dominated systems and an inferred increase in nutrient levels. These changes are coincident with large sediment influx to the lakes, perhaps as a result of increasing human activity within many of the lake catchments.

Key words: East Africa, Uganda, Late-Holocene, crater lakes, palaeolimnology, palaeoclimate, transfer function, diatoms, isotope, sediment flux.

Acknowledgements

I have quite possibly picked the worst time to write my acknowledgements…the evening that I tie all of the loose ends together, breathe a sigh of relief that I have reached the end, but a little overcome with emotion that this is it, time to let go…I have had such a fantastic (not to mention stressful!) few years in Loughborough, it seems strange that I am about to draw the line under this experience and move onto something new.

My first and biggest thank you is to Dave. I can imagine the last few years have been as steep a learning curve for you as it was for me! I am indebted to you for all of the support that you have given me throughout my research, for all the meetings we had (although I'm quite sure you enjoyed the gossip) and for all of the opportunities that you have given me. Dave, you are one of the most genuine and smartest people I have ever met, and it was a privilege to be your first Ph.D. student.

John...

To Stuart and Barry who made laboratory work straightforward and allowed me to use most of their annual budget for the mass production of diatom slides! Thanks for 'forcing' me to take to take tea breaks, and Stuart, a big thanks for all the cakes that you have supplied over the years!

To those that have helped in the wider aspects of the research, my sincerest thanks go to Immaculate Ssemmanda for her work on the pollen of my long core sites. To George, for introducing me to the weird and wonderful world of missionary archives and for allowing me the opportunity to collaborate on aspects of her research. To Angela Lamb, Melanie Leng and all of the staff at NERC (Keyworth) who have helped with the isotope preparation, analyses and understanding. To Peter Appleby, for the ^{210}Pb dating and subsequent reports. Finally to Charlotte Bryant (NERC-RCL) for her assistance with the radiocarbon dating.

Thanks are due to colleagues in Ghent, especially Hilde Eggermont who has chased water chemistry data, provided the missing data and who has, from a distance been very supportive. Similarly, a big thank you to Christine Cocquyt; for her hospitality during my visit and for her insightful discussions on East African diatom taxonomy. Thanks are also due to Dirk Verschuren, Jim Russell and Bob Rumes who have all provided samples and data that were used in this research.

I am indebted to Richard, Jimmy, Julius Leiju and the rangers and the villagers of Uganda, who, had they not carried equipment or pushed me up the side of a crater, the fieldwork would never have got off the ground.

Much of my fieldwork and many of the analyses would not have been possible without the financial support received through a number of small grants from NERC (awarded to Dave Ryves). These include Dave's new investigators award that paid for the fieldwork, and grants from NIGL and NERC-RCL for isotopic and chronological analyses. In addition to this, a number of smaller grants awarded to myself from various organisations (the British Institute in East Africa, Quaternary Research Association, Royal Society, Loughborough Graduate School and the Department of Geography travel scholarship) have alleviated fieldwork costs, paid for courses, visits to collaborating colleagues and allowed me to travel to far-flung places for conferences. Thank you also to the Ugandan Government (UNCST and UWA) for giving their permission for us to work in, and collect samples from, the Ugandan National Parks.

Thank you to all the people who have kept me smiling, who came to the pub and who were there pretty much for the long haul (Jonny, Wing Wai, Mark, Sally and Rachel). To all those I have met at British Diatomist Meetings who share this strange enthusiasm for diatoms and drinking, and more recently, thanks to Carl Sayer for making me think about my diatoms in a way I had not thought of them before!

To Mr Walton, my inspiration and the reason why I even studied geography in the first instance.

To mum and Ian, who have done all the fetching and carrying, and who probably don't understand why I wanted to be a student for nigh on 8 years and probably still don't truly understand why or what it is I actually do...

…and so begins the next chapter…

Table of Contents

List of Figures

Chapter 7

Chapter 8

List of Tables

Chapter 1

Introduction

1.1 Introduction

This thesis presents the results of neo-limnological and palaeolimnological investigations of a number of small, closed-basin crater lakes from western Uganda. The collated data have been used to infer the palaeoenvironmental history of the region over the last 1000 years. The thesis addresses a much neglected topic related to the study of modern, comparative limnology, the results of which have been used to create a new diatom-conductivity transfer function for these relatively scientifically-unknown crater lakes. In addition, this research presents detailed analyses of seven sedimentary sequences from crater lakes located within a small, regional cluster in south-west Uganda.

Diatom, organic isotope and sedimentary analyses of two core sequences obtained from a paired lake system (Lakes Nyamogusingiri and Kyasanduka) span the last 1000 years and provide an annual (last 150 years) to almost sub-decadal (2-12 years) resolution record of palaeoenvironmental history. The results are used to assess the coherence of lake records in response to documented and inferred climatic and environmental changes throughout Uganda and East Africa.

The five remaining cores span a land-use gradient in the region from 'pristine' lakes, today protected in national parks and forest reserves, to heavily impacted lakes in unprotected areas. These cores all span the last 100-150 years and are used to compare palaeolimnological (diatom and sedimentary) evidence of climatic and environmental changes directly to anecdotal (e.g. missionary records) and documentary records (e.g. Lake Victoria levels and El Niño-Southern Oscillation [ENSO] anomalies).

1.2 Research context

During the Quaternary, there have been large fluctuations in the climate of East Africa, and lake waters in this region have in turn responded to alternate periods of high and low rainfall in terms of their lake level and chemistry (Beadle, 1932; Gasse and Tekaia, 1983). The similarity of lake level trends across East Africa suggests that uniform patterns of long-term temporal variability (most likely controlled by large scale atmospheric dynamics) underlie seasonal complexities in rainfall (Nicholson, 2000). This regional

coherence also gives credibility to the use of lake levels to evaluate the regional synchronicity of climatic anomalies in the past (Verschuren, 2004).

A large number of studies concerning the palaeoclimatic and palaeoenvironmental history, spanning millennial timescales, exist for the large lakes of East Africa. The majority of the initial palaeoclimatic work from East Africa was carried out and reviewed by Gasse (2000; 2002; 2006), Gasse and Tekaia (1983) and Gasse *et al*., (1983, 1995; 1997). Other works, such as that of Barker (1990), Barker *et al*. (2000; 2001; 2002; 2003), Bessems (2007), Bessems *et al*. (2008), Nicholson (1998a; 1998b; 2000; 2001a; 2001b), Russell and Johnson (2005; 2006a; 2006b; 2007), Russell *et al*. (2003; 2007), Stager (1984), Stager and Johnson (2002), Stager *et al*. (1997; 2002; 2003; 2005; 2007), Verschuren (1994; 1997; 1999; 2001; 2002; 2003a; 2003b ; 2004) and Verschuren *et al*. (1999; 2000; 2002) have played an increasingly important role in understanding and modelling the complexity of tropical climate changes.

East Africa exhibits variability in its climate at various timescales (Figure 1.1). At the millennial scale, the climatic history of equatorial Africa can be divided into a wet Late Glacial and early Holocene, followed by a drier mid to late Holocene (deMenocal *et al*., 2000). The Holocene has also been punctuated by approximately four major dry spells over the last 15,000 years (Gasse, 2000), separated by abrupt transitions (Gasse and van Campo, 1994). It is postulated that these continent wide fluctuations in effective moisture have occurred as a result of large scale variations in the position or intensity of the tropical monsoon system (Verschuren, 2004). It has been observed in Africa that changes in precipitation have a greater environmental impact than changes in temperature (Olago and Odada, 2004), as temperature in the tropics tends to have a greater diurnal range compared to its annual range, which remains relatively constant (Nicholson, 2001a). Nicholson (1996) has also shown rainfall variability in East Africa to be closely linked to both ENSO and sea surface temperatures (SSTs, equatorial Indian and Atlantic), with an overall enhancement (i.e. increased amount of precipitation) during ENSO years.

The last 1000 years provides one of the most challenging time frames in which to understand regional climatic and environmental changes from lake sediment records in East Africa due to the issues associated with the dating of sediments spanning this timeframe as well as increasing modification of many of the catchments by anthropogenic activity, especially in terms of agriculture (with the development of nucleated, permanent settlements) and the implementation of new technologies (e.g. iron technology and associated forest clearance for the production of charcoal). The notion that African climate

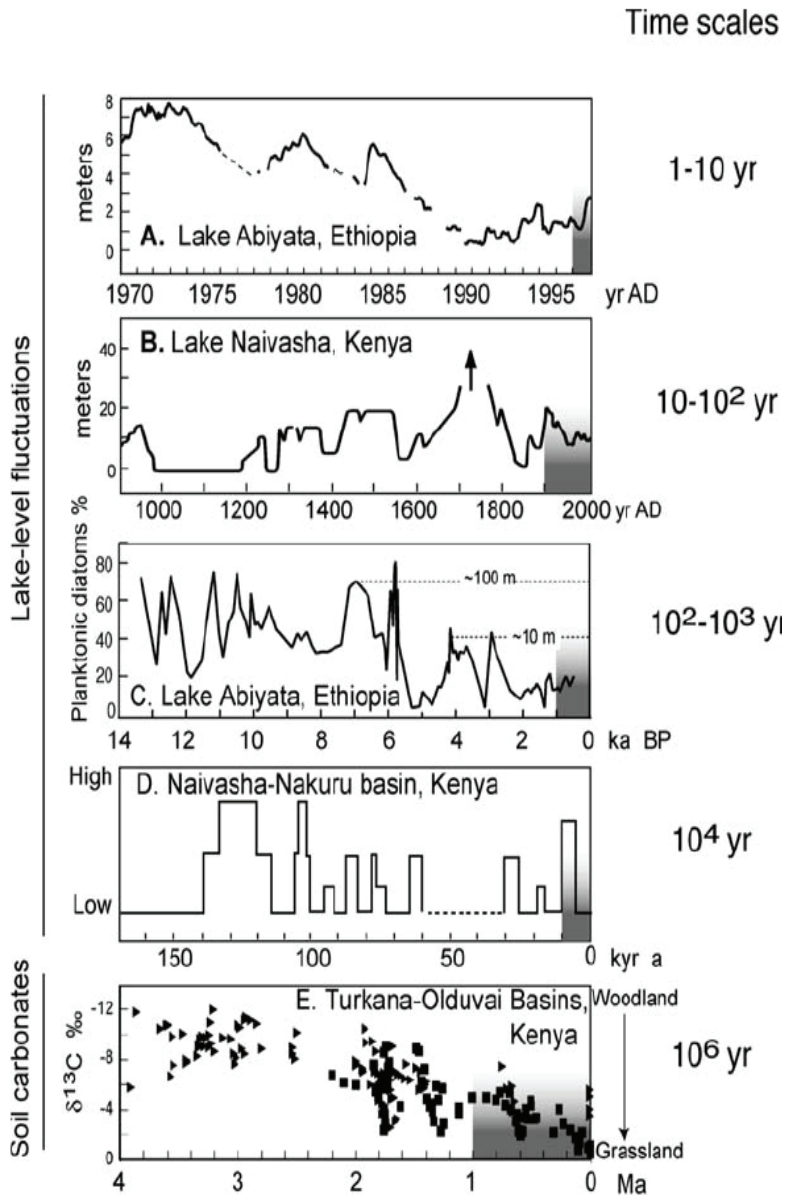

Figure 1.1 *Hydrological fluctuations in tropical Africa on different timescales.* **(A)** *Instrumental record of Lake Abiyata level (Legesse et al., 200) and* **(B-D)** *reconstructed lake level fluctuations (***B** *Lake Naivasha [Verschuren et al., 2000];* **C** *Lake Abiyata [Gasse and van Campo 1994; Chalié and Gasse, 2002];* **D** *Naivasha-Nakuru basin [Trauth et al., 2003]).* **(E)** *Isotope record of soil carbonates (Cerling and Hay, 1988; Cerling, 1992). Figure taken from Gasse, 2006.*

has been relatively stable over the last few millennia, when compared to the hydrological instability reconstructed from the early and middle Holocene (Verschuren, 2004) stems from early work on Late Quaternary vegetation and lake level variations in East Africa (e.g. Butzer *et al*., 1972; Hamilton, 1982), where a combination of poor resolution and chronology meant the last few thousand years were represented by very few data points (Verschuren, 2004). For some proxies (e.g. pollen), even high-resolution studies can provide ambiguous reconstructions of the time period due to poor precision of the proxy itself. One aspect of this thesis is therefore to study the last 1000 years of African climate at a high-resolution.

The climate of East Africa exhibits high inter-decadal variability, with high magnitude and abrupt climate events characterising the short instrumental record (e.g. rainfall variability as a result of short-term climatic perturbations, such as El Niño-Southern Oscillation; Nicholson, 1996; 2000; Nicholson and Yin, 2001; Conway, 2002). Given the instability of African climate at all time scales (Nicholson, 2000), the focus is now to try and reconstruct Africa's climate history with a resolution and precision sufficient enough to separate natural and anthropogenic climate and environmental forcing factors (Verschuren, 2004). As a result research emphasis has shifted from the need to understand the long-term dynamics of Quaternary climate fluctuations, to focus upon the comparatively shorter-term ($10^{1\text{-}2}$), more regionally specific aspects of climate variability (Verschuren, 2003a). These short-term, regional records of climate in the tropics are directly relevant to human society, in terms of ENSO and monsoonal weather systems (Thompson *et al*., 2005). However, there is currently a lack of relevant, short-term records from the tropics (Verschuren, 2003a; Thompson *et al*., 2005), considering the region is central to studies of climate change, not only in the equatorial belt, but also in the sub-tropical regions (Barker *et al*., 2004). Another aim of the thesis is to analyse records of short-term environmental change from East African lakes.

Previous studies within East Africa have shown that some of these past climatic events are synchronous across the region. However, a number of recent studies have suggested spatial complexity (cf. Verschuren *et al*. 2000; Ssemmanda *et al*., 2005; Stager *et al*., 2005), and thus regional heterogeneity of tropical palaeoenvironments in terms of responses to climatic forcing (e.g. the Little Ice Age; Russell *et al*., 2007). Current palaeoclimatic research in Africa is of immense importance as it has the means to provide an historical and pre-colonial perspective on past variability (both natural and anthropogenic). High-quality palaeodata are not only required to resolve climatic and

environmental variability, but may also help to understand the socio-political responses of past societies to such changes. The last 1000 years is a crucial period in East African history during which time there were major societal transformations and political changes, which have often been linked to fluctuations in climatic conditions (cf. Taylor *et al*., 2000; Robertshaw and Taylor, 2000; Verschuren *et al*., 2000; Robertshaw *et al*., 2004; Doyle, 2006). The data generated from this research will contribute to this ongoing debate.

There is also the potential for these records to set baselines of natural variability on which long term management plans can be based (Olago and Odada, 2004), especially as the major effects of future climate changes in Africa will be through changes in the hydrological cycle (IPCC, 2007). Many African countries are today experiencing water stress, and are likely to reach a water deficit within the next 25 years as a result of increasing population pressures coupled with climatic changes (Olago and Odada, 2004). Long-term records of change are required to assess the significance of 'historical' and modern day changes in Africa (Olago and Odada, 2004). There is a crucial need for these records in an area where there is currently a shortage of palaeodata in comparison to temperate regions (Nicholson, 2001; Barker *et al*., 2004). More high-resolution proxy records are required to differentiate between local and regional impacts and also anthropogenically induced and natural changes (Olago and Odada, 2004) and to relate to climate records from higher latitudes.

1.2.1 Proxy records of climate change from the tropics

Proxy records of climate change from areas such as Africa may provide the key to understanding the full range of tropical climate variability, its effect on earth's energy budget and water cycle, the connections between high and low latitude climate and the sensitivity of the tropics to future climate change (Gasse, 2002). However, records of climate change from tropical regions are often short (Gasse, 2002). Verschuren (2003a) identified Africa as the 'quintessential tropical continent' for studies into short-term climate change, but several problems exist in this region. Firstly, it is difficult to reconstruct documentary climatic histories older than the last 100 years, owing to the lack of instrumental or documentary records prior to the colonial period (Nicholson, 2001c). Secondly, even when such records do exist, they are often incomplete and discontinuous. Perhaps the most notable exception to this is the Rodah Nilometer, the Egyptian record of fluctuating Nile levels which dates back to AD 700. Until recently, the Rodah Nilometer was the only record of climate change (especially droughts) that could be precisely dated

(Robertshaw and Taylor, 2000). However, the exact nature of these data has been disputed by Hassan (1998) and Nicholson (1998a), who suggest that maxima and minima are explained by the inputs from the White Nile as a result of equatorial rainfall in the Ethiopian Highlands.

Whilst various proxy records do exist from the tropics and extra-tropical regions (i.e. peat/swamp sequences, lake sediment archives, ice cores, tree rings, cave speleothems and coral records, discussed below [*sections 1.2.1.1-1.2.1.6*), many of these fail to provide the high-resolution or continuous records that are required for a detailed correlation to monsoonal (e.g. the migration of the Inter-Tropical Convergence Zone [ITCZ]) and El Niño cycles and also to higher latitude climate fluctuations (e.g. Mediaeval Warm Period [MWP][1] and the Little Ice Age [LIA][2]). To understand sub-decadal and century-scale climatic variability, continuous, millennial-scale, high-resolution climate reconstructions are required. For many climate archives, the records remain limited due to the non-continuous nature of the records (often related to periods of intense aridity), the unreliable nature of their chronologies (e.g. ice cores and lake sediment sequences; Thompson *et al*., 2002; Gasse, 2002), the complication of human impacts on the sediment records and the precision associated with some proxies (e.g. pollen analyses).

1.2.1.1 Peat

Much of the previous work in Uganda has been based around pollen analysis as a climatic indicator from peat and swamp sequences (e.g. Hamilton *et al*., 1986; Marchant *et al*., 1997; Taylor *et al*., 1999; Leiju *et al*., 2005), although problems do exist. African landscapes are highly heterogeneous and high-resolution records are scarce (Ssemmanda *et al*., 2005). In addition, pollen analyses of surface sediments from Africa do not reflect the current land-use within the lake catchments or in the immediate region, which is dominated by small-scale farmland (Vincens *et al*., 1997). This is explained by the response of individual plant species to human impact but also as many of the plants grown under small-scale agriculture produce either very little or no pollen, such as banana, or produce

[1] In this thesis the MWP is defined as the period covering AD 800 to AD 1200 (Maasch *et al*., 2005).

[2] Whilst the MWP-LIA transition is suggested to have culminated c. 1400 (Maasch *et al*., 2005), there is no universally accepted or precise definition for the duration of the LIA (Maasch *et al*., 2005), however, in East Africa, the main phase of the LIA is often denoted as ~AD 1500 to AD 1800 (Verschuren *et al*., 2000; Stager *et al*., 2005; Russell *et al*., 2007) and will be referred to throughout this thesis.

pollen that cannot be distinguished from related wild species (e.g., cereals and wild grasses; Vincens *et al*., 1997). As a result natural vegetation succession, climate change and human activity may leave signals in sedimentary pollen records that are not easy to differentiate (Livingstone, 1967; Hamilton, 1972; Taylor and Marchant, 1995).

1.2.1.2 Ice cores

Ice cores provide an important proxy of climate change in the tropics (Thompson *et al*., 2005). Glaciers in tropical Africa are not as abundant as those in tropical regions of South America and Asia due to a lack of high altitude regions (Verschuren, 2004). Ice cores can provide records of hydrological and temperature changes with an annual resolution (usually confined to the uppermost sections of the cores). Ice cores recovered from Mount Kenya were amongst the first to be collected and analysed from East Africa (Verschuren, 2004). However, these early cores showed evidence of melt water percolation, which disrupted the climate signal recorded in the ice (Hastenrath, 1981). A further study at Mount Kenya by Karlén *et al*. (1999) retrieved lake sediment cores from a pro-glacial tarn to reconstruct glacial fluctuations over the last 6000 years. Six major periods of glacial advances were identified and dated. The advances, attributed to temperature changes in accordance with other climate studies (Coetzee, 1967; Bonnefille *et al*., 1995; Ricketts and Johnson, 1996; Stager *et al*., 1997), indicate a drier climate at these times (Karlén *et al*., 1999).

A study of ice cores from Kilimanjaro by Thompson *et al*. (2002) provided an 11,700 year record of climate variability for eastern equatorial Africa, based on oxygen isotopes, insoluble dust and aerosol inputs. Unfortunately, problems with poor chronology mean the precise timing of the climatic events cannot be considered absolute (Thompson *et al*., 2002; Gasse, 2002). Despite this, the Kilimanjaro ice core record presents a unique insight into the Holocene atmospheric dust inputs in equatorial Africa (Verschuren, 2004). Recent observations from the tropics show that glaciers (such as those on Kilimanjaro and the Rwenzoris) are rapidly melting and retreating (Dunbar and Cole, 1999; Thompson *et al*., 2005; Taylor *et al*., 2005; 2006). It is thus imperative to locate new records to expand understanding of past tropical climate variability to facilitate investigations into regional and global climate changes (Thompson *et al*., 2005), although with the rapid retreat of glaciers in East Africa during the 20th century (Taylor *et al*., 2005; 2006), the likelihood of retrieving ice cores in the future is unlikely.

1.2.1.3 Tree rings

Tree ring records in temperate regions offer one of the best documented, most extensively used methods of continental climate reconstructions at an annual resolution (Dunbar and Cole, 1999; Fichtler *et al*., 2004). There is a scarcity of long, dated tree ring chronologies from tropical areas. Trees from tropical areas do not always produce distinct annual growth bands due to modest variations between seasons and strong inter annual variability in wet and dry seasons (Dunbar and Cole, 1999; Verschuren, 2004). Strategies are in place to retrieve tree ring data from the tropics using microscopic techniques on anatomical structures to tease out the annual ring growth data (Dunbar and Cole, 1999). However, there is little potential to extend this technique beyond the scope of living trees, as once dead, the trees usually undergo rapid decay.

1.2.1.4 Corals

Corals from tropical oceans offer the potential for high-resolution records (seasonal to centennial scale) of past sea surface temperatures using stable isotopes and elemental analyses (Dunbar and Cole, 1999; Verschuren, 2004). A 200 year annual $\delta^{18}O$ record from coral growing off the east coast of Africa provided a history of Indian Ocean sea surface temperature (SST) change coherent with instrumental records of tropical pacific climate variability on an inter annual scale (Cole *et al*., 2000). Further studies on coral records from this region appear to provide a record of continental erosion exacerbated by colonial agricultural practices in the early 20^{th} century (Cole, 2003). However, it is likely that living corals from the Indian Ocean will cover only the last 400 years, unless fossil corals can be found for further correlation (Verschuren, 2004).

1.2.1.5 Cave speleothems

Another valuable annual proxy record of continental climate from temperate regions is cave speleothems. Although studies in South Africa (e.g. Holmgren *et al*., 1999) use high resolution records from cave stalagmites to reconstruct annual climate over the last 250 years, their use as a climate proxy within the tropics is largely unexplored. High-quality speleothems in Africa are likely to be limited to the extra-tropical north and south (Verschuren, 2004). Speleothems from the tropics are rare, and where they do occur, tend to show little variation in isotopic composition, thus attempts to reconstruct tropical climates from speleothems are scarce (Lauritzen and Lundberg, 1999).

1.2.1.6 Documentary records

Documentary evidence of climate change in East Africa include rain gauge and lake level measurements, observations of glacier fluctuations and ship observations of Indian ocean winds and currents (Hastenrath, 2001). In Uganda, such instrumental records are largely confined to the recent past (*c.* 100 years; cf. Olago and Odada, 2004, Verschuren, 2004; Endfield *et al*., 2009). The historical records of tropical African climate began with the onset of European exploration and the influx of Church missionaries (with documentary (anecdotal) records now extending back [in western Uganda] until *c*. AD 1880 [Endfield *et al*., 2009]). Similarly, Nicholson (2001c) extended the lake level history of Victoria back to the early 19th century, through the use of oral histories. Webster (1979) employed a similar method to reconstruct periods of drought in interlacustrine Africa. The earliest observed (instrumental) climate data in Uganda come from lake levels and rainfall data. For example, Lake Victoria levels from 1896 (Brooks, 1923); Lake Albert, 1904 (Hurst and Phillips, 1933-1946) and rainfall data from 1896 (Entebbe), 1903 (Fort Portal) and the majority of other stations (e.g. Butiaba, Bunyaruguru) from 1910 onwards (Hurst and Black, 1943-1949). The comprehensive instrumental records coincide with the beginning of western colonisation of Uganda and the establishment of the Protectorate (1896).

1.2.2 Lake-sediment records

One of the most widespread proxy records of climate change in East Africa is obtained from lake sediments. These archives have the potential to provide chronologically structured, ecologically integrated and (in some instances) continuous records of both local and/or regional environmental change (Anderson and Battarbee, 1994). Lakes are excellent sensors of environmental change, and sediments that accumulate in a climatically sensitive lake can provide a continuous, high-resolution record of past climate variability (Battarbee, 2000). These lake sediment archives are the principal source of information on the climate history of tropical Africa (Verschuren, 2003). Crater lakes, in particular, have the potential to provide some of the best high resolution sedimentary records of environmental change (Williams *et al*., 1993), as these lakes tend to have small, well defined catchments, simple basin morphology and in several cases rapid sediment accumulation (Lamb *et al*., 2000). With sedimentation averaging greater than 1 mm yr^{-1} in most East African lakes, (Johnson, 1996; Ssemmanda *et al*., 2005) and sedimentation rates of *c.* 10 mm yr^{-1} recorded in Ugandan crater lakes in the recent past (Lakes Kasenda and Wandakara; Ssemmanda *et al*., 2005; Ryves *et al*., submitted), sediment cores can be sub-sampled to provide

palaeoclimate data with century-scale, decadal or sub-decadal temporal resolution (Battarbee, 2000).

Despite the potential for the extraction of high-resolution, high-quality proxy records from crater lakes sequences (e.g. Verschuren *et al*., 2001; Ssemmanda *et al*., 2005; Russell *et al*., 2007; Bessems, 2007; Bessems *et al*., 2008; Ryves *et al*., submitted), these archives remain underexploited, with the focus of the majority of palaeolimnological investigations in East Africa biased towards the Great lakes – Victoria (e.g. Stager, 1984; Stager *et al*., 1997; Talbot and Laerdal, 2000; Johnson *et al*., 2000; Stager and Johnson, 2002; Stager *et al*., 2002; Stager *et al*., 2003; 2005; 2007), Albert (e.g. Beuning *et al*., 1997), Edward (e.g. Russell *et al*., 2003; Beuning and Russell, 2004; Russell and Johnson, 2005), Malawi (e.g. Filippi and Talbot, 2005), Tanganyika (Bergonzini *et al*., 1997) and Tana (e.g. Lamb *et al*., 2007).

Crater lakes are numerous in the Rift Valley and especially in the west of Uganda, where this study focuses. These small, often closed-catchment lakes are widely held to present ideal conditions for high resolution analyses of short-term events on regional and local scales (Telford and Lamb, 1999; Ssemmanda *et al*., 2005; Russell *et al*., 2007; Bessems, 2007; Bessems *et al*., 2008; Ryves *et al*., submitted). Such lakes situated in small volcanic crater basins are generally ideal sites for recovery of high-resolution palaeoclimatic records as many are thought to have a simple hydrogeological setting, thus simplifying the relationship between lake history and climate history (Gasse *et al*., 1995; Colman, 1996; Creer and Thouveny, 1996; Verschuren, 2001; Russell *et al*., 2007; Bessems *et al*., 2008). However, in some cases groundwater can complicate this relationship in Ugandan crater lakes (e.g. Lake Kasenda) by keeping the lakes fresh (salt renewal) during dry periods (Ryves *et al*., submitted). In addition, their relative depth and additional topographic wind shelter encouraging permanent/semi-permanent stratification and anoxic bottom waters allowing the accumulation and preservation of undisturbed sediment sequences.

1.2.2.1 Closed lake basins

Hydrologically closed lakes are sensitive to climatic fluctuations if net groundwater fluxes are ~0 (Fritz, 1990; Davies *et al*., 2002; Verschuren, 2003; Russell *et al*., 2007; Bessems, 2007; Bessems *et al*., 2008; Ryves *et al*., submitted). One of the main characteristics of closed basin lakes is their capacity to undergo major fluctuations in lake level and lake chemistry in response to changes in effective moisture (= $P-E_t$); the difference between the

input precipitation (P) and outputs evaporation and evapotranspiration (E_t) in response to seasonal, inter-annual or long-term climatic fluctuations (Street-Perrott and Harrison, 1985; Gasse *et al*., 1995; Laird *et al*., 1996). Variations in effective moisture, and hence water balance, are often reflected in the ionic strength and composition of lake waters through dilution and evaporative concentration of dissolved salts (Gasse *et al*., 1995; Davies *et al*., 2002).

The crater lakes in western Uganda are thought to respond to variations in precipitation and evaporation in terms of changing water depth and chemistry, influencing lake biota, as shown elsewhere in East Africa (cf. Lamb *et al*., 1995; Gasse *et al*, 1997; Chalié and Gasse, 2002). As a result the physical, chemical and biological properties of the lake and its sediments change through time; thus sediment cores from these lakes provide an opportunity to reconstruct past water chemistry (Gasse, 1986, Fritz, 1990; Fritz *et al*, 1991; Gasse *et al*., 1995; Wilson *et al*., 1996). These records can also be used to infer periods of increased or decreased effective moisture, providing valuable information on climatic variability in terms of temperature and/or rainfall (Davies *et al*., 2002). However, the hydrological sensitivity which causes closed basin lakes to respond to moderate, short-term rainfall variability also makes them prone to intermittent or complete desiccation, resulting in interruption or partial loss of the high resolution record which they accumulate (Verschuren, 2004; Russell *et al*., 2007; Bessems, 2007; Bessems *et al*., 2008).

In palaeoclimatic studies of closed basin lakes, diatom-based conductivity (or salinity) transfer functions have provided a key tool for generating-high resolution, quantitative data (Fritz, 1990; Fritz *et al*., 1991; Laird *et al*., 1996). Quantitative climate reconstructions in East Africa that use biological proxy indicators are currently focused on chironomid- and diatom-based inferences of lake water conductivity (salinity) and ionic composition (Gasse *et al*., 1995; Verschuren, 1997; Verschuren *et al*., 2000; Eggermont *et al*., 2006). Both conductivity and ionic composition reflect net precipitation. As a result, the relationship between conductivity and chironomid or diatom distributions and abundance enables fossil assemblages from sediments to be interpreted in terms of palaeosalinity and therefore indicate past precipitation-evaporation gradients (Gasse *et al*., 1995; Verschuren, 1997; Verschuren *et al*., 2000; Eggermont *et al*., 2006).

There are several other local factors (e.g. groundwater, irrigation, deforestation, agriculture) that can affect the hydrochemistry of closed basin lakes, and thus it is important that lakes are chosen carefully to minimise these factors, therefore allowing reconstructions of past water chemistry from proxy indicators (e.g. diatoms) to provide an

independent method of quantifying past changes in effective moisture (Gasse *et al*., 1995). However, a fundamental problem with diatom-based conductivity inferences is that the relationship between salinity changes and climatic forcing is indirect and complex (Gasse *et al*., 1997; Fritz, 2008).

Groundwater exerts local and regional controls on closed-basin lake level changes (Almendinger, 1990). If lake hydrology is dominated by groundwater inflow, its response to climatic variability is buffered by aquifer residence time and the geographic source area for groundwater recharge. In lakes where groundwater outflow is important, removing water and solutes, the response of lake salinity to surface evaporation is dampened (Sanford and Wood, 1991; Ryves *et al*., submitted). Similarly, lake salinity can be increased by inflows of saline groundwater. Crater lakes in active volcanic regions are subject to varying degrees of hydrothermal influence, which may result in hydrological changes that are unrelated to climate (Telford and Lamb, 1999).

Even when closed lakes do show long-term salinity variations proportional to climatic fluctuations, the relationship is often non-linear (Verschuren, 2002). In high resolution studies of fossil assemblages, sudden transitions between saline and fresh conditions are apparent (Verschuren *et al*., 2000), which may be unduly interpreted as a rapid climate transition, rather than a gradual trend exacerbated by threshold scenarios (Verschuren *et al*., 2000). In tropical systems, once river inflow and groundwater seepage decline, and fail to keep a lake fresh ($\leq$0.5 g L^{-1} TDS [total dissolved solids]), continually high temperatures and a precipitation deficit move it quickly to true salt lake conditions (>3 g L^{-1} TDS) and specialist biotic communities. This phenomenon is confirmed by the scarcity of lakes in modern Africa with intermediate salinities (Verschuren, 2002).

1.2.2.2 Lake basins with outflow

In outflow lake systems, past changes in climate may be reconstructed through the use of lake level changes; during periods of aridity, lake levels decrease, and if lake levels drop below the outflow threshold, there may also be a rise in salinity. Under wetter conditions, lake levels rise and will overflow (depending on the height of the outflow system). Whilst the potential climate signal recorded within freshwater, outflow lakes is often less sensitive compared to closed-basin (and saline) systems, studies on such systems have shown climate reconstructions are still possible (cf. work on Lake Victoria by Stager and colleagues). Furthermore, freshwater systems are likely to provide continuous sediment

records (as they are likely to be buffered towards complete desiccation) and avoid many of the preservation issues associated with closed-basin lakes.

Conductivity and habitat changes have been successfully reconstructed from Lake Victoria (Stager *et al*., 2005) even in out-flowing (or overflowing) conditions. In addition to this the same study indicated habitat changes as a result of water level fluctuations in the lake basin (inferred using the abundance of shallow water diatoms [SWD]), indicating that habitat group changes based on depth distributions (i.e. benthic vs. planktonic) produce reliable evidence of water level change within lake systems (Wolin and Duthie, 1999; Stager *et al*., 2005). In the sediment record, planktonic species, colonizing open water, are assumed to increase in abundance during periods of higher lakes levels, whilst benthic taxa will decrease, and *vice versa*. Ratios based on the abundance of planktonic versus benthic species can be successfully used to reconstruct lake level changes (Gasse *et al*., 1989, Barker *et al*, 1994; Stager *et al*., 2005; Stone and Fritz, 2004). It has been shown that this relationship of planktonic species and higher water levels can be complicated in the recent past due to human activity in lake catchments. Catchment changes due to clearance and agriculture can increase the amount of nutrients delivered to the lakes, causing blooms in planktonic taxa and perhaps erroneously leading to an inferred lake level rise (Wolin and Duthie, 1999).

Lake level changes, linked to climate forcing, can result in other signals being apparent in diatom assemblages. For example, there may be evidence of changes in the stability of the column (increasing stability with increasing water depth), and the susceptibility of the water column to turbulence, nutrient and thermal conditions (Wolin and Duthie, 1999).

1.2.2.3 Diatoms

Diatoms are microscopic, unicellular algae that have been used extensively in the reconstruction of past environmental changes, especially in lakes (Stoermer and Smol., 1999; Battarbee, 2000; Mackay *et al*., 2003). Diatom analysis is an unrivalled tool for quantitative reconstructions because diatoms (a) are extremely sensitive indicators of lake water chemistry, (b) tend to occur in high numbers in modern and sedimentary sequences, allowing sound quantitative analyses and (c) many diatom taxa are often cosmopolitan (although there are some diatoms endemic to East Africa; Richardson, 1968; Gasse, 1986; Gasse *et al*., 1995; Cocquyt, 1998). Diatoms comprise the principal proxy used in this thesis.

Diatoms have long been used as proxy indicators to reconstruct Holocene environmental changes. During the last two to three decades, the application of diatoms in Holocene environmental reconstructions has increased considerably (Stoermer and Smol, 1999). Diatoms are excellent indicators of water chemistry and contemporary studies use quantitative multivariate techniques to reconstruct past climate variables both directly and indirectly by the comparison of fossil assemblages to modern analogues (Barker, 1990). Direct approaches include the reconstruction of surface water temperature (Rosen *et al*., 2000) and air temperature (Korhola *et al*., 2000), although debate over such reconstructions is rife (Anderson, 2000). Indirect approaches reconstruct changes in the major chemical parameters such as dissolved organic carbon (DOC; Pienitz *et al*., 1995), pH (Psenner and Schmidt, 1992) and, of immediate relevance to this study, the reconstruction of salinity (Fritz, 1990; Fritz *et al*., 1991; Gasse *et al*., 1995; Laird *et al*., 1996; Verschuren *et al*., 2000; Ryves *et al*., 2002). Diatoms have also proved to be a useful proxy in non-climate related studies, e.g. in reconstructing anthropogenic eutrophication of lakes using total phosphorus (TP; Bennion *et al*., 1996; Lotter, 1998; Bradshaw and Anderson, 2001).

In closed basin system, diatoms are highly sensitive to changes in conductivity (Hecky and Kilham, 1973; Gasse *et al*., 1983), and shifts in fossil assemblages can be quantitatively interpreted in terms of past conductivity (as a proxy for climate) through the use of a transfer function (ter Braak, 1987). In arid regions of Africa, USA, Spain and West Greenland diatom models (transfer functions) have been successfully developed and used to reconstruct quantitatively changes in salinity as a direct proxy for effective moisture and to infer from fossil assemblages the nature of climate change during the late Holocene (e.g. Fritz *et al*., 1993; Cumming and Smol, 1993; Cumming *et al*., 1995; Gasse *et al*., 1995; Wilson *et al*., 1996; Gell, 1998; Reed, 1998; Davies *et al*., 2002).

In East Africa especially, the use of diatoms in reconstructing limnological variables has been shown in a number of studies. For example, correlations have been established between species composition and pH (Gasse and Tekaia, 1983; Gasse *et al*., 1995), salinity (Hecky and Kilham, 1973; Gasse *et al*., 1997), conductivity (Hecky and Kilham, 1973; Gasse *et al*., 1995) and ionic composition (Gasse *et al*., 1983; Gasse *et al*., 1995). It should be noted that the use of closed-basin, saline lakes can also be problematic in environmental reconstructions. Poor preservation as a result of silica dissolution can occur in all lake systems; however saline systems are particularly vulnerable (Barker, 1990; Barker *et al*., 1994; Ryves *et al*., 2001; Ryves *et al*., 2006; Ryves *et al*., 2009) and as

such the accuracy of environmental reconstructions will always be limited by the quality of the raw data employed. Differential preservation in saline lakes caused by the dissolution of biogenic silica can affect the composition of the microfossil assemblage (Ryves *et al*., 2001; Ryves *et al*., 2009). In extreme cases entire assemblages can be destroyed; in other systems dissolution can be incomplete, biasing the species composition towards more resistant taxa and potentially compromising the value of such records when inferring ecological and climatological changes (Ryves *et al*., 2006; Ryves *et al*., 2009). Therefore, understanding the losses associated with poor preservation is fundamental when assessing the quality of palaeoenvironmental inferences (Ryves *et al*, 2006).

Although the relationship between conductivity (salinity) and climate is complex, and depends on an array of factors including the geological, hydrological, climatological setting and the morphology of the lake (Laird *et al*., 1996), the consistency between diatom records and other independent evidence for past climates is promising (Gasse *et al*., 1995; Verschuren *et al*., 2000; Stager *et al*., 2005; Ryves *et al*., submitted).

Qualitative and quantitative reconstructions of past lake levels (often related to climatic changes) of open lakes, are possible using knowledge of diatom habitat preferences, and the physical and chemical preferences of individual diatom species. Lake level changes can also be inferred through the use of diatom species associated with turbulent, or upwelling hydrological regimes. For example, the genus *Aulacoseira* contains species which require strong turbulence in order to remain suspended (Talling, 1966; Pilskaln and Johnson, 1991). During low water levels, the increased wind-driven mixing and associated increases in nutrient upwelling can favour this genus (Wolin and Duthie, 1999). Differences in the *Aulacoseira* species present (e.g. *A. ambigua* vs. *A. granulata* v. *angustissima*) may also provide information on turbidity and water clarity, which can be related to the amount of suspended sediment present in the water column as well as the degree of mixing and productivity. For example, *A. ambigua* has higher light and silica requirements than *A. granulata v. angustissima* (Kilham *et al*., 1986). Thus assemblage changes within the *Aulacoseira* genus can aid environmental interpretations.

1.2.2.4 Organic isotopes

The geochemical composition of lacustrine sedimentary matter (e.g. $\delta^{13}C$ and C/N) are successful and widely used tools for the reconstruction of palaeoenvironments (vegetation composition and hydrological changes; Gasse and Fontes, 1989; Lister *et al*., 1991; Chivas *et al*., 1993, Lamb *et al*., 2000; Meyers and Teranes, 2001; Lamb *et al*, 2004). Bulk organic

$\delta^{13}C$ analysis, in conjunction with other organic indicators (C/N ratios and pollen analyses) can provide information about the source of organic material entering a lake system (Meyers and Teranes, 2001). C/N ratios are used as an indicator of the relative proportions of autochthonous and allochthonous sources of lacustrine organic matter (Talbot and Lærdal, 2000). The $\delta^{13}C$ composition of organic-rich lakes sediments reflects the $\delta^{13}C$ of the plant material entering the lake (e.g. Olago *et al*., 2000). The $\delta^{13}C$ composition of plants is dependent upon their photosynthetic pathway, which in turn influences the way in which they fractionate atmospheric CO_2 (O'Leary, 1988). In East Africa, when the organic matter is derived from terrestrial plants within the lake catchment, the relative proportions of C_3 and C_4 plants may be estimated (Nordt *et al*., 2002; Lamb *et al*., 2004).

Inorganic carbon isotopes ($\delta^{13}C_{TIDC}$ [total dissolved inorganic carbon]) in lake waters are incorporated into the authigenic and biogenic carbonates, and are also used by plants. Phytoplankton preferentially utilise ^{12}C to produce organic matter that averages 20‰ lower than the $\delta^{13}C$ of TIDC (i.e. more negative values; Leng *et al*., 2005). Therefore, changes in TIDC can have major effects on the $\delta^{13}C$ of bulk organic material. When drier conditions prevail, lake levels may lower and this leads to a reduction in dissolved CO_2 concentrations due to increased pH and salinity (Leng *et al*., 2005). When this occurs, aquatic plants switch metabolism from CO_2 to HCO_3^- and become enriched in ^{13}C, producing higher $\delta^{13}C$ values (plant CO_2 values recorded up to -9‰; Leng *et al*., 2005). During wetter periods, the lake carbon pool will have been refreshed from a greater influx of soil derived CO_2, which has lower $\delta^{13}C$ (Leng *et al*., 2005). In lakes the dissolved carbon pool is often changed by biological productivity, mainly by preferential uptake of ^{12}C by aquatic plants during photosynthesis. During periods of enhanced productivity the carbon pool in the water becomes enriched in ^{13}C (i.e. in-lake versus catchment productivity).

1.2.2.5 Human impacts

Establishing the level of human impacts on the environment and the nature of feedbacks are one of the most topical issues when attempting to reconstruct palaeoclimatic conditions (Taylor and Robertshaw, 2001), especially in terms of separating natural environmental changes from those which are principally anthropogenic, in lake sediment records (Taylor and Robertshaw, 2001, Anderson, 1995). The use of sediments as proxy records of human activity are based on the assumption that the associated environmental impacts are a result of major changes in human activity, such as introduction or intensification of agriculture,

which often leads to, amongst other effects (e.g. changes in pollen, increases in charcoal and increased nutrient inputs), large deposits of catchment material into the sedimentary record. However, many problems remain. For example, the clearance of catchment forests by humans and its replacement by grassland will affect the fossil pollen assemblage; however, it may also be interpreted as a period of increased aridity. As a consequence several lines of evidence are required to disentangle signals of natural and anthropogenic changes.

The exact timing of human impacts in some of the crater catchments of Uganda remains largely unknown. Studies from swamp and lake deposits from south-western Uganda identify 'human' impact in the region from pollen, charcoal and sedimentary properties, that date back to the first millennium BC and a second phase a few centuries into the second millennium AD (Taylor and Robertshaw, 2001) as a result of iron working and agriculture. Other phases include a forest disturbance episode ~1500 AD, and a recent phase dated to ~200 years BP, the earlier of which correlates with the onset of dry climates of the broadly defined LIA and thus there are uncertainties whether the increase in charcoal is a direct result of human activity or a combination of both natural and human influences (Taylor and Robertshaw, 2001).

During recent decades, Lake Victoria has undergone several ecological changes (Verschuren *et al*., 2002), the most notable of which is the explosion of the Nile perch population and the demise of endemic cichlids (Ogutu-Ohwayo, 1990; Schofield and Chapman, 2000). Observed changes in the phytoplankton community since the 1980s appear to be a consequence of bottom-up excess nutrient loading resulting from long-term, 20th century deforestation and intensified agriculture within the catchment (Hecky and Bugenyi, 1992). In more recent times silica depletion of the lake waters is important as well as a switch in diatom flora from an *Aulacoseira* to *Nitzschia* dominated assemblages as a result of increasing anoxia in the lake waters (Verschuren *et al*., 1998). The timing of the inferred productivity increase from the diatom data matches the human population growth and agricultural activity in the catchment (Verschuren *et al*., 2002). The strong chronological link between historical land use and algal production indicates that landscape disturbance is the dominant cause of eutrophication in Lake Victoria.

Similarly a study of the highland crater Lake Saaka (Crisman *et al*., 2001) in Uganda showed that the lake has been undergoing cultural eutrophication since the early 1970s, based on a variety of measured parameters (conductivity, Secchi depth and DO saturation of surface waters) and the observations of a priest who recorded an increasing

number of algal blooms. The eutrophication of the lake appears to be as a result of an expansion of a Ugandan government prison farm along the shore of the lake, where planting against the elevation contours has lead to an increase in erosion, and inorganic and nutrient loading to the lake. In addition to this, wetlands that once lay adjacent to the lake have been drained for agriculture (Crisman *et al*., 2001).

It is apparent from previous studies that human activity in many lake catchments of Uganda may be traced back a few hundred years, with a marked activity occurring since the end of colonial rule in 1962. A study by Ssemmanda *et al*. (2005) at Lakes Kasenda and Wandakara recorded pollen of agricultural origin (e.g. eucalyptus and pine) in 20th century sediments (last 50-75 years). The period following the end of colonial rule experienced rapid population growth and a need for increased agricultural expansion that has resulted in the pattern of large-scale deforestation and agricultural conversion (even on the steepest crater walls) that continues to the present day (Crisman *et al*., 2001; Verschuren *et al*., 2002). Similar pressures elsewhere in East Africa have resulted in eutrophication of crater lakes (cf. Green, 1986), the waters of which are a major resource for rural populations and degradation of lake ecosystems will continue unless land-management strategies restricting nutrient inputs are implemented (Verschuren *et al*., 2002).

1.3 Research aims

In light of the above review, the aim of this research is to provide high-resolution palaeolimnological reconstructions of short- and long-term environmental and climatic change in the western Uganda over the last 1000 years in the context of increasing human impact. The sedimentary records from a paired lake system are investigated using a multi-proxy approach to infer past changes in climate and environmental history. Records spanning the last 150 years are used to compare the palaeolimnological record to available documentary evidence in order to establish the potential impact of humans on climate history contained within lake sediments. Specific research aims are:

- To carry out a modern limnological survey of a number of crater lakes in western Uganda and to use the results to develop a new diatom-conductivity transfer function for the freshwater crater lakes.
    - How do the modern lakes function? What are their current environmental/ecological conditions?

- To establish whether sedimentary proxies from crater lakes can be used to make reliable inferences and aid the understanding and contribute to the debate surrounding the regional complexity of past regional climate and environmental changes in western Uganda and East Africa.
    - Are the crater lakes sensitive to climatic and other environmental perturbations such as the Medieval Warm Period (MWP), Little Ice Age (LIA) and changes related to El Niño-Southern Oscillation (ENSO)?
    - Is there palaeolimnological evidence for the inferred 'widespread' drought across East Africa that occurred in the late 18th century?
    - Do the results suggest regional heterogeneity or spatial complexity of climatic events (such as the LIA) across western Uganda and East Africa?

- What are the possible mechanisms controlling these spatial patterns (e.g. a result of compression of the inter-tropical convergence zone [ITCZ] or more complex involving ITCZ and ENSO interactions)?
    - Do all lakes show a similar response to such drivers? Can the theory of 'lake coherency' to common climate drivers be tested and understood?
    - Do observed in-lake changes compare to documentary and anecdotal records of climate change from the last *c.*100 years?

- To assess if and when anthropogenic impacts on the lake catchments first became apparent in the west Ugandan palaeolimnological record.
    - Does varying human influence on lake catchment over the 20th century affect the recent lake climate record?

These aims will be achieved using a multiproxy palaeolimnological approach, using analyses of diatoms, sediment properties and bulk organic ($\delta^{13}C$) isotopes. A diatom-based transfer function to reconstruct limnological parameters important to diatom ecology (e.g. conductivity, total phosphorus) will be developed from a calibration dataset from lakes in western Uganda and will be applied to all core sequences. The diatom transfer function will provide evidence of regional variations in climate (in terms of effective precipitation); the transfer function may potentially be used to explore other variables (e.g. total phosphorus enrichment due to agricultural impacts within the lake catchments).

High-resolution (sub-decadal), multiproxy investigations of lake sediment cores based on biotic assemblages (e.g. diatoms), geochemistry (e.g. stable organic isotopes: C/N and $\delta^{13}C$) and sedimentary variables (loss-on-ignition, magnetic properties and physical properties) potentially provide independent lines of evidence when reconstructing past climate and environmental changes (Lotter, 2003). Given the variation in response rates and sensitivity between proxies, a multiproxy approach provides a powerful means to reconstruct past environments, whilst a multi-lake approach assists in the identification and separation of local (catchment-scale) and regional effects (Fritz, 2008). The data collected during this research will be used to examine questions of spatial and temporal heterogeneity of climate change in the context of growing human impacts on the landscape over the last millennium.

1.4 Thesis outline

This thesis essentially consists of three parts. The first section provides a review of the study site, from the East African rift system, to the geology, climate and vegetation of Uganda. An overview of the western Uganda crater lake clusters is given alongside detailed site descriptions for each lake used in the study (**Chapter 2**). This is followed by a review of all methods employed in the investigation, from sample collection to sample analysis (water, sediment and chronological; **Chapter 3**).

The second part of the thesis presents results of a modern limnological investigation of the crater lakes of western Uganda (**Chapter 4**) before using the data to develop a diatom-conductivity model for the crater lakes (**Chapter 5**).

The final section presents results from the lake sediment records: interpreting environmental change during the last 1000 years (**Chapter 6**) and natural and cultural changes over the last 150 years (**Chapter 7**). A regional synthesis is presented in **Chapter 8**, discussing the findings and placing this research into a wider context through comparison with other published palaeoclimatic and palaeoenvironmental records from western Uganda and Eastern Africa. The thesis concludes (**Chapter 9**) by highlighting the contribution of this study to understanding of the short and long-term climatic and environmental history of western Uganda with direct reference to the original research questions proposed above.

Chapter 2

Regional Setting

2.1 Introduction

This chapter considers the major geological features which make up the physical environment of East Africa and its rift valley system before describing the crater lake clusters that run adjacent to the Western Branch of the Rift Valley in western Uganda. In addition to the physical environment, the modern monsoonal climate and hydrology of East Africa is discussed before finally detailing the modern vegetation and land-use across the field site and providing detail on the seven coring sites in the Bunyaruguru crater lake cluster.

2.2 East Africa and the Rift Valley System

The volcanically and seismically active East African rift valley system lies above a broad intercontinental swell (the East African Plateau) and consists of two branches, the Western and Kenya (Gregory) rift valleys. This system is linked to the Afar-Red Sea-Gulf of Aden rift system to the northeast (Ebinger, 1989).

The East African lakes owe their formation to the development of, and tectonic activity associated with, the Afro-Arabian rift system. The spreading associated with the formation of the East Africa Rift valley began at least 15 million years ago during the Miocene (Bahati *et al.*, 2005), though there is evidence which suggests multiple overlying phases of tectonic activity in the region, spanning the last 300 million years (Rosendahl, 1987; Braille *et al.*, 1995). The system extends from Turkey to Mozambique. The axial region of this system is the Afar triple junction (Ethiopia-Djibouti), and the rift system comprises three distinct limbs: 1) the Red Sea arm (north) and 2) eastern and 3) western branches of the Ethiopian rift which extends to the southwest into East Africa. The western branch of the divergent Ethiopian rift forms the western border of Uganda (Gregory, 1986; Figure 2.1a, b and c).

Beginning in Ethiopia, the western branch of the Rift system trends north-east, passing through Uganda and into southern Tanzania, where it rejoins the eastern rift. The western rift comprises a series of long troughs bounded by fault scarps 500-1500 m high (Arad and Morton, 1969). These normal faults constitute the basins of lakes Tanganyika, Kivu, Edward and Albert (Schlüter, 2006) with the uplifted massif (horst) of the Rwenzori

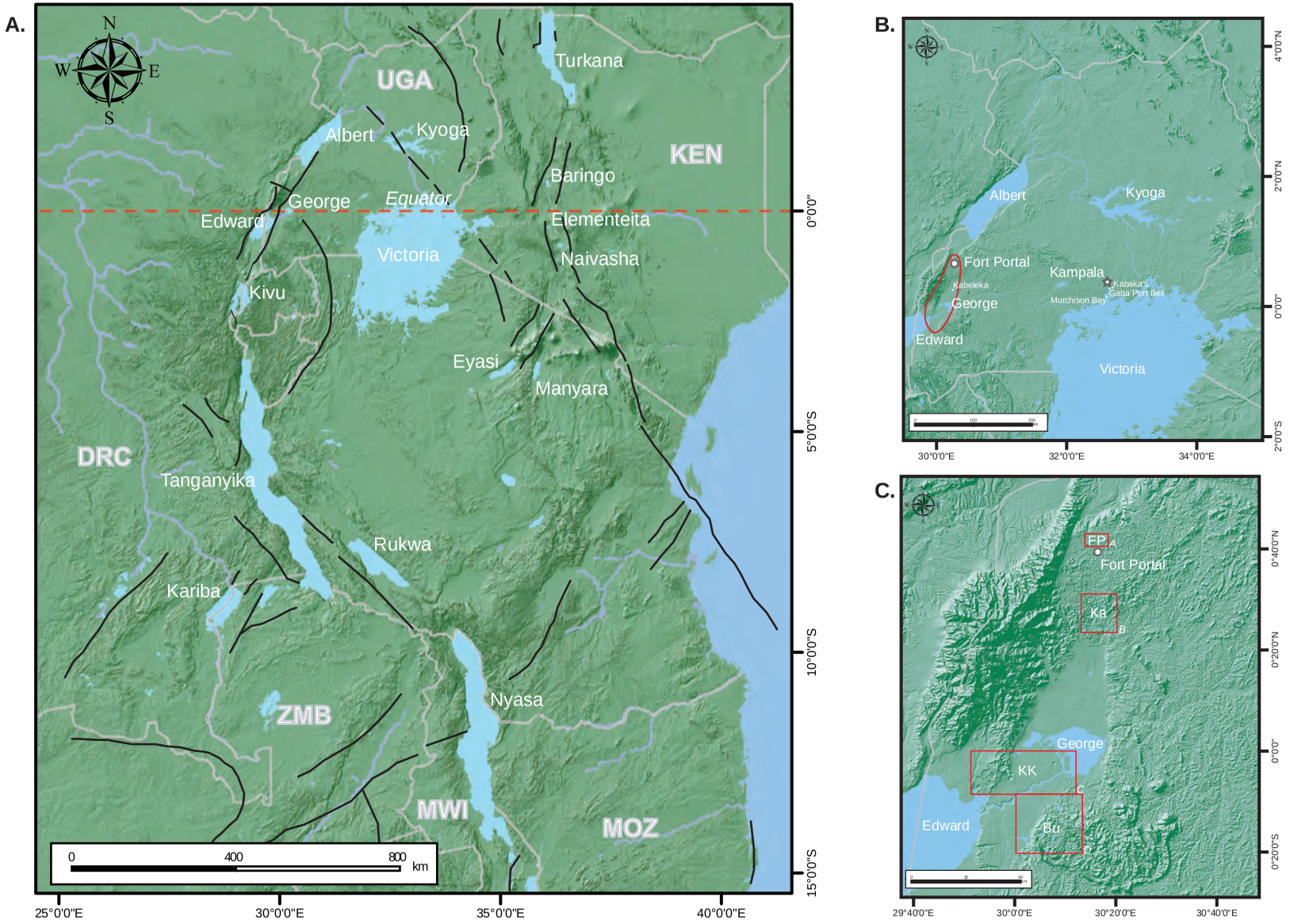

Figure 2.1 *Map of East Africa illustrating the Eastern and Western branches of the East African Rift Valley system and the major water bodies associated with this rifting* **(A)**. *The solid black lines represent the main fracture zones.* **(B)** *Map of Uganda. The red boundary shows the location of the field site in the west of the country.* **(C)** *A larger scale map of the field study area in the west of Uganda. There are four main crater lake clusters: Fort Portal (FP), Kasenda (Ka), Katwe-Kikorongo (KK) and Bunyaruguru (Bu) following those described by Melack (1978). The letters A-D correspond to the lake clusters shown in Figure 2.2*

Mountains (maximum height of 5119 m) separating the last two sections (Holmes, 1965). The majority of the lakes associated with the western rift are larger and deeper than their counterparts in the eastern rift (which includes lakes Turkana, Baringo, Elmenteita, and Naivasha; Schlüter, 1993).

In Uganda, the Western Rift also contains the Katwe, Buranga and Kibiro geothermal areas, which are thought to have formed at an early stage of the rift system development, and is younger (late Miocene–Recent) than the eastern branch (Morley and Westcott, 1999). The oldest known western rift sequences are late Miocene age (~8 Ma; Ebinger, 1989).

2.3 Geology of Uganda

The majority of Uganda is underlain by Precambrian rocks (formed between 300 and 600 Ma^{-1}). Only in the west and east are there any major developments of younger rocks: these are either Pleistocene volcanics or more recent, alluvial sedimentation (Atlas of Uganda, 1962; Schlüter, 2006).

The geology across the field region in southwest Uganda consists of Pleistocene to Recent sediments and Recent volcanics separated by a belt of Basement Complex (Figure 2.2a). The Basement Complex consists of groups of schists, marbles, gneisses and granulites, with multiple granitic and basic intrusions. The rocks within this group represent many ages, though they are most commonly attributed to a geothermal event of a post-Precambrian age (600 Ma^{-1}; Atlas of Uganda, 1962). The Pleistocene to Recent sediments/volcanics occur in the extreme north (around Fort Portal) and south (around Lakes George and Edward) of the field site. There are five main volcanic fields in southwest Uganda (from north to south): Fort Portal, Ndale (also known as the Kasenda or Kyatwa volcanic field), Katwe-Kikorongo, Bunyaruguru (or Kichwamba) and Katunga (Figure 2.2b). The western branch of the rift valley in Uganda is a classic locality for potassic alkaline magmatism. A variety of igneous lithologies are found in the Uganda segment of the rift: extrusive carbonatites to the north (FP), ultra-potassic volcanics in the central region (Katwe-Kikorongo, Bunyaruguru and Kasenyi Crater) and potassic mafic and felsic volcanics to the south (Bufumbira; Bahati, 2003).

The Fort Portal volcanic field is considered to be upper-Pleistocene to Recent in age (Nixon and Hornung, 1973), though a formation age of 6000-4000 yrs BP has also been suggested (Vinogradov *et al*., 1980). This volcanic activity resulted in the formation of around 50 morphologically youthful monogenetic tuff cones and maars, some of which

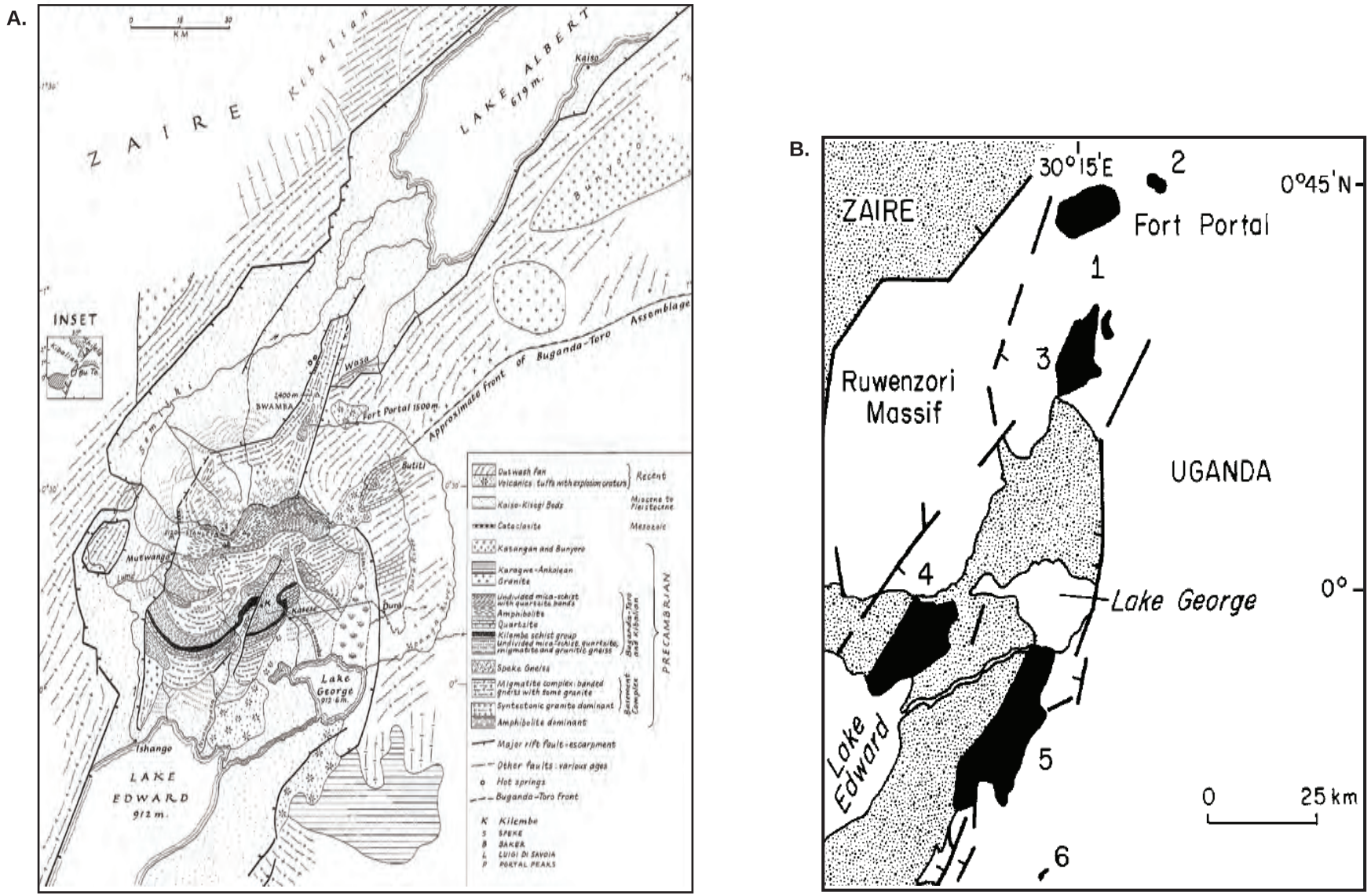

Figure 2.2 **(A)** *An outline geological map of the Rwenzori mountains and the western rift valley (from McConnell, 1972)* **(B)** *The volcanic fields of SW Uganda (in black; after Nixon & Hornung, 1973). 1=Fort Portal, 2=Kasekere, 3=Ndale, 4=Katwe-Kikorongo, 5=Kichwamba, 6=Katunga (from Barker and Nixon, 1989).*

now contain lakes, in ENE trending belts, parallel to the Precambrian basement terrain (Barker and Nixon, 1989).

South of the Fort Portal lies the Ndale, Kasenda or Kyatwa volcanic field, occupying the Western Rift Valley, east of the Ruwenzori Mountains. The tuff cones and lake-filled maars are also Pleistocene-to-Recent in age (Simkin and Seibert, 2002).

The Katwe-Kikorongo volcanic field (situated south of the Rwenzori mountains and bordered to the south by Lake Edward and the Kazinga channel) is the most extensive of a series of volcanic fields in the Western Rift Valley of Uganda, covering approximately 200 km^2, within which lies the Katwe geothermal area (Bahati *et al*., 2005). The volcanics here are mainly pyroclastic and are deposited on extensive Pleistocene lacustrine and fluvial Kaiso beds, and in some places on the Precambrian bedrock (Bahati, 2003). There are a large number of craters most of which lie on the main fault, striking NE-SW. The geology is characterized by explosion craters and ejected pyroclastics and tuffs, with abundant basement granite and gneissic rocks. Minor occurrences of lava are found mainly in the Kitigata and Kyemengo crater areas. The age of the volcanic activity has been estimated at Pleistocene to Holocene (Musisi, 1991; Bahati *et al*., 2005). The rocks in this region are largely silica-under saturated and potassic to ultra-potassic in composition (Arad and Morton, 1969; Eby *et al*., 2003). Local folklore suggest that volcanism in the Katwe-Kikorongo area has continued into historical times (Simkin and Seibert, 2002).

The southern-most volcanic field, Bunyaruguru (Kichwamba) is late Pleistocene to Holocene in age. The volcanic field lies along the eastern side of the rift valley, south of Lake George. It contains over 130 maars, 27 of which contain lakes with water ranging from fresh to saline.

An isolated tuff cone, Katunga, lies south of the Bunyaruguru volcanic field and is associated with lava flows located east of Lake Edward. The undissected tuff cone was erupted through metamorphic basement rocks and its rim and flanks are blanketed with ejected schists, its summit crater contains a freshwater lake. There is no known age of this cone but it is contemporaneous with late-Pleistocene to Recent tuff cones in the Bunyaruguru area (Simkin and Seibert, 2002).

Many of the soils in SW Uganda contain economically important minerals derived from older rocks in the region, such as detrital gold, tin ore, columbite and beryl. Of particular local importance are the salt deposits of Katwe and Kasenyi, Quaternary lacustrine limestone deposits (located north of Lake George; Mathers, 1994), glass sands, building sands and brick/pottery clays (Atlas of Uganda, 1962). In recent years there has

been the discovery of a carbon dioxide-free oil well beneath Lake Albert by Canada's Heritage Oil Company (Heritage Oil Company press release, March 2006).

2.4 The monsoonal climate

Uganda exhibits a complex regional pattern of climate regimes due to its topography, presence of large inland lakes and an eastward trend of increasing aridity related to decreasing maritime influences from the tropical Atlantic Ocean. The climate of East Africa is categorised as tropical with both wet and dry seasons, but sub-climatic zones exist and are differentiated mainly by altitude and rainfall (Bahati *et al*., 2005). Despite this spatial diversity, temporal rainfall fluctuations across the region are uniform at least at the inter-annual time scale, and seemingly driven by large-scale atmospheric dynamics linked to sea-surface temperature anomalies in the Indian Ocean (Nicholson, 1996; Nicholson and Kim, 1997; Marchant *et al*., 2006).

Rainfall in Equatorial East Africa is seasonally bimodal, driven by the biannual migration of the Inter Tropical Convergence Zone (ITCZ), bringing moisture from both the Atlantic and Indian Oceans (Nicholson, 1996). Uganda experiences two wet seasons, the first occurs between March and mid-May ('long rains' or 'latter rains'; Endfield *et al*., 2009) and the second season is October to December ('short rains'). Most of the rain falls during the first period. Precipitation is strongly affected by the discontinuous mountains along the western border of Uganda. In the northern and southern crater regions, annual rainfall varies from 1300-1600 mm yr^{-1}. By contrast, the rift floor in the region between Lakes Edward and George (Kazinga Channel) averages 750-1000 mm yr^{-1}, with extreme dry seasons (Atlas of Uganda, 1962). The highest annual rainfall is recorded for areas around Lake Victoria (~2000 mm), whilst the lowest (about 600 mm) is recorded in the northern and eastern parts of the country. The average annual precipitation for Uganda is estimated to be 1200 mm. The average annual potential evapotranspiration is 1400 mm and this exceeds precipitation during most of the year. There is little variation in temperature or day length at this latitude (mean maxima 24-27 °C, daily variation 10-15 °C; Atlas of Uganda, 1962). However, mean temperatures across the entire country can fluctuate widely, depending on elevation and landscape and thus vary from 18 to 33 ºC (Bahati *et al*., 2005).

Figure 2.3a illustrates the prevailing wind and pressure systems governing the monsoonal system over Africa during January and July/August. There are three major air streams associated with the East African monsoon system. These are the Congo air (humid,

convergent and thermally unstable), the northeast monsoon (dry conditions), and the southeast monsoon (which brings moisture from the southern ocean and is responsible for the main seasonal rainfall). The occasional moist winds from the west (Congo air) are responsible for additional rains (Langdale-Brown *et al*., 1964; Nicholson, 1996). The air streams are separated by two surface convergence zones, the Intertropical Convergence Zone (ITCZ) which separates the two monsoons, and the Congo Air Boundary (CAB on Figure 2.3a and b) which separates the easterly and westerly flows (Nicholson, 1996).

The tropical climate of Africa is governed primarily by the seasonal migration of the ITCZ in response to changes in the location of solar heating maxima. When high pressure develops over cold northern hemisphere land masses, and low pressure develops over the warm southern hemisphere, the ITCZ lies to the south (Figure 2.3b) and the southeasterly winds flow towards the area of low pressure. Conversely, when the northern hemisphere land masses heat during the summer seasons, the temperature anomaly between the land and the ocean is altered, causing a northward migration of the ITCZ (Figure 2.3b). The air above the land rises, drawing the humid air from the oceans. As the humid air rises, moisture is lost by 'monsoonal' precipitation. This results in northern and southern belts of monsoonal climates with summer wetness and winter dryness, confining a humid equatorial zone characterised by a bimodal rainfall pattern (Gasse, 2000). Nicholson (1996) has shown rainfall variability in East Africa to be closely linked to ENSO.

Long-term research into the El Niño Southern Oscillation (ENSO) show tropical climates oscillate at irregular time intervals (3-7 years), usually between El Niño and La Niña phases. However, there is growing evidence for the Indian Ocean Dipole (IOD), an independent oceanic circulation, being partly responsible for driving the climate variability of surrounding land masses (Marchant *et al*., 2006).

Many studies document links between ENSO events and precipitation over the Great Lakes region of East Africa, with an excess of precipitation in El Niño years (Nicholson, 1996), yet a considerable amount of East Africa's rainfall does originate from the Indian Ocean. During positive IOD events the Indian Ocean warm pool shifts westwards, causing a warming of SST off the east coast of Africa. This causes a change in the normal convection patterns over the eastern Indian Ocean, and thus brings heavy rainfall over the East Africa region (Marchant *et al*., 2006). The recent documented rise in level of Lake Victoria (1997-8) appeared to correlate with SST anomalies caused by

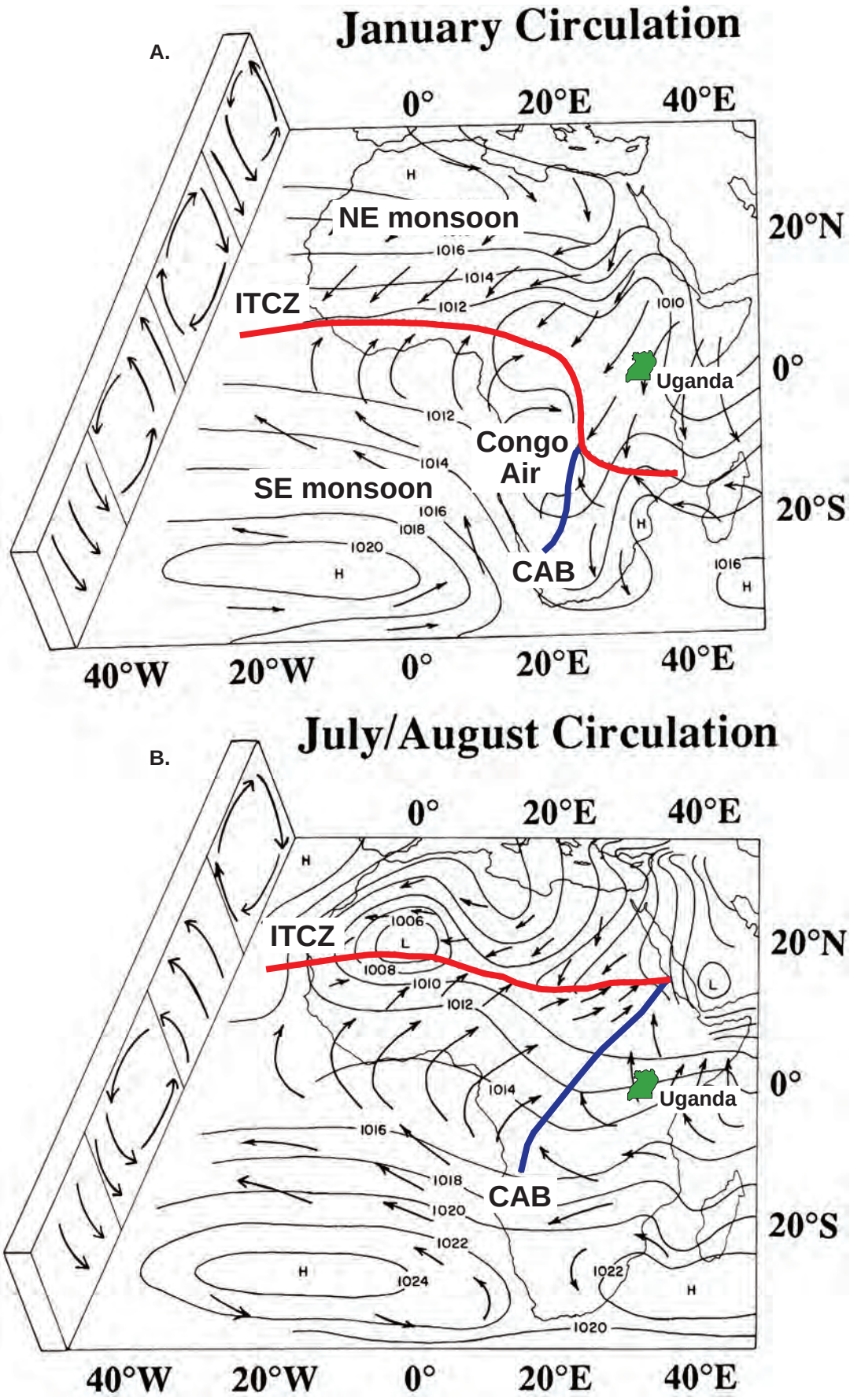

Figure 2.3 *Schematic diagram showing the general patterns of wind, pressure and convergence over East Africa during northern hemisphere winter* **(A)** *and summer* **(B)**. *The red line represents the Inter Tropical Convergence Zone (ITCZ), the blue line represesnts the Congo Air Boundary (CAB; adapted from Nicholson, 1996).*

significant warming in the western equatorial Indian Ocean following a strong El Niño event (Marchant *et al*., 2006). Conversely, recent isotope studies regarding coral SST records of the last 150 years have shown that ENSO and IOD are highly correlated (Pfeier and Dullo, 2006). Thus a degree of uncertainty does exist over the origin and potential impact of the IOD on tropical weather systems (Marchant *et al*., 2006).

2.5 The Vegetation of Uganda

2.5.1 Present day vegetation of southwest Uganda

The soils of southwest Uganda are classed as tropical eutrophic, and develop on the volcanic ash and alluvial deposits (Atlas of Uganda, 1962). These soils support a wealth of natural and secondary vegetation with the major vegetation patterns reflecting the climatic differences across the region, ranging from moist evergreen to semi-deciduous lower montane forest on the shoulders of the rift to grass savannah or thicket in the drier equatorial region of the rift valley floor (Atlas of Uganda, 1962; Kizito *et al*., 1993). Outside of National Parks (Queen Elizabeth) and forest reserves (Kibale, Maramagambo and Kasyoha-Kitomi), much of the field area has experienced heavy cultivation for the past 30-50 years or more (Figure 2.4).

Extending from Fort Portal to the Kasenda crater lake region, the vegetation consists of medium altitude forest savanna mosaic. Here the dominant vegetation is *Pennisetum purpureum* (Elephant grass), with isolated stands of forest and incoming savanna trees. This landscape is potentially a result of the partial clearance of the original forest and subsequent vegetation succession under the influence of repeated cultivation, cutting and grass fires (Langdale-Brown *et al*., 1964). Around Fort Portal are areas of dense cultivation (including tea and coffee plantations) in which natural vegetation is correspondingly sparse (Atlas of Uganda, 1962). Moving southwards and through the Kibale forest reserve the dominant vegetation is open canopy wooded savanna, consisting of moist acacia woodland and a well developed grass layer (*Hyparrhenia* spp.).

The equatorial region of southwest Uganda (near Kasese and Katunguru) is characterized by a vegetation change to a grass savanna, dominated by *Hyparrhenia* and *Themeda* species and semi deciduous thicket. These grasslands form a continuous cover from 0.5 to almost 2 m in height. In this vegetation zone trees and shrubs are generally absent (Atlas of Uganda, 1962).

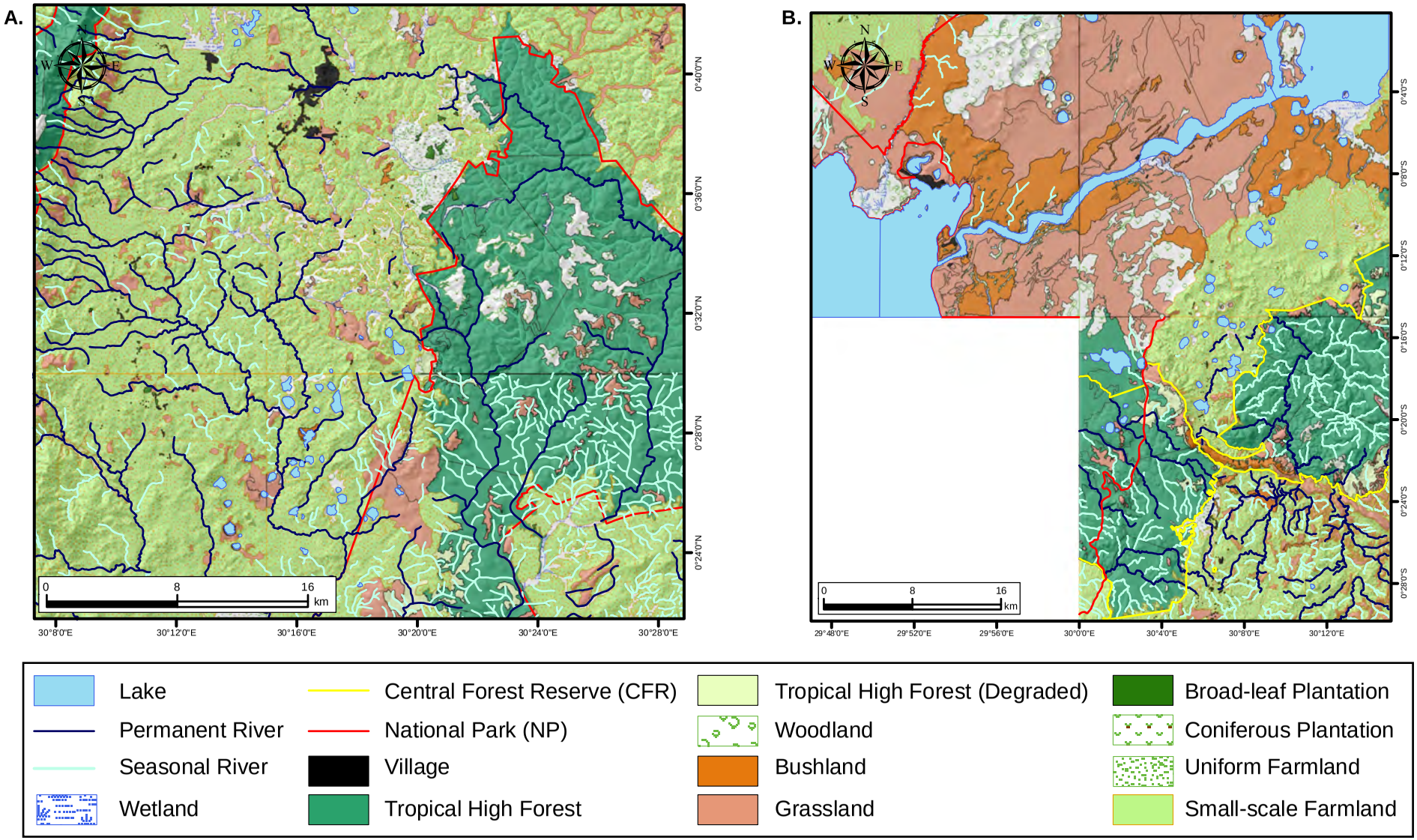

Figure 2.4 *Vegetation map across the field redion in western Uganda.* **(A)** *Northern area of field studies site (including lakes in the Fort Portal and Kasenda crater lake districts.* **(B)** *Southern area of field site including the Katwe-Kikorongo and Bunyaruguru crater lake districts.*

The vegetation of the southern-most crater lake region (Bunyaruguru) consists of a forest savanna mosaic and medium altitude moist semi-deciduous forest and moist evergreen forest. These forest types form close stands up to 30 or 40 m in height; lianas are abundant. In this region grasses are generally absent, or are broad-leaved and fire sensitive (Atlas of Uganda, 1962).

In the wetter, more densely populated areas outside of the protected areas (Fort Portal and Bunyaruguru), natural or secondary vegetation in the region has largely been replaced by an agricultural landscape and the establishment of villages, and this is especially evident within the catchments of some of the crater lakes. The steepest inner crater walls usually remain relatively undisturbed, except by firewood collection, cattle and water carrying trails. Routine burning of secondary vegetation and intense subsistence agriculture inside some of the more gently sloping crater basins may increase the phosphorus loading in the lake through the loss of phosphorous from the catchment soils. This, in conjunction with increasing pressure on the lake as a source of water for both villagers and cattle and also as a resource, in terms of establishing small fisheries with both native and introduced tilapia (*Oreochromis* spp.) species may be responsible for the exacerbating the nutrient content of these naturally eutrophic lake waters (cf. 'endless summer', Kilham and Kilham, 1990; Kizito *et al.*, 1993).

2.5.2 Agriculture and farming in southwest Uganda

The main food crops in southwest Uganda consist of banana (*Musa* spp.), finger millet (*Eleusine coracana*) and cassava (*Manihot esculenta*) accounting for up to 60% of the major food crops in the region. Of lesser importance are sweet potato (*Ipomoea batatas*), maize (*Zea mays*) and groundnuts (*Arachis hypogaea*) accounting for 5-10% of the total food crops grown (Atlas of Uganda, 1962). All are grown in and around the crater lake regions. Animal husbandry on both large and small scales is also important in Uganda, with cattle, goat and sheep the predominate livestock in the southwest of the country. Small scale commercial fisheries are becoming increasingly important, with many of the smaller crater lakes of the region yielding catches of native species including *Barbus neumayeri*, *Hypxopanchax deprimozi*, *Clarias gariepinus* and a variety of haplochromine cichlids (Crisman *et al.*, 2001). Several non-indigenous species have also been introduced to some crater lakes, including species of tilapia (*Oreochromis niloticus, O. leucostictus* and *Tilapia zillii*) in order to increase available protein resources (Kizito *et al.*, 1993; Bwanika *et al.*, 2004).

The banana that dominates plantations in Uganda is the introduced *Musa* species as opposed to the native (and inedible) banana (*Ensete*). Banana has become the major food produce, with some banana groves known to be over 50 years old. The life span of banana groves ranges from four years (central Uganda) to several decades (Kalyebara *et al*., 2007). Speijer *et al*. (1999) report plantations as old as 30 years in western Uganda, and higher ages have been reported anecdotally.

In the last 30 years, banana cultivation has undergone a recent and rapid expansion, particularly in the southwest region of Uganda. This shift has been attributed to the increasing severity of production constraints, in particular, declining soil fertility (Kalyebara *et al*., 2007). The banana plant requires good, deep soils and shelter from winds and requires ample and sustained ground water, therefore crater lake catchments present ideal conditions. The crop is also largely dependent on rainfall; hence, crops are most common in the regions experiencing biannual rainfall. Areas experiencing a single wet season denote the limit of banana growth (Atlas of Uganda, 1962).

Millet, another staple crop, is more suited to plateau areas of the rift. Millet requires rain immediately after the seeds are sown. If the wet season is late (as has been the case in recent years), crop success is greatly reduced. Furthermore in areas where there is considerable land pressure, resulting in the loss of soil fertility, the production of millet is waning (Atlas of Uganda, 1962; Kidoido *et al*., 2002).

In an attempt to limit famine in times of reduced or late rainfall, Cassava, (introduced in Uganda between 1862 and 1875), is currently one of the most important staple food crops in the country (Otim-Nape *et al*., 2005). The crop is a strategic reserve for millet, given the annual uncertainty in rainfall needed for this crop. In addition to this, cassava can be stored for long periods. In western Uganda, cassava is becoming a major crop due to its perennial nature and ability to survive on limited rainfall. It is also one of the only crops to grow successfully on the light alluvium and sands in the region (Atlas of Uganda, 1962).

Whilst the agriculture in the west of Uganda appears to be sustaining a ‘market garden’ economy, there are several economically, and internationally important farming practices. Coffee and tea (Fort Portal), fish (Nile perch, Lake Victoria), tobacco and cotton (Fort Portal, Bushenyi and Kasese) are among Uganda’s leading commodity products.

2.6 Crater lakes of western Uganda

Volcanic crater lakes are numerous and widespread throughout Africa (Melack, 1978; Beadle, 1981) occurring in Cameroon (Kling, 1988), Ethiopia (Prosser *et al*., 1968), Tanzania (Hecky, 1971; Kilham, 1971), Kenya (Melack, 1979; MacIntyre and Melack, 1982) and Uganda (Beadle, 1966; Melack, 1978; Kizito *et al*., 1993).

In Uganda, high concentrations of these crater lakes are found in association with the western branch of the rift valley system, on the border with the Democratic Republic of Congo (Beadle, 1981). Many of the lakes in western Uganda have been formed as a direct result of volcanic activity (Beadle, 1981); it is likely that the volcanic episodes responsible for the formation of the crater lakes are much younger than the main rifting event which is attributed to Tertiary rifting and warping that continued into the Pleistocene (Atlas of Uganda, 1962). Associated with the latter phases of tectonic movement was the development of volcanic activity, evident in the craters around Fort Portal, either side of the Kazinga Channel and in the Mufumbiro Mountains in the extreme south-west (Atlas of Uganda, 1962).

The majority of the smaller lakes in western Uganda comprise of explosion craters and maars (lake type 12 and 11, respectively; Hutchinson, 1957). Many of these lakes are phreatomagmatic in origin. These volcanic craters are formed by violent steam explosions occurring when magma meets water at or near the surface (Hutchinson, 1957; Crumpler and Aubele, 2001), although there are usually no volcanic flows or volcanic material associated with this type of volcanism (Schmincke *et al*., 1974; Crumpler and Aubele, 2001). In some documented cases (e.g. Lake Nkugute; Bunyaruguru; Beadle, 1966) volcanic eruptions appear to have partly blocked valleys, and subsequently water has filled not only the newly formed, deep crater, but also flooded part of the blocked valley, creating an additional shallow basin.

The crater lakes of western Uganda are hypothesised to have formed during a late Pleistocene-early Holocene period of tectonic activity associated with warping along the high-relief accommodation zone separating Lakes Edward and George (Melack, 1978; Livingstone and Melack, 1984; Lærdal and Talbot, 2002; Tiercelin and Lezzar, 2002).

Western Uganda has four distinct maar-crater districts: Fort Portal, Kasenda (Ndale), Katwe-Kikorongo, and Bunyaruguru (Figures 2.1c and 2.5a-d; Table 2.1) containing over 80 crater lakes. The lakes straddle the equator, ranging in latitude from 0° 42’N to 0°19’S. The lakes near Fort Portal lie slightly higher in altitude (1520 m asl) than those in the Kasenda cluster (1220-1400 m asl). The lakes in the Katwe-Kikorongo cluster

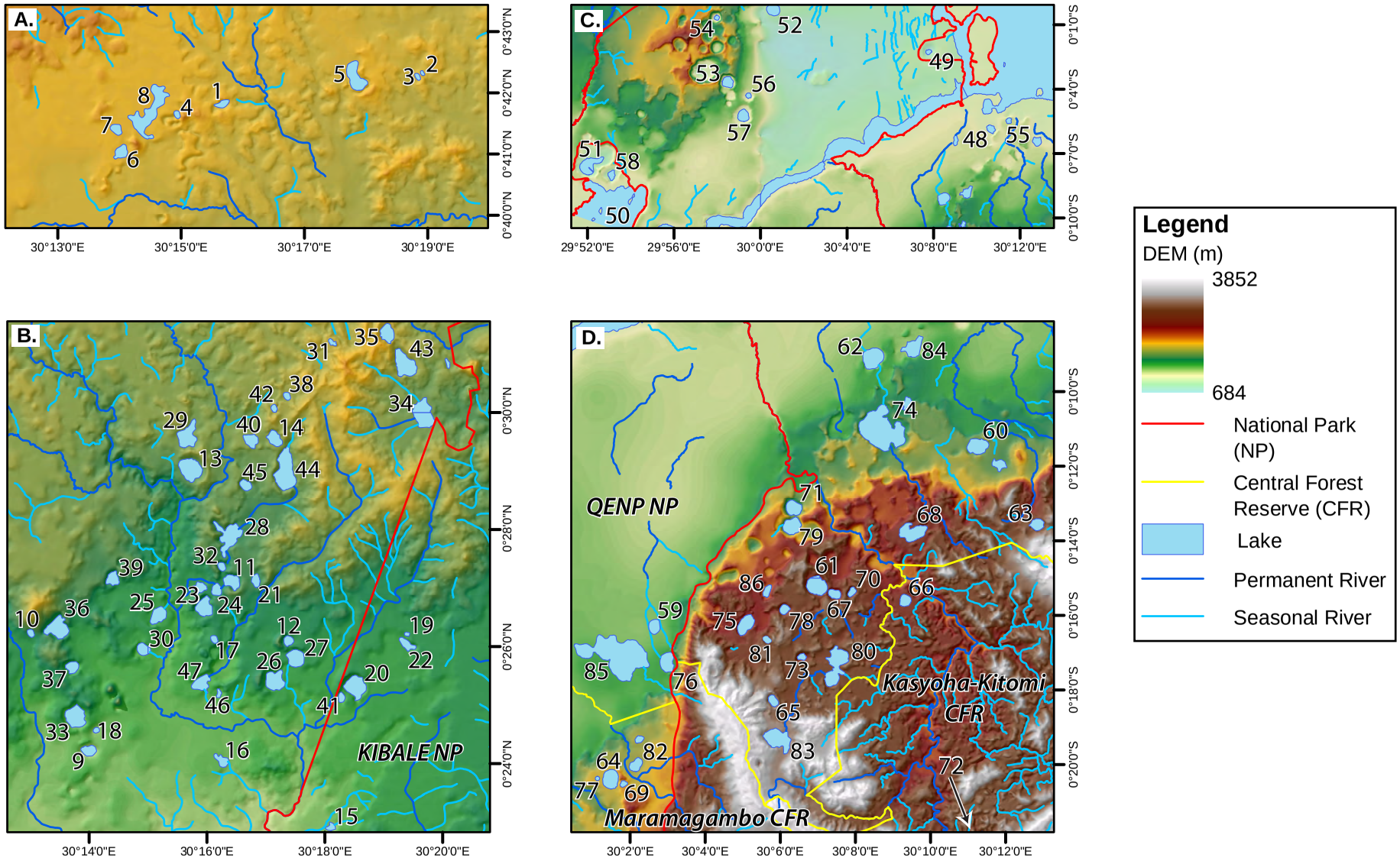

Figure 2.5 *A digital elevation model showing the four main crater lake clusters as shown in Figure 2.1c. The lakes are numbered 1-86 across the four clusters. These numbers correspond to those in Table 2.1. The lakes located in the north are shown in* **(A)** *Fort Portal and* **(B)** *Kasenda. The southern most clusters are illustrated in* **(C)** *Katwe-Kikorongo and* **(D)** *Bunyaruguru. The solid red lines represent the National Park (NP) boundaries; the solid yellow lines represent the boundaries of Central Forest reserves (CFR).*

lie on the rift valley floor (895-925 m asl), and those in the Bunyaruguru craters extend into the uplands (975-1250 m asl) floor. The lakes are spread along the strong ecotonal gradient between the moist shoulder and dry floor of the Rift valley. The crater lakes display a variety of morphological, geological, physical, chemical and biological characteristics (Tiercelin and Lezzar, 2002). There is a strong salinity gradient amongst the lakes, which vary from dilute to hypersaline (< 100 to 135,400 μS cm^{-1}), and from shallow and polymictic to deep and permanently stratified (0.25 m to >180 m; Melack, 1978, Kizito *et al*., 1993; Eggermont and Verschuren, 2004a).

2.7 Study lakes

The seven lakes chosen for detailed study belong to the Bunyaruguru cluster of crater lakes (as described by Melack, 1978), located south of the equator (Figure 2.6). The lakes range in altitude from 976 m (rift valley floor, e.g. Nyamogusingiri) to 1250 m (rift escarpment; e.g. Nyungu). The climate is tropical sub-humid with mean annual temperatures ranging from 22.5-25 °C. Annual rainfall averages 850-1200 mm and the mean annual evaporation is between 1575-1875 mm (Atlas of Uganda, 1962). The lakes are located on an east to west transect and differ in terms of the intensity of human impact within their catchments. The land-use in the region varies from protected moist semi-deciduous forest and grassland within the Queen Elizabeth National Park (QENP; established in 1954, though some reserves were established in the 1930s, cf. Ssemmanda *et al*., 2005) and two Central Forest Reserves (CFR; Maramagambo and Kasyoha-Kitomi), to a largely cleared corridor containing small-scale farmland and plantations (Figures 2.6 and 2.7). All of lakes both within and outside of this now-protected area are a primary water resource for many villages as well as being exploited for fishing and other activities.

2.7.1 Long core sites: Nyamogusingiri Crater and Kyasanduka

Lakes Nyamogusingiri and Kyasanduka (0°17’4.5” S, 30°0’46.7” E and 0°17’23.2” S, 30°0.6” E) are shallow crater lakes (depths of 2-13 m) located within the Bunyaruguru lake cluster (Figure 2.8 a, b and c). These lakes are situated within the Maramagambo CFR on the ecotone between moist semi-deciduous forest and grass savanna (Langdale-Brown *et al*., 1964). Reported annual rainfall for Lakes Nyamogusingiri and Kyasanduka is in the range of 900-1300 mm (Lock, 1967). Despite their close proximity, the two lakes differ greatly in both their physical and limnological attributes. Lake Nyamogusingiri is much

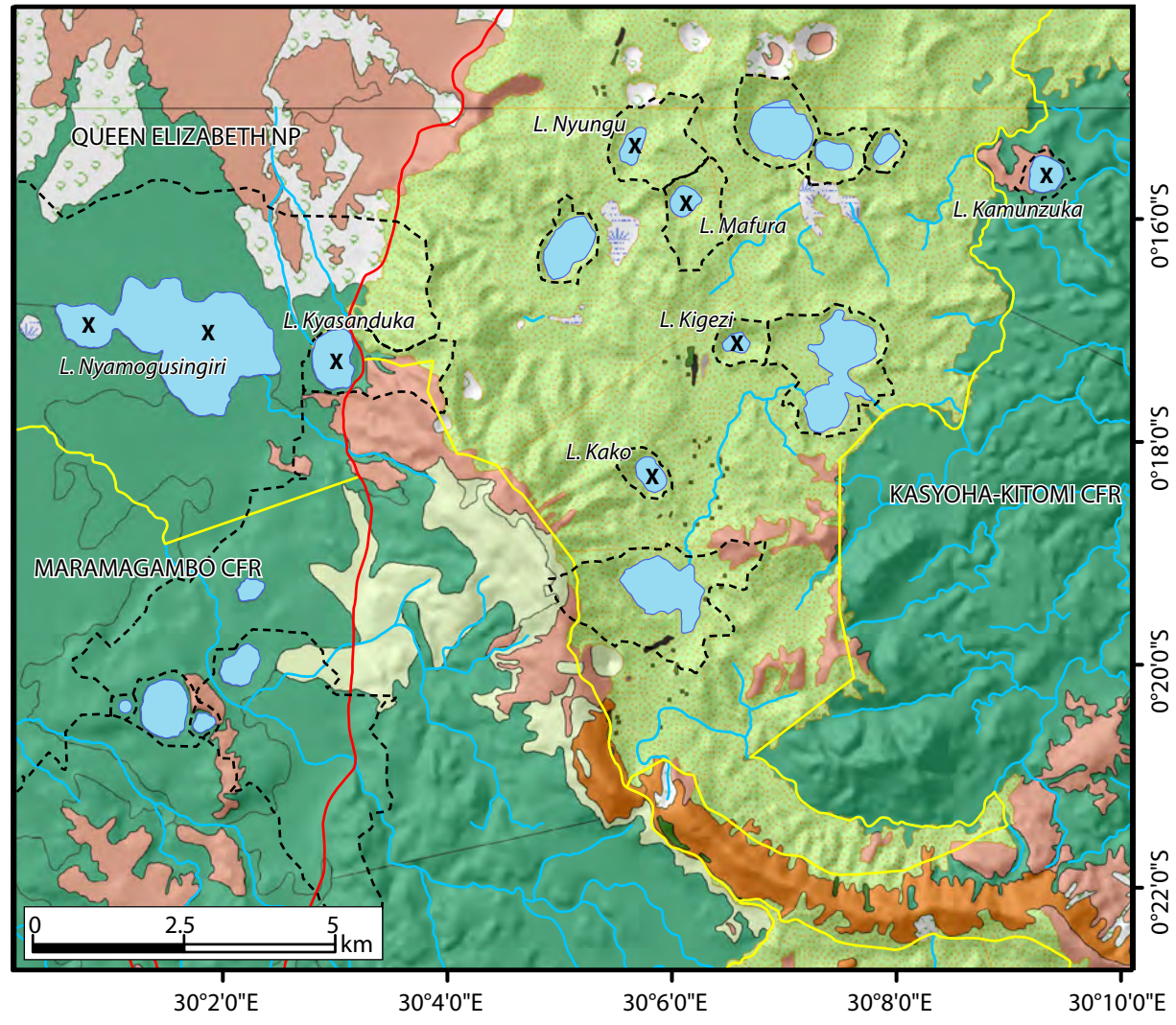

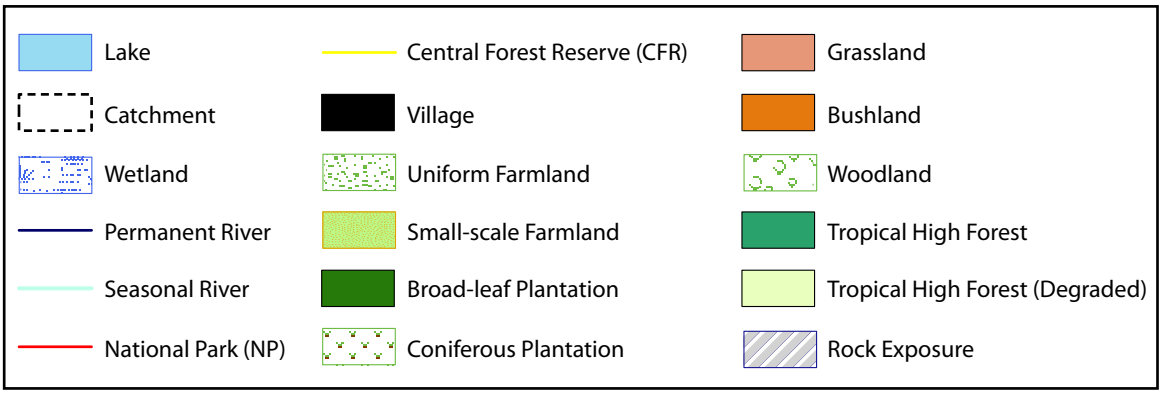

Figure 2.6 *Small scale map of the southern field area, indicating the lakes that were sampled for detailed core analyses (***X***= Kajak and Russian core sampling locations). The map highlights the main land usage across the region. It is worth noting the large scale forest clearance outside of the National Park (NP) and Central Forest Reserve (CFR) boundaries.*

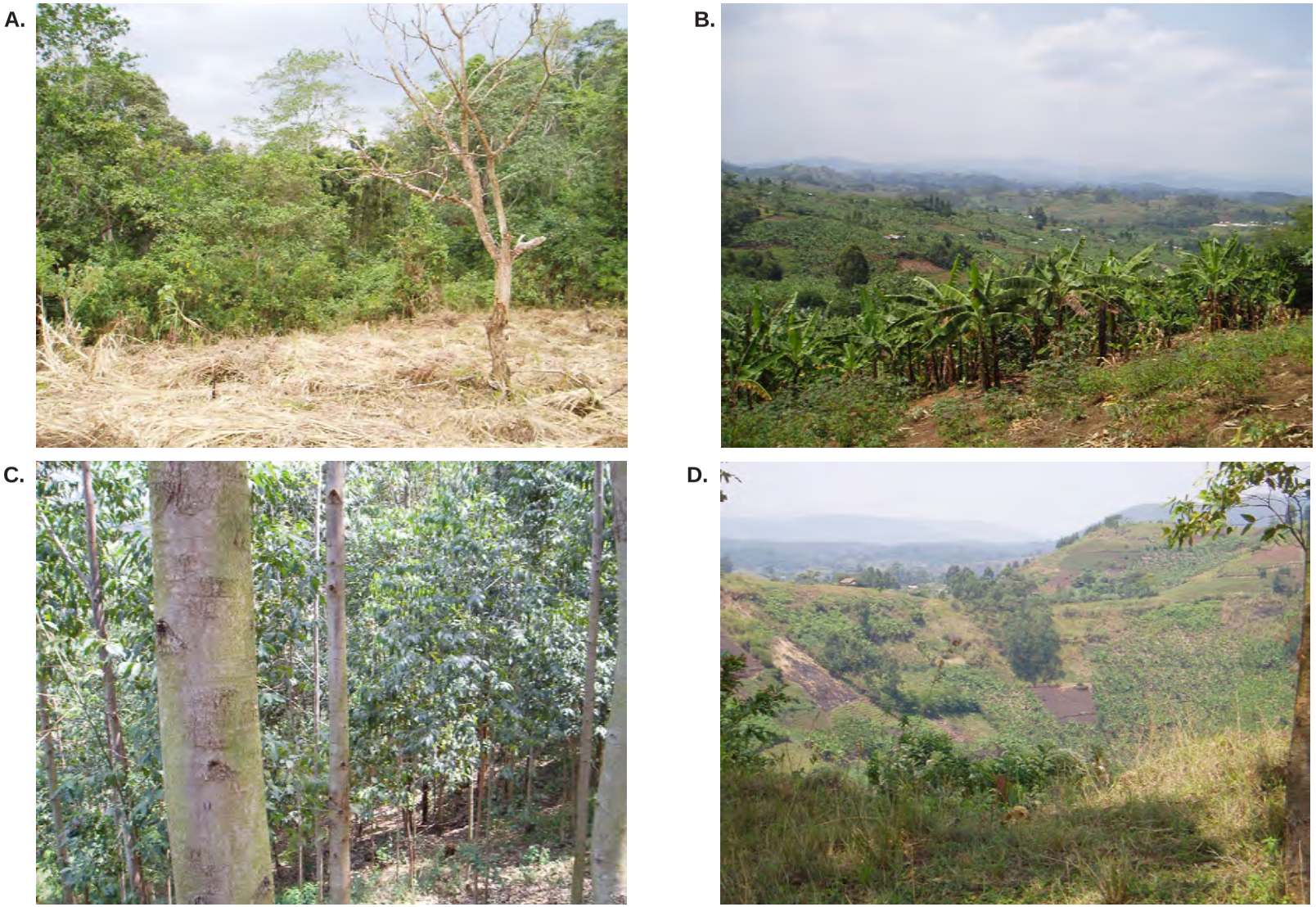

Figure 2.7 *Photographs of the various catchment types from the Bunyaruguru crater region.* **(A)** *Natural/secondary forest and grass savannah (e.g. Lakes Kamunzuka and parts of Nyamogusingiri and Kyasanduka);* **(B)** *Banana plantation (e.g. Lakes Nyungu and Mafura);* **(C)** *Eucalyptus plantation (e.g. Lake Kako) and* **(D)** *Market garden agriculture with evidence of land clearance and burning (e.g. Lakes Kigezi, Kako, Nyungu and part of Kyasanduka). Photographs taken by K. Mills.*

larger (4.3 km^2), with a minimum catchment area: lake ratio (CA: L) of 11.6* and a higher conductivity (554 µS cm^{-1}) than Kyasanduka (0.55 km^2; 204 µS cm^{-1}; CA: L = 4.1). In addition to this, Lake Nyamogusingiri has a higher Secchi disk depth than Lake Kyasanduka (**Chapter 4,** Table 4.2). Short term monitoring of Lake Kyasanduka by Bwanika *et al*. (2004) indicated that 'pronounced algal blooms' contribute to the very low Secchi transparency readings, leading to supersaturated dissolved oxygen levels in surface waters during the day, and a sharp oxycline (as found in January 2007; for full water chemistry and discussion, refer to **Chapter 4**). Furthermore, both lakes support native fish communities (including *Barbus neumayeri, Hypxopanchax deprimozi*, *Clarias gariepinus* and several haplochromine cichlids) alongside introduced, non-indigenous species (e.g. *Oreochromis niloticus*, *Oreochromis leucostictus*, and *Tilapia zillii*; Bwanika *et al*., 2004). These fish were introduced into many lakes in order to increase available protein to local villagers, and also for commercial fishing (Kizito *et al*., 1993; Bwanika *et al*., 2004). In 1988 fishing was prohibited in Lake Kyasanduka. Nyamogusingiri continues as a small-scale commercial fishery, though it is largely overexploited (Bwanika *et al*., 2004).

There has been some recent, documented human impact within the catchment of Lake Nyamogusingiri. In 1998, a new tourist eco-lodge, the 'Jacana Safari Lodge', was built on the northern shore of the larger basin of Nyamogusingiri, and is likely to have increased the amount of sediment flux and possibly nutrients to the large basin of Nyamogusingiri.

Lake Nyamogusingiri is the deeper of the two lakes. Lake Kyasanduka has a maximum recorded depth of 2 m while Nyamogusingiri has been widely reported across the years to have a maximum depth of approximately 4-5 m (Melack, 1978; Kizito *et al*, 1993; Bwanika *et al*, 2004; D.B. Ryves, unpublished data). However, in the most recent survey of Nyamogusingiri (January, 2007) the maximum depth of the lake was found to be much deeper (*c*. 12 m). Nyamogusingiri appears to be an amalgamation of several smaller craters; the majority of which form a broad, flat basin (with a depth of *c*. 3.9 m in January 2007; Table 2.1; **Chapter 4**, Table 4.2; Figure 4.2). To the extreme west of this basin lies a

* Only the minimum catchment area: lake (CA: L) ratio for Lake Nyamogusingiri is given. The actual extent of the Nyamogusingiri catchment area is unknown. The value given is that derived from digital maps, which give the northern, southern and eastern most extents of the catchment. Due to lack of available cartographic coverage in the west, the exact boundary in this direction cannot be calculated. It is expected that the CA:L would be much greater

smaller but deeper crater (~12.5 m) which is currently connected to the main basin (Figure 2.8b). A sill exists at a depth of 1.2 m between these two basins. If lake level has lowered in the recent past, then this sill may have become emergent, causing the currently adjoined basins to become two independent and isolated lakes. There is evidence within Nyamogusingiri's deep crater of previous lower lake levels. Situated around the present shoreline, several metres offshore are a series of dead trees and emerged tree stumps (Figure 2.8b). These trees are rooted at a depth of ~ 2 m and may be indicative of a long-term lower lake level in the recent past. In addition to this, local oral history tales tell of a time, reportedly in living memory, when there were 'two lakes' at this site.

2.7.2 Short core sites: Kamunzuka, Kako, Nyungu, Mafura and Kigezi

Four of the lakes under investigation: Lake Nyungu (0°15'22.9" S, 30°05'42.5" E), Lake Kako (0°18'21.18" S, 30°5'48.28" E), Lake Mafura (0°15'53.17" S, 30°6'6.09" E) and Lake Kigezi (0°17'15.1" S, 30°6'36.07" E) are located in the corridor of cleared land between the QENP and Maramagambo CFR in the west and the Kasyoha-Kitomi CFR in the east. These lakes are all subject to and differ in terms of the type and amount of human impact within their catchments (Figures 2.7 and 2.8d, e, f, g and h).

Lakes Nyungu and Mafura are very similar, relatively deep craters (*c.* 25 and 27 m, respectively) with almost identical catchments and are very heavily impacted. The vegetation within their catchments consists almost entirely of small-scale banana plantation, most likely for commercial retail. Several villages and a main road are located on the plateau between the two craters. Both lakes are used as a freshwater supply, and both are fished. Lake Nyungu experiences the most intense fishing with permanent nets in place, although these are unlikely to be used for large-scale commercial purposes.

Similarly, Lake Kako (29 m) has a heavily impacted catchment, although some stands of natural and/or secondary forest and bush do exist. The catchment surrounding Lake Kako consists of eucalyptus, pine, coffee and banana plantations and small-scale clearance mainly for subsistence agriculture (crops include sweet potato, cassava, millet and groundnuts). Lake Kigezi (26 m) has what can be described as a semi-impacted catchment. The majority of human activity in the catchment is mainly concerned with subsistence agriculture, including banana, tomato, sweet potato and ground nuts. At the time of sampling, there was also evidence of burning and clearance. Whilst it is likely that Kako and Kigezi are both exploited for small-scale fishing, unlike Nyungu there were no

Figure 2.8 *Photographs of the lakes from the Bunyaruguru crater region from which cores were collected and on which this study is based.* **(A)** *Nyamogusingiri Basin,* **(B)** *Nyamogusingiri Crater,* **(C)** *Kyasanduka and* **(D)** *Nyungu. Photographs taken by K.Mills.*

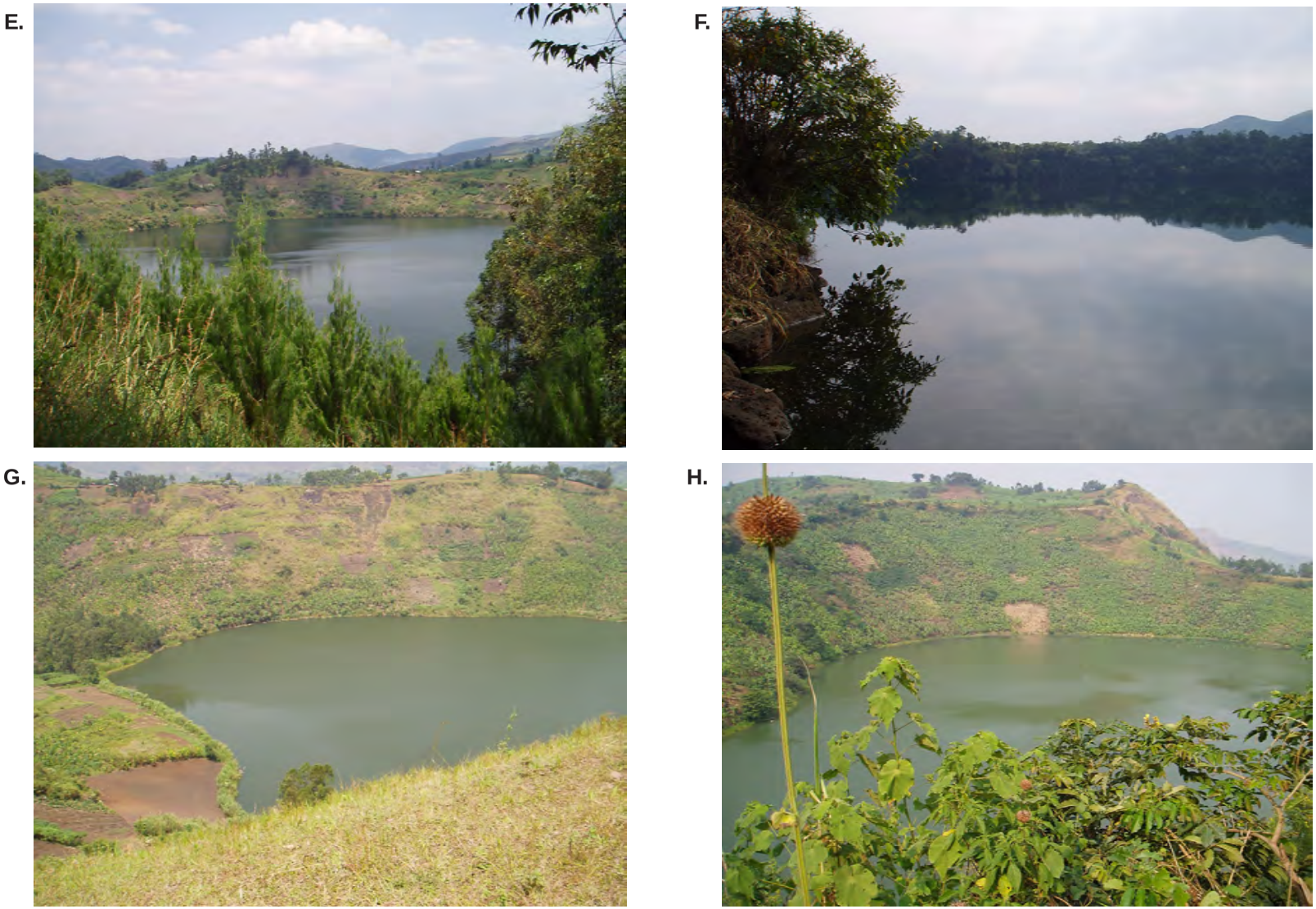

Figure 2.8 (cont'd) *Photographs of the five lakes from the Bunyaruguru crater region from which cores were collected and on which this study is based.* **(E)** *Kako,* **(F)** *Kamunzuka,* **(G)** *Kigezi and* **(H)** *Mafura. Photographs taken by K.Mills.*

signs of permanent fishing nets. However the lakes are used by several of the nearby settlements as a source of drinking water.

The remaining lake, Kamunzuka (0°15'49.8" S, 30°09'18.5" E), is a deep lake (*c.* 60 m) located just inside the Kasyoha-Kitomi CFR. Due to its protected status, Kamunzuka has a catchment largely comprising natural and/or secondary forest. To the northwest of the lake is an area of savanna grassland, which in July 2006 appeared to have experienced some recent burning (evidence of blackened trunks and cleared grasses and vegetation). As many of the existing trees were still alive, it is likely that the fire was of low intensity, though the cause (natural or as a management technique) is unknown. Human activity is evident directly outside of the protective CFR boundary, with clearance for small-scale agriculture. Despite its protected status, Kamunzuka is used as both a water and fishing resource.

2.8 Summary

- Volcanic and tectonic activity associated with the western branch of the rift valley system has resulted in the formation of ~80 crater lakes in western Uganda during the late Pleistocene.
- The crater lakes fall into four distinct clusters Fort Portal and Kasenda to the North and Katwe-Kikorongo and Bunyaruguru to the south. The positions of these clusters are related to some of the major volcanic fields in western Uganda.
- The crater lakes, which are phreatomagmatic in origin, straddle the equator and are spread along the strong ecotonal gradient between the moist shoulder and dry floor of the Rift valley.
- The climate of East Africa and the bi-modal rainfall distribution in Uganda is primarily dependent on the monsoonal weather system, which is controlled by the movement of the ITCZ. It is well documented that ENSO and perhaps the IOD can also affect regional rainfall patterns within this region.
- The present day vegetation distribution in Uganda is a reflection of both the dominating climatic conditions, with high altitude forest on the moist shoulder of the rift system and grass savanna and semi-deciduous thicket and also the extent of past and present human impact.
- Seven lakes in the southernmost crater lake cluster (Bunyaruguru) were the target for coring in this study. Whilst these lakes are in a region of similar climate and geology,

each lake varies in the amount of human activity within its catchment (from protected landscapes, to those heavily impacted by agriculture and clearance), making them suitable for analysing recent climate change and human impacts across the region.

Table 2.1 *Crater lakes of western Uganda. The numbers given below correspond to the numbered lakes on Figure 2.5. The location of the lakes are given (map sheet number, longitude and latitude) alongside the date when the individual lakes were visited and sampled (e.g. Jan-07) and by who (e.g. Lboro). The maximum depth (metres) and conductivity ($\mu S\ cm^{-1}$) of the lakes are given as well as an indication of what samples are included (X) in the transfer function (TF).*

N^o	Lake Name	Latitude	Longitude	Who	Date	Zm (m)	Cond.	TF
1	Kaitabarogo	0°41'46.8"	30°15'37.4"	RUMES	2007	70	489	
2	Kayihara	0°42'17.9"	30°18'56.1"	VERSCH.	Mar-00	65.1	498	x
2	Kayihara	0°42'17.9"	30°18'56.1"	RUMES	Jan-07	66	459	
3	Ekikoto	0°42'14.6"	30°18'46.6"	VERSCH.	Mar-00	72	484	
3	Ekikoto	0°42'14.6"	30°18'46.6"	VERSCH.	Jan-01	72	464	x
3	Ekikoto	0°42'14.6"	30°18'46.6"	RUMES	Jan-07	74	497	
4	Kanyangeye	0°42'00"	30°15'0.00"	MELACK[1]	May-71	57	456	
5	Kyaninga	0°42'8.11"	30°17'46.6"	VERSCH.	Jul-02	73	427	
5	Kyaninga	0°42'8.11"	30°17'46.6"	VERSCH.	Mar-00	57	423	
5	Kyaninga	0°42'8.11"	30°17'46.6"	VERSCH.	Jan-01	57	407	x
5	Kyaninga	0°42'8.11"	30°17'46.6"	RUMES	Jan-07	58	424	
6	Kyegere	0°41'2.9"	30°14'5.33"	RUMES	Jan-07	53	250	
7	Nyabikora	0°41'24.5"	30°13'58.8"	RUMES	Jan-07	7.7	188	
8	Saaka Crater	0°41'19.2"	30°14'34.4"	KILHAM[2]	Nov-69		535	
8	Saaka Crater	0°41'19.2"	30°14'34.4"	MELACK[1]	May-71	8.5	533	
8	Saaka Crater	0°41'19.2"	30°14'34.4"	RUSSELL	Mar-98			
8	Saaka Crater	0°41'19.2"	30°14'34.4"	CRISMAN[3]	Dec-98		623	
8	Saaka Crater	0°41'19.2"	30°14'34.4"	CHAPMAN	Dec-98	10.7	550	
8	Saaka Crater	0°41'19.2"	30°14'34.4"	RUSSELL	Jan-00			
8	Saaka Crater	0°41'19.2"	30°14'34.4"	DANIDA	Jun-00	11	714	
8	Saaka Crater	0°41'19.2"	30°14'34.4"	DANIDA	Mar-01	6	699	x
8	Saaka Crater	0°41'19.2"	30°14'34.4"	LBORO	Jul-06	7.8	662	x
8	Saaka Crater	0°41'19.2"	30°14'34.4"	RUMES	Jan-07	8	612	
9	Kanyamukali	0°24'11.4"	29°20'9.23"	VERSCH.	Mar-00	10.8	909	x
9	Kanyamukali	0°24'11.4"	29°20'9.23"	VERSCH.	Jan-02	11.0	892	
9	Kanyamukali	0°24'11.4"	29°20'9.23"	RUMES	Jan-07	11	920	
10	Kanyanchu	0°26'13.2"	30°19'19.2"	CHAPMAN	Dec-98	4.8	739	
10	Kanyanchu	0°26'13.2"	30°19'19.2"	DANIDA	Jul-00	4.7	598	
10	Kanyanchu	0°26'13.2"	30°19'19.2"	VERSCH.	Jul-02	5	700	
10	Kanyanchu	0°26'13.2"	30°19'19.2"	RUMES	Jan-07	4.8	568	
11	Kanyango	0°27'5.18"	30°16'24.6"	LBORO	Jul-06			
11	Kanyango	0°27'5.18"	30°16'24.6"	RUMES	Jan-07	58	493	
12	Kasenda	0°26'5.01"	30°17'19.6"	RUSSELL	Mar-98			
12	Kasenda	0°26'5.01"	30°17'19.6"	CHAPMAN	Dec-98	13	320	
12	Kasenda	0°26'5.01"	30°17'19.6"	DANIDA	Jul-00	13	380	x
12	Kasenda	0°26'5.01"	30°17'19.6"	DANIDA	Mar-01	13.5	275	
12	Kasenda	0°26'5.01"	30°17'19.6"	VERSCH.	Jul-02	15	321	
12	Kasenda	0°26'5.01"	30°17'19.6"	RUSSELL	May-03			
12	Kasenda	0°26'5.01"	30°17'19.6"	LBORO	Jul-06	14.2	352	x
12	Kasenda	0°26'5.01"	30°17'19.6"	RUMES	Jan-07	13	287	
13	Katanda	0°29'0.67"	30°15'42.6"	KILHAM[2]	May-05		393	
13	Katanda	0°29'0.67"	30°15'42.6"	MELACK[1]	May-71	146	375	
13	Katanda	0°29'0.67"	30°15'42.6"	KIZITO[4]	Mar-92		419	
13	Katanda	0°29'0.67"	30°15'42.6"	CHAPMAN	Dec-98	152		
13	Katanda	0°29'0.67"	30°15'42.6"	RUMES	Jan-07	>70	419	

Table 2.1 *Continued...*

N°	Lake Name	Latitude	Longitude	Who	Date	Zm (m)	Cond	TF
14	Kifuruka	0°29'33.2"	30°17'9.87"	KILHAM[2]	Nov-69		276	
14	Kifuruka	0°29'33.2"	30°17'9.87"	MELACK[1]	May-71	4	288	
14	Kifuruka	0°29'33.2"	30°17'9.87"	KIZITO[4]	Mar-92		352	
14	Kifuruka	0°29'33.2"	30°17'9.87"	RUSSELL	Mar-98			
14	Kifuruka	0°29'33.2"	30°17'9.87"	CHAPMAN	Dec-98	5	345	
14	Kifuruka	0°29'33.2"	30°17'9.87"	VERSCH.	Mar-00	5.3	347	x
14	Kifuruka	0°29'33.2"	30°17'9.87"	DANIDA	Jul-00	5	404	
14	Kifuruka	0°29'33.2"	30°17'9.87"	VERSCH.	Jul-02	2	353	
14	Kifuruka	0°29'33.2"	30°17'9.87"	RUSSELL	May-03			
14	Kifuruka	0°29'33.2"	30°17'9.87"	LBORO	Jul-06	4.5	460	x
14	Kifuruka	0°29'33.2"	30°17'9.87"	RUMES	Jan-07	3.7	411	
15	Kisibendi	0°22'56.3"	30°18'6.56"	RUMES	Jan-07	4.5	277	
16	Kitere	0°24'2.97"	30°16'13.4"	RUMES	Jan-07	51	711	
17	Kyakamihanda	0°26'4.98"	30°15'52.3"					
18	Kyanga	0°24'30.9"	29°20'15.6"	VERSCH.	Jan-01	55	1055	x
18	Kyanga	0°24'30.9"	29°20'15.6"	VERSCH.	Jan-02	57.1	1020	
18	Kyanga	0°24'30.9"	29°20'15.6"	VERSCH.	Jul-02	57	1056	
19	Kyerbwato	0°26'14.8"	30°19'20.8"	CHAPMAN	Dec-98	15.9		
19	Kyerbwato	0°26'14.8"	30°19'20.8"	DANIDA	Jul-00	13.4	450	x
19	Kyerbwato	0°26'14.8"	30°19'20.8"	VERSCH.	Jul-02	12.7	538	
19	Kyerbwato	0°26'14.8"	30°19'20.8"	RUMES	Jan-07	12.5	418	
20	Kyerere	0°25'17.8"	30°18'30.7"	CHAPMAN	Dec-98	63	256	
21	Lugembe	0°27'10.0"	30°16'48.9"	MELACK[1]	May-71	20	306	
21	Lugembe	0°27'10.0"	30°16'48.9"	KIZITO[4]	Mar-92		362	
21	Lugembe	0°27'10.0"	30°16'48.9"	CHAPMAN	Dec-98	18.9	370	
21	Lugembe	0°27'10.0"	30°16'48.9"	VERSCH.	Mar-00	18.6	395	x
21	Lugembe	0°27'10.0"	30°16'48.9"	VERSCH.	Jan-02	18.2	358	
21	Lugembe	0°27'10.0"	30°16'48.9"	VERSCH.	Jul-02	18.2	385	
21	Lugembe	0°27'10.0"	30°16'48.9"	RUSSELL	May-03	18.2	358	
21	Lugembe	0°27'10.0"	30°16'48.9"	RUMES	Jan-07	15	407	
22	Lyantonde	0°29'12.5"	30°16'50.7"	CHAPMAN	Dec-98	180	454	
22	Lyantonde	0°29'12.5"	30°16'50.7"	LBORO	Jul-06	80	512	x
22	Lyantonde	0°29'12.5"	30°16'50.7"	RUMES	Jan-07	>70	501	
23	Mahuhura	0°26'40.7"	30°15'57.2"	LBORO	Jul-06	80	633	x
23	Mahuhura	0°26'40.7"	30°15'57.2"	RUMES	Jan-07	>65	603	
24	Mpajo	0°27'0.29"	30°16'8.52"	RUSSELL	Mar-98			
24	Mpajo	0°27'0.29"	30°16'8.52"	LBORO	Jul-06			
24	Mpajo	0°27'0.29"	30°16'8.52"	RUMES	Jan-07	35	504	
25	Mubiro	0°26'30.9"	30°15'8.75"	RUMES	Jan-07	>70	718	
26	Murigamire	0°25'25.9"	30°17'8.34"					
27	Murusi	0°25'47.1"	30°17'29.3"	VERSCH.	Jul-02		366	x
27	Murusi	0°25'47.1"	30°17'29.3"	RUMES	Jan-07	57	382	
28	Mwamba	0°27'55.6"	30°16'24.6"	MELACK[1]	May-71	39	387	
28	Mwamba	0°27'55.6"	30°16'24.6"	LBORO	Jul-06			
29	Mwengenyi	0°29'34.8"	30°15'39.3"	KILHAM[2]	Nov-69		330	
29	Mwengenyi	0°29'34.8"	30°15'39.3"	MELACK[1]	May-71	101		
29	Mwengenyi	0°29'34.8"	30°15'39.3"	KIZITO[4]	Mar-92		358	
29	Mwengenyi	0°29'34.8"	30°15'39.3"	CHAPMAN	Dec-98	140	360	
29	Mwengenyi	0°29'34.8"	30°15'39.3"	RUMES	Jan-07	>70	352	
30	Njarayabana	0°25'53.8"	29°21'4.07"	VERSCH.	Jan-01	38	879	x
30	Njarayabana	0°25'53.8"	29°21'4.07"	VERSCH.	Jul-02	38	847	

Table 2.1 *Continued...*

N^{o}	Lake Name	Latitude	Longitude	Who	Date	Zm (m)	Cond.	TF
30	Njarayabana	0°25'53.8"	29°21'4.07"	RUMES	Jan-07	38	857	
31	Nkuruba	0°31'10.8"	30°18'1.53"	KIZITO[4]	Mar-92	38	341	
31	Nkuruba	0°31'10.8"	30°18'1.53"	CHAPMAN	Dec-98		325	
31	Nkuruba	0°31'10.8"	30°18'1.53"	RUSSELL	Jan-00			
31	Nkuruba	0°31'10.8"	30°18'1.53"	VERSCH.	Jul-02	34	352	
31	Nkuruba	0°31'10.8"	30°18'1.53"	VERSCH.	Mar-00	34.8	361	x
31	Nkuruba	0°31'10.8"	30°18'1.53"	DANIDA	Jul-00	38		
31	Nkuruba	0°31'10.8"	30°18'1.53"	RUMES	Jan-07	34.5	370	
32	Ntamba	0°27'23.0"	30°16'18.2"					
33	Ntambi	0°24'43.9"	29°19'56.3"	VERSCH.	Mar-00	105	5860	
33	Ntambi	0°24'43.9"	29°19'56.3"	VERSCH.	Jan-01	8	5820	x
33	Ntambi	0°24'43.9"	29°19'56.3"	VERSCH.	Jan-02	42	5380	
34	Nyabikere	0°30'5.83"	30°19'32.0"	RUSSELL	Mar-98			
34	Nyabikere	0°30'5.83"	30°19'32.0"	CHAPMAN	Dec-98	52.5	240	
34	Nyabikere	0°30'5.83"	30°19'32.0"	RUSSELL	Jan-00			
34	Nyabikere	0°30'5.83"	30°19'32.0"	VERSCH.	Mar-00	43.4	263	x
34	Nyabikere	0°30'5.83"	30°19'32.0"	RUSSELL	Jan-01			
34	Nyabikere	0°30'5.83"	30°19'32.0"	VERSCH.	Jul-02	44	239	
34	Nyabikere	0°30'5.83"	30°19'32.0"	RUSSELL	May-03			
35	Nyamirima	0°31'20.6"	30°18'58.0"	CHAPMAN	Dec-98	53.9	185	
35	Nyamirima	0°31'20.6"	30°18'58.0"	LBORO	Jul-06	51.9	216	x
36	Nyamiteza	0°26'16.5"	29°19'36.8"	VERSCH.	Jan-01	>80	1034	
36	Nyamiteza	0°26'16.5"	29°19'36.8"	VERSCH.	Jul-02	34	1057	x
37	Nyamogusani	0°26'16.5"	29°19'36.8"	RUMES	Jun-07	37	988	
37	Nyamogusani	0°25'35.9"	29°19'51.4"	VERSCH.	Jan-01	37	971	x
37	Nyamogusani	0°25'35.9"	29°19'51.4"	VERSCH.	Jul-02	36	983	
38	Nyamswiga	0°30'35.0"	30°17'4.99"	KIZITO[4]	Mar-92	11	320	
38	Nyamswiga	0°30'35.0"	30°17'4.99"	CHAPMAN	Dec-98	39.5	320	
38	Nyamswiga	0°30'35.0"	30°17'4.99"	LBORO	Jul-06	75	346	x
39	Nyamugoro	0°27'6.94"	29°20'36.5"					
40	Nyantode	0°29'29.9"	30°16'44.0"	KIZITO[4]	Mar-92	17		
41	Nyanwamba	0°25'36.7"	30°18'16.2"	CHAPMAN	Dec-98	35.7	460	
42	Nyierya	0°30'10.6"	30°17'3.39"	KIZITO[4]	Mar-92	11	463	
42	Nyierya	0°30'10.6"	30°17'3.39"	CHAPMAN	Dec-98	36	444	
42	Nyierya	0°30'10.6"	30°17'3.39"	LBORO	Jul-06	80	419	x
43	Nyinabulita	0°30'48.1"	30°19'17.4"	CHAPMAN	Dec-98	62.2	249	
43	Nyinabulita	0°30'48.1"	30°19'17.4"	LBORO	Jul-06	63.9	274	x
44	Nyinambuga	0°29'7.21"	30°17'19.5"	LBORO	Jul-06			
45	Rukwanzi	0°28'42.7"	30°16'39.1"	KIZITO[4]	Mar-92	11	413	
45	Rukwanzi	0°28'42.7"	30°16'39.1"	CHAPMAN	Dec-98	169	370	
45	Rukwanzi	0°28'42.7"	30°16'39.1"	LBORO	Jul-06			
46	Wandakara	0°25'11.3"	30°16'10.1"	DANIDA	Jul-00	12	1269	x
46	Wandakara	0°25'11.3"	30°16'10.1"	VERSCH.	Jan-01	12	1125	
46	Wandakara	0°25'11.3"	30°16'10.1"	VERSCH.	Jan-02	12.2	1057	
46	Wandakara	0°25'11.3"	30°16'10.1"	RUMES	Jan-07	10.5	1222	
47	Wankenzi	0°25'22.6"	30°15'52.4"	DANIDA	Jul-00		454	
47	Wankenzi	0°25'22.6"	30°15'52.4"	VERSCH.	Jan-01	58	496	x
47	Wankenzi	0°25'22.6"	30°15'52.4"	VERSCH.	Jul-02	51	289	
47	Wankenzi	0°25'22.6"	30°15'52.4"	RUMES	Jan-07	>60	397	
48	Bagusa	0°5'22.08"	30°10'42.4"	VERSCH.	Mar-00	0.9	61100	x
48	Bagusa	0°5'22.08"	30°10'42.4"	DANIDA	Mar-01	0.8	74100	

Table 2.1 *Continued...*

N^o	Lake Name	Latitude	Longitude	Who	Date	Zm (m)	Cond.	TF
48	Bagusa	0°5’22.08”	30°10’42.4”	RUMES	Jan-07	0.5	92300	
49	Bunyampaka	0°1’50.6”	30°7’47.98”	MELACK[1]	May-71	0.25	80000	
49	Bunyampaka	0°1’50.6”	30°7’47.98”	DANIDA	Jun-00		117500	
50	Edward	0°11’23.2”	29°49’46.6”	PHILLIPS[5]	Mar-21			
50	Edward	0°11’23.2”	29°49’46.6”	HURST[6]	Mar-24			
50	Edward	0°11’23.2”	29°49’46.6”	BEADLE[7]	Jul-31		884	
50	Edward	0°11’23.2”	29°49’46.6”	DAMAS[8]	May-35		1130	
50	Edward	0°11’23.2”	29°49’46.6”	FISH[9]	Sep-51		878	
50	Edward	0°11’23.2”	29°49’46.6”	RUSSELL	Apr-92			
50	Edward	0°11’23.2”	29°49’46.6”	RUSSELL	Dec-97			
50	Edward	0°11’23.2”	29°49’46.6”	RUSSELL	Apr-99			
50	Edward	0°11’23.2”	29°49’46.6”	VERSCH.	Jan-01	27	870	x
51	Katwe	0°7’35.45”	29°51’55.9”	PAPPE[10]	1890			
51	Katwe	0°7’35.45”	29°51’55.9”	GROVES[11]	Apr-30			
51	Katwe	0°7’35.45”	29°51’55.9”	WAY.[11]	Dec-31			
51	Katwe	0°7’35.45”	29°51’55.9”	KILHAM[2]	Nov-69	9.7		
51	Katwe	0°7’35.45”	29°51’55.9”	MELACK[1]	May-71	9	116000	
52	Kikorongo	0°1’43.7”	30°0’35.04”	GROVES[11]	Apr-30			
52	Kikorongo	0°1’43.7”	30°0’35.04”	BEADLE[7]	Jul-31		34600	
52	Kikorongo	0°1’43.7”	30°0’35.04”	KILHAM[2]	Nov-69		16300	
52	Kikorongo	0°1’43.7”	30°0’35.04”	MELACK[1]	May-71	8.5	16800	
52	Kikorongo	0°1’43.7”	30°0’35.04”	DANIDA	Jul-00		18470	
52	Kikorongo	0°1’43.7”	30°0’35.04”	VERSCH.	Jan-01	10.7	21700	x
52	Kikorongo	0°1’43.7”	30°0’35.04”	LBORO	Jul-06	11	22200	x
53	Kitagata	0°3’41.2”	29°58’26.8”	DANIDA	Jul-00		95000	
53	Kitagata	0°3’41.2”	29°58’26.8”	VERSCH.	Jan-01	7.5	135400	x
53	Kitagata	0°3’41.2”	29°58’26.8”	VERSCH.	Jul-02	8.9	127600	
53	Kitagata	0°3’41.2”	29°58’26.8”	RUSSELL	May-03			
53	Kitagata	0°3’41.2”	29°58’26.8”	RUMES	Jan-07		79600	
54	Mahega	0°0’35.78”	29°57’56.1”	MELACK[1]	May-71		112200	
54	Mahega	0°0’35.78”	29°57’56.1”	MELACK[1]	May-71		124700	
54	Mahega	0°0’35.78”	29°57’56.1”	DANIDA	Jul-00	4.1	138100	x
54	Mahega	0°0’35.78”	29°57’56.1”	LBORO	Jan-07	4.4	961000	x
55	Maseche	0°5’33.46”	30°11’26.0”	VERSCH.	Mar-00	0.05	68200	
55	Maseche	0°5’33.46”	30°11’26.0”	DANIDA	Mar-01		138100	x
55	Maseche	0°5’33.46”	30°11’26.0”	RUMES	Jan-07	0.02	32700	
56	Murumuli	0°4’18.60”	29°59’24.9”	DANIDA	Jul-00			
57	Nyamunuka	0°5’12.28”	29°59’12.0”	MELACK[1]	May-71	Dry		
57	Nyamunuka	0°5’12.28”	29°59’12.0”	LBORO	Jul-06			
58	Rwenyange	0°8’1.47”	29°53’6.98”					
59	Blue Pool	0°16’37.0”	30°2’57.07”	RUSSELL	May-99		352	
59	Blue Pool	0°16’37.0”	30°2’57.07”	DANIDA	Mar-01	2.7	460	x
60	Bugwagi	0°11’29.7”	30°11’14.7”	VERSCH.	Jan-01	85	440	x
60	Bugwagi	0°11’29.7”	30°11’14.7”	RUMES	Jan-07	85	441	
61	Chema	0°15’14.1”	30°6’59.41”	LBORO	Jul-06			
62	Chibwera	0°9’0.04”	30°8’20.25”	MELACK[1]	May-71	12.5	431	
62	Chibwera	0°9’0.04”	30°8’20.25”	DANIDA	Jul-00		513	
62	Chibwera	0°9’0.04”	30°8’20.25”	DANIDA	Mar-01	12	489	x
62	Chibwera	0°9’0.04”	30°8’20.25”	VERSCH.	Jul-02	11.7	453	
62	Chibwera	0°9’0.04”	30°8’20.25”	RUMES	Jan-07	10.5	462	
63	Kabarogi	0°13’33.3”	30°12’54.8”	RUMES	Jan-07		104	

Table 2.1 *Continued...*

N°	Lake Name	Latitude	Longitude	Who	Date	Zm (m)	Cond.	TF
64	Kacuba	0°21'40.1"	30°1'29.77"	DANIDA	Mar-01	14.5	183	
64	Kacuba	0°21'40.1"	30°1'29.77"	LBORO	Jan-07	15	126	x
65	Kako	0°18'21.1"	30°5'48.28"	LBORO	Jul-06	29	98	x
65	Kako	0°18'21.1"	30°5'48.28"	RUMES	Jan-07	29	89	
66	Kamunzuka	0°15'33.6"	30°9'19.96"	LBORO	Jul-06	61	58	x
67	Kamweru	0°15'20.6"	30°7'28.49"	KILHAM[2]	Nov-69		136	
67	Kamweru	0°15'20.6"	30°7'28.49"	MELACK[1]	May-71	33.5	129	
67	Kamweru	0°15'20.6"	30°7'28.49"	VERSCH.	Mar-00	45		
67	Kamweru	0°15'20.6"	30°7'28.49"	VERSCH.	Jul-02	33	154	x
67	Kamweru	0°15'20.6"	30°7'28.49"	LBORO	Jul-06			
67	Kamweru	0°15'20.6"	30°7'28.49"	RUMES	Jan-07	43	170	
68	Kariya	0°14'10.4"	30°9'24.83"					
69	Karolero	0°20'31.2"	30°1'44.31"	DANIDA	Mar-01	30.5	213	
69	Karolero	0°20'31.2"	30°1'44.31"	VERSCH.	Jul-02	15.5	145	x
69	Karolero	0°20'31.2"	30°1'44.31"	RUMES	Jan-07	14.5	148	
70	Kasirya	0°15'20.6"	30°7'57.57"	LBORO	Jul-06	40	323	x
70	Kasirya	0°15'20.6"	30°7'57.57"	RUMES	Jan-07	43	302	
71	Katinda	0°13'2.38"	30°6'15.82"	VERSCH.	Jan-01	17	743	x
71	Katinda	0°13'2.38"	30°6'15.82"	VERSCH.	Jan-02	17.4	661	
71	Katinda	0°13'2.38"	30°6'15.82"	RUMES	Jan-07	17	741	
72	Katunga	0°28'8.50"	30°11'17.6"					
73	Kigezi	0°17'8.0"	30°6'35.15"	LBORO	Jul-06	26	271	x
74	Kyamswiga	0°11'6.92"	30°8'44.47"	DANIDA	Jul-00		448	
75	Kyamwogo	0°16'53.3"	30°4'37.22"					
76	Kyasanduka	0°17'16.0"	30°2'57.06"	KIZITO[4]	Mar-92		307	
76	Kyasanduka	0°17'16.0"	30°2'57.06"	DANIDA	Jun-00			
76	Kyasanduka	0°17'16.0"	30°2'57.06"	DANIDA	Mar-01	2	307	x
76	Kyasanduka	0°17'16.0"	30°2'57.06"	VERSCH.	Jul-02	2	156	
76	Kyasanduka	0°17'16.0"	30°2'57.06"	LBORO	Jan-07	2	204	x
76	Kyasanduka	0°17'16.0"	30°2'57.06"	RUMES	Jan-07	2.1	269	
77	Kyogo	0°20'21.4"	30°1'7.16"	LBORO	Jan-07	3.4	55	x
77	Kyogo	0°20'21.4"	30°1'7.16"	RUMES	Jan-07	3.4	56	
78	Mafuro	0°15'53.1"	30°6'6.09"	LBORO	Jul-06	27.4	342	x
22	Mafuro	0°15'53.1"	30°6'6.09"	RUMES	Jan-07	29	259	
79	Mirambi	0°13'26.7"	30°6'20.66"	VERSCH.	Jan-01	21	652	x
79	Mirambi	0°13'26.7"	30°6'20.66"	VERSCH.	Jan-02	22	580	
79	Mirambi	0°13'26.7"	30°6'20.66"	RUMES	Jan-07	22	642	
80	Mugogo	0°17'17.7"	30°7'31.69"	LBORO	Jan-07	141	119	x
81	Muijongo	0°16'15.9"	30°5'6.31"	LBORO	Jul-06	55.4	464	x
82	Murabyo	0°20'1.96"	30°2'8.55"	DANIDA	Mar-01	16	173	
82	Murabyo	0°20'1.96"	30°2'8.55"	VERSCH.	Jul-02	14	157	x
82	Murabyo	0°20'1.96"	30°2'8.55"	RUMES	Jan-07	15	141	
83	Nkugute	0°19'14.8"	30°5'54.73"	TALLING[13]	Dec-60		86	
83	Nkugute	0°19'14.8"	30°5'54.73"	BEADLE[7]	Dec-63		75	
83	Nkugute	0°19'14.8"	30°5'54.73"	BEADLE[7]	Sep-64	58	86	
83	Nkugute	0°19'14.8"	30°5'54.73"	KILHAM[2]	Nov-69		82.7	
83	Nkugute	0°19'14.8"	30°5'54.73"	MELACK[1]	May-71	58	86	
83	Nkugute	0°19'14.8"	30°5'54.73"	DANIDA	Jul-00		150.1	
83	Nkugute	0°19'14.8"	30°5'54.73"	VERSCH.	Jan-02	58	101	x
83	Nkugute	0°19'14.8"	30°5'54.73"	RUMES	Jan-07	58	121	
84	Nshenyi	0°8'55.17"	30°9'36.19"	VERSCH.	Mar-00	0.08	31600	x

Table 2.1 *Continued...*

N°	Lake Name	Latitude	Longitude	Who	Date	Zm (m)	Cond.	TF
84	Nshenyi	0°8’55.17”	30°9’36.19”	RUMES	Jan-07	0.05	11230	
85	Nyamogusingiri Basin	0°18’55.3”	30°1’36.29”	KILHAM	Nov-69		908	
85	Nyamogusingiri Basin	0°18’55.3”	30°1’36.29”	MELACK[1]	May-71	4.9	875	
85	Nyamogusingiri Basin	0°18’55.3”	30°1’36.29”	KIZITO[4]	Mar-92			
85	Nyamogusingiri Basin	0°18’55.3”	30°1’36.29”	DANIDA	Jun-00	4.2	741	x
85	Nyamogusingiri Basin	0°18’55.3”	30°1’36.29”	DANIDA	Mar-01	4.5	669	
85	Nyamogusingiri Basin	0°18’55.3”	30°1’36.29”	VERSCH.	Jul-02	4.4	620	
85	Nyamogusingiri Basin	0°18’55.3”	30°1’36.29”	LBORO	Jan-07	3.8	554	x
85	Nyamogusingiri Basin	0°18’55.3”	30°1’36.29”	RUMES	Jan-07	4.3	681	
85	Nyamogusingiri Crater	0°18’55.3”	30°00’47.5”	LBORO	Jan-07	11.6	548	x
85	Nyamogusingiri Crater	0°18’55.3”	30°00’47.5”	LBORO	Jan-07	11.6	548	x
86	Nyungu	0°15’27.1”	30°6’0.00”	MELACK[1]	May-71	18	431	
86	Nyungu	0°15’27.1”	30°6’0.00”	LBORO	Jul-06	25.2	528	x
86	Nyungu	0°15’27.1”	30°6’0.00”	RUMES	Jan-07	25	430	
	Albert			WAY.[12]	Jan-22			
	Albert			TOTTEN.[14]	Mar-23			
	Albert			WORTH.[15]	May-28			
	Albert			FISH[9]	Aug-51		710	
	Albert			FISH[9]	Jul-53		700	
	Albert			V.D. BEN[16]	Feb-53		730	
	Albert			TALLING[13]	May-54		675	
	Albert			TALLING[13]	Feb-61		735	
	Albert			TALLING[13]	Aug-61		730	
	George (Tubengo)	0°2’42.67”	30°12’54.9”	VERSCH.	Jan-02	5.4		
	George (Tubengo)	0°2’42.67”	30°12’54.9”	RUMES	Jan-07	4.8	264	
	George			RUSSELL	Mar-00			
	George			RUSSELL	Apr-99			
	George			HURST[6]	Mar-24			
	George			BEADLE[7]	Jul-31		207	
	George			FISH[9]	Jun-51		185	
	George			FISH[9]	Jun-52		170	
	George			FISH[9]	Nov-52		165	
	George			FISH[9]	Mar-53		175	
	George			TALLING[13]	Dec-60		200	
	George			TALLING[13]	Jun-61		201	
	Kabakas	0°15’39.4”	29°21’1.08”	DANIDA	Mar-01	2.4	165	x
	Kabaleka							
	Victoria (Gaba-Port Bell)			DANIDA	Mar-01			
	Victoria (Murchison Bay)			DANIDA	Mar-01	6	119	x
	Victoria			FISH[9]	Sep-52		98	

Table 2.1 *Continued...*

N°	Lake Name	Latitude	Longitude	Who	Date	Zm (m)	Cond.	TF
	Victoria			TOTTEN.[14]	Apr-23			
	Victoria			DUKE[17]	1923			
	Victoria			GRAHAM[18]	Nov-27			
	Victoria			WORTH.[15]				
	Victoria			ANON	1951			
	Victoria			FISH[9]	1951		93	
	Victoria			TALLING[13]	Mar-61		97	

Data sources:

Direct sources

VERSCH.	= D. Verschuren and colleagues, Ghent University
DANIDA	= D. Ryves and colleagues, GEUS (Danish Geological Survey)
LBORO	= K. Mills and D. Ryves, Loughborough University
RUSSELL	= Information supplied by J. Russell, Browns University
RUMES	= B. Rumes and colleagues, Ghent University
CHAPMAN	= L. Chapman and colleagues, McGill University and MUBFS

Literature

1. Melack (1978)
2. Kilham (1971)
3. Crisman (2001)
4. Kizito *et al*. (1993)
5. Phillips (1930)
6. Hurst (1925)
7. Beadle (1932)
8. Damas (1937)
9. Fish (1953)
10. Pappe (1890)
11. Groves (1931)
12. Wayland (1925)
13. Talling and Talling (1965)
14. Tottenham (1926)
15. Worthington (1930)
16. Van Der Ben (1959)
17. Duke (1924)
18. Graham (1929)

Chapter 3

Materials and Methods

3.1 Introduction

The purpose of this chapter is to introduce the various sampling approaches and methodologies used in this study and to discuss the different statistical and interpretative methods which were employed. All of the data collection was completed by the author unless otherwise stated. A workflow for the methodology from initial sample collection to sample analysis is presented in Figure 3.1. An inventory of the samples collected and analyses performed on these samples is presented in Table 3.1. The chapter is divided into two main parts: sampling collection and sample analysis (laboratory methods). This section of thesis does not deal with the various statistical and numerical analyses of the data. Detailed numerical methods are discussed in the subsequent chapters.

3.2 Sample collection

3.2.1 Water column profiles and bathymetry

In the field, limnological profiling was carried out at regular depth intervals (0.5 to 5 m - dependent on lake depth, and restricted by the length of the probe cable; max. 50 m) on all lakes visited within the study region. Most lakes >5 m were found to be stratified (cf. Melack, 1978). Once a change in the upper water chemistry/temperature profile had had been identified (indicating the metalimnion), measurements were taken at finer intervals in order to locate the exact depth of the thermocline/chemocline in each lake. Lake bathymetry was determined using a GPS-guided and echo-sounding device (Garmin GPSMAP-188). Soundings at 10-second intervals were converted to XYZ point shapefiles, and subsequently gridded using a Natural Neighbour algorithm in ArcMap v. 9.1. The resulting grids were contoured at 5 metre increments.

Measurements of temperature (°C), pH, conductivity (μS cm^{-1}, standardised to a water temperature of 25°C) and dissolved oxygen (DO %) were all logged using a Hydrolab Quanta probe.

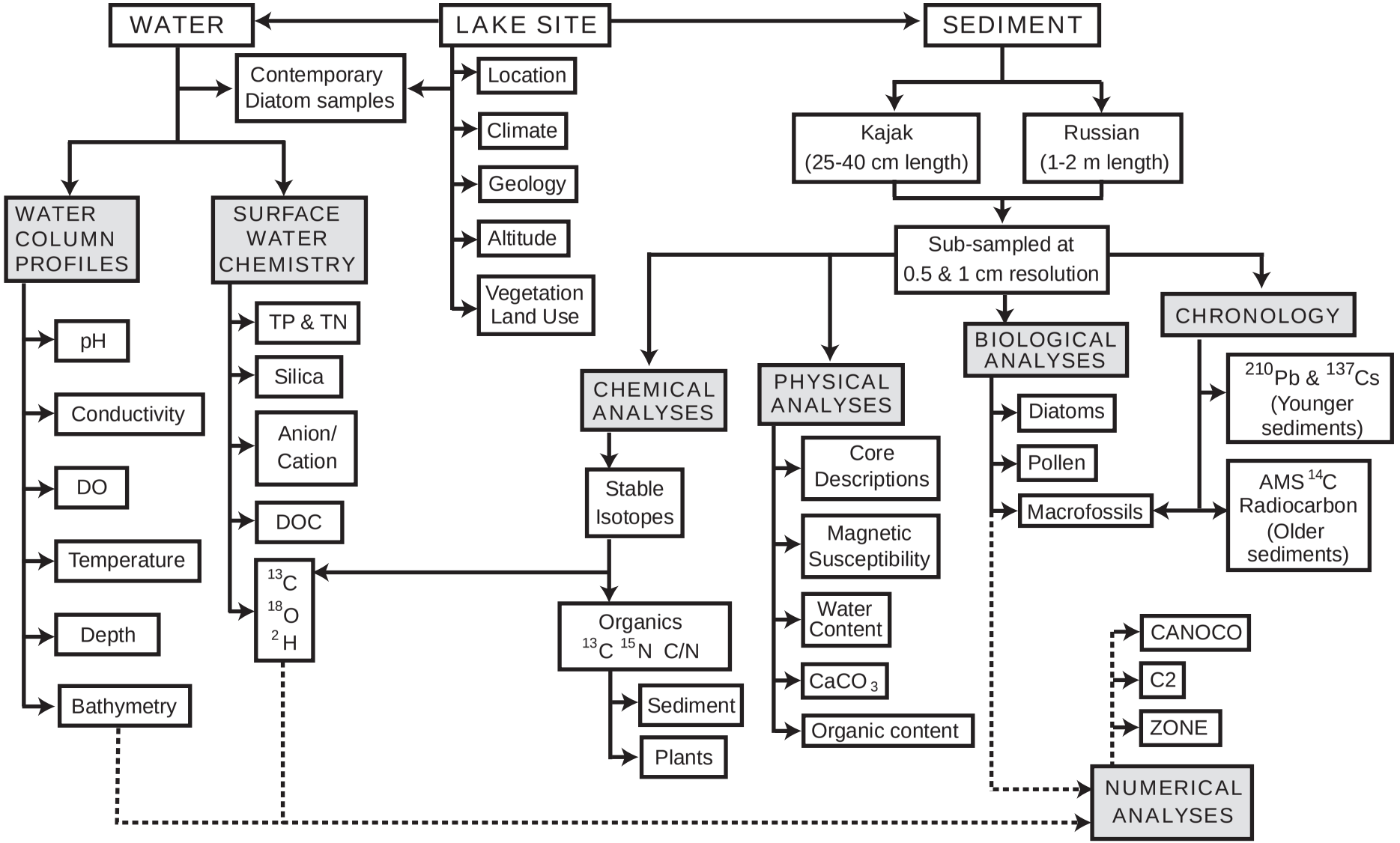

Figure 3.1 *Workflow of methods and data acquisition used in this study.*

Table 3.1 *Analysis inventory of all lakes sampled during July 2006 and January 2007 fieldwork.*

		Lake water samples					*Core sediment samples*					
Lake name	*Core code*	*Profile*	*Chemistry*	*DOC*	$\delta^{18}O$ / $\delta^{2}H$	*Live diatoms*	*LOI / $CaCO_3$*	^{210}Pb	^{14}C	*Diatoms*	*Pollen*	$\delta^{13}C$ & *C/N*
Saaka	SAAKA	X	X	X	X	P	X					
Nierya	NYA	X	X	X	X		X					
Nyamswiga	NSWIG	X	X	X	X		X					
Kifuruka	KIF	X	X	X	X		X					
Lyantonde	LYAN	X	X	X	X		X					
Mahuhura	MHURA	X	X	X	X	P	X					
Kasenda	KDA	X	X	X	X	P	X					
Nyamirima	NMIRI	X	X	X	X	P	X					
Nyinabulita	NBUL	X	X	X	X	P	X					
Kikorongo	KIK	X	X	X	X	P	X					
Nyungu	NYU-T	X	X	X	X	P	X					
	NYU-1						X	X		X	X	
	NYU-2						X					
Muijongo	MUIJ-1	X	X	X	X	P	X					
	MUIJ-2											
Kamunzuka	KAM	X	X	X	X	P	X	X		X		
Kasirya	KAS	X	X	X	X	P	X					
Kigezi	KIG-1	X	X	X	X	P	X	X		X		
	KIG-2						X					
Kako	KAK	X	X	X	X	P	X	X		X		
Mafuro	MAF	X	X	X	X	P	X	X		X		
Mugogo	MUG-1	X	X	X	X		X					
	MUG-2						X					
Kyasanduka	KYAS-1	X	X	X	X	P, L, S, ES	X	X	X	X	X	X
	KYAS-2		X	X			X	X		X		X
	KR1C1		X	X			X	X		X	X	X
	KR1C2						X	X	X	X	X	X
	KR2C1						X	X	X	X	X	X
	KR2C2						X		X	X	X	X
Nyamogusingiri	NC1	X	X	X	X	P, S, EP, EL	X					
Crater	NC2						X					
	NCR1						X			X		X
	NCR2						X	X		X	X	X
	NC5						X					
	NCR1C1						X					
	NCR2C1						X	X	X	X	X	X
Nyamogusingiri	NC6		X	X	X	P	X					
Basin	NC7						X					
	NC8						X					
Kacuba	KAC		X	X	X	P, EP	X					
Kyogo	KYO		X	X	X	P, EP	X					
Mahega	MAH		X	X	X	L	X					

Codes for live diatom samples: P=pelagic, L=littoral, S=spring/stream, EP=epiphytic, EL=epilithic, ES=epipsammic

3.2.2 Water samples

Typically, water samples were collected at the surface of the lake (0.5 m depth) and at depth below an observed thermocline/chemocline, typically in the range of 10-40 m. Samples from any springs entering the lake or streams leaving the lake were also sampled. A suite of analyses were carried out on these samples.

A pelagic water sample for cation analyses (Ca, Mg, Na, K, Li, Ba, Sr, Fe, Mn), anion analyses (F, Cl, NO_3, SO_4), dissolved silica (Si), total dissolved sulfur (TS), dissolved phosphorus (PO4-P), dissolved inorganic carbon (DIC) was filtered through Whatmann cellulose acetate filters (0.45 µm mesh). Filtrates for cation, PO_4-P and TS analysis were stabilized with a few drops of ultra-concentrated nitric acid (HNO_3) and stored in 60 ml acid pre-washed HDPE bottles. Filtered samples for analysis of anions, Si and dissolved carbon were stored, untreated, in separate bottles. For determination of total phosphorus (TP) and total nitrogen (TN), unfiltered samples were fixed by adding concentrated sulfuric acid (reducing pH to ~pH 2).

Samples for pigments, particulate organic carbon (POC) and C/N from each lake were filtered through GF/F Whatmann glass-fiber filters (0.8µm). These filters were pre-treated prior to the fieldwork by heating to 550°C for 2 hours and then weighing them. Filtering was stopped when the filter paper started to discolour and the volume of water filtered was noted. Excess water was removed from the filters which were then wrapped in aluminium foil and stored in plastic petri-dishes. All of the above water samples were stored at ~4°C (Chl-*a* samples were frozen) in a portable refrigeration unit and taken back to the UK before being shipped to Belgium for analysis.

Samples were also collected at each site for the analysis of dissolved organic carbon (DOC) from the surface (0.5 m) and from hypolimnetic water. These samples were filtered through GF/F Whatmann glass-fiber filters (0.8µm) using a hand pump (ensuring the pressure did not rise above -20 kPa). The filtered samples were transferred into 60 ml Nalgene bottles, taking care not to trap any air bubbles in the sample. The samples were labelled and sealed with PVC “electrician’s” tape and frozen until required for analysis at Loughborough University.

Two lake water samples (at 0.5 m depth) and samples from any springs, rivers and outlets around the lakes were also taken for isotopic analyses (δ^{13}C TDIC, δ^{18}O and δD). For δ^{13}C TDIC, 100 ml acid pre-washed (10% HCl for 24 hrs) Nalgene bottles were used. The bottles were rinsed out twice with the lake water prior to filling, ensuring that no plant

particles entered the bottle and no air bubbles were contained within the sample. For $\delta^{18}O$ and δD, smaller 15 ml acid pre-washed Nalgene bottles were used with the same method as carried out above. The samples were then labelled, sealed and stored cool whilst in the field. The samples were frozen on return to Loughborough and only defrosted and opened immediately prior to analysis at NERC Isotope Geosciences Laboratory (NIGL), Keyworth.

3.2.3 Contemporary diatom samples

38 samples of living diatom communities from different habitats (e.g. epiphyton, epilithon, plankton) were taken from the 25 lakes visited during fieldwork (**Chapter 4,** Table 4.13). Plankton samples were collected using a coarse phytoplankton net (60 μm), which were subsequently decanted into 60 ml Nalgene bottles. Epilithon and epiphyton samples were mainly collected by gently scrubbing the rock or plant (usually submerged logs) with a soft filament toothbrush and washing with lake water into a sample bottle; in some cases, where the plants were deemed too delicate for scrubbing, whole stems from submerged macrophytes (commonly lillies and reeds from the edge of the lakes) were collected and stored in sample bottles. Epipsammon samples consisted of coarse to fine grained sands in near shore areas. The uppermost sediment was removed and stored in sample bottle. All samples were preserved using a few drops of Lugol's Iodine and stored in dark refrigeration (4°C) at Loughborough University prior to preparation.

3.2.4 Sediment

Sampling was undertaken during two field excursions during July 2006 (four weeks) and January 2007 (two weeks). During this field work, 36 cores were collected from 24 different lakes (Table 3.2) across the field site. All of the short sediment cores (up to 43 cm long) were collected using a HON-Kajak gravity corer (9 cm diameter; Renberg, 1991) from the deepest part of the lake where possible, or from below the observed chemocline (cf. Melack, 1978). In some cases (where lake depth exceeded 50 m) cores were taken from a shallower plateau. It was imperative that, during the collection of these samples, the sediment-water interface was undisturbed as many of these samples were required for the surface sediment calibration data set for the transfer function. All of the cores were extruded in the field on a screw-threaded extruding rig at 0.5 cm or 1 cm intervals. These samples were then bagged, labelled and refrigerated (4 °C) when returned to Loughborough University until required for analysis.

Table 3.2 *Details of lakes visited and cores collected during the July 2006 and January 2007 field work. All latitudes and longitudes, unless stated, are from a GPS (Garmin 12).*

Lake name	Sample Location		Date	Core code	Lake Depth (m)	Coring Depth (m)	Core length (cm)	Sampling interval (cm)
	Latitude	Longitude						
Saaka	00°41'57.4"	030°14'41.9"	19-07-06	SAAKA	7.8	7.8	5	1
Nierya	00°29'56.9"	030°17'12.9"	21-07-06	NYA	>80	9.3	5	1
Nyamswiga	00°30'27.2"	030°17'12.5"	21-07-06	NSWIG	75	23	5	1
Kifuruka	00°30'21.9"	030°17'12.2"	22-07-06	KIF	4.5	4.5	5	1
Lyantonde	00°29'12.5"	030°16'50.7"	22-07-06	LYAN	>80	19.1	5	1
Mahuhura	00°26'24.2"	030°15'55.1"	23-07-06	MHURA	>80	8.4	5	1
Kasenda	00°25'56.7"	030°17'26.4"	23-07-06	KDA	14.2	14.2	36.5	0.5 & 0.25
Nyamirima	00°31'18.9"	030°19'05.0"	24-07-06	NMIRI	51.9	21.9	28	1
Nyinabulita	00°30'27.7"	030°19'32.0"	24-07-06	NBUL	63.9	21.9	5	1
Kikorongo	-00°00'34.8"	030°00'42.7"	26-07-06	KIK	11	9.8	39.25	0.25
Nyungu	-00°15'23.1"†	030°06'0"†	27-07-06	NYU-T	25.2	22	15	0.5
	-00°15'22.9"	030°05'42.5"	28-07-06	NYU-1	25.2	25	27.5	0.5
	-00°15'22.0"†	030°05'57.6"†	28-07-06	NYU-2	25.2	25	15	0.5
Muijongo	-00°16'35.4	030°05'00.7"	29-07-06	MUIJ-1	55.4	42	47	0.5
	-00°16'35.4"	030°05'03.4"	01-08-06	MUIJ-2	55.4	42	42	0.5
Kamunzuka	-00°15'49.8"	030°09'18.5"	30-07-06	KAM	61	50.4	43	0.5
Kasirya	-00°15'31.4"	030°07'57.5"	30-07-06	KAS	40	38.9	28	0.5
Kigezi	-00°17'15.1"	030°06'36.7"	31-07-06	KIG-1	26	25.7	33.5	0.5
	-00°17'15.2"	030°06'36.9"	31-07-06	KIG-2	26	25.6	33	0.5
Kako	-00°18'21.8"†	030°05'48.2"†	31-07-06	KAK	29	28.6	33	0.5
Mafuro	-00°16.023'	030°06.118'	01-08-06	MAF	27.4	27.4	27.5	0.5
Mugogo	-00°17'8.6"	030°17'47.1"	09-01-07	MUG-1	141	11	46	0.5
	-00°17'7.3"	030°17'24.4"	09-01-07	MUG-2	141	12	16	1
Kyasanduka	-00°17'23.2"	030°3'0.8"	11-01-07	KYAS-1	2	2	39.5	0.5
	-00°17'23.1"	030°3'0.6"	11-01-07	KYAS-2	2	2	28.5	0.5
	-00°17'23.2"	030°3'0.8"	11-01-07	KR1C1	2	2	70	RC*

Table 3.2 *Continued…*

Lake Name	Sample location		Date	Core code	Lake Depth (m)	Coring Depth (m)	Core length (cm)	Sampling interval (cm)
	Latitude	Longitude						
Kyasanduka	-00°17'23.2"	030°3'0.8"	11-01-07	KR1C2	2	2	97	RC*
	-00°17'23.1"	030°3'0.6"	11-01-07	KR2C1	2	2	80	RC*
	-00°17'23.1"	030°3'0.6"	11-01-07	KR2C2	2	2	100	RC*
Nyamogusingiri	-00°17'4.5"	030°00'46.7"	13-01-07	NC1	13.5	12.5	30.5	0.5
Crater	-00°17'3.0"†	030°00'46.7"†	13-01-07	NC2	13.5	13.5	16.5	0.5
	-00°17'3.9"	030°00'47.5"	13-01-07	NCR1	13.5	13	29.5	0.5
	-00°17'3.9"	030°00'47.5"	13-01-07	NCR2	13.5	13	35.5	0.5
	-00°16'56.5”	030°00'48.3"	13-01-07	NC5	13.5	6.6	30	0.5
	-00°17'3.9"	030°00'47.5"	13-01-07	NCR1C1	13.5	13.5	85	RC*
	-00°17'3.9"	030°00'47.5"	13-01-07	NCR2C1	13.5	13.5	100	RC*
Nyamogusingiri	-00°16'45.9"	030°00'34.0"	15-01-07	NC6	3.8	3.4	41	0.5
Basin	-00°17'38.2"	030°01'45.9"	15-01-07	NC7	3.8	3.4	30	1
	-00°17'36.7"	030°01'48.8"	15-01-07	NC8	3.8	3.4	47	1
Kacuba	-00°20'33.4"	030°1'33.3"	16-01-07	KAC	15	14.5	47.5	1
Kyogo	-00°20'30.7"	030°01'11.5"	17-01-07	KYO	3.4	3.4	45.5	0.5
Mahega	-00°00'35.7"†	029°57'56.1"†	18-01-07	MAH	4.4	0.5	5	0.5

RC - Russian core – not sectioned in field, sub-sampled in laboratory at 0.5 & 1 cm intervals.*
† *- Latitude/longitude estimated from map*

Two lakes (Kyasanduka and Nyamogusingiri; **Chapter 2,** Figure 2.6) within the field site were selected to retrieve longer core sequences. In these lakes the uppermost, unconsolidated sediments were retrieved using the HON-Kajak corer (sectioned in the field at 0.5 cm intervals). The deeper, consolidated sediments were collected using a Russian peat corer (1 m long, 7.5 cm diameter; Belokopytov and Beresnevich, 1955; Jowesy, 1966). This coring was carried out from a raft, either roped tightly to three points on shore (Kyasanduka) or strongly anchored on four points (Nyamogusingiri). Multiple cores were taken to ensure overlap between adjacent core sections. Russian cores were kept intact and placed in half drain-pipes and wrapped in cling-film immediately after collection and stored in the dark. After shipping to the UK (2-3 weeks after collection) the samples were kept in dark refrigeration (4 °C) until required for analyses.

3.3 Sample analysis

3.3.1 Water chemistry

3.3.1.1 TP, TN, Chlorophyll-a, anions and cations

Cations and Si were analysed by Inductively Coupled Plasma Atom Emission Spectrometry (ICP-AES; IRIS, Thermo Elemental). F, Cl, NO_3 and SO_4 were analysed by ion-exchange chromatography (DX100, Dionex). TP was determined by wet oxidation in an acid persulphate solution (120°C, 30 min), and TN (as nitrate plus nitrite) by wet oxidation in an alkaline persulphate solution (120°C, 30 min), both following Grasshoff *et al*. (1983). Chl-*a* was determined by high-pressure liquid chromatography (HPLC) following the protocol of Wright *et al*., (1991, 1997). Particulate organic carbon (POC) and particulate organic nitrogen (PON) were measured by flash combustion/thermal conductivity in a CE Instruments NC2100 elemental analyzer (H. Eggermont, *pers. comm.*).

All of the water chemistry analyses were completed at external laboratories in collaboration with colleagues from Ghent. This ensured that all water chemistry results were standardised and comparable. Samples for anion and cation analyses were completed at GeoForschungsZentrum under the supervision of Dr. Georg Schettler. TP and TN analyses were carried out by Prof. Lei Chou at the Université Libre de Bruxelles and pigment analyses were completed by Renaat Dasseville (Ghent University, Belgium).

3.3.1.2 Dissolved Organic Carbon (DOC)

Samples for DOC analyses were defrosted overnight in a refrigerator before use. The samples were analysed at Loughborough University using a Shimadzu Total Organic Carbon analyser (TOC-VCSN) and an ASI-V auto sampler. The standards (50 ppm to 100 ppm) were automatically calibrated using the TOC analyzer. Analyses were carried out under the supervision of Fengjuan Xiao.

3.3.1.3 Isotopes ($\delta^{13}C$ TDIC, $\delta^{18}O$ and δD)

Following sample collection (see *section 3.2.2*), and prior to analyses, all samples were frozen until needed. Following a thorough defrost, total dissolved inorganic carbon (TDIC) for $\delta^{13}C$ analysis was precipitated by the addition of $BaCl_2$ NaOH solution and then filtered and washed with de-ionised water. The smaller (15 ml) untreated sample was used for the analysis of $\delta^{18}O$ and δD.

The analyses were performed following standard procedures. The isotope ratios are reported in per thousand (‰) versus V-SMOW. The precision of carbonate analysis (1 SD), based on analysis of the laboratory standard, is better than 0.1 ‰ for $\delta^{13}C$. The precision for water $\delta^{18}O$ is 0.02 ‰.

The samples were prepared for analysis by the author using the facilities at the NIGL under the supervision of Dr. Angela Lamb and Prof. Melanie Leng. The analyses were carried out by the technical staff at NIGL.

3.3.2 Contemporary diatom samples (periphyton: phytoplankton, epiphyton, epilithon and epipsammon)

Samples from the contemporary diatom communities were prepared following the standard technique of diatom analysis as set out by Battarbee (1986), as beakers were more suitable for the oxidization of samples that were too organic for the water bath technique of Renberg (1990).

The samples (water and plant material) were placed into large beakers with 20 ml cold H_2O_2 (30%) for one week prior to heating to try and minimize the reaction caused by oxidation when the samples were heated. The H_2O_2 was refreshed regularly. After a week had elapsed the samples were heated for 2-3 hours on a hotplate. When plant material was oxidized, the large plant matter was removed after 1 hour on the hotplate; a gentle scrub with a toothbrush/spatula aided the removal of any diatoms that remained attached to the plant material. Once oxidized, the samples were washed four times after the chemical

treatments, and allowed to settle for 24 hours between each wash. After the last wash the samples were decanted into test tubes. The samples were then diluted (where necessary) to a suitable concentration, and an aliquot of the sample was left to evaporate on a coverslip at room temperature (approximately 48 hours). These strewn slides were mounted in Naphrax (refractive index of 1.73).

Where possible, 300-500 valves were counted per sample (though this was considerably lower in some of the pelagic samples) in parallel transects under oil-immersion phase-contrast light microscopy (LM) at x1000 magnification on a Leica DMRE research microscope.

3.3.3 Sediment analysis

3.3.3.1 Core descriptions

Initial core sediment descriptions (of the longer, intact Russian cores) were carried out in the field immediately after collection, and prior to the storing of the samples in order to record the gross lithology, colour changes and macrofossil presence. This was to ensure that key stratigraphic units were noted in case sediments were subject to diagenetic alteration and oxidization whilst in storage. In addition to this, detailed core descriptions were also carried out on clean cores in the laboratory after they were shipped back to the UK. A more detailed description, in terms of colour changes (identified using a Munsell colour chart) and stratigraphic changes and a more detailed inventory of both floral and faunal macrofossils within the cores were documented.

The initial field-based descriptions proved fruitful, as they identified stratigraphic units (in the form of distinct red, brown and black banding) that provided a key correlation tool (confirmed by LOI analysis, see below) for the overlapping sections of cores from Lake Kyasanduka. Unfortunately, this banding had all but degraded/oxidised, by the time they had returned to the laboratory for further analyses, with only some of the darker bands left intact.

3.3.3.2 Magnetic susceptibility

After description, non-destructive bulk magnetic susceptibility was measured on freshly cleaned Russian core sections using a Bartington MS2E high resolution surface scanning sensor and a MS2 magnetic susceptibility meter (Lees *et al*., 1998), through a thin layer of cling-film at every 0.5 cm. This analysis was carried out prior to any other sub-sampling.

3.3.3.3 Organic and carbonate content

Loss-on-ignition (LOI) was used to estimate the organic content (C_{org}) and carbonate content (CO_3) of all the sediment samples from the lakes included in this study. LOI provides an approximate measure of the organic content of the lake sediments (Dean, 1974). Known sample weights (typically in the range of 1 – 2 g) of the lake sediment were placed in a crucible and dried overnight at 105 °C. The samples were reweighed to estimate the water content. The sediments were then placed in the furnace and kept at 550 °C for 2 hours. The resulting weight loss following heating at this temperature derives values of 'loss-on-ignition' (a proxy for the sample C_{org}). The ashed samples were then used to estimate the carbonate content of the sediment by heating the sediment to 925 °C for 4 hours. The amount of carbon dioxide lost in the process can be used to determine the original carbonate content of the sediment (cf. Dean, 1974). Whilst simple, this analysis often overestimates the C_{org} and CO_3 as other components, such as interstitial water in clays, can contribute to the mass loss (Snowball and Sandgren, 1996; Leong and Tanner, 1999). The error associated with the analytical technique can pose challenges with interpretation (Heiri *et al.*, 2001).

3.3.3.4 Sedimentary diatom analysis

The standard technique of diatom analysis follows the method as set out by Battarbee (1986). When a large number of fossil diatom samples are to be prepared, the method is typically modified to that of Renberg (1990) which uses a water bath. In this study, samples from the core sequences for diatom analysis were prepared following the Renberg (1990) water bath method. Approximately 0.1 g of wet weight material per sample was used for the analysis, to which 10% HCl was added to remove carbonates. Following this, organic material was oxidized using 30% H_2O_2, heated to 90°C for 4 hours. Samples were washed four times after the chemical treatments, and allowed to settle for 24 hours between each wash. After the last wash, a few drops of dilute ammonia were added to the sample to keep any clay in suspension (deflocculation).

As with the contemporary diatom preparation (*section 3.3.2*) after washing the samples were diluted and placed on coverslips and allowed to dry for approximately 48 hours. These strewn slides were mounted in Naphrax (refractive index of 1.73), and at least 300 valves per sample (for fossil core samples) and 500 valves per surface sediment sample (for the transfer function) were counted in parallel transects under oil-immersion phase-contrast light microscopy (LM) at x1000 magnification on a Leica DMRE research

microscope. A variety of general (e.g. Krammer and Lange-Bertalot, 1986-1991; Patrick and Reimer, 1966, 1975; Germain, 1981) and regional floras (e.g. Gasse, 1986; Cocquyt, 1998) were consulted, and valves identified to species level where possible. The dissolution of the diatom valves was assessed using a two-scale system (pristine and dissolved; cf. Ryves *et al*., 2001). This ratio varies from 0 (all valves partly dissolved) to 1 (perfect preservation). Diatom concentrations were estimated by adding a known number of inert microspheres to the samples (Battarbee and Kneen, 1982).

3.3.3.5 Stable isotope analysis ($\delta^{13}C$)

Percentage carbon and nitrogen, used to calculate C/N, were measured on bulk sediments treated with 5% HCl to remove carbonates, using a Carlo Erba elemental analyser, calibrated through an internal acetanilide standard. $^{13}C/^{12}C$ analyses were performed by combustion using a Carlo Erba 1500 on-line to a VG Triple Trap and Optima dual-inlet mass spectrometer. $\delta^{13}C_{organic}$ values were calculated to the VPDB scale using a within-run laboratory standard (calibrated against NBS-19 and NBS-22).

All of the samples were prepared for analysis by the author using the facilities at NIGL under the supervision of Dr Angela Lamb and Prof. Melanie Leng. The analyses were carried out by the technical staff at NIGL. All of the NIGL isotope analyses were allocated through the NIGL Steering Committee (award IP/884/1105 to D.B. Ryves).

3.3.4 Chronological analyses

3.3.4.1 ^{210}Pb, ^{226}Ra and ^{137}Cs analyses

Recent sediment samples from the two long core (Lakes Nyamogusingiri and Kyasanduka) and five short core sequences (Lakes Nyungu, Kako, Kamunzuka, Mafura and Kigezi) were analysed for ^{210}Pb, ^{226}Ra, and ^{137}Cs by direct gamma assay (Appleby *et al.* 1986; Appleby, 2001). The analyses were carried out using Ortec HPGe GWL series well-type coaxial low background intrinsic germanium detectors (Appleby *et al*. 1986). ^{210}Pb was determined via its gamma emissions at 46.5keV, and ^{226}Ra by the 295keV and 352keV γ-rays emitted by its daughter isotope ^{214}Pb following 3 weeks storage in sealed containers to allow radioactive equilibration. ^{137}Cs was measured by its emissions at 662keV (Appleby *et al*. 1992).

Radiometric dates for each core were calculated using the constant rate of supply (CRS) and constant initial concentration (CIC) ^{210}Pb dating models where appropriate (Appleby and Oldfield, 1978), and compared with stratigraphic dates determined from the ^{137}Cs record. Tentative radiometric dates were calculated for the short core sequences (Kamunzuka, Nyungu, Kako, Mafura and Kigezi) using the CRS ^{210}Pb dating model (Appleby *et al*. 1978), and compared with the best estimate of the 1963 stratigraphic date suggested by the ^{137}Cs record. Best chronologies for Kyasanduka and Nyamogusingiri were determined using the procedures described in Appleby (2001).

24 samples (taken between 0-53 cm) from Nyamogusingire and 29 samples (taken between 0-150 cm) from Kyasanduka were analysed at 2 cm and 4 cm intervals respectively, in order to obtain a detailed chronology for the upper sections of the longer core sequences. Five samples were analysed from each of the short cores in order to obtain a general indication of the age of recent sediments. The lakes were sampled at regular intervals.

All of the cores were sub-sampled, dried and weighed at Loughborough University. The ^{210}Pb, ^{226}Ra, and ^{137}Cs were carried out at Liverpool University Environmental Radioactivity Laboratory (under the supervision of Prof. Peter Appleby).

3.3.4.2 AMS ^{14}C analyses

Both longer core sequences from Kyasanduka and Nyamogusingiri were dated using AMS ^{14}C dating of large terrestrial macrofossils or charcoal (both >250 µm). Initially six range-finder dates were processed in December 2007 (1 from Nyamogusingiri and 5 from Kyasanduka) from the two cores. In May/June 2008 a further 8 dates were obtained (3 from Nyamogusingiri and 5 from Kyasanduka) to establish a full chronology for both sediment sequences. Two additional samples from the basal sediments of both Nyamogusingiri and Kyasanduka were submitted in July 2008 to the Poznań radiocarbon laboratory. Precise details regarding the samples sent for analyses are presented in Table 3.3.

A 1 cm thick sediment sample was taken from the selected horizon and wet sieved through a 250 µm, 125 µm and 63 µm mesh with de-ionised water. The various residues were transferred into labelled petri-dishes, and samples were picked using metal tweezers under a Leica dissecting microscope (x10 – x50 magnification). The picked samples were transferred into sterile glass bottles and dried at 40°C.

All of the samples for radiocarbon dating, submitted to NERC-RCL were subject to an acid-alkali-acid (AAA) pre-treatment before analysis; however this method was slightly modified for very small samples (given in parentheses after the standard procedure has been described). The larger samples were digested in 2M HCl at 80°C for 4 hours (1M HCl at 80°C for 30 minutes for smaller samples). The sample residue was then rinsed free from mineral acid with de-ionised water and then digested in 0.5M KOH at 80°C for 30 minutes (0.2M KOH at 80°C for up to 20 minutes). The residue was rinsed free of alkali before being digested in 1 M HCl at 80°C for 2 hours (1M HCl at 80°C for 1 hour). Following the AAA procedure, all samples were rinsed free of acid, dried and homogenised. The total carbon from a known weight of sample was recovered as CO_2 by heating with CuO in a sealed quartz tube. The CO_2 was then converted to graphite (by Fe/Zn reduction) for AMS analyses (C. Bryant, *pers. comm.*). The results were reported as conventional radiocarbon years before present (BP, relative to AD 1950). Calibrated ages were derived from ^{14}C dates using the CALIB 5.0 program (Stuiver *et al*., 1998).

After the extracting and drying of samples by the author at Loughborough University, all of the samples for radiocarbon dating were prepared by the NERC Radiocarbon Laboratory (RCL) and analysed by the SUERC AMS radiocarbon laboratory in East Kilbride (supervised by Dr. Charlotte Bryant). The radiocarbon dating was carried out under the NERC-RCL awards 1233.0407 and 1264.1007 to D.B. Ryves. Sediments analysed at the Poznań radiocarbon laboratory were carried out under the supervision of Tomasz Goslar.

Table 3.3 *Details of samples submitted for AMS radiocarbon dating.*

Laboratory sample code	Date of Analysis	Lake	Nature of Sample	Core	Stratigraphic position (cm)	
					Top	Bottom
SUERC-16173	Dec ‘07	Kyasanduka	Wood / Reed	KR1C2	202	203
SUERC-16174	Dec ‘07	Kyasanduka	Leaf	KR2C1	90	91
SUERC-16175	Dec ‘07	Kyasanduka	Charcoal / Wood	KR2C2	164	165
SUERC-16176	Dec ‘07	Kyasanduka	Wood fragment	KR2C2	172	174
SUERC-18396	May ‘08	Nyamogusingiri	Wood fragment	NR2C1	121	122
SUERC-18397	May ‘08	Kyasanduka	Leaf	KR1C2	167	168
SUERC-18398	May ‘08	Kyasanduka	Charred wood	KR1C2	192	192.5
SUERC-18988	Jun ‘08	Kyasanduka	Wood	KR2C2	181	182
SUERC-18991	Jun ‘08	Nyamogusingiri	Leaf / Charcoal	NR2C1	61	62
SUERC-19065	Jun ‘08	Kyasanduka	Charcoal	KR2C2	181	182
SUERC-19066	Jun ‘08	Nyamogusingiri	Leaf / Charcoal	NR2C1	92	93
SUERC-19067	Jun ‘08	Nyamogusingiri	Wood / Charcoal	NR2C1	108	109
SUERC-19070	Jun ‘08	Kyasanduka	Charcoal	KR1C2	134	135
SUERC-19071	Jun ‘08	Kyasanduka	Wood	KR2C2	184	185
Poz-26360	Sept ‘08	Kyasanduka	Charcoal	KR1C2	206	207
Poz-26361	Sept ‘08	Nyamogusingiri	Charcoal	NR2C1	126	127

Chapter 4

Contemporary Limnology of the Crater Lakes

4.1 Introduction

This chapter describes the physical, chemical and some biological aspects of 48 crater lakes in western Uganda, with the aim to provide an understanding of the contemporary functioning of these under-studied tropical lake systems. The data are discussed in relation to previous studies in tropical East Africa (especially the crater lakes of Uganda) and theoretical concepts surrounding tropical limnology.

4.2 Background

4.2.1 Historical context

The investigation and understanding of tropical limnology is largely a product of research carried out during the latter half of the 20th century (Talling and Lemoalle, 1998). The motives of early European exploration of East Africa during the nineteenth century was most likely related to economic profits, expansion of trade, national prestige along with humanitarian and scientific curiosity as well as the general expansion of geographical knowledge; much was known (and mapped) of the African coastline (cf. 1821), though very little was know of the interior (Beadle, 1974). Early German missionaries to East Africa (e.g. Krapf, 1848-9) recorded the presence of an immense lake interior of Africa, and the myths surrounding the source of the Nile led to an increase in the number of scientific expeditions funded by the Royal Geographical Society (e.g. the expedition to search for the source Nile; Burton and Speke, 1857-8).

The European colonisation of much tropical Africa by the late 1880s provided additional incentives for the scientific exploration of Africa by specialist scientific societies (*c*. 1890s; Beadle, 1974). During the early 1900s, when temperate limnology was emerging as a scientific discipline, the majority of the research in tropical regions was based upon short-term expeditions (periods of months to years; cf. Worthington and Worthington, 1933) that produced mostly descriptive reports on the floral, faunal and taxonomic aspects of these scientifically, poorly known regions. These early expeditions (pre-1925), described by Beadle (1974) as ‘short-term investigations to some remote

place', required little in the way of specialist equipment, with scientists carrying only collecting jars, preservatives and portable weather instruments, and did little to advance the science of tropical limnology (Beadle, 1974). However, notable exceptions were the systematic collection of plankton from Malawi in 1899 by the Fülleborn expedition (Fülleborn, 1900).

The increasing sophistication of limnological techniques during the 1930s, involving the use of chemical measurements began to complicate expeditions, with the transportation of more equipment and the need for makeshift laboratories, often set up in tents, on the back of lorries and occasionally outside exposed to the elements (e.g. wind and dust; Worthington and Worthington, 1933; Beadle, 1974). It was not until the publication of these more sophisticated scientific expeditions in the 1930s that the scientific knowledge of these tropical regions was advanced. Far from being descriptive, work carried out by the Cambridge expeditions (Beadle, 1932; Worthington and Worthington, 1933), Percy Sladen expedition (Jenkin, 1936) and Damas (1934-35) to East Africa (specifically Kenya, Uganda, DRC and Rwanda) provided some of the first physical, chemical and biological data from tropical lakes. Almost all of the large lakes were investigated, including the Great Lakes Rudolf (now Lake Turkana), Nyasa (Malawi), Kivu, Albert Nyanza (Albert) and Victoria and Lakes Edward, George, Kioga and Bunyoni. The Cambridge expeditions also provided some of the first reports on the crater lakes of rift valley floor: Baringo and Hannington (Bogoria) in Kenya and the hypersaline crater lakes Bagusa, Maseche and Kikorongo (Uganda).

During the late 1930s work slowly began to emerge on the hydrological fluxes of the Nile river system (Hurst and Phillips, 1933-1946), but it was not until the 1960s and 1970s that an expansion in scientific knowledge relating to functioning of tropical lake systems began. During this time numerous studies were completed on the physical limnology of tropical African lakes (e.g. stratification: Talling, 1963; Baxter, 1965; Beadle, 1966; Wood *et al*., 1976; 1984; and circulation: Beadle, 1967; Moss and Moss, 1969; Ganf, 1974a; Melack, 1978; Lewis Jr., 1987), the chemical composition of tropical lake waters (Talling and Talling, 1965; Melack, 1978; Schlüter, 1993) and the zooplankton and phytoplankton (e.g. Ganf, 1974b; Hecky and Fee, 1981, Green, 1986; and with special reference to diatoms: Richardson, 1968; Kilham, 1971; Gasse, 1986; Kalff and Watson, 1986; Kilham *et al*., 1986; Talling, 1986). Specific studies were also completed on the numerous saline lake systems of equatorial Africa (e.g. Arad and Morton, 1969; Dixon and Morton, 1970; Melack and Kilham, 1972, 1974; Hecky and Kilham, 1973).

More recently a number of studies have focused specifically on the limnology of the crater lakes in western Uganda (e.g. Chapman *et al*, 1998; Kizito *et al*., 1993; Crisman *et al*., 2001) and the lakes of the Rwenzori mountains (Eggermont *et al*., 2007).

4.2.2 Tropical limnology

Lakes systems respond physically, chemically and biologically to changes in climate and these responses are registered in various ways in lake sediment records (Battarbee, 2000); as a result lakes are excellent sensors of environmental change. However, climate and environmental changes influence lakes in many ways and the direct and indirect links between climate and the lake water column must be understood to realise the potential of lake sediments as recorders of past climate variability (Battarbee, 2000).

The lakes of Uganda have outstanding characteristics in terms of their limnological variety (Melack, 1978). Therefore, western Uganda provides a unique opportunity to study comparative limnology and with past research, there are several baselines to which new data can be compared (e.g. Beadle, 1932; Worthington and Worthington, 1933; Jenkin, 1936; Talling and Talling, 1965; Beadle, 1966; Melack, 1978; Kizito *et al*., 1993).

The inter-annual variability of lakes, both physically and chemically, is well known and has been intensively studied in temperate regions, with many long-term monitoring stations in place. In comparison, tropical lakes are under-studied, with many of the published studies based on just a single sample per lake. The lack of knowledge regarding the functioning of these lake systems has led to generalisations regarding the irregular and unpredictable process of lake functioning in tropical regions (Ruttner, 1937; Hutchinson and Löffler, 1956; Hutchinson, 1957; Lewis Jr., 1984), though more thorough studies have supported the idea that many (larger) tropical lakes do indeed show seasonality in mixing, stratification and phytoplankton and zooplankton succession (Talling, 1969; Lewis Jr., 1973).

Since the 1960's, monthly sampling of some of the more accessible crater lakes in Uganda has been undertaken (e.g. Lake Nkugute, Beadle, 1966; Lake Nkuruba, Chapman *et al*., 1998; Saaka crater, Crisman *et al*., 2001), though the duration of these studies is short-term, lasting between 12 months and 5 years. However, the documented data published across the years provide a useful comparison for more recently collected data (cf. Crisman *et al*., 2001). Care must be taken when comparing recent water chemistry data to those collected in the 1960s and 1970s. Kizito *et al.* (1993) noted large discrepancies in some of the measured nutrient values (especially phosphorus concentrations in lakes

Kifuruka, Katanda and Lugembe) when comparing to earlier results of Melack (1978). Kizito *et al*. (1993) suggested that these variations could perhaps be attributed to strong temporal fluctuations (though due to a lack of data, this claim could not be substantiated). More likely, the differences were probably attributable to the unreliable and less accurate analyses (compared to the accuracy of today's technology) carried out by Melack (1978), where 'low concentrations' of P were denoted as <100 $\mu g\ l^{-1}$ (Kizito *et al*., 1993). Furthermore, discrepancies can arise due to differences in laboratory procedures which can lead to a lack of coherence in results processed in different laboratories (D. Verschuren, *pers. comm*.).

Although many of the principals are the same, the physical, chemical and biological properties and processes of tropical lakes are somewhat different to those in temperate lakes (Lewis Jr., 1987). Some of the crater lakes in Uganda have been described as polymictic (Eggermont and Verschuren, 2004a). In these lakes, the period of stratification ranges from one to several days, and is usually prevalent in shallow tropical lakes with a small heat storage capacity, subject to high daytime winds or night time cooling (Kalff, 2003). Many researchers have suggested that the small, deep, steep-sided crater lakes are likely to be permanently stratified, with partial overturn occurring in the upper waters only (meromictic; Beadle, 1966; Melack, 1978). Despite this, tropical lakes in general (and many of the Ugandan crater lakes) are only weakly stratified thermally; the temperature difference (thermocline) between the epilimnia and hypolimnia is much smaller for tropical lakes than their temperate counterparts (Kalff, 2003). Thus only moderate changes in temperature and wind are needed to mix these lakes. The stability of stratification is more likely a consequence of increased concentrations of organic matter decomposing to inorganic salts at depth too large to be overcome by wind mixing (Beadle, 1981).

Dissolved oxygen (DO) concentrations reflect the balance between oxygen supply from the atmosphere and photosynthesis, and the metabolic processes that consume oxygen. Low DO levels affect the distribution of aquatic biota and have a major influence on the solubility of nutrients. The DO content of the water column is affected by water temperature, barometric pressure (both altitude and hydrostatic) and salinity. The high temperatures of the hypolimnia of tropical lakes means they are likely to hold less DO per litre than temperate lakes, in addition to this, high productivity in the upper waters can lead to a larger biochemical oxygen demand (BOD) in the hypolimnia throughout the year, resulting in nearly all tropical lakes becoming anoxic at depth (Thornton, 1987). Similarly, the oxygen holding capacity of saline lakes is lower than freshwater, which combined with

the temperature effects means tropical lakes are more prone to anoxic conditions. As a result hypoxia is widespread in the deep waters of many tropical lakes (Wetzel, 1975; Beadle, 1981).

A limnological survey of 48 lakes spread across the field site in western Uganda (over a number of years) is reported in terms of their physical, chemical and biological attributes. The data collected in recent years (2000-2007) will be compared to historical data recorded between 1960 and 2000 by other researchers (e.g. Beadle, 1966; Talling and Talling, 1965, Melack, 1978, Chapman *et al*., 1998 and Crisman *et al*., 2001).

4.3 Study Sites

The location and general information regarding the crater lake clusters in western Uganda are described in **Chapter 2**. The data are based on a representative sample of lakes across the field site, with 21 lakes from the northern clusters (Fort Portal and Kasenda) and 27 from the southern part of the field site. Of these southern lakes, six are from the saline Katwe-Kikorongo cluster; the remaining lakes form a subset of the dilute (<1000 μS cm^{-1}, Melack, 1978) lakes in the Bunyaruguru cluster. A full list of lakes included in this chapter is given in Tables 4.1 and 4.2. The data for this study were collected during the years 2000-2001 (DANIDA), 2006-2007 (LBORO) and 2007 (RUMES and colleagues in Ghent; please refer to **Chapter 2** for details). All of the water chemistry analyses (from samples collected between 2006 and 2007) were carried out in a single laboratory to ensure compatibility between the results. For details regarding the methods of collection and analysis of the water and biological samples, please refer to **Chapter 3**).

4.4 Physical properties

4.4.1 Lake morphometry and transparency

The morphometry of the craters above water level and the lake basins are listed in Table 4.1, with several illustrations in Figures 4.1 and 4.2. Lake catchments ranged in size from 0.02 km^2 (Lake Kayihara) to 109 km^2 (Lake Maseche; with an average catchment size of *c*. 8.15 km^2 and a median of 0.48km^2). The area of catchment containing Lake Nyamogusingiri and Kikorongo were also amongst the largest (>49 and 81 km^2, respectively), though exact catchments could not be estimated due to the lack of available map data in these generally very flat catchments. Therefore it is likely that the measurements here represent the minimum catchment size for the two lakes. Lakes

Table 4.1 *Continued...*

Lake	Latitude	Longitude	Date	Who	Altitude (m)	Lake area (km^2)	Catchment area (km^2)	CA:L ratio	Height crater rim (m)		Angle of slope (°)	
									Min	Max	Min	Max
Mahega[1]	0°0’35.78”	29°57’56.1”	18-Jul-00	DANIDA	908	0.14	1.50	10.7:1	114	243	19.53	30.27
Mahega[2]	0°0’35.78”	29°57’56.1”	18-Jan-07	LBORO	908	0.14	1.50	10.7:1	114	243	19.53	30.27
Mahuhura	0°26’40.7”	30°15’57.2”	23-Jul-06	LBORO	1205	0.20	0.80	4:1	38	101	6.93	27.51
Maseche	0°5’33.46”	30°11’26.0”	22-Feb-07	RUMES	948	0.19	108.84	572.8:1	12	21	0.97	27.9
Mirambi	0°13’26.7”	30°6’20.66”	31-Jan-07	RUMES	1036	0.57	2.61	4.6:1	86	201	3.33	39.07
Mugogo	0°17’17.7”	30°7’31.69”	09-Jan-07	LBORO	1322	1.32	3.08	2.3:1	11	70	0.55	29.73
Muijongo	0°16’15.9”	30°5’6.31”	01-Aug-06	LBORO	1237	0.56	0.95	1.7:1	42	127	4.4	23.86
Murabyo	0°20’1.96”	30°2’8.55”	29-Jan-07	RUMES	1088	0.31	9.13	29.5:1	42	127	4.4	23.86
Murusi	0°25’47.1”	30°17’29.3”	17-Jan-07	RUMES	1229	0.24	1.30	5.4:1	13	43	1.73	28.73
Njarayabana	0°25’53.8”	29°21’4.07”	17-Feb-07	RUMES	1169	0.12	9.20	76.7:1	25	69	3.69	29.13
Nkugute	0°19’14.8”	30°5’54.73”	01-Feb-07	RUMES	1395	1.01	4.34	4.3:1	29	133	0.64	34.83
Nkuruba[1]	0°31’10.8”	30°18’1.53”	16-Jul-00	DANIDA	1535	0.04	0.90	22.5:1	46	32	2.17	17.4
Nkuruba[2]	0°31’10.8”	30°18’1.53”	16-Feb-07	RUMES	1535	0.04	0.90	22.5:1	46	32	2.17	17.4
Nshenyi	0°8’55.17”	30°9’36.19”	26-Jan-07	RUMES	951	0.62	3.61	5.8:1	7	60	1.511	19.74
Nyamogusingiri Basin	0°18’55.3”	30°1’36.29”	14-Jan-07	LBORO	984	4.28	49.75*	13.3:1*	9	114	4.67	35.13
Nyamogusingiri Crater	0°18’55.3”	30°00’47.5”	13-Jan-07	LBORO	984	4.28	49.75*	93.9:1*	9	114	4.67	35.13
Nyamirima	0°31’10.8”	30°18’1.53”	24-Jul-06	LBORO	1465	0.19	0.40	2.1:1	19	85	17.77	29.55
Nyamogusani	0°25’35.9”	29°19’51.4”	16-Feb-07	RUMES	1152	0.12	0.56	4.7:1	61	218	17.16	46.2
Nyamswiga	0°30’35.0”	30°17’4.99”	21-Jul-06	LBORO	1448	0.99	0.99	1:1	35	52	7.66	14.4
Nyierya	0°30’10.6”	30°17’3.39”	21-Jul-06	LBORO	1454	0.04	0.41	10.3:1	16	23	3.38	27.33
Nyinambulita	0°30’48.1”	30°19’17.4”	24-Jul-06	LBORO	1408	0.40	1.11	2.8:1	13	75	15.59	37.7
Nyungu	0°15’27.1”	30°6’0.00”	27-Jul-06	LBORO	1190	0.17	1.83	10.8:1	9	114	4.67	35.13
Saaka[1]	0°41’19.2”	30°14’34.4”	26-Jun-00	DANIDA	1568	0.64	7.35	114.8:1	5	92	0.51	36.06
Saaka[2]	0°41’19.2”	30°14’34.4”	20-Jul-06	LBORO	1568	0.64	7.35	114.8:1	5	92	0.51	36.06
Wandakara[1]	0°25’11.3”	30°16’10.1”	15-Jul-00	DANIDA	1172	0.03	0.67	22.3:1	3	83	6.35	31.9
Wandakara[2]	0°25’11.3”	30°16’10.1”	19-Jan-07	RUMES	1172	0.03	0.67	22.3:1	3	83	6.35	31.9
Wankenzi	0°25’22.6”	30°15’52.4”	19-Jan-07	RUMES	1176	0.20	0.56	2.8:1	0	49	0.48	34.83
*Nyamogusingiri inlet	No reading	No reading	15-Jan-07	LBORO	984	--	--	--	--	--	--	--
*Kyasanduka inlet	0°15’15.3”	30°03’10.8”	12-Jan-07	LBORO	994	--	--	--	--	--	--	--
*Kyasanduka outlet	0°17’26.1”	30°02’50.4”	16-Jan-07	LBORO	994	--	--	--	--	--	--	--

Table 4.1 *Geographical features of 48 lakes sampled (* catchment areas are likely underestimated given the lack of map coverage in these regions).*

Lake	Latitude	Longitude	Date	Who	Altitude (m)	Lake area (km^2)	Catchment area (km^2)	CA:L ratio	Height to crater rim (m)		Angle of slope (°)	
									Min	Max	Min	Max
Bagusa	0°5’22.08”	30°10’42.4”	22-Feb-07	RUMES	903	3.57	10.03*	2.8:1*	5	26	0.58	15.06
Bugwagi	0°11’29.7”	30°11’14.7”	24-Feb-07	RUMES	1055	0.65	1.15	1.8:1	7	33	0.18	23.91
Chibwera	0°9’0.04”	30°8’20.25”	26-Jan-07	RUMES	955	0.85	1.84	2.2:1	15	35	0.34	12.38
Ekikoto	0°42’14.6”	30°18’46.6”	18-Jan-07	RUMES	1525	0.19	0.07	0.4:1	3	41	2.86	26.53
Kacuba	0°21’40.1”	30°1’29.77”	16-Jan-07	LBORO	1112	0.60	1.22	2:1	7	78	0.06	38.24
Kako	0°18’21.1”	30°5’48.28”	31-Jul-06	LBORO	1375	0.20	0.48	2.4:1	22	109	17.89	37.41
Kamunzuka	0°15’33.6”	30°9’19.96”	30-Jul-06	LBORO	1258	0.27	1.64	6.1:1	14	20	0.09	3.98
Kamweru	0°15’20.6”	30°7’28.49”	20-Feb-07	RUMES	1212	0.23	0.75	3.3:1	62	154	20.52	42.96
Kanyanmukali	0°24’11.4”	29°20’9.23”	14-Jan-07	RUMES	1069	0.12	0.67	5.6:1	84	111	28.97	47.52
Karolero	0°20’31.2”	30°1’44.31”	21-Feb-07	RUMES	1155	0.09	9.00	100:1	0	59	0.07	32.86
Kasenda[1]	0°26’5.01”	30°17’19.6”	08-Jul-00	DANIDA	1254	0.08	1.49	18.6:1	0	81	3.33	35.28
Kasenda[2]	0°26’5.01”	30°17’19.6”	18-Mar-01	DANIDA	1254	0.08	1.49	18.6:1	0	81	3.33	35.28
Kasenda[3]	0°26’5.01”	30°17’19.6”	23-Jul-06	LBORO	1254	0.08	1.49	18.6:1	0	81	3.33	35.28
Kasirya	0°15’20.6”	30°7’57.57”	30-Jul-06	LBORO	1256	0.13	0.36	2.8:1	73	81	21.15	34.93
Katinda	0°13’2.38”	30°6’15.82”	31-Jan-07	RUMES	996	0.46	2.17	4.7:1	47	189	3.28	31.72
Kayihara	0°42’17.9”	30°18’56.1”	24-Mar-00	DIRK	1544	0.05	0.02	0.4:1	0	19	1.37	10.81
Kifuruka[1]	0°29’33.2”	30°17’9.87”	16-Jul-00	DANIDA	1408	0.16	1.25	7.8:1	17	82	4.23	33.01
Kifuruka[2]	0°29’33.2”	30°17’9.87”	22-Jul-06	LBORO	1408	0.16	1.25	7.8:1	17	82	4.23	33.01
Kigezi	0°17’8.0”	30°6’35.15”	31-Jul-06	LBORO	1247	0.11	0.59	5.4:1	87	121	28.28	36.01
Kikorongo	0°1’43.7”	30°0’35.04”	26-Jul-06	LBORO	930	0.96	81.42*	84.8:1*	0	5	0.96	5.28
Kitagata	0°3’41.2”	29°58’26.8”	10-Jan-01	DIRK	930	0.72	2.12	2.9:1	16	220	15.36	41.43
Kyaninga	0°42’8.11”	30°17’46.6”	10-Feb-07	RUMES	1567	0.32	8.77	27.4:1	0	64	1.41	33.04
Kyasanduka[1]	0°17’16.0”	30°2’57.06”	20-Mar-01	LBORO	994	0.55	2.27	4.1:1	5	554	0.06	39.17
Kyasanduka[2]	0°17’16.0”	30°2’57.06”	11-Jan-07	LBORO	994	0.55	2.27	4.1:1	5	554	0.06	39.17
Kyasanduka[3]	0°17’16.0”	30°2’57.06”	12-Jan-07	LBORO	994	0.55	2.27	4.1:1	5	554	0.06	39.17
Kyerbwato[1]	0°26’14.8”	30°19’20.8”	12-Jul-00	DANIDA	1239	0.02	0.37	18.5:1	3	3	0.866	13.42
Kyerbwato[2]	0°26’14.8”	30°19’20.8”	23-Jan-07	RUMES	1239	0.02	0.37	18.5:1	3	3	0.866	13.42
Kyogo	0°20’21.4”	30°1’7.16”	17-Jan-07	LBORO	1120	0.69	1.22	1.8:1	3	4	0.48	2.08
Lugembe	0°27’10.0”	30°16’48.9”	15-Jan-07	RUMES	1254	0.18	0.84	4.7:1	47	154	3.31	38.4
Lyantonde	0°29’12.5”	30°16’50.7”	22-Jul-06	LBORO	1202	0.11	0.38	3.5:1	10	49	1.18	26.58
Mafura	0°15’53.1”	30°6’6.09”	01-Aug-06	LBORO	1247	0.18	1.36	7.6:1	29	117	5.72	30.31

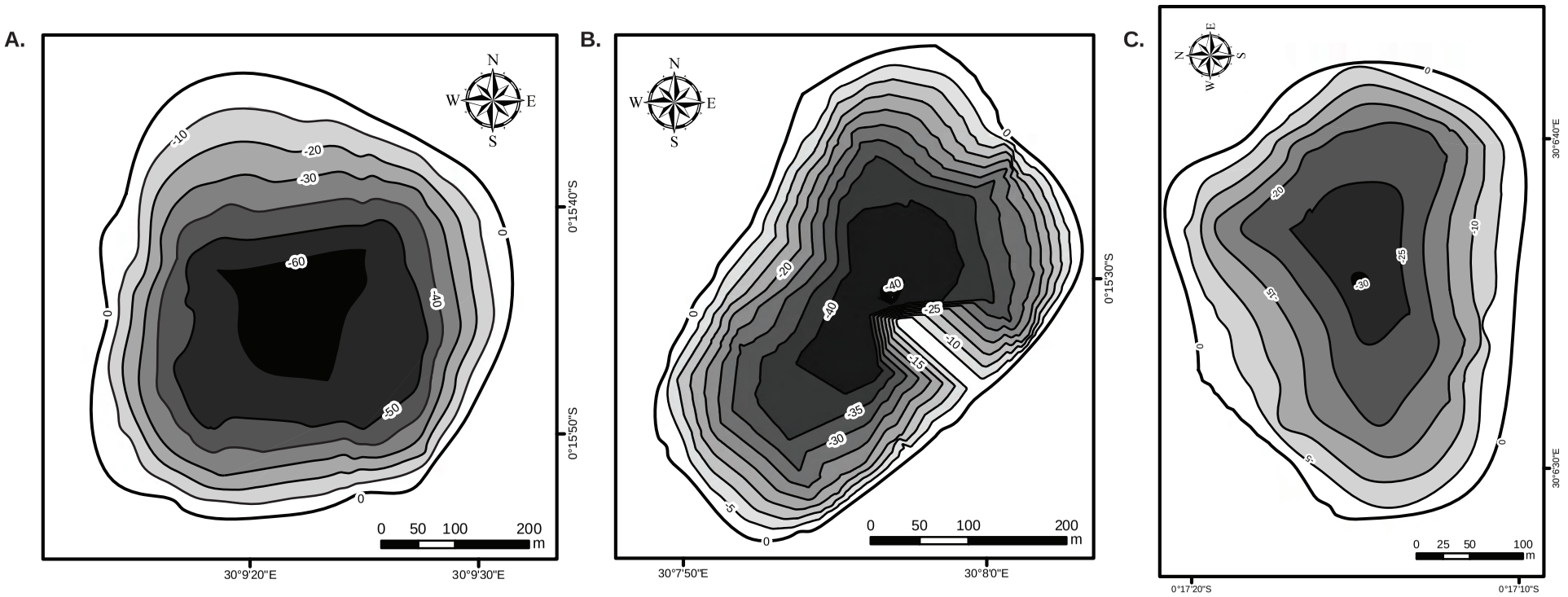

Figure 4.1 *Lake bathymetries (contours in metres) of* **(A)** *Kamunzuka,* **(B)** *Kasirya and* **(c)** *Kigezi (NB. the rotation of the axes on figure* **C**, *indicated by the position of the North arrow).*

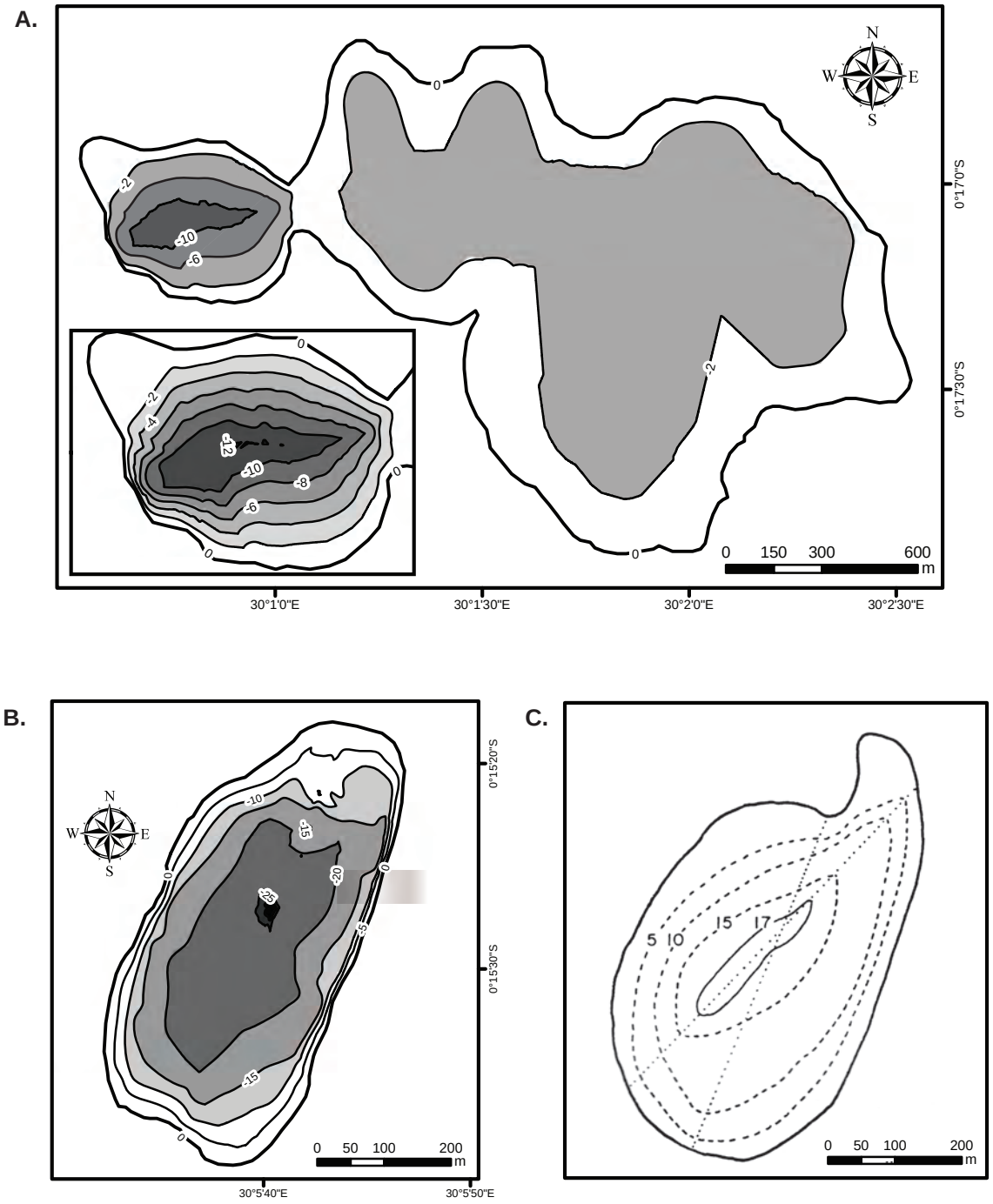

Figure 4.2 *Lake bathymetries (contours in metres) of* **(A)** *Nyamogusingiri, the inset shows an enlargement of the crater lake bathymetry* **(B)** *Nyungu (as measured by Mills in 2006) and* **(C)** *Nyungu (as sampled by Melack in 1971; Melack, 1978).*

Kayihara and Ekikoto (a paired lake system in the Fort Portal cluster) had the smallest catchment area (0.02 and 0.07 km^2, respectively). The height of the crater rim above the lake was greatest for lakes Kyasanduka and Mahega (554 and 243 m, respectively), and the least for lakes Kyerbwato and Kyogo (3 m and 5 m). The most substantial forest cover occurred around the lakes located within the Maramagambo Central Forest Reserve (Lakes Kacuba, Karolero and Kyogo), whilst open scrub savannah lined the craters containing the saline lakes (e.g. Kikorongo) except in the case of Lake Mahega, which contained bush/scrub vegetation. The lakes with the smallest and largest surface areas were Kyerbwato (0.02 km^2) and Nyamogusingiri (crater and basin combined, 4.28 km^2), with an average lake surface area of *c*. 1.27 km^2 and a median of 0.2 km^2.

The catchment area: lake ratio (Table 4.1) was calculated for each of the lakes as an indicator of the relative role of the catchment on the lake system. Lakes reflect the topography, geology, land-use and vegetation of its catchment (watershed). In addition to this there is a relationship between the CA:L and nutrient loading (WOW, 2004) tends to decrease with increasing catchment area. Lake Ekikoto has the smallest CA:L (0.36:1) and Lake Maseche the largest (572:1), the mean and median of the CA:L of all lakes was 27.9:1 and 4.69:1 respectively.

Water transparency was measured using a Secchi disk (Table 4.2). The Secchi depth varied from 2 cm in the hypersaline Lake Maseche to 7.7 m in the freshwater Lake Kamunzuka. The saline lakes had the lowest Secchi readings (ranging from 2-30 cm; median of 14.5 cm). Lake Kikorongo (22,200 µS cm^{-1} in 2006) was the exception with a relatively high Secchi depth of 1.6 m. The Secchi depths recorded in the dilute lakes ranged from 17.5 cm in the shallow Lake Kyasanduka, 2007 to 7.7 m in Lake Kamunzuka. The median Secchi depth for these lakes was *c*. 1.35 m.

4.4.2 Thermal stratification

The temperatures of the surface waters (taken between 1000 and 1400 hours) during the dry seasons of 2000, 2001, 2006 and 2007 ranged from 18.7°C (Lake Kasenda, 2000) and 32.3°C (Lake Maseche; Table 4.2 and Figures 4.3 and 4.4). The lower temperatures were generally recorded in the fresher lakes, with a median temperature of *c*. 25°C (ranging from 18.7°C to 29.1°C, Lakes Kasenda and Kyasanduka, respectively). The saline lakes had a median temperature of *c*. 30°C, with a range of 26.9°C (Lake Kikorongo) and 32.3°C (Lake Maseche).

Table 4.2 *Measured temperature, oxygen (mg l^{-1} and percent saturation), Secchi depth, total phosphorous (TP) and total nitrogen (TP) and chlorophyll-a concentrations for the lakes sampled by DANIDA and LBORO (-- missing data/ data not collected). The column 'profile' indicates whether a limnological profile was obtained using the Hydrolab Quanta probe (refer to* ***Figures 4.3 and 4.4****).*

Lake	Sampling date	Depth (m)	Temperature (°C)	Oxygen (mg l^{-1})	Oxygen saturation (%)	Profile	Secchi depth (cm)	TP (µg l^{-1})	TN (µg l^{-1})	Chl-a (µg l^{-1})
Bagusa	22-Feb-07	0.9	31.2	0.3	--		24	--	--	497.41
Bugwagi	24-Feb-07	85	26.3	5.58	--		245	18.10	334.70	3.84
Chibwera	26-Jan-07	12	26.0	6.58	--		135	24.75	295.78	6.74
Ekikoto	18-Jan-07	72	24.7	10.8	--		180	--	--	5.03
Kacuba	16-Jan-07	15	27.0	--	--		235	21.23	248.71	--
Kako	31-Jul-06	29	25.2	5.52	77.2	X	292.5	4.62	86.10	1.19
Kamunzuka	30-Jul-06	61	24.8	6.13	86.5	X	770	1.68	66.22	0.69
Kamweru	20-Feb-07	33	25.7	5.65	--		43	32.14	656.42	13.85
Kanyanmukali	14-Jan-07	10.8	27.2	8.29	121		94	187.96	443.66	7.16
Karolero	21-Feb-07	15.5	26.8	4.74	--		149	20.49	373.60	5.42
Kasenda[1]	08-Jul-00	13	24.6	5.59	78.8	X	--	--	--	--
Kasenda[2]	18-Mar-01	13	26.1	8.25	104.8	X	--	--	--	--
Kasenda[3]	23-Jul-06	14.2	18.7	8.5	70.3		175	18.48	662.20	2.96
Kasirya	30-Jul-06	40	24.6	3.23	44.9		175	--	--	1.84
Katinda	31-Jan-07	17	27.0	11.14	--		35	19.36	767.97	25.43
Kayihara	24-Mar-00	55.2	24.0	7.67	104		129.5	--	--	1.76
Kifuruka[1]	16-Jul-00	5	23.3	5.63	73.3	X	500	--	--	--
Kifuruka[2]	22-Jul-06	4.5	23.2	8.02	94.6	X	115	35.28	496.72	8.63
Kigezi	31-Jul-06	26	24.8	4.87	67.7	X	135	16.36	282.51	6.64
Kikorongo	26-Jul-06	11	26.9	3.24	44	X	160	1372	11914.00	3.95
Kitagata	10-Jan-01	7.5	--	--	--		5	42.75	1821.39	25.53
Kyaninga	10-Feb-07	57	23.9	7.3	--		660	5.32	103.78	0.81
Kyasanduka[1]	20-Mar-01	2	25.4	14.33	175.1	X	--	--	--	--
Kyasanduka[2]	11-Jan-07	2	29.1	13.72	177.1	X	130	210.98	892.56	203.03
Kyasanduka[3]	12-Jan-07	2	25.9	10.55	130	X	17.5	210.98	892.56	203.03
Kyerbwato[1]	12-Jul-00	13.4	25.3	5.61	79.9	X	63.5	--	--	--
Kyerbwato[2]	23-Jan-07	13.4	25.3	6.28	--		63.5	11.34	228.31	1.72
Kyogo	17-Jan-07	3.4	27.5	--	--		290	272.66	342.87	2.04
Lugembe	15-Jan-07	18.6	25.2	9.43	133		77.5	21.42	529.28	5.69
Lyantonde	22-Jul-06	80	23.9	7.18	85.7	X	280	5.46	258.30	2.27
Mafura	01-Aug-06	27.4	24.3	4.28	59	X		11.48	245.00	3.30

Table 4.2 *Continued…*

Lake	Sampling date	Depth (m)	Temperature (°C)	Oxygen (mg l^{-1})	Oxygen saturation (%)	Profile	Secchi depth (cm)	TP (µg l^{-1})	TN (µg l^{-1})	Chl-a (µg l^{-1})
Mahega[1]	18-Jul-00	4.1	30.8	--	--	X	--	--	--	--
Mahega[2]	18-Jan-07	4.4	31.0	--	--		30	1355.38	2080.83	--
Mahuhura	23-Jul-06	80	26.7	9.08	114.3		660	49.98	86.10	1.17
Maseche	22-Feb-07	0.01	32.3	0.75	--		2	--	--	4.97
Mirambi	31-Jan-07	21	25.3	12.21	--		100	18.01	633.07	11.07
Mugogo	09-Jan-07	141	25.8	7.31	59	X	212	7.39	282.51	--
Muijongo	01-Aug-06	55.4	24.9	4.24	59.1	X	270	6.58	331.10	2.04
Murabyo	29-Jan-07	14	27.4	6.41	--		203	9.78	321.72	0.00
Murusi	17-Jan-07	57	26.1	6.9	--		140	5.09	308.74	1.32
Njarayabana	17-Feb-07	38	26.6	7.7	--		75	359.68	498.15	3.75
Nkugute	01-Feb-07	58	24.5	6.66	--		90	--	--	7.70
Nkuruba[1]	16-Jul-00	34.8	24.6	6.41	96	X	148.5	--	--	--
Nkuruba[2]	16-Feb-07	34.8	24.6	6.41	96		148.5	25.03	659.01	5.89
Nshenyi	26-Jan-07	0.08	29.9	--	--		2	--	--	26.31
Nyamogusingiri Basin	14-Jan-07	3.8	27.0	--	--		52.5	26.99	2003.01	--
Nyamogusingiri Crater	13-Jan-07	11.6	27.5	--	--		50	29.6	1535.98	14.79
Nyamirima	24-Jul-06	51.9	20.9	6.8	76.7		440	4.06	245.00	2.35
Nyamogusani	16-Feb-07	37	26.3	8.2	--		120	152.33	285.39	3.46
Nyamswiga	21-Jul-06	75	23.7	7.82	93	X	180	33.32	390.74	3.99
Nyierya	21-Jul-06	80	23.6	6.91	82.2	X	135	16.1	470.26	14.03
Nyinambulita	24-Jul-06	63.9	19.4	7.09	77.6		427.5	25.9	165.62	1.78
Nyungu	27-Jul-06	25.2	25.8	7.27	101.6	X	46.5	119.14	1498.00	57.25
Saaka[1]	26-Jun-00	11	21.4	6.85	78.8	X	--	--	--	--
Saaka[2]	20-Jul-06	7.8	22.2	6.15	71.2	X	60	36.54	894.04	32.51
Wandakara[1]	15-Jul-00	12	24.7	7.72	105.5	X	--	--	--	--
Wandakara[2]	19-Jan-07	10.5	24.3	7.73	--		31	25.97	752.42	9.08
Wankenzi	19-Jan-07	>60	24.2	9.37	--		36	24.47	835.44	11.35
*Nyamogusingiri inlet	15-Jan-07	0.1	22.0	--	--		--	126.30	354.96	--
*Kyasanduka inlet	12-Jan-07	0.1	22.0	--	--		--	83.80	183.51	--
*Kyasanduka outlet	16-Jan-07	0.1	23.0	--	--		--	261.02	3170.54	--

In lakes with persistent thermoclines (those lakes deeper than 5 m; cf. Melack, 1978), the bottom temperatures of the lake waters varied from 19.9°C (Lake Nyierya) to 25.9°C (Lake Kikorongo; Table 4.3 and Figures 4.3 and 4.4). Lake Kikorongo is rather peculiar in its thermal stratification (Figure 4.4x) and thus a potential outlier when understanding bottom water temperatures as the lake experiences a temperature inversion at *c*. 9 m, coincident with a sharp increase in the measured conductivity. This high temperature at depth could be due to geothermal heat flux and inflow of saline waters from a subterranean geothermal spring; a similar phenomenon to that observed in Lake Kivu, where heat input from below causes a stepwise form in the temperature and salinity gradients (Newman, 1976; Talling and Lemoalle, 1998). With this lake removed, the highest recorded bottom temperature is *c*. 25°C (this occurs in a number of lakes: Bagusa [0.9 m], Karolero [15. m], Murabyo [14 m], Bugwagi [85 m] and Kanyanmukali [10.8 m]). Generally, the higher bottom temperatures were recorded in lakes at lower altitudes, the lower bottom temperatures occurred in lakes of higher altitude (cf. Melack, 1978; Eggermont *et al.*, 2007).

Where full limnological profiles were measured, the lakes appear to show some form of stratification, which can be classified as transient, superficial or deep-seated (cf. Melack, 1978; Table 4.4; Figures 4.3 and 4.4). A transient thermocline is evident in Lake Kyasanduka, where diurnal measurements exist, taken in the morning (*c*. 0900 hours) and late afternoon (*c*. 1500 hours; Figure 4.4xv). The morning measurements indicate near isothermy at Kyasanduka, and an intensification of thermal stratification in the afternoon. Superficial thermoclines occur in the majority of lakes, where a shallow layer of the uppermost waters were at higher temperatures. In some instances deep-seated thermoclines occur (e.g. in lakes > 25 m depth) and are inferred from the temperature profiles (Figures 4.3 and 4.4). These deeper thermoclines can be inferred from their position below the superficial thermocline, and in some instances are linked to chemoclines, the presence of anoxic water beneath them, and the sheltered setting of small, deep, steep-sided lakes (cf. Melack, 1978). These deep-seated thermoclines can be observed in Kamunzuka, Kasirya, Kigezi, Lyantonde, Mafura, Mugogo, Muijongo and Nyierya (Figures 4.3 and 4.4). Deep-seated thermoclines are more apparent in the southern lakes (Bunyaruguru cluster), than those in the north (Kasenda cluster). Multiple thermoclines are more likely to exist in tropical lakes than in temperate regions, though their occurrence is thought to be rare (Lewis Jr., 1973). Out of 19 lakes where full limnological profiles exist, 8 of the lakes show evidence of multiple thermoclines, 6 of which are located in the south.

Table 4.3 *Temperature, pH, conductivity and oxygen concentrations (mg l^{-1} and % saturation) from the bottom water samples of the crater lakes (-- missing data/data not collected).*

Name	Date	Max. Depth	Sample Depth	Bottom Temp. (°C)	Bottom pH	Bottom Cond. (µS cm^{-1})	Bottom Sat. %	Bottom Oxygen (mg l^{-1})
Bagusa	22-Feb-07	0.9	0.9	24.9	10.66	60900	120	10.55
Bugwagi	24-Feb-07	85	85	25.3	7.06	549	--	0
Chibwera	26-Jan-07	12	12	25.6	8.27	--	--	0.2
Ekikoto	18-Jan-07	72	72	22.8	7.04	666	--	0
Kacuba	16-Jan-07	15	15	--		--	--	
Kako	31-Jul-06	29	28	23.4	6.68	125	3.6	0.27
Kamunzuka	30-Jul-06	61	48.6	23.8	6.67	76	4.5	0.33
Kamweru	20-Feb-07	33	33	--	5.59	227	--	0
Kanyanmukali	14-Jan-07	10.8	10.8	25.3	8.41	940	--	0.72
Karolero	21-Feb-07	15.5	15.5	25.0	7	145	---	0.2
Kasenda[1]	08-Jul-00	13.5	13.5	23.2	6.54	--	35.5	2.61
Kasenda[2]	18-Mar-01	13.5	13.4	23.2	6.72	483	1.5	0.12
Kasenda[3]	23-Jul-06	14.2	13.5	--	8.45	352	60.4	5.6
Kasirya	30-Jul-06	40	38	23.1	6.57	954	6.3	0.47
Katinda	31-Jan-07	17	17	24.3	7.53	837	--	0
Kayihara	24-Mar-00	55.2	--	21.7	6.78	737	9	0.65
Kifuruka[1]	16-Jul-00	5	4.2	21.9	6.7	--	31.2	2.47
Kifuruka[2]	22-Jul-06	4.5	--	22.7	8.71	469	69.6	5.96
Kigezi	31-Jul-06	26	--	22.7	6.52	862	4.5	0.33
Kikorongo	26-Jul-06	11	--	25.9	9.99	51900	5.5	0.36
Kitagata	10-Jan-01	7.5	7.5	--		143800	--	
Kyaninga	10-Feb-07	57	57	22.5	6.56	705	--	0.46
Kyasanduka[1]	20-Mar-01	2	1.8	23.9	7.16	588	1.8	0.15
Kyasanduka[2]	11-Jan-07	2	1.8	24.6	7.39	374	12.4	1.09
Kyasanduka[3]	12-Jan-07	2	1.7	24.5	6.8	392	4.8	0.4
Kyerbwato[1]	12-Jul-00	13.4	12.5	24.2	7.98	--	37.2	2.7
Kyerbwato[2]	23-Jan-07	13.4	13	--	7.67	--	--	0
Kyogo	17-Jan-07	3.4	--	--	6.77	--	--	3.06
Lugembe	15-Jan-07	18.6	18	24.6	7.33	444	24	1.15

Table 4.3 *Continued…*

Name	Date	Max. Depth	Sample Depth	Bottom Temp. (°C)	Bottom pH	Bottom Cond (µS cm^{-1}).	Bottom Sat %	Bottom Oxygen (mg l^{-1})
Lyantonde	22-Jul-06	80	30.1	21.5	7.39	760	13	1.14
Mafura	01-Aug-06	27.4	27.2	22.6	6.5	1292	3.5	0.26
Mahega[1]	18-Jul-00	4.1	--	--	--	--	--	--
Mahega[2]	18-Jan-07	4.4	--	--	9.07	144200	--	--
Mahuhura	23-Jul-06	80	--	--	--	--	--	--
Maseche	22-Feb-07	0.01	--	--	--	--	--	--
Mirambi	31-Jan-07	21	21	24.4	8.49	686		0
Mugogo	09-Jan-07	141	15	23.1	7	130	1.6	0.15
Muijongo	01-Aug-06	55.4	42	23.4	7.07	657	4.1	0.3
Murabyo	29-Jan-07	14	14	25.0	6.43	158	--	0.1
Murusi	17-Jan-07	57	57	22.4	6.58	768	--	0
Njarayabana	17-Feb-07	38	38	23.8	7.83	932	--	0
Nkugute	01-Feb-07	58	58	22.5	6.68	145	--	0
Nkuruba[1]	16-Jul-00	34.8	11.9	22.0	6.81	--	25.1	1.98
Nkuruba[2]	16-Feb-07	34.8	--	--	--	--	--	--
Nshenyi	26-Jan-07	0.08	--	--	--	--	--	--
Nyamogusingiri Basin	14-Jan-07	3.8	--	--	--	--	--	2.71
Nyamogusingiri Crater	13-Jan-07	11.6	--	--	--	--	--	--
Nyamirima	24-Jul-06	51.9	--	--	8.73	216	73.9	6.55
Nyamogusani	16-Feb-07	37	--	24.7	8.52	1032	--	--
Nyamswiga	21-Jul-06	75	10.1	23.2	8.02	353	18.3	1.56
Nyierya	21-Jul-06	80	48.1	19.9	7.12	971	4.2	0.38
Nyinambulita	24-Jul-06	63.9	--	--	9.04	274	76.9	7.05
Nyungu	27-Jul-06	27	25.4	22.5	7.75	624	5	0.38
Saaka[1]	26-Jun-00	11	11	22.0	6.32	--	35.1	3.03
Saaka[2]	20-Jul-06	7.8	7	21.5	6.94	--	7.4	0.65
Wandakara[1]	15-Jul-00	12	--	--	--	--	--	--
Wandakara[2]	19-Jan-07	10.5	--	22.9	7.68	--	--	0
Wankenzi	19-Jan-07	60	--	22.5	6.27	920	--	0

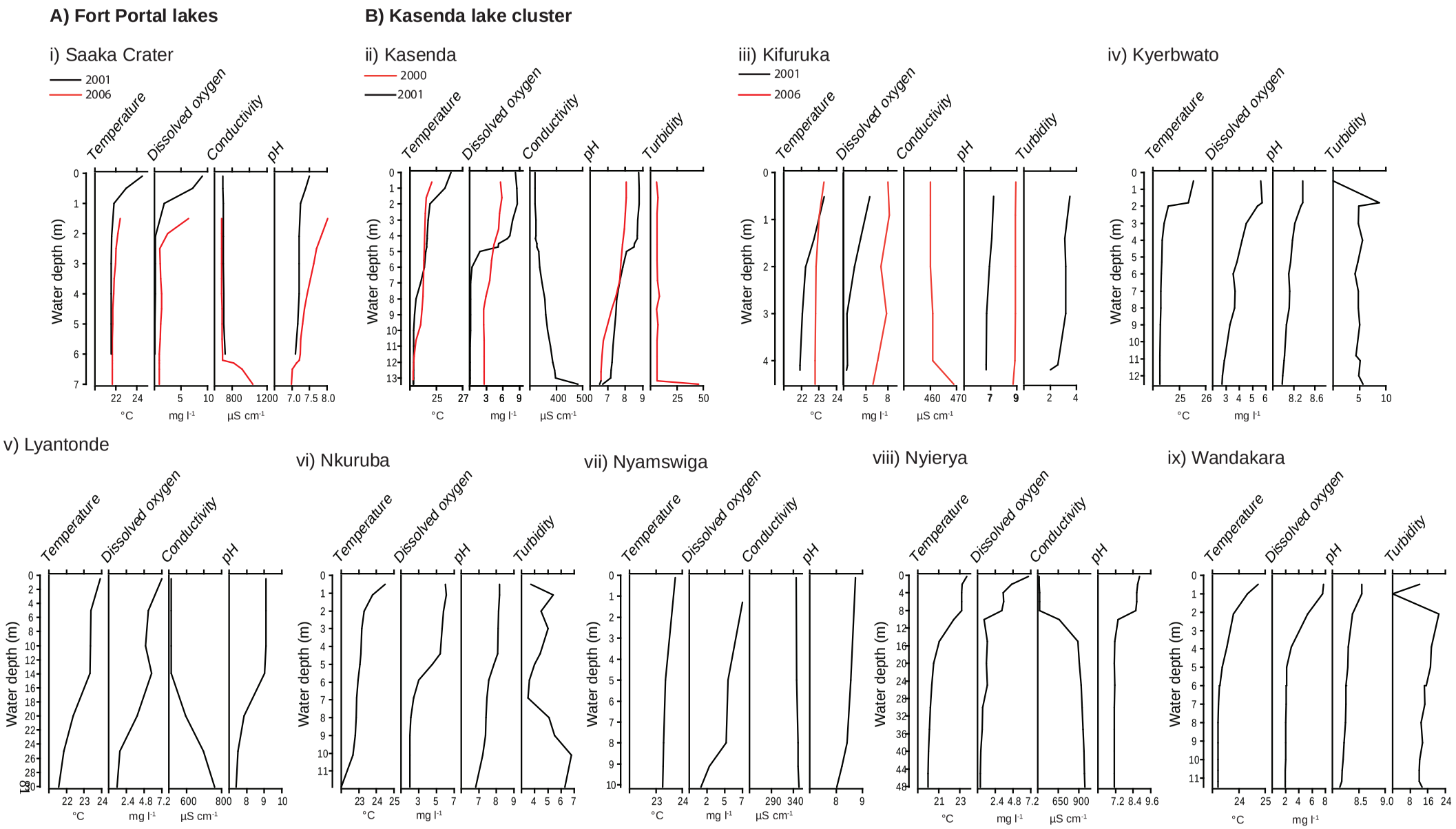

Figure 4.3 *Limnological profiles showing temperature, oxygen, conductivity, pH and turbidity (where data are available) for a selected number of lakes from the north of the field site:* **(A)** *Fort Portal cluster* **(i)** *and* **(B)** *Kasenda lake cluster* **(ii-ix)**. *Depths to the thermocline and chemocline for each lake are given in* **Table 4.4**.

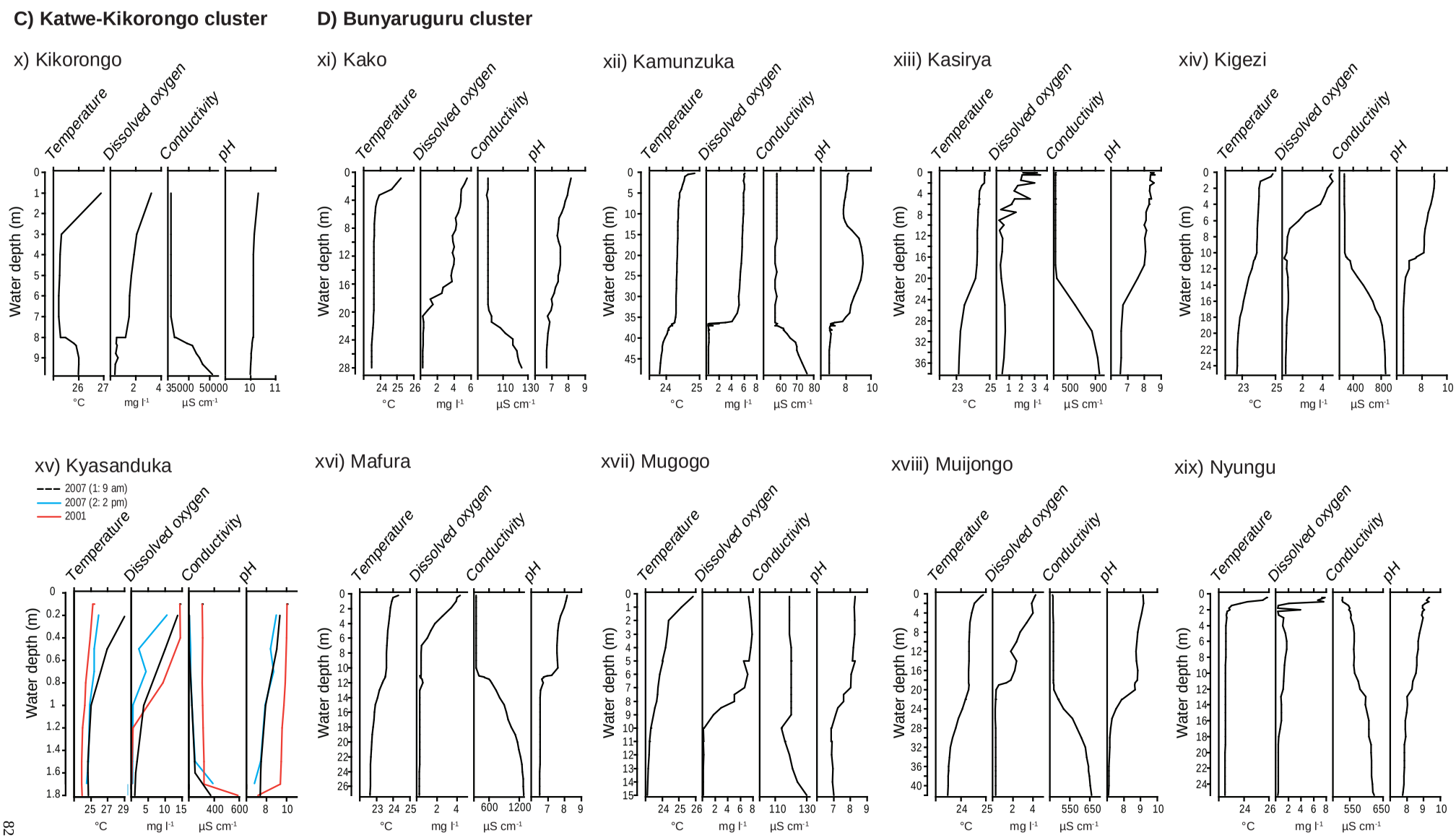

Figure 4.4 *Limnological profiles showing temperature, oxygen, conductivity, pH and turbidity (where data are available) for a selected number of lakes from the south of the field site:* **(C)** *Katwe-Kikorongo cluster* **(x)** *and* **(D)** *Bunyaruguru lake cluster* **(xi-ixx)**. *Depths to the thermocline and chemocline for each lake are given in* **Table 4.4**.

4.4.3 Chemical stratification

The electrical conductivities of the surface waters range from 55-138,100 µS cm^{-1}. The conductivity of the freshwater lakes ranges from 55 µS cm^{-1} (Kyogo) to 1269 µS cm^{-1} (Wandakara), with a median conductivity of *c*. 400 µS cm^{-1}. The lakes in the north of the field site (Fort Portal and Kasenda clusters), although fresh, generally have a higher conductivity than those in southern cluster (Bunyaruguru). The lakes in the north have a conductivity range of 216 µS cm^{-1} (Nyamirima) to 1269 µS cm^{-1} (Wandakara; median conductivity of 421 µS cm^{-1}). The conductivity range of the southern sites is 55-741 µS cm^{-1} (Kyogo and Katinda, respectively). Unlike the findings of Melack (1978) on his study of 16 lakes across the crater lake clusters, it is noted that the lakes in the north are more variable and have a greater conductivity range than lakes in the south (a range of 1053 µS cm^{-1} compared to 686 µS cm^{-1}, north and south respectively).

The lakes with the highest conductivity are those located on the rift valley floor. Values of conductivity in these saline lakes range from 11,230 µS cm^{-1} (Lake Nshenyi) to 138,100 µS cm^{-1} (Lake Mahega). The conductivity of these lakes is governed primarily by the climate of the rift valley floor. The plains between Lakes Edward and George have a low rainfall as they lie in the rain shadow of the Rwenzori Mountains which traps much of the western rainfall (~500 mm yr^{-1}; Atlas of Uganda, 1962; Beadle, 1974). The electrical conductivity in the saline lakes Bagusa, Maseche and Nshenyi over the course of 6 years (2000-2006, data from this research) differed by *c*. 30-50%, providing an indication of the variation in these closed-basin, saline lakes (Melack, 1978).

The maximum percent saturation of dissolved oxygen in the upper waters of the dilute lakes varied between 44.9% and 177.1% (super-saturation; 3.23-14.33 mg l^{-1}; Lakes Kasirya and Kyasanduka, respectively). Only three measurements of oxygen saturation in the saline lakes were taken. The dissolved oxygen ranged from 0.3 mg l^{-1} (Bagusa) to 3.24 mg l^{-1} (Kikorongo). All lakes (where data exist; Table 4.2 and 4.4; Figures 4.3 and 4.4) show anoxia or near anoxia (<2 mg l^{-1}) in the deeper waters; even the shallow lakes Kyasanduka and Kifuruka show near anoxic conditions (Figure 4.3iii and Figure 4.4xv). It is likely that lakes >5 m deep are permanently anoxic at depth, with many lakes being meromictic (cf. Melack, 1978).

4.4.4 Summary

The water-column profiles of temperature, dissolved oxygen, conductivity and pH indicate that all of the surveyed lakes undergo stratification (including some of the shallower lake

Table 4.4 *Depth of thermocline, and depths to anoxia (or near anoxic conditions) and increases in conductivity (chemocline) for 19 crater lakes in western Uganda. Several lakes have multiple readings taken during different field campaigns (2000-2007). The data in this table compliments the limnological profiles in* ***Figures 4.3*** *and* ***4.4****. Data was collected by K. Mills and D.B. Ryves (LBORO;* ***Table 2.1****) using a Hydrolab Quanta probe (see* ***Chapter 3****, section 3.2.1).*

Cluster		Lake	Latitude	Longitude	Date	Thermocline (m)		Max. depth (m)	Anoxia (m)	Conductivity (m)
						Top	Bottom			
A) Fort Portal	i	Saaka	0°41'19.2"	30°14'34.4"	26-Jun-00	0.2	1	11	2.1	--
	i	Saaka	0°41'19.2"	30°14'34.4"	20-Jul-06	--	--	7.8	2.5	6.2
B) Kasenda	ii	Kasenda	0°26'5.01"	30°17'19.6"	08-Jul-00	1	2	13	8.7*	No data
	ii	Kasenda	0°26'5.01"	30°17'19.6"	18-Mar-01	1	2	13	6	13
	iii	Kifuruka	0°29'33.2"	30°17'9.87"	16-Jul-00	0.5	2	5	3*	No data
	iii	Kifuruka	0°29'33.2"	30°17'9.87"	22-Jul-06	--	--	4.5	--	4
	iv	Kyerbwato	0°26'14.8"	30°19'20.8"	12-Jul-00	1.8	2	13.4	6*	No data
	v	Lyantonde	0°29'12.5"	30°16'50.7"	22-Jul-06	0.2	5	80	2.5*	13.9
	vi	Nkuruba	0°31'10.8"	30°18'1.53"	16-Jul-00	1.1	2	34.8	5.0*	No data
	vii	Nyamswiga	0°30'35.0"	30°17'4.99"	21-Jul-06	--	--	75	9*	--
	viii	Nyierya	0°30'10.6"	30°17'3.39"	21-Jul-06	8	15	80	10	8
	ix	Wandakara	0°25'11.3"	30°16'10.1"	15-Jul-00	2	6	12	5	No data
C) Katwe-Kikorongo	x	Kikorongo	0°1'43.7"	30°0'35.04"	26-Jul-06	0.5	3	11	8	8
D) Bunyaruguru	xi	Kako	0°18'21.1"	30°5'48.28"	31-Jul-06	0.2	2	29	19.5	19.5
	xii	Kamunzuka	0°15'33.6"	30°9'19.96"	30-Jul-06	1	5	61	37	37
	xiii	Kasirya	0°15'20.6"	30°7'57.57"	30-Jul-06	2	3.5	40	9	20
	xiv	Kigezi	0°17'8.0"	30°6'35.15"	31-Jul-06	0.5	1.1	26	7	10
	xv	Kyasanduka	0°17'16.0"	30°2'57.06"	20-Mar-01	0.5	1	2	1.6	1
	xv	Kyasanduka	0°17'16.0"	30°2'57.06"	11-Jan-07	--	--	2	1.5	1
	xv	Kyasanduka	0°17'16.0"	30°2'57.06"	12-Jan-07	--	--	2	1.2	1.7
	xvi	Mafura	0°15'53.1"	30°6'6.09"	01-Aug-06	0.2	0.5	27.4	10	7
	xvii	Mugogo	0°17'17.7"	30°7'31.69"	09-Jan-07	0.2	2	141	10*	--
	xviii	Muijongo	0°16'15.9"	30°5'6.31"	01-Aug-06	0.2	2	55.4	19	20
	xix	Nyungu	0°15'27.1"	30°6'0.00"	27-Jul-06	0.8	2	25.2	4	13

* *Dissolved oxygen concentration reduces to c. 2 mg* l^{-1} *creating a very low oxygen environment, but not fully anoxic conditions.*

-- *No distinct change in profile for this limnological variable.*

Table 4.5 *Criteria used for lake classification (see **Table 4.6**) based on thermal stratification, dissolved oxygen content and the presence and attributes of a chemocline.*

Class	Description				
	Thermal	Dissolved oxygen (D.O.)	Conductivity	Conductivity and D.O.	Other
I	**Strong** thermal stratification (>1.5°C temperature change)	**Anoxic** conditions at depth (dissolved oxygen <1 mg l^{-1})	**Increase** in conductivity at depth	**Change** in **conductivity** and **dissolved oxygen** at **same depth**	n/a
II	**Strong** thermal stratification (>1.5°C temperature change)	**Oxygenated** water at depth (dissolved oxygen >1 mg l^{-1})	**Increase** in conductivity at depth	**Change** in **conductivity** and **dissolved oxygen** occur at **different depths**	n/a
III	**Weak** thermal stratification (<1.5°C temperature change)	**Oxygenated** water at depth (dissolved oxygen >1 mg l^{-1})	**No change** in conductivity at depth	**Change** in **conductivity** and **dissolved oxygen** occur at **different depths**	n/a
IV	**Strong** thermal stratification (>1.5°C temperature change)	**Anoxic** conditions at depth (dissolved oxygen <1 mg l^{-1})	**Increase** in conductivity at depth	**Change** in **conductivity** and **dissolved oxygen** occur at **different depths**	n/a
V	**Strong** thermal stratification (>1.5°C temperature change)	**Anoxic** conditions at depth (dissolved oxygen <1 mg l^{-1})	**Increase** in conductivity at depth	**Change** in **conductivity** and **dissolved oxygen** at same depth	**Temperature inversion** at depth

systems). It is possible to discern several classes of lakes based on the type and magnitude of surface-bottom measurements of the above parameters (Table 4.5 and 4.6). It should be stressed that these classifications have been made on the measured parameters at the time of sampling. Type I represents lakes with both a strong thermo- and chemocline, in particular those lakes with a strongly clinograde oxygen profile, whose shift to anoxic conditions is concurrent with a rise in conductivity (e.g. Lakes Lyantonde, Kako, Kamunzuka and Kigezi). Type II and III are lakes that have dissolved oxygen at depth (>2 mg l^{-1}) and whose thermal stratification is weak. Type III lakes appear to have experienced complete mixing (e.g. Type II: Lakes Kasenda, Nkuruba; Type III: Lake Kifuruka). Type IV comprises lakes that have a strong thermocline with anoxic conditions at depth, but the change in conductivity is not concurrent with the switch to anoxia (e.g. Lakes Kasirya, Mafura and Nyungu). The final class (V) comprises just a single lake (Kikorongo) is it representative of saline lake systems with a temperature inversion at depth, concurrent with a rise in conductivity and a switch to anoxic conditions. Lake Mahega is also known to exhibit similar properties to Lake Kikorongo (Melack, 1978) and would also fit into this classification system (class V).

Table 4.6 *Classification of lakes based on their limnological characteristics (data colleted using a Hydrolab Quanta probe). A description of the characteristics of each class is given in* ***Table 4.5****.*

Lake	Weak thermal	Strong thermal	D.O. <1 mg l^{-1}	D.O. >1 mg l^{-1}	Cond. change	Cond / D.O.	Temp. inversion	Class
Lyantonde		X	X		X	X		1
Nyierya		X	X		X	X		1
Kako		X	X		X	X		1
Kamunzuka	X		X		X	X		1
Kigezi		X	X		X	X		1
Mugogo		X	X		X	X		1
Muijongo		X	X		X	X		1
Kasenda		X		X	X			2
Kyerbwato		X		X	No data	No data		2
Nkuruba		X		X	No data	No data		2
Wandakara		X		X	No data	No data		2
Kifuruka	X			X				3
Nyamswiga	X			X				3
Saaka		X	X		X			4
Kasirya		X	X		X			4
Kyasanduka		X	X		X			4
Mafura		X	X		X			4
Nyungu		X	X		X			4
Kikorongo		X	X		X	X	X	5

Melack (1978) used the results of his limnological survey of 16 lakes to try and assess the importance of lake morphometry on the depth of vertical mixing. Table 4.4 and Figures 4.3 and 4.4 show a wide variation in the depth of, what is likely to be, a persistent thermocline and subsequent depth to anoxia. Based on the morphometric descriptions of lakes (e.g. Table 4.1), Melack (1978) proposed an index of the exposure of such crater lakes to wind-induced mixing. In order to calculate this index, Melack used the ratio $D\ H^{-1}$ (D = maximum diameter of lakes, calculated in this study from the digital maps in ArcGIS; H = minimum height of the crater rim above lake level). To simplify the exposure index, the crater vegetation in Melack's study was ignored. A reproduction of Melack's (1978) original figure illustrating the relationship of $D\ H^{-1}$ to the depth of anoxia (AX) is shown in Figure 4.5. New data from this research has been added to the figure, alongside Melack's original lakes (1-16) and his comparison to the Ethiopian and Australian crater lakes (A-J; Melack, 1978). This figure was originally based on the observations of Walker and Likens (1975) who had suggested the need for quantitative evaluation of local catchment topography on the extent of mixing, but had not cited examples (Melack, 1978). Melack chose the depth to anoxia as the indication of the vertical mixing depth, as the thermocline is often ill-defined. Furthermore, Melack (1978) selected lakes with very slight or no chemoclines and well-defined crater rims. All lakes with appropriate data from this research are displayed on Figure 4.5; those with a strong chemocline are highlighted in red.

The regression equation for Melack's lakes (minus his outlier Lake Kanyangeye) alongside the Ethiopian and Australian lakes and all of the lakes from this research (i-xix) is $\ln AX = 9.8 + 7 \times 10^{-3} \ln (D\ H^{-1})$ and has a coefficient (r^2) of 0.035. When all lakes from this study with a well-defined chemocline are removed (red triangles, Figure 4.5), the regression equation becomes $\ln AX = 9.8 + 7 \times 10^{-3} \ln (D\ H^{-1})$ with an $r^2 = 0.35$. The increase in the regression coefficient after the removal of lakes with a well defined chemocline make the results comparable to those of Melack (1978; $r^2 = 0.31$ and 0.47, the latter r^2 was obtained in Melack's study after the addition of the Australian lakes) and also suggest the effect that strong chemoclines have on the depth of mixing in these small shallow lakes, perhaps lending support to permanent anoxia and stratification in lakes with strong chemoclines (see *sections 4.4.2* and *4.4.3*).

The addition of lakes from this research to Melack's original figure (Figure 4.5) does little to alter the original patterns observed by Melack, with the majority of the new data complementing the existing data, and supporting Melack's (1978) conclusion that the scatter is an expected result of well known determinants of stratification (e.g. wind speed,

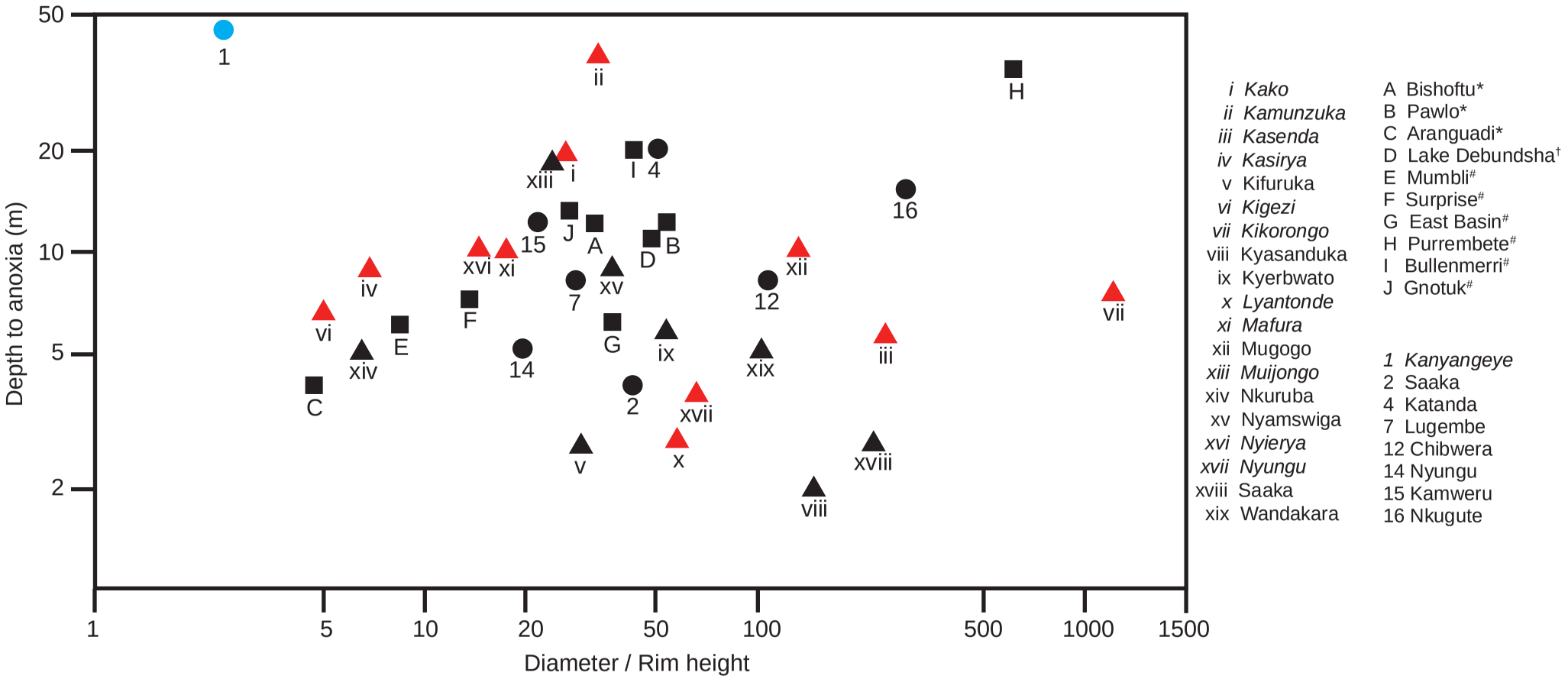

Figure 4.5 *Scatter diagram of the ratio of the maximum diameter of the lake divided by the minimum height of the crater rim versus the depth of anoxic water. Diagram based on Melack (1978).* **i-xix** *data from this study (Ugandan crater lakes). Symbols highlighted in red are those that have evidence for a strong chemocline and therfore do not conform to the criteria used by Melack (1978).* **A-C** *Ethiopian lakes (*Wood et al. [1976] and Prosser et al. [1968]; † Green et al. [1973]);* **D-J** *Australian lakes (Yimms and Brand [1973]; Timms [1975] and Timms [1976].* **1-16** *Ugandan crater lakes (Melack et al. [1978]; Melack's outlier Lake Kanyangeye is highlighted in blue).*

evaporative cooling and turbidity) and the result of only a single measurement per lake (which may be unrepresentative). The addition of new sites may give credibility to the use of a single morphometric ratio (D H^{-1}) in volcanic crater lakes to indicate the depth to anoxia (Melack, 1978).

4.5 Chemical properties

4.5.1 Ionic composition

Table 4.7 lists the major chemical features of the lake waters. All of the saline lakes were alkaline, and the pH of the surface waters varied between 9.3 and 10.62 (median pH of 10.2). The pH in the dilute lakes is similar between the northern and southern clusters, with pH ranging from 7.09 (Kyogo) and 10.62 (Kyasanduka) with a median pH of 8.64. Talling and Talling (1965) split the African lake waters into three classes on the basis of their pH. Class I consists of lakes with a pH range of 7-8.7. Class II included lakes with a pH 8.8-9.5, the final class included lakes with pH 9.5. If this classification system is applied to the Ugandan crater lakes, classes I and II mainly comprise the dilute lakes (although it does include one of the saline lakes, Mahega). All of the other saline lakes belong to class III, as does a single measurement from Lake Kyasanduka (2001, pH 10.2). It is likely that the high pH measured at Kyasanduka is the result of photosynthesis is the upper waters (as photosynthesis increases the pH of lake waters), especially given the occurrence of pronounced algal blooms (Bwanika *et al*., 2004; *section 2.7.1*). However, classification of the current data based on the system of Talling and Talling (1965) should be approached with caution. Talling and Talling (1965) based their system on averages of multiple pH measurements, the data presented here consist of a single sample only.

Amongst the dilute lakes, Njarayabana (north) has the highest Mg and Ca concentrations (22.7 mg l^{-1} and 22.8 mg l^{-1}, respectively) and the ultra-dilute lakes Kyogo and Kamunzuka (south) have the lowest values of Mg (Kyogo, 1.96 mg l^{-1}) and Ca (Kamunzuka, 3 mg l^{-1}; Figure 4.6). Na varies from 1.3 mg l^{-1} (Kako) to 124 mg l^{-1} (Wandakara). Lake Mahega, one of the saline lakes on the rift valley floor has the highest Mg recorded (134 mg l^{-1}) and the highest Ca value of the saline lakes (15 mg l^{-1}), which replicate the findings of Melack (1978); Lake Nshenyi had the lowest Mg and Ca values of the saline lakes (1.99 mg Mg l^{-1} and 17.50 mg Ca l^{-1}). As expected in the saline lakes, Na was particularly high ranging from 384 mg l^{-1} to 40,720 mg l^{-1} (Lakes Kitigata and Mahega).

Table 4.7 *Measured conductivity, pH and ionic composition for the lakes sampled by DANIDA and LBORO (-- missing data/ data not collected).*

Lake	Sampling date	Conductivity ($\mu S\ cm^{-1}$)	pH	F ($mg\ l^{-1}$)	Cl ($mg\ l^{-1}$)	SO_4 ($mg\ l^{-1}$)	Na ($mg\ l^{-1}$)	K ($mg\ l^{-1}$)	Mg ($mg\ l^{-1}$)	Ca ($mg\ l^{-1}$)	Si ($mg\ l^{-1}$)
Bagusa	22-Feb-07	92300	10.62	40.39	4779.68	800.92	40278.97	15473.95	70.66	9.65	12.18
Bugwagi	24-Feb-07	441	8.64	0.48	3.88	--	20.71	20.66	37.68	20.48	24.10
Chibwera	26-Jan-07	462	8.91	0.46	5.92	--	22.15	29.12	24.28	15.31	7.34
Ekikoto	18-Jan-07	497	8.58	0.79	3.90	10.02	39.05	17.57	21.18	35.95	11.98
Kacuba	16-Jan-07	126	7.4	0.31	3.45	--	3.78	10.43	7.78	12.59	9.66
Kako	31-Jul-06	98	8.16	0.11	1.56	0.34	1.30	4.00	6.00	6.50	3.30
Kamunzuka	30-Jul-06	58	8.23	0.04	1.56	0.32	1.50	3.10	3.70	3.00	0.37
Kamweru	20-Feb-07	170	8.4	0.26	2.71	0.49	2.98	4.19	13.53	16.73	11.61
Kanyanmukali	14-Jan-07	920	8.78	2.09	20.69	--	32.87	55.70	48.73	40.27	13.58
Karolero	21-Feb-07	148	8.75	0.29	3.25	--	3.62	9.89	7.55	12.71	9.68
Kasenda[1]	08-Jul-00	380	8.05	--	--	--	--	--	--	--	--
Kasenda[2]	18-Mar-01	320	8.77	--	--	--	--	--	--	--	--
Kasenda3	23-Jul-06	352	8.5	1.07	2.51	0.39	8.90	4.30	12.30	29.70	15.90
Kasirya	30-Jul-06	323	8.58	0.20	2.10	0.17	3.30	7.60	24.10	22.80	12.30
Katinda	31-Jan-07	741	9.23	0.56	14.05		94.34	70.33	27.72	11.98	18.54
Kayihara	24-Mar-00	459	8.39	0.78	1.57	1.73	10.84	8.08	15.70	30.24	13.15
Kifuruka[1]	16-Jul-00	404	7.27	--	--	--	--	--	--	--	--
Kifuruka[2]	22-Jul-06	460	8.92	1.07	4.83	0.32	9.50	15.00	27.10	44.40	18.90
Kigezi	31-Jul-06	271	9	0.22	1.15	0.24	2.00	6.00	19.50	22.80	10.40
Kikorongo	26-Jul-06	22200	10.31	4.89	1659.00	354.00	3628.00	659.90	5.70	7.70	16.00
Kitagata	10-Jan-01	135400	9.63	0.97	70.87	19.76	384.39	172.79	29.82	8.20	4.97
Kyaninga	10-Feb-07	424	8.18	0.90	1.27	1.05	16.50	12.20	27.50	36.60	12.87
Kyasanduka[1]	20-Mar-01	307	10.2	--	--	--	--	--	--	--	--
Kyasanduka[2]	11-Jan-07	204	9.3	0.31	6.42	5.03	12.09	15.94	15.28	19.87	15.01
Kyasanduka[3]	12-Jan-07	204	9.3	0.31	6.42	5.03	12.09	15.93	15.28	19.87	15.01
Kyerbwato[1]	12-Jul-00	538	8.37	--	--	--	--	--	--	--	--
Kyerbwato[2]	23-Jan-07	418	8.47	0.84	1.46	--	9.26	10.76	41.06	21.65	10.41
Kyogo	17-Jan-07	55	7.09	0.04	1.58	--	7.77	7.38	1.96	4.79	6.34
Lugembe	15-Jan-07	407	8.78	1.09	5.08	--	15.60	14.10	22.70	22.40	9.67
Lyantonde	22-Jul-06	512	9.09	2.68	5.78	1.07	9.60	11.10	46.30	29.10	15.30
Mafura	01-Aug-06	342	8.16	0.21	3.77	0.18	3.90	16.40	19.70	27.60	13.70

Table 4.7 *Continued…*

Lake	Sampling date	Conductivity ($\mu S\ cm^{-1}$)	pH	F ($mg\ l^{-1}$)	Cl ($mg\ l^{-1}$)	SO^{2}_{4} ($mg\ l^{-1}$)	Na ($mg\ l^{-1}$)	K ($mg\ l^{-1}$)	Mg ($mg\ l^{-1}$)	Ca ($mg\ l^{-1}$)	Si ($mg\ l^{-1}$)
Mahega [1]	18-Jul-00	138100	--	--	--	--	--	--	134.00	15.00	28.00
Mahega[2]	18-Jan-07	96100	9.3	19.67	37992.89	34988.73	40719.81	8862.23	126.52	9.55	11.06
Mahuhura	23-Jul-06	633	9.19	4.63	7.11	2.57	23.50	24.20	47.40	35.60	22.20
Maseche	22-Feb-07	32700	10.19	22.55	2371.46	960.00	15218.06	2374.07	5.99	7.77	11.76
Mirambi	31-Jan-07	642	8.98	0.49	9.05	5.87	69.93	52.24	27.02	9.93	13.16
Mugogo	09-Jan-07	119	8.29	0.15	2.47	0.94	3.26	3.65	9.65	14.30	5.89
Muijongo	01-Aug-06	464	9.15	0.31	3.13	0.19	12.50	34.70	33.80	17.80	13.00
Murabyo	29-Jan-07	141	8.42	0.16	1.59	--	2.46	8.42	8.33	11.88	6.69
Murusi	17-Jan-07	382	8.54	0.86	1.98	--	13.12	8.26	26.17	29.84	19.42
Njarayabana	17-Feb-07	857	8.58	3.72	5.50	0.50	18.10	24.20	79.40	61.60	21.50
Nkugute	01-Feb-07	121	8.72	0.17	2.13	0.14	3.29	3.50	7.56	11.27	0.11
Nkuruba[1]	16-Jul-00	361	8.4	--	--	--	--	--	--	--	--
Nkuruba[2]	16-Feb-07	370	8.4	1.11	1.45	--	3.80	4.95	24.65	43.28	6.27
Nshenyi	26-Jan-07	11230	10.21	14.28	720.87	262.58	11602.12	3326.86	1.99	7.50	36.76
Nyamogusingiri Basin	14-Jan-07	554	9.16	0.32	26.68	1.44	48.57	101.90	30.75	10.60	13.16
Nyamogusingiri Crater	13-Jan-07	548	9.1	0.36	26.52	0.58	47.76	101.28	30.89	11.04	13.29
Nyamirima	24-Jul-06	216	8.89	0.17	1.42	0.18	4.10	5.20	9.30	24.40	10.10
Nyamogusani	16-Feb-07	988	8.61	4.52	31.33		79.62	50.21	58.29	49.32	20.63
Nyamswiga	21-Jul-06	346	8.74	0.86	2.57	0.24	4.60	8.70	17.40	39.50	8.50
Nyierya	21-Jul-06	419	8.84	1.13	3.40	0.60	5.50	4.10	21.20	24.80	9.30
Nyinambulita	24-Jul-06	274	9.15	0.43	1.92	0.19	1.80	2.90	7.10	12.60	9.80
Nyungu	27-Jul-06	528	9.31	0.53	71.30	16.20	40.30	36.00	41.30	27.20	21.50
Saaka[1]	26-Jun-00	699	7.24	--	--	--	--	--	--	--	--
Saaka[2]	20-Jul-06	662	7.98	0.93	2.39	2.82	29.40	14.90	36.40	58.00	9.10
Wandakara[1]	15-Jul-00	1269	8.56	--	--	--	--	--	--	--	--
Wandakara[2]	19-Jan-07	1222	8.75	3.05	50.95	--	123.98	54.62	42.76	22.81	22.12
Wankenzi	19-Jan-07	397	8.65	1.05	5.37	2.96	10.05	5.36	12.04	25.44	18.75
*Nyamogusingiri inlet	15-Jan-07	631	8.00	0.37	26.79	1.58	47.48	102.84	31.48	14.72	13.40
*Kyasanduka inlet	12-Jan-07	372	7.70	0.52	10.42	3.49	12.84	15.95	15.27	20.21	15.40
*Kyasanduka outlet	16-Jan-07	233	8.00	0.50	11.38	36.53	27.20	35.28	42.58	72.26	27.09

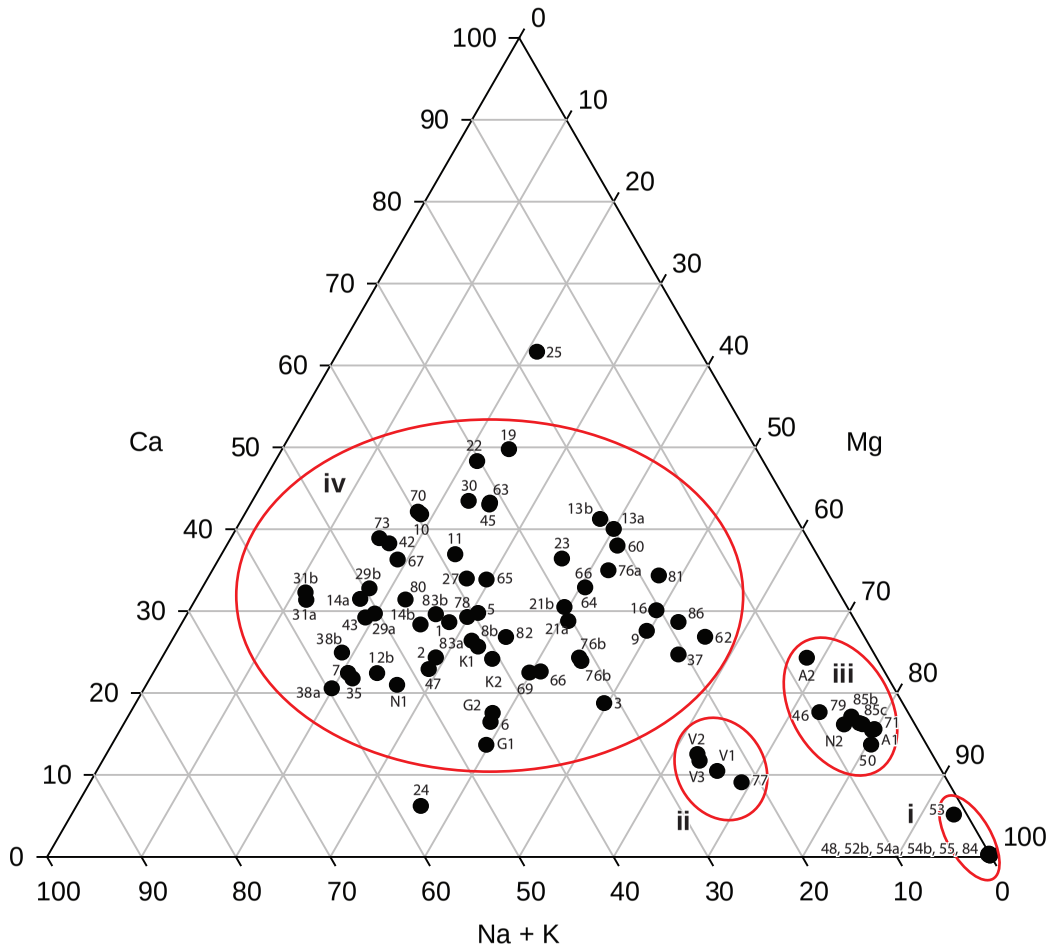

1	Kaitabarogo	31a	Nkuruba	71	Katinda
2	Kayihara	31b	Nkuruba	73	Kigezi
3	Ekikoto	35	Nyamirima	76a	Kyasanduka
5	Kyaninga South	37	Nyamogusani	76b	Kyasanduka
6	Kyegere	38a	Nyamswiga	77	Kyogo
7	Nyabikora	38b	Nyamswiga	78	Mafuro
8b	Saaka Crater	42	Nyierya	79	Mirambi
9	Kanyamukali	43	Nyinabulita	80	Mugogo
10	Kanyanchu	45	Rukwanzi	81	Muijongo
11	Kanyango	46	Wandakara	82	Murabyo
12b	Kasenda	47	Wankenzi	83a	Nkugute
13a	Katanda	48	Bagusa	83b	Nkugute
13b	Katanda	50	Edward	84	Nshenyi
14a	Kifuruka	52b	Kikorongo	85b	Nyamogusingiri Basin
14b	Kifuruka	53	Kitagata	85c	Nyamogusingiri Crater
16	Kitere	54a	Mahega	86	Nyungu
19	Kyerbwato	54b	Mahega	A1	Albert
21a	Lugembe	55	Maseche	A2	Albert
21b	Lugembe	60	Bugwagi	G1	George
22	Lyantonde	62	Chibwera	G2	George
23	Mahuhura	63	Kabarogi	V1	Victoria
24	Mpajo	64	Kacuba	V2	Victoria
25	Mubiro	65	Kako	V3	Victoria
27	Murusi	66	Kamunzuka	K1	Kyasanduka Spring
29a	Mwengenyi	67	Kamweru	K2	Kyasanduka Outlet
29b	Mwengenyi	69	Karolero	N1	Nyamogusingiri 10m
30	Njarayabana	70	Kasirya	N2	Nyamogusingiri Inlet

Figure 4.6 *Ternary diagram of major cation proportions from 64 lakes in Uganda. Four groups can be identified on the ternary diagram:* **(i)** *hypersaline lakes,* **(ii)** *Lake Victoria and Lake Kyogo (forest lake),* **(iii)** *Lakes Albert, Edward, Nyamogusingiri, Wandakara and Mirambi* **(iv)** *All other crater lakes, except Lakes Mpajo and Mubiro (which are appear to sit outside of this main dataset). Data collected by K. Mills and D. Ryves and colleagues in Ghent (D. Verschuren and B. Rumes)*

The concentration of total Fe and Mn are not systematically studied, and in many lake are below the limits of detection (Talling and Talling, 1965). In some African lake waters, Fe concentrations of *c*. 500 µg l^{-1} have been noted in lakes >10m depth (regardless of lake salinity). The distribution of manganese generally follows that of Fe. The iron concentration of surface waters ranged from 3.44 µg l^{-1} (Maseche) to 1153 µg l^{-1}; manganese varied from 0.1µg l^{-1} (Kanyanmukali) to 61 µg l^{-1} (Kamunzuka). The Fe and Mn concentrations of the saline lakes were, on average lower and less variable (Fe range of 3.46 mg l^{-1} to 14 mg l^{-1} and Mn range 0.71 mg l^{-1} to 2.7 mg l^{-1}) than the more dilute lakes (Fe 4.32 mg l^{-1} to 1153 mg l^{-1} and Mn 0.1 mg l^{-1} to 61.14mg l^{-1}).

The silica values across all of the lakes ranges from 0.11 mg l^{-1} (Nkugute) to 36.8 mg l^{-1} (Nshenyi), and the dissolved silica (DSi) content of the lakes does not vary between the dilute and saline lakes. Kilham (1971) suggested that silica values of *c*. 20 mg l^{-1} are typical of regions such as western Uganda with abundant volcanic rocks. However, only 12 of 50 sampled lakes have values in the region of 20 mg l^{-1} (average Si content of 13.5 mg l^{-1} and a median of *c*. 13 mg l^{-1}). These lower values are likely a result of diatom uptake or limited catchment input (Kilham, 1971; Melack, 1978).

4.5.2 Dissolved Inorganic Carbon (DIC) and Non-Purgeable Organic Carbon (NPOC)

The DIC of 48 lake waters ranges from 5 mg l^{-1} (Kyogo) to 12,222 mg l^{-1} (Bagusa), with a median value of 47 mg l^{-1} and an average of 507 mg l^{-1}. The saline lakes record the highest DIC values, ranging from 215 mg l^{-1} (Kitigata) to 12,222 mg l^{-1}, compared to the low range of the dilute lakes (5 mg l^{-1} to 112 mg l^{-1}). The NPOC ranges from 0.86 mg l^{-1} (Kamunzuka) to 70 mg l^{-1} (Mahega). Again, the saline lakes generally record the highest values (Kikorongo 30 mg l^{-1} and Mahega 70 mg l^{-1}), though the value of Kikorongo is exceeded by the dilute Lake Kyasanduka (36 mg l^{-1}). Values of NPOC of samples below the observed chemocline (see Table 4.8) do not reveal any significant differences when compared to the values of the surface waters.

Dissolved Organic Carbon (DOC) can have a major effect of the structure and function of lake ecosystems (Sobek *et al*., 2007). Currently the majority of work on lake water DOC has been undertaken in temperate zones, and many of the assumptions and interpretations in the literature are based on such studies, and gaps still exist with regards to tropical systems (Sobek *et al*., 2007). Lake DOC is made up of autochthonous and allochthonous components. Autochthonous DOC can be released from phytoplankton (extra cellular DOC from their photosynthate; Nalewajko and Marin, [1969]) and

Table 4.8 *Results of DOC and water isotopes ($\delta^{18}O$ and $\delta^{13}C_{TDIC}$. The data were collected by LBORO during 2006 and 2007 (see* ***Table 2.1****). Samples for non-purgeable organic carbon (NPOC) were taken from the surface waters and at depth (anoxic water where present). Samples for isotopic analyses were retrieved from the surface waters only.*

Lake	Sampling date	TOC (mg l^{-1})	DIC (mg l^{-1})	$NPOC_{surface}$ (mg l^{-1})	$NPOC_{anoxia}$ (mg l^{-1})	$\delta^{18}O$	δD	$\delta^{13}C_{tdic}$
Bagusa	22-Feb-07	228.38	12221.68	--	--	--	--	--
Bugwagi	24-Feb-07	3.23	56.35	--	--	--	--	--
Chibwera	26-Jan-07	1.91	50.99	--	--	--	--	--
Ekikoto	18-Jan-07	3.97	42.98	--	--	--	--	--
Kacuba	16-Jan-07	5.49	15.25	2.41	--	6.43	38.80	--
Kako	31-Jul-06	1.50	11.00	1.32	1.35	5.76	29.70	--
Kamunzuka	30-Jul-06	1.00	6.50	0.86	0.99	5.57	34.20	--
Kamweru	20-Feb-07	12.56	22.49	--	--	--	--	--
Kanyanmukali	14-Jan-07	8.21	107.13	--	--	--	--	--
Karolero	21-Feb-07	4.22	14.71	--	--	--	--	--
Kasenda[1]	08-Jul-00	--	--	--	--	--	--	--
Kasenda[2]	18-Mar-01	--	--	--	--	--	--	--
Kasenda[3]	23-Jul-06	4.80	37.70	3.61	3.54	4.66	30.20	-1.38
Kasirya	30-Jul-06	2.10	36.10	2.22	2.22	5.68	34.30	-4.23
Katinda	31-Jan-07	7.95	73.20	--	--	--	--	--
Kayihara	24-Mar-00	6.73	29.04	--	--	--	--	--
Kifuruka[1]	16-Jul-00	--	--	--	--	--	--	--
Kifuruka[2]	22-Jul-06	4.30	47.50	4.27	--	6.30	38.40	1.24
Kigezi	31-Jul-06	4.50	31.50	2.60	1.66	5.67	33.70	-0.80
Kikorongo	26-Jul-06	51.30	1187.00	29.76	29.90	8.95	53.00	1.01
Kitagata	10-Jan-01	22.00	215.40	--	--	--	--	--
Kyaninga	10-Feb-07	0.57	51.73	--	--	--	--	--
Kyasanduka[1]	20-Mar-01	--	--	--	--	--	--	--
Kyasanduka[2]	11-Jan-07	--	--	--	--	--	--	--
Kyasanduka[3]	12-Jan-07	79.89	28.84	35.62	33.28	4.33	26.90	--
Kyerbwato[1]	12-Jul-00	--	--	--	--	--	--	--
Kyerbwato[2]	23-Jan-07	5.61	42.05	--	--	--	--	--
Kyogo	17-Jan-07	3.67	4.89	2.23	--	5.82	37.20	--
Lugembe	15-Jan-07	2.26	48.19	--	--	--	--	--
Lyantonde	22-Jul-06	2.90	58.10	2.34	3.22	4.86	31.90	-4.64
Mafura	01-Aug-06	4.60	37.70	4.20	3.49	5.96	35.60	-6.23

Figure 4.8 *Continued…*

Lake	Sampling date	TOC (mg l^{-1})	DIC (mg l^{-1})	$NPOC_{surface}$	$NPOC_{anoxia}$	$\delta^{18}O$	δD	$\delta^{13}C_{tdic}$
Mahega[1]	18-Jul-00	--	--	--	--	--	--	--
Mahega[2]	18-Jan-07	115.81	1257.87	69.65	--	7.15	31.30	
Mahuhura	23-Jul-06	2.30	72.40	1.74	1.45	5.99	37.40	-2.14
Maseche	22-Feb-07	668.87	2970.76	--	--	--	--	--
Mirambi	31-Jan-07	3.72	54.39	--	--	--	--	--
Mugogo	09-Jan-07	6.24	16.60	3.35	--	2.99	20.10	-4.33
Muijongo	01-Aug-06	3.60	52.60	3.24	3.77	5.99	37.40	-4.43
Murabyo	29-Jan-07	6.27	15.25	--	--	--	--	--
Murusi	17-Jan-07	8.61	36.78	--	--	--	--	--
Njarayabana	17-Feb-07	11.23	111.55	--	--	--	--	--
Nkugute	01-Feb-07	5.24	12.86	--	--	--	--	--
Nkuruba[1]	16-Jul-00	--	--	--	--	--	--	--
Nkuruba[2]	16-Feb-07	5.85	45.95	--	--	--	--	--
Nshenyi	26-Jan-07	503.43	4463.01	--	--	--	--	--
Nyamogusingiri Basin	14-Jan-07	17.13	64.24	16.13	--	6.52	39.50	10.10
Nyamogusingiri Crater	13-Jan-07	17.31	62.97	15.38	14.60	6.66	40.70	10.44
Nyamirima	24-Jul-06	1.30	15.20	1.68	1.68	5.47	33.80	-6.78
Nyamogusani	16-Feb-07	1.66	112.48	3.56	5.38	5.36	32.10	-1.20
Nyamswiga	21-Jul-06	4.00	39.20	2.99	2.88	4.00	25.80	-1.90
Nyierya	21-Jul-06	3.70	42.10	--	--	--	--	--
Nyinambulita	24-Jul-06	1.70	30.40	1.41	1.80	5.57	35.40	-2.00
Nyungu	27-Jul-06	6.60	102.00	3.33	2.84	2.32	21.20	-4.72
Saaka[1]	26-Jun-00	--	--	--	--	--	--	--
Saaka[2]	20-Jul-06	7.30	80.40	7.54	--	2.70	22.20	9.61
Wandakara[1]	15-Jul-00	--	--	--	--	--	--	--
Wandakara[2]	19-Jan-07	6.88	107.05	--	--	--	--	--
Wankenzi	19-Jan-07	7.59	46.54	--	--	--	--	--
*Nyamogusingiri inlet	15-Jan-07	1.35	78.02	--	--	-2.04	-2.60	-9.23
*Kyasanduka inlet	12-Jan-07	79.73	28.55	23.76	--	-2.27	-4.70	-9.68
*Kyasanduka outlet	16-Jan-07	4.25	83.72	1.12	--	4.43	27.60	--

macrophytes. However, this form of DOC is often colourless and is usually rapidly broken down by bacteria (Gergel *et al*. 1999). It also only constitutes a small proportion of lake DOC; allochthonous DOC is believed to represent the largest fraction of DOC in lakes, and is often much darker in colour. This form of DOC can enter lake systems through precipitation, leaching, and decomposition, in addition highly productive wetlands can generate large amounts of organic matter that enter lakes in dissolved form (Wetzel 1990, 1992). This DOC is often composed of fulvic and humic acids, which result from the decomposition of lignin and cellulose (Engstrom, 1987). The fulvic and humic acids of DOC can influence the acid-base chemistry of freshwaters (Sullivan *et al.* 1989), affecting the cycling of metals such as copper, mercury, and aluminum (Campbell *et al*. 1992). Where darker coloured DOC exists, it can affect the thermal structure and mixing depth of the lakes (Fee *et al*., 1996), it can also affect ecosystem production as it can hinder photosynthesis through the attenuation of solar radiation (Sobek *et al*., 2007).

Climatic conditions are important for the DOC concentration in lakes. For example, under arctic conditions, the permafrost conditions limit the amount of carbon exported from the soil to the lake ecosystem, resulting in generally low DOC concentrations. Conversely, in boreal regions, organic rich soils coupled with low microbial metabolism, lead to high DOC in lakes. The closed lakes of the Northern Great Plains are subject to high evaporative concentration of solutes, causing high conductivities (74,000 $\mu S\ cm^{-1}$; Curtis and Adams, 1995). These lakes also exhibit high DOC concentrations. As a result it is postulated that climate affects both the production and mobilization of organic carbon from terrestrial soils and the hydrological balance of lakes and therefore plays an important role in the regulation of DOC concentrations in lakes (Sobek *et al*., 2007).

The results from the Ugandan crater lakes show that DOC (measured here as NPOC) are higher in the saline lakes, and very low in the majority of freshwater lakes. Freshwater lakes with known algal blooms (e.g. Saaka and Kyasanduka) have higher DOC than other lakes. It is likely that large amounts of DOC are delivered to the lake from the productive catchment soils, but given the warm waters of these systems, the breakdown and or recycling in these systems is probably rapid enough to keep concentrations low.

4.5.3 Water isotopes ($\delta^{18}O$, δD and $\delta^{13}C_{TDIC}$)

The Global Meteoric Water Line (GMWL, Figure 4.7) was defined by Craig (1961) and was designed to illustrate the average (global) relationship between hydrogen and oxygen isotope ratios in natural terrestrial waters. A meteoric water line can also be calculated for

a given area (Local Meteoric Water Line, LMWL) with variations from this model due to isotope effects of kinetic fractionation. Lakes in tropical regions (both open- and closed-basin), where water loss is mainly through evaporation, have waters with variable and elevated oxygen isotope composition. Measured $\delta^{18}O$ (and δD) values are always higher than those of ambient precipitation as the lighter isotopes of ^{16}O and (^{1}H) are preferentially lost to evaporation (Leng and Marshall, 2004; Figure 4.7). In addition, hydrologically closed lakes often show $\delta^{18}O$ vs. $\delta^{13}C_{TDIC}$ (Total Dissolved Inorganic Carbon) covariance, the higher values reflecting different degrees of equilibration of the TDIC with atmospheric carbon dioxide and preferential evaporative loss of the lighter ^{16}O. Groundwater and river water tend to have low values of $\delta^{13}C_{TDIC}$ (usually between –10‰ and –15‰) from plant respiration and production of CO_2 in catchment soils (Leng and Marshall, 2004).

The results from the isotopic analyses of lake waters indicate that the crater lakes of western Uganda lie on an evaporative local meteoric water line (Figure 4.7). Lakes Saaka, Nyungu and Mugogo have the lowest lake $\delta^{18}O$ and δD values ($\delta^{18}O$: +2.7, +2.3 and +2.99, respectively; δD: +22.2, +21.2 and +20.1, respectively) and lie closer to the GMWL. The two saline lakes analysed (Kikorongo and Mahega), as expected, lie the furthest from the GMWL, indicating greater evaporative concentration of these lakes. The remainder of the dilute lakes lie between the values of Kikorongo ($\delta^{18}O$ = +8.95 and δD = +53) and the lowest values of Saaka, Nyungu and Mugogo (with a $\delta^{18}O$ range of +4 to +6.66 and a δD range of +25.8 to +40.7).

The lowest $\delta^{18}O$ and δD belong to the two spring water samples, one feeding Lake Kyasanduka ($\delta^{18}O$ –2.27; δD –4.7), the other feeding Lake Nyamogusingiri ($\delta^{18}O$ –2.04; δD –2.6). These low values, plotting almost on the GMWL (Figure 4.7) suggest that the source of this spring water is precipitation, which has not undergone any evaporative enrichment. Only 10 samples have results for $\delta^{13}C_{TDIC}$ which can be compared to the $\delta^{18}O$ values (Table 4.8 and Figure 4.8). The results indicate that the spring feeding Kyasanduka has the lowest $\delta^{13}C_{TDIC}$ value (–1.2‰). Although not at the low values suggested by Leng and Marshall (2004; groundwater typically has values of −10‰ to −15‰), the values are still indicative of an extremely freshwater source, most likely precipitation. Similarly, the results for the saline lake Kikorongo conform to the expected distribution (cf. Figure 4.8). The remaining eight results represent the dilute lakes across the field region. All of these lakes indicate an increasing amount of organic matter oxidation, with Lakes Kigezi and Kyasanduka recording the lowest $\delta^{13}C_{TDIC}$ values. The positive $\delta^{18}O$ values of all of the

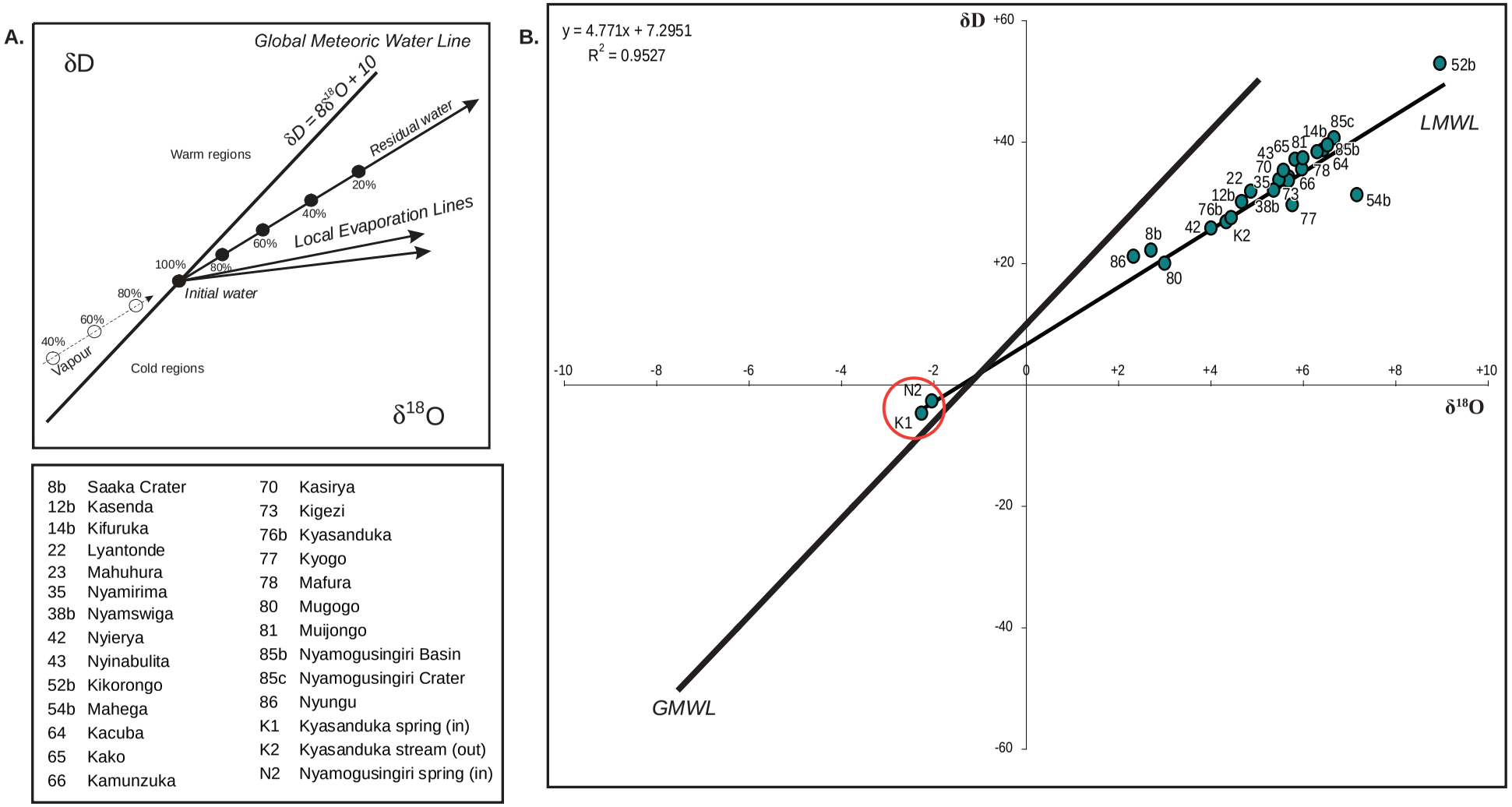

8b	Saaka Crater	70	Kasirya
12b	Kasenda	73	Kigezi
14b	Kifuruka	76b	Kyasanduka
22	Lyantonde	77	Kyogo
23	Mahuhura	78	Mafura
35	Nyamirima	80	Mugogo
38b	Nyamswiga	81	Muijongo
42	Nyierya	85b	Nyamogusingiri Basin
43	Nyinabulita	85c	Nyamogusingiri Crater
52b	Kikorongo	86	Nyungu
54b	Mahega	K1	Kyasanduka spring (in)
64	Kacuba	K2	Kyasanduka stream (out)
65	Kako	N2	Nyamogusingiri spring (in)
66	Kamunzuka		

Figure 4.7 *Oxygen and hydrogen isotopes of the surface waters of 24 crater lakes, 2 springs and 1 stream.* **(A)** *The main controls governing the $\delta^{18}O$ vs δD of precipitation and lake waters. The Global Meteoric Water Line (GMWL) is an average of a multitude of local meteoric water lines (taken from Leng and Marshall, 2004).* **(B)** *Results of $\delta^{18}O$ vs δD from the Ugandan crater lakes. The LMWL indicates the lakes in the west of Uganda are evaporatively enriched in comparison to the GMWL. It is worth noting that the two spring samples (K1 and N2; highlighted in red circle) plot almost on the GMWL, showing their relationship to global precipitation.*

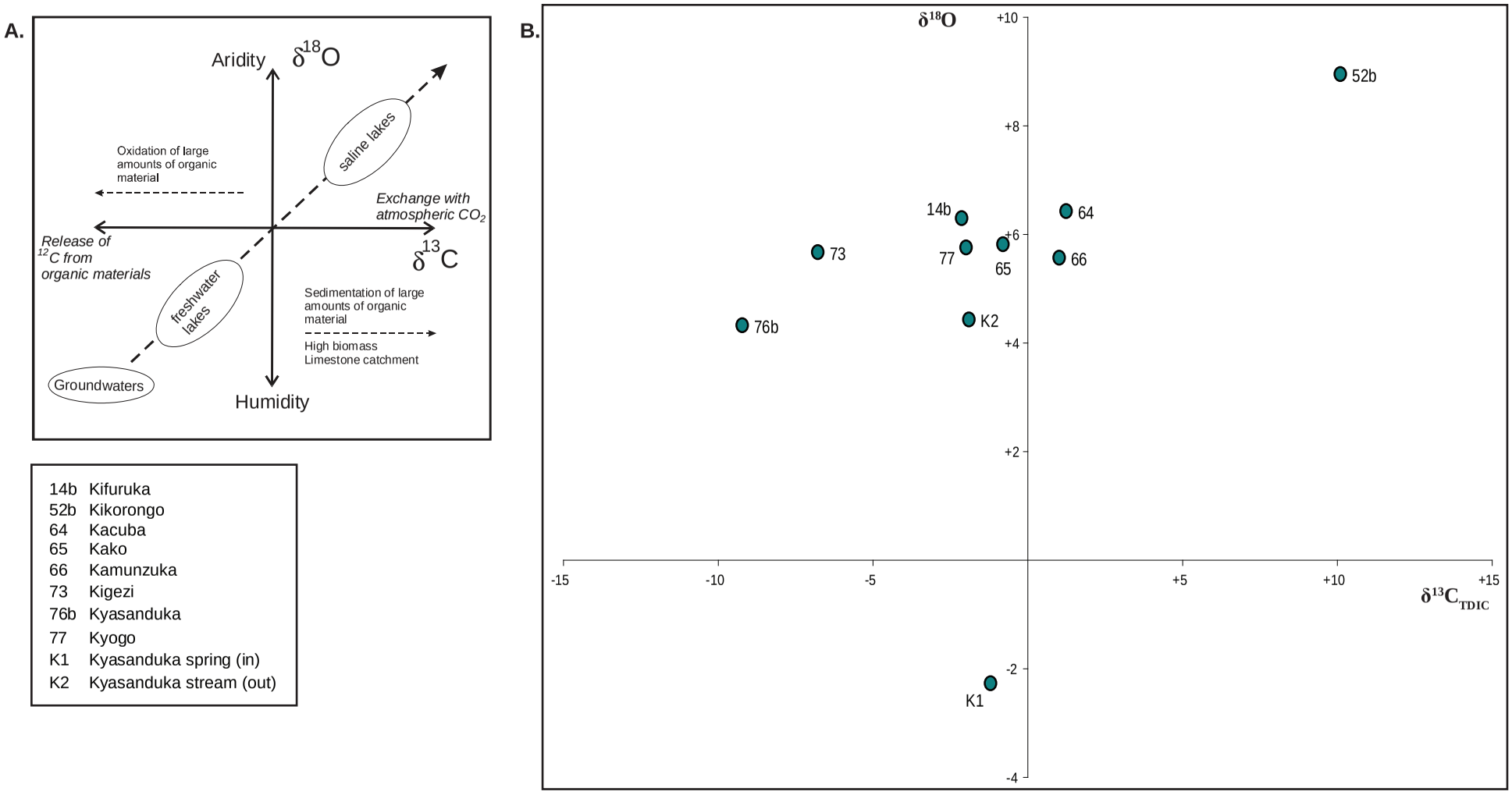

Figure 4.8 **(A)** *$\delta^{13}C_{TDIC}$ vs. $\delta^{18}O$ of lake waters (taken from Leng and Marshall, 2004).* **(B)** *Results of $\delta^{13}C_{TDIC}$ vs. $\delta^{18}O$ from the Ugandan crater lakes.*

dilute lakes suggest that they experience some degree of evaporative enrichment, as would generally be expected in these tropical lakes (see Figure 4.7 also).

4.6 Nutrients and lake trophic status

The total phosphorus (TP) concentration in surface waters across all lakes sampled ranges from 1.7 µg l^{-1} (Lake Kamunzuka) to 13,720 µg l^{-1} (Lake Kikorongo; median value of 25 µg l^{-1}). The TP in the dilute lakes ranges from 1.7-360 µg l^{-1} (highest value is recorded in Lake Njarayabana). The dilute lakes located to the north have a greater TP range (4-360 µg l^{-1}; Nyamirima and Njarayabana, respectively) than those in the south (1.7-273 µg l^{-1}; Kamunzuka and Kyasanduka, respectively), although average TP values between the north and the south are similar (the medians differ somewhat, 25 and 20 µg l^{-1}; north and south, respectively). The saline lakes have the highest recorded TP values. Results only exist for three of the saline lakes: 43 µg l^{-1} (Kitigata), 1355 µg l^{-1} (Mahega) and 13,720 µg l^{-1} (Kikorongo). Talling and Talling (1965) suggested that phosphorus values of >1000 µg l^{-1} are common in saline lakes whilst values of >150 µg l^{-1} are usual in shallow, productive lakes. Whilst this is true for two of the saline lakes (Mahega and Kikorongo) and two of the dilute lakes (shallow lakes Kyasanduka and Kyogo), it does not hold true for some of the other lakes with extremely high TP values. Therefore the higher TP (>150 µg l^{-1}) levels in some of the deeper, dilute lakes may be attributable to human activity in the catchment with internal cycling of the phosphorus (Talling and Talling, 1965).

Similarly, total nitrogen (TN) values are more variable in the northern than in the southern lakes with ranges of 86 µg l^{-1} (Mahuhura) to 894 (Saaka) and 66 µg l^{-1} (Kamunzuka) to 273 µg l^{-1} (Kyogo) respectively. The saline lakes have values of 1821 µg l^{-1} (Kitigata), 2081 µg l^{-1} (Mahega) and 11914 µg l^{-1} (Kikorongo). Tables 4.2 and 4.8 also show chlorophyll-*a* concentrations in the lakes studied. Across the field site, Chl-*a* varies from 0.69 µg l^{-1} (Kamunzuka) to 497 µg l^{-1} (Bagusa). The majority of lakes sampled (31) had Chl-*a* concentrations of <10 µg l^{-1}; the remaining 12 had values greater than 10 µg l^{-1}. The highest recorded values occur in the saline Lake Bagusa and the shallow lake Kyasanduka (203 µg l^{-1}).

The linear relationship (r^2 = 0.93) between total phosphorus (TP and total nitrogen (TN) is illustrated in Figure 4.9. The red and blue lines represent the ratios (TN:TP)15:1 and 7:1 (Vollenweider and Kerekes, 1982). Lakes are typically P limited when the ratio is >15, and N limited when the ratio <7. The majority of the Ugandan crater lakes appear to be phosphorus limited (27 of 41, where both TP and TN data were available; Table 4.9), 9

Table 4.9 *Limiting nutrients for the Ugandan crater lakes based on TN: TP thresholds outlined by Vollenweider and Kerekes (1982;* ***Figure 4.9****). A ratio > 15 suggests a lake is phosphorus limited, a ratio <7 suggests that nitrogen is the limiting nutrient. Where ratios are 7-15, either P or N can be the limiting nutrient.*

Lake name	Date	Who	TP (µg/L)	TN (µg/L)	TN:TP	Limiting nutrient		
						P	N	N or P
Bagusa	22-Feb-07	RUMES	--	--	--	--	--	--
Bugwagi	24-Feb-07	RUMES	18.10	334.70	18.49	X		
Chibwera	26-Jan-07	RUMES	24.75	295.78	11.95			X
Ekikoto	18-Jan-07	RUMES	--	--	--	--		
Kacuba	16-Jan-07	LBORO	21.24	248.71	11.71			X
Kako	31-Jul-06	LBORO	4.62	86.10	18.64	X		
Kamunzuka	30-Jul-06	LBORO	1.68	66.22	39.42	X		
Kamweru	20-Feb-07	RUMES	32.14	656.42	20.42	X		
Kanyanmukali	14-Jan-07	RUMES	187.96	443.66	2.36		X	
Karolero	21-Feb-07	RUMES	20.50	373.60	18.23	X		
Kasenda[3]	23-Jul-06	LBORO	18.48	662.20	35.83	X		
Kasirya	30-Jul-06	LBORO	--	--	--	--	--	--
Katinda	31-Jan-07	RUMES	19.36	767.97	39.66	X		
Kayihara	24-Mar-00	DIRK	--	--	--	--		
Kifuruka[2]	22-Jul-06	LBORO	35.28	496.72	14.08			X
Kigezi	31-Jul-06	LBORO	16.37	282.51	17.26	X		
Kikorongo	26-Jul-06	LBORO	13720.00	11914.00	0.87		X	
Kitagata	10-Jan-01	DIRK	42.76	1821.39	42.60	X		
Kyaninga	10-Feb-07	RUMES	5.32	103.78	19.51	X		
Kyasanduka[2]	11-Jan-07	LBORO	210.98	892.56	4.23		X	
Kyerbwato[2]	23-Jan-07	RUMES	11.34	228.31	20.13	X		
Kyogo	17-Jan-07	LBORO	272.66	342.87	1.26		X	
Lugembe	15-Jan-07	RUMES	21.42	529.28	24.71	X		

Table 4.9 *Continued…*

Lake name	Date	Who	TP (µg/L)	TN (µg/L)	TN:TP	Limiting nutrient		
						P	N	N or P
Lyantonde	22-Jul-06	LBORO	5.46	258.30	47.31	X		
Mafuro	01-Aug-06	LBORO	11.48	245.00	21.34	X		
Mahega[2]	18-Jan-07	LBORO	1355.38	2080.83	1.54		X	
Mahuhura	23-Jul-06	LBORO	49.98	86.10	1.72		X	
Maseche	22-Feb-07	RUMES	--	--	--	--	--	--
Mirambi	31-Jan-07	RUMES	18.02	633.07	35.14	X		
Mugogo	09-Jan-07	LBORO	7.39	282.51	38.22	X		
Muijongo	01-Aug-06	LBORO	6.58	331.10	50.32	X		
Murabyo	29-Jan-07	RUMES	9.79	321.72	32.88	X		
Murusi	17-Jan-07	RUMES	5.10	308.74	60.59	X		
Njarayabana	17-Feb-07	RUMES	359.69	498.15	1.38		X	
Nkugute	01-Feb-07	RUMES	--	--	--	--	--	--
Nkuruba[2]	16-Feb-07	RUMES	25.03	659.01	26.33	X		
Nshenyi	26-Jan-07	RUMES	--	---	--	--	--	--
Nyamogusingiri Basin	14-Jan-07	LBORO	26.99	245.00	60.34	X		
Nyamogusingiri Crater	13-Jan-07	LBORO	29.60	285.39	1.87		X	
Nyamirima	24-Jul-06	LBORO	4.06	2003.01	74.21	X		
Nyamogusani	16-Feb-07	RUMES	152.33	1535.98	51.90	X		
Nyamswiga	21-Jul-06	LBORO	33.32	390.74	11.73			X
Nyierya	21-Jul-06	LBORO	16.10	470.26	29.21	X		
Nyinambulita	24-Jul-06	LBORO	25.90	165.62	6.39		X	
Nyungu	27-Jul-06	LBORO	119.14	1498.00	12.57			X
Saaka Crater[2]	20-Jul-06	LBORO	36.54	894.04	24.47	X		
Wandakara[2]	19-Jan-07	RUMES	25.97	752.42	28.97	X		
Wankenzi	19-Jan-07	RUMES	24.47	835.44	34.14	X		
*Nyamogusingiri inlet	15-Jan-07	LBORO	279.65	--	--	--	--	--
*Kyasanduka inlet	12-Jan-07	LBORO	185.57	--	--	--	--	--
*Kyasanduka outlet	LBORO	16-Jan-07	577.964	--	--	--	--	--

are nitrogen limited and 5 fall between the two ratios and can be either nitrogen or phosphorus limited. Talling and Talling (1965) suggested that N-limitation rather than P-limitation might be regionally prevalent in East Africa (with regards to larger lake systems and multiple samples from several years). The analysis of one sample from each of the crater lakes suggests that these small systems are (or were, at the point of sampling) most likely to be P-limited (Figure 4.9 and Table 4.9). It is likely that one of the major sources of nitrogen to the Ugandan crater lakes is either from atmospheric nitrogen deposition (Lewis Jr. *et al*., 2008) from the fixation (conversion of molecular N to N oxides and ammonia) or atmospheric N_2 by blue-green algae, which in some lakes can be attested to due to the presence of diatoms that are known nitrogen heterotrophs (e.g. *Nitzschia palea*) and thus require a nitrogen fixing host (e.g. Microcystis; Talling and Lemoalle, 1998). This increase in nitrogen in the lake waters may then lead to the observed P-limitation.

Using the TP, TN and Chl-*a* data, an indication of lake trophic status was obtained using Carlson's (1977) trophic status index (TSI; Tables 4.10 and 4.11). The use of TSI does not define a lake's trophic status, as chlorophyll or total phosphorus (for example) are not considered the basis of a definition of trophic state, rather they are indicators of a more broadly defined concept (Carlson, 1977). In conjunction with this, the best indicator of trophic status can vary between lakes, and within lakes depending on the season.

Table 4.10 *Lake trophic status as defined by Carlson (1977) and OECD (based on Vollenweider and Kerekes [1982]).*

Trophic state	Carlson's TSI (TSI 0-100)	OECD		
		P (μg l^{-1})	Chl-*a* (μg l^{-1})	Secchi (m)
Ultra-oligotrophic	--	< 4	< 1	> 12
Oligotrophic	< 40	< 10	< 2.5	> 6
Mesotrophic	40 – 50	10 – 35	2.5 – 8	6 – 3
Eutrophic	50 – 70	35 – 100	8 – 25	3 – 1.5
Hyper -eutrophic	> 70	> 100	> 25	< 1.5

The trophic state index (TSI) of Carlson (1977) uses algal biomass as the basis for trophic state classification. Three variables, Secchi depth (SD), chlorophyll-*a* (CHL) and total phosphorus (TP), independently estimate algal biomass. There are no lake types (e.g. oligotrophic, eutrophic, acidotrophic; cf. Naumann, 1929), rather Carlson's TSI is based on

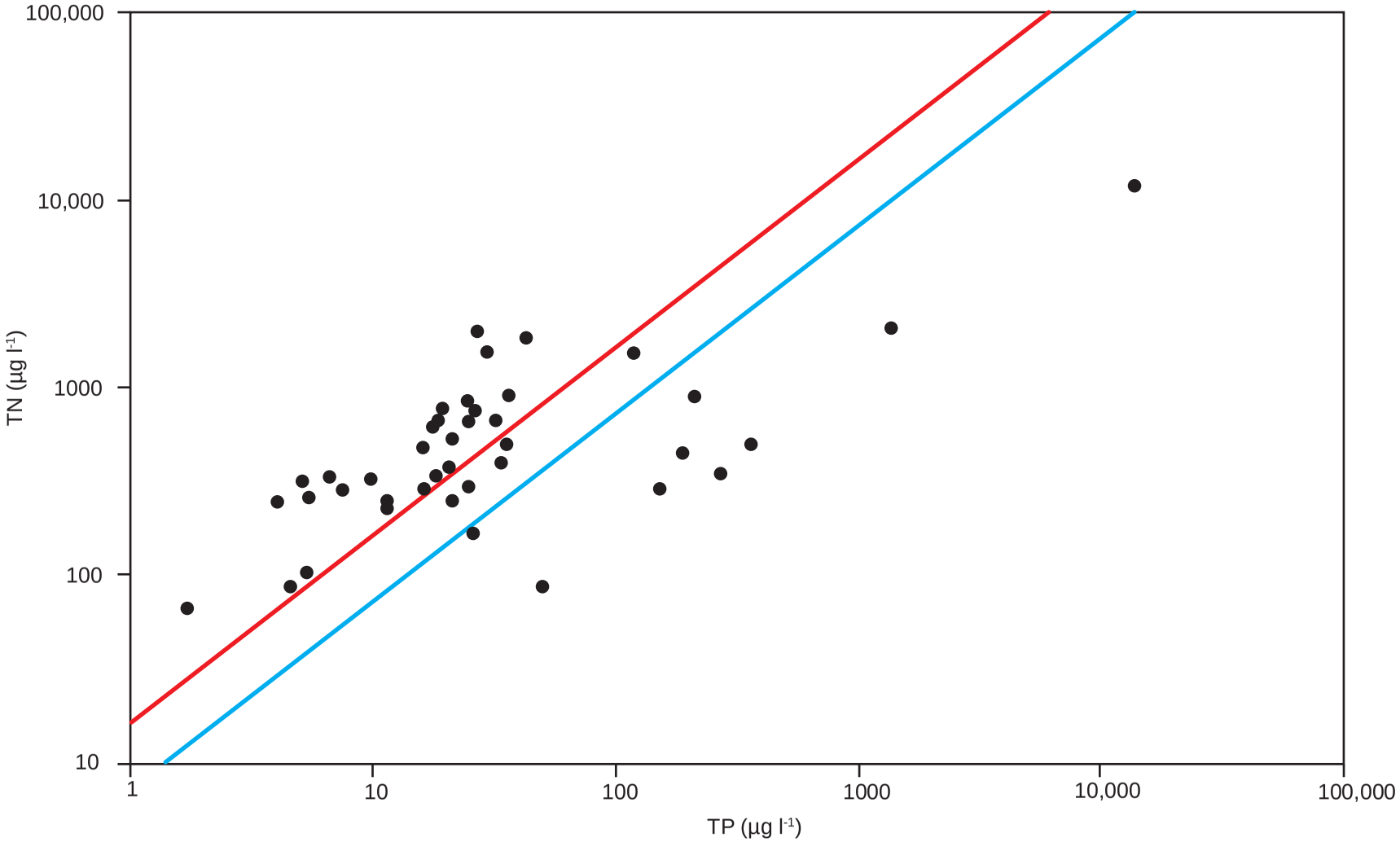

Figure 4.9 Total phosphorus (*TP) vs. Total nitrogen (TN) of the Uganda crater lakes. The solid lines represent 7:1 (blue) ratio and 15:1 (red) ratio. Lakes that are phosphorus limited (ratio N:P > 15:1) plot above the red line, those that are nitrogen limited (ratio N:P <7:1) plot below the blue line. Lakes that plot between the two lines may be limited by either phosphorus or nitrogen (Vollenweider and Kerekes, 1982). Refer to* ***Table 4.9c*** *for a list of the limiting nutrient for each of the crater lakes.*

a trophic continuum and is based on a base-2 logarithmic transformation of Secchi depth. TSI ranges along a scale from 0-100 that is based upon relationships between Secchi depth and surface water concentrations of chlorophyll-*a* and total phosphorus. A set of equations describe these relationships:

$$\begin{aligned} \text{TSI (SD)} &= 60 - 14.41 \ln \text{SD (meters)} \\ \text{TSI (CHL)} &= 9.81 \ln \text{Chl-}a\ (\mu g\ l^{-1}) + 30.6 \\ \text{TSI (TP)} &= 14.42 \ln \text{TP}\ (\mu g\ l^{-1}) + 4.15 \end{aligned}$$

In Carlson's (1977) classification system, an increase in TSI of 10 units corresponds to a halving of Secchi depth and a doubling of phosphorus concentration, and higher TSI values correspond with nutrient enriched conditions. With regards to the calculated TSI, Secchi depth alone is likely to give an inaccurate TSI, especially in highly-coloured and very clear lakes (Carlson, 1977). Chlorophyll-*a* values are more likely to be free from interference, as well as providing a good estimate of algal biomass, so it is likely to be the better indicator of lake trophic state. The use of total phosphorus depends on the assumption that it is a limiting factor for algal growth. However, nitrogen has often been shown to be the limiting factor in many Africa lake waters (Kalff, 1983), though in the crater lakes of western Uganda, phosphorus is more often the limiting nutrient (Table 4.9). Where TSI values diverge between those generated by biological values and those predicted by phosphorus (cf. Table 4.11), it is unwise to average the values (Carlson, 1977). In cases where there is a discrepancy between the various trophic indicators, priority is usually given to the chlorophyll-*a* index (during summer months) and TP during the rest of the year. However, many African lake waters tend to have high TP year round ("endless summer hypothesis", Kilham and Kilham, 1990) due to the within lake cycling of phosphorus, causing many lakes to be naturally eutrophic.

An alternative classification of lake trophic status is that of Vollenweider and Kerekes (1982; OECD). Similar to the classification of Carlson (1977), this system is based on total phosphorus (TP), Chl-*a* and Secchi depth (Tables 4.9b and 4.9c), but rather than computing a trophic continuum (0-100) the OECD classification uses lake types based on actual values of total phosphorus, Chl-*a* and Secchi depth (fixed boundary system). The results generated by both classification systems (Tables 4.9 and 4.9c) are in relatively good agreement, especially the TP and Chl-*a*. Where results do differ in these two categories (TP and Chl-*a*) Carlson's TSI overestimates TP in the eutrophic category and

Table 4.11 *Lake trophic status calculated using the trophic status index (TSI; Carlson, 1977). Results are shown for each of the three potential criteria: Secchi depth, total phosphorous (TP) and Chl-a. The numerical TSI values for defining each status are: <40 = Oligotrophic (oligo); 40-50 = Mesotrophic (Meso); 50-70 = Eutrophic (Eutro) and >70 = hyper-eutrophic (Hyper).*

Lake name	Date	Who	Secchi (m)	TP (µg/L)	Chl-a (µg/L)	Secchi Depth		Total Phosphorous		Chlorophyll-a	
						TSI value	Status	TSI value	Status	TSI value	Status
Bagusa	22-Feb-07	RUMES	0.24	--	497.41	80.55	Hyper	--	--	91.51	Hyper
Bugwagi	24-Feb-07	RUMES	2.45	18.10	3.84	47.10	Meso	45.91	Meso	43.80	Meso
Chibwera	26-Jan-07	RUMES	1.35	24.75	6.74	55.68	Eutro	50.42	Eutro	49.31	Meso
Ekikoto	18-Jan-07	RUMES	1.80	--	5.03	51.54	Eutro	--	--	46.44	Meso
Kacuba	16-Jan-07	LBORO	2.35	21.24	--	47.70	Meso	48.21	Meso	--	--
Kako	31-Jul-06	LBORO	2.93	4.62	1.19	44.54	Meso	26.22	Oligo	32.30	Oligo
Kamunzuka	30-Jul-06	LBORO	7.70	1.68	0.69	30.61	Oligo	11.63	Oligo	26.90	Oligo
Kamweru	20-Feb-07	RUMES	0.43	32.14	13.85	72.15	Hyper	54.19	Eutro	56.38	Eutro
Kanyanmukali	14-Jan-07	RUMES	0.94	187.96	7.16	60.89	Eutro	79.66	Hyper	49.91	Meso
Karolero	21-Feb-07	RUMES	1.49	20.50	5.42	54.26	Eutro	47.70	Meso	47.18	Meso
Kasenda[3]	23-Jul-06	LBORO	1.75	18.48	2.96	51.94	Eutro	46.21	Meso	41.25	Meso
Kasirya	30-Jul-06	LBORO	1.75	--	1.84	51.94	Eutro	--	--	36.58	Oligo
Katinda	31-Jan-07	RUMES	0.35	19.36	25.43	75.12	Hyper	46.88	Meso	62.34	Eutro
Kayihara	24-Mar-00	DIRK	1.30	--	1.76	56.28	Eutro	--	--	36.14	Oligo
Kifuruka[2]	22-Jul-06	LBORO	1.15	35.28	8.63	57.99	Eutro	55.53	Eutro	51.74	Eutro
Kigezi	31-Jul-06	LBORO	1.35	16.37	6.64	55.68	Eutro	44.46	Meso	49.18	Meso
Kikorongo	26-Jul-06	LBORO	1.60	13720.00	3.95	53.23	Eutro	141.52	Hyper	44.07	Meso
Kitagata	10-Jan-01	DIRK	0.05	42.76	25.53	103.14	Hyper	58.30	Eutro	62.38	Eutro
Kyaninga	10-Feb-07	RUMES	6.60	5.32	0.81	32.83	Oligo	28.25	Oligo	28.54	Oligo
Kyasanduka[2]	11-Jan-07	LBORO	0.18	210.98	203.03	85.10	Hyper	81.32	Hyper	82.72	Hyper
Kyerbwato[2]	23-Jan-07	RUMES	0.64	11.34	1.72	66.54	Eutro	39.17	Oligo	35.92	Oligo
Kyogo	17-Jan-07	LBORO	2.90	272.66	2.04	44.67	Meso	85.02	Hyper	37.60	Oligo
Lugembe	15-Jan-07	RUMES	0.78	21.42	5.69	63.67	Eutro	48.34	Meso	47.66	Meso

Table 4.11 *Continued…*

Lake name	Date	Who	Secchi (m)	TP (µg/L)	Chl-a (µg/L)	Secchi Depth		Total Phosphorous		Chlorophyll-a	
						TSI value	Status	TSI value	Status	TSI value	Status
Lyantonde	22-Jul-06	LBORO	2.80	5.46	2.27	45.17	Meso	28.63	Oligo	38.65	Oligo
Mafuro	01-Aug-06	LBORO	1.15	11.48	3.30	57.99	Eutro	39.34	Oligo	42.30	Meso
Mahega[2]	18-Jan-07	LBORO	0.30	1355.38	--	77.34	Hyper	108.14	Hyper	--	--
Mahuhura	23-Jul-06	LBORO	6.60	49.98	1.17	32.83	Oligo	60.56	Eutro	32.11	Oligo
Maseche	22-Feb-07	RUMES	0.00	--	4.97	182.65	Hyper	--	--	46.33	Meso
Mirambi	31-Jan-07	RUMES	1.00	18.02	11.07	60.00	Eutro	45.84	Meso	54.19	Eutro
Mugogo	09-Jan-07	LBORO	2.12	7.39	--	49.18	Meso	33.00	Oligo	--	--
Muijongo	01-Aug-06	LBORO	2.70	6.58	2.04	45.70	Meso	31.32	Oligo	37.60	Oligo
Murabyo	29-Jan-07	RUMES	2.03	9.79	0.00	49.80	Meso	37.04	Oligo	--	--
Murusi	17-Jan-07	RUMES	1.40	5.10	1.32	55.15	Eutro	27.63	Oligo	33.32	Oligo
Njarayabana	17-Feb-07	RUMES	0.75	359.69	3.75	64.14	Eutro	89.02	Hyper	43.56	Meso
Nkugute	01-Feb-07	RUMES	0.90	--	7.70	61.52	Eutro	--	--	50.63	Eutro
Nkuruba[2]	16-Feb-07	RUMES	1.49	25.03	5.89	54.31	Eutro	50.58	Eutro	48.00	Meso
Nshenyi	26-Jan-07	RUMES	0.02	--	26.31	116.33	Hyper	--	--	62.68	Eutro
Nyamogusingiri Basin	14-Jan-07	LBORO	0.53	26.99	--	69.28	Eutro	51.67	Eutro	--	--
Nyamogusingiri Crater	13-Jan-07	LBORO	0.50	29.60	14.79	69.98	Eutro	53.00	Eutro	57.03	Eutro
Nyamirima	24-Jul-06	LBORO	4.40	4.06	2.35	38.66	Oligo	24.36	Oligo	38.99	Oligo
Nyamogusani	16-Feb-07	RUMES	1.20	152.33	3.46	57.37	Eutro	76.63	Hyper	42.78	Meso
Nyamswiga	21-Jul-06	LBORO	1.80	33.32	3.99	51.54	Eutro	54.71	Eutro	44.17	Meso
Nyierya	21-Jul-06	LBORO	1.35	16.10	14.03	55.68	Eutro	44.22	Meso	56.51	Eutro
Nyinambulita	24-Jul-06	LBORO	4.28	25.90	1.78	39.08	Oligo	51.08	Eutro	36.27	Oligo
Nyungu	27-Jul-06	LBORO	0.47	119.14	57.25	71.03	Hyper	73.08	Hyper	70.31	Hyper
Saaka Crater[2]	20-Jul-06	LBORO	0.60	36.54	32.51	67.36	Eutro	56.04	Eutro	64.75	Hyper
Wandakara[2]	19-Jan-07	RUMES	0.31	25.97	9.08	76.87	Hyper	51.12	Eutro	52.24	Eutro
Wankenzi	19-Jan-07	RUMES	0.36	24.47	11.35	74.71	Hyper	50.26	Eutro	54.43	Eutro
*Nyamogusingiri inlet	15-Jan-07	LBORO	--	279.65	--	--	--	85.39	Hyper	--	--
*Kyasanduka inlet	12-Jan-07	LBORO	--	185.57	--	--	--	79.47	Hyper	--	--
*Kyasanduka outlet	LBORO	16-Jan-07	--	577.964	--	--	--	95.85	Hyper	--	--

underestimates oligotrophic lakes when compared to the OECD system. Similarly, Carlson's TSI tends to underestimate a lake's trophic state based on Chl-*a*, with lakes identified as eutrophic (Carlson's TSI) being classified as hyper-eutrophic using the OECD system (Tables 4.10 and 4.12). This discrepancy appears to result from lakes that have TP and Chl-*a* values very close to the OECD boundaries (Table 4.12).

The largest discrepancies between the two classification systems is concerned with the results produced for the Secchi depth. The Carlson TSI appears to underestimate the lake's trophic status in comparison to the OECD system, which consistently gives a higher trophic state (e.g. hyper-eutrophic [OECD] rather than eutrophic [Carlson]; Table 4.12). Many of the Ugandan crater lakes have low Secchi depth readings, which may not be a result of increases in algal biomass as a result of eutrophication, but rather a result of low light conditions related to suspended particulate matter or DOC in the lake waters (see *section 4.5.2*).

4.7 Phytoplankton: Diatoms

This section is based on the results of a trawl from a phytoplankton net to sample diatoms currently living in the open water as well as samples from shore communities (littoral water samples, rock scrapes and plant samples). For the sample collection and preparation procedures, please refer to **Chapter 3** (*sections 3.2.3* and *3.3.2*).

Thirty-six samples were collected from 21 lakes across the field study area, 21 of the samples were pelagic (phytoplankton net trawl) and 13 were periphytic samples. The remaining two samples were taken from Nyamogusingiri crater: one from floating pom-poms of organic matter and the other from the sediment-water interface where there was an orange bacterial mat present. In total 155 species were recorded across the 36 samples, with 134 identified from the pelagic samples and 88 from the periphytic samples.

Detrended Correspondence Analysis (DCA) was carried out on the diatom data, to see if any trends or clusters in the data could be identified (the results of which are displayed in Figure 4.10). Four samples were omitted from the analyses. Three of these samples belonged to the saline lakes Mahega (2 samples) and Kikorongo, as each of these samples only contained a single diatom valve. The fourth sample omitted was the sample from the spring feeding Kyasanduka, which was a clear outlier amongst the samples from the dilute lakes (Figure 4.10), owing to its unusual assemblage dominated by *Nitzschia frustulum*.

Table 4.12 *Lake trophic status calculated using the parameters defined by Vollenweider and Kerekes (1982). The final two columns indicate whether there is agreement (Y/N) between the classification of the lakes based on the scheme of Vollenweider and Kerekes (1982) compared to the TSI of Carlson (1977;* ***Table 4.9****). Where the two systems produce different results (N), the result of Carlson's TSI is given in parentheses.*

Lake name	Date	Who	TP (µg/L)	Chl-a (µg/L)	Secchi (m)	TP	Chl-a	Secchi	Comparison to Carlson		
									TP	Chl-a	Secchi
Bagusa	22-Feb-07	RUMES	--	497.41	0.24	--	Hyper	Hyper	--	Y	Y
Bugwagi	24-Feb-07	RUMES	18.10	3.84	2.45	Meso	Meso	Eutro	Y	Y	N [Meso]
Chibwera	26-Jan-07	RUMES	24.75	6.74	1.35	Meso	Meso	Hyper	Y	Y	N [Eutro]
Ekikoto	18-Jan-07	RUMES	--	5.03	1.80	--	Meso	Eutro	--	Y	Y
Kacuba	16-Jan-07	LBORO	21.24	--	2.35	Meso	--	Eutro	Y	--	N [Meso]
Kako	31-Jul-06	LBORO	4.62	1.19	2.93	Oligo	Oligo	Eutro	Y	Y	N [Meso]
Kamunzuka	30-Jul-06	LBORO	1.68	0.69	7.70	Ultra-oligo	Ultra-oligo	Oligo	N [Oligo]	N [Oligo]	Y
Kamweru	20-Feb-07	RUMES	32.14	13.85	0.43	Meso	Eutro	Hyper	N [Eutro]	Y	Y
Kanyanmukali	14-Jan-07	RUMES	187.96	7.16	0.94	Hyper	Meso	Hyper	Y	Y	N [Eutro]
Karolero	21-Feb-07	RUMES	20.50	5.42	1.49	Meso	Meso	Hyper	Y	Y	N [Eutro]
Kasenda[3]	23-Jul-06	LBORO	18.48	2.96	1.75	Meso	Meso	Eutro	Y	Y	Y
Kasirya	30-Jul-06	LBORO	--	1.84	1.75	--	Oligo	Eutro	--	Y	Y
Katinda	31-Jan-07	RUMES	19.36	25.43	0.35	Meso	Hyper	Hyper	Y	N [Eutro]	Y
Kayihara	24-Mar-00	DIRK	--	1.76	1.30	--	Oligo	Hyper	--	Y	N [Eutro]
Kifuruka[2]	22-Jul-06	LBORO	35.28	8.63	1.15	Eutro	Eutro	Hyper	Y	Y	N [Eutro]
Kigezi	31-Jul-06	LBORO	16.37	6.64	1.35	Meso	Meso	Hyper	Y	Y	N [Eutro]
Kikorongo	26-Jul-06	LBORO	13720.00	3.95	1.60	Hyper	Meso	Eutro	Y	Y	Y
Kitagata	10-Jan-01	DIRK	42.76	25.53	0.05	Eutro	Hyper	Hyper	Y	N [Eutro]	Y
Kyaninga	10-Feb-07	RUMES	5.32	0.81	6.60	Oligo	Ultra-oligo	Oligo	Y	N [Oligo]	Y
Kyasanduka[2]	11-Jan-07	LBORO	210.98	203.03	0.18	Hyper	Hyper	Hyper	Y	Y	Y
Kyerbwato[2]	23-Jan-07	RUMES	11.34	1.72	0.64	Meso	Oligo	Hyper	N [Oligo]	Y	N [Eutro]
Kyogo	17-Jan-07	LBORO	272.66	2.04	2.90	Hyper	Oligo	Eutro	Y	Y	N [Meso]
Lugembe	15-Jan-07	RUMES	21.42	5.69	0.78	Meso	Meso	Hyper	Y	Y	N [Eutro]

Table 4.12 *Continued…*

Lake name	Date	Who	TP (µg/L)	Chl-a (µg/L)	Secchi (m)	TP	Chl-a	Secchi	Comparison to Carlson		
									TP	Chl-a	Secchi
Lyantonde	22-Jul-06	LBORO	5.46	2.27	2.80	Oligo	Oligo	Eutro	Y	Y	N [Meso]
Mafuro	01-Aug-06	LBORO	11.48	3.30	1.15	Meso	Meso	Hyper	N [Oligo]	Y	N [Eutro]
Mahega[2]	18-Jan-07	LBORO	1355.38	--	0.30	Hyper	--	Hyper	Y	--	Y
Mahuhura	23-Jul-06	LBORO	49.98	1.17	6.60	Eutro	Oligo	Oligo	Y	Y	Y
Maseche	22-Feb-07	RUMES	--	4.97	--	--	Meso	Hyper	--	Y	Y
Mirambi	31-Jan-07	RUMES	18.02	11.07	1.00	Meso	Eutro	Hyper	Y	Y	N [Eutro]
Mugogo	09-Jan-07	LBORO	7.39	--	2.12	Oligo	--	Eutro	Y	--	N [Meso]
Muijongo	01-Aug-06	LBORO	6.58	2.04	2.70	Oligo	Oligo	Eutro	Y	Y	N [Meso]
Murabyo	29-Jan-07	RUMES	9.79	0.00	2.03	Oligo	--	Eutro	Y	--	N [Meso]
Murusi	17-Jan-07	RUMES	5.10	1.32	1.40	Oligo	Oligo	Hyper	Y	Y	N [Eutro]
Njarayabana	17-Feb-07	RUMES	359.69	3.75	0.75	Hyper	Meso	Hyper	Y	Y	N [Eutro]
Nkugute	01-Feb-07	RUMES	--	7.70	0.90	--	Meso	Hyper	--	N [Eutro]	N [Eutro]
Nkuruba[2]	16-Feb-07	RUMES	25.03	5.89	1.49	Meso	Meso	Hyper	N [Eutro]	Y	N [Eutro]
Nshenyi	26-Jan-07	RUMES	--	26.31	0.02	--	Hyper	Hyper		N [Eutro]	Y
Nyamogusingiri Basin	14-Jan-07	LBORO	26.99	--	0.53	Meso	--	Hyper	N [Eutro]	--	N [Eutro]
Nyamogusingiri Crater	13-Jan-07	LBORO	29.60	14.79	0.50	Meso	Eutro	Hyper	N [Eutro]	Y	N [Eutro]
Nyamirima	24-Jul-06	LBORO	4.06	2.35	4.40	Oligo	Oligo	Meso	Y	Y	N [Oligo]
Nyamogusani	16-Feb-07	RUMES	152.33	3.46	1.20	Hyper	Meso	Hyper	Y	Y	N [Eutro]
Nyamswiga	21-Jul-06	LBORO	33.32	3.99	1.80	Meso	Meso	Eutro	N [Eutro]	Y	Y
Nyierya	21-Jul-06	LBORO	16.10	14.03	1.35	Meso	Eutro	Hyper	Y	Y	N [Eutro]
Nyinambulita	24-Jul-06	LBORO	25.90	1.78	4.28	Meso	Oligo	Meso	N [Eutro]	Y	N [Oligo]
Nyungu	27-Jul-06	LBORO	119.14	57.25	0.47	Hyper	Hyper	Hyper	Y	Y	Y
Saaka Crater[2]	20-Jul-06	LBORO	36.54	32.51	0.60	Eutro	Hyper	Hyper	Y	Y	N [Eutro]
Wandakara[2]	19-Jan-07	RUMES	25.97	9.08	0.31	Meso	Eutro	Hyper	N [Eutro]	Y	Y
Wankenzi	19-Jan-07	RUMES	24.47	11.35	0.36	Meso	Eutro	Hyper	N [Eutro]	Y	Y
*Nyamogusingiri inlet	15-Jan-07	LBORO	279.65	--	--	Hyper	--		Y	--	--
*Kyasanduka inlet	12-Jan-07	LBORO	185.57	--	--	Hyper	--		Y	--	--
*Kyasanduka outlet	LBORO	16-Jan-07	577.964	--	--	Hyper	--	--	Y	--	--

The DCA revealed an axis 1 gradient length of 3.602 (explaining 12.6% of the variation in the species data) and an axis 2 gradient length of 2.895 (7.4% of species variance). Several groups can be identified in the DCA (Figure 4.10, groups A-F). The first group (A) represents epiphytic samples from the forest lake Kyogo (*Cabomba* spp. and lily), the major composition of these two assemblages consists of *Gomphonema* cf. *gracile* (45% and 57% respectively), *Eunotia pectinalis* (10% and 12%) and *Pinnularia gibba* (*c.* 1%). The largest cluster of samples (B) represents the majority of pelagic samples from the dilute lakes. The majority of these samples come from the 20 m phytoplankton trawls and the 5 m and 7 m samples from lakes Kasenda and Saaka. The samples from these lakes are associated with planktonic species such as *Aulacoseira ambigua*, *A. granulata* and *Nitzschia lancettula* and littoral/epiphytic species such as *Achnanthidium minutissimum*, *Amphora copulata* and *A. pediculus*. Lake Muijongo is also closely related to this group, though it is dominated by *Nitzschia gracilis* (*c.* 91%). Group C includes samples from the forest lakes Kacuba (epiphytic samples from a reed and a lily) and Kyogo (2 m phytoplankton sample), it also includes samples from Lakes Kigezi (15 m) and Mafura (20 m). These samples are closely related to those samples in group B, with *A. ambigua* and *A. granulata*, *N. palea*, and *Gomphonema parvulum* being amongst the more dominant species. Similarly, group D is closely related to B and C, with the *Aulacoseira* species being important, as are the littoral/periphytic species *Achnanthidium minutissimum* and *Nitzschia palea*. The differences in the position of samples with groups B, C and D are driven by the differences in the relative proportions of the most common taxa. The final two groups, E and F, are related to lakes Nyamogusingiri and Kyasanduka respectively. Group E consists of samples from the Lake Nyamogusingiri basin and crater (including an epilithic sample and epiphytic sample from a submerged tree). Samples of the orange bacterial mat and the small free-floating algal pom-poms from the crater site are also included in this group. This group is dominated by *Nitzschia* species, specifically *N. amphibia*, *N. gracilis* and *N. palea* and also *Achnanthidium minutissimum*. The final group, F, is composed of two littoral samples and a sample from a trawl from 1 m from Lake Kyasanduka and is dominated by the epiphytic species *Hantzschia amphioxys*, *Nitzschia palea* and *N. amphibia*.

A Canonical Correspondence Analysis (CCA) was performed on the live diatom samples and 29 measured environmental variables (Figure 4.11). There was some degree of co-linearity between some of the environmental variables, indicated by a high Variance Inflation Factor (VIF; e.g. between conductivity, Na, Cl, F). Manual forward selection

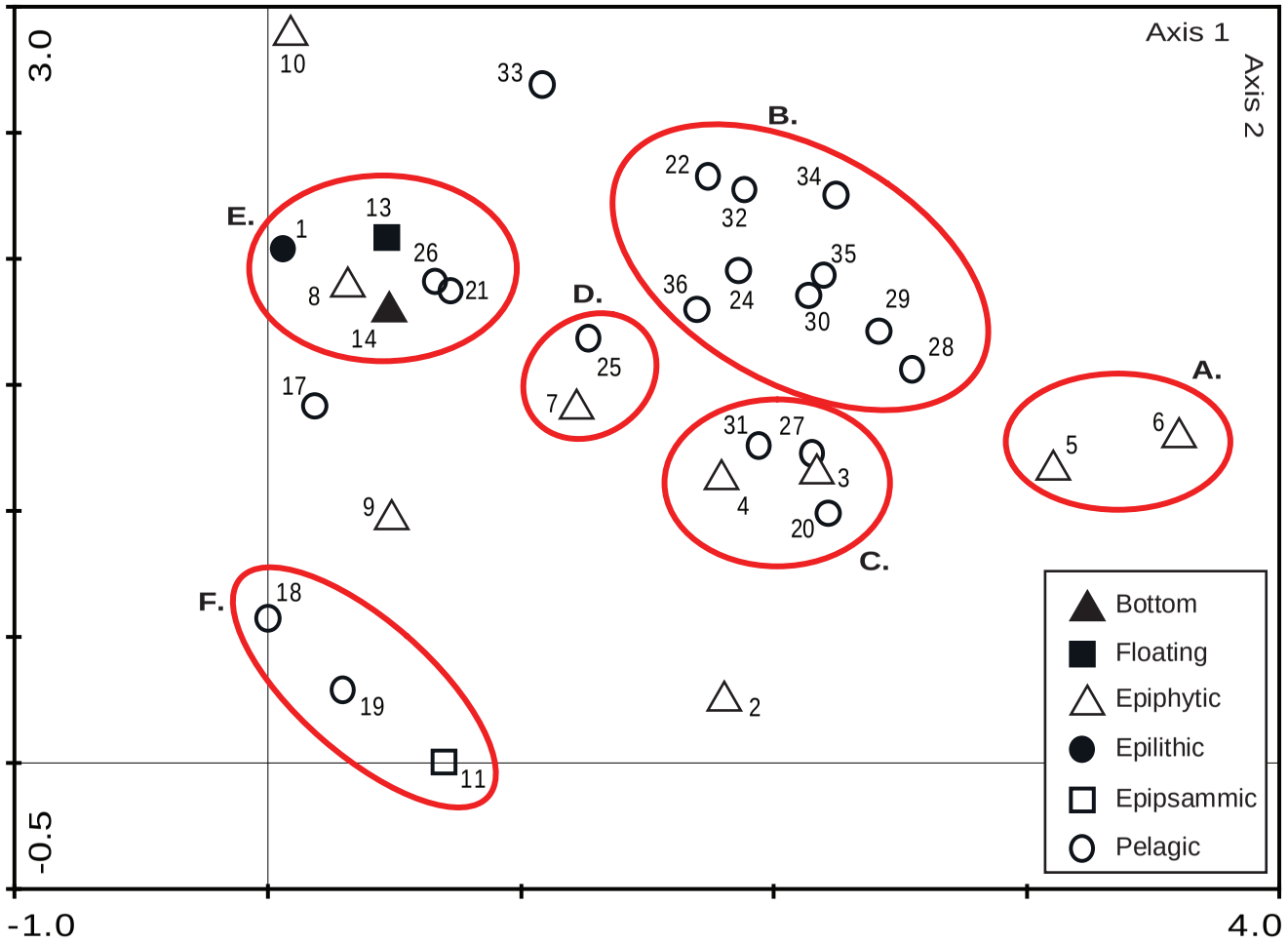

Figure 4.10 *Detrended Correspondence Analysis (DCA) of the live diatom samples. The numbered samples correspond to the sample numbes in* **Table 4.#.** *The data have been split into six groups* **A-F**. *These groups are discussed in the text.*

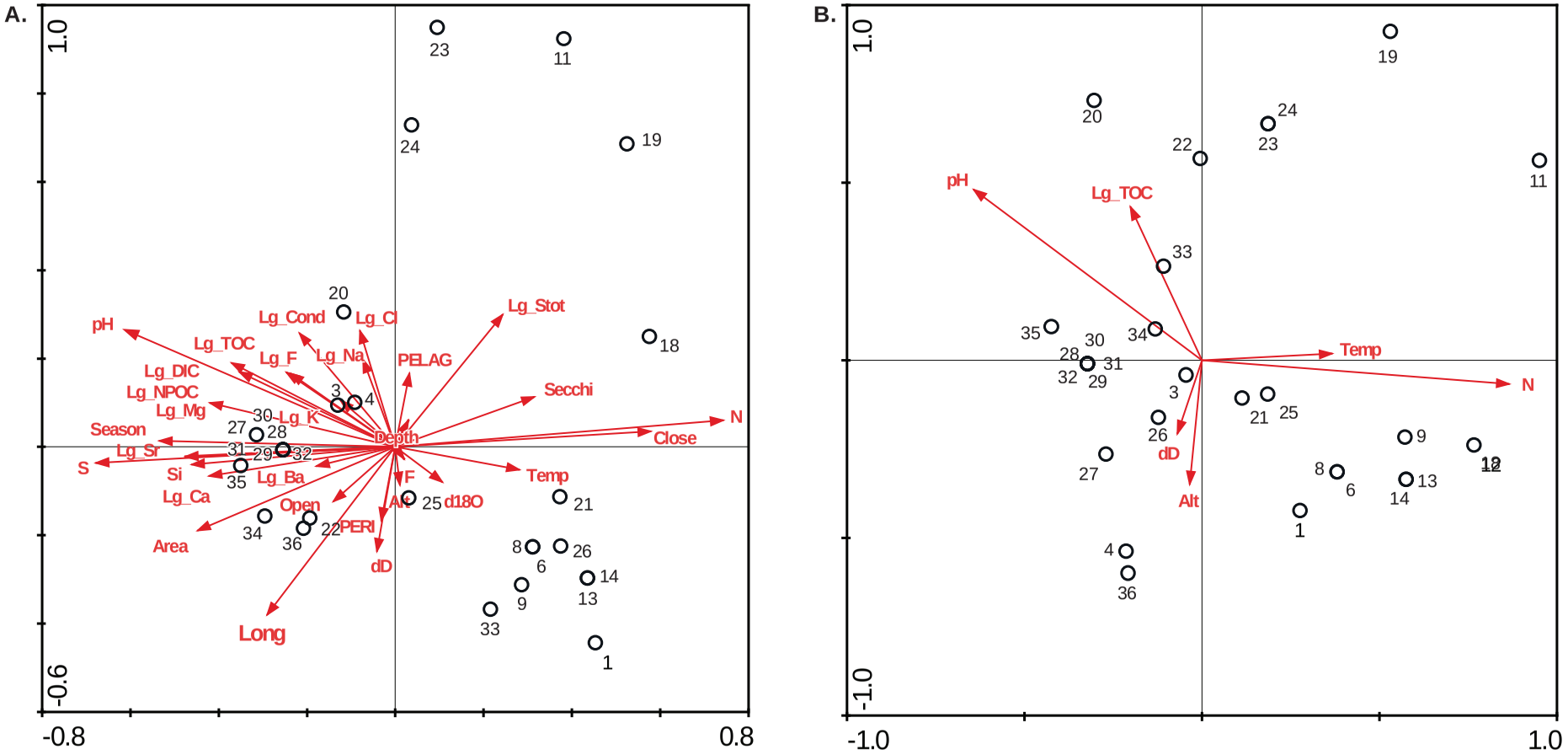

Figure 4.11 *CCA of live diatom samples and measured environmental variables (with outliers Mahega [15] and Kyogo [5] removed).* **(A)** *All 32 environmental variables and* **(B)** *six significant ($p < 0.001$) forward selected environmental variables. The sample numbers correspond to the names and numbers in* ***Table 4.9***.

indicated that N was the only significant environmental variable (accounting for 7.7 % of the variation in the diatom data); however this did not appear representative of the scatter in the diatom data. Automatic forward selection of 6 environmental variables showed N, temperature, altitude, δD, TOC and pH to be the significant drivers behind the variation in the diatom data (with both the first axis and sum of all canonical axes being significant [$p < 0.05$]).

4.7.1 Pelagic samples

In the net samples from 18 lakes (Table 4.13) approximately 130 diatom taxa were found, of which 92 occurred in abundances >0.5%. The most common species were *Nitzschia palea* (15 samples, maximum abundance 26.86%), *Navicula cryptonella* (14 samples, maximum 8% abundance) and the *Aulacoseira* species *A. granulata* and *A. ambigua* (14 and 13 samples, maximum abundance 42.6 and 20% respectively). Out of the pelagic samples (trawled at varying depths, depending on the lake depth; Table 4.13). Lake Kyogo (3.4 m deep, trawl at 2 m) had the most 'diverse' assemblage, with 56 species recorded, the most common species of which was *Diadesmis contenta* (13%), Lake Kyogo was also unique in its floral assemblage, with over 5% of the total counts consisting of *Eunotia* species (predominantly *E. paludosa*) and >2% consisting of *Pinnularia* (mostly *P. gibba* and *P. acrosphaeria*). After the removal of this sample, Lake Kyasanduka (2 m deep, trawl from a depth of 1 m) had the lowest number of recorded species (10), the most abundant being *Hantzschia amphioxys* (*c.* 28%).

4.7.2 Periphytic samples

The periphytic samples were less diverse than the pelagic samples, with only 84 taxa being identified across the 18 samples; 74 of these species occurred in abundances >0.5 % in any one sample. The most diverse sample was an epiphytic sample from Lake Kacuba (submerged reed stem). Thirty species were recorded, the main species being *Aulacoseira ambigua* (24% of the total count), *A. granulata* (25%), and *Gomphonema parvulum* (*c.*10%). Lake Mahega was not included in the analyses as the two samples obtained from this lake (one a water sample, the other a sample from a floating algal/carbonate mat) contained only a single diatom valve per sample (*Nitzschia frustulum* and *Anomoeoneis sphaerophora*). With this saline lake being identified as an outlier, samples from the freshwater lakes Chibwera (submerged plant) and Kyasanduka (sample from a spring/inlet to the lake) had the lowest diversity in this group. Both samples recorded only 8 species,

Table 4.13 *List of pelagic and periphytic samples from the Ugandan crater lakes. The number refers to the sample number as shown in the DCA (**Figures 4.9** and **4.10**). The total count represents the total number of diatoms counted from each sample. The number of species recorded in each sample is also given.*

Number	Lake	Year	Description	Sample type	Total count	No. species
1	Nyamogusingiri	2007	Epilithic	Rock	613	14
2	Chibwera	2001	Epiphytic	Submerged Plant	502	8
3	Kacuba	2007	Epiphytic	Lily	193	26
4	Kacuba	2007	Epiphytic	Reed	310	31
5	Kyogo	2007	Epiphytic	Cacomba	549	15
6	Kyogo	2007	Epiphytic	Lily	560	10
7	Nyamogusingiri Crater	2001	Epiphytic	Plant	30	10
8	Nyamogusingiri Crater	2007	Epiphytic	Log	609	14
9	Nyamogusingiri Crater	2007	Epiphytic	Reed/Outlet	604	10
10	Wanadakara	2001	Epiphytic	Reed	514	17
11	Kyasanduka	2007	Epipsammic	Littoral Sediments	300	11
12	Mahega	2007	Periphytic?	Floating Mat	1	1
13	Nyamogusingiri Crater	2007	Floating	Pom Pom	602	23
14	Nyamogusingiri Crater	2007	Bottom	Interface	516	19
15	Mahega	2001	Periphytic?	Littoral mat	1	1
16	Kyasanduka	2007	Pelagic	0m Inlet (spring)	1578	8
17	Kyasanduka	2007	Pelagic	0m Outlet (stream)	307	14
18	Kyasanduka	2007	Pelagic	Littoral	773	11
19	Kyasanduka	2007	Pelagic	0-1m depth*	67	10
20	Kyogo	2007	Pelagic	0-2m depth*	522	57
21	Nyamogusingiri Basin	2007	Pelagic	0-2m depth*	526	35
22	Kasenda	2007	Pelagic	0-5m depth*	336	27
23	Kikorongo	2007	Pelagic	0-6m depth*	1	1
24	Saaka	2007	Pelagic	0-7m depth*	611	15
25	Kacuba	2007	Pelagic	0-9m depth*	529	32
26	Nyamogusingiri Crater	2007	Pelagic	0-10m depth*	301	19
27	Kigezi	2007	Pelagic	0-15m depth*	80	16
28	Kako	2007	Pelagic	0-20m depth*	524	30
29	Kamunzuka	2007	Pelagic	0-20m depth*	543	45
30	Kasirya	2007	Pelagic	0-20m depth*	310	41
31	Mafuro	2007	Pelagic	0-20m depth*	125	27
32	Mahuhura	2007	Pelagic	0-20m depth*	314	37
33	Muijongo	2007	Pelagic	0-20m depth*	560	11
34	Nyamirima	2007	Pelagic	0-20m depth*	514	36
35	Nyinabulita	2007	Pelagic	0-20m depth*	513	46
36	Nyungu	2007	Pelagic	0-20m depth*	430	25

** Tow of phytoplankton net (0-maximum depth in metres), using a 60 μm mesh.*

with *Nitzschia frustulum* (87%) and *Navicula minima* (*c.* 9%) being the most abundant species in the Kyasanduka spring sample and *Synedra rumpens* (86%) and *Gomphonema parvulum* (10%) being the two most dominant species in the Chibwera sample. All other species recorded in these two samples occurred at less than 1% abundance.

4.8 Discussion

Two outstanding characteristics of the crater lakes of western Uganda are their limnological variety and their natural division into groups with gradients of one or two factors (e.g. salinity gradient across all lakes and TP gradient across dilute lakes; cf. Melack, 1978). The most obvious gradient amongst these lakes is the natural salinity gradient, with dilute lakes in the north and the south, on the shoulder of the rift valley, and the saline lakes located on the rift valley floor, in the rain shadow of the Rwenzori Mountains. It has further been suggested that even though many other regions in Africa have diverse lakes, such as the Bishoftu craters (Prosser *et al.*, 1968) and the craters of central Kenya (Jenkin, 1936; Beadle, 1936), none are as varied as those in Uganda (in such a small geographical area; Melack, 1978).

4.8.1 Lake stratification

In the majority of lakes sampled, the thermal stratification of the lake waters is weak, even though hypolimnic temperatures can still be high >25°C. This is attributed to the high insolation and a lack of distinct seasonal changes experienced in tropical regions (Gunkel, 2000). Despite this weak thermal stratification, once established it is likely to be very stable (Ruttner, 1931; 1932; Beadle, 1966). This is largely attributable to the density of these warmer waters. In the temperature range of 20-25°C, the density difference of the upper waters is much larger than water at a lower temperature (e.g. 0-5°C), causing pronounced stratification due to unusually small temperature differences (Talling, 1963). In some lakes the density difference at depth is enhanced by the rise in conductivity between the epilimnion and hypolimnion.

There is some evidence (though limited) in this dataset for the intensification of thermal stratification near the surface due to daily heating. For example, limnological profiles from the shallow Lake Kyasanduka taken early morning (*c.* 0900 hours) and mid-afternoon (*c.* 1500 hours) highlight this event. The intensity of solar heating causes rapid heating of the surface waters, leading to a superficial thermocline (Beadle, 1966; Melack,

1978). In these shallow systems, nocturnal cooling of the epilimnic waters is most likely sufficient to cause complete mixing (Beadle, 1966; Baxter *et al.*, 1965).

Melack (1978) observed that all lakes (11) deeper than 5 m have persistent deep-seated thermoclines, inferred by their location beneath the superficial thermocline, an observation also made in this study. Frequently, these deeper thermoclines are concurrent with chemoclines, with anoxic waters beneath them. In several of the deeper lakes there appears to be the formation of multiple thermoclines. This is assumed to occur when a relatively cool epilimnion is subjected to a period of surface warming in a time of calm conditions, during which a second thermocline develops above the first (Kling, 1988), with the likely erosion of the lower thermocline over time.

The circulation of tropical lakes is predominantly controlled by wind, rainfall, and humidity rather than seasonal temperature changes as seen in temperate lakes and lakes at higher altitudes (Beadle, 1966; Wood *et al*., 1976; Beadle, 1981). It is therefore likely that small sheltered lakes that are deep relative to their surface area (such as many of the crater lakes in western Uganda) are more likely to be permanently stratified and less productive than shallow lakes with high exposure (Beadle, 1966; 1981). These volcanic crater lakes with steep-sided walls provide wind-sheltered conditions and ideal conditions for the prolonged stratification of the lake waters (Beadle, 1981; Lewis Jr., 1983).

It is likely that complete mixing in the deeper crater lakes is rare (lakes >5 m; Beadle, 1966; Melack, 1978). The data presented here are single (point) samples only and therefore it is difficult to draw conclusions regarding the seasonal and longer-term variation and the incidence of vertical mixing in these lakes. However, given that oxygen depletion in deeper lake waters is often a long-term phenomenon; the data presented here do give credence to the idea of stability of the water column and the occurrence of permanent stratification. Long-term studies of the crater lakes Nkugute (Melack, 1978) and Nkuruba (Chapman *et al*., 1998), permanently stratified lakes with a deoxygenated hypolimnion, provided no evidence for deep mixing or complete mixing (based on a 12 month temperature record; Melack, 1978; 2 year temperature and dissolved oxygen record, Chapman *et al*., 1998). Nonetheless, it is probable that some form of ‘seasonal’ mixing of the upper waters occurs in most lakes (most notably after periods of heavy rains during the wet seasons), although the steep-sided nature of many of the crater lake affords some protection from the wind (Gunkel, 2000). Therefore, in some instances wind effect is likely to be greater in equatorial regions than in temperate regions, and the smallest change in

wind strength may be enough to cause mixing in shallow lakes and the upper layers of strongly stratified lakes (Gunkel, 2000).

Considering the hypothesised lack of overturn in some of these deeper, sheltered lake systems, the current mechanism for cooler waters (usually several degrees less than the surface temperature) at depth is not known. Talling (1963) suggested that cool waters in the hypolimnion of Lake Albert are caused by the nocturnal cooling of waters in shallow zones, which slide down the shore slope under the warmer water, providing a regular source of cool bottom water. This mechanism has not yet been recognised in the crater lakes of western Uganda, and is unlikely given the steep nature of many of the lake shores, and the lack of shallow inshore areas where sufficient amounts of water could cool to replenish the deep water (Beadle, 1966; Kizito *et al.*, 1993). Kizito *et al.* (1993) suggest that cooler hypolimnetic waters may indicate groundwater inputs, and in many lakes, the lack of significant changes in seasonal lake levels may also attest to this (e.g. Nyierya and Nyamswiga [Kizito *et al.*, 1993]).

The tropical climate appears to favour the prolonged stratification of lake waters in East Africa causing many of the lakes to be permanently anoxic (Beadle, 1966). Hypoxia is widespread in many tropical freshwaters, especially given low-light conditions and reduced mixing (Chapman *et al.*, 1998), though it has been shown that the dissolved oxygen content of shallow pools can vary with seasonal rainfall (Chapman and Kramer, 1991). As a consequence, the hypolimnia of deep, stratified tropical lakes are unlikely to be disturbed by any diurnal or seasonal mixing. Rather deep mixing is more likely to occur at irregular intervals following abnormally violent weather (Ruttner, 1931; 1932). This extreme form of lake stratification is known to occur in the in the larger, deeper lakes of East Africa (e.g. Lakes Tanganyika and Malawi). These lakes are permanently stratified, with a large anoxic hypolimnion. Periodic fish kills attest to full mixing of these lakes, where large quantities of deoxygenated waters and toxic elements are brought to the surface. This phenomenon has also been seen in a number of lakes of volcanic origin (e.g. Lake Kivu, cf. Bootsma and Hecky, 1993; Lake Nkugute, Beadle, 1966; Lake Bunyoni, Beadle, 1981; Lake Nyos, Kling *et al.*, 1987). Baxter *et al.* (1965) describe these lakes as oligomictic (lakes that circulate at rare, irregular intervals after abnormal climate; for example after unusually cold or violent storms/winds or volcanic or seismic activity [Lake Nyos]) as local conditions reduce the wind fetch required for overturn.

In the crater lakes, the oxygen content of the surface waters differs greatly between lakes, but the majority reach anoxic or near anoxic conditions very quickly and in the

majority of cases there is no oxygen below 10 m (cf. Kizito *et al.*, 1993). In addition the majority of lakes exhibit a clinograde profile in their dissolved oxygen distributions. Large rates of change in oxygen concentrations between the surface and deep waters (such as that seen at Lake Nyungu) are likely due to dense phytoplankton blooms causing oxygen super-saturation of surficial waters. This gradient can cause a barrier to turbulent mixing and can further isolate water at depth from gaseous exchange with the atmosphere. It can also be noted that conductivity increases with depth, with some of the more rapid changes occurring in the upper part of the oxygen free zones, an observation also made by Beadle (1966) during his research on Lake Nkugute. Whilst this is usually observed under meromictic conditions, the large changes in the conductivity at depth aid the density stratification of the lake waters, further preventing potential overturn that may occur due to thermal instability. The lake water density stratification associated with increasing concentrations of dissolved salts, is usually only important in saline systems, or lakes that are influenced by deep-water hydrothermal springs (e.g. Lake Kivu, Degens *et al* [1973]). The density stratification in the Ugandan crater lakes may perhaps be indicative of groundwater influence in these lakes; the lack of temperature inversion at depth suggests that any groundwater springs feeding these lakes are not hydrothermal.

4.8.2 Chemical composition

Melack (1978) suggests that high phosphate and potassium levels are more usual in the saline lake waters of western Uganda and are rarely seen in more dilute lake waters (Prosser *et al.*, 1968; MacIntyre, 1975). It has been suggested that the causal mechanism behind these extreme values lies with the large populations of hippopotamus and buffalo that frequent the shores of these saline lake systems (an observation also made in the field, e.g. Lake Kikorongo). It is suggested that these large populations of mega-fauna fertilise the lake waters (cf. Hippo pool; MacIntyre, 1975). In this study these extremely high potassium values are seen in all of the saline lakes (Kitigata [buffalo], Kikorongo [hippopotamus and buffalo], Maseche [hippopotamus], Nshenyi [hippopotamus], Mahega [buffalo] and Bagusa [hippopotamus]) and in these instances enrichment of K as a result hippopotamus pollution almost certainly, in part, accounts for the high values (172-15473 mg l^{-1}). The majority of lakes (all except Nyinabulita) have K values >3 mg l^{-1}, suggesting that geology also plays an important role in the concentrations of K in the dilute lakes; the western branch of the East African rift system is noted for its abundance of potassic alkaline rocks, comprising mafic and ultramafic lavas and plugs (Eby *et al.*, 2003).

Interestingly, the dilute Lake Nyamogusingiri (crater and basin) exhibits very high potassium levels. Whilst these high values may be attributable to the local geology (neighbouring Lake Kyasanduka does not record such high concentrations) it was noted during field work that this lake had a high presence of hippopotamus along the shores, again, perhaps contributing to, and explaining in part, the high K values recorded.

The ratios of K:Na and Mg:Ca are relatively high in some lakes (Kako and Mafura [K:Na], and Bagusa and Kitigata [Mg:Ca]), particularly in the more saline lakes, though high values do occur in some of the more dilute lakes. These higher values are unusual in most lake waters, but seem to occur in several lakes in the western rift (Talling and Talling, 1965). These ratios in conjunction with Mg being the dominating cation in many lakes and high K and F values, suggests that, in some lakes, the ionic composition is most likely influenced by the surrounding volcanic rocks (Kilham and Hecky, 1973; Kizito *et al*., 1993).

In accordance with the findings of Talling and Talling (1965) in their research on the chemical composition of African lake waters, Fe and Mn (Fe in particular) appeared to have higher concentrations in the shallower lake systems (Talling & Talling, 1965); in many instances both Fe and Mn were below the limits of detection. Whilst the presence of iron and manganese is not systematically studied in limnology, the tendency for higher values in shallow lakes is well known from other regions (Gorham, 1955). Current explanations for the high concentrations in shallow lakes relate to the upward movement of particulate Fe and Mn by turbulence and the liberation of ferrous ions under reducing conditions at the sediment water interface (Talling and Talling, 1965). In many of the crater lakes, iron was present in the poorly oxygenated deeper waters experiencing stratification. Although quantitative analyses were not completed, the presence was noted due to the colour change of the water extracted and the ferrous residue on filter papers. This observation is common amongst the African lakes (cf. Lakes Victoria and Albert; Talling and Talling, 1965).

4.8.3 Lake nutrients

Most tropical lakes have phosphorus levels that suggest that they are naturally eutrophic. Such natural examples of eutrophication do occur, especially with high fluxes of phosphorus from lake catchments in the volcanic regions of East Africa (high amounts of silica can also attest to these high catchment inputs, Golterman, 1973; Melack, 1978). Tropical African waters have high phosphorus concentration in comparison to unpolluted

European waters. The reason for this excess could be due to phosphorus being limited in its availability to algae, or that there is insufficient demand by algae to exhaust supplies, suggesting an alternative nutrient (e.g. nitrogen) is the limiting growth factor (Kalff, 1983). Nitrogen limitation is unlikely in the crater lakes surveyed during this research, as the results suggest the majority of the lakes are P limited (see *section 4.6*).

The high concentrations of nitrogen in lake systems may attest to pollution from animal waste. In the present dataset, lakes not impacted by current human activity values tend to range from 100-1500 μg l^{-1}, with values between 1500-6000 μg l^{-1} indicating a pollution source (such as animal waste and human activities). However, the majority of measured nitrogen concentrations in the crater lakes are well below 1500 μg l^{-1}.Those lakes with high total nitrogen are the saline lakes Kitigata, Mahega and Kikorongo. In addition to these, two dilute lakes have nitrogen values approaching 1500 μg l^{-1}: Lakes Nyamogusingiri and Nyungu. The high nitrogen values in the saline lakes and Lake Nyamogusingiri are possibly attributable to animal waste (hippopotami are known to frequent the shores of these lakes on the rift valley floor). The high values of Lake Nyungu are perhaps attributed to the large amount of human impact in the lake catchment as there is little evidence of pollution by animal waste. However, the distribution of phosphorus values with regards to the quantity of human impact with in the lake catchment is not as expected, as high values in lakes with heavily impacted catchments are not routinely observed. This suggests that the relationship between catchment agricultural activity and total phosphorus values are far more complex, and may be due to several confounding factors such as catchment geology and within-lake processes (such as phosphorus cycling, affecting deposition and subsequent release of phosphorus from sediments under anoxic hypolimnia).

Despite this, the input of phosphorus to lake systems has almost certainly increased in the recent past due to the observed catchment disturbance through the clearance and burning of the natural forest for subsistence agriculture. This in conjunction with periods of intense rainfall and the steep crater slopes aids the transport of nutrients to lakes. The retention of phosphorus and nitrogen by undisturbed, well-vegetated catchments means very little is transported to lakes (Borman and Likens, 1970; Ahl, 1975). Conversely, lakes situated in agricultural drainage basins with rich soils (and those receiving e.g. animal manure fertilisers) receive extremely high nutrient loads (Kalff, 2003). Human impacts, such as deforestation can result in a huge response in the aquatic systems due to the modification of catchment hydrology (Borman and Likens, 1970) and through nutrient loss

from land to water through erosion and runoff. Subsequent effects are dependent on land-use e.g. bare soil, cultivation or regrowth of 'natural' vegetation. In East Africa, the impact of human disturbance is thought to increase in proportion to population growth (Verschuren *et al*., 2002). Climate changes can also influence the loss of nutrients from a catchment to a lake through changes in rainfall, soil moisture, and changes in runoff and erosion; the separation of these factors from anthropogenic factors is complex (Anderson, 1995).

The crater lakes were classified according to their trophic state (Carlson, 1977). A eutrophic lake has a high nutrient content with associated increased aquatic plant growth, conversely oligotrophic lakes have low nutrient concentrations and low aquatic plant growth. The three factors regulating a lake's trophic state are: (1) nutrient supply (geology, soil, vegetation, human land-use); (2) climate (sunlight, temperature and hydrology) and (3) basin morphometry (depth, volume and surface area). The onset of lake eutrophication can invoke many water quality issues, such as blooms of blue-green algae, low dissolved oxygen concentrations (which has implications for the lake biota), fish kills, degraded fish habitats and changes in the type and composition of the plankton and the loss of water clarity (which affects the light penetration and therefore photosynthesis). Perhaps one of the most important water quality issues in the crater lake region of western Uganda is the degradation of drinking water which may lead to human health problems, especially with relation to schistosomiasis (John *et al*., 2008).

With regards to the calculated trophic index of the crater lakes, in accordance with the results of Kizito *et al*. (1993), the Chl-*a* content suggests that most of the sampled crater lakes are oligotrophic or mesotrophic (<10 µg l^{-1}) despite their high phosphorus and low Secchi values. The phosphorus and Secchi measurements would suggest that the majority of lakes are either eutrophic or hyper-eutrophic (Carlson, 1977). The low TSI calculated by the Chl-*a* in many lakes is likely a testament to the relatively low algal biomass in the photic zone of many of these lakes. Lakes which are known to have pronounced algal blooms (e.g. Kyasanduka) or some of the hypersaline lakes (e.g. Bagusa) where other algae (e.g. cyanobacteria) might be important, had a Chl-*a* TSI indicative of eutrophic conditions. Similarly, high Secchi TSI is likely the result of other factors influencing the lake, and not a result of algal biomass. Factors such as DOC content and suspended sediments in the lake waters may cause the low Secchi readings in the fresher water lakes, whereas bacteria is possibly the most important factor in the more saline lakes.

Carlson (1977) suggests that results from Secchi, TP and Chl-*a* TSI should not be averaged. Secchi depth is often problematic when calculating trophic status as it may be influenced by other factors (as suggested above). Therefore inference of the lake's trophic status should be calculated using either TP or Chl-*a*. Chl-*a* is more likely to be free from interference, as well as providing a good estimate of algal biomass, and is thus a better indicator of lake trophic state indicator although TP can be reliable if P is the limiting factor for algal growth.

4.8.4 Lake phytoplankton

The planktonic diatom communities of many of the lakes appear simplistic in nature, mostly dominated by *Aulacoseira* and *Nitzschia* species. The majority of the lakes are dominated by a few (usually two or three) relatively widespread taxa. Hustedt (1949) and Talling and Talling (1965) have classified lakes through their differences in chemistry or by the major aspects of their algal or macrophytic floras. The chemical classification of Talling and Talling, (1965) is closely related to the biological aspects of the lake. In the African lakes, it has long been suggested that the major determinant of the floral distributions is controlled by alkalinity (Richardson, 1968). Hustedt classified the flora of African lakes based on alkalinity: Class I (acid waters) dominated by the genera *Eunotia* and *Pinnularia*, with a weak representation of *Nitzschia*; Class II represented more alkaline waters and this class was split into 2 subsets. Class IIa lakes were those in which *Aulacoseira* (*Melosira*) plankton dominate, alkalinity rarely exceed 1.5 meq l^{-1}, whilst class IIb lakes were those in which a *Nitzschia*-plankton dominate, alkalinity is usually greater than 1.5 meq l^{-1}. It was further suggested that Hustedt's classification system should be extended to include the hyper-alkaline lakes of East Africa (Class III; Beadle, 1932; Jenkin, 1936; Talling and Talling, 1965). Class III is also rich in *Nitzschia* species (Richardson, 1968). More recently, the work of Hustedt (1949) and Richardson (1968) on the diatoms of East Africa has been updated through the detailed work of Gasse *et al*. (1983) who defined 17 diatom assemblages in 5 major groups from lake across East Africa. Gasse *et al*., (1983) show that diatom assemblages in East Africa are linked to the major ionic composition of the lake waters, based on statistically derived relationships between living diatom communities and environmental variables. Despite this important work, the factors controlling diatom assemblage distribution in East Africa are still not fully understood, as there are so many potential influences that have not been fully explored (e.g. N and P).

The classification of African lakes using their diatom flora is a useful method (Richardson, 1968). The current diatom data in this study appear to reaffirm Hustedt's classification, as the lakes can be identified as *Aulacoseira* (*Melosira*) or *Nitzschia* dominated. The majority of lakes can be classed as type II; although the lack of alkalinity data does not allow the investigation into the relationship between alkalinity and the observed diatom flora, but perhaps the diatom flora could be utilised to infer lake alkalinity. However, an exception to this majority is Lake Kyogo, which is dominated by *Aulacoseira*, but also has a large presence of *Eunotia* and *Pinnularia* (not really observed in any other lake system), suggesting that Class I may be a more appropriate class for this particular lake, and perhaps suggests that alkalinity alone does not control the distribution of the diatom flora (cf. Richardson, 1968).

Interestingly, unlike *Melosira* lakes that are a familiar and widespread occurrence in both tropical and temperate regions (Richardson, 1968); *Nitzschia* lakes are restricted to the warm tropics. This is likely due to the organic requirement of the species; only in warmer waters would sufficient decomposition occur within the photosynthetic zone to satisfy the nutrient requirements of this genus (Richardson, 1968). Richardson (1968) also suggested that *Nitzschia* are uncommon in the plankton of lakes where blue-green algae dominate or where lakes are very turbid (Beadle, 1932; Richardson, 1968). Rather, in these conditions *Nitzschia* species are important as a benthic form (cf. Cholnoky, 1953), this would especially hold true with species such as *N. palea* and *N. frustulum* that are obligate nitrogen heterophs, and would rely on the fixation of nitrogen by blue-green algae (e.g. microcystis).

4.9 Lake classifications

There are many criteria on which lakes may be classified, only a handful of which were utilised in this research: physical properties (e.g. depth to anoxia and thermocline), trophic status, pH and their dominant phytoplankton, and many have been used within this research. Table 4.14 summarises all of the various methods of classification used in this study, and shows how each lake is classified within each of the methods. Lake classifications are rarely holistic, and are based on certain aspects of the lake, either its physical or chemical properties or biota. These classifications allow the understanding of relationships within and between lakes in a single region, and also to allow them to be easily compared to other lake systems.

Table 4.14 *Summary of lake classification schemes used in this study (where relevant data exists). For the TSI where there are two possible outcomes for the lake trophic status based on TP and Chl-a, they are marked as such. Black units denote that both TP and Chl-a gave the same TSI.*

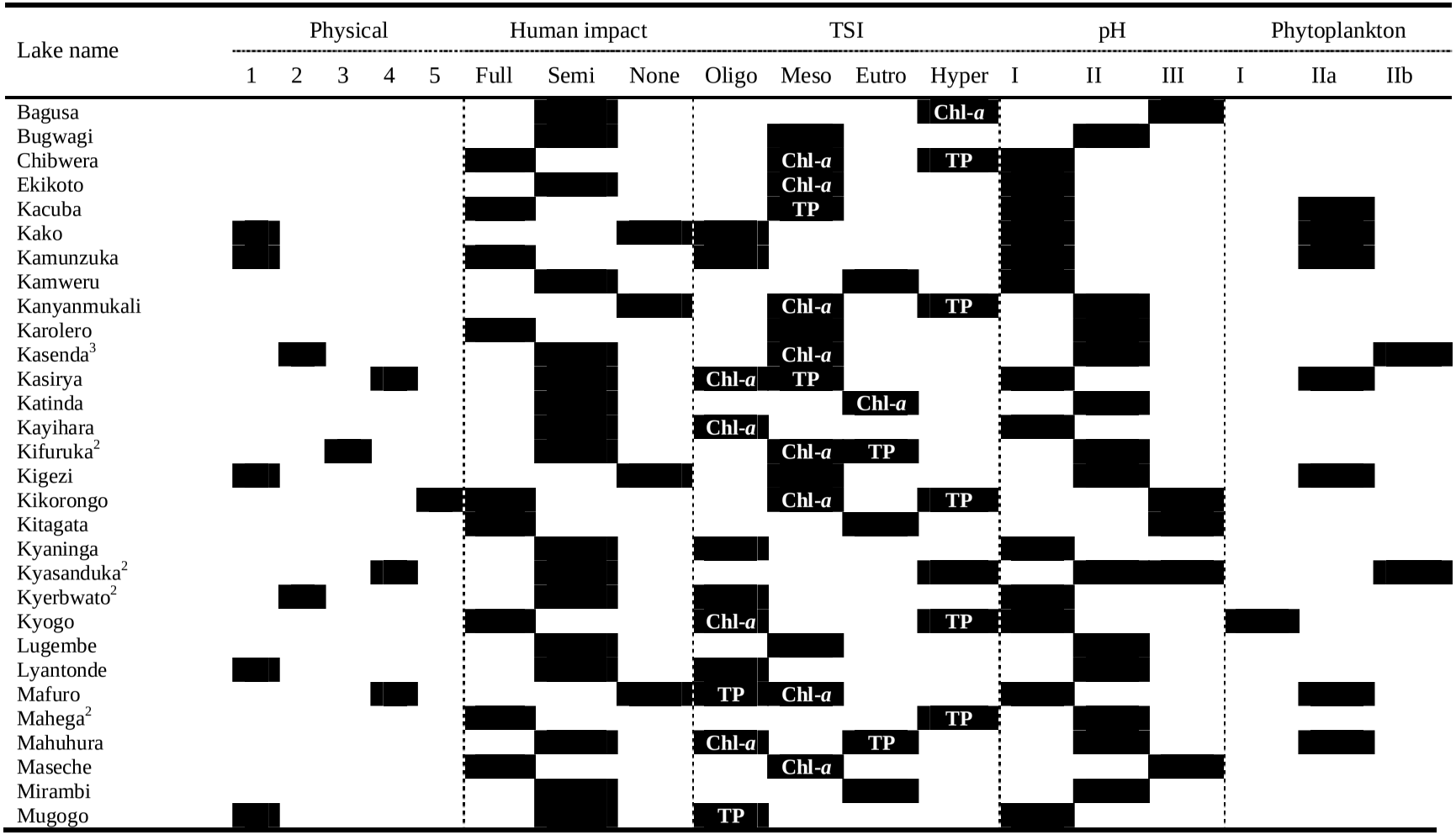

Table 4.14 *Continued…*

Lake name	Physical					Human impact			TSI				pH			Phytoplankton		
	1	2	3	4	5	Full	Semi	None	Oligo	Meso	Eutro	Hyper	I	II	III	I	IIa	IIb
Muijongo									TP									
Murabyo									TP									
Murusi																		
Njarayabana										Chl-*a*								
Nkugute																		
Nkuruba[2]										Chl-*a*	TP							
Nshenyi											Chl-*a*							
Nyamogusingiri Basin											TP							
Nyamogusingiri Crater																		
Nyamirima																		
Nyamogusani										Chl-*a*		TP						
Nyamswiga										Chl-*a*	TP							
Nyierya										TP	Chl-*a*							
Nyinambulita									Chl-*a*		TP							
Nyungu																		
Saaka Crater[2]											TP	Chl-*a*						
Wandakara[2]																		
Wankenzi																		

Problems can arise in lake classification when defining boundaries, as many aspects of limnology that are classified, in reality, are a continuum, and in some cases lakes may just sit on, or a little either side of these boundaries. This can cause lakes on or near defined boundaries to be separated into different groups, when in reality they might be physically and ecologically similar. Furthermore, some classification systems used here were developed based on temperate lakes (e.g. trophic status) and may need adjusting in order for them to be applicable and produce meaningful results in tropical lake systems. A particular problem encountered during this research is categorising lakes based on a single sample. Ideally many of these lake systems would require several samples across a year and/or seasons in order to ensure the lakes were correctly classified, especially if there are seasonal differences following, for example, periods of heavy rainfall.

The classification of tropical lake systems is largely unexplored, and the lack of short- and long-term monitoring is another hindrance. The preliminary results presented here suggest that there is certainly scope to expand temperate lake classification systems to tropical regions. Areas such as western Uganda, where there are a high number of lakes in a small geographical area spanning an altitudinal, climatic and human impact gradient provide the ideal conditions for comparative limnology. Improving our understanding of lake ecosystem responses to changes in climate and human impact today, will allow the management of these vulnerable systems in the future, and would aid researchers trying to understand lake response to past climate changes.

4.10 Summary

- A limnological survey of 48 lakes spread across western Uganda (sampled over a number of years) has investigated their physical, chemical and biological attributes.
- Water-column profiles of temperature, dissolved oxygen, conductivity and pH indicate that all of the surveyed lakes undergo stratification (including some of the shallower lake systems). Four classes of lake can be identified based on these data.
- Outstanding characteristics of the crater lakes are their limnological variety and their natural division into groups with gradients of one or two factors. The chemical composition of the lakes reflects variously the regional geology, nutrient inputs by hippopotamus, and in-lake processes.
- The input of phosphorous to the lakes has increased in the recent past, though the relationship between catchment agricultural activity and total phosphorus values are

complex, and may be due to several confounding factors such as catchment geology and within lake processes and large herbivores.

- The contemporary diatom assemblages can be classified according to Hustedt's (1949) classification system, with the majority of lakes falling into class II. On the basis of their planktonic assemblage, the lakes can be further split into those lakes dominated by *Aulacoseira* (*Melosira*) or those dominated by *Nitzschia* species. The presence of such species is likely to be a reflection of the alkalinity content of the lake waters.

Chapter 5

Diatom-Conductivity Transfer Function

5.1 Introduction

This chapter focuses on the development of the diatom-conductivity transfer function based on a dataset mainly comprising samples from the crater lake region of western Uganda. A brief review of the use of transfer functions in palaeoecology is given before moving on to the development of the transfer function. A description of the datasets is provided followed by an overview of the various numerical methods employed for the analyses. Results of indirect and direct ordinations and the various model performances are given. A short discussion follows highlighting some of the issues encountered when developing a regional diatom transfer function.

5.2 Context

Diatom analysis is amongst the most frequently used palaeolimnological tool for understanding climate and environmental changes as recorded in lake sediments. In East Africa, quantitative diatom models are often used to trace changes in past water chemistry (Gasse *et al*., 1995). Calibrating the present day distributions of diatoms in lakes across a known environmental gradient (e.g. water chemistry, such as conductivity or pH) provides a tool for inferring changes in that particular environmental variable from sedimentary records in lake basins. Clear correlations have been demonstrated across a range of lake types and in different regions of the world between diatom species composition and pH (e.g. Gasse and Tekaia, 1983; Birks *et al*., 1990), salinity (e.g. Fritz, 1990; Cumming and Smol, 1993; Reed, 1998; Davies *et al*., 2002); nutrient content (Bennion, 1994; Bradshaw *et al*., 2002) and ionic composition (e.g. Gasse *et al*., 1983; Fritz *et al*., 1993). Modern calibration datasets have been established for a number of regions, including East and North Africa (Gasse *et al*., 1995), North America (Fritz *et al*., 1993); western Canada (Cumming and Smol, 1993; Cumming *et al*., 1995; Wilson *et al*., 1996), Spain (Reed, 1998), Australia (Gell, 1998) and Mexico (Davies *et al*., 2002). Some of these European and African datasets have been combined and harmonised in the European Diatom Database (EDDI; http://craticula.ncl.ac.uk/eddi).

The interpretation of fossil diatom assemblages is reliant on knowledge of the modern autecology of the biota and assumes uniformitarianism of the response of the diatom species over time (i.e. they respond today as they did in the past). Where a strong replacement of species occurs along an environmental gradient (e.g. freshwater to saline), the response of the taxa can be used to create a transfer function (Anderson, 1993). Diatoms are known to respond to changes in conductivity (salinity) even below the true saline threshold (gradient < 3 g l^{-1}; Hammer, 1986; Wilson *et al*., 1996; Ryves *et al*., 2002). This relationship between modern diatom assemblages and environmental variables is used to create quantitative models to infer past environmental conditions from fossil diatom assemblages (using calibration and single variable regression [*x*] with multiple responses [*y*]).

There are various approaches to reconstructing quantitatively past environments using fossil diatom assemblages (Birks, 1998); (a) the indicator species approach; (b) an assemblage approach and (c) a multivariate indicator species approach ("transfer function"). All of these techniques require contemporary diatom ecologies to create 'modern analogues' for the fossil assemblages. The fossil assemblages are then compared to the modern analogues, which in turn allows an inference of the environment at the time the sample was deposited (Birks and Birks, 1980; Barker, 1990).

The occurrence of fossil taxa in a lake sediment record that have known modern tolerances provide the basis for the indicator species approach. The information is obtained through the comparison of fossil assemblages to the modern-day distributions of species with selected environmental/climatic variables (e.g. conductivity or total phosphorus [TP]); if the trend between the variable and the species distribution covaries, a cause-and-effect relationship is assumed (Birks and Birks, 2003). However, when using this technique, only a small number of taxa are examined ("indicator species") and little attention is directed towards the numerical frequencies of the different taxa within an assemblage. This has led to an alternative approach which utilises the entire species assemblage (Modern Analogue Technique, MAT; Birks and Birks, 2003).

MAT numerically compares the fossil assemblage with modern assemblages, and finds the most similar modern analogue to the fossil sample, inferring the modern environmental variable for that assemblage (Overpeck *et al*., 1997). This is repeated for all fossil samples and the environmental reconstruction is based on the modern

sample(s) that most closely resembles the fossil assemblage. The technique can also be based on a weighted mean: the sample with the least dissimilarity has the greatest weight in the reconstruction. For these reconstructions high-quality, taxonomically consistent modern analogues from comparable environments are required (Birks and Birks, 2003). However, in many cases 'no analogue' or 'multiple analogue' scenarios exist (Birks, 1995; Birks and Birks, 2003), an issue which transfer functions attempt to resolve (Birks and Birks, 2003).

Transfer functions quantify the modern relationship between an environmental proxy (e.g. diatoms) and an environmental variable (e.g. conductivity) in a modern calibration ("training") set (ter Braak, 1987; Racca *et al*., 2004). They are routinely used in the quantitative reconstruction of past climate and hydrochemical changes from lake sediment archives (Racca *et al*., 2004). A transfer function approach assumes; (1) that the environmental variable to be inferred is highly correlated with diatom distribution; (2) that the ecological preferences of taxa can be accurately assessed based on their occurrences in the training set; (3) that the ecological preferences of the taxa have not changed over time and (4) that fossil taxa are well represented in the modern taxa-based training set (Fritz *et al*., 1999).

A two step process of regression and calibration is required when inferring past changes in water chemistry from a lake sediment sequence (Gasse *et al*., 1995). Relationships between modern diatom taxa and their preferred environmental conditions using surface sediment samples and corresponding water chemistry data are explored. These data are used to form a calibration or training set (Birks, 1995). The training set generally includes a range of lakes from the geographical region under investigation (e.g. western Uganda), which span the limnological gradient of the variable of interest (in this case, conductivity; c.f. Gasse *et al*., 1995; Reed, 1998). Based on the distribution of taxa preserved in the surface sediments of training-set lakes, regression techniques can be used to quantify the response of each diatom taxon to the given environmental variable (Gasse *et al*., 1995; Fritz *et al*., 1999).

When developing the transfer function, the diatom-environment training sets are statistically analysed to determine which environmental variables are most strongly correlated with species distributions. This is usually carried out through the use of ordination techniques (Birks, 1995; 1998): the indirect analyses of principal components analysis (PCA) and detrended correspondence analysis (DCA) are first used to explore the relationships between the samples, species and environmental variables. Following

this, direct ordination (constrained), such as canonical correspondence analysis (CCA) can be applied to quantify the relationship between the species and the environment (ter Braak, 1986), where the CCA axes are constrained to be linear combinations of the measured environmental variables (Eggermont *et al*., 2006).

The vectors generated during the CCA analysis indicate the direction of maximum variation of each environmental variable, and their length is directionally proportional to their importance in explaining variation in the data set (Battarbee *et al*., 1999). When a transfer function is developed for a particular environmental variable, it is imperative that the variable in question uniquely explains a significant potion of the total variation in the diatom data (Birks, 1995; Battarbee *et al*., 2001). This can be established through the use of Monte Carlo permutation tests with a Bonferroni-adjustment. However, in most instances there are confounding effects between some variables (such as conductivity and the major ions) which can cause redundancy of variables in the environmental dataset.

There are a range of regression and calibration techniques available. The most widely used is the weighted averaging (WA) approach (Birks *et al*., 1990). WA has been established as the primary technique in the construction of transfer functions for a whole range of physio-chemical variables (ter Braak & Looman, 1986). It assumes that taxa display a unimodal response to the environmental variable of interest (in this study, conductivity) and works on the principle that for a given value of the environmental variable, taxa with their optima closest to that value will be the most abundant. The taxon's optimum is the average value of the environmental variable from the training set across all sites in which the taxon occurred, weighted by its relative abundance (WA regression). Taxa with a small tolerance to the environmental variable (those species that have a small standard deviation [in their abundance] with regards to the environmental variable ['niche' concept in ecology]) can be given more 'weight' in the WA approach than taxa with larger tolerances (ter Braak and van Dam, 1989). This method is known as tolerance down-weighting (WA_{tol}; ter Braak and Barendregt, 1986; ter Braak and Looman, 1986; ter Braak and Prentice, 1988; Birks, 1995). When applied to core sediment samples, estimates of past surface water conductivity are based on the computed estimates of each taxon's optimum and tolerance weighted by their relative abundances in the sediment sample. This procedure involves taking averages twice, which shrinks the absolute range of inferred values. The effect can be corrected through the use of classical deshrinking (where the initial inferred values for the training set are

regressed on the observed values and provides the highest accuracy at the endpoints of the gradient), or inverse deshrinking (where the observed values are regressed on the initial inferred values which provides the highest accuracy in the middle of the gradient [in the 'apparent' validation]; Birks *et al*., 1990).

A weakness of the WA approach is that it ignores correlations in the species data that remain after fitting the environmental variable of interest, especially in cases where the species response is influenced by secondary environmental variables (which are not taken into account in WA; ter Braak and Juggins, 1993; Birks, 1995). In these cases the WA-PLS (weighted averaging – partial least squares) technique may be applied (ter Braak and Juggins, 1993). This allows successive components to be extracted from the training set to increase the predictive power of the regression model (Battarbee *et al*., 2001).

The predictive ability of a transfer function is defined by the strength of the relationship between the measured and inferred values of the environmental variable in the training set. However, the calculation of the correlation coefficient (r^2) and root mean squared error (RMSE) on the basis of the training set alone can be misleading as the same data which are used in the creation of the model are also being employed to test the model (Birks, 1995). A particularly robust method for approximating the errors is the root mean squared error of prediction (RMSEP) that is calculated using computer intensive, randomised resampling procedures (most often jack-knifing or bootstrapping; Birks *et al*., 1990; ter Braak and Juggins, 1993). Jack-knifing (leave-one-out validation) creates new training sets from the initial calibration set, each of which excludes one of the original lake samples. In each jack-knife, the value of the environmental variable of the excluded sample is calculated based on the optima and tolerance of the taxa in the remaining set of samples (Battarbee *et al*. 2001). Bootstrapping is a complex statistical resampling procedure. This process randomly generates a number of 'new' training sets from the original training set, using replacement. These new training sets are the same size as the original dataset (as some samples are chosen twice). Some samples are not selected during this process, and they are used to form an independent test set (Birks *et al*., 1990; Stoermer and Smol, 1999). This procedure is repeated (e.g. 100 or 1000 cycles), so that various combinations of 'training' sets and 'test' sets are created (Stoermer and Smol, 1999). The overall estimate of the predictive ability of the transfer function (RMSEP) is based on the estimates of the environmental variable (e.g. conductivity) in each test set (Stoermer and Smol, 1999).

Estimates derived from transfer functions are all subject to bias (value specific deviation of inferred against observed values over different parts of the environmental gradient). This is usually assessed as both the mean and maximum value under cross-validation (ter Braak and Juggins, 1993; Birks, 1998). The mean bias is the average difference between jack-knifed and observed values across the whole gradient; the maximum bias is the highest absolute value of the mean jack-knifed residuals in any section of the gradient (Ryves *et al*., 2002).

5.3 Datasets

Collection of modern diatom samples was carried out during several independent field campaigns: 2000-2002 (Verschuren), 2000-2001 (DANIDA) and 2006-2007 (Lboro). In all cases the sampling was undertaken during the dry season. For some lakes in the dataset a number of habitat types (e.g. periphytic and pelagic) were sampled (see **Chapter 4**, *section 4.7*). However for the purpose of this study, only the surface sediments have been included in the crater lake calibration sets as these are considered to be most analogous to the core assemblages, representing the average composition of species within the lake (Davies *et al*., 2002). Surface sediment samples collected by DANIDA and Lboro were extracted using a HON-Kajak corer from the deepest part of the lake, Verschuren and colleagues used a gravity corer (D. Verschuren, *pers. comm.*). Care was taken to ensure that the sediment-water interface was undisturbed (see **Chapter 3**, *section 3.2.4*) and water chemistry samples for the crater lake dataset are single, mid-lake measurements. The chosen sampling sites across the crater lake clusters (and hence the salinity gradient) was designed to represent a good range of physical and chemical properties. However, it proved particularly difficult to find and sample lakes with conductivities between 1000 and 20,000 µS cm^{-1} (3 to 4.4 log units; Figure 5.1). This phenomenon was highlighted by Eggermont *et al* (2006) during the development of a chironomid-salinity transfer function for East Africa and is confirmed by the scarcity of lakes in modern Africa with intermediate salinities (Verschuren, 2003).

A number of problems were encountered when creating the calibration datasets, causing the various numerical analyses to be carried out on separate datasets. All samples (25) from the Lboro 2006-2007 field work have diatom samples with (almost) complete water chemistry that was sampled simultaneously. Samples collected by D. Ryves (DANIDA) during 2000-2001 have basic water chemistry data, although conductivity and depth data do exist in all cases. Samples collected during 2000-2002

Table 5.1 *Lakes sampled for inclusion in the crater lake diatom-conductivity transfer function. The numbers given below correspond to the numbered lakes on Figure 2.5. The location of the lakes are given (map sheet number, longitude and latitude) alongside the date when the individual lakes were visited and sampled (e.g. Jan-07) and by who (e.g. Lboro). The maximum depth (metres) and conductivity (μS cm^{-1}) of the lakes are given as well as an indication of whether the samples prepared yielded diatoms (Y/N).*

N^{o}	Lake Name	Latitude	Longitude	Who	Date	Zm (m)	Cond.	Diatoms (Y/N)
2	Kayihara	0°42’17.9”	30°18’56.1”	VERSCH.	Mar-00	65.1	498	Y
3	Ekikoto	0°42’14.6”	30°18’46.6”	VERSCH.	Jan-01	72	464	Y
5	Kyaninga	0°42’8.11”	30°17’46.6”	VERSCH.	Jan-01	57	407	Y
8A	Saaka Crater	0°41’19.2”	30°14’34.4”	DANIDA	Mar-01	6	699	Y
8B	Saaka Crater	0°41’19.2”	30°14’34.4”	LBORO	Jul-06	7.8	662	Y
9	Kanyamukali	0°24’11.4”	29°20’9.23”	VERSCH.	Mar-00	10.8	909	Y
12A	Kasenda	0°26’5.01”	30°17’19.6”	DANIDA	Jul-00	13	380	Y
12B	Kasenda	0°26’5.01”	30°17’19.6”	LBORO	Jul-06	14.2	352	Y
14A	Kifuruka	0°29’33.2”	30°17’9.87”	VERSCH.	Mar-00	5.3	347	Y
14B	Kifuruka	0°29’33.2”	30°17’9.87”	LBORO	Jul-06	4.5	460	Y
18	Kyanga	0°24’30.9”	29°20’15.6”	VERSCH.	Jan-01	55	1055	Y
19	Kyerbwato	0°26’14.8”	30°19’20.8”	DANIDA	Jul-00	13.4	450	Y
21	Lugembe	0°27’10.0”	30°16’48.9”	VERSCH.	Mar-00	18.6	395	Y
22	Lyantonde	0°29’12.5”	30°16’50.7”	LBORO	Jul-06	80	512	Y
23	Mahuhura	0°26’40.7”	30°15’57.2”	LBORO	Jul-06	80	633	Y
27	Murusi	0°25’47.1”	30°17’29.3”	VERSCH.	Jul-02	63	366	Y
30	Njarayabana	0°25’53.8”	29°21’4.07”	VERSCH.	Jan-01	38	879	Y
31	Nkuruba	0°31’10.8”	30°18’1.53”	VERSCH.	Mar-00	34.8	361	Y
33	Ntambi	0°24’43.9”	29°19’56.3”	VERSCH.	Jan-01	8	5820	Y
34	Nyabikere	0°30’5.83”	30°19’32.0”	VERSCH.	Mar-00	43.4	263	Y
35	Nyamirima	0°31’20.6”	30°18’58.0”	LBORO	Jul-06	51.9	216	Y
36	Nyamiteza	0°26’16.5”	29°19’36.8”	VERSCH.	Jul-02	34	1057	Y
37	Nyamogusani	0°25’35.9”	29°19’51.4”	VERSCH.	Jan-01	37	971	Y
38	Nyamswiga	0°30’35.0”	30°17’4.99”	LBORO	Jul-06	75	346	Y
42	Nyierya	0°30’10.6”	30°17’3.39”	LBORO	Jul-06	80	419	Y
43	Nyinabulita	0°30’48.1”	30°19’17.4”	LBORO	Jul-06	63.9	274	Y
46	Wandakara	0°25’11.3”	30°16’10.1”	DANIDA	Jul-00	12	1269	Y
47	Wankenzi	0°25’22.6”	30°15’52.4”	VERSCH.	Jan-01	58	496	Y
48	***Bagusa***	***0°5’22.08”***	***30°10’42.4”***	***VERSCH.***	***Mar-00***	***0.9***	***61100***	***N***
50	Edward	0°11’23.2”	29°49’46.6”	VERSCH.	Jan-01	27	870	Y
52A	***Kikorongo***	***0°1’43.7”***	***30°0’35.04”***	***VERSCH.***	***Jan-01***	***10.7***	***21700***	***N***
52B	***Kikorongo***	***0°1’43.7”***	***30°0’35.04”***	***LBORO***	***Jul-06***	***11***	***22200***	***N***
53	Kitagata	0°3’41.2”	29°58’26.8”	VERSCH.	Jan-01	7.5	135400	Y
54A	Mahega	0°0’35.78”	29°57’56.1”	DANIDA	Jul-00	4.1	138100	Y
54B	***Mahega***	***0°0’35.78”***	***29°57’56.1”***	***LBORO***	***Jan-07***	***4.4***	***961000***	***N***
55	***Maseche***	***0°5’33.46”***	***30°11’26.0”***	***DANIDA***	***Mar-01***	***0.01***	***138100***	***N***
59	Blue Pool	0°16’37.0”	30°2’57.07”	DANIDA	Mar-01	2.7	460	Y
60	Bugwagi	0°11’29.7”	30°11’14.7”	VERSCH.	Jan-01	85	440	Y
62	Chibwera	0°9’0.04”	30°8’20.25”	DANIDA	Mar-01	12	489	Y
64	Kacuba	0°21’40.1”	30°1’29.77”	LBORO	Jan-07	15	126	Y
65	Kako	0°18’21.1”	30°5’48.28”	LBORO	Jul-06	29	98	Y
66	Kamunzuka	0°15’33.6”	30°9’19.96”	LBORO	Jul-06	61	58	Y
67	Kamweru	0°15’20.6”	30°7’28.49”	VERSCH.	Jul-02	33	154	Y
69	Karolero	0°20’31.2”	30°1’44.31”	VERSCH.	Jul-02	15.5	145	Y
70	Kasirya	0°15’20.6”	30°7’57.57”	LBORO	Jul-06	40	323	Y

Table 5.1 *Continued...*

N°	Lake Name	Latitude	Longitude	Who	Date	Zm (m)	Cond.	Diatoms (Y/N)
71	Katinda	0°13'2.38"	30°6'15.82"	VERSCH.	Jan-01	17	743	Y
73	Kigezi	0°17'8.0"	30°6'35.15"	LBORO	Jul-06	26	271	Y
76A	Kyasanduka	0°17'16.0"	30°2'57.06"	DANIDA	Mar-01	2	156	Y
76B	Kyasanduka	0°17'16.0"	30°2'57.06"	LBORO	Jan-07	2	204	Y
77	Kyogo	0°20'21.4"	30°1'7.16"	LBORO	Jan-07	3.4	55	Y
78	Mafuro	0°15'53.1"	30°6'6.09"	LBORO	Jul-06	27.4	342	Y
79	Mirambi	0°13'26.7"	30°6'20.66"	VERSCH.	Jan-01	21	652	Y
80	Mugogo	0°17'17.7"	30°7'31.69"	LBORO	Jan-07	141	119	Y
81	Muijongo	0°16'15.9"	30°5'6.31"	LBORO	Jul-06	55.4	464	Y
82	Murabyo	0°20'1.96"	30°2'8.55"	VERSCH.	Jul-02	14	157	Y
83	Nkugute	0°19'14.8"	30°5'54.73"	VERSCH.	Jan-02	58	101	Y
84	***Nshenyi***	***0°8'55.17"***	***30°9'36.19"***	***VERSCH.***	***Mar-00***	***0.08***	***31600***	***N***
85A	Nyamogusingiri Basin	0°18'55.3"	30°1'36.29"	DANIDA	Jun-00	4.2	741	Y
85B	Nyamogusingiri Basin	0°18'55.3"	30°1'36.29"	LBORO	Jan-07	3.8	554	Y
85A	Nyamogusingiri Crater	0°18'55.3"	30°1'36.29"	LBORO	Jan-07	11.6	548	Y
85B	Nyamogusingiri Crater	0°18'55.3"	30°1'36.29"	LBORO	Jan-07	11.6	548	Y
86	Nyungu	0°15'27.1"	30°6'0.00"	LBORO	Jul-06	25.2	528	Y
	Kabakas	0°15'39.4"	29°21'1.08"	DANIDA	Mar-01	2.4	165	Y
	Victoria (Murchison Bay)			DANIDA	Mar-01	6	119	Y

Data sources:

Direct sources

VERSCH. = D. Verschuren and colleagues, Ghent University

DANIDA = D. Ryves and colleagues, GEUS (Geological Survey of Denmark and Greenland)

LBORO = K. Mills and D. Ryves, Loughborough University

A. Mills_58 dataset

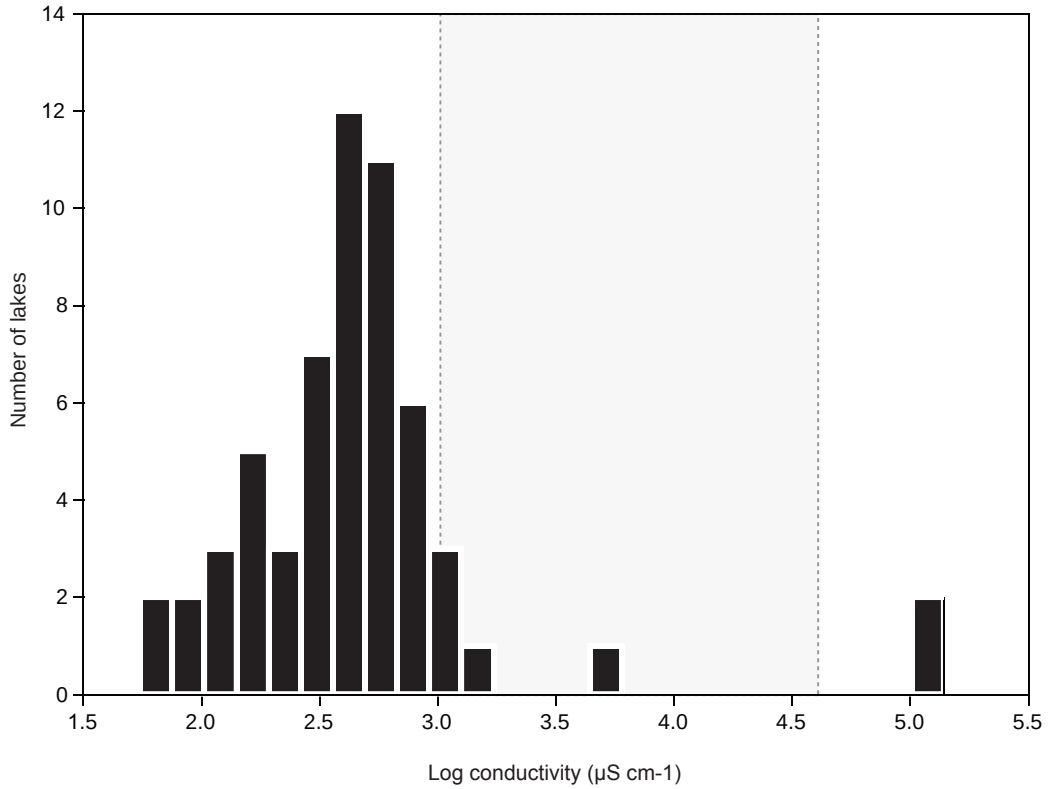

B. Combined_76 dataset

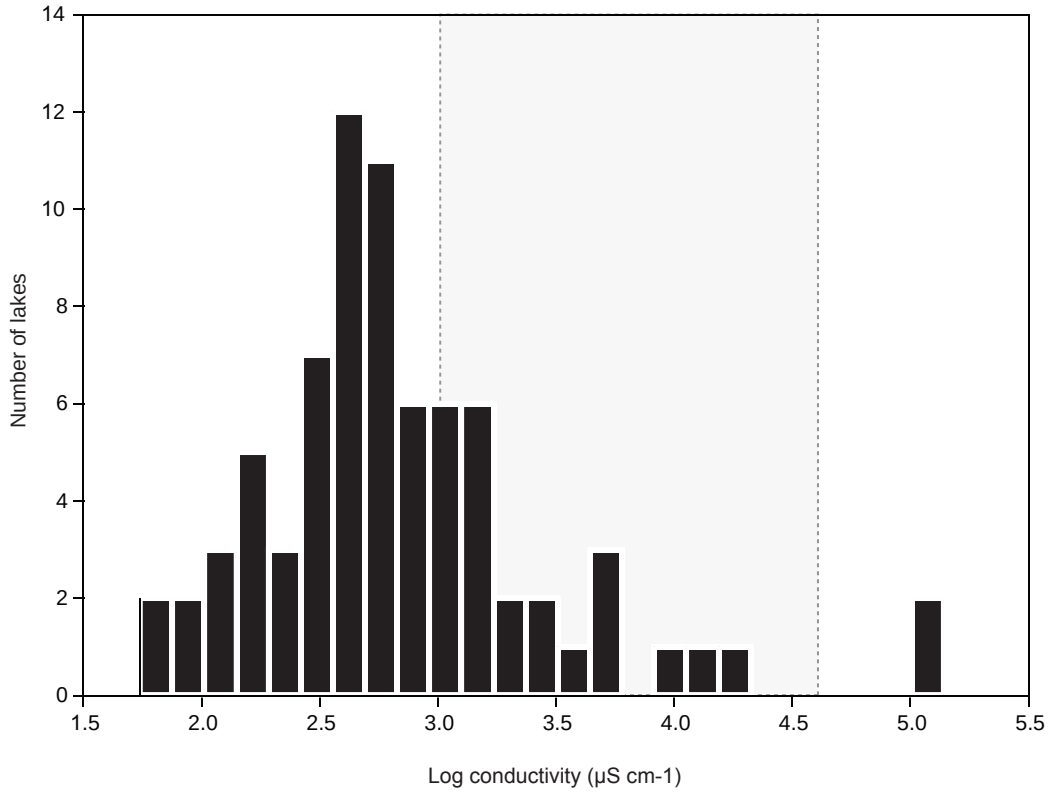

Figure 5.1 *Diagrams showing the gap in the conductivity data in* **(A)** *the Mills_58 dataset and* **(B)** *the attempt at reducing the conductivity gap after adding sites from EDDI to create the Combined_76 dataset..*

by Verschuren and colleagues have 'offset' water chemistries (c.f. Gasse, 1986). Although, sediment samples and water chemistry samples were taken simultaneously during this field work campaign, differences in the water chemistry preparation procedures in the original laboratories (in Belgium) led to some discrepancies in the output and an incompatibility between the old and new samples (D. Verschuren, *pers. comm.*). As a result the lakes from this dataset were re-sampled for water chemistry during 2007, thus creating an offset between the sediment samples and water chemistry. Exploration of the old (2001-2002) and new (2007) measured conductivities of these samples, show little variation (Figure 5.2) in the majority of the lakes. The largest discrepancies are noted in the hypersaline lakes. In addition Eggermont *et al*. (2006) note that a single sample water chemistry measurements in sub-humid western Uganda can be considered representative for the modern annual mean value, given that lakes measured in different seasons and in consecutive years showed relatively stable water chemistry, lending support to the use of these offset data (although sometimes problems may exist with some saline lakes, see **Chapter 4**, *section 4.4.3*).

The full dataset consists of 64 sediment samples from 56 different lakes (Table 5.1). Multiple samples for one site exist and are included in the dataset (i.e. 8 lakes: Kifuruka, Kikorongo, Kasenda, Kyasanduka, Mahega, Nyamogusingiri Basin, Nyamogusingiri Crater and Saaka). Of these 64 sediment samples, 58 contained diatoms and the remaining six sites did not contain any diatoms (Table 5.1). These six sites: Lakes Bagusa, Kikorongo (1 and 2), Mahega (2), Maseche and Nshenyi, are all hypersaline (96,100 to 217,000 µS cm^{-1}) and all except Lake Kikorongo (11 m) are (sometimes extremely) shallow (0.01–4.4 m). Of the 58 samples with diatoms (from 53 lakes), 40 have full water chemistry data (representing 39 different lake sites; Nyamogusingiri Crater provides the extra sample). As a result, for analysis, two crater lake datasets were created: Mills_40 (40 samples from 39 lakes; Table 5.2), representing the lakes with full water chemistry and fossil diatom data and Mills_58 (58 samples from 53 lakes; Table 5.2), representing all lakes with fossil diatom counts and basic limnological data (such as conductivity and depth).

Table 5.2 *Number of sites and taxa in each of the three datasets.*

Dataset	N° samples	N° lakes	N° taxa (all)	N° taxa (>0.5%)
Mills_40	40	39	200	143
Mills_58	58	53	227	165
Combined_76	76	71	279	198

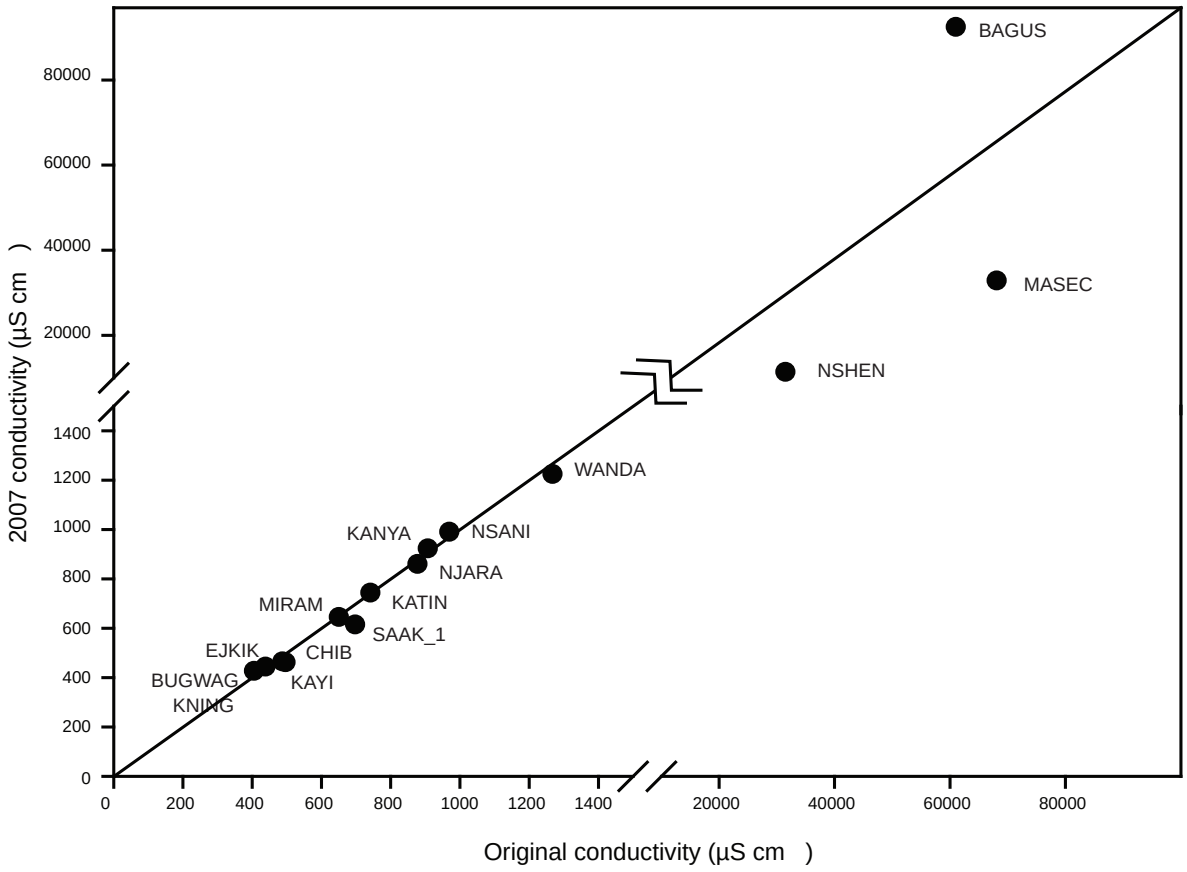

Figure 5.2 *Scatter plot showing the relationship between the original measured conductivity and conductivity measurements made in 2007. This set of lakes were not initially sampled for detailed water chemistry. The lakes were resampled for water chemistry only in 2007 (by B. Rumes, Ghent University). The solid line represents the 1:1 line. On the basis of little change in the conductivity data, the new water chemistry was used in conjunction with the older surface sediment samples. The largest variation in the data occurs in the hyper-saline lakes, subject to greater seasonal variation.*

Table 5.3 *Information regarding the European Diatom Database (EDDI) sites added into the crater lake conductivity transfer function.*

EDDI Code	Site Name	Country	Site Type	Sample Type	Latitude	Longitude	Date	Zm (m)	Cond. ($\mu S\ cm^{-1}$)
AFE004	Oudoudda	Dijibouti	Well	Periphytic	11° 34’ 0”	42° 4’ 0”	Nov-73	n/a	4060
AFE011	Awassa	Ethiopia	Lake	Plankton	6° 58’ 0”	38° 22’ 0”	Mar-80	21.6	1050
AFE012	Langano	Ethiopia	Lake	Plankton	7° 31’ 0”	38° 40’ 0”	Apr-80	47.9	1900
AFE013	Biete Mengest	Ethiopia	Lake	Plankton	8° 46’ 0”	38° 58’ 0”	Apr-80	38	2500
AFE017	Abiyata	Ethiopia	Lake	Bottom mud	7° 32’ 0”	38° 27’ 0”	Apr-80	14.20	10700
AFE021	Kilotes	Ethiopia	Lake	Plankton	8° 48’ 0”	39° 4’ 0”	Mar-80	6.4	5930
AFE035	Wadi Kalou	Dijibouti	River	Mud	11° 34’ 0”	42° 19’ 0”	Nov-75	0.1	1540
AFE036	Wadi Kalou	Dijibouti	River	Mud	11° 34’ 0”	42° 19’ 0”	Nov-75	0.1	1720
AFE037	Wadi Kalou	Dijibouti	River	Mud	11° 34’ 0”	42° 19’ 0”	Nov-75	0.1	1720
AFE055	Gadeb/Geradila	Ethiopia	Lake	Mud	7° 0’ 0”	39° 15’ 0”	Feb-77	0.2	2000
AFE061	Ol Bolossat	Kenya	Swampy lake	Littoral mud	0° 9’ 0”	36° 25’ 0”	Mar-79	0.5	1390
AFE073	Marairs ol Bolossat	Kenya	Lake	Littoral mud	0° 9’ 0”	36° 25’ 0”	Dec-79	0.1	1500
AFE080	Turkana	Kenya	Lake	Plankton	2° 25’ 0”	35° 49’ 0”	Jan-79	120	2630
AFE090	Awassa	Ethiopia	Lake	Bottom mud	6° 58’ 0”	38° 22’ 0”	Mar-64	21.6	1050
AFE115	Kenke swamp	Tanzania	Lake	Bottom mud	4° 40’ 0”	34° 40’ 0”	Jul-69	n/a	1200
AFE116	Kindai	Tanzania	Lake	Bottom mud	4° 50’ 0”	34° 43’ 0”	Jul-69	n/a	4800
AFE122	Kikorongo	Uganda	Lake	Bottom mud	0° 0’ 0”	30° 01’ 0”	Nov-69	0.3	16300
AFE175	Gawani	Ethiopia	Swamp	Littoral mud	11° 40’ 0”	40° 40’ 0”	Nov-72	0.1	14300

In an attempt to fill the gap between the freshwater and hypersaline sites in the full crater lake dataset (Mills_58), 18 additional lake sites were integrated into the dataset using sites and samples from the European Diatom Database (EDDI; Table 5.3). These sites were explored and selected on the basis of their conductivity and whether the diatom species in the samples overlapped with those from the crater lake dataset.

The species names presented in this chapter are based on updated diatom taxonomy with the assignation of existing diatom species (e.g. Navicula) to new genera (e.g. Diadesmis, Luticola; cf. Round *et al*., 1990). A list of synonyms and their authorities is given in **Appendix A**. All species recorded during this research were coded according to EDDI and were based on the old taxonomy to ensure consistency between the EDDI sites and the samples analysed here (e.g. Navicula contenta = Diadesmis contenta = EDDI code NA046A).

The predictor variables (e.g. water chemistry data) that exhibited skewed distributions were transformed in order to reduce the influence of extreme values, necessary for all variables except for Si, surface water temperature and pH. Depth and altitude were square-root transformed (Table 5.5). The data transformations were carried out using CALIBRATE (version 0.81; Juggins and ter Braak, 1997).

5.4 Methods

Surface sediment samples (0-0.5 cm, Lboro; 0-1 cm, DANIDA and 0-1 cm and 0-3 cm, Verschuren), physical limnological measurements and corresponding water samples for the analysis of nutrients, anions and cations were taken from 56 lakes across a natural salinity gradient (see Table 5.6 and Table 5.7 for a summary of the physical and chemical attributes). For details regarding the laboratory preparation and analysis techniques of these samples please refer to **Chapter 3**.

5.4.1 Numerical methods

Detrended correspondence analysis (DCA) was used in the exploratory analysis of all of the crater lake diatom data (>0.5% in any one sample) in order to determine the gradient length of axis one to assess whether unimodal or linear ordination techniques were most appropriate. Where unimodal models were identified as the most suitable response model, biplots of the first two DCA axes were compared with correspondence analysis (CA) ordinations to ascertain whether there was an arch in the data (ter Braak, 1995).

Table 5.4 *Lakes included in the 3 datasets: Mills_40 with full water chemistry data, Mills (58) with conductivity and basic physical data (e.g. depth, altitude) and Combined_76 with conductivity only (this dataset includes samples from EDDI). Six sites were omitted from all datasets (highlighted) as these samples did not contain any diatoms.*

N^{o}	Lake Name	Latitude	Longitude	Mills (40)	Mills (58)	Comb. (76)	Cond.	Diatoms (Y/N)
2	Kayihara	0°42’17.9”	30°18’56.1”		X	X	498	Y
3	Ekikoto	0°42’14.6”	30°18’46.6”		X	X	464	Y
5	Kyaninga	0°42’8.11”	30°17’46.6”	X	X	X	407	Y
8A	Saaka Crater	0°41’19.2”	30°14’34.4”		X	X	699	Y
8B	Saaka Crater	0°41’19.2”	30°14’34.4”	X	X	X	662	Y
9	Kanyamukali	0°24’11.4”	29°20’9.23”	X	X	X	909	Y
12A	Kasenda	0°26’5.01”	30°17’19.6”		X	X	380	Y
12B	Kasenda	0°26’5.01”	30°17’19.6”	X	X	X	352	Y
14A	Kifuruka	0°29’33.2”	30°17’9.87”		X	X	347	Y
14B	Kifuruka	0°29’33.2”	30°17’9.87”	X	X	X	460	Y
18	Kyanga	0°24’30.9”	29°20’15.6”		X	X	1055	Y
19	Kyerbwato	0°26’14.8”	30°19’20.8”	X	X	X	450	Y
21	Lugembe	0°27’10.0”	30°16’48.9”	X	X	X	395	Y
22	Lyantonde	0°29’12.5”	30°16’50.7”	X	X	X	512	Y
23	Mahuhura	0°26’40.7”	30°15’57.2”	X	X	X	633	Y
27	Murusi	0°25’47.1”	30°17’29.3”	X	X	X	366	Y
30	Njarayabana	0°25’53.8”	29°21’4.07”	X	X	X	879	Y
31	Nkuruba	0°31’10.8”	30°18’1.53”	X	X	X	361	Y
33	Ntambi	0°24’43.9”	29°19’56.3”		X	X	5820	Y
34	Nyabikere	0°30’5.83”	30°19’32.0”		X	X	263	Y
35	Nyamirima	0°31’20.6”	30°18’58.0”	X	X	X	216	Y
36	Nyamiteza	0°26’16.5”	29°19’36.8”		X	X	1057	Y
37	Nyamogusani	0°25’35.9”	29°19’51.4”	X	X	X	971	Y
38	Nyamswiga	0°30’35.0”	30°17’4.99”	X	X	X	346	Y
42	Nyierya	0°30’10.6”	30°17’3.39”	X	X	X	419	Y
43	Nyinabulita	0°30’48.1”	30°19’17.4”	X	X	X	274	Y
46	Wandakara	0°25’11.3”	30°16’10.1”	X	X	X	1269	Y
47	Wankenzi	0°25’22.6”	30°15’52.4”	X	X	X	496	Y
48	***Bagusa***	***0°5’22.08”***	***30°10’42.4”***				***61100***	***N***
50	Edward	0°11’23.2”	29°49’46.6”		X	X	870	Y
52A	***Kikorongo***	***0°1’43.7”***	***30°0’35.04”***				***21700***	***N***
52B	***Kikorongo***	***0°1’43.7”***	***30°0’35.04”***				***22200***	***N***
53	Kitagata	0°3’41.2”	29°58’26.8”	X	X	X	135400	Y
54A	Mahega	0°0’35.78”	29°57’56.1”		X	X	138100	Y
54B	***Mahega***	***0°0’35.78”***	***29°57’56.1”***				***961000***	***N***
55	***Maseche***	***0°5’33.46”***	***30°11’26.0”***				***138100***	***N***
59	Blue Pool	0°16’37.0”	30°2’57.07”		X	X	460	Y
60	Bugwagi	0°11’29.7”	30°11’14.7”	X	X	X	440	Y
62	Chibwera	0°9’0.04”	30°8’20.25”	X	X	X	489	Y
64	Kacuba	0°21’40.1”	30°1’29.77”	X	X	X	126	Y
65	Kako	0°18’21.1”	30°5’48.28”	X	X	X	98	Y
66	Kamunzuka	0°15’33.6”	30°9’19.96”	X	X	X	58	Y
67	Kamweru	0°15’20.6”	30°7’28.49”	X	X	X	154	Y
69	Karolero	0°20’31.2”	30°1’44.31”	X	X	X	145	Y
70	Kasirya	0°15’20.6”	30°7’57.57”		X	X	323	Y
71	Katinda	0°13’2.38”	30°6’15.82”	X	X	X	743	Y
73	Kigezi	0°17’8.0”	30°6’35.15”	X	X	X	271	Y
76A	Kyasanduka	0°17’16.0”	30°2’57.06”		X	X	156	Y

Table 5.4 *Continued...*

N^o	Lake Name	Latitude	Longitude	Mills (40)	Mills (58)	Comb. (76)	Cond.	Diatoms (Y/N)
76B	Kyasanduka	0°17'16.0"	30°2'57.06"	X	X	X	204	Y
77	Kyogo	0°20'21.4"	30°1'7.16"	X	X	X	55	Y
78	Mafuro	0°15'53.1"	30°6'6.09"	X	X	X	342	Y
79	Mirambi	0°13'26.7"	30°6'20.66"	X	X	X	652	Y
80	Mugogo	0°17'17.7"	30°7'31.69"	X	X	X	119	Y
81	Muijongo	0°16'15.9"	30°5'6.31"	X	X	X	464	Y
82	Murabyo	0°20'1.96"	30°2'8.55"	X	X	X	157	Y
83	Nkugute	0°19'14.8"	30°5'54.73"		X	X	101	Y
84	***Nshenyi***	***0°8'55.17"***	***30°9'36.19"***				***31600***	***N***
85A	Nyamogusingiri Basin	0°18'55.3"	30°1'36.29"		X	X	741	Y
85B	Nyamogusingiri Basin	0°18'55.3"	30°1'36.29"	X	X	X	554	Y
85A	Nyamogusingiri Crater	0°18'55.3"	30°1'36.29"	X	X	X	548	Y
85B	Nyamogusingiri Crater	0°18'55.3"	30°1'36.29"	X	X	X	548	Y
86	Nyungu	0°15'27.1"	30°6'0.00"	X	X	X	528	Y
	Kabakas	0°15'39.4"	29°21'1.08"		X	X	165	Y
	Victoria (Murchison Bay)				X	X	119	Y
AFE004	Oudoudda	11° 34' 0"	42° 4' 0"			X	4060	Y
AFE011	Awassa	6° 58' 0"	38° 22' 0"			X	1050	Y
AFE013	Biete Mengest	8° 46' 0"	38° 58' 0"			X	2500	Y
AFE021	Kilotes	8° 48' 0"	39° 4' 0"			X	5930	Y
AFE055	Gadeb/Geradila	7° 0' 0"	39° 15' 0"			X	2000	Y
AFE073	Marairs ol Bolossat	0° 9' 0"	36° 25' 0"			X	1500	Y
AFE090	Awassa	6° 58' 0"	38° 22' 0"			X	1050	Y
AFE122	Kikorongo	0° 0' 0"	30° 01' 0"			X	16300	Y
AFE012	Langano	7° 31' 0"	38° 40' 0"			X	1900	Y
AFE017	Abiyata	7° 32' 0"	38° 27' 0"			X	10700	Y
AFE035	Wadi Kalou	11° 34' 0"	42° 19' 0"			X	1540	Y
AFE036	Wadi Kalou	11° 34' 0"	42° 19' 0"			X	1720	Y
AFE037	Wadi Kalou	11° 34' 0"	42° 19' 0"			X	1720	Y
AFE061	Ol Bolossat	0° 9' 0"	36° 25' 0"			X	1390	Y
AFE080	Turkana	2° 25' 0"	35° 49' 0"			X	2630	Y
AFE115	Kenke swamp	4° 40' 0"	34° 40' 0"			X	1200	Y
AFE116	Kindai	4° 50' 0"	34° 43' 0"			X	4800	Y
AFE175	Gawani	11° 40' 0"	40° 40' 0"			X	14300	Y

Data sources:

All AFE coded samples were taken form the European Diatom Database (EDDI)

Table 5.5 *Summary of the 19 environmental variables measured from the 42 lakes in the diatom surface sediment training set, indicating units of measurement, summary statistics (average, minimum, maximum and median), data transformations (trans.) applied prior to numerical analyses (e.g. log or square root) and the abbreviated code.*

Type	Variable	Unit	Average	Max.	Min	Median	Trans.	Code
Major ion chemistry	Conductivity	$\mu S\ cm^{-1}$	9456	138100	55	464	Log(x)	Lg_COND
	pH	$mg\ l^{-1}$	9.81	10.62	7.09	8.75	None	pH
	Sodium	$mg\ l^{-1}$	2301	40719.81	1.3	12.5	Log(x)	Lg_Na
	Potassium	$mg\ l^{-1}$	650	15473.95	2.9	14.9	Log(x)	Lg_K
	Calcium	$mg\ l^{-1}$	22	61.6	3	20.18	Log(x)	Lg_Ca
	Magnesium	$mg\ l^{-1}$	28.96	134	1.96	24.18	Log(x)	Lg_Mg
	Fluoride	$mg\ l^{-1}$	2.91	40.39	0.04	0.78	Log(x)	Lg_F
	Chloride	$mg\ l^{-1}$	979	37991.89	1.15	3.88	Log(x)	Lg_Cl
	Strontium	$mg\ l^{-1}$	1.18	6.56	0.06	0.52	Log(x)	Lg_Sr
	Barium	$mg\ l^{-1}$	0.39	5.85	0.004	0.08	Log(x)	Lg_Ba
	Total S	$mg\ l^{-1}$	276.85	12380	0.091	2.31	Log(x)	Lg_Stot
	Silica	$mg\ l^{-1}$	13.25	36.76	0.11	12.58	None	Si
Nutrient	Total P	$\mu g\ l^{-1}$	406.25	13720	1.68	24.61	Log(x)	Lg_TP
	Total N	$\mu g\ l^{-1}$	877.69	11914	66.22	417.2	Log(x)	Lg_TN
Physical	Altitude	m.a.s.l	1186	1568	903	1176	Square root	SQ_ALT
	Max. depth	m	32.05	141	0.01	19.8	Square root	SQ_DEPTH
	Secchi depth	cm	154.87	770	0.02	115	None	SECCHI
	Temperature	°C	25.82	32.3	18.71	25.82	None	TEMP_S
	DIC	$mg\ l^{-1}$	497	12221.68	4.89	47.5	Log(x)	Lg_DIC
	TOC	$mg\ l^{-1}$	38.92	668.87	0.56	5.48	Log(x)	Lg_TOC
	Catchment impact	Dummy[1]*	n/a	n/a	n/a	n/a	None	NONE / SEMI / FULL
	Lake status	Dummy[2]*	n/a	n/a	n/a	n/a	None	OPEN / SEASON / CLOSE

* Dummy variable – is used to denote the presence or absence of the variable using 0 or 1 codes. For example, a closed lake system would be represented as: CLOSE = 1, open = 0, seasonal = 0.

[1] Catchment impact (based on contemporary lake setting): whether the lake catchment was subject to human activity. Categories include NONE (usually those protected in forest reserves and national parks with no visible signs of human modification), SEMI (signs of human activity, e.g. clearance) and FULL (over 50% of the catchment heavily impacted by plantations, farming and homesteads). Status assigned according to field observations and map data

[2] Lake status: whether the lake system is OPEN (permanent inflow and outflow), SEASON (outflow following seasonal rains) or a hydrologically closed (CLOSE) system

Following these exploratory analyses, constrained ordination (canonical correspondence analysis; CCA) was applied to the diatom data with all predictor variables (19) included to explore the relationships amongst and between species and their environment (Mills_40 dataset). A subset of the environmental variables was selected based on the inspection of variance inflation factors (VIF; ter Braak and Šmilauer, 1998). A variable with a large VIF (>20) suggests that the variable is redundant with regards to other variables in the data set. For example, conductivity may have a large VIF; however, this would be expected given that conductivity would contain some of the same information as Na, K and Ca (i.e. anions). Environmental variables with a VIF of 1 are uncorrelated with the other measured variables.

Principal components analysis (PCA) of the environmental data was also used to explore redundancy (co-linearity) within the predictors. Ordinations with species data as untransformed percentages were compared with both log% and square root percentage transformations to assess the robustness of the observed patterns (c.f. Ryves *et al*., 2002). Ordinations were carried out using CANOCO 4.5 (ter Braak and Šmilauer, 2002).

Detrended CCA (DCCA) was used to estimate conductivity gradient length (Birks, 1995) to determine whether linear or unimodal techniques were appropriate. Canonical correspondence analysis, on untransformed data with down-weighting of rare species, was applied to the datasets using manual forward selection (Monte Carlo permutation tests, n=999) to identify a subset of significant variables (partial CCA). To restrict the number of explanatory variables included in the final model and to avoid a type I error, a Bonferroni-adjustment was applied to the forward-selection process (Manly, 1992). The use of forward selection can result in the occurrence of a type I error, as the selection of variable is based on a large number of significant tests (one for each variable). As a consequence the probability of a false positive result (type I error) increases with the number of significance tests (Rabe-Hesketh and Everitt, 2004). A type I error therefore occurs when a non-significant predictor is identified as significant. The occurrence of a type I error can be reduced by adjusting (reducing) the *p*-value for statistical significance (Manly, 1992). The simplest form of adjustment is Bonferroni, where the *p*-value is divided (and hence adjusted) by the number of variables included in the forward selection process. Using 0.05 as the initial threshold (*p*) value, the first significant variable must have a *p*-value of <0.05 (0.05/1); the second significant

variable must have a *p*-value of <0.025 (0.05/2) for it to be significant and included, and so on.

Following this forward selection procedure, variance inflation factors (VIF) were inspected to ensure that the selected variables did not exhibit a high degree of co-linearity with each other (ter Braak and Šmilauer, 1998). The significance of the first axis and the sum of all canonical axes (from the forward selected variables) was tested using a Monte Carlo permutation test (n=999 unrestricted permutations) under the reduced model.

The strength and independence amongst the significant variables was tested using a series of CCAs and partial CCAs to establish their relative contributions to the variance observed in the diatom data (ter Braak 1988; Borcard *et al*., 1992). To assess the unique contribution of each of the significant variables, the effect of the other variables were removed (partialled out) by including them as covariables during the partial CCA analysis. This process was repeated on paired sets of variables to calculate the intersect (interaction) between the environmental variables. The proportion of the variation was transformed into percentages following the procedure outlined by Borcard *et al*. (1992).

When CCA is run with a single environmental variable, there will be one constrained axis and a series of unconstrained axes (Kingston *et al*., 1992). The more important an environmental variable is in explaining the variation in the diatom data, the larger the first constrained axis (λ_1) will be compared to the unconstrained axis ($\lambda_{2.}$)

In addition to this, the response of taxa occurring at least 10 times in a dataset to conductivity is assessed by fitting their distribution (log-transformed) to a hierarchical set of models using the maximum likelihood method of Huisman-Olff-Fresco (Huisman *et al*., 1993) implemented using HOF 2.3 with a binomial error distribution (http://www.cc.oulu.fi/~jarioksa/; Oksanen and Minchin, 2002). These models include a skewed unimodal distribution (model V), a symmetric unimodal distribution (model IV), a monotonic relationship with a plateau (model III), a monotonic increase or decrease (model II) and, null model (model I). Conductivity optima and tolerances for all species were estimated as weighted averages (Birks *et al*., 1990) using C2 (Juggins, 2003).

Table 5.6 *42 lakes and the physical data included in the ordination. Lakes listed here contain full water chemistry data. 58 actual Mills lakes in training set (see* ***Table 5.4****) of which these 42 contain complete physical data.*

Lake name	Code	Altitude m	Zm m	Secchi cm	Temp. °C	Impact*	System status[+]	DIC mg/l	TOC mg/l
Bugwagi	BUGWAG	1055	85	245	26.3	S	C	56.35	3.23
Chibwera	CHIB	955	12	135	26.01	N	S	50.99	1.91
Kacuba	KACUB	1112	15	235	27	N	C	15.25	5.49
Kako	KAKO	1375	29	292.5	25.22	F	C	11.00	1.50
Kamunzuka	KAMUN	1258	61	770	24.85	N	C	6.50	1.00
Kamweru	KAMWER	1212	33	43	25.7	S	C	22.49	12.56
Kanyanmukali	KANYA	1069	10.8	94	27.2	F	C	107.13	8.21
Karolero	KARO	1155	15.5	149	26.89	N	C	14.71	4.22
Katinda	KATIN	996	17	35	27	S	C	73.20	7.95
Kyerbwatoi	KBWAT	1239	13.4	63.5	25.3	S	C	42.05	5.61
Kifuruka (2)	KIFU_2	1408	4.5	115	23.28	S	C	47.50	4.30
Kigezi	KIGEZ	1247	26	135	24.83	F	C	31.50	4.50
Kikorongo (2)	***KIKO_2***	***930***	***11***	***160***	***26.9***	***N***	***S***	***1187.00***	***51.30***
Kitigata	KITIG	930	7.5	5	28	N	C	215.40	22.00
Kyaninga	KNING	1567	57	660	23.9	S	C	51.73	0.57
Kasenda (2)	KSEN_2	1254	14.2	175	18.71	S	C	37.70	4.80
Kyasanduka (2)	KYAS_2	994	2	17.5	29.11	S	S	28.84	79.89
Kyogo	KYOG	1120	3.4	290	27.5	N	C	4.89	3.67
Lugembe	LUGEM	1254	18.6	77.5	25.2	S	C	48.19	2.26
Lyantonde	LYAN	1202	80	280	23.93	S	C	58.10	2.90
Mafura	MAFU	1247	27.4	115	24.31	F	C	37.70	4.60
Mahega (2)	***MAH_2***	***908***	***4.4***	***30***	***31***	***N***	***C***	***1257.87***	***115.81***
Mahuhura	MAHUH	1205	80	660	26.75	S	C	72.40	2.30
Mirambi	MIRAM	1036	21	100	25.3	S	C	54.39	3.72
Mugogo	MUGO	1322	141	212	25.84	S	O	16.61	6.24
Muijongo	MUIJO	1237	55.4	270	24.9	S	C	52.60	3.60
Murabyo	MURAB	1088	14	203	27.48	N	C	15.25	6.27

Table 5.6 *Continued*

Lake name	Code	Altitude m	Zm m	Secchi cm	Temp. °C	Impact*	System status†	DIC mg/l	TOC mg/l
Murusi	MURU	1229	57	140	26.13	S	S	36.78	8.61
Nyinambulita	NBULIT	1408	63.9	427.5	19.43	S	C	30.40	1.70
Njarabanya	NJARA	1169	38	75	26.6	S	S	111.55	11.23
Nkuruba	NKUBA	1535	34.8	148.5	24.6	S	C	45.95	5.85
Nyamirima	NMIRI	1465	51.9	440	20.95	S	C	15.20	1.30
Nyamogusani	NSANI	1152	37	120	26.3	S	C	112.48	1.66
Nyamswiga	NSWIG	1448	75	180	23.73	S	C	39.20	4.00
Nyamogusingiri Basin (2)	NYAMB_2	984	3.8	52.5	27	S	S	64.24	17.13
Nyamogusingiri Crater (1)	NYAMC_1	984	11.6	50	27.5	S	S	62.98	17.31
Nyamogusingiri Crater (2)	NYAMC_2	984	11.6	50	27.5	S	S	62.98	17.31
Nyierya	NYIER	1454	80	135	23.65	S	C	42.10	3.70
Nyungu	NYUN	1190	25.2	46.5	25.82	F	C	102.00	6.60
Saaka (2)	SAAK_2	1568	7.8	60	22.24	S	O	80.40	7.30
Wandakara	WANDA	1172	12	31	24.31	S	C	107.05	6.88
Wankenzi	WANZI	1176	58	36	24.27	S	O	46.54	7.59

** Impact: All lake catchments were allocated a code (N, S, F) depending on the amount of human activity within the lake catchment. N = no visible human activity; S = semi-impacted catchment, with some natural vegetation remaining or areas of land that cannot be cultivated (e.g. steep rock faces); F = fully impacted, no natural vegetation remaining.*

† System status: This category refers to whether the lake system is open (O), closed (C) or temporarily open after the wet season (seasonally; S).This information was derived from field data and Ugandan Government maps using ArcGIS.

Table 5.7 *42 lakes and the water chemistry data included in the ordination. Lakes listed here contain full water chemistry data. 58 actual 'Mills' lakes in training set (see* ***Table 5.4****) of which these 42 contain complete chemistry data. The highlighted samples (Lakes Kikorongo and Mahega) does not have a corresponding diatom count (no diatom valves in the sediment).*

Lake name	Code	pH	Cond. µS cm^{-1}	TP µg/l	TN µg/l	Na mg/l	K mg/l	Ca mg/l	Mg mg/l	F mg/l	Cl mg/l	Si mg/l
Bugwagi	BUGWAG	8.64	440	18.10	334.70	20.71	20.66	20.48	37.68	0.48	3.88	24.10
Chibwera	CHIB	8.91	489	24.75	295.78	22.15	29.12	15.31	24.28	0.46	5.92	7.34
Kacuba	KACUB	7.40	126	21.24	248.71	3.78	10.44	12.59	7.78	0.31	3.45	9.66
Kako	KAKO	8.16	98	4.62	86.10	1.30	4.00	6.50	6.00	0.11	1.56	3.30
Kamunzuka	KAMUN	8.23	58	1.68	66.22	1.50	3.10	3.00	3.70	0.04	1.56	0.37
Kamweru	KAMWER	8.40	154	32.14	656.42	2.98	4.19	16.73	13.53	0.26	2.71	11.61
Kanyanmukali	KANYA	8.78	909	187.96	443.66	32.87	55.70	40.27	48.73	2.09	20.69	13.58
Karolero	KARO	8.75	183	20.50	373.60	3.62	9.89	12.71	7.55	0.29	3.25	9.68
Katinda	KATIN	9.23	743	19.36	767.97	94.34	70.33	11.98	27.72	0.56	14.05	18.54
Kyerbwatoi	KBWAT	8.47	538	11.34	228.31	9.26	10.76	21.65	41.06	0.84	1.46	10.41
Kifuruka (2)	KIFU_2	8.92	460	35.28	496.72	9.50	15.00	44.40	27.10	1.07	4.83	18.90
Kigezi	KIGEZ	9.00	271	16.37	282.51	2.00	6.00	22.80	19.50	0.22	1.15	10.40
Kikorongo (2)	***KIKO_2***	***10.31***	***22200***	***13720.00***	***11914.00***	***3628.00***	***659.90***	***7.70***	***5.70***	***4.89***	***1659.00***	***16.00***
Kitigata	KITIG	9.63	135400	42.76	1821.39	384.39	172.79	8.20	29.82	0.97	70.87	4.97
Kyaninga	KNING	8.18	407	5.32	103.78	16.50	12.20	36.60	27.50	0.90	1.27	12.87
Kasenda (2)	KSEN_2	8.50	352	18.48	662.20	8.90	4.30	29.70	12.30	1.07	2.51	15.90
Kyasanduka (2)	KYAS_2	9.30	204	210.98	892.56	12.10	15.94	19.88	15.28	0.31	6.42	15.01
Kyogo	KYOG	7.09	55	272.66	342.87	7.78	7.39	4.80	1.97	0.04	1.59	6.34
Lugembe	LUGEM	8.78	395	21.42	529.28	15.60	14.10	22.40	22.70	1.09	5.08	9.67
Lyantonde	LYAN	9.09	512	5.46	258.30	9.60	11.10	29.10	46.30	2.68	5.78	15.30
Mafura	MAFU	8.16	342	11.48	245.00	3.90	16.40	27.60	19.70	0.21	3.77	13.70
Mahega (2)	***MAH_2***	***9.30***	***96100***	***1355.38***	***2080.83***	***40719.81***	***8862.23***	***9.55***	***126.53***	***19.67***	***37992.89***	***11.07***
Mahuhura	MAHUH	9.19	633	49.98	86.10	23.50	24.20	35.60	47.40	4.63	7.11	22.20
Mirambi	MIRAM	8.98	652	18.02	633.07	69.93	52.24	9.93	27.02	0.49	9.05	13.16
Mugogo	MUGO	8.29	119	7.39	282.51	3.27	3.66	14.30	9.66	0.15	2.48	5.90
Muijongo	MUIJO	9.15	464	6.58	331.10	12.50	34.70	17.80	33.80	0.31	3.13	13.00

Table 5.7 *Continued*

Lake name	Code	pH	Cond. µS cm^{-1}	TP µg/l	TN µg/l	Na mg/l	K mg/l	Ca mg/l	Mg mg/l	F mg/l	Cl mg/l	Si mg/l
Murabyo	MURAB	8.42	157	9.79	321.72	2.46	8.42	11.88	8.33	0.16	1.59	6.69
Murusi	MURU	8.54	366	5.10	308.74	13.12	8.26	29.84	26.17	0.86	1.98	19.42
Nyinambulita	NBULIT	9.15	274	25.90	165.62	1.80	2.90	12.60	7.10	0.43	1.92	9.80
Njarabanya	NJARA	8.58	879	359.69	498.15	18.10	24.20	61.60	79.40	3.72	5.50	21.50
Nkuruba	NKUBA	8.40	361	25.03	659.01	3.80	4.95	43.28	24.65	1.11	1.45	6.27
Nyamirima	NMIRI	8.89	216	4.06	245.00	4.10	5.20	24.40	9.30	0.17	1.42	10.10
Nyamogusani	NSANI	8.61	971	152.33	285.39	79.62	50.21	49.32	58.29	4.52	31.33	20.63
Nyamswiga	NSWIG	8.74	346	33.32	390.74	4.60	8.70	39.50	17.40	0.86	2.57	8.50
Nyamogusingiri Basin (2)	NYAMB_2	9.16	554	26.99	2003.01	48.57	101.90	10.60	30.75	0.32	26.68	13.17
Nyamogusingiri Crater (1)	NYAMC_1	9.10	548	29.60	1535.98	47.76	101.29	11.04	30.90	0.36	26.52	13.30
Nyamogusingiri Crater (2)	NYAMC_2	9.10	548	29.60	1535.98	47.76	101.29	11.04	30.90	0.36	26.52	13.30
Nyierya	NYIER	8.84	419	16.10	470.26	5.50	4.10	24.80	21.20	1.13	3.40	9.30
Nyungu	NYUN	9.31	528	119.14	1498.00	40.30	36.00	27.20	41.30	0.53	71.30	21.50
Saaka (2)	SAAK_2	7.98	662	36.54	894.04	29.40	14.90	58.00	36.40	0.93	2.39	9.10
Wandakara	WANDA	8.75	1269	25.97	752.42	123.98	54.62	22.81	42.76	3.05	50.95	22.12
Wankenzi	WANZI	8.65	496	24.47	835.44	10.05	5.36	25.44	12.04	1.05	5.37	18.75

5.4.2 Diatom-inferred conductivity models

Transfer function development was carried out in the program C2 (version 1.5.1; Juggins, 2003). Diatom assemblage data were analysed as percentages. The data were otherwise untransformed. Conductivity (expressed as µS cm^{-1}) was log-transformed to approximate normality and to reduce the influence of large values, in keeping with many other salinity transfer functions (e.g. Fritz *et al*., 1990; Wilson *et al*. 1996; EDDI; Ryves *et al*., 2002).

Several models were created using weighted averaging (WA) regression and calibration (ter Braak and van Dam, 1989). WA and weighted averaging with tolerance down-weighting (WA_{tol}) were performed using both inverse and classical deshrinking. Models based on WA partial least squares (WA-PLS; ter Braak and Juggins, 1993) were also developed for comparison. All models were validated using the leave-one-out jack-knifing cross-validation method (ter Braak and Juggins, 1993) and were compared on the basis of their root mean squared error of prediction (RMSEP). Bias was estimated as both the mean and maximum value under cross-validation (ter Braak and Juggins, 1993; Birks, 1998) to assess the systematic differences between inferred and measured conductivity (Birks, 1998). Apparent and predicted root-mean square errors (RMSE and RMSEP) values are reported as $\log_{10}$ conductivity. Conductivity optima of the diatom species were derived using WA. Models were developed for all three datasets (Mills_40, Mills_58 and Combined_76) for comparison of model performance.

Possible outliers in the dataset were identified as those with a jack-knifed residual (inferred-observed) greater than the standard deviation of the environmental parameter (in this case conductivity; Gasse *et al*., 1995). To ascertain whether these samples were "true" outliers, the method of Racca and Prairie (2004) was employed, which can reduce the apparent bias in the residual data, thus instilling greater confidence in the models predictive capabilities. Once these true outliers were detected, the influence of these samples on the model was assessed using Cook's *D* (Cook and Weisberg, 1982; calculated in SigmaPlot 9.0) and compared against the critical value of $n/4$ (where n= number of sites in the model; Jones and Juggins, 1995). Samples with a low Cook's *D* could be deleted safely, and those with high Cook's *D* (and especially those >1) should be investigated fully. As well as employing statistical methods for the deletion of outlying samples, every sample that was a candidate for deletion was assessed in terms of its effect on the species optima if the sample was removed; i.e., whether it affected the representation of certain species known to be important in

particular sections of the fossil core data (e.g. *Thalassiosira rudolfi*, see *section 5.6* and **Chapter 6**) in the training set and whether it improved the performance of the conductivity model. Logical reasons for and against the deletion of samples were also employed such as lake type (e.g. some hypersaline sites were removed), general unconformity of samples (e.g. the unusual flora associated with Lake Kyogo) or whether sample type (e.g. pool or rock scrape as opposed to a lake surface sediment) may have been an issue (i.e. Blue Pool sample was not a lake, rather a very slow flowing river).

5.5 Results

5.5.1 Exploratory analyses of the training set

Of the 227 taxa identified during diatom analysis of the all surface sediments, 7 species (given '9999' coding in CANOCO; see **Appendix A**) could not be resolved to species level and were excluded from further analysis, after the transformation of counts to percentages. The remaining 220 taxa represent over 98% of all valves counted.

Exploratory ordination analyses were carried out on the Mills_40 dataset, as this particular dataset had 'full' corresponding water chemistry (not just basic limnological variables [e.g. conductivity, depth and human impact] cf. Mills_58). The ordination was applied to 0.5% screened data, which included 140 taxa (of 173 in this smaller dataset, and after the removal of the 7 taxa not resolved to species level). The initial analyses suggested that Lakes Kitigata and Kyogo (samples 13 and 17; Figure 5.3 and 5.4) were potential outliers. Lake Kitigata is the only hypersaline lake in this dataset and Lake Kyogo has a unique flora not shared by other lakes (e.g. dominated by *Eunotia* species). As such, these lakes were removed and the analyses rerun. Initial DCA of the Mills_40 diatom data on untransformed, square root and log transformed percentages data (species >0.5%, rare species down-weighted and Kitigata and Kyogo removed) revealed axis 1 gradient lengths of 3.34 (√) – 5.66 (none) SD units. The resultant gradient lengths for all data transformations were greater than >2 SD, suggesting unimodal methods were the most appropriate for further analysis (CA and DCA; Hill and Gauch, 1980; ter Braak, 1995; Table 5.8).

The CA indicated an arch in the data (Figure 5.3). The arch is a distortion or artifact in an ordination diagram, in which the second axis is an arched function of the first axis and is caused by the unimodal distribution of species along gradients (Leps

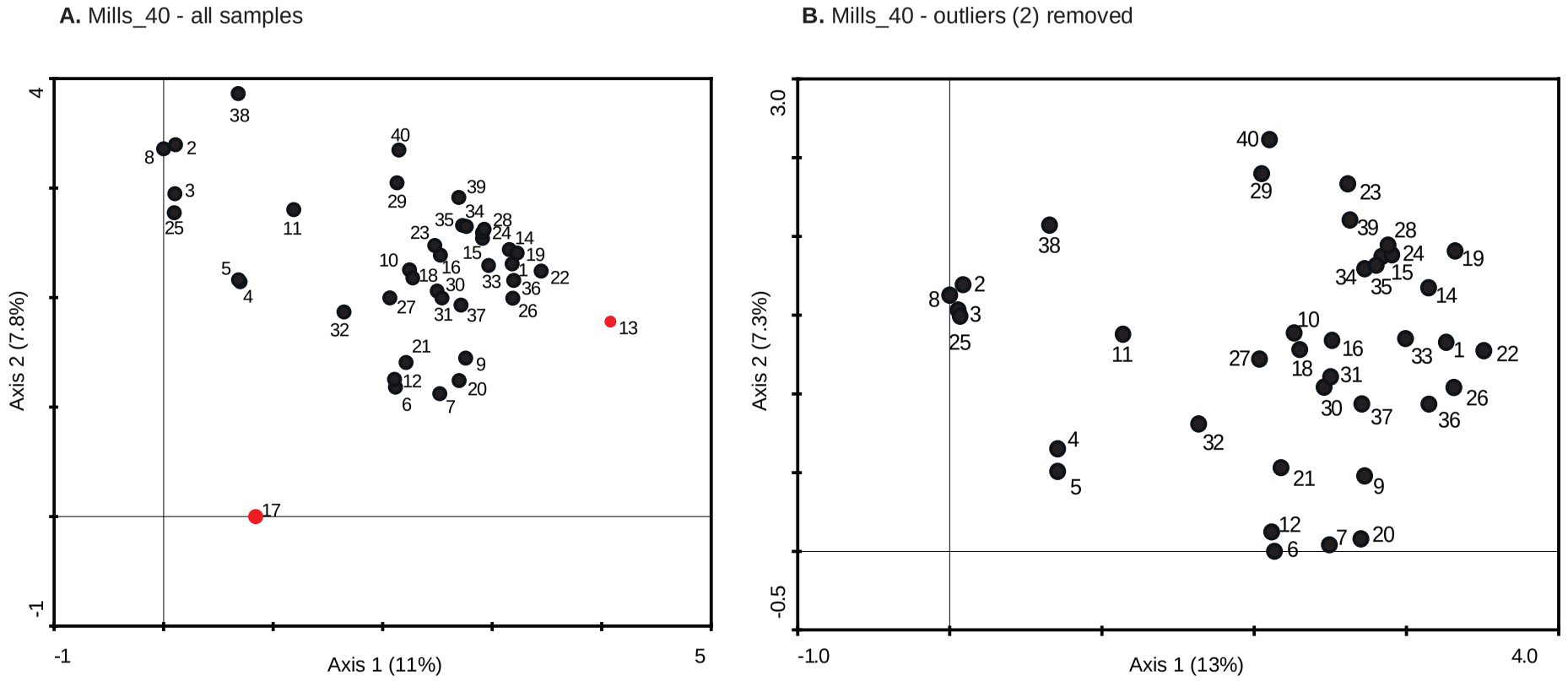

Figure 5.3 *Detrended Correspondence Analysis (DCA) with log transformation (see **Table 5.8**) on* **(A)** *the Mills_40 dataset (40 samples), the samples highlighted in red have been identified as outliers and* **(B)** *Mills_40 after the removal of outliers Kitigata and Kyogo (13 and 17).*

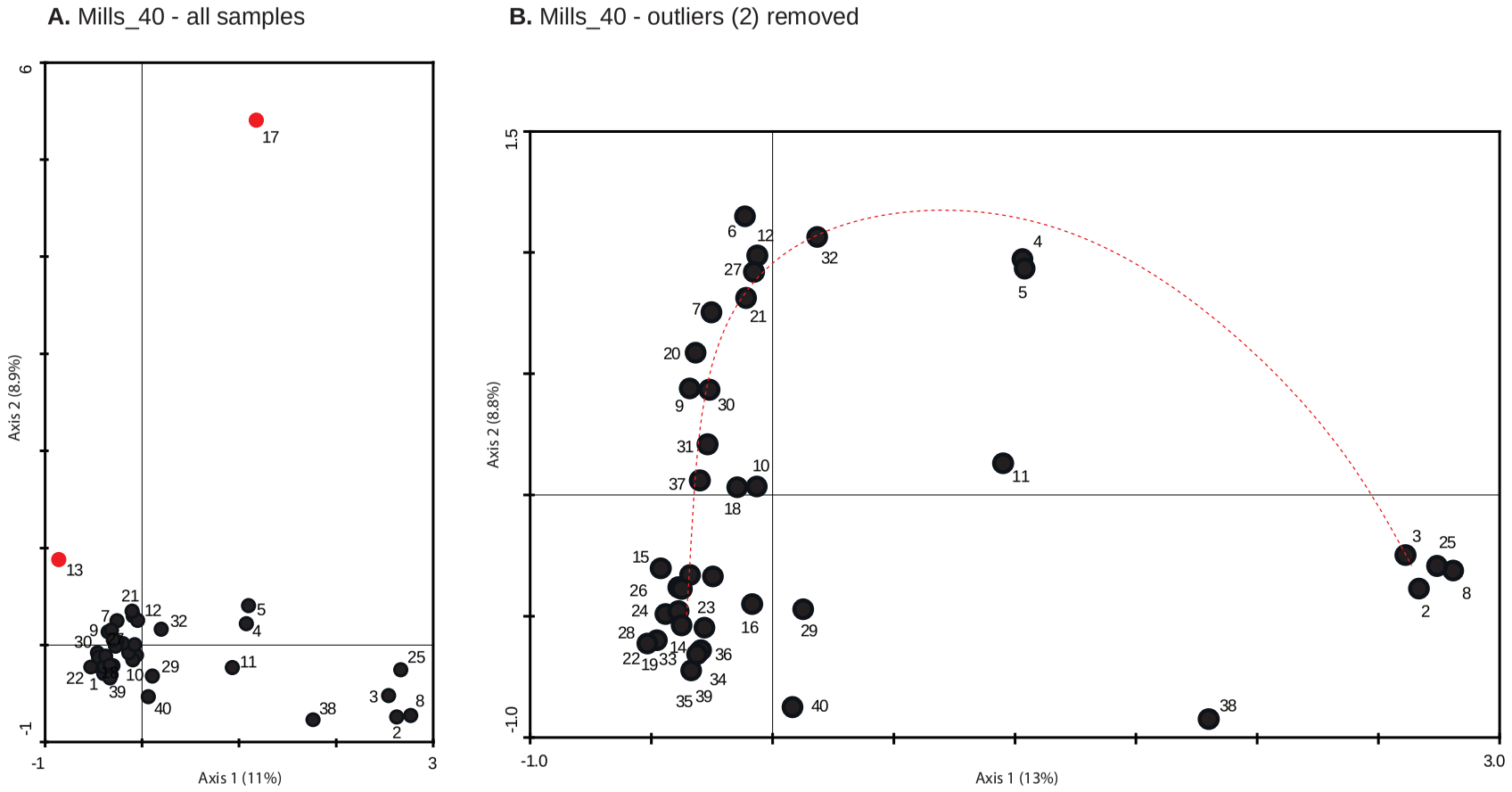

Figure 5.4 *Correspondence Analysis (CA) with log transformation on* **(A)** *the Mills_40 dataset (40 samples), outliets are highlighted in red* **(B)** *Mills_40 after the removal of outliers Kitigata and Kyogo (13 and 17). After the removal of the two outliers, the arch in the data is evident, suggesting detrending of the data and the use of DCA as an exploratory tool is a more appropriate technique.*

Table 5.8 *Comparison of DCA gradient lengths and percentage variance explained by axes 1 and 2 using different data transformations. >0.5%*

Dataset	Outliers omitted		Transformations - Axis 1			Transformations – Axis 2		
			None	√	Log	None	√	Log
Mills_40		Eigenvalues	0.858	0.560	0.562	0.694	0.359	0.344
		Gradient length	5.890	3.764	4.079	6.828	3.838	3.863
		% variance	8.7	11.4	11.3	7.0	7.3	7.0
		Total inertia	***9.874***	***4.909***	***4.957***			
Mills_40	Kitigata	Eigenvalues	0.857	0.559	0.561	0.640	0.353	0.341
		Gradient length	5.743	3.391	3.551	4.729	3.702	3.869
		% variance	9.3	12.3	12.3	7.0	7.8	7.4
		Total inertia	***9.183***	***4.538***	***4.571***			
Mills_40	Kitigata, Kyogo	Eigenvalues	0.859	0.561	0.563	0.574	0.276	0.306
		Gradient length	5.662	3.340	3.509	3.714	2.117	2.615
		% variance	10.2	13.4	13.5	6.8	6.6	7.3
		Total inertia	***8.445***	***4.180***	***4.185***			

and Šmilauer, 2003). Therefore DCA was more appropriate for further analyses. DCA was used to reveal major patterns of variation within the diatom data (Figure 5.4). Detrending was by segments and rare taxa were down-weighted. Between 10.2% (none) and 13.5% (%) of species variance was explained on axis 1, and a further 6.6 (√) to 7.3% (%) on axis 2 in the DCA ordinations (Table 5.8). Broken stick analyses revealed that axes 1 and 2 were both significant (**Appendix B**).

Principal components analysis (PCA) of all of the environmental variables is shown in Figure 5.5. Axis 1 (explaining 32.9% of the environmental data) is highly correlated with conductivity and the major ion concentrations, as well as TP and TN, whilst axis 2 (21.4%) contrasts lakes with no human impact in their catchments with those whose catchments are partially impacted. To ensure that axis 1 was not driven by the hypersaline lake Kitigata, and axis 2 not driven by Lake Kyogo, both of these outliers were removed from the PCA ordination. The removal of the outliers Lakes Kitigata and Kyogo do little to change the main drivers or percentage variance explained on either axes 1 (35.8%) and 2 (20.1%; Figure 5.5 and Table 5.9). Broken stick analyses revealed that axes 1 and 2 were both significant (**Appendix B**).

Table 5.9 *Comparison of PCA percentage variance explained by axes 1 and 2 when outliers are included and omitted from the ordination.*

Dataset	No Sites	Outliers		Axis 1	Axis 2
Mills_40	40		Eigenvalues	0.329	0.214
	40		Variance (%)	32.9	21.4
Mills_40	38	Kitigata, Kyogo	Eigenvalues	0.358	0.200
	38	Kitigata, Kyogo	Variance (%)	35.8	20.1

5.5.2 Constrained ordinations

Despite the indirect gradient analysis CA suffering from the arch effect (corrected using DCA; Gauch, 1982), it was not apparent in the CCA analysis (cf. Figure 5.6), so detrending of the data (DCCA) was not employed. CCA is a far more robust technique, and is not seriously affected by the arch effect (although in some circumstances it can occur; Palmer, 1993).

Sites were originally chosen for the construction of a conductivity model and DCCA was used to estimate conductivity gradient length (Birks, 1995). Results of the

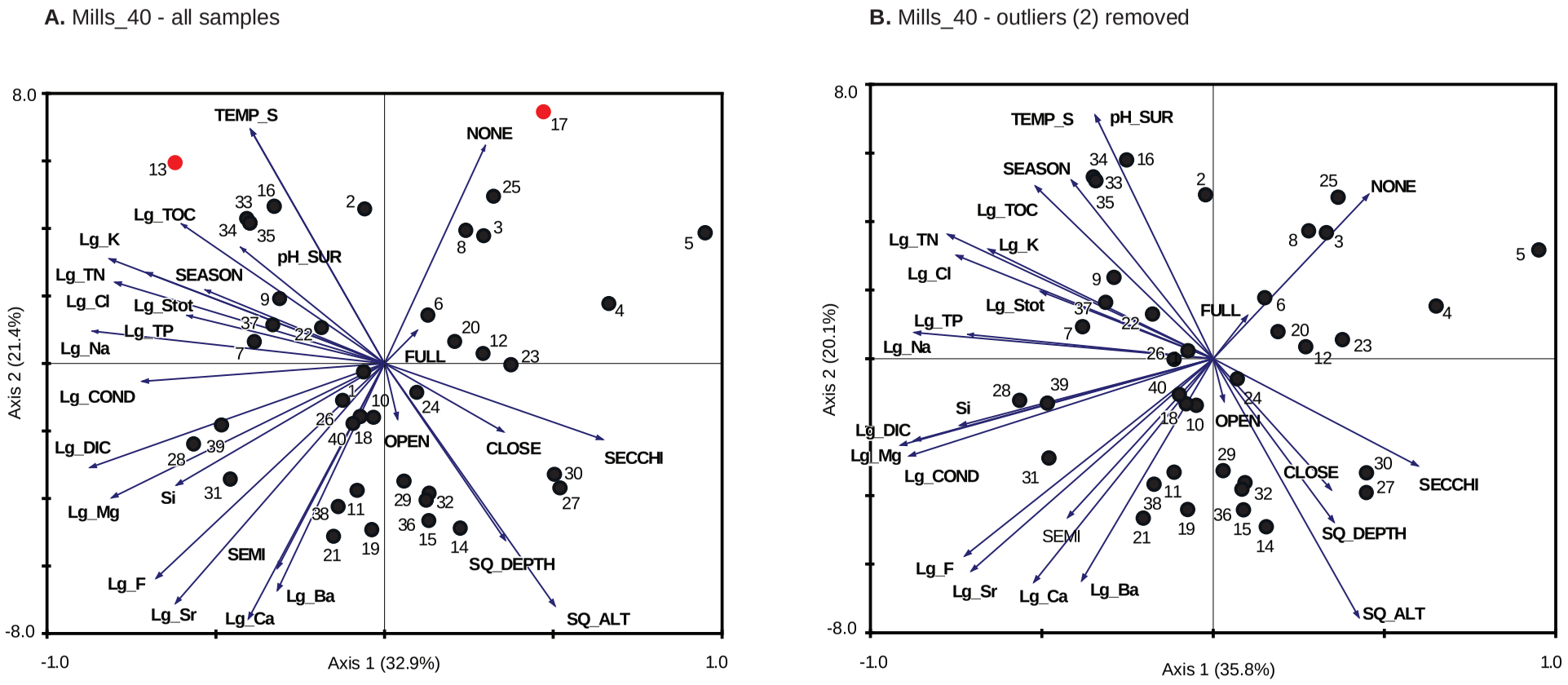

Figure 5.5 *Principal Components Analysis (PCA) of all the measured environmental variables from the crater lake training set.* **(A)** *illustrates the relationship between samples and environmental variables for the full 40 lake taining set (Mills_40), the outliers are higlighted in red.* **(B)** *illustrates the same analysis but with the outliers Lake Kitigata (13) and lake Kyogo (17) removed.*

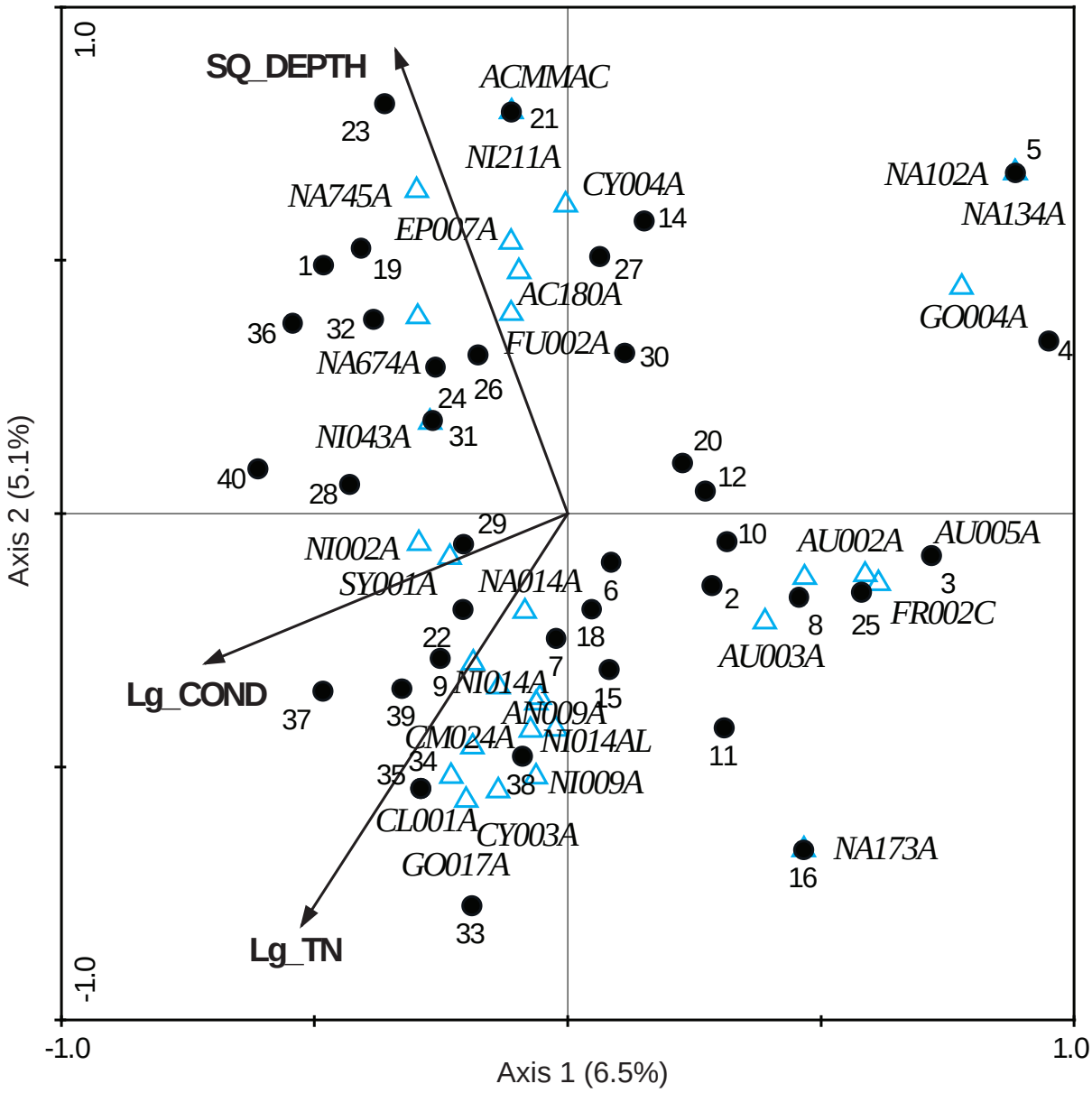

Figure 5.6 *Canonical Correspondence Analysis (CCA) triplot of Mills_40 (with outliers Kitigata and Kyogo removed) showing (1) three forward-selected environmental variables (vectors); (2) surface sediment samples; (3) WA optima of 32 diatom taxa (>10% abundance; open triangles). Diatom species are given as codes, full names can be found in* ***Appendix A****.*

DCCA analysis on Mills_40 (with these 2 outliers removed above) revealed an axis 1 gradient length of 3.649 and CCA revealed eigenvalues of 0.531 (λ_1) and 0.296 (λ_2), accounting for 19.7% of the total variation in the diatom data (Table 5.10). This low percentage explained is relatively typical of such noisy datasets with large numbers of taxa and many zero values in the species matrix (cf. Davies *et al*., 2002). The patterns of species and sites under CCA were similar regardless of the species transformation used and showed close correspondence to the unconstrained ordinations with 19% explained on the first two CCA axes (log transformation) using the full data set (18.3% on first two DCA axes) and 19.7% explained on the corresponding first 2 CCA axes with Lakes Kitigata and Kyogo omitted from the analyses (compared to 20.8% on the first two DCA axes).

Table 5.10 Results of CCA analyses on the Mills_40 dataset (with outliers Kitigata and Kyogo removed). DCCA was used to estimate the gradient length of axis 1.

Dataset	Outliers omitted		Axis 1	Axis 2
Mills_40	Kitigata, Kyogo	Eigenvalues	0.531	0.296
		% variance	12.7	7.0
		Total inertia	***4.15***	
		DCCA Gradient length	*3.649*	

When all 26 environmental variables were included in the CCA (manual forward selection, n = 999 Monte Carlo permutations) using the Mills_40 dataset with the two outliers omitted, there was redundancy amongst some of the variables. These variables were identified as those with high variance inflation factors (VIFs >20; Table 5.11). In the Mills_40 dataset, conductivity (Lg_COND) exhibited one of the highest VIFs. This is perhaps unsurprising given that conductivity is a measure of the ionic content of the water (and is likely explained by and has a positive correlation with Na, K, Mg, F, Sr, Ba and DIC; Table 5.12). As conductivity is the more ecologically plausible and the most widely understood variable for explaining diatom variance, the major ions and DIC were removed from the CCA. This caused a reduction in the VIF for conductivity (<10; Table 5.13). This subset of variables with low VIFs were reduced to a smaller subset of environmentally significant variables using forward selection with Monte Carlo permutations.

Table 5.11 *Variance inflation factors (VIF) for all 26 environmental variables (Mills_40). Those highlighted have critical VIF values (>20).*

Variable	Weighted mean	SD	VIF
NONE	0.14	0.35	6.04
SEMI	0.72	0.45	8.90
FULL	0.14	0.35	0.00
OPEN	0.06	0.24	2.16
SEASON	0.19	0.40	2.32
CLOSE	0.74	0.44	0.00
SQ_DEPTH	5.42	2.32	5.48
SECCHI	181.07	179.38	7.12
pH_SUR	25.28	2.04	10.44
TEMP_S	25.28	2.04	0.00
Lg_COND	***2.58***	***0.29***	***44.91***
SQ_ALT	34.70	2.35	9.90
Lg_TP	1.34	0.50	7.24
Lg_TN	2.61	0.35	18.56
Lg_Na	***1.07***	***0.54***	***31.84***
Lg_K	***1.19***	***0.45***	***41.45***
Lg_Ca	1.31	0.27	14.95
Lg_Mg	***1.34***	***0.31***	***32.32***
Lg_Sr	***-0.10***	***0.47***	***41.48***
Lg_Ba	***-0.94***	***0.76***	***25.66***
Lg_F	***-0.23***	***0.46***	***80.45***
Lg_Cl	0.70	0.48	15.76
Lg_DIC	***1.62***	***0.30***	***136.32***
Si (mg/l	13.26	5.62	4.65
Lg_Stot	0.10	0.63	6.09
Lg_TOC	0.69	0.39	8.44

Table 5.12 *Correlation matrix of all environmental variables. The coefficients highlighted are those that have are significant (tested using Pearson's product moment) with conductivity, causing the variable to have a high VIF.*

	None	Semi	Full	Open	Season	Close	Depth	Secchi	pH	Temp	**Cond**	Alt.	TP	TN	Na	K	Ca	Mg	Sr	Ba	F	Cl	DIC	Si	Stot	TOC	
None	1.00																										
Semi	-0.65	1.00																									
Full	-0.16	-0.64	1.00																								
Open	-0.11	0.16	-0.10	1.00																							
Season	0.01	0.14	-0.20	-0.13	1.00																						
Close	0.05	-0.22	0.24	-0.44	-0.83	1.00																					
Depth	-0.15	0.20	-0.11	0.21	-0.33	0.18	1.00																				
Secchi	0.26	-0.13	-0.10	-0.13	-0.30	0.34	0.54	1.00																			
pH	0.23	-0.21	0.04	-0.15	0.45	-0.32	-0.27	-0.26	1.00																		
Temp	0.23	-0.21	0.04	-0.15	0.45	-0.32	-0.27	-0.26	1.00	1.00																	
Cond	-0.51	0.45	-0.07	-0.01	0.17	-0.15	-0.17	-0.42	0.03	0.03	1.00																
Alt.	-0.24	0.15	0.05	0.19	-0.52	0.36	0.42	0.38	-0.68	-0.68	-0.22	1.00															
TP	-0.23	0.11	0.10	-0.02	0.29	-0.25	-0.37	-0.51	0.35	0.35	0.52	-0.32	1.00														
TN	-0.30	0.31	-0.11	0.14	0.41	-0.45	-0.51	-0.79	0.20	0.20	0.45	-0.40	0.49	1.00													
Na	-0.34	0.40	-0.18	-0.03	0.32	-0.27	-0.31	-0.38	0.28	0.28	**0.84**	-0.49	0.47	0.55	1.00												
K	-0.18	0.15	-0.01	-0.21	0.42	-0.27	-0.44	-0.38	0.50	0.50	**0.71**	-0.65	0.45	0.52	0.88	1.00											
Ca	-0.48	0.35	0.03	0.13	-0.09	0.01	0.09	-0.23	-0.23	-0.23	0.58	0.37	0.51	0.13	0.24	0.05	1.00										
Mg	-0.54	0.42	0.00	-0.12	0.23	-0.14	-0.08	-0.35	0.20	0.20	**0.90**	-0.19	0.53	0.35	0.75	0.67	0.63	1.00									
Sr	-0.51	0.56	-0.21	0.00	0.02	-0.02	0.07	-0.17	-0.10	-0.10	**0.78**	0.15	0.45	0.14	0.53	0.30	0.80	0.79	1.00								
Ba	-0.32	0.41	-0.21	0.06	-0.12	0.08	0.10	-0.02	-0.19	-0.19	0.39	0.36	0.36	-0.04	0.15	-0.08	0.68	0.41	0.82	1.00							
F	-0.42	0.47	-0.19	0.00	-0.02	0.01	0.06	-0.20	-0.06	-0.06	**0.79**	0.05	0.55	0.15	0.55	0.31	0.77	0.76	0.95	0.80	1.00						
Cl	-0.22	0.10	0.08	-0.09	0.30	-0.22	-0.34	-0.44	0.39	0.39	0.63	-0.59	0.57	0.61	0.82	0.83	0.06	0.55	0.28	0.05	0.38	1.00					
DIC	-0.55	0.42	0.01	0.00	0.20	-0.18	-0.14	-0.43	0.10	0.10	**0.96**	-0.22	0.62	0.49	0.83	0.71	0.62	0.93	0.77	0.38	0.78	0.68	1.00				
Si	-0.47	0.41	-0.06	-0.04	0.12	-0.09	0.01	-0.27	0.11	0.11	0.70	-0.28	0.51	0.33	0.65	0.49	0.53	0.68	0.60	0.33	0.66	0.56	0.72	1.00			
Stot	0.02	0.20	-0.29	0.01	0.26	-0.24	-0.22	-0.40	0.39	0.39	0.36	-0.33	0.32	0.32	0.45	0.27	0.18	0.35	0.29	0.10	0.35	0.25	0.33	0.32	1.00		
TOC	-0.20	0.19	-0.04	0.11	0.55	-0.55	-0.49	-0.70	0.48	0.48	0.18	-0.50	0.52	0.75	0.27	0.35	0.05	0.21	0.03	-0.02	0.03	0.38	0.24	0.26	0.27	1.00	1.00

Table 5.13 *Variance inflation factors (VIF) for 19 environmental variables after the removal of those variable with high colinearity (**Table 5.12**).*

Variable	Weighted mean	SD	VIF
NONE	0.14	0.35	3.38
SEMI	0.72	0.45	3.04
FULL	0.14	0.35	0.00
OPEN	0.06	0.24	1.34
SEASON	0.19	0.40	1.95
CLOSE	0.74	0.44	0.00
SQ_DEPTH	5.42	2.32	2.45
SECCHI	181.07	179.38	4.80
pH_SUR	25.28	2.04	3.41
TEMP_S	25.28	2.04	0.00
Lg_COND	2.58	0.29	6.55
SQ_ALT	34.70	2.35	6.85
Lg_TP	1.34	0.50	3.75
Lg_TN	2.61	0.35	7.36
Lg_Ca	1.31	0.27	7.72
Lg_Cl	0.70	0.48	6.30
Si (mg/l	13.26	5.62	4.18
Lg_Stot	0.10	0.63	1.99
Lg_TOC	0.69	0.39	6.69

5.5.3 Forward selection and variance partitioning

After the direct gradient technique of CCA was performed on the full dataset, a subset of significant environmental variables was determined using forward selection with a Bonferroni adjustment and Monte Carlo permutation tests (n = 999). This analysis identified three environmental variables that are independently significant in explaining variation in the diatom data: conductivity, total nitrogen (TN) and depth.

The results of the partial CCA using the three environmental variables are given in Tables 5.14 and 5.15, which explains 15.8% of the variation in the whole dataset. Monte Carlo permutations performed on axis 1 and all canonical axes demonstrate that all models are significant ($p < 0.001$). Relationships between the 3 significant variables, the 38 surface sediment samples and the dominant species (>10%) are shown in a CCA triplot (Figure 5.6). In the CCA triplot, surface sediment samples located close to each other are similar in species composition, and species located near to them in the ordination are the dominant taxa within those samples. The order of the sample along the environmental vector approximates the order of the sample along the measured environmental gradient. The origin represents the mean value of the environmental variable in the dataset. The position of a species also approximates its weighted average (WA) optimum relative to other species and approximates its relationship to the environmental variables (Pienitz *et al*., 1995). Where small angles exist between the environmental vectors, the environmental variables are closely related. Angles of 90° suggest there is little correlation between the variables and angles closer to 180° are indicative of a negative correlation between the measured variables.

Table 5.14 *CCA of diatom (all species > 0.5%) and reduced environmental dataset after forward selection.*

	CCA axes			Reduced model (total)
	1	2	3	
Eigenvalues	0.376	0.221	0.185	
p-value				0.001
% variance of species data	7.6	4.5	3.7	15.8
Sum of all canonical eigenvalues				0.783
Total inertia				4.957

The results of the variance partitioning are shown in Figure 5.7 and Table 5.15. The three significant environmental variables used in the variance partitioning account for a total of 15.8% of the variance in the diatom data. The total explained variance is

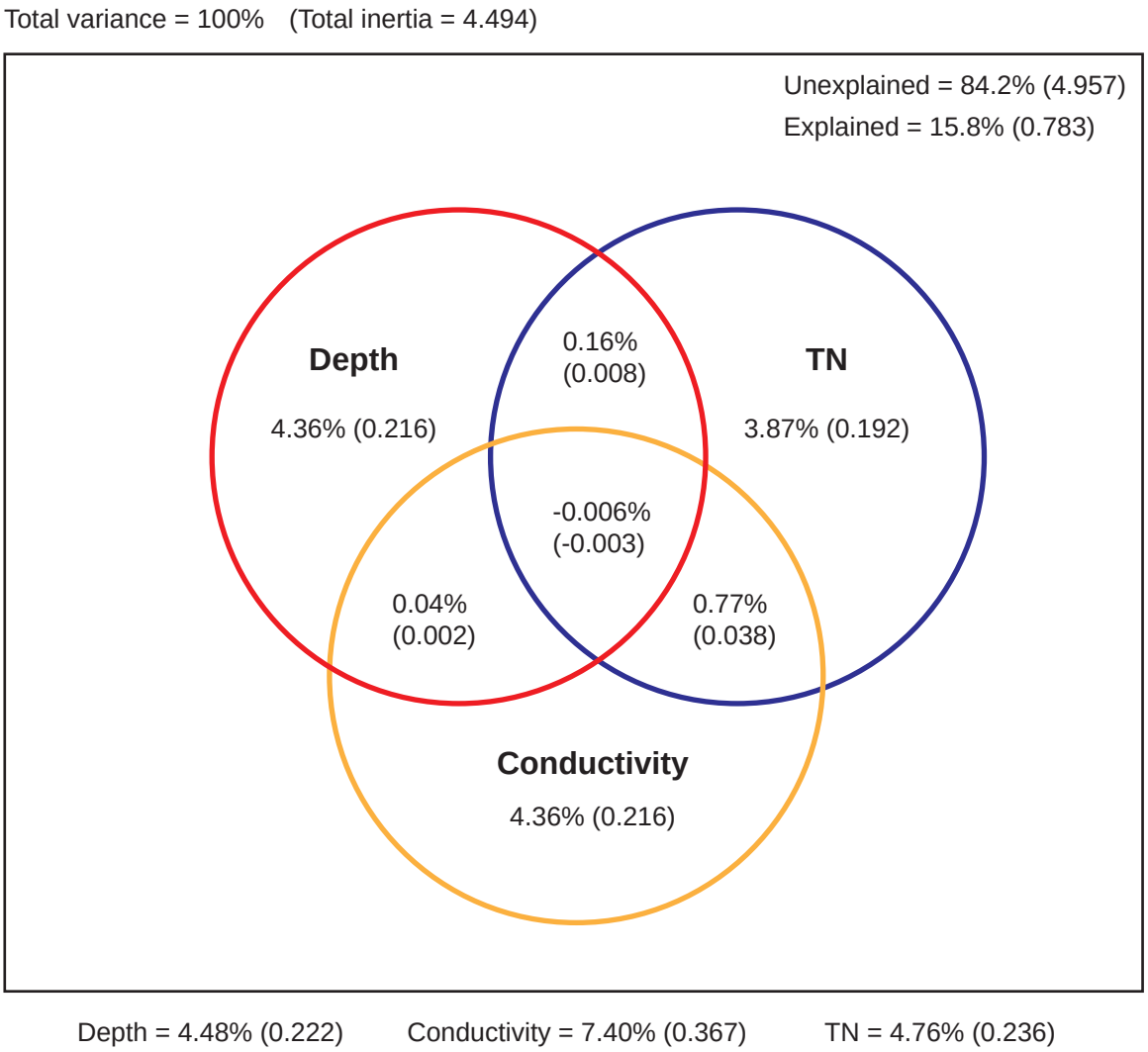

Figure 5.7 *Diagram showing the results of variance partitioning for the three environmental variables for the Mills_40 training set. All of the environmental variables were significant in the partial CCA ($p < 0.05$; see **Table 5.15**).*

predominantly composed of unique contributions from variables representing conductivity (4.21%), total nitrogen (TN; 4.53%) and depth (5.29%; Table 5.15 and 5.16). The variance due to interactions or conditional effects between pairs of gradients is low (the very small negative number [-0.006%] representing the overlap between conductivity, TN and depth is likely the result of a rounding error). This suggests the three variables make large and unique contributions to the explained variance. These results also indicate that there is the potential for independent transfer functions to be developed for each of the variables.

Table 5.15 *Results of variance partitioning of the 3 forward selected environmental variables calculated using CCA (see **Tables 5.15**, **5.16** and **Figure 5.7**).*

Explanatory variable	Co-variable	Eigenvalue	% explained	*P* value
Depth	n/a	0.222	4.48	0.004
Conductivity	n/a	0.367	7.40	0.001
TN	n/a	0.236	4.76	0.006
Depth	Conductivity	0.224	4.52	0.002
Depth	TN	0.217	4.38	0.006
Depth	Conductivity, TN	0.216	4.36	0.003
Conductivity	Depth	0.369	7.44	0.001
Conductivity	TN	0.332	6.70	0.001
Conductivity	Depth, TN	0.330	6.66	0.001
TN	Conductivity	0.200	4.03	0.020
TN	Depth	0.231	4.66	0.008
TN	Conductivity, Depth	0.192	3.87	0.013
Total inertia		*4.957*		
Sum of canonical axes		*0.783*		

Table 5.16 *Unique variance explained by significant variables using Canonical Correspondence analysis (CCA) variance partitioning for the 40 lake diatom dataset.*

Dataset	Unique explanation			
	Variable	λ_{var}	Variance (%)	*p* level (n = 999)
Mills_40	Log Conductivity (µS cm^{-1})	0.358	4.21	0.002
	Log TN (µg l^{-1})	0.385	4.53	0.001
	Sq Depth (m)	0.449	5.29	0.001

5.5.4 Diatom response to conductivity

Unimodal models assume that diatom taxa respond with a distinct single peak (optima), with symmetric distributions (tolerance) along the environmental gradient under investigation. Whilst the gradient length of the first unconstrained and constrained axes (DCA = 5.89 SD; CCA = 8.878 SD) of the diatom data indicates that diatom species' responses were largely unimodal for the Combined_76 dataset, the form of response of individual species was tested using the maximum-likelihood method of Huisman-Olff-Fresco (HOF; Huisman *et al.* 1993; Figure 5.8; Table 5.17). Statistical analyses of species response, using HOF for species present in at least 10 samples, indicated a range of responses, from symmetric unimodal responses (e.g. *Amphora copulata*, *Fragilaria tenera* and *Gomphonema pumilum*) to skewed unimodal responses (e.g. *Amphora pediculus* and *Aulacoseira granulata*) and sigmoidal responses (e.g. *Amphora veneta* and *Aulacoseira ambigua*). The HOF analyses included 57 taxa from the Combined_76 training set. Almost 70% of the 57 taxa included have a unimodal response (HOF types IV and V; Table 5.17) to conductivity, whereas only ~7% show a monotonic decrease or increase; 24% do not show any relationship to this variable according to the HOF analyses. However, it should be noted this may be a result of a failure in the analysis, which can occur in two ways: (1) an error due to illegal mathematical operation if the function deviates too far from the solution or (2) the fitted curve is trapped in a local minimum (which manifests as a flat line; Oksanen and Minchin, 2002).

Table 5.17 *The response of 56 taxa (occurring at least 10 times) to conductivity using HOF (version 2.3; binomial distribution). The number of species fitting each model is given along with the percentage of the total responses analysed (see* ***Figure 5.8*** *also).*

HOF Model	Description	N° species	Percent (%)
V	Skewed unimodal distribution	9	15.79
IV	Symmetric unimodal distribution	30	52.63
III	Monotonic relationship with plateau	1	1.75
II	Monotonic increase or decrease	3	5.36
I	No relationship, null model	14	24.56

There is a good relationship between the distribution of diatom taxa and conductivity in the Mills training set (all 58 sites with measured conductivities; Figure 5.9), and this relationship is also apparent with the addition of more saline sites from EDDI (to form the Combined_76 model; Figure 5.10). Whilst the assumption of a

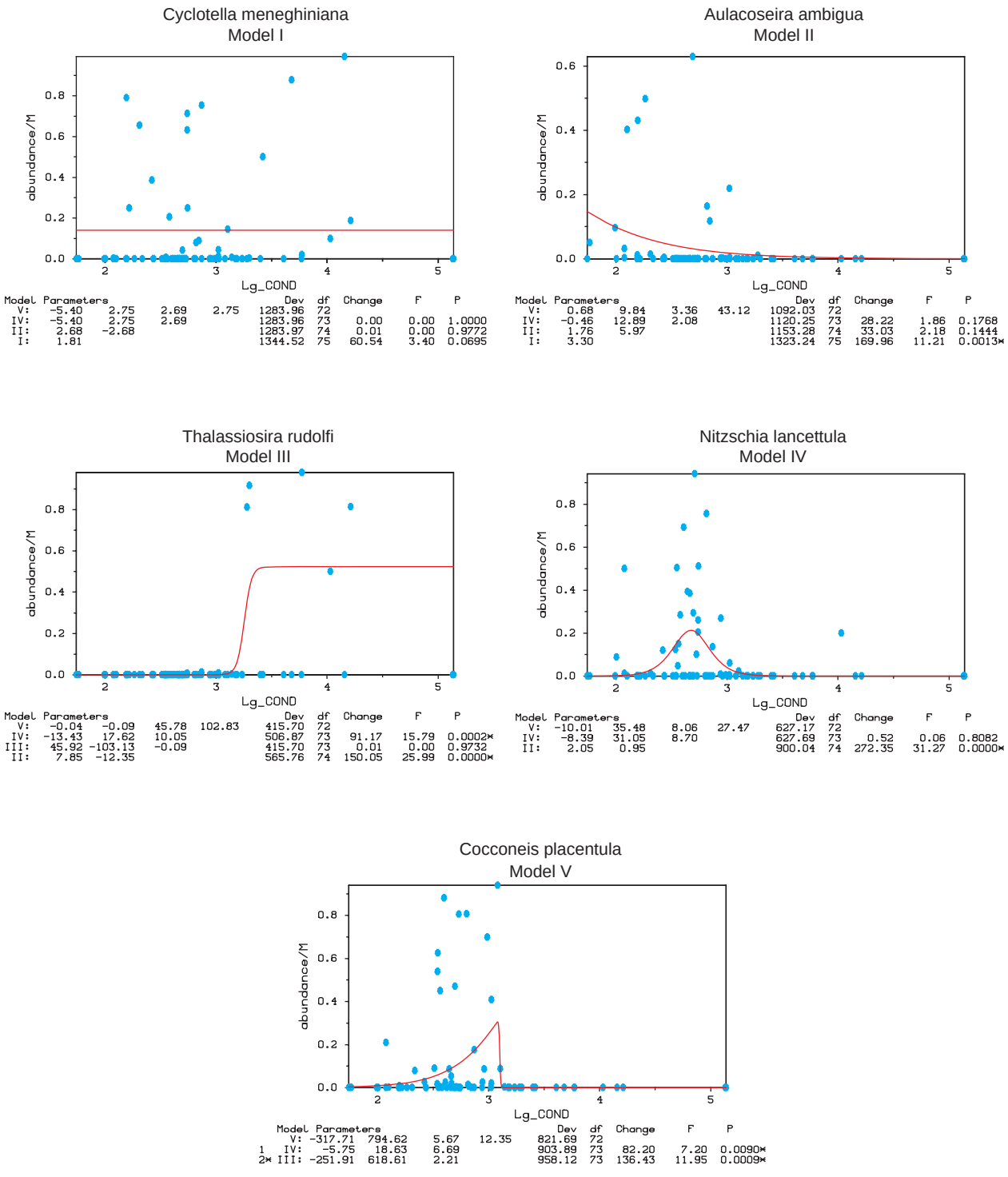

Figure 5.8 *Examples of HOF response curves I-V (Huisman et al., 1993. The relative abundance of 5 selected taxa (occurring more than 10 times in the training set and representing the response curves) are plotted against conductivity (see* ***Table 5.16****).*

unimodal response for all taxa is an oversimplification in a complex system, there is a distinct turnover over species as conductivity increases (Figures 5.9 and 5.10). In addition to this, many species demonstrate distinct optima across this gradient, although some taxa appear indifferent or eurytopic in their response to salinity across much of the gradient (e.g. *Nitzschia fonticola* and *Cyclotella meneghiniana*). Samples with the highest and lowest conductivity waters support distinct diatom floras (e.g. low conductivity sites: Lakes Kamunzuka and Kyogo and high conductivity sites Lakes Mahega and Kitigata).

5.5.5 Inference models

After exploration of the Mills_40 dataset (for which a full set of environmental variable were available), CCAs of the Mills_58 and Combined_76 were carried out to test the significance of conductivity within these datasets (ter Braak, 1986). CCA with down-weighting of rare species and log-transformed conductivity as the sole explanatory variable was performed to calculate the ratio between the eigenvalues of the first (λ_1; constrained) CCA axis and the second ($\lambda_{2;}$ unconstrained) DCA axis on all three datasets (Mills_40, Mills_58 and Combined_76; Table 5.18). This value reflects the strength of conductivity as an explanatory variable for diatom species distributions (ter Braak, 1988; Kingston *et al.*, 1992; ter Braak and Juggins, 1993). The more important an environmental variable is in explaining the variation in the diatom data, the larger the first constrained axis (λ_1) will be compared with the first unconstrained axis (λ_2; Kingston *et al*., 1992), and therefore the greater the ratio. The eigenvalue ratios for all datasets (Mills_40 [0.53], Mills_58 [0.47] and Combined_76 [0.71]) with conductivity as the sole variable suggested that the Mills_40 and Combined_76 datasets were

Table 5.18 *Results of Canonical Correspondence Analysis (CCA) for all three datasets (with outliers removed). Eigenvalue ratios (λ_1 vs λ_2) are also given (Kingston et al., 1992). The results are all based on conductivity as the sole explanatory variable.*

Dataset	Gradient length	Variance explained (%)		Eigenvalues		Ratio	Total inertia	*P*-value
	Axis 1	Axis 1	Axis 2	λ_1	λ_2			
Mills_40	0.829	5.1	9.8	0.435	0.820	0.53	8.445	0.001
Mills_58	0.806	3.5	7.3	0.386	0.809	0.47	11.065	0.001
Combined_76	0.878	4.1	5.8	0.557	0.783	0.71	13.501	0.001

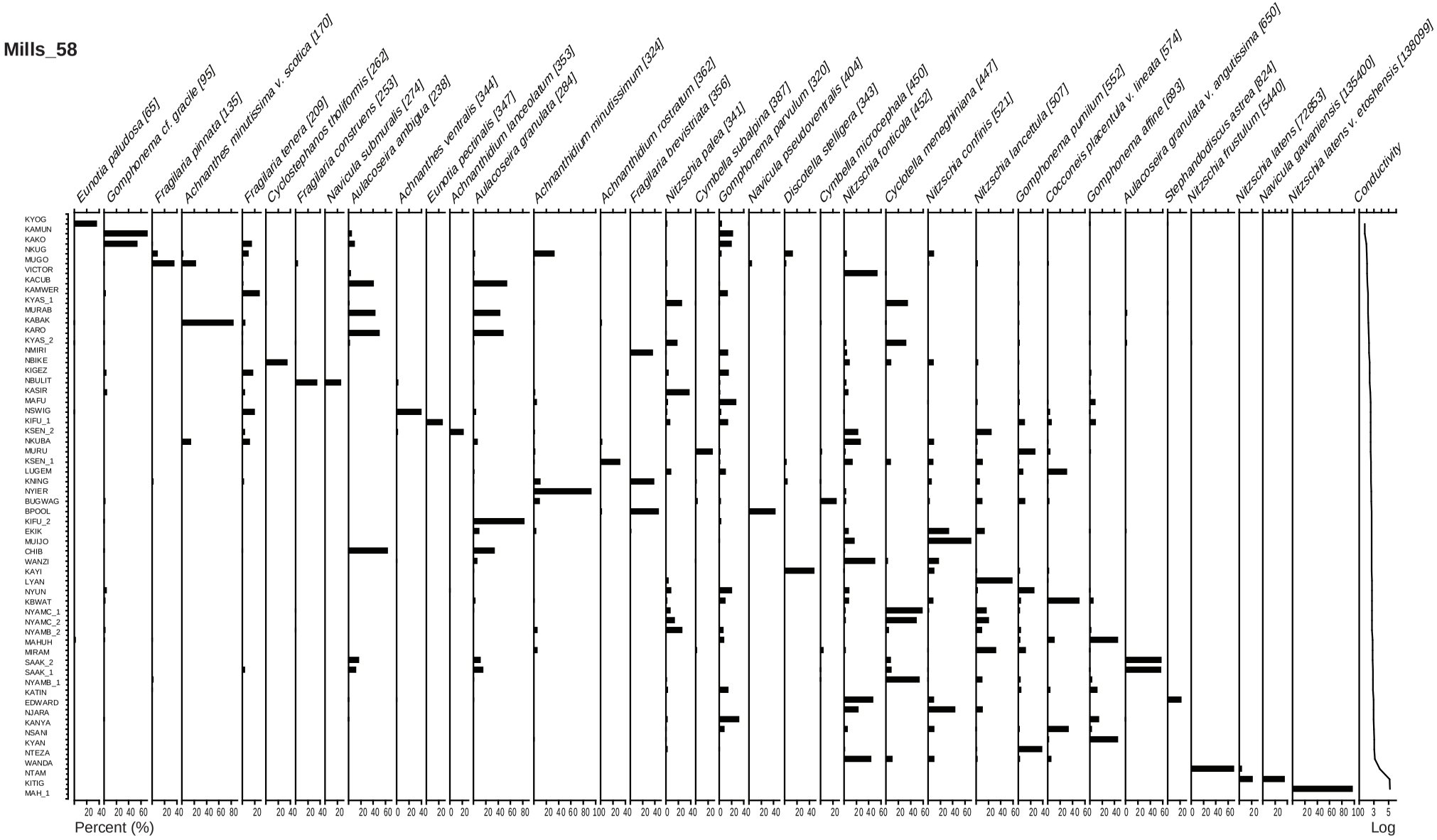

Figure 5.9 *Diatom distributions of selected taxa in surface sediments of 58 lakes, plotted as relative abundance (%). All 35 taxa >20% in any sample are shown. Sites are ordered according to their conductivity optimum from top to bottom (values shown in µS cm^{-1}), and species are ordered according to their weighted average distribution (closely corresponding to their condutivity optimum, shown in parantheses as µS cm^{-1}). Lakes are shown with lake codes, for full lake name, refer to* ***Table 5.6****.*

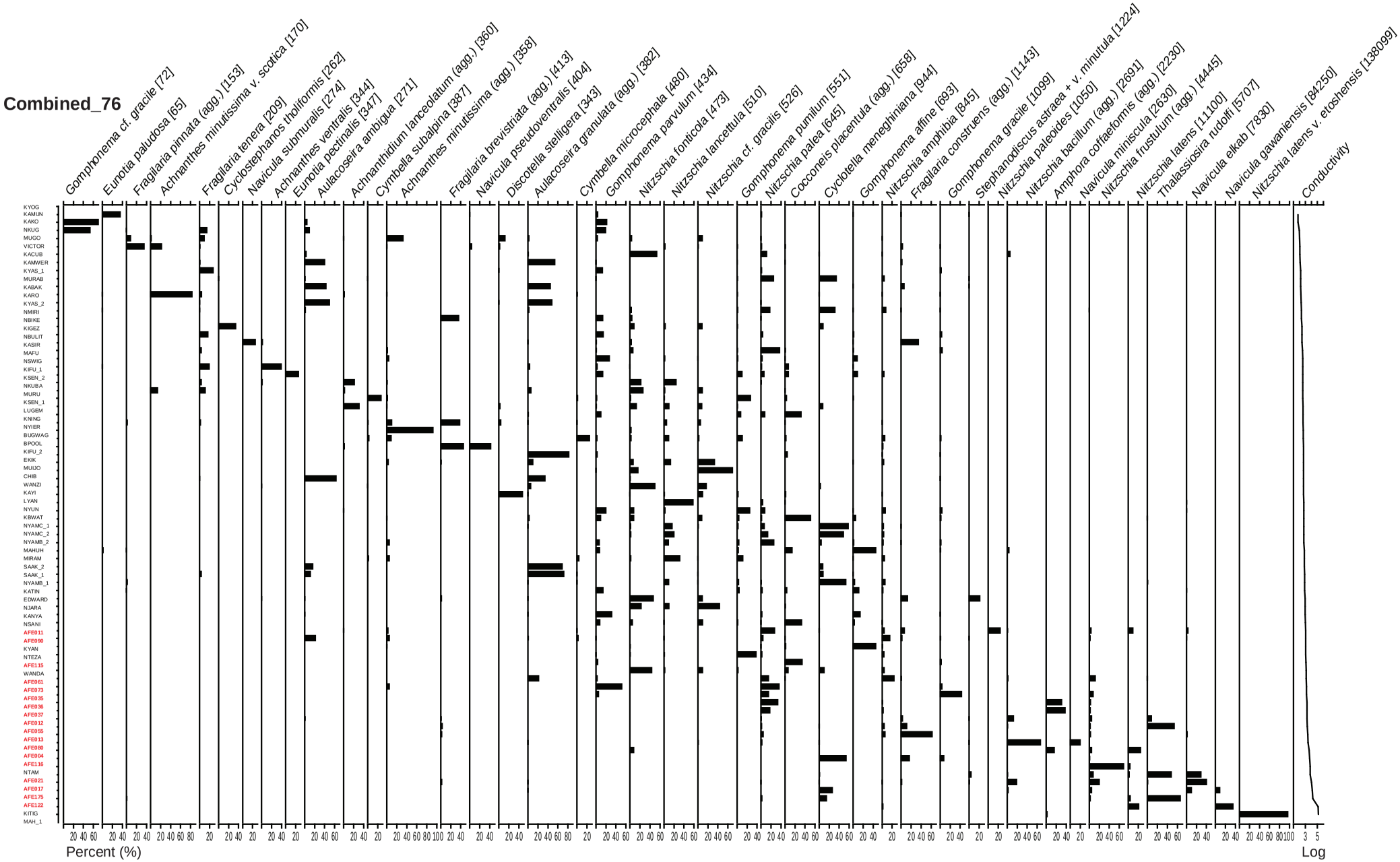

Figure 5.10 *Diatom distributions of selected taxa in surface sediments of 76 lakes, plotted as relative abundance (%). All 41 taxa >20% in any sample are shown. Sites are ordered according to their conductivity optimum from top to bottom (values shown in µS cm^{-1}), and species are ordered according to their weighted average distribution (closely corresponding to their condutivity optimum, shown in parantheses as µS cm^{-1}). Lakes are shown with lake codes, see* ***Tables 5.3*** *and* ***5.6*** *for lake names.*

suitable for the development of a transfer function. Both of these datasets had an eigenvalue ratio >0.5, suggesting that the relationship between diatom species distribution and conductivity was sufficiently strong to generate a diatom-conductivity calibration dataset (Kingston *et al*., 1992). For the Mills_40 dataset, all three forward selected variables were shown to be potentially strong enough for the development of a transfer function (all eigenvalue ratios >0.5; Table 5.19).

The gradient length for conductivity (CCA axis 1) in all datasets was >4 SD units, suggesting unimodal models (WA and WA-PLS; ter Braak and Juggins, 1993) were the most appropriate. Weighted Averaging models with and without tolerance downweighting were tested using classical and inverse deshrinking (Birks, 1995). All models were internally validated using the leave-one-out jack-knife method (Birks, 1995) and critically compared according to their root mean square error of prediction (RMSEP).

For all models two clear outliers were identified: the hypersaline lakes Mahega (1) and Kitigata. These lakes both support unique flora, with Lake Mahega (littoral sample) dominated by a form of *Nitzschia latens* v. *etoshensis* (97% of total count) and Lake Kitigata dominated by *Navicula gawaniensis* and *N. latens* (35% and 21% of total count, respectively). Other potential outliers in the training set were identified as those with a jack-knifed residual (inferred-observed) greater than the standard deviation of the environmental parameter in question (Gasse *et al*., 1995) after the removal of Lakes Mahega and Kitigata (SD = 0.52; Figure 5.11). This highlighted six other sites that were potential outliers in the dataset. Four sites were from the original crater lake dataset (Lakes Victoria, Kyogo, Nkugute and Blue Pool) and two were those added from the EDDI East Africa dataset (Marairs ol Bolossat and Lake Kikorongo).

An alternative method exists for the identification of ‘true outliers’ (Racca and Prairie, 2004) where residuals (observed-inferred) are plotted against predicted conductivity values (Figure 5.11). This method (with Kitigata and Mahega omitted) again indicates that the same six lakes in the dataset are potential outliers (Figure 5.12). All of these sites were critically inspected in terms of their flora and sample type to try and understand why they were identified as outliers in the model (Table 5.20). In all cases the reason was attributed to the diatom assemblage recorded in the surface sediment as a result of sample (or lake) type (e.g. Victoria a large lake, not a crater; Blue Pool, not a lake, rather a flowing river and Kyogo had unusual diatoms; see *section 5.4.2* [Table

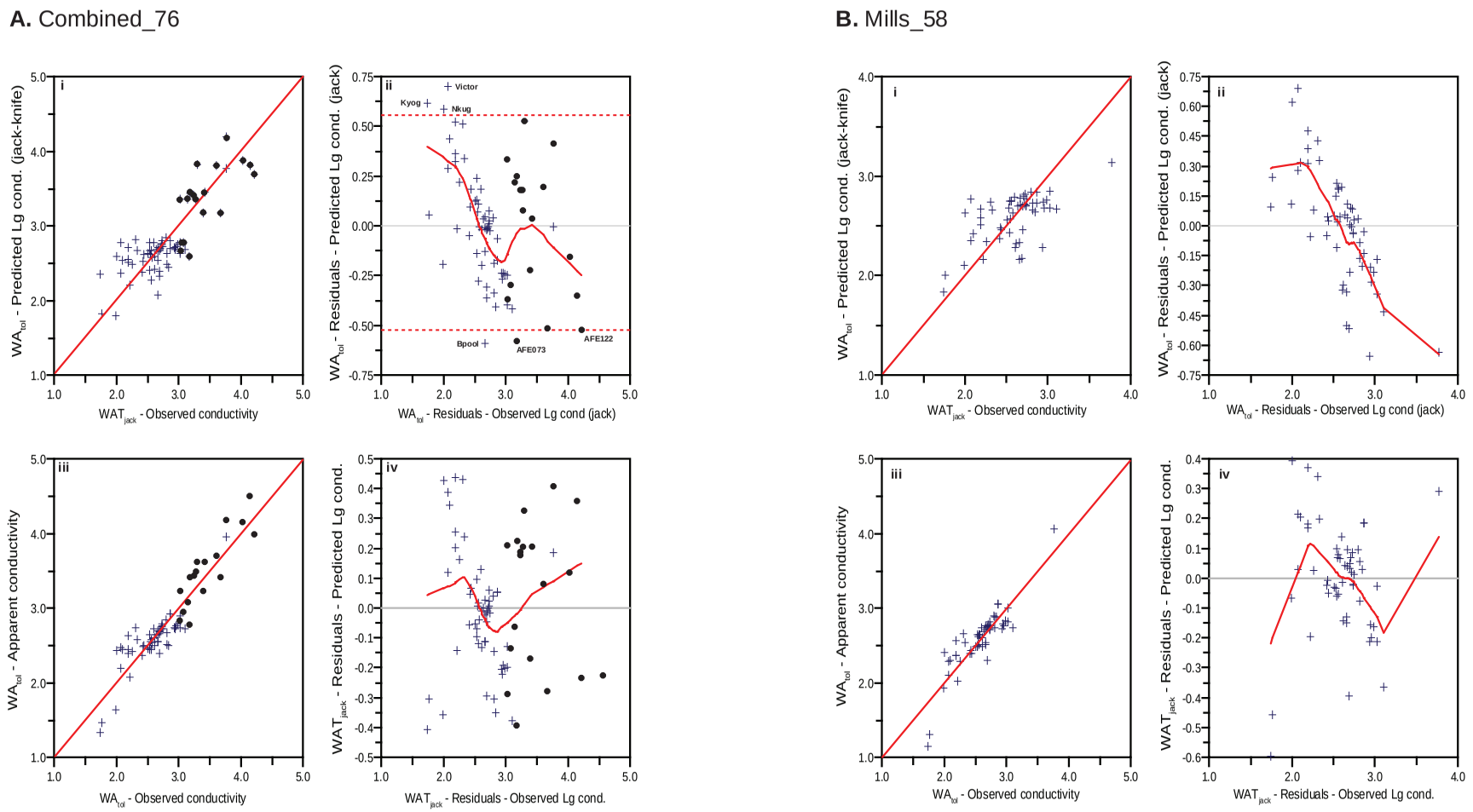

Figure 5.11 *Diatom based inference model - comparison of the best models for both the* **(A i-iv)** *Combined_76 (EDDI sites denoted as black filled circles) and* **(B i-iv)** *Mills_58 dataset. Both datasets present the results of weighted averaging model with tolerance downweighting and classical deshrinking (with leave-one-out jack-knife). The problems with the middle part of the conductivity gradient is evident im the Mills-58 model* **(A i-iv)**, *which is improved by the addition of the EDDI sites* **(A i-iv)**. *The outliers in the final model Combined_76 were identified using the standard deviation of the conductivity data (0.52 Lg conductivity units), these lakes are coded on* **(Bi)** *(refer to* ***Tables* 5.3** *and* **5.6** *for full lake names).*

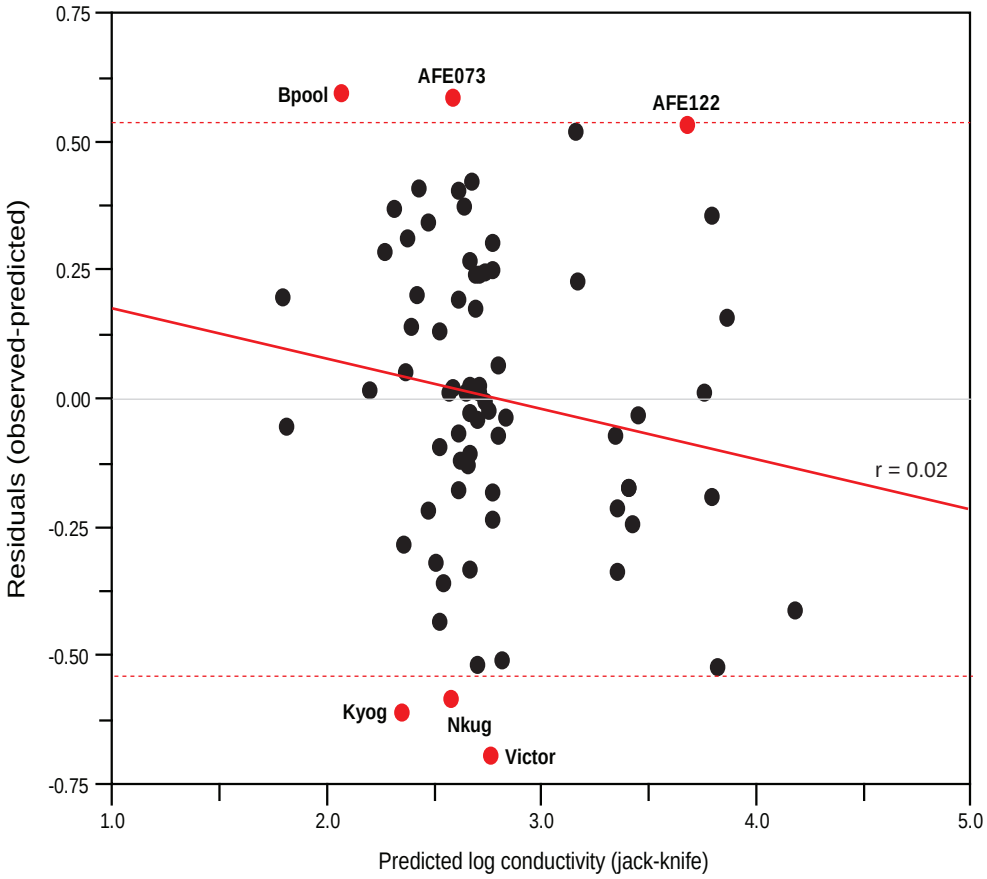

Figure 5.12 *Figure based on the method of Racca and Prairie (2004). Identification of outliers in the final diatom-conductivity model (Combined_76; weighted averaging with tolerance down-weighting [jack-knife]); saline sites Kitigata and Mahega were removed from the analysis. The dashed red line denotes the standard deviation of the conductivity data (0.52 Lg conductivity units). Potential outliers are highlighted in red. This alternative method aims to identify 'true outliers' whilst reducing the trend in the data. This method highlights the same six outliers identified in* ***Figure 5.11****.*

Table 5.19 *Results of Canonical Correspondence Analysis (CCA) for Mills_40 (with outliers removed). Eigenvalue ratios are also given (Kingston et al., 1992).*

Variable	Gradient length	Variance explained (%)		Eigenvalues		Ratio	Total inertia	*P*-value
	λ_1	λ_1	λ_2	λ_1	λ_2			
Conductivity (Cond)	0.829	5.1	9.8	0.435	0.820	0.53	8.445	0.001
Total Nitrogen (TN)	0.893	5.3	10.1	0.448	0.853	0.52	8.445	0.001
Depth	0.845	5.1	9.6	0.431	0.806	0.53	8.445	0.001

Table 5.20 *Samples omitted from the Combined_76 model. Samples were identified as their residual value was greater than the conductivity standard deviation. The reasons for omission are also based on the criteria outlined in the text (section 5.#.#).*

Sample	Dominant species	Omitted	Reason
Victoria	*Nitzschia fonticola* (53%) *Cyclostephanos dubius* (16%)	Y	Lake Victoria supports a flora recording eutrophic conditions in terms of *C. dubius*. This particular eutrophic species is not seen in any of the other crater lakes (usually species such as *C. meneghiniana*).
Nkugute	*Achnanthidium minutissimum* (32%) *Cyclotella stelligera* (12%)	Y	Lake Nkugute is a large deep lake, supporting an *A. minutissimum* assemblage, again a unique assemblage in the training set.
Blue Pool	*Fragilaria brevistriata* (45%) *Navicula pseudoventralis* (42%)	Y	Blue Pool is dominated by 2 species. Blue pool is not a true lake sample, rather a wet 'pool' in the middle of the Maramagambo forest reserve.
Kyogo	*Eunotia paludosa* (35%) *Navicula subrotundata* (18%)	Y	This lake supports a unique flora, with an assemblage dominated by *Eunotia* and oversized *Sellaphora.*
Marairs ol Bolossat	*Gomphonema parvulum* (52%) *Nitzschia paleacea* (36%)	Y	Again, this dataset is dominated by only 2 species and presents an unusual assemblage not seen elsewhere in the training set.
Kikorongo	*Cyclotella meneghiniana* (15%) *Thalassiosira rudolfi* (65%)	N	Deletion would cause under representation of *T. rudolfi* in the training set. Important fossil core species (see Chapter 6)

5.20]). Before any of these sites were deleted, the influence (leverage) of these samples on model parameters was assessed using Cook's *D* (Cook and Weisberg, 1982) and compared to the critical value of 4/n (where n = number of sites in the model; Jones and Juggins, 1995; Table 5.21). After inspection of the outlying samples, poorly fitted samples with a low (<1) Cook's *D* could be deleted safely (cf. Ryves *et al*., 2002; Mackay *et al*., 2003). Out of the six potential outliers, five were removed (Victoria, Kyogo, Nkugute, Blue Pool and Marairs ol Bolossat) from the model based on the following criteria: (1) whether removal of the outliers actually improved the model performance (r^2_{jack}) and (2) whether the removal of the outlying sample would cause some species common to the fossil core data (see **Chapter 6**) to be under represented. Only if an outlying sample fulfilled both criteria, was it removed from the model with confidence (Table 5.21). Although Lake Kikorongo could be safely deleted on the basis of the Cook's *D* analysis, it was kept in the model, as the deletion of this sample altered the conductivity optima of the taxa in the Combined_76 model. In addition to this, the removal of this site would have caused certain taxa (e.g. *Thalassiosira rudolfi*), important in the fossil core data (**Chapter 6**) to be under-represented in the training set.

Table 5.21 *Estimated Cook's D for the six potential outliers (Combined_76) as identified using the conductivity SD (0.05 critical value = 4/74).*

Sample	Residual	Cook's D	Delete Safely
Victoria	0.6989	0.0758	Y
Nkugute	0.5859	0.0531	Y
Blue Pool	-0.5898	0.0192	N*
Kyogo	0.6146	0.0583	Y
Marairs ol Bolossat	-0.5808	0.0307	N*
Kikorongo	-0.5288	0.1627	Y

* Values do not exceed the critical threshold, so samples must be carefully examined before deletion. All other samples can be deleted safely with no further considerations if necessary.

Several conductivity models were developed, based on the three datasets (Mills_40, Mills_58 and Combined_76) and using different techniques (WA, WAPLS and MAT; Tables 5.22 and 5.23). This was carried out to highlight the importance of the additional EDDI sites to the original Mills dataset. In the majority of cases, for all datasets, WA models with tolerance down-weighting proved the strongest statistically (Tables 5.23 and 5.24).

Simple weighted averaging (WA) and weighted averaging-partial least squares (WA-PLS) models out performed MAT techniques (both simple MAT and weighted averaging MAT [WMAT]). MAT and WMAT had a low r^2 for the Mills_40 and Mills_58 training sets; RMSE and maximum bias values were large. Although the Combined_76 model performed much better with an r^2 of 0.62 (WMAT), however, the RMSE and maximum bias are large (>0.3 and >0.8 log conductivity units respectively).

Weighted averaging and WA-PLS performed well on all three training sets, with an r^2 >0.75 in all cases (Table 5.22). However, WA performed much better when leave-one-out cross-validation techniques (jack-knifing) were employed. The r^2_{jack} for the WA-PLS components in many cases was much less than 0.5, although WA-PLS r^2_{jack} for the Combined_76 training set was good (r^2_{jack} = 0.67). However, this improvement was related to WA-PLS-1 component (which is the same as simple weighted averaging). As a result weighted averaging models were investigated further (Table 5.23).

Table 5.23 shows the performance of the three training sets with various outliers removed. The best model in each situation is highlighted. In all models (where outliers were omitted) WA with tolerance down-weighting performed well, though there was very little difference between samples with tolerance down-weighting and those without. Jack-knifing caused a significant reduction in the r^2_{jack} in both the Mills_40 and Mills_58 training sets, but had less of an effect on the Combined_76 training set (r^2 = 0.87, r^2_{jack} =0.74).

Weighted averaging with tolerance down weighting (WA_{tol}) models produced lower jack-knifed RMSEP for the Combined_76 model, whereas WA-PLS showed no improvement at all. In all cases, the Combined_76 dataset performed better than either of the smaller datasets. The model that was chosen performed well in terms of the best r^2_{jack} and lowest RMSEP and was based on the Combined_76 dataset using WA_{tol} with classical deshrinking (Tables 5.23 and 2.24; r^2_{jack} = 0.74, RMSEP = 0.256 log conductivity units), although the WA_{tol} with inverse deshrinking gave an almost comparable performance (r^2_{jack} = 0.737, RMSEP = 0.257). The model using classical deshrinking was also selected as it has a lower maximum bias than that using inverse deshrinking (Table 5.23). The results of the diatom conductivity model of Gasse *et al.* (1995) are displayed in table 5.23 to highlight the comparable performance of the crater lake training set to that developed for Africa. The r^2 and r^2_{jack} of both the Combined_76

Table 5.22 *Comparison of MAT, WA (see Table 5.23 also) and WAPLS for the 3 datasets (Mills_40, Mills_58 and Combined_76) with outliers removed. All modelling was carried out on 0.5% screened data (to ensure consistency with the EDDI dataset). The best model in each set is highlighted. The final model is highlighted in bold.*

Model	Method	N° Sites	N° Species	r^2	RMSE	Max bias	r^2_{jack}	RMSEP	Max bias
Mills_40 (1 outlier#)	MAT	39	138	0.14	0.3060	0.8069	--	--	--
	WMAT	39	138	0.22	0.2879	0.6947	--	--	--
Mills_58 (2 outliers*)	MAT	56	159	0.10	0.3400	1.1606	--	--	--
	WMAT	56	159	0.21	0.3171	1.1630	--	--	--
Combined_76 (7 outliers†)	MAT	69	198	0.53	0.3604	0.8944	--	--	--
	WMAT	69	198	0.62	0.3275	0.8565	--	--	--
Mills_40 (1 outlier#)	WA_Inv	39	138	0.75	0.1577	0.2934	0.33	0.2603	0.5216
	WA_Cla	39	138	0.75	0.1819	0.3151	0.36	0.2709	0.4429
	WA_{tol}_Inv	39	138	0.79	0.1443	0.2899	0.44	0.2394	0.4012
	WA_{tol}_Cla	39	138	0.79	0.1623	0.3862	0.46	0.2352	0.4054
Mills_58 (2 outliers*)	WA_Inv	56	159	0.75	0.1776	0.2544	0.14	0.3314	1.4236
	WA_Cla	56	159	0.75	0.2056	0.7462	0.15	0.3461	1.5106
	WA_{tol}_Inv	56	159	0.78	0.1662	0.2507	0.35	0.2843	0.7817
	WA_{tol}_Cla	56	159	0.78	0.1885	0.5261	0.37	0.2816	0.6339
Combined_76 (7 outliers†)	WA_Inv	69	198	0.82	0.2111	0.2733	0.66	0.2897	0.4932
	WA_Cla	69	198	0.82	0.2331	0.3838	0.67	0.3111	0.3410
	WA_{tol}_Inv	69	198	0.87	0.1797	0.2639	0.74	0.2567	0.4937
	WA_{tol}_Cla	**69**	**198**	**0.87**	**0.1927**	**0.2812**	**0.74**	**0.2560**	**0.3611**
Mills_40 (1 outlier#)	WAPLS 1	39	138	0.75	0.1577	0.2934	0.33	0.2606	0.5310
	WAPLS 2	39	138	0.82	0.1355	0.2335	0.34	0.2695	0.4214
	WAPLS 3	39	138	0.88	0.1089	0.1431	0.22	0.3618	0.5139
	WAPLS 4	39	138	0.92	0.0909	0.1086	0.19	0.4319	0.5682
	WAPLS 5	39	138	0.94	0.0767	0.1000	0.18	0.4887	0.5986
Mills_58 (2 outliers*)	WAPLS 1	56	159	0.75	0.1776	0.2540	0.14	0.3310	1.4227
	WAPLS 2	56	159	0.84	0.1406	0.1674	0.15	0.3692	1.6309
	WAPLS 3	56	159	0.89	0.1180	0.1361	0.09	0.4563	1.9320
	WAPLS 4	56	159	0.92	0.1003	0.0772	0.05	0.5702	2.3199
	WAPLS 5	56	159	0.94	0.0837	0.0593	0.05	0.6688	2.5932
Combined_76 (7 outliers†)	WAPLS 1	69	198	0.82	0.2111	0.2731	0.67	0.2858	0.5032
	WAPLS 2	69	198	0.89	0.1658	0.2072	0.59	0.3362	0.5808
	WAPLS 3	69	198	0.92	0.1374	0.1450	0.46	0.4316	0.6725
	WAPLS 4	69	198	0.94	0.1189	0.1331	0.37	0.5252	0.7389
	WAPLS 5	69	198	0.96	0.1004	0.1117	0.31	0.6247	0.7328

Outliers omitted for Mills models (*) and the combined model (†). The values in brackets indicate the lake conductivity (in $\mu S\ cm^{-1}$)

 # Lake Kitigata (134,000)
** Lakes Kitigata and Mahega (138,100)*
† Lakes Kitigata, Mahega, Victoria (119), Blue Pool (460), Nkugute (101), Kyogo (55), Marairs ol Bolossat (1500)

Table 5.23 *Comparison of methods for various weighted averaging (WA) diatom-conductivity models. Results are shown for the original crater lake models (Mills_40 and Mills_58) and for the Combined_76 model (Mills-EDDI), supplementing the original dataset with sites of 'intermediate salinities' (1000-10,000 μS cm^{-1}) from the European Diatom Database (EDDI). All modelling was carried out on 0.5% screened data (to ensure consistency with the EDDI dataset). The best model in each set is highlighted. The final model is highlighted in bold. The performance of the East African diatom-conductivity model of Gasse et al. (1995) is also included for comparison.*

Model	Method	N^o Sites	N^o Species	r^2	RMSE	Max bias	r^2_{jack}	RMSEP	Max bias
Mills_40	WA_Inv	40	143	0.90	0.1587	0.3411	0.32	0.4336	2.2218
	WA_Cla	40	143	0.90	0.1670	0.4022	0.37	0.4178	2.1026
	WA_{tol}_Inv	40	143	0.91	0.1552	0.3696	0.45	0.4157	2.1188
	WA_{tol}_Cla	40	143	0.91	0.1629	0.3775	0.50	0.3977	1.9968
Mills_40 (1 outlier[#])	WA_Inv	39	138	0.75	0.1577	0.2934	0.33	0.2603	0.5216
	WA_Cla	39	138	0.75	0.1819	0.3151	0.36	0.2709	0.4429
	WA_{tol}_Inv	39	138	0.79	0.1443	0.2899	0.44	0.2394	0.4012
	WA_{tol}_Cla	39	138	0.79	0.1623	0.3862	0.46	0.2352	0.4054
Mills_58	WA_Inv	58	165	0.90	0.1873	0.4205	0.58	0.4500	0.4205
	WA_Cla	58	165	0.90	0.1979	0.4188	0.59	0.4335	0.4188
	WA_{tol}_Inv	58	165	0.91	0.1743	0.4280	0.28	0.5227	0.4280
	WA_{tol}_Cla	58	165	0.91	0.1827	0.4273	0.29	0.5169	0.4273
Mills_58 (2 outliers*)	WA_Inv	56	159	0.75	0.1776	0.2544	0.14	0.3314	1.4236
	WA_Cla	56	159	0.75	0.2056	0.7462	0.15	0.3461	1.5106
	WA_{tol}_Inv	56	159	0.78	0.1662	0.2507	0.35	0.2843	0.7817
	WA_{tol}_Cla	56	159	0.78	0.1885	0.5261	0.37	0.2816	0.6339
Combined_76	WA_Inv	76	206	0.86	0.2383	0.3795	0.61	0.4003	1.5657
	WA_Cla	76	206	0.86	0.2574	0.3954	0.62	0.3927	1.4209
	WA_{tol}_Inv	76	206	0.89	0.2107	0.3227	0.68	0.3687	1.3003
	WA_{tol}_Cla	76	206	0.89	0.2235	0.2886	0.69	0.3572	1.1597
Combined_76 (7 outliers[†])	WA_Inv	69	198	0.82	0.2111	0.2733	0.66	0.2897	0.4932
	WA_Cla	69	198	0.82	0.2331	0.3838	0.67	0.3111	0.3410
	WA_{tol}_Inv	69	198	0.87	0.1797	0.2639	0.74	0.2567	0.4937
	WA_{tol}_Cla	**69**	**198**	**0.87**	**0.1927**	**0.2812**	**0.74**	**0.2560**	**0.3611**
Gasse et al. (1995)	WA_Inv	179	332	0.86	0.3238	0.3064	0.78	0.4101	0.4610
	WA_Cla	179	332	0.86	0.3483	0.3391	0.78	0.4224	0.4790

Outliers omitted for Mills models (*) and the combined model (†). The values in brackets indicate the lake conductivity (in μS cm^{-1})

 # Lake Kitigata (134,000)
** Lakes Kitigata and Mahega (138,100)*
† Lakes Kitigata, Mahega, Victoria (119), Blue Pool (460), Nkugute (101), Kyogo (55), Marairs ol Bolossat (1500)

dataset and that of Gasse *et al*. (1995) are very similar, whilst the RMSEP and maximum bias are lower in the Combined_76 model. The slightly lower r^2 and r^2_{jack} in the Combined_76 is likely a result of a lower number of samples in the training set (69 compared to 274 [Gasse *et al*., 1995]).

The model based on the Combined-76 jack-knife WA_{tol} (classical deshrinking; Table 5.24) was applied to the sediment fossil diatom data to produce conductivity reconstructions (see **Chapters 6** and **7**).

Table 5.24 *Model performance for the Combined_76 dataset (with outliers removed).*

	WA Inverse	WA Classical	WA_{tol} Inverse	***WA_{tol} Classical***
RMSE	0.2111	0.2331	0.1797	***0.193***
R^2	0.8201	0.8201	0.8697	***0.870***
Average bias	$9.65x10^{-18}$	$6.11x10^{-17}$	$-4.22x10^{-16}$	***$-3.67x10^{-16}$***
Maximum bias	0.2733	0.3838	0.2639	***0.281***
Jack r^2	0.6635	0.6672	0.7374	***0.740***
Jack average bias	-0.0043	-0.0057	0.0030	***0.003***
Jack maximum bias	0.4932	0.3411	0.4937	***0.361***
RMSEP	0.2897	0.3111	0.2567	***0.256***

5.6 Discussion

The apparent predictability of the conductivity transfer function based on 76 sites (58 [Mills] and 18 [EDD]) is high ($r^2 = 0.86$) and comparable to other diatom conductivity transfer functions for other geographical regions: Africa ($r^2 = 0.87$; Gasse *et al*., 1995), Great Plains ($r^2 = 0.83$; Fritz *et al*., 1993), British Columbia ($r^2 = 0.89$; Cumming and Smol, 1993), Spain ($r^2 = 0.91$; Reed, 1998) and Mexico ($r^2 = 0.91$, Davies *et al*., 2002). By comparing the Combined_76 dataset with those from other regions, it is possible to explore the degree of consistency between datasets in the ecological optima derived for different species.

The diatom flora in the original crater lake training set (Mills_40 and Mills_58) are mostly comprised of freshwater species, with a tolerance for more saline conditions (e.g. *Amphora coffeaeformis*; Figure 5.10 and 5.13). There were some exceptions, notably the flora from the hypersaline Lakes Kitigata and Mahega (e.g. *Nitzschia latens* + varieties and *Navicula gawanensis*). The accepted definition of true saline systems that marks an ecological threshold for many groups of organisms is 3 g l^{-1} (Hammer, 1986). Using this definition, of the 56 sites (originally sampled) in the original crater lake training set, 49 were freshwater (<1500 µS cm^{-1}), one had an intermediate salinity

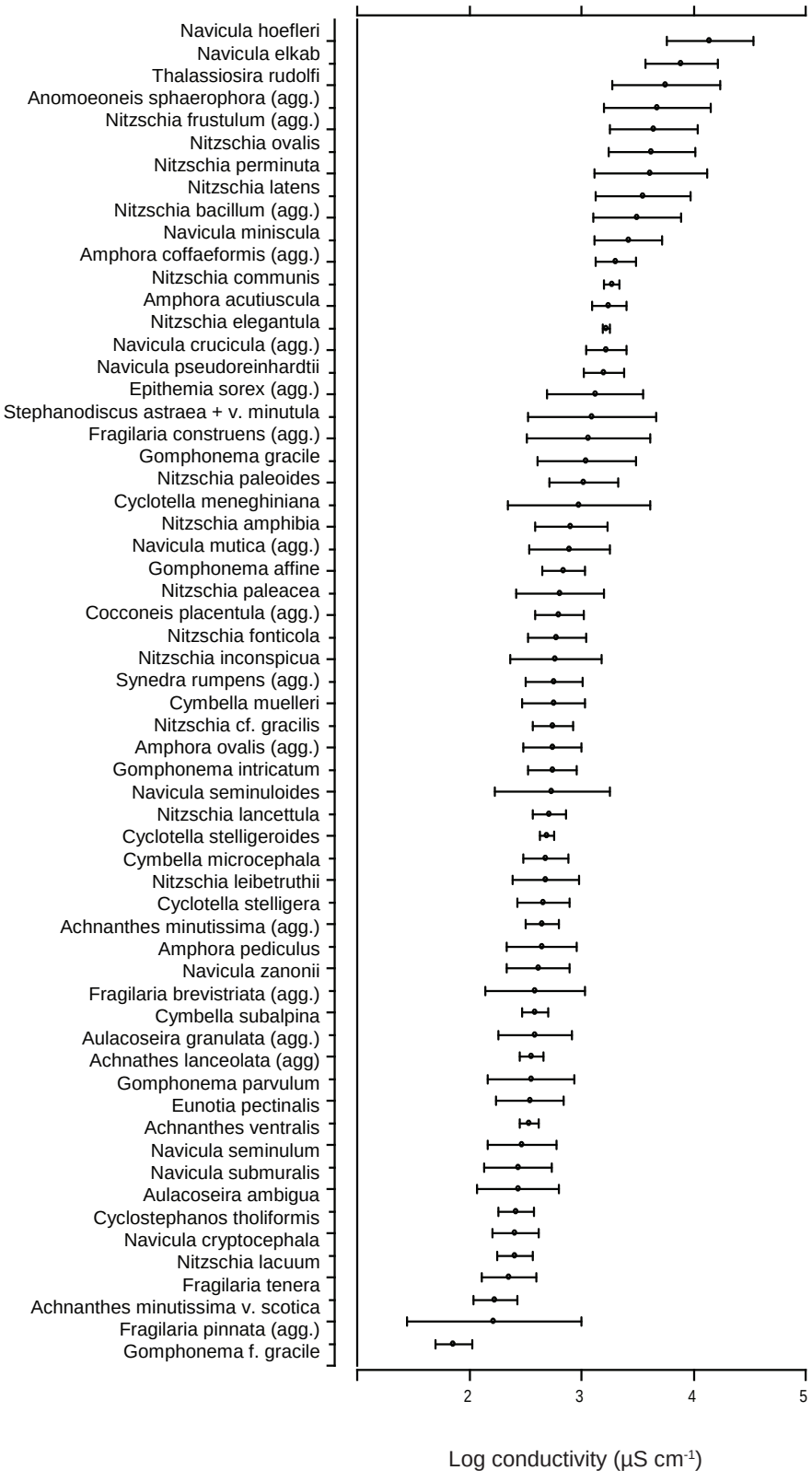

Figure 5.13 *Weighted average conductivity optima and tolerances for species >10% in any one sample from the Combined_76 dataset.*

(5900 µS cm^{-1}) and one very high salinity (31,600 µS cm^{-1}) and four were (hyper)saline (range 61,100-138,100 µS cm^{-1}). Regionally, the vast majority of crater lakes in western Uganda are dilute (freshwater), however analyses do suggest that conductivity is still an important variable in these fresh lakes (<1500 as cm^{-1}).

There are a small number of (hyper)saline crater lakes situated on the rift valley floor (between Lakes Edward and George), straddling the equator (Lakes Bagusa, Kikorongo, Kitigata, Mahega, Maseche; see **Chapter 2**, Figure 2.5). Lake Nshenyi, although a hypersaline site (31,600 µS cm^{-1}) is not found with the above lake cluster, but is located slightly further south in the Buyaruguru lake cluster, although still near the rift valley floor (altitude 950 m asl; see **Chapter 2**). However, several of these hypersaline sites (a) did not record any diatom flora in their sediments (Lakes Bagusa, Kikorongo_1 and 2, Mahega_2, Maseche and Nshenyi) or (b) supported a unique flora, which caused the samples to appear as outliers in the exploratory analyses and were therefore removed from the conductivity models.

The lack of diatoms in some of the lake sediments may be attributable to poor preservation of the diatom valves in these saline systems (cf. Barker, 1990; Barker *et al*., 1991; Barker *et al*., 1994; Gasse *et al*., 1997; Ryves *et al*., 2002; Ryves *et al*., 2006; Ryves *et al*., 2009). Whilst the Lake Mahega_2 sample (collected in 2007 with a lake conductivity of 96,100 µS cm^{-1}) failed to yield diatoms, the sample from the same lake in 2001 (Mahega_1; 138,100 µS cm^{-1}) produced a count of 509 diatom valves (although this was an epilithic sample). Likewise, the two samples from Lake Kikorongo (2001, 21,700 µS cm^{-1}; 2007, 22,200 µS cm^{-1}) did not yield diatoms, but a sample from the same lake analysed by F. Gasse (Lake *Kirongoro*[1], May 1969, 16,300 µS cm-1 [Gasse *et al*., 1983]) did contain diatoms (EDDI)[2]. Lake Kikorongo is periodically fed by flood waters from Lake George (Beadle, 1932), and this may partially explain the occurrence of diatoms in Kikorongo in the late 1960s. Bishop (1969) documented that a rapid rise in Lake George had resulted in the flooding of the Kikorongo crater. Furthermore, from 1962 until *c.* 1967, Lake Kikorongo was at a high-stand (Bishop, 1969). This could

[1] Note the discrepancy in the spelling; the lake referred to by Gasse is Lake *Kikorongo*, confirmed by its longitude and latitude. This error appears to be common place in Uganda, with map names having been mistranslated by overseas cartographers and the reliance on the local villagers/landowners to provide lake names and spellings, which in itself can provide an array of choices.

[2] Data provided as percentage abundance only. Actual count data are unknown.

account for the lower conductivity of Kikorongo when sampled in 1969 and the presence of diatoms in the lake sediment.

In the hypersaline lakes where diatoms were recorded (Lakes Kitigata and Mahega_1, with counts of *c.* 500) the diatom assemblages were unique to the training set, though the two sites did have species in common. Lake Mahega_1 (2001; 138,100 µS cm^{-1}) was dominated by *Nitzschia latens* v. *etoshensis* (97% of total count), with some form of *Amphora* species (aff. *coffeaeformis*) present; high dissolution (**F** index = 0) prevented this species from being confidently resolved to species level. Similarly, Lake Kitigata (2001, 135,400 µS cm^{-1}, **F** index = 0.38) supported an assemblage with a high prevalence of *Nitzschia latens* (21%) and also the hypersaline species *Navicula gawaniensis* (35%; Gasse *et al*., 1983; Barker *et al*., 1991).

Lake conductivity does not appear to be a predictor of the presence of diatoms preserved in the surface sediments as samples from higher salinity sites (e.g. Kitigata) contained diatoms, whilst other sites (e.g. Bagusa, which had a salinity lower than Kitigata) did not. Similarly, the diatom occurrence in some of the saline systems appears to differ during different sampling years. This is quite possibly a result of the season in which the lakes were sampled (and perhaps critically, the length of time since the wet season). Temporal variation in salinity can be as high as 50% in this particular crater lake region (Katwe-Kikorongo; Beadle 1932). This is also clear in Figure 5.2 (comparison of original conductivities against those collected in 2007), where the biggest changes are observed in the hypersaline lakes (Maseche and Bagusa); the fresher lakes exhibit a (close to) 1:1 relationship. This discrepancy did not affect the development of the diatom-conductivity model as sediments from Bagusa did not contain any diatom valves and Mahega was identified as a clear outlier in all of the analyses (and was always omitted). It does however highlight some of the potential problems that may be encountered when using water chemistry data which was not sampled at the same time as surface sediment samples in extremely sensitive lake systems when developing training sets.

One of the most significant problems encountered whilst amalgamating samples for the crater lake training set was the paucity of modern lakes with ‘intermediate salinities’ (i.e. log 3-4 conductivity units; Talling and Talling, 1965; Wood and Talling, 1988; Verschuren, 2003; Eggermont *et al*., 2006). This is a phenomenon that occurs throughout East Africa (Talling and Lemoalle, 1998; Verschuren, 2003). Lakes across the study area (from Fort Portal in the north to Bunyaruguru in the south) are either

fresh (typically <1500 µS cm^{-1}) or (hyper)saline (>20,000 µS cm^{-1}), thus few lakes lie close to the biologically important freshwater-saline transition (*c.* 3000 µS cm^{-1}; Hammer 1986). This is perhaps not unexpected from the perspective of lake water balance (cf. Kalff, 2003) and the local role of groundwater in keeping the lakes wet and allowing the renewal and removal of salts.

This was also a problem encountered by Eggermont *et al*. (2006) during their development of a chironomid-salinity transfer function for East Africa. The saline lakes in Uganda are often concentrated soda lakes of Na-K-HCO_3 type (Talling and Talling, 1965; Kilham, 1971; Eggermont *et al*., 2006). Many of the lakes of Uganda sampled at the higher end of the conductivity scale, and with atypical water chemistries, were omitted from the analyses as diatom valves were not recovered from the surface sediment sample.

In order to overcome this issue and to enhance the representation of some of the fossil core taxa in the training set (see **Chapter 6**), additional sites were added to the crater lake training set from EDDI. Only sites from East Africa were reviewed for inclusion. This was to ensure that there was an overlap in the diatom flora and to ensure a biogeographical consistency. Sites from EDDI were chosen primarily on their conductivity measurement. Sites selected ranged in salinity from 1050 to 16,300 µS cm^{-1}. With the omission of the two hypersaline crater lake from the original dataset, hypersaline sites from EDDI were also avoided to try and prevent the addition of more specialised flora associated with these unusual sites. Following this process, sites were also examined to ensure that the dominant flora were similar to that of the crater lake training set in order to create an ecologically continuous combined training set[3].

However, the merging of different datasets is not without problems, one of which is the taxonomic and methodological inconsistencies in the datasets for merging due to different analysts (cf. Birks, 1995). In this instance the EDDI diatom taxonomy was updated to match that of the crater lakes (e.g. *Amphora libyca* became *Amphora copulata*), however this was completed using the images and morphologic descriptions available online, the original slides were not consulted. It was important to try and select EDDI sites from East Africa to try and prevent the combining of species with

[3] The original EDDI slides were not analysed or consulted as part of this research. The taxonomic information (descriptions and photographs) were obtained from the EDDI website (www.craticula.ncl.ac.uk/eddi)

different environmental optima, which may be particularly problematic when merging datasets from more than one biogeographical region (Duigan and Birks, 1997; Eggermont *et al*., 2006). Furthermore it may cause secondary environmental gradients to become more prominent (cf. Eggermont *et al*., 2006).

It was also important to try and include sites of intermediate conductivities into the transfer function, not only because it improved the model performance, but also because intermediate conductivities may have existed in the past in western Uganda, when climatic regimes were different (during extreme wet or dry periods).There is always the possibility that the crater lakes of western Uganda have never experienced intermediate conductivities, with only abrupt changes characterising the fossil record and thus rendering the reconstruction of intermediate conductivities less useful. The reconstruction of these intermediate conductivities will be tested through the application of the transfer function to sediment cores spanning a time period with known and well-documented climatic fluctuations (see **Chapters 6** and **7**). For further discussion, refer to **Chapter 8**.

The distributions of some well-represented taxa from the combined training set can be compared with those from the African training set (Gasse *et al*., 1995). The distributions and conductivity optima of 10 well-represented taxa spanning the conductivity gradient from the Combined_76 training set are compared and shown in Table 5.25 and Figure 5.14 (from low to high conductivity: *Aulacoseira ambigua, A. granulata, Nitzschia lancettula, Amphora copulata, N. fonticola, Cocconeis placentula, N. amphibia, Cyclotella meneghiniana, Gomphonema gracile, Amphora coffeaeformis* and *Thalassiosira rudolfi*). Whilst broadly there is some agreement between the two training sets (key freshwater and saline species are identified as such, even though their tolerances are similar), there is a distinct lack of agreement between the optima calculated during the development of the crater lake training set and of those calculated by Gasse *et al*. (1995).

There are a number of potential reasons why this may be the case. Firstly, and perhaps the most important reason for the differences in the species optima is the size of the training set. Gasse *et al*. (1995) use a 276-lake dataset from across Africa (167 of

Figure 5.14

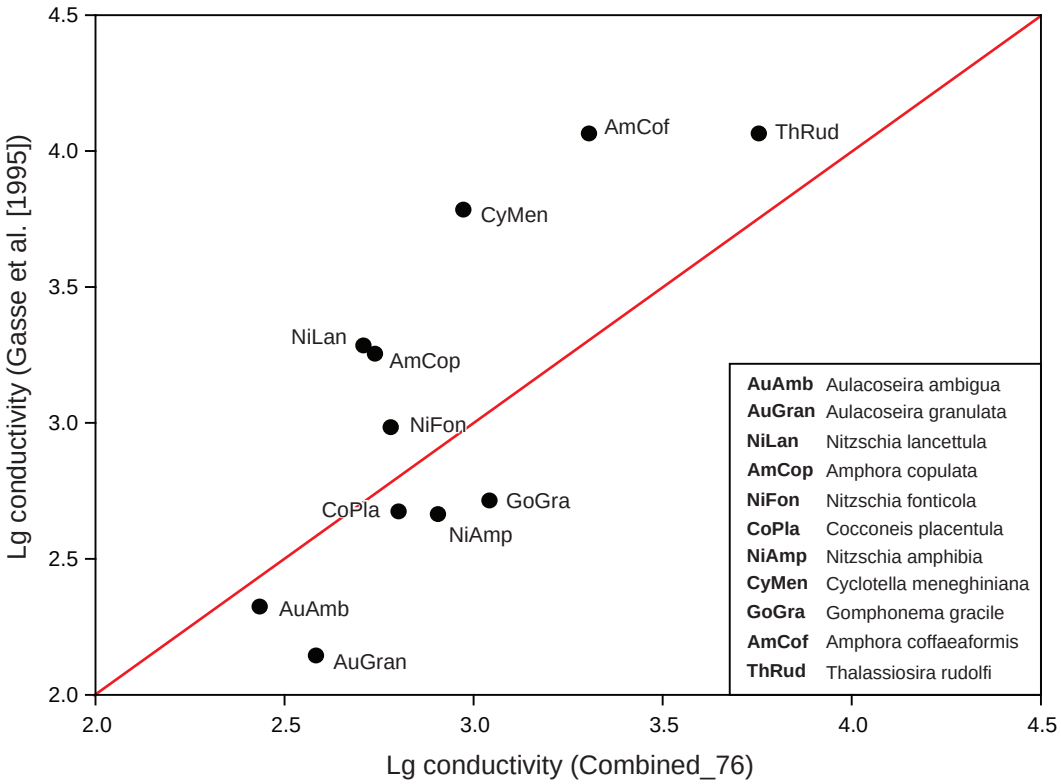

Figure 5.14 *Comparison of species optima for 10 taxa spanning the salinity gradient in the Combined_76 model to optima calculated by the Gasse et al. (1995) diatom-conductivity (salinity) transfer function (see* ***Table 5.21*** *also). The solid red line represents the 1:1 ratio.*

which are from East Africa). The crater lake training set here is relatively small in size (76 including the EDDI sites), and the lakes sampled cover a smaller conductivity gradient than the African training set. Summary statistics show that the minimum recorded conductivity for the African training set is 40 µS cm^{-1} (55 µS cm^{-1} in the crater lake training set), with a maximum of 99,060 µS cm^{-1} (16,300 µS cm^{-1} in the crater lake set after the removal of the two hypersaline outliers) and the median conductivity for the African training set is 925 µS cm^{-1} (520 µS cm^{-1}; crater lakes). These results highlight the fact that the crater lake transfer function contains more samples from and is therefore biased towards the fresher end of the conductivity gradient. It is also likely that the true optima for some species may not have been identified in the crater lake training set, given the short conductivity gradient (especially with species such as *Cyclotella meneghiniana* where there is a particularly large discrepancy between optima). *Cyclotella meneghiniana*, a cosmopolitan facultatively-planktonic species is described as a euryhaline (Caljon and Cocquyt, 1992), but its salinity preference varies amongst studies (Tuchman *et al*., 1984; Roubiex and Lancelot, 2008).

Table 5.25 *Comparison of species optima for 10 taxa spanning the salinity gradient in the Combined_76 model to optima as calculated for the East Africa diatom-conductivity/salinity transfer function of Gasse et al. (1995; see* ***Figures 5.9*** *and* ***5.14****).*

Species name	Combined_76	Gasse et al. (1995)
Aulacoseira ambigua	273.28	208.93
Aulacoseira granulata	385.26	138.04
Nitzschia lancettula	514.15	1905.46
Amphora copulata	551.38	1778.28
Nitzschia fonticola	606.62	954.99
Cocconeis placentula	636.93	467.74
Nitzschia amphibia	809.19	457.09
Cyclotella meneghiniana	944.80	6025.60
Gomphonema gracile	1106.68	512.86
Amphora coffeaeformis	2028.62	11481.54
Thalassiosira rudolfi	5707.16	11481.54

C. meneghiniana is a species most often associated with waters of higher conductivity in East Africa (Gasse, 1986), but has also been shown to bloom in eutrophic lakes (Dong *et al*., 2008) and lakes with a high water temperature (Mitrovic *et al*., 2008). Despite this, the optimum generated for the crater lake training set is more plausible than the African dataset optimum. There are only a handful of sites (where *C.*

meneghiniana occurs in significant abundance) within the African dataset with extremely high conductivities, and this clearly exerts a large influence on the dataset and calculated conductivity optima (cf. Gasse, 1986; EDDI). Furthermore, all but one of the high salinity sites (with high *C. meneghiniana* abundance) included in the African dataset are either hot springs or salt swamps. Whilst the inclusion of these sites increases the salinity gradient, and therefore betters the performance of the transfer function (r^2), it is highly unlikely that the reconstructions would improve. The lakes used to validate the transfer function (**Chapter 6**) are all from western Uganda, and whilst exhibiting floral changes that suggest increasing conductivity over time, the recorded species are not of the specialist flora usually associated with (hyper)saline lakes. Furthermore, in the present crater lake training set, all except one site, are taken from lake surface sediments. It is likely that the discrepancy between the optima calculated for the crater lake transfer function and that which exists in the African model (Gasse *et al*., 1997) is perhaps attributed to an overestimation of optima in the latter dataset, caused by a low number of high salinity swamp sites. Alternatively, other factors which influence the presence/abundance of *C. meneghiniana* (eutrophication and high water temperatures; Dong *et al*., 2008; Mitrovic *et al*., 2008) and the robust nature of *C. meneghiniana* valves allowing them to be preferentially preserved and identified (cf. Barker, 1990) may be confounding factors in the distribution of *C. meneghiniana*.

It is possible that, in some cases, the 0-0.5 cm surface sediment sample in some lakes does not integrate any seasonal fluctuations in diatom species assemblage composition and water chemistry samples are perhaps more representative of shorter-term limnological conditions than the surface sediments (e.g. the sediments may integrate a signal spanning 6 months or more, whilst the sampled water chemistry may only be representative of the last 1-2 months). Sedimentation rates in Uganda are known to range between *c.* 0.2-2 cm y^{-1} (rates of *c.* 2 cm yr^{-1} calculated in lakes Wandakara [Ssemmanda *et al*., 2005] and Kyasanduka [this study, **Chapter 6** and **Appendix C**).

There are a number of limitations to quantitative palaeoecological reconstructions in western Uganda using the crater lake training set (even with additional EDDI sites included). For example, a number of important fossil species in Ugandan lake sediments are often poorly represented. For instance, *Thalassiosira rudolfi*, *Amphora coffeaeformis* and *A. veneta* are abundant in analysed core sections (**Chapter 6**), but they are rarely found in the modern environment. This can result in problems when applying the transfer function to palaeoecological data. Another

potential issue when applying the transfer function to core sediments is the potential modification of modern lakes and their respective surface sediment samples due to human impact. Many lake basins in western Uganda have experienced significant human impact in the recent past (*c.* last 50-100 years; cf. Ssemmanda *et al*., 2005).

During CCA analysis of all environmental variables, sites with no contemporary human impact ('NONE') appeared to be a significant driver of diatom assemblages. However, it appears that this gradient is driven by only a small number of sites (Lakes Kyogo, Karolero, Kacuba, Chibwera and Murabyo) and does not present a realistic ecological variable that can be easily reconstructed using a transfer function. A more viable explanatory variable would be a nutrient signal such as total phosphorus (TP) or total nitrogen ('TN'). Out of the two nutrient variables TN was identified as a variable that explained a significant proportion of variation in the diatom data, making this a possible candidate for a diatom model. Its significance in explaining diatom assemblage variation, and its eigenvalue ratio in the Mills_40 training set ($\lambda_1/\lambda_2 = 0.52$) was comparable to that of conductivity (in the same dataset; Kingston *et al.*, 1992). Unfortunately, the importance of TN in the combined dataset could not be assessed as TN data were not available for the EDDI sites that were added.

The results of exploratory analyses during a partial CCA and variance partitioning on the Mills_40 dataset indicated that conductivity does make an independent and significant contribution to the total variance in the diatom data. A CCA of the Combined-76 dataset with salinity only also suggested that the data are appropriate for the derivation of a reliable transfer function. The apparent predictive ability of the conductivity transfer function (using the Combined_76 dataset) was high ($r^2 = 0.86$), and the performance under jackknifing was also good ($r^2_{jack} = 0.74$).

The results from the development of a crater lake transfer function indicate a strong and highly significant relationship between diatoms and conductivity. A transfer function quantifying this relationship can be used to reconstruct down core changes in conductivity from fossil diatom assemblages. However, the application of transfer functions should always be treated with caution, especially when inferring past climatic conditions using the model. Water chemistry can be affected by multiple factors such as the seepage of groundwater and catchment modification by anthropogenic activity (e.g. agriculture). More importantly, the relationship between salinity (conductivity) change and climate forcing is indirect and complex (Gasse *et al*., 1997) with in-lake processes also playing an important role (see **Chapter 8** for further discussion).

5.7 Summary

- Exploratory data analyses in the form of indirect ordinations (PCA, CA and DCA) show trends and variation in the diatom data that can be attributed to hydrochemical gradients across which the lakes were sampled.
- The application of constrained ordination techniques with forward selection on the original crater lake dataset (Mills_40) suggest there are three independent and significant environmental variables that can explain the variation in the diatom dataset: conductivity, TN and depth.
- A diatom-conductivity model was developed for the East African crater lakes. However, due to a paucity of sites with conductivities between log 3 and 5, additional sites were selected from the EDDI (East African) dataset.
- Weighted averaging (WA), with tolerance down-weighting and classical deshrinking, provided the strongest model. This model was internally validated using the jackknife procedure. During this process a number of 'outliers' were identified. The influence of these outliers on the diatom model was assessed using Cook's *D* and a number of other criteria before they were rejected.
- The transfer function has been applied to fossil sediment core samples, the results and interpretation of which are available in **Chapters 6** and **7**.

Chapter 6

Long Cores: Environmental change during the Last 1000 years

6.1 Introduction

This chapter focuses on results obtained from the analyses of two long sediment cores spanning the last *c.* 900 years from Lakes Nyamogusingiri and Kyasanduka. The chapter begins by providing a brief account of the numerical methods employed. Details regarding the site locations are given in **Chapter 2**.

For each lake, the core correlations are first established using a range of techniques including organic content (loss-on-ignition, LOI), magnetic susceptibility, core physical properties and the diatom biostratigraphy, following which the core chronology, based on a combination of ^{210}Pb dating and AMS ^{14}C dating is presented. The results of diatom analyses are presented, as well as diatom habitat summaries and the results of indirect ordination analyses as are the results of the bulk organic stable isotope analyses (C/N ratio and δ^{13}C). Dry mass accumulation rates (DMAR) were calculated for the sediment data to infer the flux of organic and minerogenic material to the lake as well as to calculate the flux of diatoms to the sediment. Each section is completed with a summary of the various 'in-lake' records in an effort to tie together analyses of the various proxy data. Results tables for the ^{210}Pb and multivariate analyses are presented in **Appendix C**.

6.2 Numerical methods

6.2.1 ZONE

The stratigraphical diatom data from each core were divided into assemblage zones using optimal sum of squares partitioning (Birks and Gordon, 1985) by the program ZONE (version 1.2; Juggins, 2002).

6.2.2 Stratigraphic diagrams (C2)

For all stratigraphic diagrams, all diatom species >5% in any sample are shown as percentage abundance and ordered according their down-core weighted averaging abundance (species ordered in terms of their occurrence in the core). The cores are plotted against calendar years AD and composite core depth (cm). The dissolution index (**F**-

index), total concentration of diatoms ($x10^6$ valves g^{-1} dry sediment), reconstructed salinity, DCA axis 1 and 2 sample scores and testate amoeba counts (as a testate amoeba: diatom ratio) are also displayed. The diatom zones presented are based on the output of ZONE (see *section 6.2.1*). A habitat summary for each of the cores is also provided.

6.2.3 CANOCO

Indirect ordination analyses were carried out using CANOCO 4.5 (ter Braak and Šmilauer, 2002) to identify the predominant trends within the data. Initially a Detrended Correspondence Analysis (DCA; Hill and Gauch, 1980) with detrending by segments, and down-weighting of rare species, was used to explore the main patterns of taxonomic variation among sites and to estimate the compositional gradient lengths of the first few DCA axes. The diatom percentage data were transformed using log transformation in an attempt to reduce clustering of abundant or common taxa at the centre of origin (Leps and Šmilauer, 2003). The gradient lengths allow the determination of the most appropriate response model for further analysis. If the gradients were sufficiently long (>1.5 s.d.), it indicated that numerical methods based on a unimodal response model were most appropriate (e.g. [Detrended] Correspondence Analysis; CA or DCA; ter Braak and Prentice, 1988). Where gradient lengths were <1.5 s.d. a linear response model (e.g. Principal Components Analysis; PCA) was deemed the most appropriate.

6.2.4 Sediment flux

Dry mass accumulation rates (DMAR in g cm^{-2} yr^{-1}) were calculated for the two sediment sequences. For the upper sediments, dated by ^{210}Pb and ^{137}Cs, dry mass accumulation rates were provided by P.G. Appleby (University of Liverpool; see **Appendix C** for ^{210}Pb and ^{137}Cs data). For the lower core sequences (where AMS ^{14}C dates exist), DMAR was calculated by first linearly extrapolating the dates to create an age model and to provide a date for each sample included in the analysis. This in turn allowed the estimation of the bulk dry density of each sample using known sample dry weights (based on percentage water content; N.J. Anderson, unpublished data). The DMAR (g cm^{-2} yr^{-1}) was then derived from the dry bulk density estimate divided by the numbers of years taken for the sediment sample to accumulate (in 1 cm slices). The results were further transformed in order to calculate both the organic and inorganic sediment flux to the lakes (using the organic matter estimated by LOI at 550°C, CO_3 at 925°C and minerogenic content of the

sediments) and the diatom flux (for the different habitats, dominant species and total diatom flux).

6.3 Lake Nyamogusingiri

6.3.1 Core correlation

Four cores were collected from Lake Nyamogusingiri: two Kajak cores (NCR1 0-29 cm; NCR2 0-35 cm) and two Russian cores (NCR1C1 0-85 cm; NCR2C1 0-100 cm). Both Kajak cores were sampled for LOI analysis, but only the longer NCR2 was used to construct a core chronology and for the analyses of diatoms and organic isotopes as this core provided a larger overlap with the top of the Russian cores (*c.* 8 cm). During the first attempt at retrieving a long core (NCR1C1) the core chamber failed to close correctly, causing the loss of the bottom 15 cm of the core and almost one third of the volume of the remaining core sediments. As the integrity of this core was compromised and the risk of contamination with modern lake water was high, NCR1C1 was not considered for any further analyses. The second drive, the recovery of NCR2C1, was successful and the entire core was recovered intact with no sediment loss. This second core (NCR2C1) was selected for chronological, diatom and isotope analyses.

Due to the lack of any obvious defining stratigraphic or sedimentological indicators (e.g. banding) in the Nyamogusingiri cores, the Kajak (NCR2) and Russian (NCR2C1) cores were first correlated on the basis of the field calculations of the coring depths. This correlation was subsequently corrected and finalised based on the loss-on-ignition analyses (organic content; Figure 6.1 and 6.5). Further confirmation of these overlapping sections was provided in both the analyses of the organic isotopes and diatoms, with *Thalassiosira rudolfi* being a key species in the confirmation of the overlap (Figure 6.7 and 6.8). The continuous ^{210}Pb chronology through the Kajak core and into the upper sections of the Russian core provided the final verification of the overlapping sections (P.G. Appleby, *pers. comm.*). The composite core length for Lake Nyamogusingiri was 1.27 m.

6.3.2 ^{210}Pb dating and ^{14}C chronology

^{210}Pb activity in Nyamogusingiri reaches equilibrium with the supporting ^{226}Ra at a depth of ~50 cm. The unsupported ^{210}Pb activity declines steeply and almost exponentially with depth in the upper 10 cm, but at a slower rate than in deeper sections (Figure 6.2a). This gradient change indicates a recent reduction in the sedimentation rate, but may also be

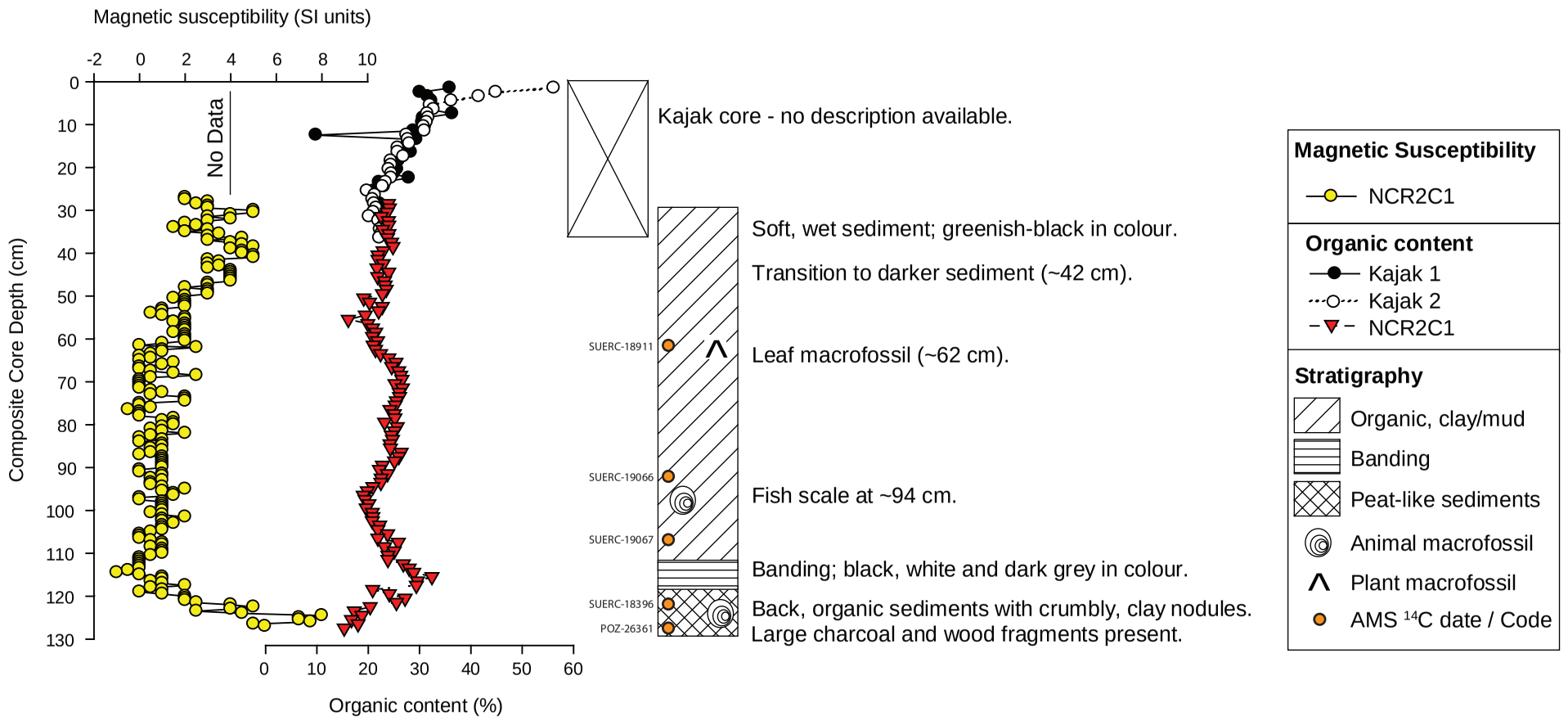

Figure 6.1 *Correlation of the overlapping core sections recovered from Lake Nyamogusingiri. Results of magnetic susceptibility, loss-on-ignition (LOI; a measurement of the organic content of the sediment). Core stratigraphies are also displayed alongside brief descriptions.*

Lake Nyamogusingiri

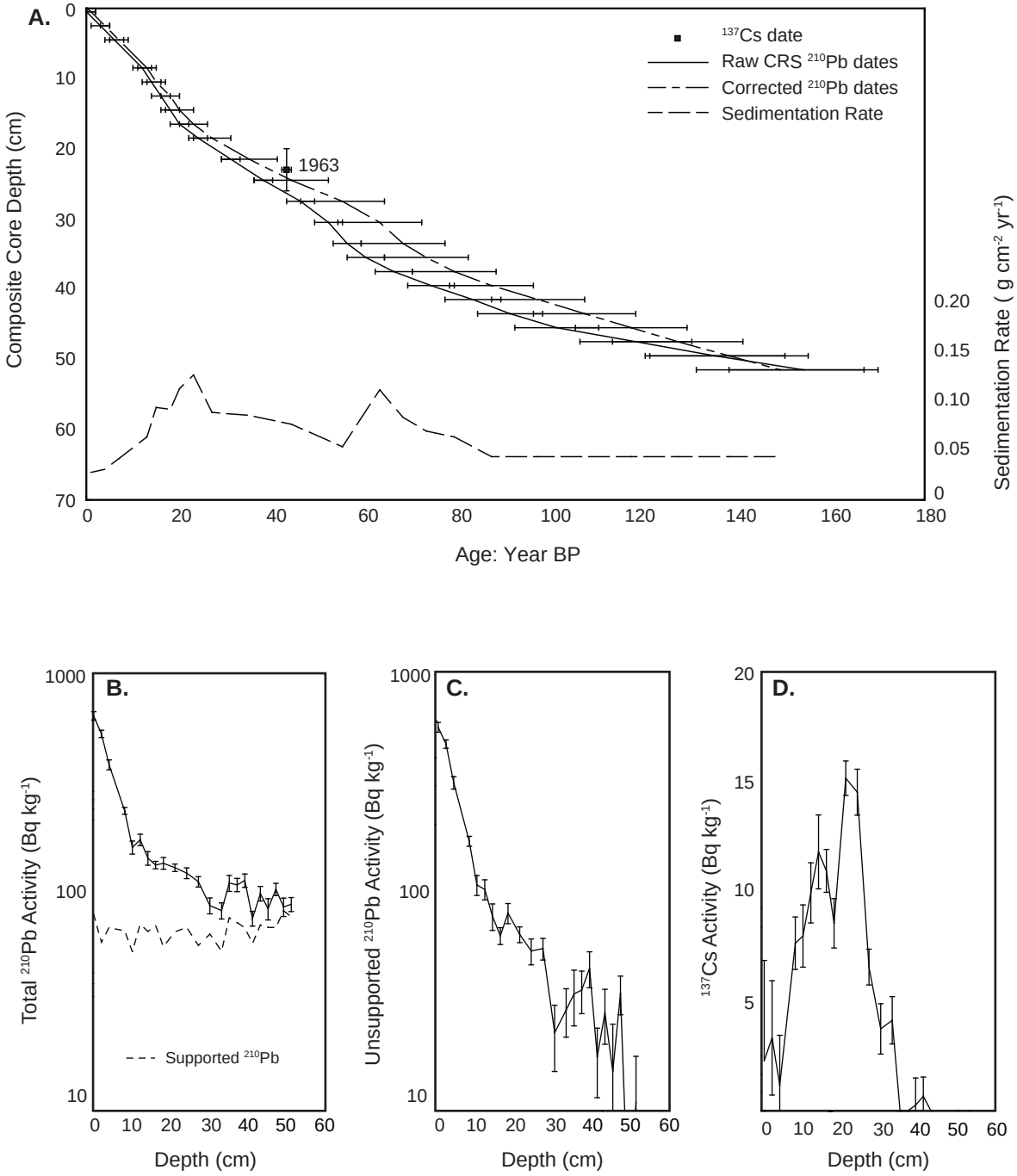

Figure 6.2 *^{210}Pb and ^{137}Cs data for Lake Nyamogusingiri.* **(A)** *^{210}Pb chronology for Nyamogusinigiri (using linear extrapolation between the dated horizons). Filled circles represent actual dated horizons (see* ***Appendix #****), the filled square is the base of the sequence, dated by linear extrapolation.* **(B-D)** *Fallout radionuclides in the Nyamogusingiri core showing* **(B)** *total and supported ^{210}Pb,* **(C)** *unsupported ^{210}Pb and* **(D)** *^{137}Cs concentrations versus depth (Figures are adapted from dating report supplied by P.G. Appleby, unpublished report).*

attributed to the shift to lower density sediments in the upper 10 cm of the core (results tables for ^{210}Pb and ^{137}Cs can be found in **Appendix C**).

The ^{137}Cs activity versus depth profile of Nyamogusingiri shows a relatively well defined peak at 20-26 cm (Figure 6.2b-d) and this peak almost certainly records the 1963 fallout maximum from the atmospheric testing of nuclear weapons (P.G. Appleby, *pers. comm.*). The ^{210}Pb chronology for Nyamogusingiri places 1963 at 27 cm, a little below the depth indicated by the ^{137}Cs record (Figure 6.2a-d). The Constant Initial Concentration model (CIC) was not used due to the large discrepancy between the calculated 1963 depth and the inferred ^{137}Cs date. The Constant Rate of Supply model (CRS) provided a better estimate of the 1963 ^{210}Pb depth, the small discrepancy using this model is likely due to a small reduction in the ^{210}Pb supply rate in the upper part of the core (P.G. Appleby, *pers. comm.*). The revised dates were calculated by applying the CRS model in a piecewise way using the 1963 ^{137}Cs date as a reference point. The results suggest a relatively high sedimentation rate from *c.* AD 1930 through to the early 1990s, with peak values occurring in the mid 1940s and mid 1980s (P.G. Appleby, *pers. comm.*). The mean accumulation rate during this period is 0.083 g cm^{-2} yr^{-1}. Since the mid-1990s sediment accumulation rates appear to have significantly decreased (mean accumulation rate of 0.041 g cm^{-2} yr^{-1}). It is also likely that sedimentation rates were lower in the 19th and earlier 20th century, although the disturbances in the early 1920s have led to uncertainties for the earlier results (P.G. Appleby, *pers. comm.*).

Five AMS ^{14}C dates were obtained from terrestrial plant macrofossils from Lake Nyamogusingiri's composite core sequence, below the ^{210}Pb equilibrium depth (*c.* 52 cm; Tables 6.1 and 6.2; Figure 6.3a). All dates were calibrated using CALIB 5.0 (Stuiver and Reimer, 1993) using the IntCal04 calibration curve (Reimer *et al.*, 2004). Two dates from near the base of the core sequence (494 ± 37 ^{14}C yr BP; 121-122 cm and 415 ± 30 ^{14}C yr BP; 126-127 cm) were rejected; the dates for these lower samples were obtained on two wood/charcoal fragments (SUERC-18396 and POZ-26361) and produced erroneously young radiocarbon ages, and hence a younger calibrated date compared to the other three dates above, which all occurred in stratigraphic sequence. The anomalously young ages of these two samples compared to the others perhaps indicates that they were probably from an intrusive root fragment during a period of lower lakes levels (Krider, 1998). These lower two samples were extracted from a soil-like deposit at the base of the core.

Three radiocarbon dates were used in conjunction with the ^{210}Pb dated core sequence (0-52 cm) to construct an age model for Nyamogusingiri (Figure 6.3b). The

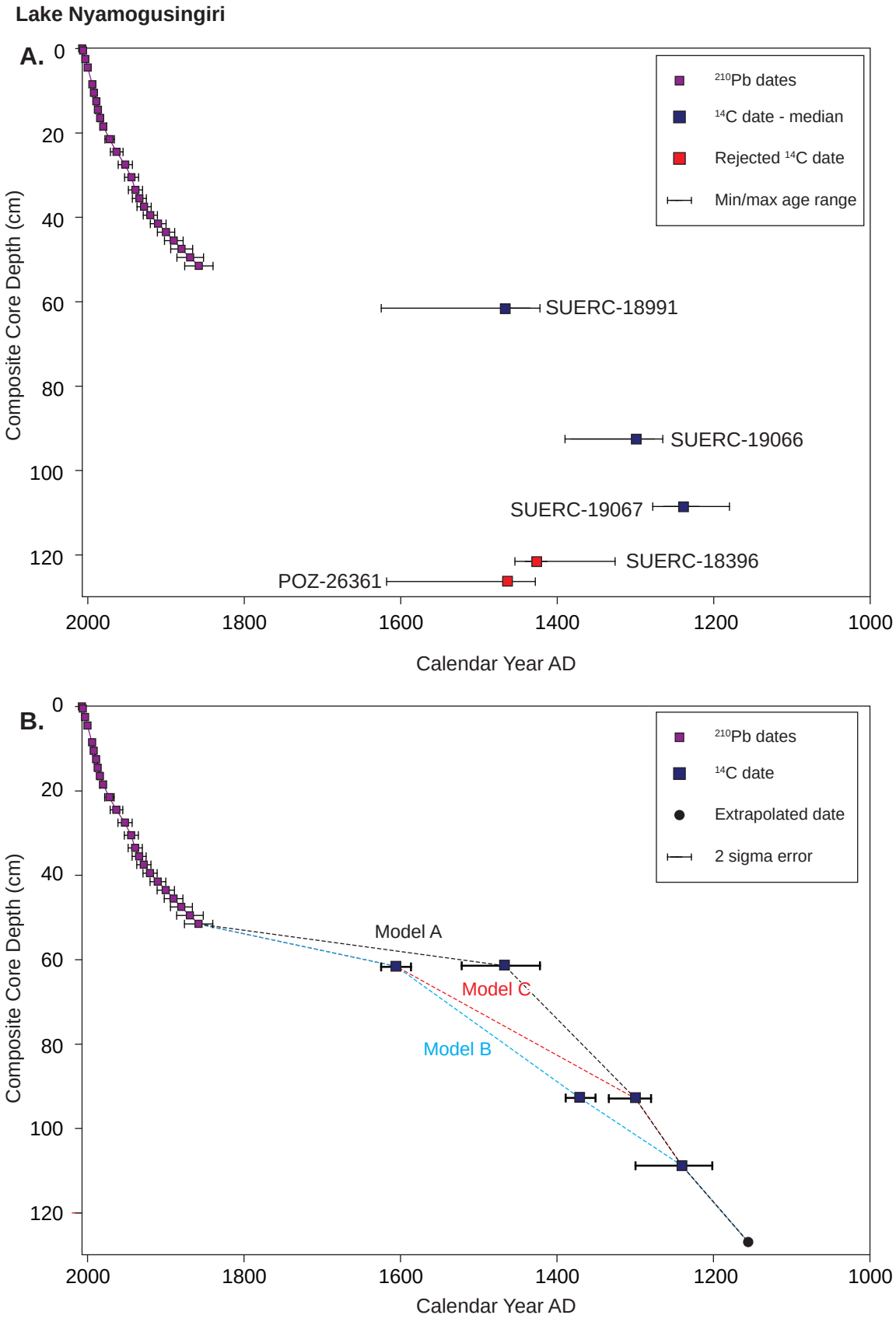

Figure 6.3 *All dates from Lake Nyamogusingiri sediment cores.* **(A)** *^{210}Pb dates and all calibrated ^{14}C dates plotted against composite core depth. Radiocarbon dates were calibrated using CALIB 5.0. All error bars are given for ^{210}Pb (see* ***Appendix #****). For the radiocarbon dates the square denotes the median age as calculated in CALIB 5.0. The error bars represent the absolute maximum and minimum ages for each sample at two sigma error (see* ***Table 6.#*** *and* ***section 6.#*** *for additional information).* **(B)** *Final age models (A, B and C) for Lake Nyamogusingiri, with some radiocarbon dates excluded (see* ***Table 6.#*** *and* ***section 6.#*** *for explanation). The error bars represent the age range at two sigma error.*

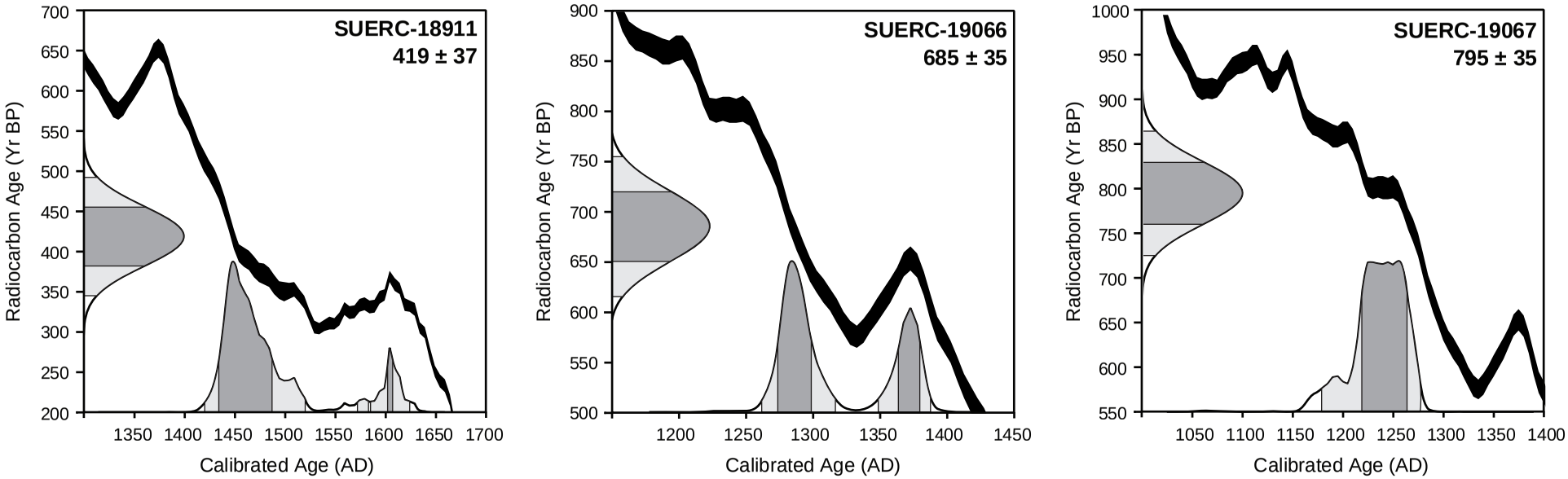

Figure 6.4 *Probability distributions of the three accepted radiocarbona dates used in the age-model for Lake Nyamogusingiri.The probability distributions were calculated using CALIB 5.0.*

median age (as calculated in CALIB 5.0) was used to represent the age of the sample and 2 sigma error ranges are given for each date. The dating of such young sediments (< 1000 years) has been problematic, as many of the dates have multiple possibilities for calibrated ages at both one and two sigma error. Figure 6.4 shows the probability distributions of each calibrated age accepted for use in the age model (SUERC-18911, SUERC-19066 and SUERC-19067). The problem of multiple possibilities in the calibrated age and possible age reversals is attributed to the 'de Vries' effect, which affects the calibration of radiocarbon samples from the recent past (*c.* 500 years; Stuiver and Becker, 1993). For a full discussion, please see **Chapter 8** (*section 8.8.2*).

Three potential age models (A, B and C) are presented for Lake Nyamogusingiri sediments. All three age models are constrained at depth by the same date which has 100% probability distribution (AD 1239, 108.5 cm; SUERC-19067) and differ only in their upper sections. Model A provides the maximum age model for the sediments and is based on the calibrated ages with the maximum possibilities (Tables 6.1 and 6.2), where as Model B provides the minimum age model for the dated sediments (Figure 6.3); Model C provides a compromise between models A and B. Model B was chosen as the final age model for the sediments, denoting the absolute minimum ages that could be assigned to any event. The selection of this model uses the lowest probability age for the uppermost radiocarbon date (SUERC-18991). There was no obvious reason for this date to be rejected outright (in terms of the material dated, its stratigraphic order, or problems with the ^{14}C analysis itself, C. Bryant, NERC-RCL, *pers. comm.*). Therefore, this lower probability age was accepted on the basis that the older of the two dates ('Range 1'; Table 6.2) seemed implausible, yielding a spuriously low sedimentation rate over a *c.* 400 year interval. At worst it would imply a hiatus in the sediment sequence. With no evidence (both physical or biological, see *sections 6.3.3* and *6.3.4* below) to support an hiatus, or a seemingly low sedimentation rate in the core, and to maintain coherence between the ^{210}Pb-dated sediments and the lower core sections, the youngest calibrated date was used (AD 1587-1625). The youngest date still assumes a period of low sedimentation, but over a shorter time period, which coincides with a period of inferred aridity from other crater lake sediment sequences in western Uganda (cf. Bessems, 2007; Russell *et al*., 2007, Bessems *et al*., 2008) and an inferred period of lower sedimentation in Lake Kyasanduka (see *section 6.4.2*).

Table 6.1 *All AMS ^{14}C radiocarbon dates from Lake Nyamogusingiri. Dates are reported as conventional radiocarbon years BP, relative to AD 1950. The samples were prepared at the NERC radiocarbon laboratory and passed onto the SUERC AMS laboratory for ^{14}C analyses. The samples highlighted in bold italics are dates that have been excluded from subsequent age models. Please refer to the text for details.*

Code	Nature of sample	Core	Correlated Depth		Radiocarbon Age	1σ error	2σ error	^{14}C enrichment (% modern)	Enrichment ± 1σ	Carbon content (% by wt.)	Sample wt. (mg)	$\delta 13C_{VPDB}$‰ ± 0.1
			Top	Bottom								
SUERC-18911	Leaf/Charcoal	NR2C1	61	62	419	37	74	94.91	0.44	60.3	2.40	-30.80*
SUERC-19066	Leaf/Charcoal	NR2C1	92	93	685	35	70	91.80	0.28	53.2	3.66	-20.80
SUERC-19067	Wood/Charcoal	NR2C1	108	109	795	35	70	90.60	0.28	56.3	1.69	-21.10
SUERC-18396	***Wood***	***NR2C1***	***121***	***122***	***494***	***37***	***74***	***94.04***	***0.43***	***58.3***	***29.3***	***-28.00***
POZ-26361	***Charcoal***	***NR2C1***	***126***	***127***	***415***	***30***	***60***	--	--	--	--	--

* Sample produced insufficient CO_2 for an independent measurement of $\delta^{13}C$. -25 $\delta^{13}C_{VPDB}$ ‰ was applied in calculating the ^{14}C result for these samples.

Table 6.2 *Calibrated radiocarbon dates from Lake Nyamogusingiri. Radiocarbon ages were calibrated using CALIB 5.0 (Stuiver and Reimer, 1993) using the calibration curve IntCal04.14c (Reimer et al., 2004). All calibrated ages are given as calendar years AD.*

Code	Correlated Depth		Radiocarbon Age	2σ error	Range 1			Range 2			Range 3		
	Top	Bottom			Lower	Upper	Probability	Lower	Upper	Probability	Lower	Upper	Probability
SUERC-18911	61	62	419	74	1422	1522	85.03%	1574	1585	1.53%	1587	1625	13.44%
SUERC-19066	92	93	685	70	1265	1319	64.48%	1351	1390	35.52%	--	--	--
SUERC-19067	108	109	795	70	1180	1278	100%	--	--	--	--	--	--
SUERC-18396	***121***	***122***	***494***	***74***	***1326***	***1343***	***4.18%***	***1394***	***1454***	***95.82%***	--	--	--
POZ-26361	***126***	***127***	***415***	***60***	***1429***	***1518***	***90.25%***	***1594***	***1618***	***9.74%***	--	--	--

6.3.3 Physical properties

The sediments from Lake Nyamogusingiri consist of homogenous, dark greenish-black gyttja for the majority of the core (0-115 cm; Figure 6.5). Towards the bottom of the core (between 115 and 122 cm) is a sequence of laminations: black, white and dark grey in colour. Below the banding (122-127 cm) is a very black, compact, peat-like deposit. Crumbly clay nodules are present in the lower 2 cm of this section (cf. Russell *et al*., 2007). There was a lack of visible macrofossils in the Russian core. A leaf fragment was located at ~62 cm and a fish scale at ~94 cm. Charcoal (125-250 μm) was abundant throughout the core, and provided the main material for dating. In the peat-like layer at the base of the core larger fragments of charcoal were found (~5 mm).

The sediments from Nyamogusingiri are organic-rich, with an organic content generally between 20% and 40% (uppermost core section), CO_3 around 1-15% and non-carbonate residue typically accounts for up to a maximum of *c.* 70% Figure 6.1 and 6.5). The organic content is at its lowest (*c.* 7%) in the early part of the record (127 cm; AD 1085), after which it increases to ~30% (119 cm; AD 1150) before briefly dropping and rising to its highest value (32%) in this lower section of the core. The organic content steadily decreases between 114 and 95 cm (AD 1190-1350), before steadily rising to ~25% at 86 cm. The organic content is then relatively stable and fluctuates around 25% in the mid-part of the record (85-65 cm; AD 1425-1580) From AD 1585 (64 cm) values once again decline, reaching a value of *c.* 16% (54 cm; AD 1795). The organic content begins to increase, but tends to fluctuate between ~19 and 23% until AD 1965 (23 cm) when the organic content steadily rises to the present day (60%). The CO_3 record shows a generally decreasing trend towards the present day; however there are some excursions in the data in the earlier part of the sequence. Peaks in the carbonate record occur at AD 1145 (120 cm; ~15%) and AD 1305 (100 cm, ~10%), with low values (~5%) in between.

The bulk magnetic susceptibility from Nyamogusingiri has three distinct zones with a major spike during the low organic period (base of the sequence), and values rising towards the top of the Russian core sequence (magnetic susceptibility measurements are not available for the Kajak core). The earliest part of the record (127-115 cm; AD 1085-1185) has very high values, in comparison to the rest of the core. These high values coincide with a low organic content in the sediments and a period of soil-like deposition in the core stratigraphy. As the organic content increases, the magnetic susceptibility of the sediments drops and remains relatively stable for the majority of the record (115-50 cm). After AD 1865 (50 cm), the magnetic susceptibility fluctuates, but increases and reaches

peaks at AD 1915 (40 cm) and AD 1945 (30 cm), with periods of lower magnetic susceptibility at AD 1935 (35 cm) and AD 1950 (27 cm).

The dry mass accumulation rates (DMAR) from Lake Nyamogusingiri show clear trends, though one of the features is perhaps attributable to the dating applied to the core (Figure 6.5; see *section 6.3.2* for detail). The DMAR is very high at the beginning of the record (127-120 cm; AD 1085-1145), after which a drop in values occurs (*c.* 120 cm; AD 1145). The values rise steadily between 116-95 cm (AD 1175-AD 1350). After *c.* 95 cm (AD 1350) the DMAR is relatively constant until 63 cm (AD 1595) when there is a sharp reduction, though this feature is partly due to the artifact of the AMS ^{14}C date from this section of the longer core sequence (the extrapolation of the ^{14}C dates). The DMAR remains low between 91-53 cm (AD 1380-1820).The dry mass accumulation increases *c.* 51 cm (AD 1860), and this coincides with the start of the ^{210}Pb record, which forces the observed change in the calculated sedimentation rate. DMAR is steady until *c.* 40 cm (AD 1915) after which there is a double peak in the sedimentation rate, marked by the first rapid increase, peaking at *c.* 30 cm (AD 1950) and the second peak is centred on 16 cm (AD 1985). The double peak is separated by a drop in DMAR at 27 cm (AD 1950). From 10 cm (AD 1990) DMAR declines towards the present day.

The inferred values of both the organic and inorganic sediment fluxes to Lake Nyamogusingiri are strongly influenced by the calculated dry mass accumulation rates and thus the pattern of organic and inorganic fluxes are extremely similar. Both organic and inorganic sediment flux is high at the beginning of the record (127-121 cm; AD 1085-1135), after which both flux records decline. The organic flux stabilizes at *c.* 0.012 g cm^{-2} yr^{-1} between 121-62 cm (AD 1135-1365), the inorganic flux follows the pattern of the DMAR, with a brief rise at 117 cm (AD 1170) and a steady increase until *c.* 95 (AD 1350) after which the inorganic flux stabilizes (*c.* 0.04 g cm^{-2} yr^{-1}). Both the organic and inorganic flux records indicate a drop between 62 cm and 52 cm (AD 1600-AD 1845), as observed in the DMAR record (a consequence of the extrapolation of the core chronology). At the onset of detailed ^{210}Pb dating (52 cm), both the organic and inorganic flux appear to increase. The organic and inorganic flux records are stable between 51-40 cm (AD 1860-1915), after which several excursions appear in both records. The organic flux records three peaks 36, 31 and 17 cm (AD 1930, 1940 and 1980, respectively). The inorganic sediment flux records two of these peaks at 31 cm and 17 cm (AD 1940 and AD 1980). The organic and inorganic sediment flux records both decline towards the present day.

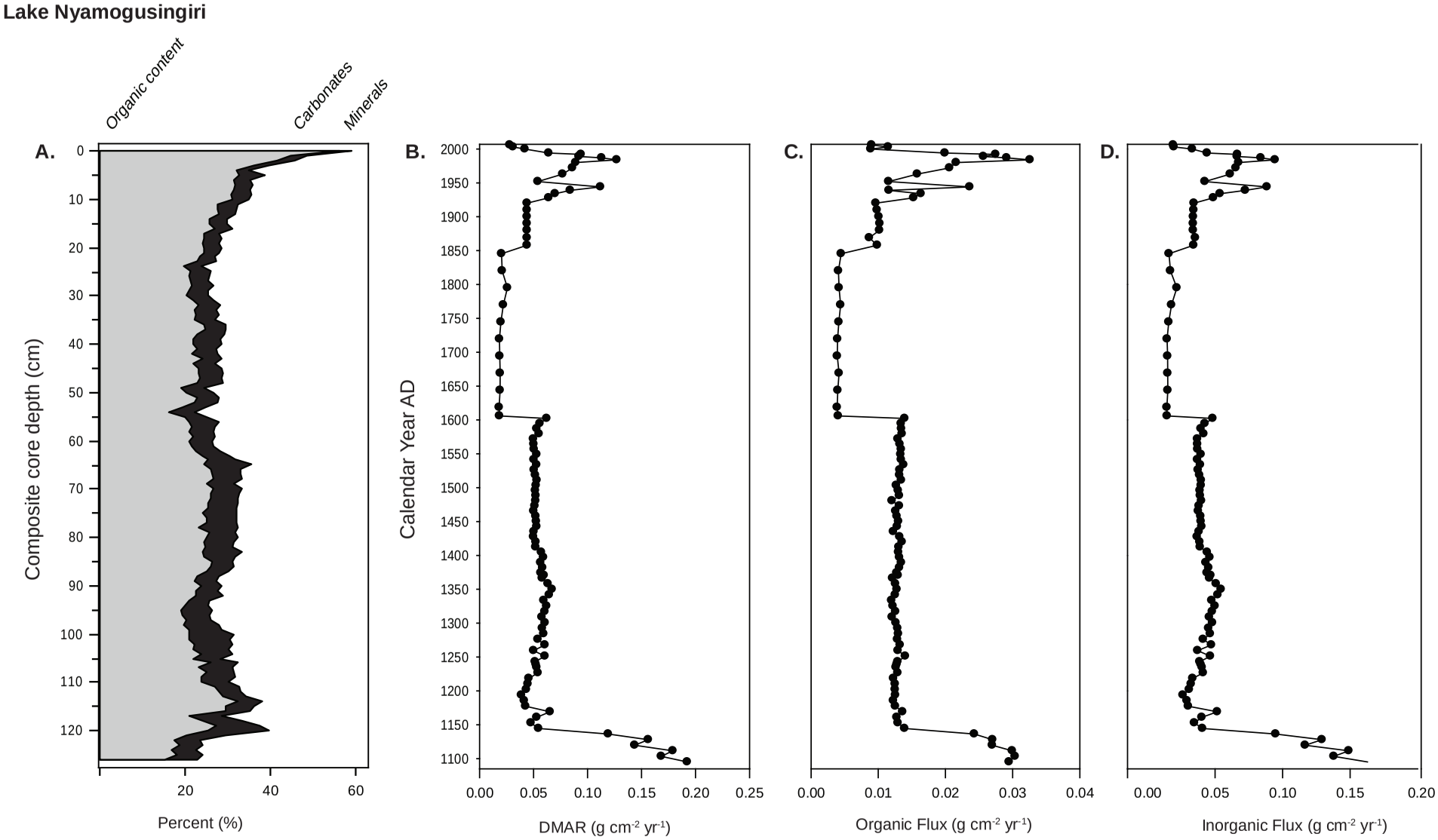

Figure 6.5 *Calculated flux data for Lake Nyamogusingiri.* **(A)** *Stacked organic content (loss-on-ignition) and carbonate percentages versus depth (cm),* **(B)** *dry mass accumulation rate (DMAR) calculated using the dry bulk density and ^{210}Pb dates,* **(C)** *Loss-on-ignition (organic content) displayed as flux (g cm^{-2} yr^{-1}) and* **(D)** *inorganic (minerogenic) flux (g cm^{-2} yr^{-1}).*

Lake Nyamogusigiri

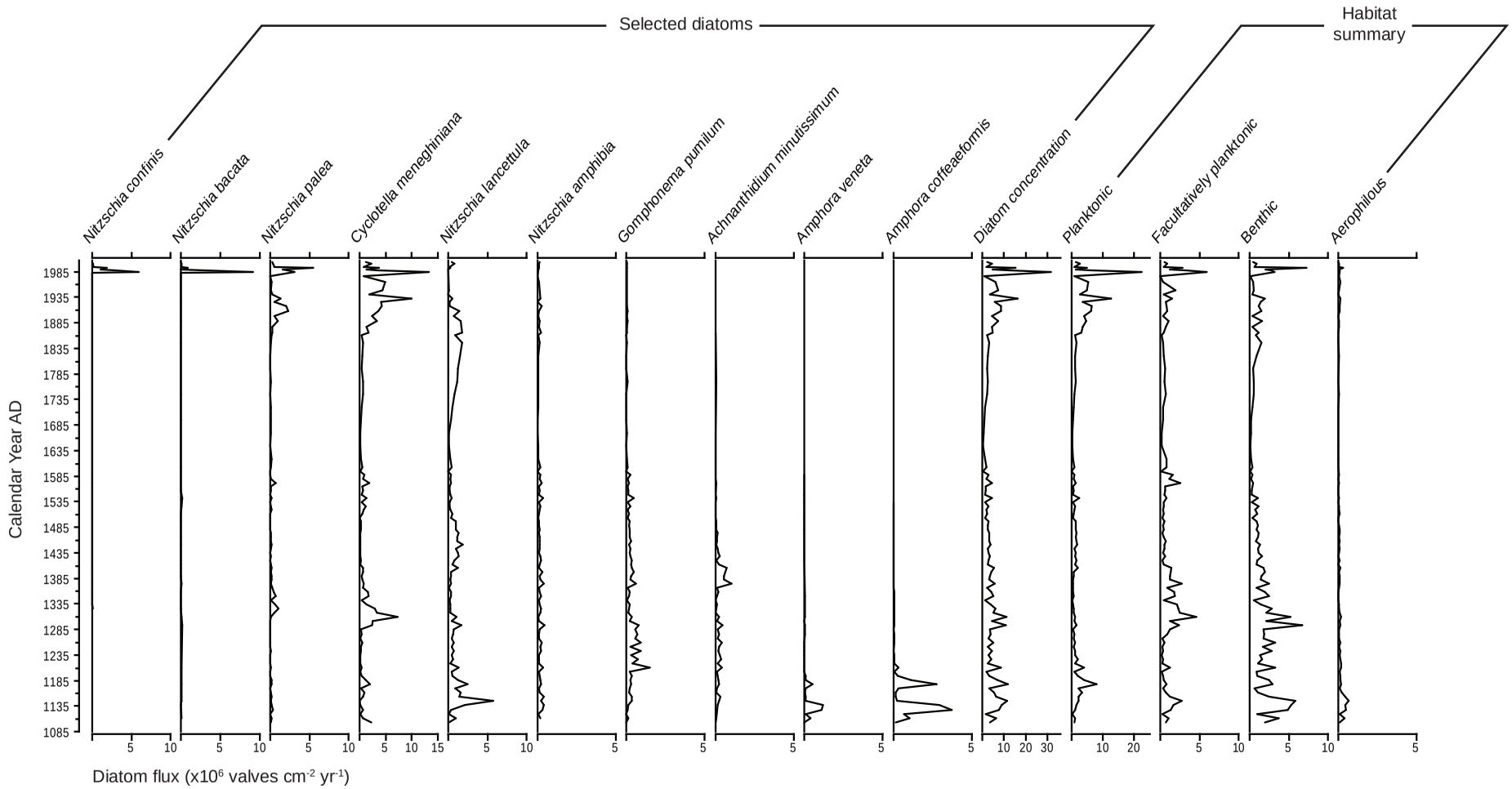

Figure 6.6 *Diatom flux for selected dominant taxa from Lake Nyamogusingiri displayed alongside the total diatom flux for each sample (left). The flux of diatoms within the habitat categories are also shown (right).*

The total diatom flux is quite low (generally <5 x 10^6 valves cm^{-2} yr^{-1}) for the majority of the record, with the largest increase in values occurring in the last *c.* 150 years (generally >5 x 10^6 valves cm^{-2} yr^{-1}), concomitant with the increase in the amount of sediments delivered to the lake (Figure 6.6). There is not a clear relationship between the DMAR and diatom flux, suggesting that any increases in the diatom flux are independent of the sediment accumulation rates. There is a slight elevation in the total diatom flux in the earliest part of the record (*c.* 10 x 10^6 valves cm^{-2} yr^{-1}), driven by the flux of *Amphora coffeaeformis* and *Nitzschia lancettula* (see *section 6.3.4*) to the sediments. The total diatom flux declines until *c.* AD 1650 after which it begins to increase gradually. The largest increase in diatoms occurs from *c.* AD 1850, primarily driven by the large amounts of *Nitzschia palea* (2-5 x 10^6 valves cm^{-2} yr^{-1}) and *Cyclotella meneghiniana* (2-13 x 10^6 valves cm^{-2} yr^{-1}) to the sediments. The total diatom flux exhibit a sharp decline towards the present.

6.3.4 Diatom analyses

The diatom record from Lake Nyamogusingiri is shown in Figure 6.7, 6.8 and 6.9. A total of 130 samples were counted in 0.5 cm sections at a resolution of 1 cm; 174 species were recorded. Using ZONE, eleven assemblage zones were identified for Nyamogusingiri (Ny1-11). The diatom ecologies are largely based upon the information provided in Gasse (1986).

The earliest zone Ny1 (127-114 cm; AD 1085-1190) has been split into 2 sub-zones as this zone comprises two different assemblages. Ny1a (127-125 cm; AD 1085-1105) includes the bottom three samples, and contains an assemblage dominated by the planktonic *Cyclotella meneghiniana* (~55%). The presence of the salt-tolerant, littoral species *Amphora coffeaeformis* (13%) is also important in this zone. There are low abundances of other littoral and benthic taxa present in this zone, such *Hantzschia amphioxys*, *Nitzschia inconspicua* and *Encyonema muelleri*. The benthic, N-heterotrophic species *Nitzschia palea* and the planktonic, freshwater *Aulacoseira ambigua*, peak in abundance over the transition between the two sub-zones. Sub-zone Ny1b (125-114 cm; AD 1105-1190) again has *C. meneghiniana* present (10-15%) and also has high abundances of the salt-tolerant taxa *Amphora veneta* and *A. coffeaeformis* (*c.* 13 and >40%, respectively). At *c.* 120-121 cm (*c.* AD 1140), *C. meneghiniana*, *A. veneta*, *A. coffeaeformis* almost disappear (<2%), and are replaced by a peak in the abundance of *Nitzschia lancettula* (which reaches a maximum of 50%). After this peak, *C.*

meneghiniana, *A. veneta* and *A. coffeaeformis* increase once again, though do not reach the abundances seen at the start of the zone. The benthic/littoral species *Nitzschia amphibia*, *N. inconspicua*, *Encyonema muelleri* and the periphytic *Gomphonema pumilum* appear in this zone. The littoral/benthic species *Achnanthidium minutissimum*, *Nitzschia aequalis* and the periphytic or aerophilous species *Caloneis bacillum* appear in this zone. *Synedra ulna* peaks towards the upper boundary of Ny1b. The diatom preservation **F** index at the beginning of the record is 0.5, and increases throughout Ny2b (**F** = 0.7-0.8). Diatom concentrations are also low at *c.* 39 x 10^6 valves g^{-1} at the base of the sequence, and this increases towards the top of Ny1b to *c.* 180 x 10^6 valves g^{-1}.

Zone Ny2 (114-102 cm; AD 1190-1290) is characterised by a peak in the abundance of *Gomphonema pumilum* (~20%). *Cyclotella meneghiniana* is present in low numbers (<5%) and *Nitzschia lancettula* is also a prominent feature of this zone (~15%). There is a small peak in *Achnanthidium minutissimum* (7%), *Encyonopsis microcephala* (9%) and *Cocconeis placentula* (agg.) (~5%). The benthic and littoral taxa *Nitzschia amphibia*, *Navicula cryptonella*, *Sellaphora pupula*, *Encyonema muelleri*, *Amphora copulata* and the periphytic or aerophilous *Caloneis bacillum* are consistently present throughout this zone. The **F** index is relatively high (**F** = 0.7-0.8) and concentrations fluctuate between 50-75 x 10^6 valves g^{-1}.

In zone Ny3 (102-92 cm; AD 1290-1375) the record is dominated by *Cyclotella meneghiniana* (~60%) and *Nitzschia palea* (~17%), although both species decrease in abundance towards the top of the zone. The planktonic *Nitzschia lancettula* is low in abundance, and its lowest values are coincident with the peak in *C. meneghiniana*. As in Ny2, there is a consistent presence of *Encyonema muelleri*, *Nitzschia amphibia* and *Amphora copulata*, with a decline in the abundance of *Gomphonema pumilum* and *Achnanthidium minutissimum* and *Cocconeis placentula* (agg.).

Ny4 (92-86 cm; AD 1375-1420) is a small zone characterised by a peak in *Achnanthidium minutissimum* (15%) and the epiphytic/benthic species *Encyonopsis microcephala* (~4%). *Gomphonema pumilum* increases in percentage in comparison to the previous zone (>10%). *Amphora copulata*, *Encyonema muelleri* and *Nitzschia amphibia* are still present, and there is a small peak in *Navicula cryptonella*. The **F** index is high at the beginning of the zone (**F** = 0.7) and increases to 0.87 towards the top of the zone. Diatom concentrations fluctuate between 55-70 x 10^6 valves g^{-1}.

The major characteristic of zone Ny5 (86-74 cm; AD 1420-1510) is the peak in *Nitzschia lancettula* (~40%), coincident with a low abundance of *Cyclotella meneghiniana*

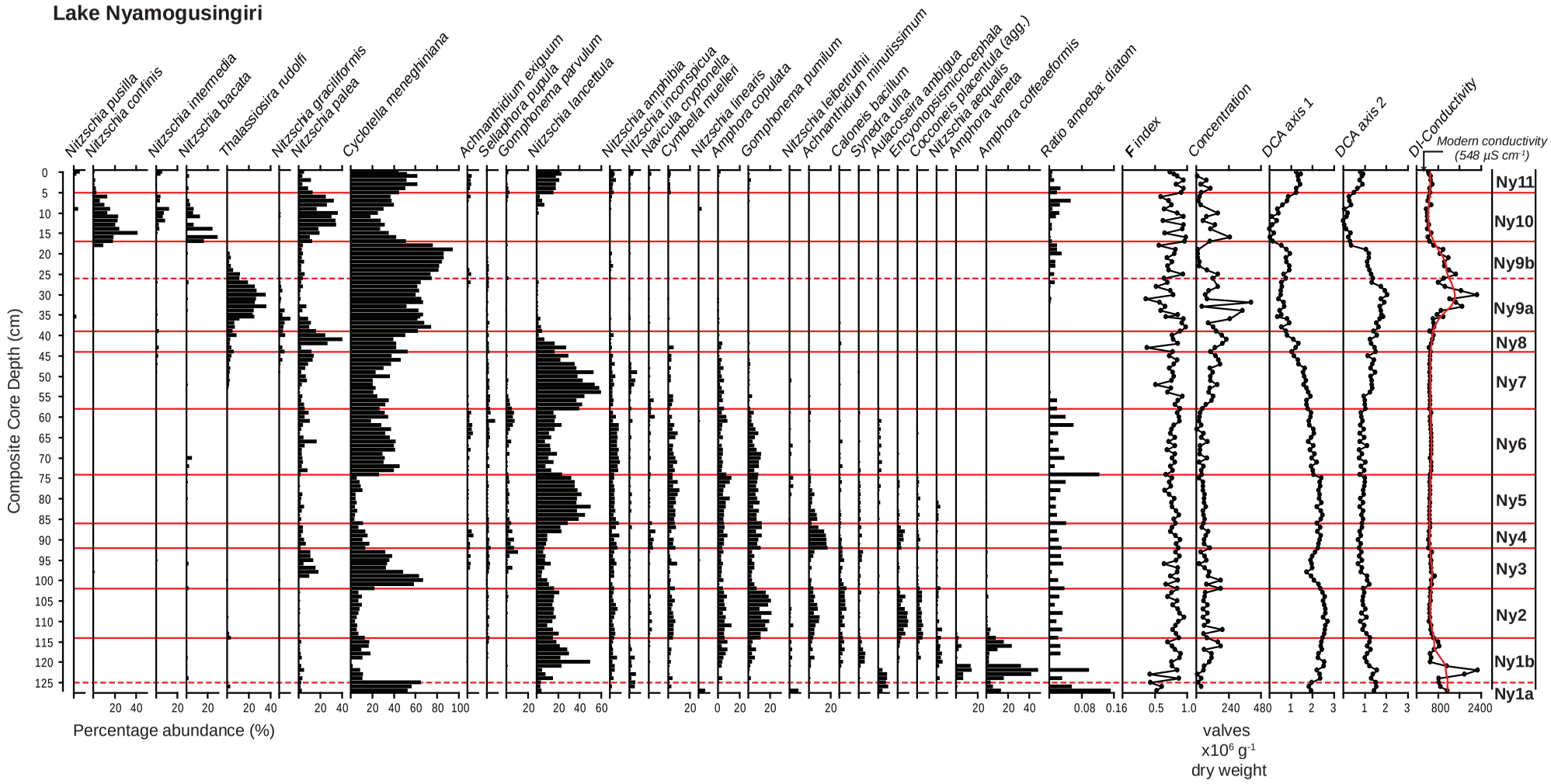

Figure 6.7 *Diatom stratigraphy from Lake Nyamogusingiri plotted against depth. All species > 5% in any one sample are displayed. The diatom taxa have been ordered according to their weighted average abundance in the core (ascending) and are split into assemblage zones Ny1-11. The ratio of testate amoeba scales to diatoms are displayed alongside the diatom preservation index (**F** index), diatom concentrations and the axis 1 and axis 2 sample scores from Detrended Correspondance Analaysis (DCA). Reconstructed conductivities are based on the crater lake transfer function (Combined_76; see **Chapter 5**), a lowess smoother has been added to the reconstruction.*

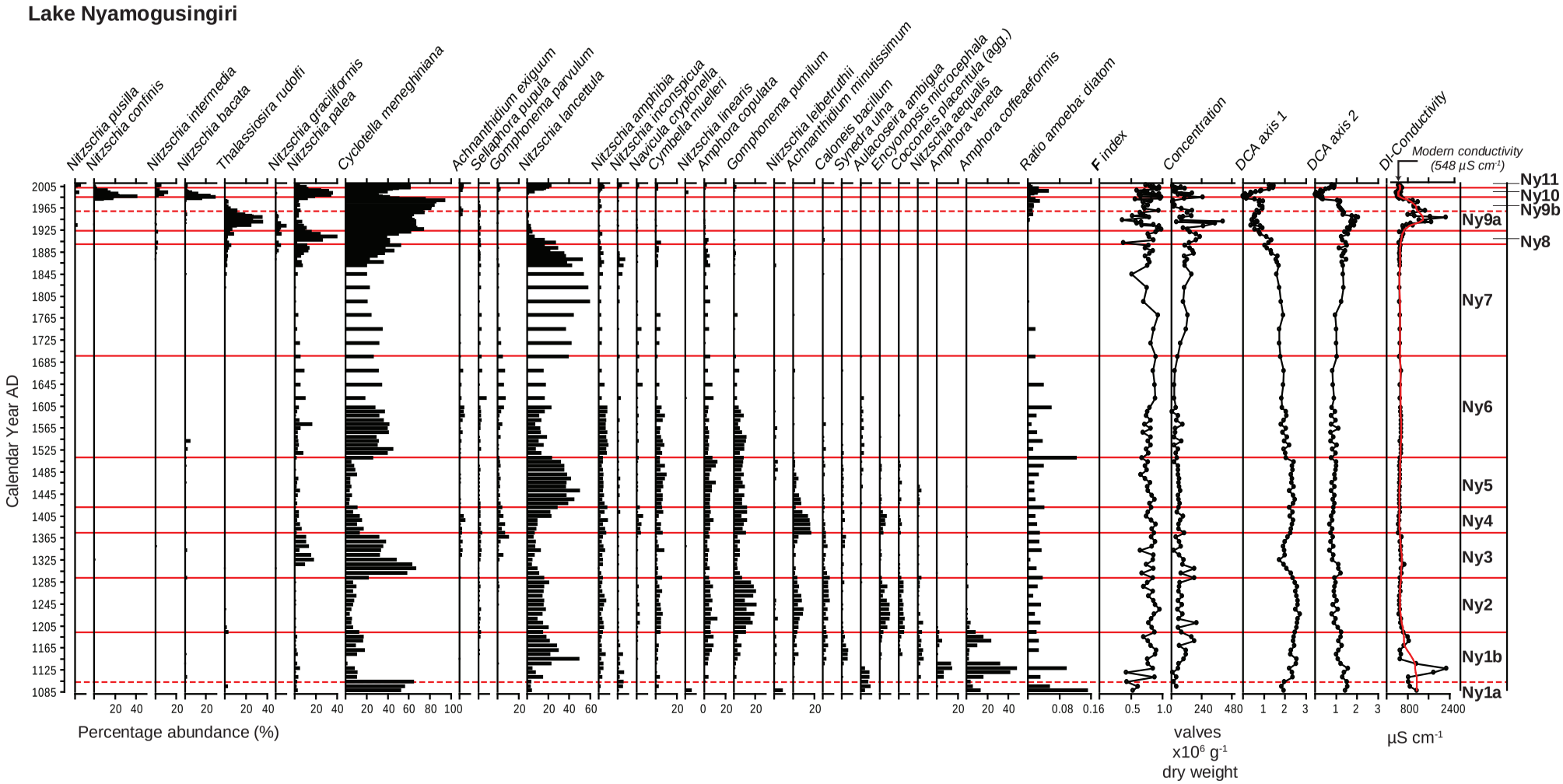

Figure 6.8 *Diatom stratigraphy from Lake Nyamogusingiri. All species > 5% in any one sample are displayed. The diatom taxa have been ordered according to their weighted average abundance in the core (ascending) and are split into assemblage zones Ny1-11. The ratio of testate amoebae scales to diatoms are displayed alongside the diatom preservation index (**F** index), diatom concentrations and the axis 1 and axis 2 sample scores from Detrended Correspondance Analaysis (DCA). Reconstructed conductivities are based on the crater lake transfer function (Combined_76; see **Chapter 5**), a lowess smoother has been added to the reconstruction.*

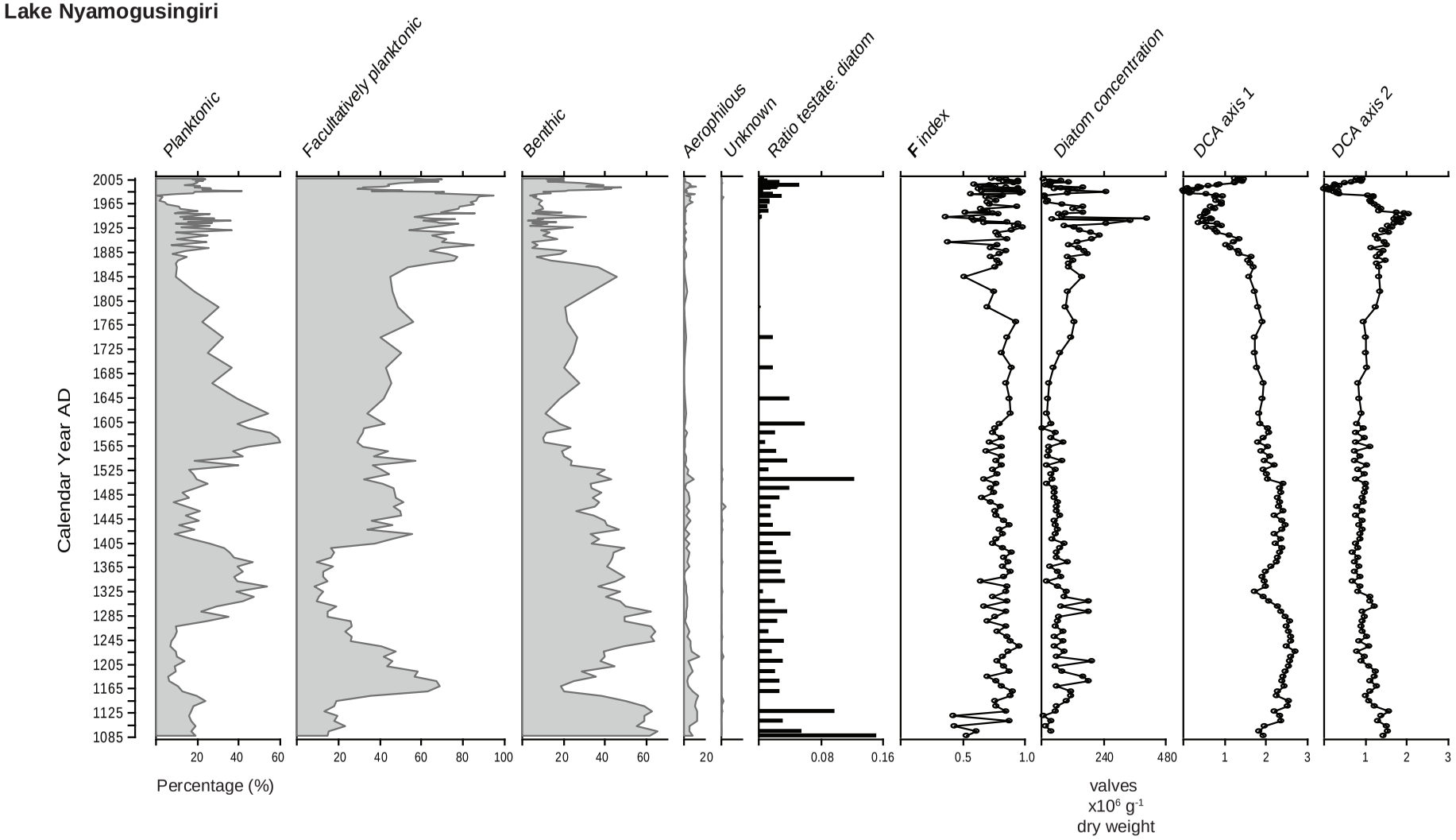

Figure 6.9 *Habitat summary of all diatom species from lake Nyamogusingiri displayed alongside the ratio of testate amoeba scales to diatoms, dissolution index (**F** index), diatom concentration and sample scores from DCA axes 1 and 2.*

(~3%). *Nitzschia palea* is very low in abundance and *Gomphonema parvulum* decreases to ~1%. *Nitzschia amphibia, Encyonema muelleri, Amphora copulata* and *Gomphonema pumilum* are all present at *c.* 4%. There is a small peak in *Amphora pediculus* and a reduction (~1%) of *Achnanthidium minutissimum, Caloneis bacillum, Synedra ulna* and *Encyonopsis microcephala*. *Aulacoseira ambigua* reappears *c.* 81-82 cm (AD 1455). The preservation of diatoms is very good (**F** = 0.8-0.93) and concentrations vary from 80-100 x 10^6 valves g^{-1}.

Ny6 (74-58 cm; AD 1510-1695) returns to a planktonic, *Cyclotella meneghiniana*-dominated assemblage (40%) with a low abundance of *Nitzschia lancettula* (12%). *Gomphonema parvulum* starts the zone with a low percentage and increases towards the top of the zone. *Nitzschia amphibia* also increases to *c.* 8% and there is a slight increase in *Aulacoseira ambigua* (maximum of 2%). The benthic/littoral species *Encyonema muelleri, Amphora copulata* and *Gomphonema pumilum* almost disappear after this zone. The diatom preservation is good (**F** >0.6), but diatom concentrations are variable (4-100 x 10^6 valves g^{-1}).

The assemblage switches from one dominated by *Cyclotella meneghiniana* to a *Nitzschia lancettula* dominated assemblage in zone Ny7 (58-44 cm; AD 1695-1895). Towards the top of the zone, *N. lancettula* decreases as *C. meneghiniana* increases. *Nitzschia palea* is still low in abundance, but increases towards the top of the zone with *Cyclotella meneghininana*. *N. amphibia* is still present and there is a small peak of *Nitzschia inconspicua* midway through (53-48 cm). The species *Encyonema muelleri, Amphora copulata* and *Gomphonema pumilum* disappear. There is also the appearance of the alkaliphilous, planktonic species *Thalassiosira rudolfi* in low percentages (1-2%) at 52 cm. Preservation is good (**F** = 0.8), and diatom concentrations increase from 70-170 x 10^6 valves g^{-1} throughout the zone.

Zone Ny8 (44-39 cm; AD 1895-1920) is characterised by a peak in *Nitzschia palea* (reaching a maximum of 40%). *Cyclotella meneghiniana* is present at *c.* 40% and *N. lancettula* at 20%. The abundance of *N. lancettula* declines to ~1% when *N. palea* reaches its maximum abundance (41 cm). Ny8 represents the last zone in which some benthic and littoral taxa are present (e.g. *N. amphibia*, *Encyonema muelleri* and *Amphora copulata*). The diatom preservation is poor (**F** = 0.3) at the start of the zone and increases (**F** = 0.9) towards the top of the zone.

Zone Ny9 (39-17 cm; AD 1920-1980) has been split into two sub-zones: Ny9a (39-26 cm; AD 1920-1955) and Ny9b (26-17 cm; AD 1955-1980). Both zones have a similar

species assemblage, but Ny9a is characterised by a prominent increase in the saline taxa *Thalassiosira rudolfi* (~25%). *Cyclotella meneghiniana* is high (*c.* 60%), *Nitzschia palea* is low and *N. lancettula* is absent. *Nitzschia graciliformis* (planktonic) occurs at the start of the zone, but declines as *T. rudolfi* peaks. Ny9b demonstrates a rise in *C. meneghiniana* to *c.* 85%, and this coincides with a significant decrease in *T. rudolfi* which disappears at 20 cm (AD 1975). *N. palea* is present, but in low quantities. *N. amphibia* makes a brief recovery in the middle of this zone (~1%, 24 cm; AD 1965).

Ny10 (17-5 cm; AD 1980-2000) is characterised by a drop in the percentage of *Cyclotella meneghiniana*, which is coincident with the appearance of the planktonic species *Nitzschia confinis*, *N. intermedia*, *N. bacata* and a peak in the periphytic *N. palea* (~33%). There is a small peak in *Aulacoseira granulata* v. *angustissima* (~4%). The **F** index varies between 0.6 and 0.9, suggesting good preservation of diatom valves. Diatom concentrations are high at the beginning of the zone (248 x 10^6 valves g^{-1}) and declines to 18 x 10^6 valves g^{-1} at the top of the zone.

The most recent zone Ny11 (5-0 cm; AD 2000-2007) records a decrease in the *Nitzschia* species prominent in the previous zone - *Nitzschia confinis*, *N. bacata* and *N. palea*. There is a peak in *Cyclotella meneghiniana* (60%), *Nitzschia lancettula* (20%) and a small peak in *Achnanthidium exiguum* (3%). The benthic/littoral taxa *Nitzschia amphibia*, *N. inconspicua* and *Encyonema muelleri* reappear during this zone. The diatom preservation is high (0.8-0.9). Diatom concentrations are *c.* 75 x 10^6 valves g^{-1}.

The inferred conductivity from Lake Nyamogusingiri is relatively stable for the majority of the sequence, but does exhibit two major excursions during the *c.* 900 year record. The earliest zone (Ny1) contains the first excursion in the conductivity record. At the very base of the record, the conductivity is higher than the majority of the record (*c.* 1100 µS cm^{-1}; AD 1085) and dips to *c.* 800 µS cm^{-1} at the boundary of sub-zones Ny1a and Ny1b. Following the boundary, the diatom inferred (DI) conductivity reaches one of its highest values (2200 µS cm^{-1}; AD 1130), before declining (500 µS cm^{-1}) and rising to 855 µS cm^{-1} at the boundary of Ny1b and Ny2. The reconstructed conductivity for the middle part of the record (Ny2-Ny8; AD 1218-1913) is extremely stable with conductivities fluctuating around 500 µS cm^{-1}. At the boundary of Ny8 and Ny9a, diatom-inferred conductivities start to increase, reaching a maximum of ~2300 µS cm^{-1} at AD 1950. Values then decline, just before the Ny9a-Ny9b transition (~800 µS cm^{-1}; AD 1955). AD 1960 sees a rise in conductivity to ~1400 µS cm^{-1}, after which values decline, reaching a minimum at AD 1988 (400 µS cm^{-1}; Ny10). The most recent zone (Ny11) exhibits a

slight rise in reconstructed conductivity, reaching a present day value of 400 µS cm^{-1} (just slightly lower than the recorded modern lake conductivity of 500 µS cm^{-1}).

Fossil data are very well covered by the crater lake conductivity model, with 97-100% of species abundance data included. Similarly, there are very good analogues for most levels, with average minimum dissimilarity coefficients of 39, and no samples >83 (Jones and Juggins, 1995; Juggins, 2001).

6.3.5 Indirect ordination – Detrended Correspondence Analysis (DCA)

DCA on all taxa >0.5% abundance (174) revealed a gradient of 2.719 S.D. units; therefore a unimodal response model was appropriate for further analysis. Correspondence Analysis (CA) indicated an arch in the data, thus DCA was deemed the most appropriate response model. A DCA plot of all the core samples and diatom species >5% are shown in Figure 6.10. Comparison to the broken stick model indicated that the four DCA axes were significant in explaining the variance in the diatom data (**Appendix B**), though axes 1 and 2 explained the majority of the variance in the dataset (28.5%); axes 3 and 4 explained only 9.2%. Eigenvalues for axes 1 and 2 are 0.353 and 0.142, respectively whereas those for axes 3 and 4 are only 0.105 and 0.056, and are not considered further (see **Appendix C** for CANOCO output). The first two axes capture 28.5% of the variation in the diatom data set. The gradient represented by axes 1 and 2 appear to reflect the variation in the habitat preferences of the diatoms in the lake sediment sequences. Axis 1 sample scores are positively correlated to the abundance of benthic species (Pearson's correlation coefficient, $r = 0.59$) and negatively correlated to the abundance of facultatively planktonic species ($r = -0.55$). Axis 2 appears to be correlated to the reconstructed conductivity ($r = 0.60$). It is likely that these changes are driven by changes in the abundance of the species *Cyclotella meneghiniana* (coded CY003A) and the introduction and relatively high abundances of species such as *Thalassiosira rudolfi* (TH003A) and *Nitzschia confinis* (NI082A), *N. palea* (NI009A) and *N. bacata* (NIBACC) in the upper parts of the core.

Samples in the DCA ordination diagrams (Figure 6.13) can be split into four groups: (i) 127-48 cm (AD 1085-1875); (ii) 47-19 cm (AD 1875-1980); (iii) 18-6 cm (AD 1980-2000) and (iv) 5-0 cm (AD 2000-2007). Species that dominate group (i) include the planktonic *Nitzschia lancettula*, the facultatively planktonic *Cyclotella meneghiniana* (CY003A) and a large number of benthic and periphytic species (such as *Gomphonema pumilum* (GO080A), *Amphora copulata* (AM011A), *A. coffaeaformis* (AM006A), *A. veneta* (AM004A) and *Nitzschia amphibia* (NI014A). Group (ii) contains many samples that have

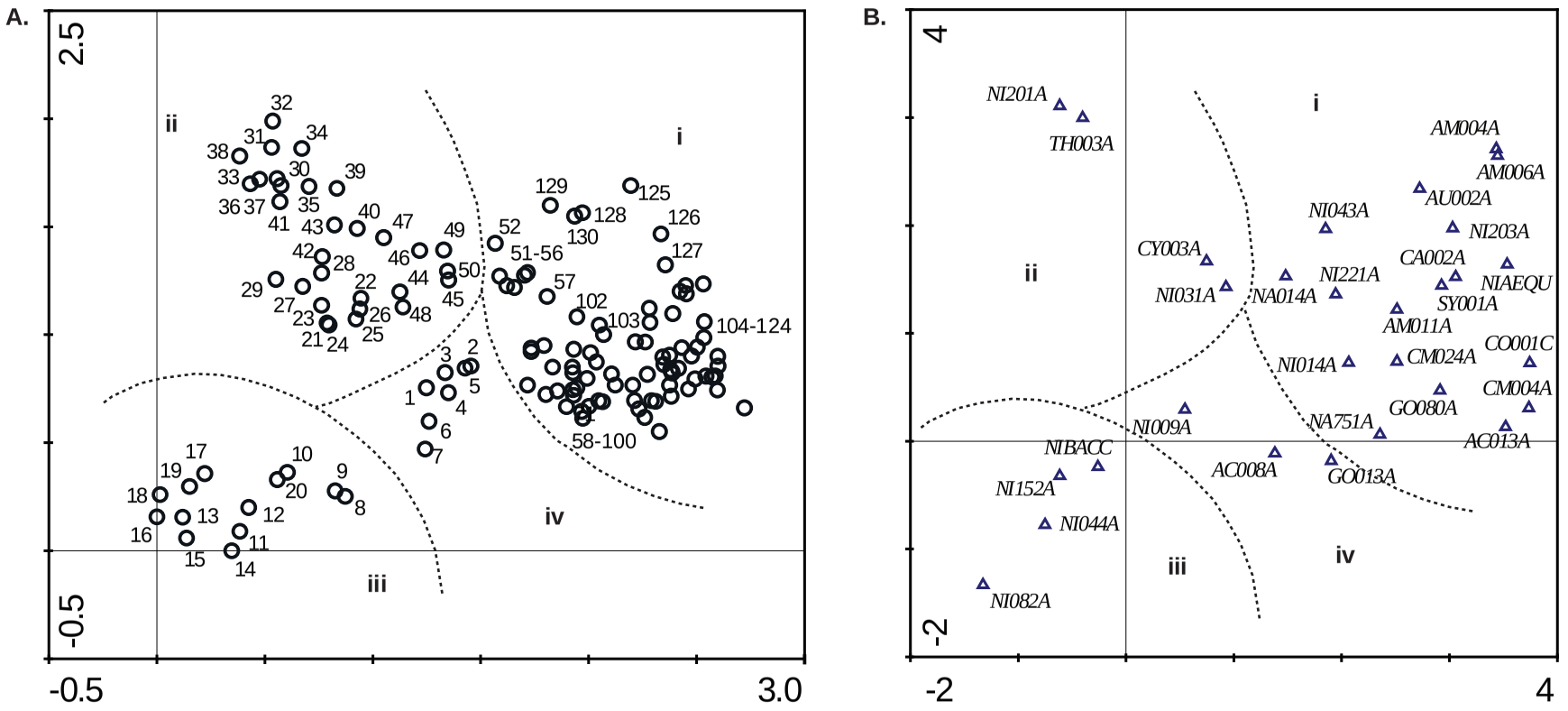

Figure 6.10 *Indirect ordination of diatom samples from Lake Nyamogusingiri. The DCA of* **(A)** *samples (in depth, cm) and* **(B)** *species >5% from Lake Nyamogusinigiri are shown.*

a large abundance of *Cyclotella meneghiniana* (CY003A), but the group is also dominated by the planktonic *Thalassiosira rudolfi* (TH003A) and the benthic *Nitzschia graciliformis* (NI201A). Groups (iii) and (iv) have similar species present, though group (iii) is dominated by the presence of planktonic *Nitzschia* spp., such as *N. confinis* (NI082A), *N. intermedia* (NI044A) and *N. bacata* (NIBACC). The youngest group, (iv), is dominated by the periphytic *N. palea* (NI009A).

6.3.6 Organic isotope analyses

Stable carbon isotope analysis is a widely used technique for determining the source of organic matter and is used to determine the relative proportions of phytoplankton and terrestrial carbon in lacustrine sedimentary sequences (Tyson, 1995). The organic matter of lacustrine sediments is comprised of detritus contributed from terrestrial higher plants in the catchment (C_3 and C_4), aquatic higher plants growing in and around the lakes and algae within the lake (Meyers and Ishiwatari, 1993; Ficken *et al.*, 1998; Ficken *et al*., 2000; Street-Perrott *et al*., 2004). C/N ratios are often used to distinguish whether the source of carbon is predominantly comprised of algae or terrestrial (Tyson, 1995), with values less than 10-12 indicative of a mainly algal source, values >20 suggest carbon of terrestrial plant origin. Whilst it is acknowledged that the use of C/N ratios as an indicator of the source of organic matter should be used with care, they do provide a relatively reliable indication of organic origin.

Figure 6.11 shows the results from the bulk organic isotope analyses ($\delta^{13}C$) and C/N from Lake Nyamogusingiri. C/N ratios are expressed as atomic mass ratios (cf. Meyers and Teranes, 2001). The earliest part of the organic isotope record at Lake Nyamogusingiri (127-120 cm; AD 1085-1145) has sediment with high C/N (~16-20), indicating that the source of the deposited carbon is a mix of both terrestrial vegetation and aquatic algae, though given the higher values, it is likely that terrestrial material is the more dominant source of the deposited carbon. Talbot and Livingstone (1989) found that the $\delta^{13}C_{organic}$ composition of C_3-dominated sediments from lakes in East Africa varied between −20‰ and −30‰, whereas C_4-dominated lake sediments varied from −10‰ to −15‰. The high C/N at this depth coincides with $\delta^{13}C$ values of –22‰ to –17‰, which, given the high terrestrial input is perhaps related to lower lake levels, and may be interpreted as an increased input of $\delta^{13}C$ from aquatic macrophytes or C_4 plants. The $\delta^{13}C$ values become more negative towards AD 1145 (120 cm; −23‰) and C/N decreases (~14). The carbon is still from a mixed source, and the low $\delta^{13}C$ may be a result of terrestrial

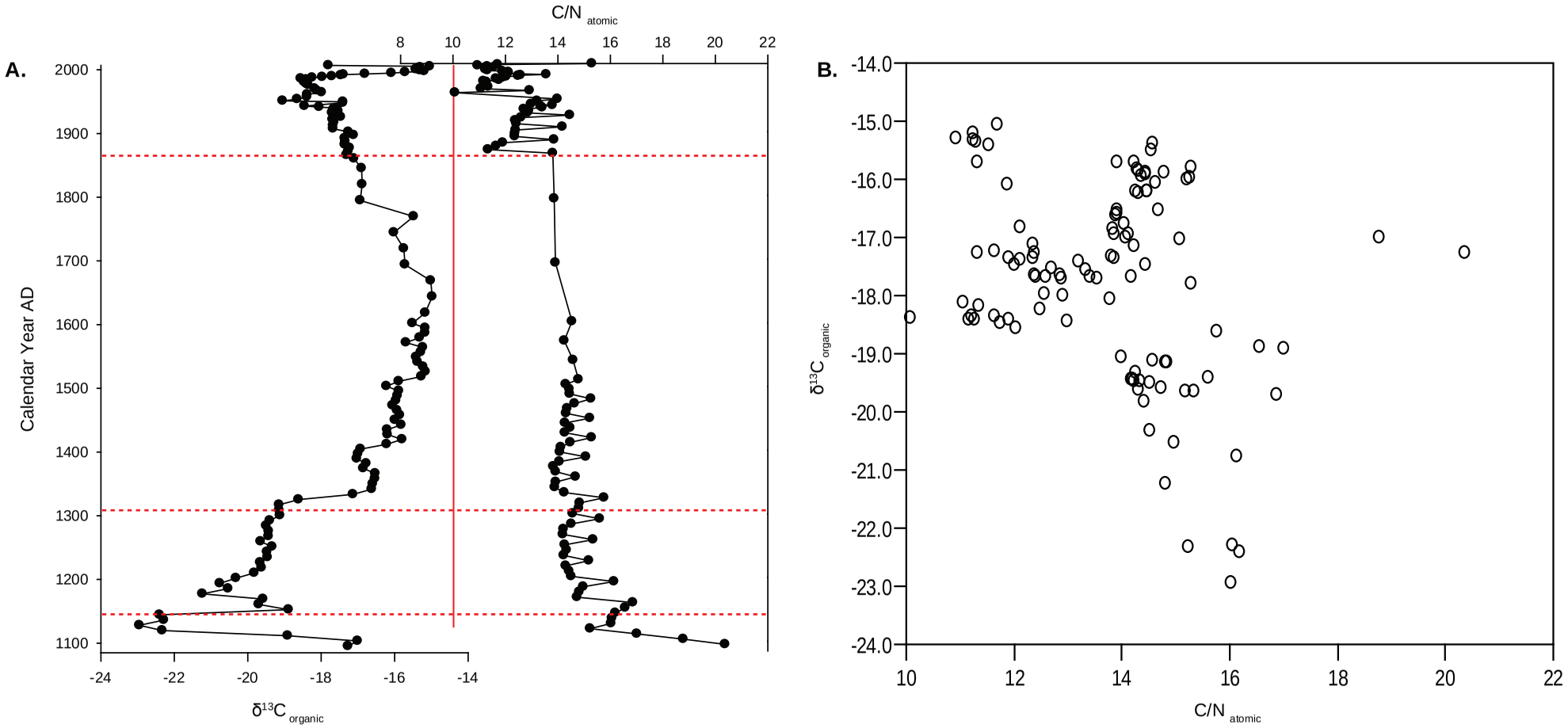

Figure 6.11 **(A)** *Organic isotope stratigraphy from Lake Nyamogusingiri - $\delta^{13}C_{organic}$ (left) and C/N_{atomic} ratios (right). The vertical solid red line (C/N ratio) indicates the boundary between algal (<10) and terrestrial (>10) dominated productivity (Meyers and Lallier-Vergès, 1999). The dashed lines represent key zones discussed in the text.* **(B)** *Scatter plot of C/N vs. $\delta^{13}C$.*

input (C_3 woody plants), or perhaps the increasing importance of aquatic algae (plankton $\delta^{13}C$: −19 to −23‰ [Lamb et al., 2004], −22 to −36‰ [Tyson, 1995]; cyanobacteria $\delta^{13}C$: −13 to −17‰ [Tyson, 1995], especially given the drop in C/N towards the aquatic/terrestrial boundary (C/N = 10; Tyson, 1995; Horiuchi *et al*., 2000).

The record between AD 1146-1305 (120-100 cm) is typical of lacustrine sediments, indicating a mixed carbon source. C/N oscillates between 14 and 15, perhaps a result of carbon input from both C_3 plants and macrophytes. The low $\delta^{13}C$ values (−21 to −19‰) are indicative of C_3 woody vegetation and perhaps phytoplankton. The C/N follows a similar oscillating pattern between AD 1305-1865 (100-50 cm), though it should be noted that there are fewer C/N measurements over this period. During this section the $\delta^{13}C$ values rise quite sharply to values between −17 to −13‰, which may be associated with the deposition of carbon from C_4 plants. However, given the low C/N values, it is more likely that these values arise from an aquatic carbon source (macrophytes and algae). At 50 cm (AD 1865), C/N values reach one of the lowest seen in the record, dipping to *c.* 11, perhaps indicating a brief period when algal-dominated productivity is more prevalent than inputs from the terrestrial system. This is confirmed by the higher $\delta^{13}C$ (−18‰) suggesting an important input from the lake phytoplankton.

After AD 1865 (50 cm), the C/N increases (12-13), and resumes the oscillating pattern seen earlier in the record. Whilst still indicative of a mixed carbon source, these lower C/N values and high $\delta^{13}C$ (*c.* −18‰) highlight the increasing importance of phytoplankton to the carbon being deposited in the lake. At ~25 cm (AD 1960), the C/N drops to 10 (the lowest value in the record). In conjunction with a $\delta^{13}C$ of −19‰, this suggests phytoplankton productivity is driving the carbon signal recorded in the sediments. In the uppermost samples (10-0 cm; AD 1990-2007) the C/N fluctuates between 11 and 13.5 (maximum of 15 in the surface sediment sample), again reflecting a typical lacustrine sediment with a mixed carbon source, but certainly indicating the importance of the aquatic macrophytes and phytoplankton as carbon sources in this recent period. This is in turn supported by the high $\delta^{13}C$ (*c.* −14%).

6.3.7 Interpretation of records from Lake Nyamogusingiri

Ny1: AD 1085 – AD 1190

The earliest part of the Nyamogusingiri record is split into two subzones. Initially the diatom assemblage is dominated by *Cyclotella meneghiniana* and low abundances of the

salt-tolerant taxon *Amphora coffeaeformis*, indicating a shallow, saline environment (Gasse, 1986; Gasse *et al*., 1997). The appearance of *Aulacoseira ambigua* and a slight increase in the abundance of *Nitzschia lancettula* across the sub-zone boundary and a subsequent reduction in the abundances of *A. coffaeaformis* and *C. meneghiniana* attest to a short-lived fresher, open-water phase.

The abundance of *A. coffeaeformis* increases in conjunction with the appearance of the salt-tolerant *A. veneta* (*c.* AD 1110), both of which show a double peak in this zone, suggesting two periods of higher salinity (centred on AD 1120 and AD 1180). These two saline events are punctuated by a freshwater event (*c.* AD 1150) characterised by a deepening of the lake, indicated by a rise in *Nitzschia lancettula* (Stager *et al*., 2005) and *Synedra ulna*. The latter species has a wide ecological tolerance, but clearly favours fresh water environments (Gasse, 1986; Telford and Lamb, 1999), whereas there is little literature surrounding the ecological preferences of the former. Ecological inference of *N. lancettula* is therefore based on a small number of studies by Stager and colleagues (e.g. Stager *et al*., 2005) who report this taxon in cores from the freshwater Lake Victoria at times of inferred higher lake levels.

The earliest peak in the reconstructed conductivity (and supported by the diatom ecology) is greater than the latter event (lower conductivity), when the lake appears to be somewhat deeper and fresher (low *C. meneghiniana* and high flux of *N. lancettula*) perhaps allowing the colonisation of inundated shallower areas by aquatic vegetation, as indicated by the appearance of the periphytic taxa *Amphora copulata*, *Nitzschia amphibia*, *Gomphonema pumilum* and *Achnanthidium minutissimum* (AD 1140; Gasse, 1986) and the mixed input of carbon from terrestrial and aquatic ecosystems (including a contribution from aquatic macrophytes).

This very early period is coincident with sediments indicative of a more terrestrial environment, where the catchment has a large influence on the lake habitat, there is a large flux of minerogenic sediments to the lake at this time with a low organic content and high magnetic susceptibility, perhaps suggestive of catchment inwash due to reduced catchment stability (e.g. decline of stable forest vegetation during an arid phase). Similarly the organic isotopes suggest that terrestrial plants are the most dominant source of deposited carbon in the sediments. The high testate amoebae: diatom ratio earlier in the record also suggests that littoral areas are important. The testate: diatom ratio decreases during the inferred freshwater period *c.* AD 1150 and is coincident with a rise in the organic content of the sediments (119 cm) and a reduction in the flux of minerogenic matter to the lake.

The sediment stratigraphy has a section of laminations, perhaps indicative of deeper, stratified waters during this fresh period (and supports the interpretation of the presence of the diatom taxon *N. lancettula*).

Ny2: AD 1190 – AD 1290

The dominance of *Gomphonema pumilum* during this period perhaps attests to little catchment disturbance (catchment stability; cf. Leira and Sabater, 2005). Freshwater and a deepening of the lake are inferred by the higher abundance (*c.* 15%) of *Nitzschia lancettula* and low *Cyclotella meneghiniana* although the presence of benthic and periphytic species *Encyonopsis muelleri* and *Cocconeis placentula* (agg.) suggest that marginal lake areas are important, especially as benthic species tend to dominate in this zone (Figure 6.9). The sediment stratigraphy is comprised of organic lake mud and organic isotopes suggest a mixed carbon source (C/N 13-15).

Ny3 – Ny7: AD 1290 – AD 1890

From *c.* AD 1200 to *c.* AD 1890, the diatom record is seemingly characterised by lake level fluctuations and perhaps by changes in the mixing regime of the lake. Higher lake levels with a stratified water column are indicated by high abundances of the freshwater, planktonic *Nitzschia lancettula* (Stager *et al*., 2005); the presence and the high flux of the epiphytic *Achnanthidium minutissimum* is also indicative of a well oxygenated lake (Cholnoky, 1968) and suggests that the core site at this time was closer to the littoral zone. Throughout this period the isotopic record is typical of an East African lacustrine system dominated by a mixed carbon source of C_3 plants and phytoplankton (Lamb *et al*., 2004). Using *N. lancettula* as a proxy for higher lake level, inferred high-stands are centred on AD 1140, AD 1285, AD 1470 and AD 1820. Lower lake levels, increasing inputs of organic matter and low oxygen levels characterise the periods between the high-stands centred on AD 1300, AD 1560, AD 1925, AD 1980 and AD 2005. These low light, low oxygen and possibly nutrient rich phases are typified by high abundances and fluxes of *C. meneghiniana* and *Nitzschia palea* (Leland and Porter, 2000; Tuchman *et al*., 2006) and may attest to poor health of this aquatic ecosystem (Lange-Bertalot, 1979; van Dam *et al*., 1994; Charles *et al*., 2006). *Nitzschia palea* follows a similar pattern to *C. meneghiniana*, diverging only in the uppermost core section (AD 1980-2007).

During the period AD 1135 to AD 1890, littoral taxa are also important, suggesting persistent aquatic vegetation, especially due to the continuous presence of *Encyonema*

muelleri (Stager and Johnson, 2000). The sediment stratigraphy throughout this period consists of organic lake mud, with the presence of floral and faunal macrofossils (leaves and fish scales). The fish scales located at *c.* 94 cm (*c.* AD 1350) perhaps attests to a long history of fish in this lake system. A period of low sedimentation is inferred between AD 1600 and AD 1850, a period coincident with higher lake levels (*N. lancettula*) and the climatic perturbation known as the Little Ice Age (Bradley, 2000), which may be indicative of a well vegetated catchment (and thus catchment stability) restricting the amount of sediment delivered to the lake.

Ny8 – Ny11: AD 1890 – AD 2007

During the last *c.* 120 years, major changes are observed in all records. The overall diatom flux (Figure 6.6) is relatively low prior to AD 1860 (generally $<5 \times 10^6$ valves cm^{-2} yr^{-1}), after which it increases to *c.* 8×10^6 valves cm^{-2} yr^{-1} (an a maximum of *c.* 30×10^6 valves cm^{-2} yr^{-1}). The dominance of *N. palea* is perhaps related to the influx of sediments and organic matter as a result of catchment disturbance (Sabater, 2000; Figures 6.6 and 6.8). Recent studies have shown that *Nitzschia palea* thrives in habitats that are organically enriched and as a consequence *N. palea* is capable of living and sustaining large populations in very turbid (low light) conditions (Tuchman *et al*., 2006). Where light levels (solar radiation) are too low for photosynthesis, *N. palea* are able to utilize heterotrophic metabolism organic carbon sources to sustain growth (Tuchman *et al*., 2006).

The sediments suggest a highly productive lake system (AD 1860-AD 1995), due to the increasing organic matter and indicators of lower lakes levels (*C. meneghiniana* and *N. palea*). The increase in the flux of catchment sediments (both organic and minerogenic) to the lake coincides with an increase in the flux of *Nitzschia palea* and *Cyclotella meneghiniana*. An increase in the flux of catchment sediments to the lake system would be expected to dilute the diatom concentrations, which is not the case in the Nyamogusingiri record. Thus it is likely that the influx of these sediments, perhaps as a result catchment destabilisation (vegetation removal) in response to climatic stressors (e.g. a more arid climate) and anthropogenic impacts (clearance for agriculture) led to the delivery of a large quantity of nutrients to the lake. This nutrient input may have caused a large increase in turbidity and diatom productivity and hence the influx of total diatoms, which is primarily driven by *N. palea* and *C. meneghiniana*. This increase in diatom productivity also coincides with a change/drop in the C/N to <12 and $\delta^{13}C$ values in the range of phytoplankton (diatoms), suggesting the importance of algae as a source of carbon.

The disappearance of littoral/periphytic taxa after AD 1920 suggests conditions were unsuitable for the growth of aquatic vegetation, as a consequence of high turbidity and rising salinity, whilst a rise in the abundance of *Cyclotella meneghiniana*, *Nitzschia palea* and the concurrence of *Thalassiosira rudolfi* may indicate a more saline lake. The association of *C. meneghiniana* with *T. rudolfi* is thought to indicate higher alkalinity/hyper-alkalinity and may be linked to very low lake levels (Stager, 1984; Gasse, 1986); this inferred period of alkalinity coincides with a low dissolution index (**F** = 0.3). *Nitzschia lancettula* disappears almost completely from the record between AD 1950 and AD 1990 and *N. palea* dominates. In addition to this, the lowering of lake levels would perhaps induce more frequent mixing of the lake waters, causing the mixing of the lower, nutrient enriched waters which may lead to a bloom in *Cyclotella meneghiniana*. Lower lake levels would lead to a greater concentration of total phosphorus (TP; through evaporative enrichment), and with a lack of outflow during times of lower lake level, water residence time would be increased leading to the recycling of phosphorus.

Around AD 1980 *Cyclotella meneghiniana* decreases and there is a peak in the long thin, needle-like *N. confinis* and *N. bacata* which may attest to deeper, stable lake conditions with stratification. *Nitzschia bacata* in Lake Kivu, for example, has been shown to form distinct near-surface populations under daily (thermal) stratification (Sarmento *et al*., 2006). *Nitzschia palea* increases in abundance, coincident with a decline in *N. confinis* and *N. bacata*, reaching a peak *c.* AD 1995. This increase in *N. palea* in the very recent past may be a result of increasing nutrient inputs to the lake as a consequence of human induced catchment disturbance. The construction of a safari lodge (Jacana, completed in 1998; see **Chapter 2**, *section 2.7.1*) on the shores of the larger basin would have delivered large amounts of minerogenic and organic sediments into the lake system.

The most recent period (AD 1995-AD 2007) is once again dominated by *Cyclotella meneghiniana* and *Nitzschia lancettula*, which up until the present have not occurred simultaneously. The increase in *N. lancettula* is most likely a result of increasing lake levels and chemical stratification in the lake. The co-occurrence of the more saline tolerant taxon (*C. meneghiniana*) and the freshwater taxon (*N. lancettula*) is extremely unusual and could be attributed to the wide tolerance of environmental conditions that *Cyclotella meneghininana* can withstand (Gasse, 1986). However this co-dominance may be for several other reasons. For example, in this part of the sediment record, the samples most likely incorporate taxa from several seasons, especially given the near-annual resolution in the upper 50 cm of the core (^{210}Pb dating, see *section 6.3.2*). The lake may support

different diatom communities on a seasonal basis, with *Nitzschia lancettula* the dominating taxon during the wet season, and *Cyclotella meneghiniana* prevailing during the dry season. This mixing of seasonal signals has been observed elsewhere in the tropics, where extreme seasonality has in a single sample, brought together seemingly incompatible diatom species (cf. Barker, 1990).

6.4 Lake Kyasanduka

6.4.1 Core correlation

Six cores were collected from Lake Kyasanduka: two Kajak cores (KYAS-1 0-39 cm; KYAS-2 0-28 cm) and four Russian cores (KR1C1 31-99 cm; KR2C1 20-100 cm; KR1C2 4-97 cm and KR2C2 0-100 cm). Preliminary core correlations were made using the field notes related to coring depths. Detailed core correlations were completed through the use of the core descriptions, loss-on-ignition (organic content) profiles, magnetic susceptibility profiles and high-resolution diatom analysis on overlapping sections. Finally, ^{210}Pb and AMS ^{14}C dating validated the core correlations, and formed a composite core chronology.

Core descriptions made in the field immediately after collection and the supplementary descriptions taken in the laboratory identified several laminated sections in all four of the Russian cores. These sections of banding provided a key tool for the visual correlation of the four core sequences (Figure 6.12). They included a section of discontinuous banding in the middle of R2C1 (*c.* 45-50 cm) which was correlated with a thin black band in R1C1 (at *c.* 85 cm). A section of banding consisting of orange, brown, red and grey laminations was identified at the base of R2C1 (80-84 cm) and the upper sections of R1C2 and R2C2 (14-18 cm and 14-17 cm), providing a clear tie point for the correlation of these lower core sequences.

The correlations based on the core stratigraphy were confirmed by the loss-on-ignition analyses (organic content) and the magnetic susceptibility (Figure 6.12 and 6.13). The correlation for the three cores R1C2, R2C1 and R2C2 was extremely tight in the upper sections, with a series of oscillations in the organic content being repeated exactly in all three cores (Figure 6.12). However, the lower sections of R1C2 and R2C2 were slightly more difficult to correlate, due to several deviations in the organic content and magnetic susceptibility in R2C2 (Figures 6.12, 6.13 and 6.14).

The correlation of the Kyasanduka cores R1C2 and R2C2 highlighted potential problems when relying on LOI as the sole tool for correlation (Figure 6.14a). The two core

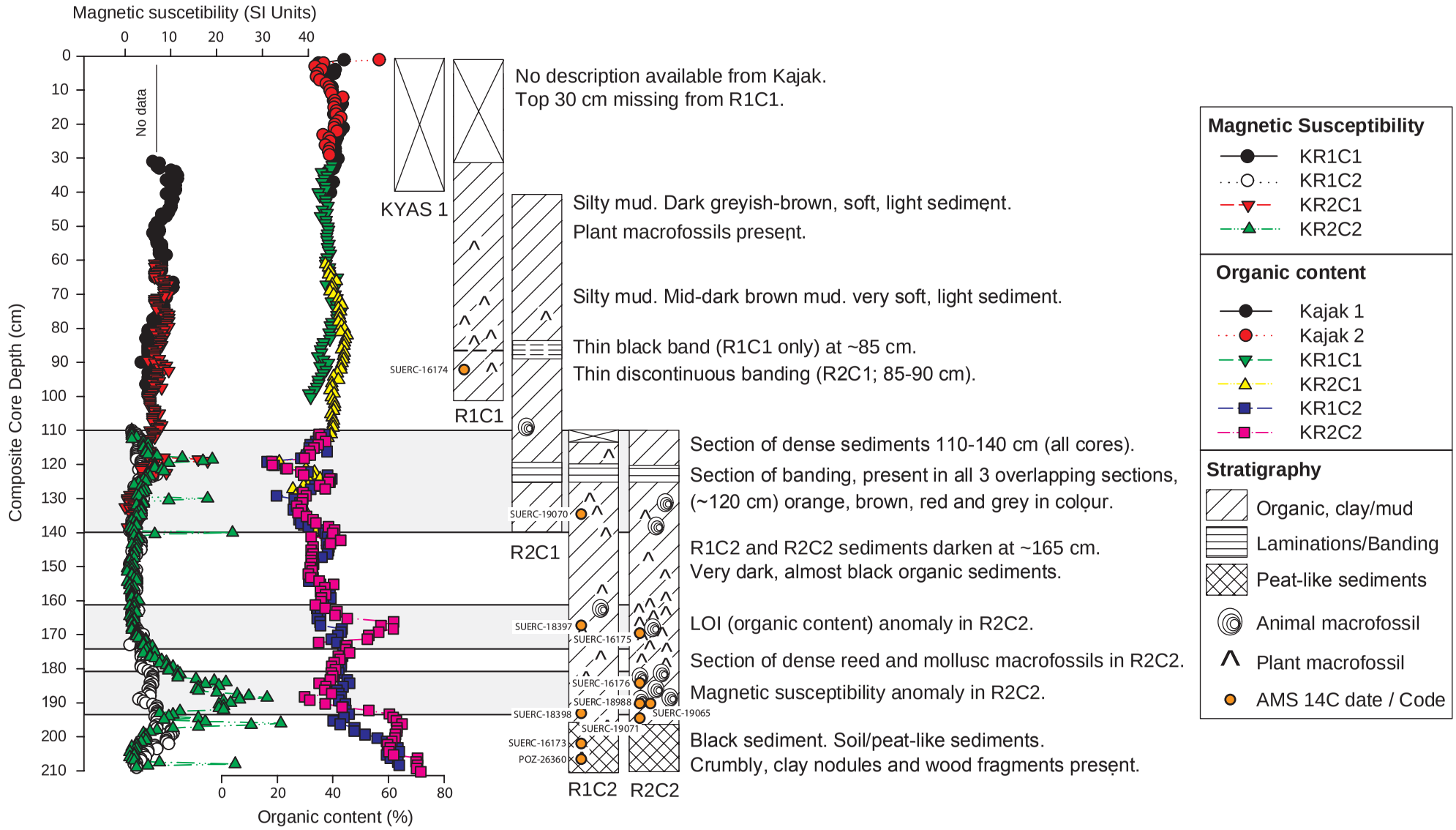

Figure 6.12 *Correlation of the overlapping core sections recovered from Lake Kyasanduka. Results of magnetic susceptibility, loss-on-ignition (LOI; a measurement of the organic content of the sediment). Core stratigraphies are also displayed alongside brief descriptions, highlighting how a series of laminations across all cores was used as a tie-point for the correlation of the cores.*

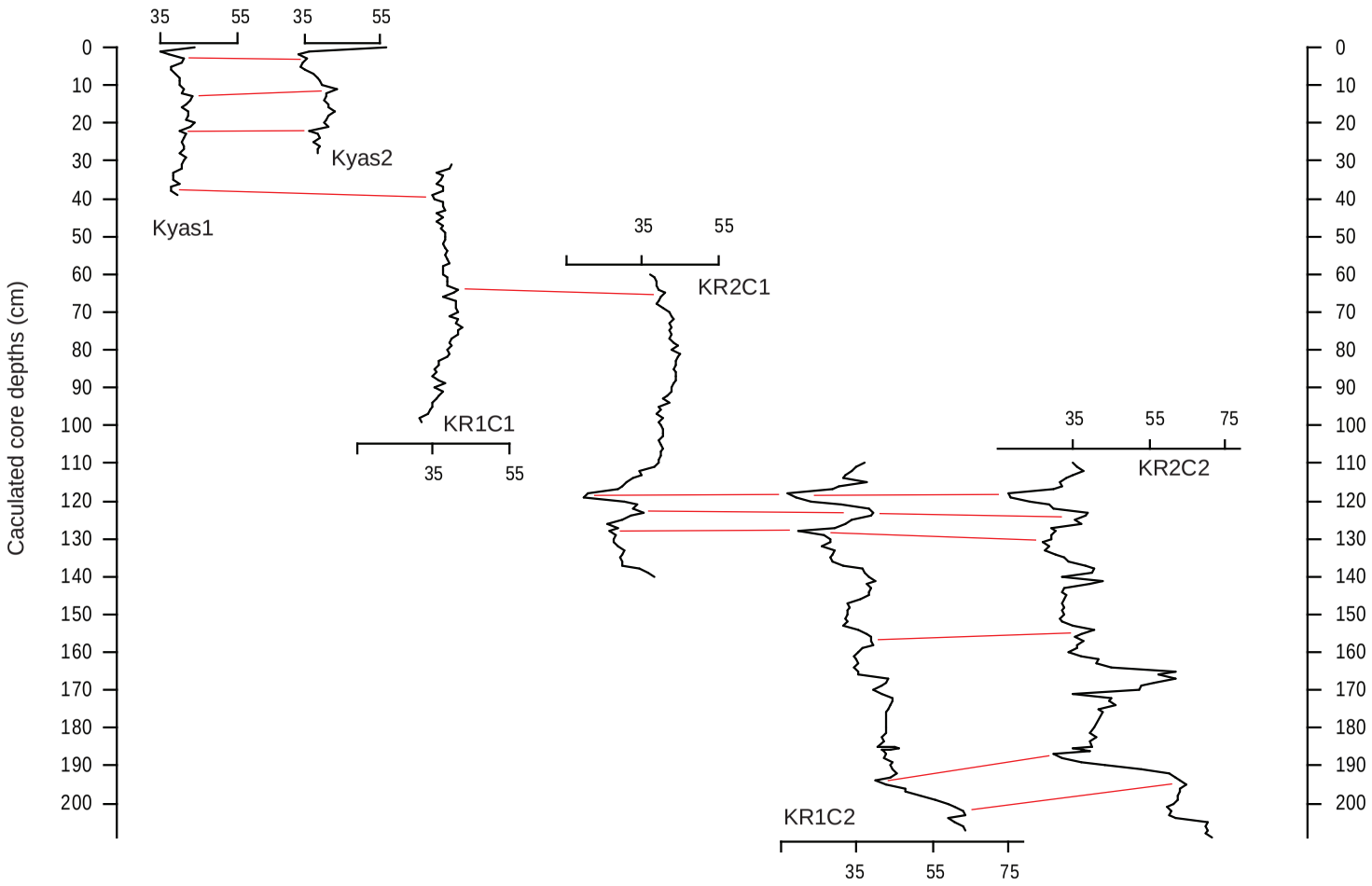

Figure 6.13 *Loss-on-ignition (organic content) profiles for the six cores (2 Kajak and 4 Russian) recovered from Lake Kyasanduka. The cores are displayed against their calculated coring depths (based on measurements made in the field). The red lies indicate tie points between the various core sections. The large oscillations in the organic content between c. 120 cm and 130 cm provided a key index in the correlation of the three lower cores (R2C1, R1C2 and R2C2). The compaction of R2C2 relative to R1C2 can also be observed (see* ***section 6.#.#*** *for details).*

records, although covering the same period, have differing LOI profiles, with R2C2 seemingly presenting a number of differences between 160-190 cm. The two notable data excursions in R2C2 manifest as a peak in the LOI profile (160-170 cm), a peak in the magnetic susceptibility coincident with a drop in the LOI record *c.* 180-190 cm. It appears that R2C2, in its lower sections (from *c.* 160 cm) has a compacted record, relative to R1C2. In order to resolve the correlation in these lower sections, high resolution diatom analyses were completed on the problematic section of R2C2 (Figure 6.14).

The diatom record showed an almost identical stratigraphy in both cores, with several prominent features identified. The disappearance and reappearance of *Aulacoseira* spp. evident in both records as well as the appearance of subaerial taxa (e.g. *Orthoseira roeseana*) in the lower parts of both of the cores (Figure 6.14b) highlighted a 5-10 cm offset in the R2C2 record. This offset is almost certainly due to lower sedimentation in R2C2. Figure 6.15 presents a Shaw diagram to aid the understanding and comparison of features in the lower cores (R1C2 and R2C2). Numerous features, common to both cores (e.g. peaks and troughs in LOI and key diatom assemblage changes) were selected and their cores depths noted. In Shaw diagrams (Shaw, 1964) uniform accumulation rates are presented by a 1:1 straight line (y=x). Changes of slope indicate between core differences of accumulation rate, whilst deviations from a straight line (e.g. “dog-legging”) suggest relative changes in the accumulation rate for a given time period (Anderson, 1986). The Shaw diagram (Figure 6.15) for cores R1C2 and R2C2 indicates that in the upper sections of the two cores (110-160 cm) the accumulation rate is uniform (points sit on the 1:1 line). After 160 cm, all points deviate (‘dog-leg’) from this 1:1, indicating a period of lower sedimentation in R2C2, relative to R1C2.

Using these key tie points from the Shaw diagram and the offset between the accumulation rates in the two cores, the R2C2 sequence was stretched relative to R1C2. The results of this stretch and the correlation of R2C2 relative to R1C2 are shown in Figures 6.16. The adjustment of the R2C2 record resulted in the composite core sequence being 2.17 m in length.

The LOI peak in R2C2 (160-170 cm) is almost certainly due to the presence of a high number of reed macrofossils, not observed in R1C2. Although care was taken when sampling for LOI, given the high abundance of the reed macrofossils, it is more than likely that some fragments were incorporated into the sample for combustion. The high organic content of these plants would almost certainly account for the spike in LOI over this core section as well as the high abundance of mollusc, which would likely have thrived in a

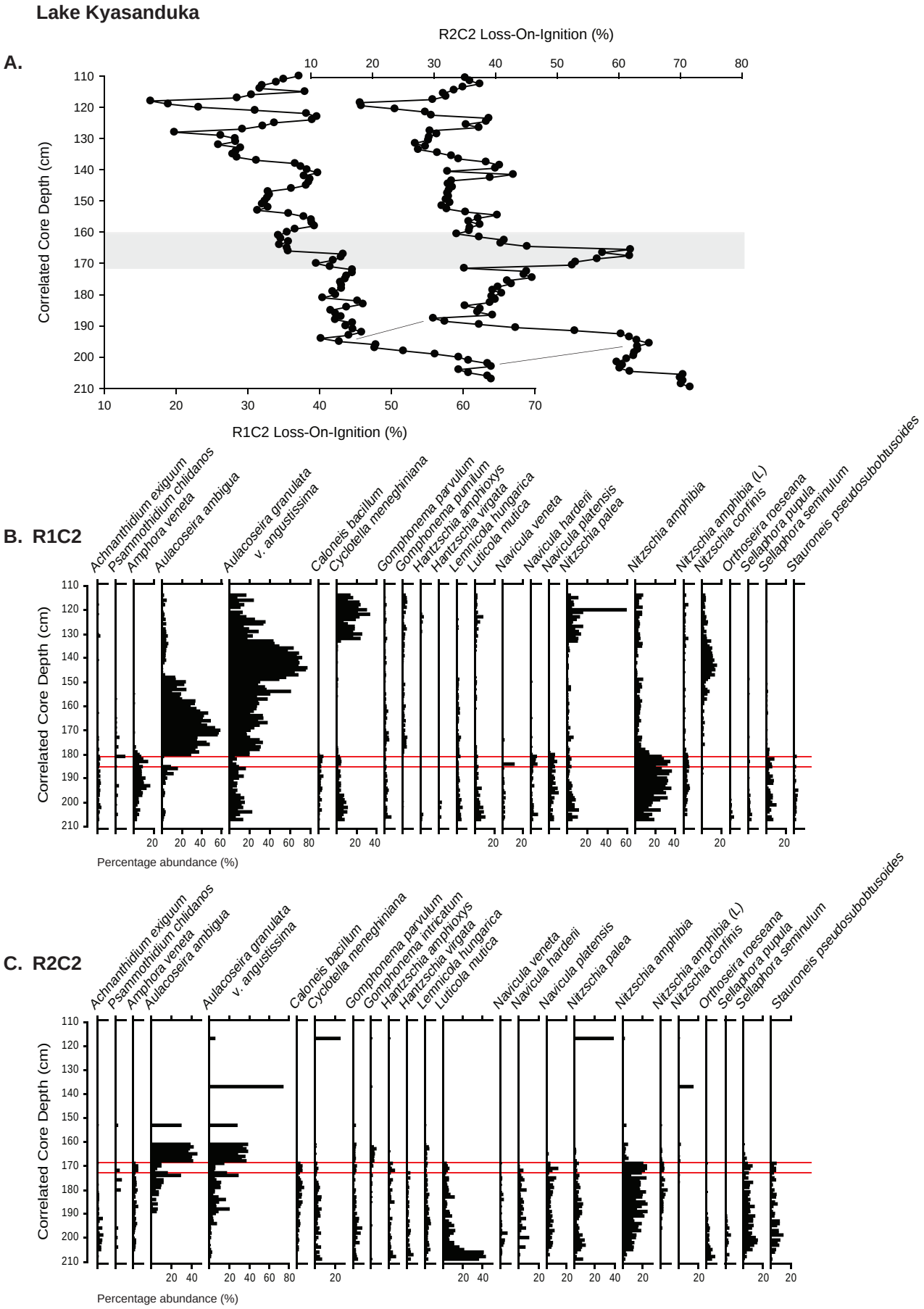

Figure 6.14 *Detailed correlation of the lower core sequences (R1C2 and R2C2) from Lake Kyasanduka.* **(A)** *Loss-on-ignition profiles of cores R1C2 and R2C2. The shaded box indicates the excursion in the LOI profile as noted in R2C2 only, which corresponds to a reed mat deposit in the core.* **(A and C)** *Detailed diatom counts from core R1C2* **(B)** *and R2C2* **(C)**. *The red boundaries highlight the key feature, a significant reduction in the percentage of Aulacoseira species (A. ambigua and A. granulata), that was used to confirm the core correlation.*

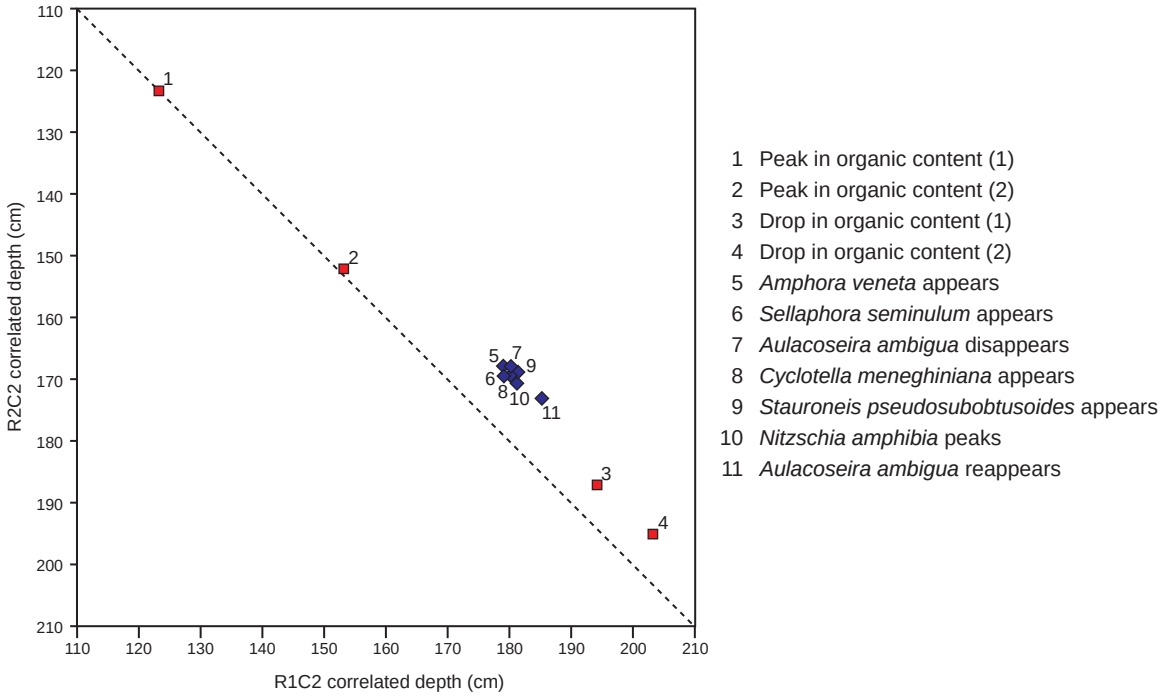

Figure 6.15 *Shaw diagram for the overlapping cores R1C2 and R2C2. Each point (1-11) represents an assumed synchronous feature for both cores, dervived using the loss-on-ignition (organic content) curves and the diatom biostratigraphy. The deviation from the 1:1 line towards the bottom of both cores suggests a change in sedimentation rate between the two cores and their depositional environments (see* ***Figure 6.#*** *and text for details).*

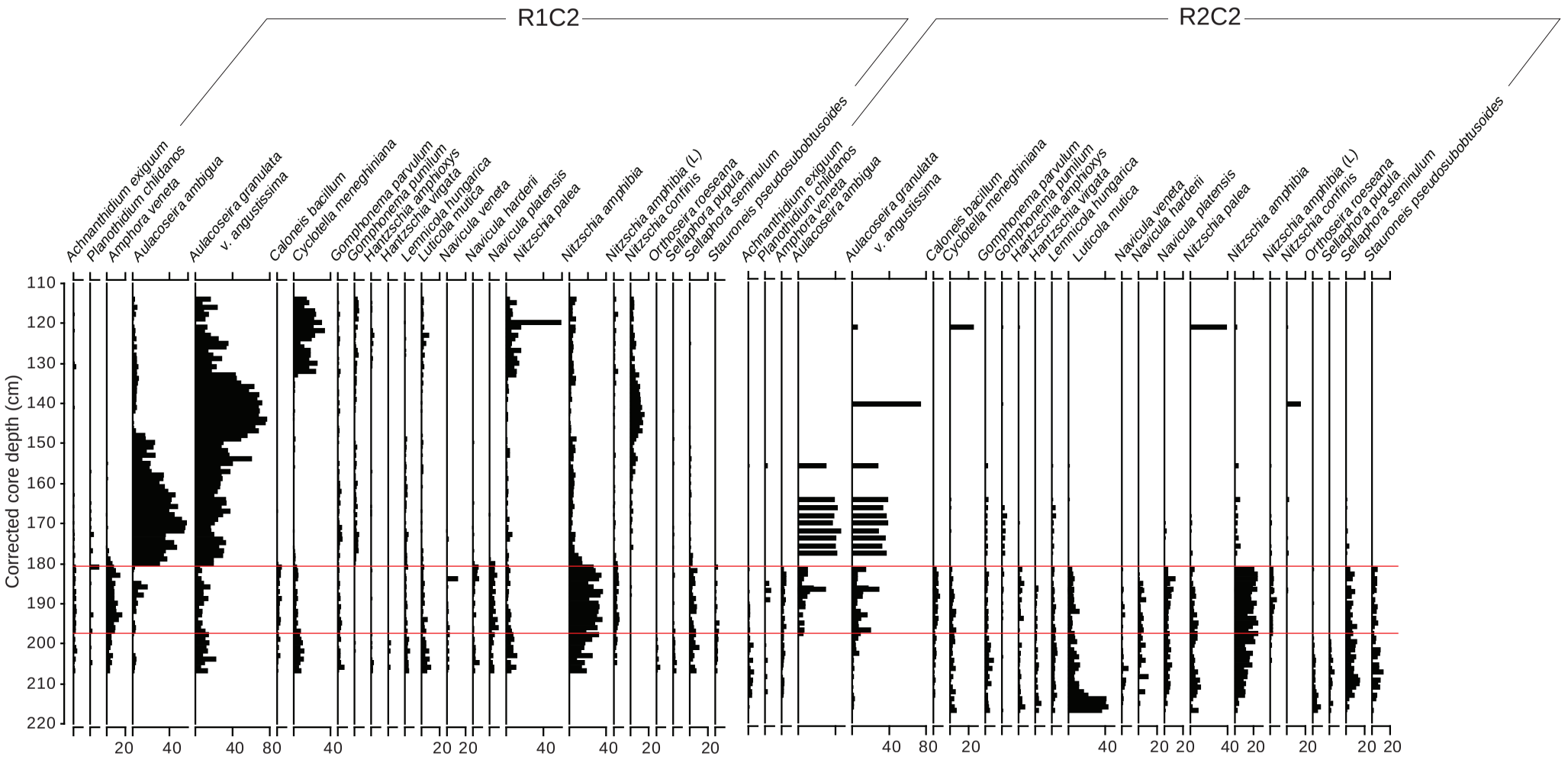

Figure 6.16 *Detailed correlation of the lower core sequences (R1C2 and R2C2) from Lake Kyasanduka. Core R2C2 has been corrected relative to R1C2 (N.B. the stretching of the core sequence has caused several gaps in the R2C2 record) The red lines indicate tie points which confirm the correction of the core R2C2. The upper line indicates the reduction of both Aulacoseira species and a significant increase in Nitzschia amphibia. The lower red line indicates the appearance of the aerophilous species Orthoseira roeseana.*

reed macrophyte habitat. Similarly the peak in magnetic susceptibility (180-190 cm) may be accounted for by the littoral core position with the inwash of magnetic minerals from local catchment soils being incorporated into the marginal sediments of the section (perhaps trapped by littoral vegetation), but not reaching the lake centre (Boreham *et al*., 1999; Figure 6.17).

6.4.2 ^{210}Pb dating and ^{14}C chronology

The ^{210}Pb inventory from Lake Kyasanduka is not comparable to the value supported by the atmospheric flux; rather it is double the fallout value (P.G. Appleby, *pers. comm.*). This high value may be the result of strong sediment focusing, or catchment erosion. As a large part of the lake's catchment lies outside of the QENP boundary and is today subject to large-scale clearance of natural vegetation for subsistence agriculture, the high value is most likely attributed to significant inputs as a result of catchment erosion. Kyasanduka has a number of irregularities in its unsupported ^{210}Pb activity (versus depth), suggesting several periods of major disturbances in the recent past. Concentrations reach a maximum value at 8.5 cm below the top of the core and there is an additional non-monotonic feature at 24-50 cm. The presence of a layer of dense sediment at ~110-140 cm may be related to the virtual absence of unsupported ^{210}Pb below 110 cm, which is coincident with a possible hiatus in the sequence, or a period of extremely low sedimentation (P.G. Appleby, *pers. comm.*). Total ^{210}Pb reaches equilibrium with the supporting ^{226}Ra (Figure 6.18) at a depth of around 120 cm.

The ^{137}Cs activity versus depth profile of Kyasanduka shows a relatively well defined peak between 44 cm and 53 cm and almost certainly records the 1963 fallout maximum from the atmospheric testing of nuclear weapons (P.G. Appleby, *pers. comm.;* **Appendix C**). There is some uncertainty with the ^{137}Cs peak recorded in Kyasanduka due to the rapid changes in ^{210}Pb occurring at the same interval in the core, and it is likely that the factors driving these changes have also modified the ^{137}Cs profile (P.G. Appleby, *pers. comm.*). Thus a more appropriate guide to the 1963 depth may be obtained by using the ^{137}Cs/^{210}Pb ratio (which peaks at 38-49 cm). ^{137}Cs concentrations were very low and the ^{137}Cs inventory suggests values of ~462±45 Bq m^{-2}, significantly below that observed at sites in Europe and North America (cf. Ssemmanda *et al*., 2005). The use of the CRS model places 1963 at a depth of *c.* 60 cm, significantly below the depth indicated by the ^{137}Cs record (~48 cm). This discrepancy is attributed to high rates of supply prior to 1963; the post 1963 ^{210}Pb flux is less than 40% of the pre-1963 sediments. Revised dates

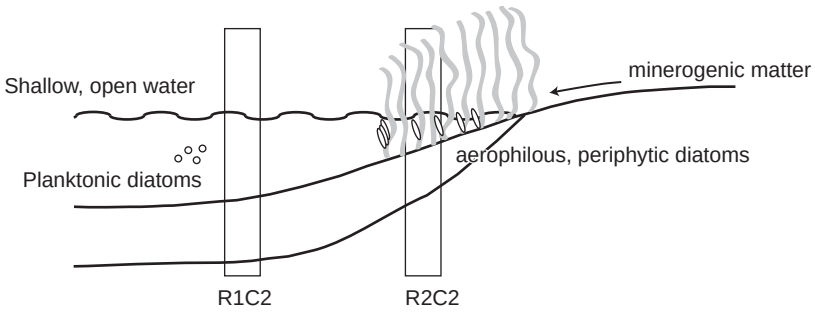

Loss-on-ignition	Low values	High values
Magnetic susceptibility	Low values	High values
Planktonic diatoms	Dominate	Low
Shallow benthos	Common	Common
Aerophilous diatoms	Absent	Dominate
Commonalities	*Nitzschia amphibia*, *Amphora veneta*, *Achnanthes* spp.	

Figure 6.17 *Schematic diagram showing proposed coring locations of cores R1C2 and R2C2. Both cores were taken from the middle of the lake. However, during the sediment deposition in R2C2 the lake was most likely a shallow system, resulting in the core being retrieved from a littoral area*

calculated by applying the CRS model in a piecewise way using the 1963 ^{137}Cs date as a reference point suggest a relative uniform sedimentation rate of around 0.047 g cm^{-2} y^{-1} since the later part of the 19th century, punctuated by episodes of rapid accumulation in the 1920s, the late 1960s/early 1970s, and most recently during the past few years (P.G. Appleby, *pers. comm.;* **Appendix C**).

Eleven AMS ^{14}C dates were obtained from terrestrial plant macrofossils or charcoal from Lake Kyasanduka's composite core sequence (Tables 6.3 and 6.4; Figure 6.19). All dates were calibrated using CALIB 5.0 (Stuiver and Reimer, 1993) using the IntCal04 calibration curve (Reimer *et al*., 2004). Out of the eleven dates, six were rejected. Five of the six rejected dates were charcoal fragments (SUERC-19070, SUERC-16175, SUERC-19065, SUERC-18398 and POZ-26360; cf. Russell *et al*., 2007). Whilst the charcoal fragments selected for analysis were >250 µm in length, suggesting a local source, and those with rounded edges were avoided to try and limit errors due to the reworking of charcoal in the sediments, the dates all produced consistently older ages than the sediments dated above and below, or in the case of SUERC-19065, the charcoal date produced an older age than a second date obtained from the same horizon from a piece of wood. These older charcoal ages could be due to 'old wood' (containing old carbon) having been partially burned and deposited in the lake, or the reworking of older charcoal remaining within the catchment and was deposited in the lake during periods of high sedimentation as a result of rainfall events or catchment disturbance. Problems with the dating of charcoal in the East African crater lakes has recently been reported (cf. Russell *et al*., 2007), but the occurrence of terrestrial macrofossils in these cores were rare, limiting the available material for dating. Dating of bulk sediment samples is not optimal in these closed crater lakes, as many bulk samples have been shown to demonstrate a carbon reservoir age (see **Chapter 8**, *section 8.8.2* for discussion). The final rejected date (SUERC-19071) was omitted on the basis that it appeared to be an outlier when compared to all of the samples from the bottom 50 cm of the composite core record.

Initially the five accepted dates were considered for the age model, only three of which were used to construct the final age model (SUERC-18397, SUERC-16176/18988 and SUERC-16173; illustrated in Figure 6.19). SUERC-18397 and SUERC-16173 were accepted without any complications, and the dates with the highest probabilities (50.76% and 100%, respectively; Figure 6.20) were used in the age model. Three of the other dates were manipulated in order for them to be used, leading to the omission of one date

Lake Kyasanduka

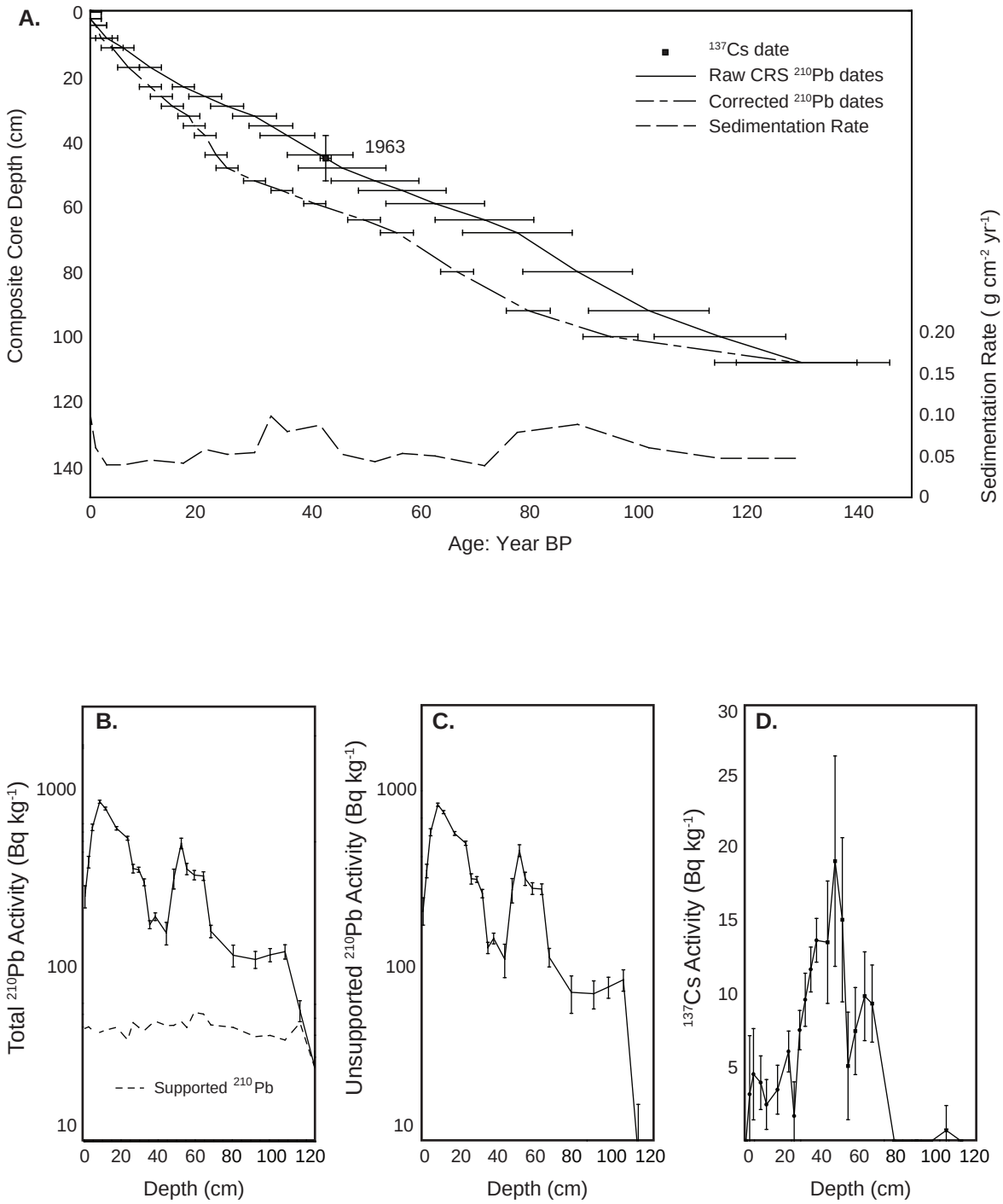

Figure 6.18 *^{210}Pb and ^{137}Cs data for Lake Kyasanduka.* **(A)** *^{210}Pb chronology for Kyasanduka (using linear extrapolation between the dated horizons). Filled circles represent actual dated horizons (**Appendix #**), the filled square is the base of the sequence, dated by linear extrapolation.* **(B-D)** *Fallout radionuclides in the Kyasanduka core showing* **(B)** *total and supported ^{210}Pb,* **(C)** *unsupported ^{210}Pb and* **(D)** *^{137}Cs concentrations versus depth (Figures are adapted from dating report supplied by P.G. Appleby, unpublished report).*

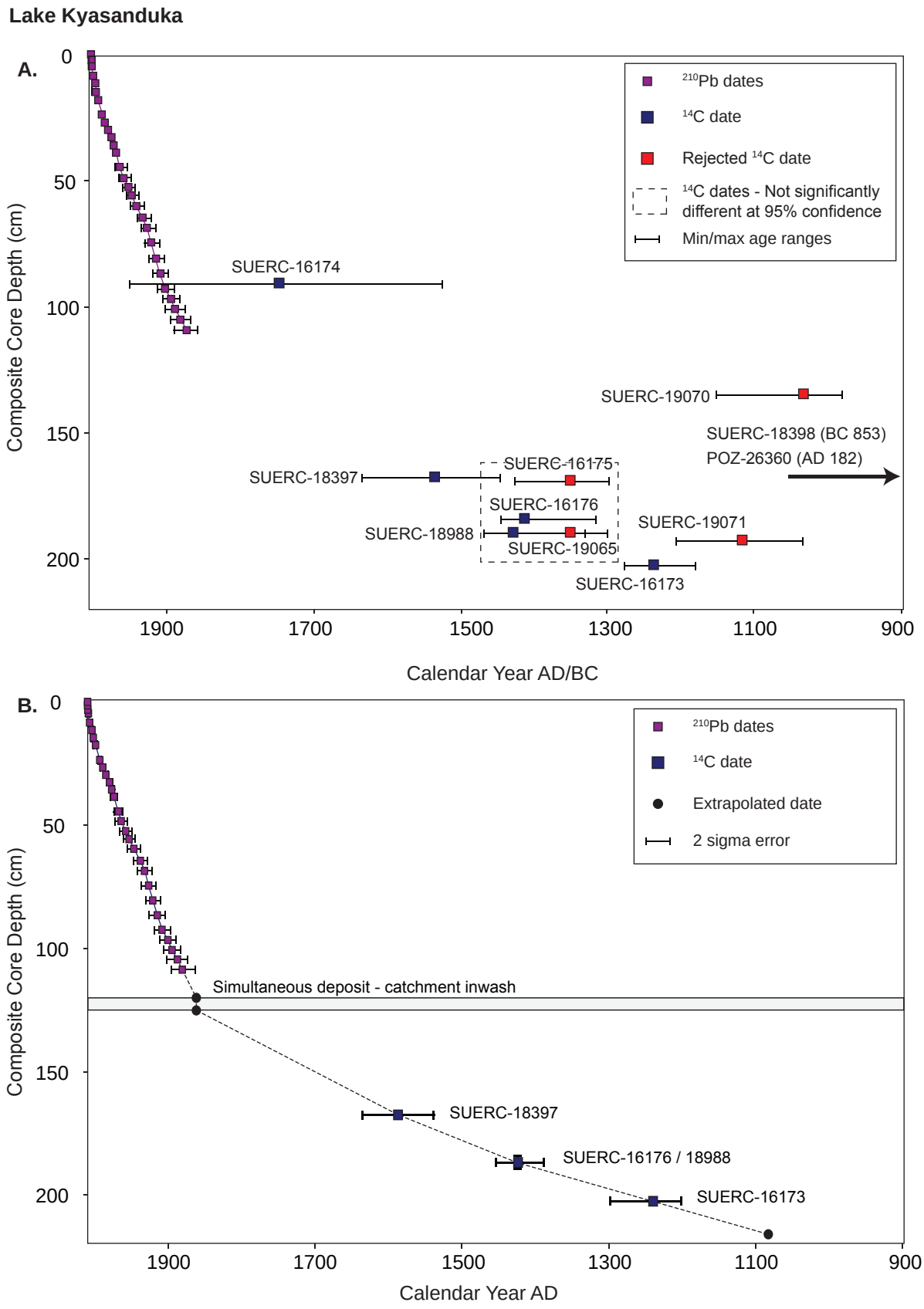

Figure 6.19 *All dates from Lake Kyasanduka sediment cores.* **(A)** *^{210}Pb dates and all calibrated 14C dates plotted against composite core depth. Radiocarbon dates were calibrated using CALIB 5.0. All error bars are given for ^{210}Pb (see* ***Appendix #****). For the radiocarbon dates the square denotes the median age as calculated in CALIB 5.0. The error bars represent the absolute maximum and minimum ages for each sample at two sigma error (see* ***section 6.#*** *for additional information). The dates contained within the dashed lines are not significantly different at the 95% confidence interval. Samples SUERC-18398 and POZ-26360 are not shown on the diagram, due to their erroneously old ages.* **(B)** *Final age model for Lake Kyasanduka, with some radiocarbon dates excluded (see* ***Table 6.#*** *and* ***section 6.#*** *for explanation). The error bars represent the age range at two sigma error.*

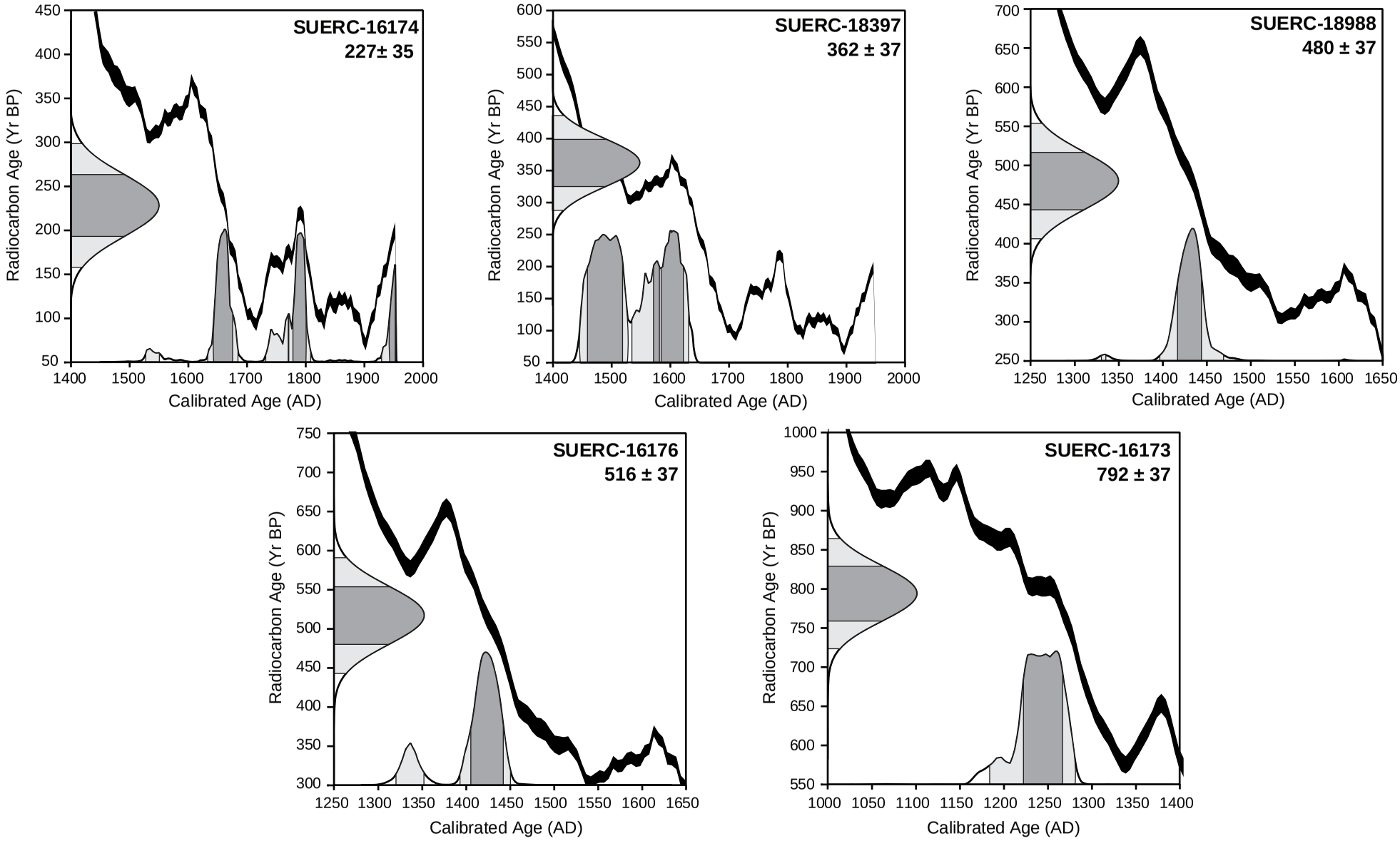

Figure 6.20 *Probability distributions of the five accepted dates used in the age-model for Lake Kyasanduka. The probability distributions were calculated using CALIB 5.0.*

(SUERC-16174) and the amalgamation of the remaining two (SUERC-16176 and SUERC-18988).

The youngest radiocarbon date obtained (SUERC-16174) does not appear in the final age model (Figure 6.19). This sample was taken from an horizon also dated by ^{210}Pb (90-91 cm; *c.* AD 1907). Within a two sigma error, the radiocarbon age overlapped with the ^{210}Pb age, and given that the ^{210}Pb is a more robust method of dating young sediments, the radiocarbon age from this depth was corrected to, and assumed to be, the same age as the ^{210}Pb date.

The remaining dates (SUERC-16176 and SUERC-18988) were amalgamated for use in the age model. After testing the statistical significance of the dates (using a t-test) within the calibration program CALIB 5.0, it was shown that the dates obtained from the two horizons (183-185 cm and 189-190 cm) were not significantly different at the 95% confidence interval. Therefore, the dates with the highest probability were amalgamated, and an average age of this section of the core (with associated two sigma error) is reported. As a result of amalgamating these two samples, the errors in the precise depth of the age are also given (as minimum and maximum). The average depth is also displayed (Figure 6.16b).

6.4.3 Physical properties

The uppermost section of the Kyasanduka stratigraphy consists of dark greyish-brown gyttja (*c.* 0-165 cm; Figure 6.12). The sediment is soft and light and there are several plant macrofossils present. At *c.* 85 cm a single black band (R1C1) and a small section of discontinuous banding (R2C1) occurs in the sediment cores. Below the banding the sediment is dark brown gyttja. At *c.* 120 cm (composite core depth) a section of laminations occurs in the three overlapping sections. The laminations were orange, brown, red and grey in colour. At *c.* 165 cm, the sediments in the lower cores (R1C2 and R2C2) begin to darken, before turning to an almost black, silty mud. There were very few macrofossils are present in R1C2. Core R2C2 has an overwhelming abundance of reed fragments and associated mollusc shells, perhaps indicative of shallower conditions and the deposition of a reed mat. At *c.* 200 cm the sediment exhibits soil-like properties. The sediments are black and appear condensed. Crumbly clay nodules and large fragments of wood and charcoal are present in the basal layer (cf. Russell *et al*., 2007).

Table 6.3 *All AMS ^{14}C radiocarbon dates from Lake Kyasanduka. Dates are reported as conventional radiocarbon years BP, relative to AD 1950. The samples were prepared at the NERC radiocarbon laboratory and passed onto the SUERC AMS laboratory for ^{14}C analyses. The samples highlighted in bold italics are dates that have been excluded from subsequent age models. Please refer to the text for details.*

Code	Material	Core	Correlated Depth		Radiocarbon Age	1σ error	2σ error	^{14}C enrichment (% modern)	Enrichment ± 1σ	Carbon content (% by wt.)	Sample wt. (mg)	$\delta 13C_{VPDB}$‰ ± 0.1
			Top	Bottom								
SUERC-16174	Leaf	KR2C1	90	91	227	35	70	97.21	0.42	65	--	-25.0*
SUERC-19070	***Charcoal***	***KR1C2***	***134***	***135***	***95***	***35***	***70***	***88.33***	***0.26***	***61***	***2.54***	***-15.1***
SUERC-18397	Leaf	KR1C2	167	168	362	37	74	95.59	0.44	-	5.68	-28.4
SUERC-16175	***Charcoal/Wood***	***KR2C2***	***168***	***170***	***568***	***37***	***74***	***93.17***	***0.43***	***49***	**--**	***-25.5***
SUERC-16176	Wood fragment	KR2C2	183	185	516	37	74	93.77	0.43	62	--	-28.1
SUERC-18988	Wood	KR2C2	189	190	480	37	74	94.20	0.43	52.8	6.23	-30.8
SUERC-19065	***Charcoal***	***KR2C2***	***189***	***190***	***565***	***35***	***70***	***93.24***	***0.29***	***46.5***	***6.34***	***-25.3***
SUERC-18398	***Charred wood***	***KR1C2***	***192***	***192.5***	***2700***	***37***	***74***	***71.45***	***0.33***	***-***	***18.28***	***-27.2***
SUERC-19071	***Wood***	***KR2C2***	***192***	***193***	***905***	***35***	***70***	***89.34***	***0.28***	***51.3***	***7.62***	***-29.5***
SUERC-16173	Wood fragment	KR1C2	202	203	792	35	70	90.61	0.39	54	--	-16.1
POZ-26360	***Charcoal***	***KR1C2***	***206***	***207***	***1830***	***30***	***60***	--	--	--	--	--

* Sample produced insufficient CO_2 for an independent measurement of $\delta^{13}C$. -25 $\delta^{13}C_{VPDB}$ ‰ was applied in calculating the ^{14}C result for these samples.

Table 6.4 *Calibrated radiocarbon dates from Lake Kyasanduka. Radiocarbon ages were calibrated using CALIB 5.0 (Stuiver and Reimer, 1993) using the calibration curve IntCal04.14c (Reimer et al., 2004). All calibrated ages are given as calendar years AD.*

Code	Correlated Depth		Radiocarbon Age	2σ error	Range 1			Range 2			Range 3		
	Top	Bottom			Lower	Upper	Probability	Lower	Upper	Probability	Lower	Upper	Probability
SUERC-16174	90	91	227	70	1634	1685	41.46%	1732	1808	44.06%	1928	1952	11.72%
SUERC-19070	***134***	***135***	***95***	***70***	***1069***	***1071***	***0.29%***	***1076***	***1154***	***37.96%***	--	--	--
SUERC-18397	167	168	362	74	1449	1530	49.24%	1538	1635	50.76%	--	--	--
SUERC-16175	***168***	***170***	**568** †	***74***	***1300***	***1368***	***58.94%***	***1381***	***1429***	***41.06%***	--	--	--
SUERC-16176	183	185	516 †	74	1319	1351	15.742%	1390	1447	84.26%	--	--	--
SUERC-18988	189	190	480 †	74	1332	1337	0.60%	1397	1470	99.30%	--	--	--
SUERC-19065	***189***	***190***	***565*** †	***70***	***1302***	***1366***	***56.86%***	***1383***	***1429***	***43.13%***	--	--	--
SUERC-18398	***192***	***192.5***	***2700***	***74***	***-914***	***-802***	***100%***	--	--	--	--	--	--
SUERC-19071	***192***	***193***	***905***	***70***	***1037***	***1209***	***100%***	--	--	--	--	--	--
SUERC-16173	202	203	792	70	1182	1279	100%	--	--	--	--	--	--
POZ-26360	***206***	***207***	***1830***	***60***	***86***	***107***	***3.62%***	***120***	***252***	***96.38%***			

† Calibrated ages not significantly different at the 95% confidence interval

The organic content from the Lake Kyasanduka cores has two distinct parts (Figure 6.12 and 6.21). In the earlier part of the record (base to *c*115 cm; prior to AD 1860) the organic content of the sediment is highly variable with values fluctuating between 15% (120 cm; AD 1850) to ~65% (217 cm). The record begins (217 cm; AD 1070) with high LOI values in both of the overlapping sequences (R1C2 and R2C2; 65-70%). The organic content declines to ~50% at 202 cm (AD 1240). Values then remain high (~45%) and stable until 170 cm (AD 1560), when there is a large excursion in the data (to values *c.* 60%) in one of the overlapping sequences (R2C2). The excursion to higher values in R2C2 is likely a result of the presence of a massive reed deposit in the core (see above) parts of which were combusted during LOI, forcing a peak to higher values at this point in the record. At 160 cm (AD 1630) the overlapping records regain their synchroneity, and co-vary, with values fluctuating between 40% (156 cm) and 30% (150 cm). At 140 cm (AD 1755) a third sequence (R2C1) overlaps with cores R1C2 and R2C2. All records co-vary, indicating a strong coherence of the overlapping lake sediment records. Between 140-115 cm (AD 1755-1865), the LOI record has several notable data excursions in all of the overlapping core records. The first occurs at *c.* 130 cm (AD 1810) when LOI values drop to ~25%. The organic content increases to ~38% (123 cm; AD 1850) before an extremely low organic content occur immediately above at 124-120 cm (<20%, AD 1850). This short-lived period of low organic content may be a result of rapid sedimentation, or an instantaneous input from the catchment. After 115 cm (AD 1860) the organic content of the sediments is much less variable with an almost stable organic content of ~40% until the present day (Figure 6.21).

In a similar manner to the organic content, the carbonate record from Lake Kyasanduka is slightly more variable below 115 cm (prior to AD 1860). During the earliest part of the record (217-167 cm; AD 1075-1590), CO_3 values are low (~8%) with an increasing trend towards higher values upcore. A small peak in CO_3 values occurs between 170 and 160 cm (AD 1560 and AD 1630), though the peak is less evident than the coeval peak in LOI, as the carbonate records from the overlapping sequences (R1C2 and R2C2) are more variable. In conjunction with the low LOI at 130 cm, CO_3 values peak in all three records (*c.* 24%), before decreasing to ~10% at 115 cm. After AD 1860, the CO_3 record co-varies with the LOI record, with values fluctuating between *c.* 5 and 15%.

The magnetic susceptibility record from Lake Kyasanduka is, in the main, stable and non-fluctuating throughout, with a gentle increasing trend towards the top of the Russian core sequence. Notably there are three major excursions in the magnetic record.

The first peak occurs at the beginning of the sequence (217 cm; AD 1070), where the peat-like deposit with crumbly clay-nodules is observed. The second excursion is evident in sequence R2C2 only, and this is located just below the peak in the organic content and the section of reed mat noted in the core stratigraphy above, and is also coincident with a high concentration of mollusc shells. The final peak occurs at 120 cm (AD 1850) and is coincident with a drop in LOI values. The peak in the magnetic susceptibility lends support to the possibility of an instantaneous deposit of minerogenic catchment sediments into the lake system.

The dry mass accumulation rate (DMAR) from Lake Kyasanduka is relatively stable for the earlier part of the record (*c.* 0.02 g cm^{-2} yr^{-1}; 217 cm to 128 cm; AD 1070-AD 1830), with a slightly decreasing trend through time (Figure 6.21). There are several smaller deviations between 217-128 cm (AD 1070-1830), with a small rise in DMAR *c.* 188-177 cm (AD 1400-AD 1500) and a slight increase *c.* 169 cm (AD 1570). The most notable increase in the DMAR occurs at 121 cm (AD 1850; >0.05 g cm^{-2} yr^{-1}) at the onset of the detailed ^{210}Pb dating. From AD 1850 onwards there are three major excursions in the DMAR, with peaks at 117 cm (0.06 g cm^{-2} yr^{-1}), *c.* 80 cm (0.09 g cm^{-2} yr^{-1}) and *c.* 35 cm (0.1 g cm^{-2} yr^{-1}; AD 1860, AD 1920 and AD 1975, respectively). After the final peak, values decline towards the present day. However, unlike the DMAR record from Lake Nyamogusingiri, the most recent samples indicate a rise in dry mass accumulation towards the present. The inferred values of both the organic and inorganic sediment fluxes to Lake Kyasanduka are strongly influenced by the calculated dry mass accumulation rates. The organic flux starts relatively high at 217 cm (AD 1070) and declines steadily until 186 cm (AD 1425). Conversely, the inorganic flux is low and stable, but with a slightly increasing trend towards 186 cm (AD 1420). Between 186-177 cm (AD 1420-1500) there is a small peak in both the organic and inorganic flux records. Whilst the onset of this deviation occurs with a ^{14}C dated horizon, the end of the excursion in the data is not associated with a dated horizon or a change in DMAR. Both records more or less stabilise between 176-127 cm (AD 1510-1830), with a change observed at the onset of the ^{210}Pb dating. A small peak in the flux of inorganic matter to the lake occurs at *c.* 137-132 cm (AD 1770-AD 1800). After 120 cm (AD 1850) the organic and inorganic flux records co-vary, and record three major excursions centered on 117, 80 and 35 cm (AD 1860, AD 1920 and AD 1970); the earliest peak (AD 1860) is more pronounced in the inorganic record. After *c.* 35 cm (AD 1970) values from both records decline, though do increase in the most recent samples (1-0 cm; AD 2007).

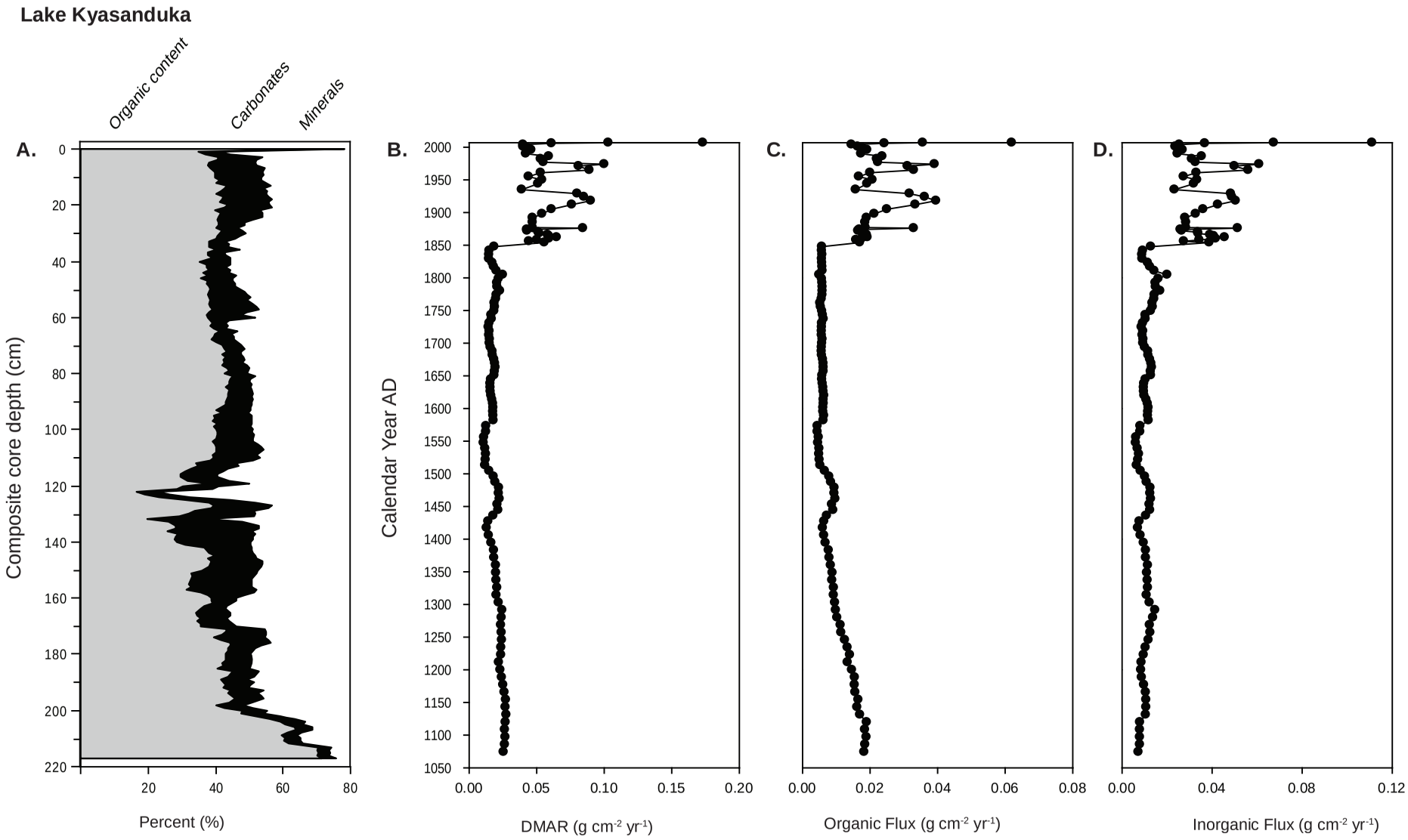

Figure 6.21 *Calculated flux data for Lake Kyasanduka.* **(A)** *Stacked organic content (loss-on-ignition) and carbonate percentages versus depth (cm),* **(B)** *dry mass accumulation rate (DMAR) calculated using the dry bulk density and ^{210}Pb dates,* **(C)** *Loss-on-ignition (organic content) displayed as flux (g cm^{-2} yr^{-1}) and* **(D)** *inorganic (minerogenic) flux (g cm^{-2} yr^{-1}).*

Lake Kyasanduka

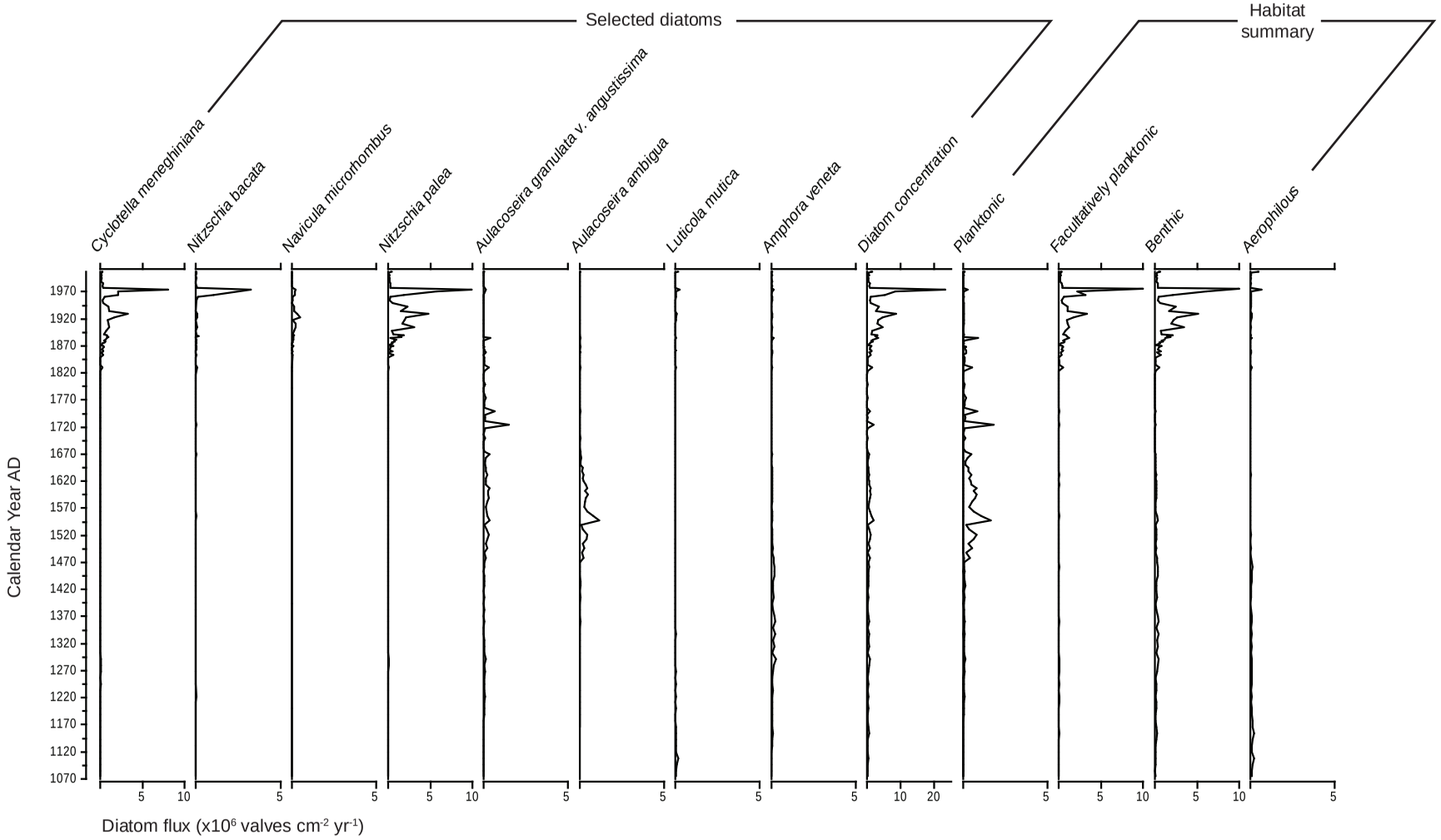

Figure 6.22 *Diatom flux for selected dominant taxa from Lake Kyasanduka displayed alongside the total diatom flux for each sample (left). The flux of diatoms within the habitat categories are also shown (right).*

The total diatom flux is extremely low for the majority of the record (generally <0.4 x 10^6 valves g cm^{-2} yr^{-1}), with a slight peak *c.* AD 1480-AD 1500 due to the influx of *Aulacoseira ambigua* (*c.* 2 x 10^6 valves g cm^{-2} yr^{-1}; Figure 6.22). Again, bearing similarities to the Nyamogusingiri record, the largest flux of diatoms to the lake sediments occurs after *c.* AD 1870, where diatom the flux dramatically increases (to a maximum of 23 x 10^6 valves g cm^{-2} yr^{-1}). This large influx is driven by the flux of *Cyclotella meneghiniana* and *Nitzschia palea* to the lake sediments, which is coincident with the delivery of large amounts of sediments from the catchment, after a period of very low organic input (*c.* AD 1840).

6.4.4 Diatom analyses

A total of 278 samples were counted from the composite core sequence from Kyasanduka in 0.5 cm thick samples at 1 cm intervals (including a number of overlapping sections to aid the correlation of the lower core sequences; see *section 6.4.1*) and 192 species were recorded. Nine assemblage zones were identified for Kyasanduka (Ks1-9) using ZONE (see *section 6.2.1*). The results of diatom analysis from Lake Kyasanduka are shown in Figures 6.23, 6.24 and 6.25.

The diatom record from Lake Kyasanduka has two distinct parts. In the earliest part of the record (prior to AD 1860; 115 cm) the assemblage is dominated by planktonic *Aulacoseira* species and aerophilous, benthic and littoral taxa. After AD 1860, and at what is interpreted as a period of low sedimentation as a result of a lower lake level (see *section 6.4.2*), there is a rapid switch in the assemblage to one dominated by *Cyclotella-Nitzschia* species. Towards the top of the sequence, aerophilous and benthic/littoral taxa become more important.

Zone Ks1 (217-207 cm; AD 1070-1180); the earliest zone consists of a *Cyclotella meneghiniana* (6%) and *Nitzschia palea* (8%) assemblage. Aerophilous and benthic/littoral species are also important in this zone (e.g. *Orthoseira roeseana*, *Hantzschia amphioxys*, *H. virgata*, *Gomphonema parvulum* and *Stauroneis pseudosubobtusoides*). Of particular importance within this group is *Luticola mutica*, which reaches abundances of ~43%. Diatom preservation is good within zone Ks1 (**F** = 0.8), although diatom concentrations are particularly low with only *c.* 12 x 10^6 valves g^{-1}.

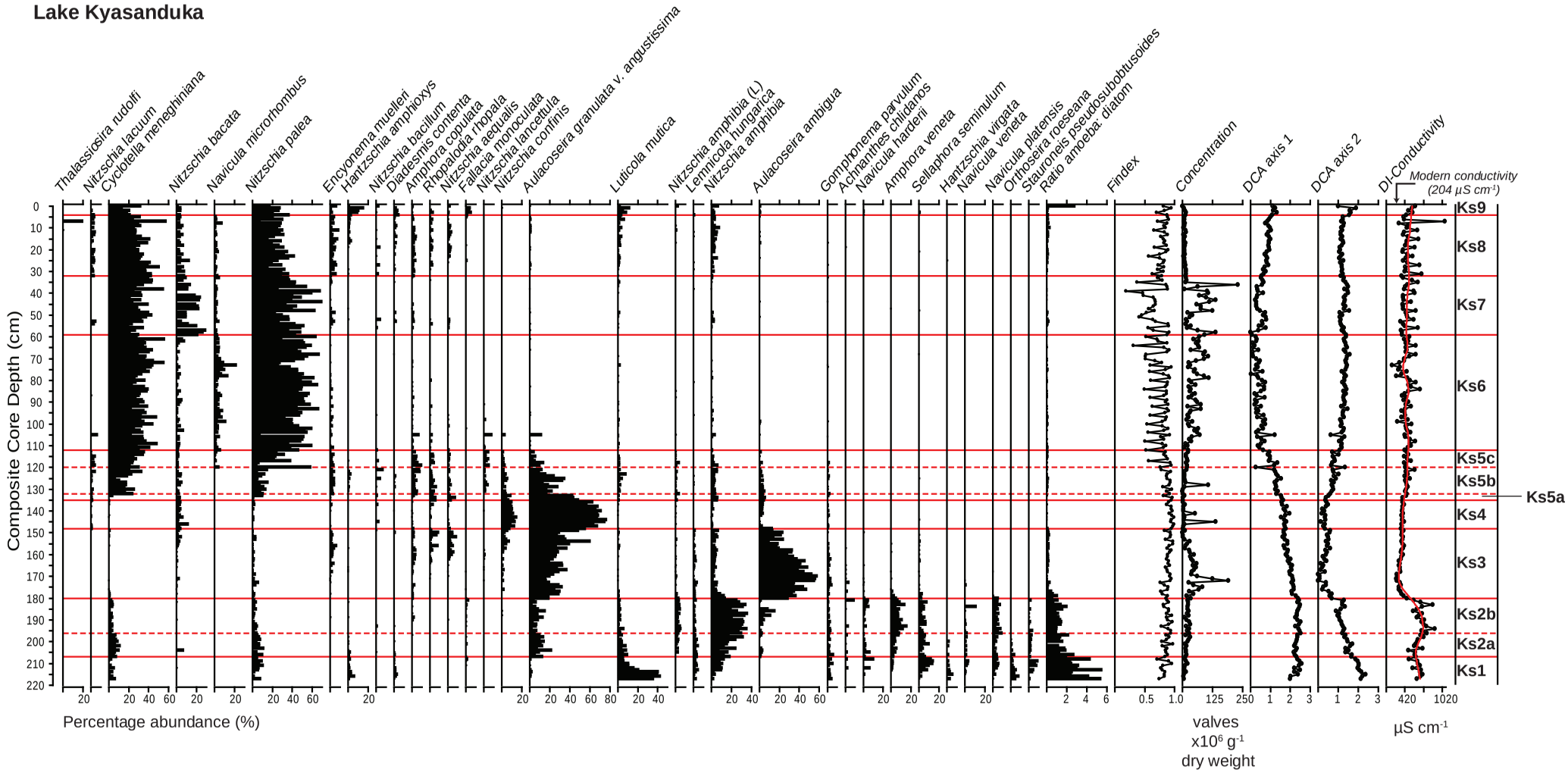

Figure 6.23 *Diatom stratigraphy from Lake Kyasanduka plotted against depth. All species > 5% in any one sample are displayed. The diatom taxa have been ordered according to their weighted average abundance in the core (ascending) and are split into assemblage zones Ks1-9. The ratio of testate amoebae scales to diatoms are displayed alongside the diatom preservation index (**F** index), diatom concentrations and the axis 1 and axis 2 sample scores from Detrended Correspondance Analaysis (DCA). Reconstructed conductivities are based on the crater lake transfer function (Combined_76; see* **Chapter 5***), a lowess smoother has been added to the reconstruction.*

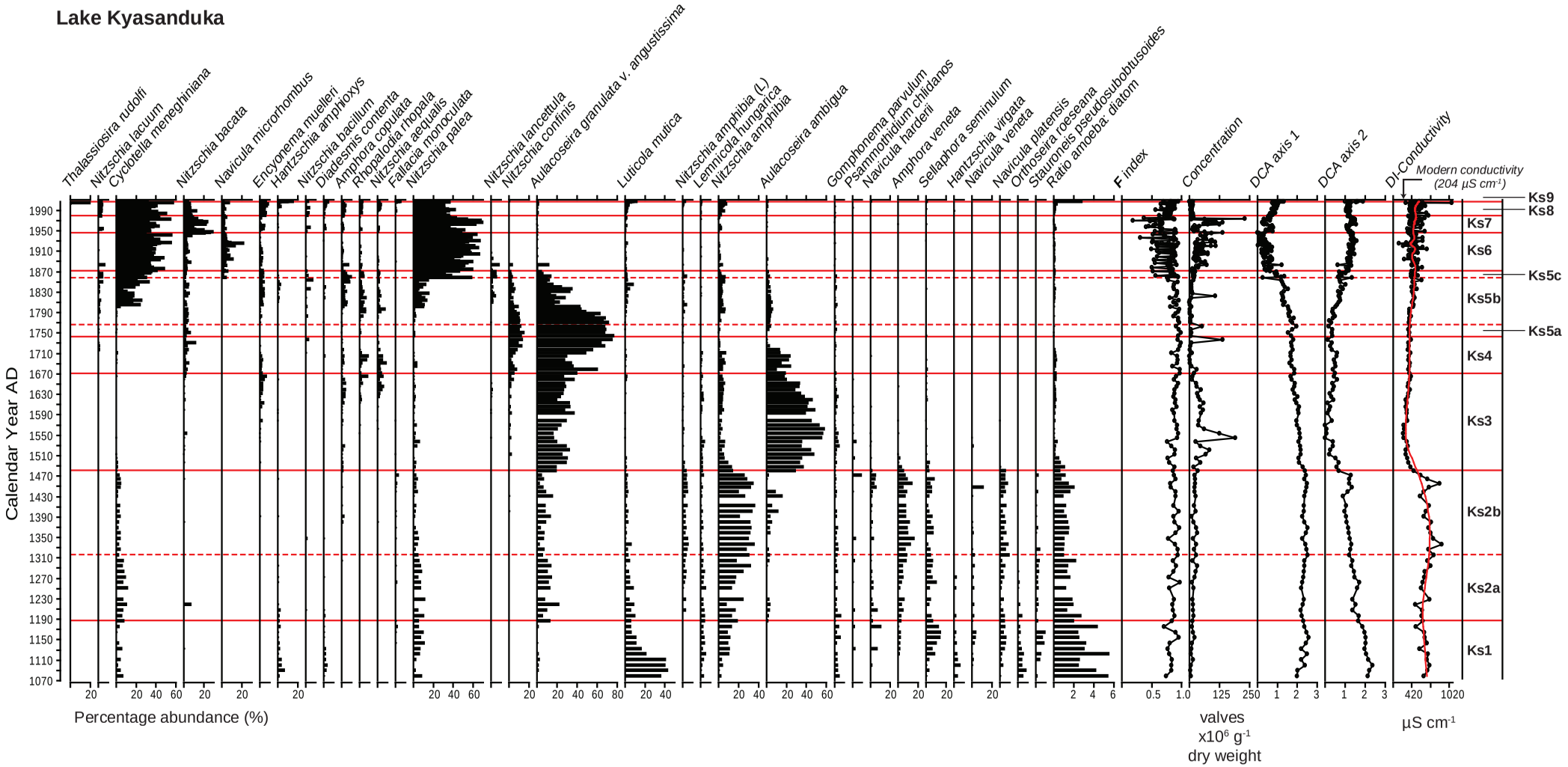

Figure 6.24 *Diatom stratigraphy from Lake Kyasanduka. All species > 5% in any one sample are displayed. The diatom taxa have been ordered according to their weighted average abundance in the core (ascending) and are split into assemblage zones Ks1-9. The ratio of testate amoebae scales to diatoms are displayed alongside the diatom preservation index (**F** index), diatom concentrations and the axis 1 and axis 2 sample scores from Detrended Correspondence Analaysis (DCA). Reconstructed conductivities are based on the crater lake transfer function (Combined_76; see **Chapter 5**), a lowess smoother has been added to the reconstruction.*

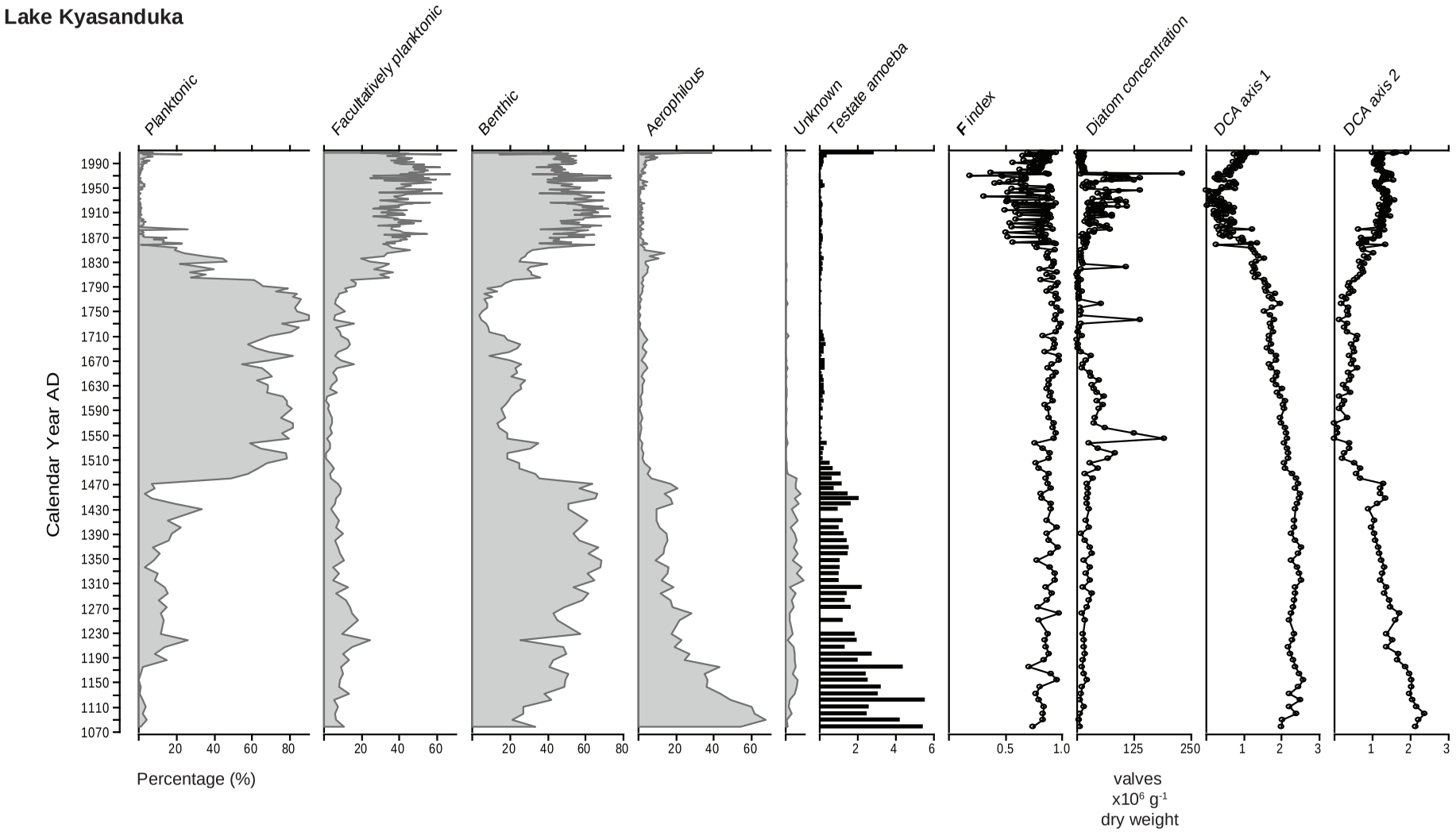

Figure 6.25 *Habitat summary of all diatom species from lake Kyasanduka displayed alongside the ratio of testate amoeba scales to diatoms, dissolution index (**F** index), diatom concentration and sample scores from DCA axes 1 and 2.*

Ks2 (207-180 cm; AD 1180-1470) consists of 2 sub-zones: Ks2a (207-196 cm; AD 1185-1315) Ks2b (196-180 cm; AD 1315-1475). Aerophilous and benthic/littoral species are consistently present throughout this zone, but there is an appearance of (tycho)planktonic *Aulacoseira* species. Zone Ks2a contains aerophilous species such as *H. amphioxys*, *Diadesmis contenta* and *O. roeseana* along with increasing percentages of *C. meneghiniana* and *N. palea*. *Aulacoseira granulata* v. *angustissima* becomes increasingly important in this sub-zone reaching an abundance of *c.* 15%, and *A. ambigua* is present in small quantities (~3%). *Nitzschia amphibia* is one of the more dominant species in this sub-zone, with abundances of *c.* 30%. *Planothidium chlidanos, Caloneis bacillum, Navicula harderii, N. platensis, Sellaphora seminulum* and *Amphora veneta* are also important species that characterise this zone. Zone Ks2b is identical in species composition to Ks2a, however the relative abundance of the various taxa differs. *Cyclotella meneghiniana* (planktonic) and *Nitzschia palea* (periphytic) decrease in abundance, and towards the top of this sub-zone aerophilous taxa almost disappear. *Aulacoseira granulata* v. *angustissima* decreases slightly in abundance, whilst *A. ambigua* appears to peak. *Nitzschia amphibia* reaches its maximum abundance (35%) in the entire record in Ks2b. *Planothidium chlidanos, Navicula minima, N. harderii, N. platensis* and *Sellaphora seminulum* are all present in low quantities. The slightly saline tolerant taxon *Amphora veneta* reaches its peak in this sub-zone (>15%), before disappearing almost entirely from this record. Diatom preservation is extremely good (maximum of **F** = 0.97) and diatom concentrations remain low (maximum of 27 x 10^6 valves g^{-1}).

Ks3 (180-148 cm; AD 1470-1700) sees a marked shift in the dominant taxa. There is almost a total reduction of aerophilous and littoral/benthic taxa to <1%, and several taxa completely disappear. There is an appearance of littoral and periphytic taxa in small quantities throughout this zone (e.g. *Encyonema muelleri*, *Amphora copulata*, *Rhopalodia rhopala* and *Gomphonema pumilum*). *Nitzschia confinis* appears and begins to increase through this zone as does the planktonic *Aulacoseira granulata* v. *angustissima*. *A. ambigua* rapidly increases at the start of this zone to its highest recorded abundance (~58%) before gradually declining through the zone to abundances of *c.* 20%. Conversely, *Nitzschia amphibia* rapidly decreases to <5%. The earlier part of this zone also sees a short-lived appearance of the planktonic taxon *Fragilaria tenera*. In the upper part of this zone *Nitzschia bacata* becomes increasingly important and there is a peak in the planktonic species *Aulacoseira granulata* v. *angustissima* and *N. confinis* and the periphytic species *Rhopalodia rhopala* and *Nitzschia aequalis*; the percentage abundance of *A. ambigua*

decreases. Diatom concentrations increase slightly in this zone, with a peak concentration of 190 x 10^6 valves g^{-1} at 173 cm (AD 1530), though values do decline towards the top of the zone (<10 x 10^6 valves g^{-1}).

Aulacoseira granulata v. *angustissima* reaches its highest abundance within Ks4 (~80%; 148-135 cm, AD 1700-1780). *Nitzschia bacata* increases in abundance and *N. lacuum* (plankton) becomes more prominent in the record. There is a reduction in the abundance of littoral and epiphytic species (such as *Encyonema muelleri*, *Amphora copulata*, *Rhopalodia rhopala*, *Nitzschia aequalis*, *Gomphonema pumilum*, *Luticola mutica* and *Nitzschia amphibia*). Diatom concentrations in this zone are generally low (*c.* 3 x 10^6 valves g^{-1}), though the record is punctuated by several samples with high (52-138 x 10^6 valves g^{-1}) values.

Zone Ks5 (135-112 cm; AD 1780-1870) consists of three sub-zones and represents the transition zone between the two contrastingly different assemblages evident in the record. Ks5a (135-132 cm; AD 1780-1800) is a very small sub-zone, consisting of only 3 samples, and probably represents the point of transition. The abundance of *Cyclotella meneghiniana* and *Nitzschia palea* are low, and taxa such as *Luticola mutica*, *Amphora copulata*, *Rhopalodia rhopala* and *Nitzschia aequalis* are present in abundances just under 5%. *Aulacoseira granulata* v. *angustissima* is present in high abundances, though it does start to decrease through the zone. *Nitzschia amphibia* reappears and there is a small rise in *A. ambigua*. Diatom concentrations in this zone are low (9 x 10^6 valves g^{-1}). Zone Ks5b (132-120 cm; AD1800-1850) sees the reappearance of *C. meneghiniana* to abundances >20%. *Nitzschia palea* also begins to increase (~10%). Aerophilous and benthic/littoral species are still present, and there is the appearance of the more freshwater taxon *Nitzschia lancettula*. Other *Nitzschia* species such as *N. bacata* and *N. confinis* decrease in this zone. The abundance of *Luticola mutica* peaks at the boundary of Ks5b and Ks5c (*c.* 8% at AD 1850) before declining to <5% in Ks5c. The final sub-zone, Ks5c (120-112 cm; AD 1850-1870) shows increasing abundances of *Cyclotella meneghiniana* and *Nitzschia palea*, and is also the last zone in which the *Aulacoseira* species *A. granulata* v. *angustissima* and *A. ambigua* are present in any significant quantities. Many aerophilous and benthic/littoral taxa disappear in this zone. The top of Ks5c (112 cm, AD 1870) marks the full transition from the *Aulacoseira* dominated assemblage to the *Cyclotella-Nitzschia* assemblage.

Ks6 (112-59 cm; AD 1870-1940) is dominated entirely by *Cyclotella meneghiniana* (*c.* 40%) and *Nitzschia palea* (*c.* 50%). Aerophilous, littoral, benthic and epiphytic taxa are present, but in low quantities (<1%). The freshwater benthic (or occasionally planktonic;

Kelly *et al*., 2005) taxon *Nitzschia bacata* is consistently present in low quantities (<5%) and the freshwater species *Navicula microrhombus* becomes increasingly important (~10%). Similarly, zone Ks7 (59-32 cm; AD 1940-1970) is dominated by *Cyclotella meneghiniana*, though there is a slight decrease in the absolute abundance. *Nitzschia palea* also dominates this zone, though percentages do fluctuate (40-60%). The most prominent feature of this zone is the double peak in *Nitzschia bacata* (57 cm and 44 am; AD 1940 and 1960), a rise in *Encyonema muelleri* and the reappearance of *N. amphibia*. The preservation in zones Ks7 and Ks8 is much more variable than the earlier zones, with an **F** index between 0.3 and 0.9. Diatom concentrations are also variable, fluctuating between 13 and 140 x 10^6 valves g^{-1}.

Zone Ks8 (32-4 cm; AD 1970-2005) continues to be dominated by *Cyclotella meneghiniana* and *Nitzschia palea*, though the percentage abundance of both is lower than in previous zones (abundance 30% and 20% respectively). *Navicula microrhombus* is still consistently present throughout this zone and there is a reduction in the abundance of *Nitzschia bacata*. There is a reappearance of aerophilous, benthic and littoral taxa such as *Amphora copulata, A. pediculus, Diadesmis contenta*, *Encyonema muelleri*, *Gomphonema pumilum*, *Hantzschia amphioxys*, *Luticola mutica*, *Nitzschia amphibia* and *Rhopalodia rhopala*. There is also a prominent peak in the saline tolerant species *Thalassiosira rudolfi* at 9 cm (AD 2000).

Throughout the most recent zone Ks9 (4-0 cm; AD 2005-2007), *Cyclotella meneghiniana* and *Nitzschia palea* are still important in the assemblage, and aerophilous, benthic and littoral taxa maintain their importance throughout this zone, with peaks in *Hantzschia amphioxys*, *Diadesmis contenta*, *Luticola mutica*, *Fallacia monoculata* and *Nitzschia amphibia*.

Kyasanduka has an interesting division in the reconstructed conductivity, with high reconstructed conductivities prior to AD 1480 and lower conductivities after this date. The record is highly variable in the most recent part of the record (last *c.* 130 years; Ks6-9), though some of this variability is likely due to the extremely high temporal resolution in these upper sediments (top *c.* 120 cm). A LOWESS smoother (0.1 moving average) has been used to try and reduce the noise in the data and extract the main patterns.

Zone Ks1 shows a slightly decreasing trend in the reconstructed conductivity, with values between *c.* 700 µS cm^{-1} (AD 1090) and ~500 µS cm^{-1} (AD 1170). Throughout Ks2a, the conductivity increases to 800 µS cm^{-1} (AD 1310; boundary with Ks2b). Values continue to increase (900 µS cm^{-1}; AD 1330), before decreasing towards the boundary of

Ks2b and Ks3. There is a small excursion in the data to higher values at AD 1450 (900 µS cm^{-1}), though this is not highlighted in the applied LOWESS smoother. The reconstructed conductivity values drop to <450 µS cm^{-1} immediately after the Ks2b-Ks3 boundary. Zone Ks3 is relatively stable, though there is a slight peak in the reconstructed conductivity at AD 1530 (300 µS cm^{-1}) followed by a drop in conductivity to *c.* 250 µS cm^{-1}; conductivity does increase slightly throughout the zone (300-500 µS cm^{-1}). The relative stability of the reconstructed conductivity continues into zones Ks4 and Ks5a, with values fluctuating around 350 µS cm^{-1}. AD 1800 (Ks5b) marks a slight increase in conductivity to 400 µS cm^{-1}, after which conductivity continues to steadily rise through the zone to a maximum at the Ks5c boundary (conductivity of *c.* 600 µS cm^{-1} at AD 1850). Zones Ks6-Ks9 are extremely variable in their reconstructed conductivities, and thus patterns are described using the smoothed data. Zone Ks6 shows variation in the reconstructed conductivity with peaks centred on AD 1910 and AD 1930 (*c.* 700 and *c.* 600 µS cm^{-1}, respectively) and troughs centred on AD 1890 and AD 1920 (*c.* 300 and *c.* 200 µS cm^{-1}). Towards the top of Ks6, the conductivity stabilizes and begins to rise steadily throughout Ks7 (to a maximum of *c.* 700 µS cm^{-1} at AD 1980). Ks8 sees a slight dip in the reconstructed conductivity values (c 400 µS cm^{-1}; early 1990s). The reconstructed values increase slightly towards the present day, and produce a modern value of *c.* 400 µS cm^{-1}, double the actual recorded value of 204 µS cm^{-1}.

Fossil data are very well covered by the crater lake conductivity model, with an average 97% of species abundance data included. Similarly, there are very good analogues for most levels, with average minimum dissimilarity coefficients of 51, and no samples >127. Samples that lie beyond a value of 150 are suggested to have poor or no-analogues in the diatom training set (Jones and Juggins, 1995; Juggins, 2001).

6.4.5 Indirect ordination – Detrended Correspondence Analysis (DCA)

DCA revealed a gradient of 2.569 S.D. units; therefore a unimodal response model was appropriate for further analysis. Correspondence Analysis (CA) indicated an arch in the data, thus DCA was deemed the most appropriate response model.

A DCA plot of all the core samples and diatom species >5% is shown in Figure 6.26. Eigenvalues for axes 1 and 2 are 0.375 and 0.124, respectively whereas those for axes 3 and 4 are only 0.063 and 0.043, respectively, and are not considered further (broken stick analyses; **Appendix B**). The first two axes account for 28.3% of the variation in the diatom data set. The gradients represented by both axes 1 and 2 can be correlated to variations in

the habitat preferences of the diatoms recorded in the sediment sequences. Axis 1 is negatively correlated with benthic and facultatively planktonic species (r = -0.43 and r = -0.86, respectively, based on Pearson's correlation coefficient) and positively correlated to aerophilous species (r = 0.51). Axis 2 is positively correlated to benthic species (r = 0.66) and reconstructed conductivity (r = 0.50) and negatively correlated with planktonic species (r = -0.86). The changes in the axis 1 sample scores are likely driven by changes in the benthic *Nitzschia palea* (NI009A), the facultatively planktonic *Cyclotella meneghiniana* (CY003A) and littoral and benthic species such as *Nitzschia amphibia* (NI014A), *Amphora veneta* (AM004A), *Sellaphora pupula* (NA014A) and *Stauroneis pseudosubobtusoides* (SAPSEUD). Axis 2 changes are most likely driven by the dominance of the freshwater species *Aulacoseira granulata* v. *angustissima* (AU003A) and *A. ambigua* (AU002A) in the lower sections of the core, and the benthic *Nitzschia palea* (NI009A) in the upper sections of the core.

The DCA ordination diagram (Figure 6.26) can be split into three groups: (i) 217-180 cm (AD 1070-1470); (ii) 179-113 cm (AD 1470-1860) and (iii) 112-0 cm (AD 1870-2007). The samples from the earliest group (i) are related to aerophilous and benthic taxa such as *Orthoseira roeseana* (OS005A), *Hantzschia* spp., *Fallacia monoculata* (NA739A), *Diadesmis contenta* (NA046A) and *Lemnicola hungarica* (AC032A). Group (ii) is related to planktonic species such as *Aulacoseira ambigua* (AU002A), *A. granulata* v. *angustissima* (AU003A) and *Nitzschia confinis* (NI082A). The most recent group of samples (iii) are related to facultatively planktonic species such as *Cyclotella meneghiniana* (CY003A), planktonic species such *as Nitzschia lancettula* (NI221A) and benthic species such as *Navicula microrhombus* (NAMICR).

6.4.6 Organic isotope analyses

Lacustrine organic matter is a complex mixture of compounds synthesized by terrestrial plants, aquatic macrophytes, algae and bacteria (Tyson, 1995; Ficken et al., 2000; Street-Perrott et al., 2004). Terrestrial plants and emergent macrophytes use atmospheric CO_2 as their main carbon source, whereas lacustrine algae and submerged macrophytes utilise CO_2 (dissolved) and in some cases HCO_3 due to high water temperature, changes in pH, salinity or enhanced productivity caused by an increase in nutrients (Meyers and Ishiwatari, 1993).

The results of bulk organic isotope analyses ($\delta^{13}C$ and C/N) from Lake Kyasanduka are shown in Figure 6.27. Overall, the C/N ratio in the sedimentary record from

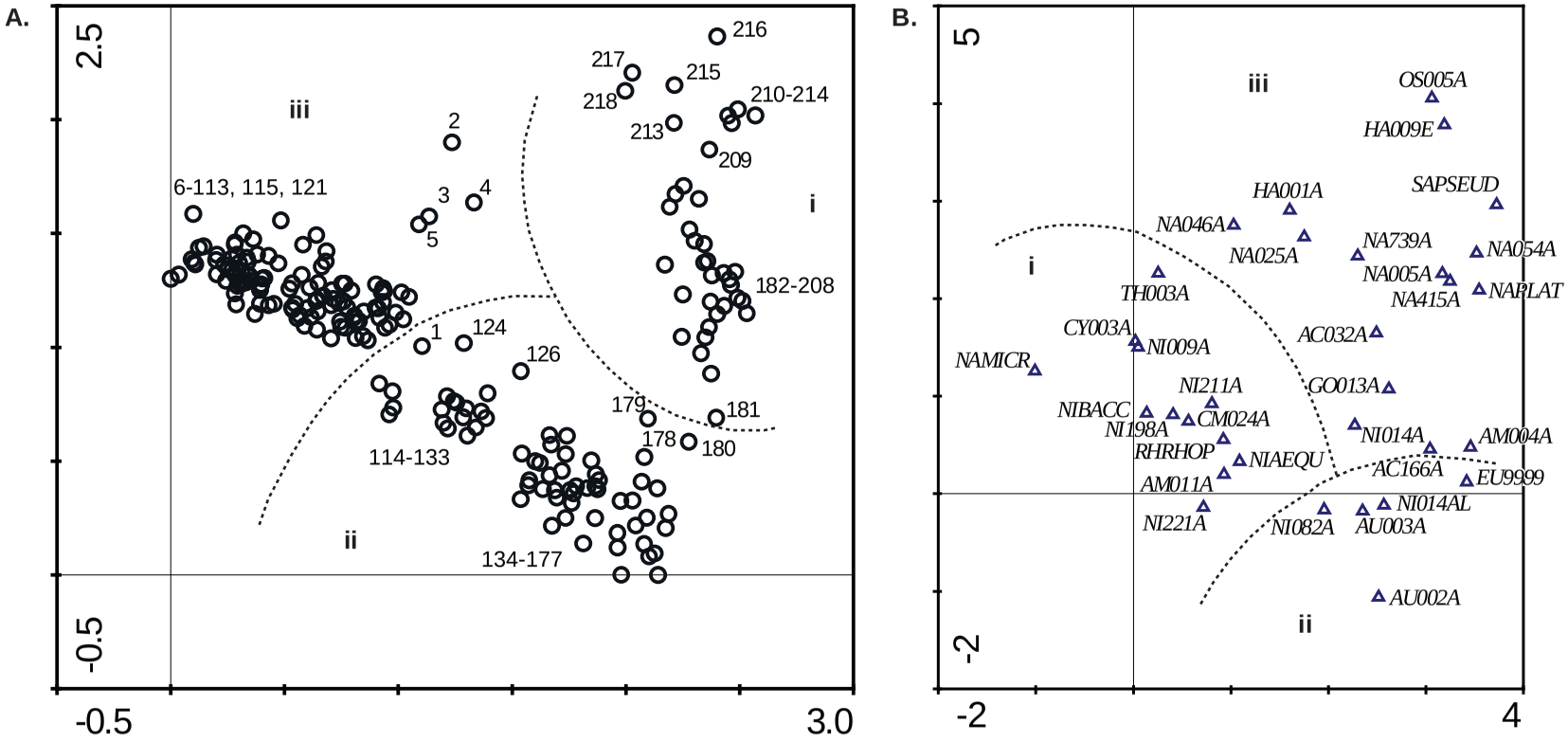

Figure 6.26 *Indirect ordination of diatom samples from Lake Kyasanduka. The DCA of* **(A)** *samples (in depth, cm) and* **(B)** *species >5% from Lake Kyasanduka are shown.*

Kyasanduka is relatively stable (e.g. compared to Lake Nyamogusingiri) with the majority of the record (AD 1200 to present) displaying a C/N of 10-20, suggesting a mixture of algae and terrestrial higher-plant detritus (Olago, 1995; Ficken *et al*., 1998). There are two excursions in the data between AD 1070-1180 (217-207 cm) and AD 1830-1860 (125-115 cm).

The organic isotope record from AD 1070-1180 exhibits extremely high C/N (*c.* 22 to > 65). These extreme C/N values are coincident with low $\delta^{13}C$ values of *c.* −25 to −20‰ suggesting that the predominant source of carbon is likely from higher terrestrial plants (cf. Tyson, 1995) and aquatic macrophytes (cf. Ficken *et al*., 2000). Culture studies suggest that some green algae (such as *Botryococcus*) can produce C/N values of >30, which may also contribute to the high C/N values observed in the early record Huang *et al*., 1995). However, without biomarker or palynological evidence for the presence of these algae, a predominantly terrestrial carbon source is assumed. The terrestrially sourced carbon is likely a weighted averaged mix of woody vegetation (C_3) and perhaps C_4 plants and/or aquatic macrophytes. The catchment morphology, topography and relative abundances of the terrestrial and lake plants strongly influence the relative contributions from terrestrial and aquatic sources to lake sediments (Meyers AND Ishiwatari, 1993). The diatom assemblage indicates that lake level was almost certainly lower at this time, increasing the available habitat for terrestrial C3 and C4 vegetation and increasing the available habitat for emergent macrophytes (with $\delta^{13}C$ values of c. −27 to −22‰; Ficken *et al*., 2000). In some marginal areas of East African lakes C_4-type macrophytes, such as *Cyperaceae papyrus* can dominate and may also contribute to the observed $\delta^{13}C$ values (Hillaire-Marcel *et al*., 1989; Lamb *et al*., 2004).

C/N exhibits a gradually decreasing trend between AD 1180-1630 (207-160 cm; C/N 17-13.5), where it stabilises at ~14, again indicative of a mixed source of carbon input to the lake system. With lake levels increasing during this period the relative input of terrestrially derived carbon may decrease, and the proportion of carbon contributed from the aquatic environment (microalage) has most likely increased (Tyson, 1995). In conjunction with this, $\delta^{13}C$ values of −23 to −18‰ suggest C_3 vegetation, aquatic macrophytes and microalgae (cyanobacteria [−13 to −27‰] and diatoms [−19 to −23‰]) are the likely sources of carbon input (Tyson, 1995).

Between AD 1630 and AD 1810 (160 cm to 131 cm), $\delta^{13}C$ rises sharply (c. −10‰) coincident with a sustained decrease in C/N values to *c.* 12. These lower C/N values might be indicative of an increasingly important aquatic carbon source (e.g. diatoms,

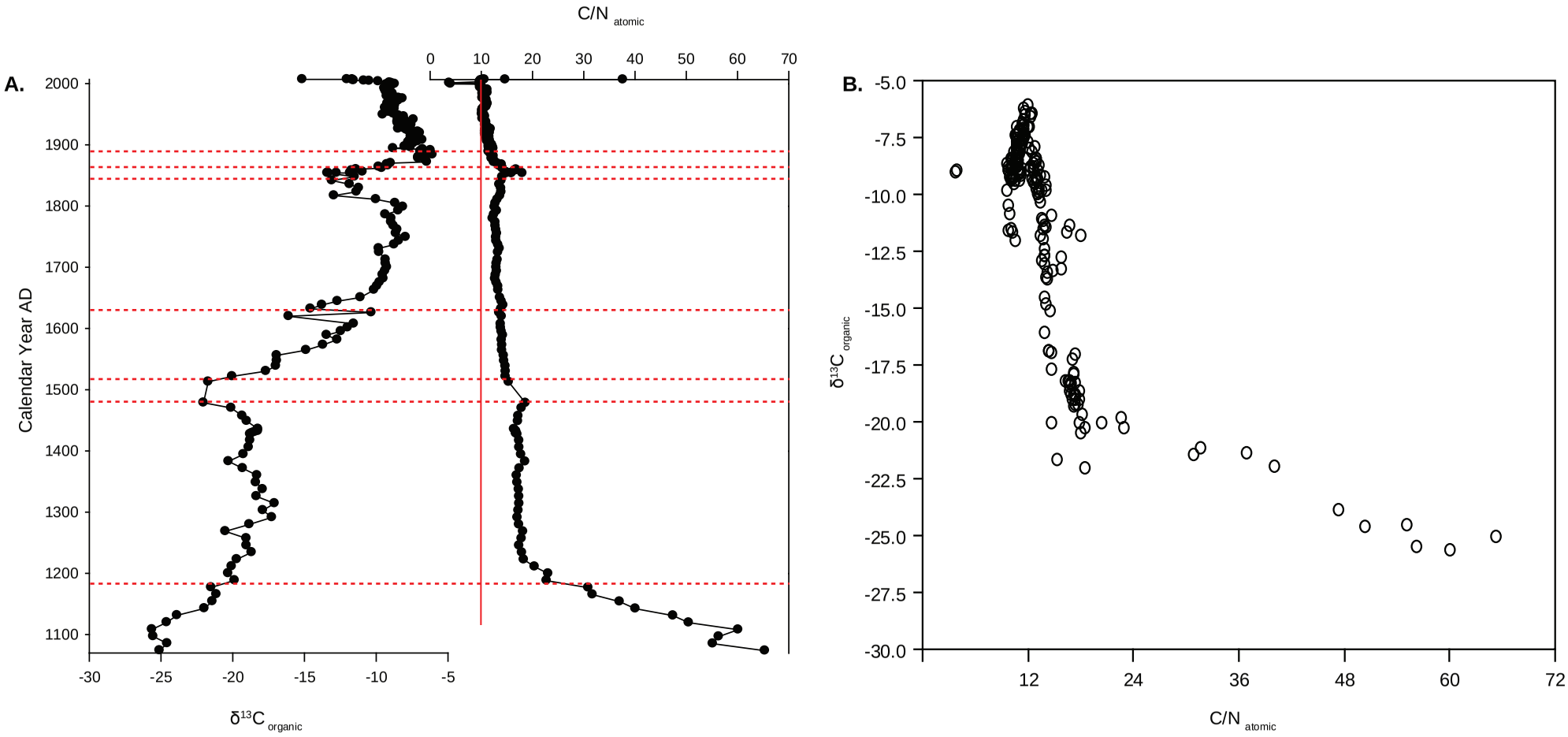

Figure 6.27 **(A)** *Organic isotope stratigraphy from Lake Kyasanduka - $\delta^{13}C_{organic}$ (left) and C/N_{atomic} ratios (right). The vertical solid red line (C/N ratio) indicates the boundary between algal (<10) and terrestrial (>10) dominated productivity (Meyers and Lallier-Vergès, 1999). The dashed lines highlight key zones discussed in the text.* **(B)** *Scatter plot of C/N vs. $\delta^{13}C$.*

macrophytes), but still with a proportion of the carbon contributed from terrestrial higher plants (Meyers and Ishiwatari, 1993; Tyson, 1995; Ficken *et al*., 2000; Street-Perrott *et al*., 2008). The higher $\delta^{13}C$ values (c. −11‰) may be indicative of the presence of diatoms and cyanobacteria in the lake waters and input from terrestrial C_4 plants or emergent macrophytes (e.g. *Cyperus* [−9‰]; Ficken *et al*., 2000).

An excursion in the data occurs between *c.* AD 1840-1860 (125-115 cm). This period is coincident with a period of inferred catchment inwash (high magnetic susceptibility, low organic content and an increase in the number of aerophilous taxa in the core). There is also a switch in the diatom flora to species indicative of higher nutrient content and the presence of N-fixing algae. The C/N rises to *c.* 18 and $\delta^{13}C$ is lower (−13‰). This section of the core is perhaps affected by the inwash of terrestrial and/or littoral vegetation or could be related to a short-lived period of aridity and lower lake level. Algae and submerged macrophytes, as well as the submerged leaves use dissolved CO_2 and in some cases, HCO_3 as opposed to atmospheric CO_2. Algae and aquatic plants that can actively take up HCO_3 are favoured at times of low dissolved CO_2 availability, which may be a result of increased aridity (which may increase water temperatures) side effects of aridity such as high water temperatures, or high aquatic productivity resulting from an enhanced nutrient supply (Street-Perrott *et al*., 2004).

Immediately after this excursion (AD 1860-1890; 113-100 cm) $\delta^{13}C$ rises to −6 to −7‰ and C/N drops to 11. The C/N record steadily decreases and the $\delta^{13}C$ increases and stabilise towards the present (AD 1890-2006; 100-2 cm). This part of the record suggests a system where the predominant carbon source is aquatic. The diatom stratigraphy is indicative of enriched nutrient conditions, concomitant with a period of lower lake level as a result of elevated aridity in the region. During this period the lake appears to be functioning similar to that during the period AD 1630 to AD 1810. The most recent samples (AD 2006-2007; 2-0 cm) see a return to low values of $\delta^{13}C$ (-15‰) and high C/N (37). The excursion in the values of the uppermost sample (0-1cm) may be attributed to the fact that these sediments are very recent and have not been subjected to any diagenetic alteration or degradation.

6.4.7 Interpretation of records from Lake Kyasanduka

Ks1: AD 1070 – AD 1180

The earliest period in the Kyasanduka diatom record (AD 1070-1180) suggests a lake environment with shallower conditions than seen today, perhaps with some of the littoral areas consisting of swamp or water logged conditions, as suggested by the presence of the aerophilous species *Orthoseira roeseana*, *Stauroneis pseudosubobtusoides*, *Hantzschia amphioxys* and *Luticola mutica* (enhanced by the flat nature of the lake basin; Gasse, 1986). The organic isotope data suggest a lake environment dominated by a terrestrial carbon source (very high C/N and very low $\delta^{13}C$), whilst the fluxes of sediments and diatoms to the lake system are very low. The organic content of the sediments is very high (*c.* 70%) and coincides with soil/peat like sediments in the basal *c.* 15 cm of the core sequence.

Ks2: AD 1180 – AD 1470

The lake is dominated by aquatic vegetation during the period AD 1180-1470, suggested by the high abundances of *Nitzschia amphibia* and other periphytic species (*Amphora veneta* and *Encyonema muelleri*). The isotopic data suggest a well mixed source for the deposited carbon (both terrestrial and aquatic). The sediment and diatom fluxes remain low. The presence of *Amphora veneta* and *Cyclotella meneghiniana* may attest to slightly more saline conditions at this time (in conjunction with the low lake level), with periphytic species (such as *N. amphibia*) being widely salt tolerant and thus supporting this interpretation (Gasse, 1986). The majority of the species present during this period suggest slightly alkaline waters, with a pH *c.* 8-8.5 (Gasse, 1986). There are three small perturbations in this relatively uniform phase, centred on AD 1220, AD 1300 and AD 1430, where there is a short-lived peak in the abundance of *Aulacoseira ambigua*, perhaps suggesting a rapid increase in water levels and more open conditions (coincident with small decreases in some of the benthic/periphytic taxa; Chalié and Gasse, 2002; Stager *et al*., 2005). The low abundances of *Aulacoseira granulata* v. *angustissima* suggest that where a body of water did exist, the water was well mixed and turbid as this taxon thrives in low light conditions. The presence of this taxon may also be indicative of slightly eutrophic conditions (Kilham *et al*., 1986; Kilham and Kilham, 1975; Owen and Crossley, 1992; Stager *et al*, 1997; Barker *et al*., 2003), with total phosphorus optimum of *c.* 28.5 µg l^{-1} TP (Kilham *et al*., 1986). Again, this taxon is indicative of slightly higher conductivity

(it has a higher conductivity optima higher than other *Aulacoseira* species; Gasse *et al*., 1995) and lower lake levels; *A. granulata* v. *angustissima* has optimal growth in shallow lakes with highly turbid waters (Lamb *et al*., 2007). Furthermore, this taxon supports the suggestion of alkaline waters, as it is often found in East African waters with a pH of 8-8.5 (Gasse, 1986).

Ks3 – Ks4: AD 1470 – AD 1780

At *c.* AD 1480 there is a drop in the C/N and $\delta^{13}C$ becomes more negative, which is concurrent with a switch in the lake ecosystem to more open lake conditions, where *Aulacoseira ambigua* becomes the dominant taxon (and has a high flux rate). There is an abrupt decline in *N. amphibia*, the diatom that previously dominated (AD 1480) and the disappearance of benthic/periphytic species such as *Amphora veneta, Hantzschia virgata* and *Orthoseira roeseana*. The appearance of *Aulacoseira ambigua* and decline in the periphytic species indicates an opening of the lake waters, and a reduction in the available habitat for littoral vegetation. Some benthic and periphytic taxa do persist (e.g. *Encyonema muelleri*, *Amphora copulata* and *Nitzschia aequalis*) attesting to improved light penetration in the lake. *Aulacoseira granulata* v. *angustissima* is still present, but in lower quantities, and *A. ambigua* dominates (Stager *et al*., 2005). The isotopic record suggests a lake system that is increasingly dominated by algal productivity. *Aulacoseira ambigua* has a high light requirement and is indicative of well mixed, but less turbid conditions. The availability of silica (in particular a high Si: P ratio) is also likely responsible for the dominance of *A. ambigua* (Kilham *et al*., 1986; Owen and Crossley, 1992; Fritz *et al*., 1993; Barker *et al*., 2002). *Aulacoseira granulata* is a poor competitor for Si, and in the absence of turbid waters, *A. ambigua* may simply out compete *A. granulata* v. *angustissima*.

A switch to *Aulacoseira granulata* v. *angustissima* dominance (AD 1710) suggests a less shallow (*c.* 3 m), well mixed, turbid lake (Stager *et al*., 1997), and the very high (less negative) $\delta^{13}C$ values may be indicative of a long lake water residence time, in a closed lake system, that is becoming progressively shallow with a rise in both pH and conductivity. This inferred turbid and shallow lake system is coincident with an increase in the flux of minerogenic sediments to the lake. The influx of sediments is likely due to catchment instability due to vegetation removal (perhaps as a result of a more arid climate). The removal of catchment vegetation would also leave the shallow lake system unsheltered and vulnerable to wind-induced mixing. The increase in turbidity is responsible for a decline in *A. ambigua* due to the reduction of light intensity. The

appearance of long, thin *Nitzschia* (*N. bacata* and *N. confinis*) does suggest that the lake may also be polymictic at this stage, undergoing periodic stratification, both daily through thermal stratification (cf. *Nitzschia bacata* in Lake Kivu, Sarmento *et al*., 2006; see **Chapter 4**, *section 4.4.2*), and perhaps even for a few weeks. This period almost certainly indicates an increase in water depth (Stager *et al*., 2003; Stager *et al*., 2005).

Ks5: AD 1780 – AD 1860

This period marks the beginning of a major change in the diatom flora. The abundance of *Aulacoseira granulata* v. *angustissima* declines to *c.* 20% and there is an increase in *Cyclotella meneghiniana* and *Nitzschia palea*. Although in decline, the presence of *Aulacoseira granulata* v. *angustissima* (AD 1850) in conjunction with a rise and reappearance of aerophilous and shallow water species *Diadesmis contenta*, *Hantzschia amphioxys* and *Nitzschia amphibia* suggesting a turbid, shallow environment. The turbidity is likely caused by either the resuspension of sediments from the lake bottom (though there is little evidence in the core and diatom stratigraphy for this) or more likely the littoral areas (given the occurrence of benthic and aerophilous taxa) and perhaps the mixing of inwashed catchment sediments (thus increasing the number of aerophilous taxa delivered to the core site).

At *c.* AD 1850 there is a switch from an *Aulacoseira* dominated assemblage to one dominated by *Nitzschia* and *Cyclotella*. The possibility of an hiatus in the core (*c.* AD 1850) can be dismissed (see *section 6.4.1*) on the basis of the diatom stratigraphy; the changes in the flora starts to occur prior to the biggest change. Furthermore there is no evidence for the reworking of sediments and the continuous presence of species such as *Nitzschia confinis* and *N. amphibia* does not support an hiatus or desiccation surface.

This period is interpreted as an extremely low lake level, which also coincides with a section of laminated sediments and a drop in the organic content of the sediments and a peak in the magnetic susceptibility. A change occurs in the isotopes also, with C/N rising to levels which suggest an increasing input of terrestrial material, and $\delta^{13}C$ becomes more negative, indicating an input of C_3 vegetation.

Ks6 – Ks9: AD 1860 – AD 2007

The upper section of the core (AD 1860-2007) is less diverse than the lower core sections. This drop in diversity is likely due to the disappearance of periphytic taxa (Gasse *et al*., 2002). The occurrence of *Cyclotella meneghiniana* (AD 1850) is indicative of a shallowing

of the lake system (rapid infilling of the lake occurred from this point, with *c.* 1.5 metres of sediment deposited over the last *c.* 140 years) and perhaps lower lake levels, longer water residence time or perhaps stagnant water (Patrick, 1948; Stager, 1984). The co-dominance of *Nitzschia palea* is perhaps indicative of large quantities of particulate organic matter entering the lake system (Sabater, 2000). *Nitzschia palea* is a species highly tolerant of pollution (Sabater, 2000), as well as being suggestive of eutrophic/hyper-eutrophic conditions (van Dam *et al.*, 1994). This may be the result of an increase in nutrients and organic matter from the catchment following deforestation and/or the onset of agriculture.

Both *C. meneghiniana* and *N. palea* are indicators of polysaprobic waters (waters with a heavy load of decomposed organic matter, with little or no free oxygen). *Nitzschia palea* is also a nitrogen-heterotroph, and requires the presence of a nitrogen fixing host (e.g. cyanophytes such as microcystis; Kilham *et al*., 1986; Leland and Porter, 2000). Both of the dominant species have the ability to harvest light energy in very turbid environments and have the capacity to sustain a rapid population growth through the heterotrophic utilisation of organic carbon (Leland *et al*., 2001; Tuchman *et al*., 2006). *Nitzschia palea* is a species common in water bodies draining agricultural land (Leland and Porter, 2000). Overall the total diatom flux to the Lake Kyasanduka is very low (and much lower than Lake Nyamogusingiri; Figure 6.22). The largest increase in the total diatom flux occurs at *c.* AD 1884 through to the late 1970s. At the same time fluxes of *Nitzschia palea* and *Cyclotella meneghiniana* increase, showing two distinct peaks (with a drop in the 1940s). These increases in the diatom flux data are coincident with the increase in the fluxes of organic and minerogenic materials to the lake. Again, the large influx of sediments is most likely responsible for the delivering of a large quantity of nutrients to the lake system, causing diatom blooms (increasing productivity), similar to the record at Nyamogusingiri. This increase in productivity is matched by the C/N of the sediments (*c.* 10), suggesting an algal source of carbon is very important.

The appearance of *Navicula microrhombus* (AD 1855) is also worthy of note and perhaps denotes the introduction of fish to the lake. Cholnoky (1970) reported *N. microrhombus* (previously recorded as *Fragilaria microrhombus*) as endemic to (South) Africa and was reported to have occurred in a shallow pool to which fish had recently been introduced. However, more recently Gasse (1986) recorded its presence in East Africa as an aerophilous species in the moss of a peat bog on Mt. Badda.

Towards the top of the sediment record (AD 1950) the presence of *Nitzschia bacata* becomes increasingly important. These long, thin *Nitzschia* in African lakes are often

indicative of increased lake stability and suggest a reduced mixing regime (Stager *et al*., 1997). At *c.* AD 1960, there is a brief reappearance of littoral/aerophilous taxa (*Encyonema muelleri, Diadesmis contenta* and *Amphora copulata*) and a short-lived reduction in *Nitzschia bacata*, which recovers immediately after this short dry phase and expansion of aquatic vegetation. The most recent part of the record (from AD 1980) sees a decline in the abundance of *Cyclotella meneghiniana* and *Nitzschia palea*, though they are still the most dominant taxa. This reduction is concurrent with an increase in littoral/benthic/aerophilous taxa (*Nitzschia amphibia, Luticola mutica, Rhopalodia rhopala, Diadesmis contenta, Hantzschia amphioxys* and *Encyonema muelleri*). The appearance of these taxa may well be related to a slight reduction in water level and/or the stabilisation of littoral vegetation (supported by the presence of *E. muelleri*), more frequent mixing (reduction of *Nitzschia bacata*) and thus the frequent oxygenation of bottom waters (Stager, 1984).

6.5 Summary

- Two long (2.3m and 1.3 m) sediment cores spanning the last *c.* 1000 years were retrieved from a paired lake system in western Uganda (Lakes Kyasanduka and Nyamogusingiri)
- Multiproxy analyses (organic content, diatoms, organic stable isotopes and calculation of flux data) were completed on both composite core sequences.
- Whilst both lakes differ somewhat in their overall diatom species composition and their response to both external and internal factors, they do share some common features.
- The earliest phase in both sediment records suggest an arid period, characterised by low lake levels and elevated salinity and a carbon source that is predominantly terrestrial.
- Both lakes record a number of high- and low-stands between the 12^{th} and 19^{th} centuries which occur roughly at the same time (given the possible errors in the chronology). Both lakes also exhibit a similar organic isotope ($\delta^{13}C$ and C/N) profiles. This period is likely related more natural changes linked to changes in the climatic regime, perhaps as a result of changes in regional rainfall patterns.
- During the last *c.* 150 years there has been a major change in both lake ecosystems. There is a major switch to assemblages dominated by *Cyclotella meneghiniana* and *Nitzschia palea* coincident with a period of climatic changes and large organic and minerogenic sediment influx causing both lakes to become highly productive (increase

in the diatom flux and organic isotopes). This influx of diatoms and sediments manifests itself as a double peak. It is likely that this period represents a major phase of human activity within the lake catchments.

Chapter 7

Short Cores: Natural and cultural changes over the last 150 years

7.1 Introduction

This chapter focuses on results obtained from the analyses of five short sediment cores spanning the last *c.* 150 years from Lakes Kamunzuka, Nyungu, Kako, Mafura and Kigezi. The five lakes are located on a land-use gradient ranging from pristine (natural/secondary forest), to lakes whose lake catchments have been fully impacted by human activity (e.g. burning and clearance, market-garden agriculture and small-scale banana, pine and eucalyptus plantations). These lakes were chosen in order to try and understand 'time' (long- and short-term dynamics) and space (lakes with differing characters across a landscape) simultaneously. The numerical methods employed are described in **Chapter 6** and details regarding the site locations are given in **Chapter 2**.

For each lake, the core chronology, based on ^{210}Pb dating is presented, followed by results of physical analyses (based on loss-on-ignition). Dry mass accumulation rates (DMAR) were calculated for the sediment data to infer the flux of organic and minerogenic material to the lake. The results of diatom analysis, diatom habitat summaries and indirect ordinations are presented from three of the five cores (Kamunzuka, Nyungu and Kako). For these lakes, the diatom flux was also calculated. Where necessary each section is completed with a summary of the 'in-lake' records in an effort to tie together analyses of the proxy data (Kamunzuka, Nyungu and Kako). Results tables for the ^{210}Pb and multivariate analyses are presented in **Appendix D**.

7.2 Lake Kamunzuka

7.2.1 ^{210}Pb chronology

Lake Kamunzuka has a very good ^{210}Pb record, with a high surface concentration (~1730 Bq kg^{-1}) which declines regularly with depth, reaching equilibrium with the supporting ^{226}Ra at approximately 40 cm (P.G. Appleby, *pers. comm.*; Figure 7.1). The highest ^{137}Cs concentration occurs in the 14-15 cm sample, which is in relatively good agreement with the depth of 1963 as calculated from the ^{210}Pb dates using the CRS model (at 17-18cm). Thus sediments around this depth almost certainly date from the early 1960s (P.G.

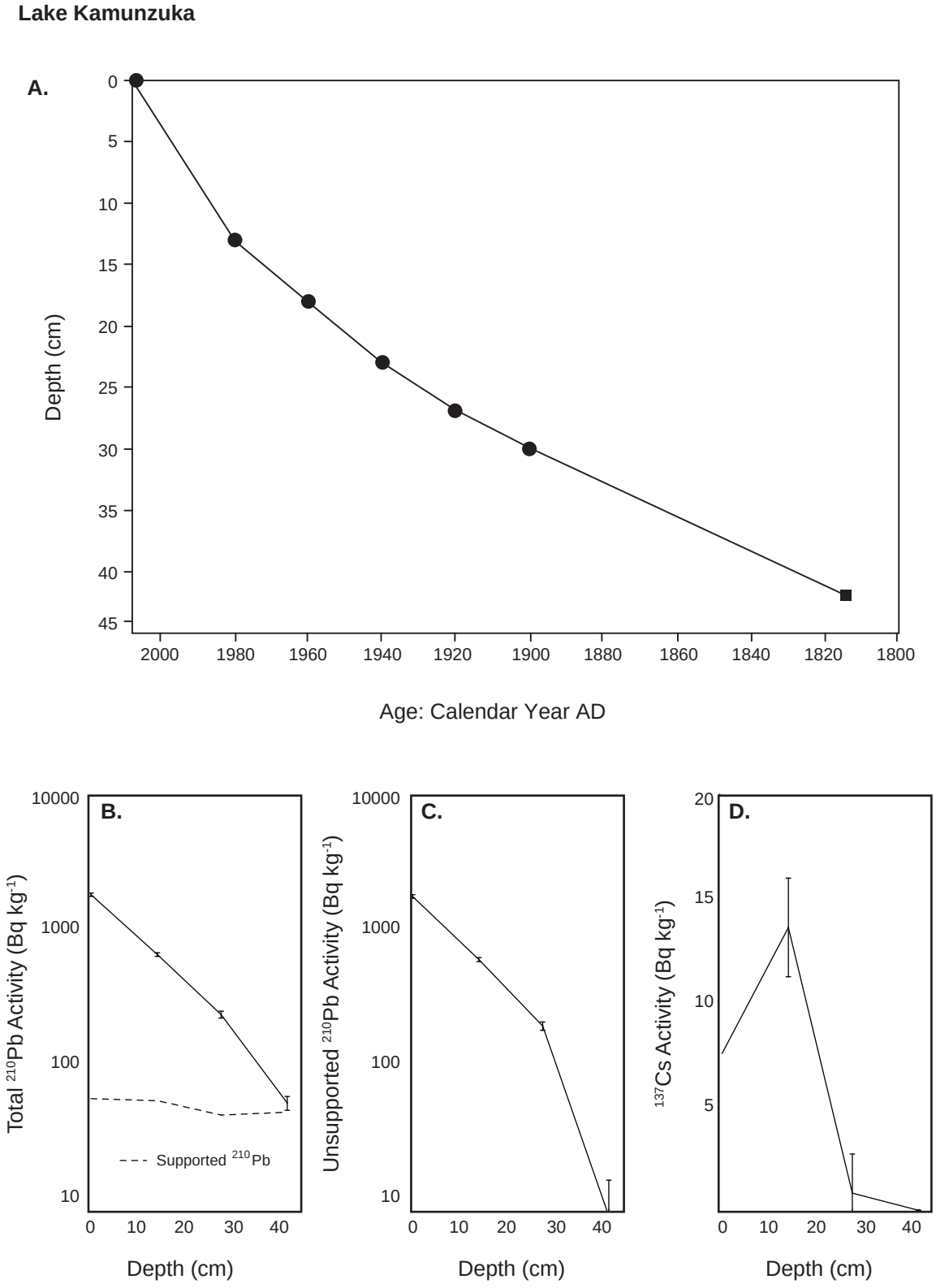

Figure 7.1 *^{210}Pb and ^{137}Cs data for Lake Kamunzuka.* **(A)** *^{210}Pb chronology for Kamunzuka (using linear extrapolation between the dated horizons). Filled circles represent actual dated horizons, the filled square is the base of the sequence, dated by linear extrapolation. (b-d) Fallout radionuclides in the Kamunzuka core showing* **(B)** *total and supported ^{210}Pb,* **(C)** *unsupported ^{210}Pb and* **(D)** *^{137}Cs concentrations versus depth.*

Appleby, *pers. comm.*). Accumulation rates in Kamunzuka are constant prior to the mid-1940s (~0.025 g cm^{-2} yr^{-1}), after which the rates begin to increase. Since the 1980s the accumulation rate is double the pre-1920s value (~0.049 g cm^{-2} yr^{-1}). Tentative radiometric dates were calculated using the CRS ^{210}Pb dating model (Appleby *et al.* 1978), and compared with the best estimate of the 1963 stratigraphic date suggested by the ^{137}Cs record (P.G. Appleby, *pers. comm.*).

7.2.2 Physical properties

The sediments from Kamunzuka are organic-rich, with loss-on-ignition values generally between 20% and 40%, carbonate values of 1-5% and minerogenic residue accounting for up to almost 80% (Figure 7.2). The organic content is relatively stable and fluctuates around 20% in the earlier part of the record (40-15.5 cm; AD 1810-1970). After AD 1970, the organic content increases steadily to 40%. The carbonate content, although fluctuating between 1 and 5%, is relatively stable throughout the entire record, with no significant excursions seen in the data. The DMAR in Kamunzuka is relatively stable in the earliest part of the record (42.5-30 cm; AD 1810-1900). After 30 cm (AD 1900) the DMAR dips slightly before generally increasing between AD 1920-1930 (27-25 cm). The values fall once again during the period AD 1930-1942 before increasing at 22 cm (AD 1940). Between 22-14 cm (AD 1940-1975) the values fluctuate but exhibit an overall decreasing trend. At 13 cm (AD 1980) there is a large excursion in the data to the highest DMAR seen in the record from Kamunzuka. After 12 cm (AD 1985) the values fluctuate but with a decreasing trend towards the present day.

Lake Kamunzuka has a highly variable DMAR and therefore variable organic and minerogenic flux records. None-the-less, several excursions can be identified in the data. In the earliest part of the record (42.5-30 cm; AD 1840-1900) values for the organic and minerogenic flux records are relatively stable fluctuating around ~0.007 g cm^2 yr^{-1} (organic flux) and ~0.05 g cm^2 yr^{-1} (minerogenic flux). After this period the organic and minerogenic fluxes decline slightly, reaching a low at *c.* AD 1910 (*c.* 28 cm; 0.004 and 0.03 g cm^2 yr^{-1}, respectively). At AD 1930, all records peak before briefly dropping to values similar to those at AD 1910. From the early 1940s (23 cm) there is a prominent shift within the data. Both of the records become noisier, and two excursions (to peak values; *c.* 20 cm, AD 1950 and 13 cm, AD 1980) are noted in the data. After AD 1980, the organic and minerogenic fluxes decline towards the present day.

The total diatom flux is quite high (generally >20 x 10^6 valves cm^{-2} yr^{-1}) for the majority of the record, with two peaks occurring in the last 60 years (centred on AD 1950 and AD 1995), concomitant with the increase in the amount of sediments delivered to the lake (Figures 7.2 and 7.3). There is not a clear relationship between the DMAR and diatom flux, suggesting that any increases in the diatom flux are independent of the sediment accumulation rates. The peaks in diatom flux are primarily driven by the large amounts of *Aulacoseira granulata* and *Gomphonema* cf. *gracile* (74 x 10^6 valves cm^{-2} yr^{-1} and 4 x 10^6 valves cm^{-2} yr^{-1}, AD 1950) and also *Gomphonema parvulum* (14 x 10^6 valves cm^{-2} yr^{-1}, AD 1995) to the sediments. Total diatom flux declines towards the present.

7.2.3 Diatom Analyses

The results of diatom analysis are shown in Figure 7.4, habitat summaries are given in Figure 7.5. Twenty-two samples at 2 cm intervals were analysed from Lake Kamunzuka. In total 43 species were identified. Three assemblage zones were identified for Kamunzuka (Km1-3).

The diatom stratigraphy from Kamunzuka is dominated by a form of *Gomphonema* cf. *gracile* (**Appendix E**, **Plate 4**), which generally increases up core, and which constitutes between 60-90% of the total diatom count in all samples. The diatom preservation within the core is generally good (**F**-index values between 0.7 and 0.95), the lowest values (more dissolved valves) associated with the oldest samples. The occurrence of testate amoeba scales in the Kamunzuka record is much lower than at other sites examined (e.g. Kyasanduka, Nyamogusingiri and Nyungu), with counts of <10 in any one sample. However, it is worthy to note that the highest counts of testate amoeba scales occur in zones Km1 and Km2.

Zone Km1 (42-34 cm; AD 1810-1870), as with the majority of the core, is dominated by the epiphytic diatom *Gomphonema* cf. *gracile*. A second *Gomphonema* spp. (*G. parvulum*) is also present in this zone. Both *G. gracile* and *G. parvulum* are at (relatively) low abundances in this zone (~60% and 5% maximum, respectively) but generally increase towards the top of the zone and into zone Km2. The taxa *Aulacoseira ambigua*, *Pseudostaurosira brevistriata*, *Staurosira construens* and *Fragilaria tenera* are also important at the beginning of this zone, but decline towards the top of the zone, with *A. ambigua* and the littoral taxa *P. brevistriata* disappearing from the record entirely. The diatoms *Encyonema minuta* and *A. granulata* are continuously present throughout this zone

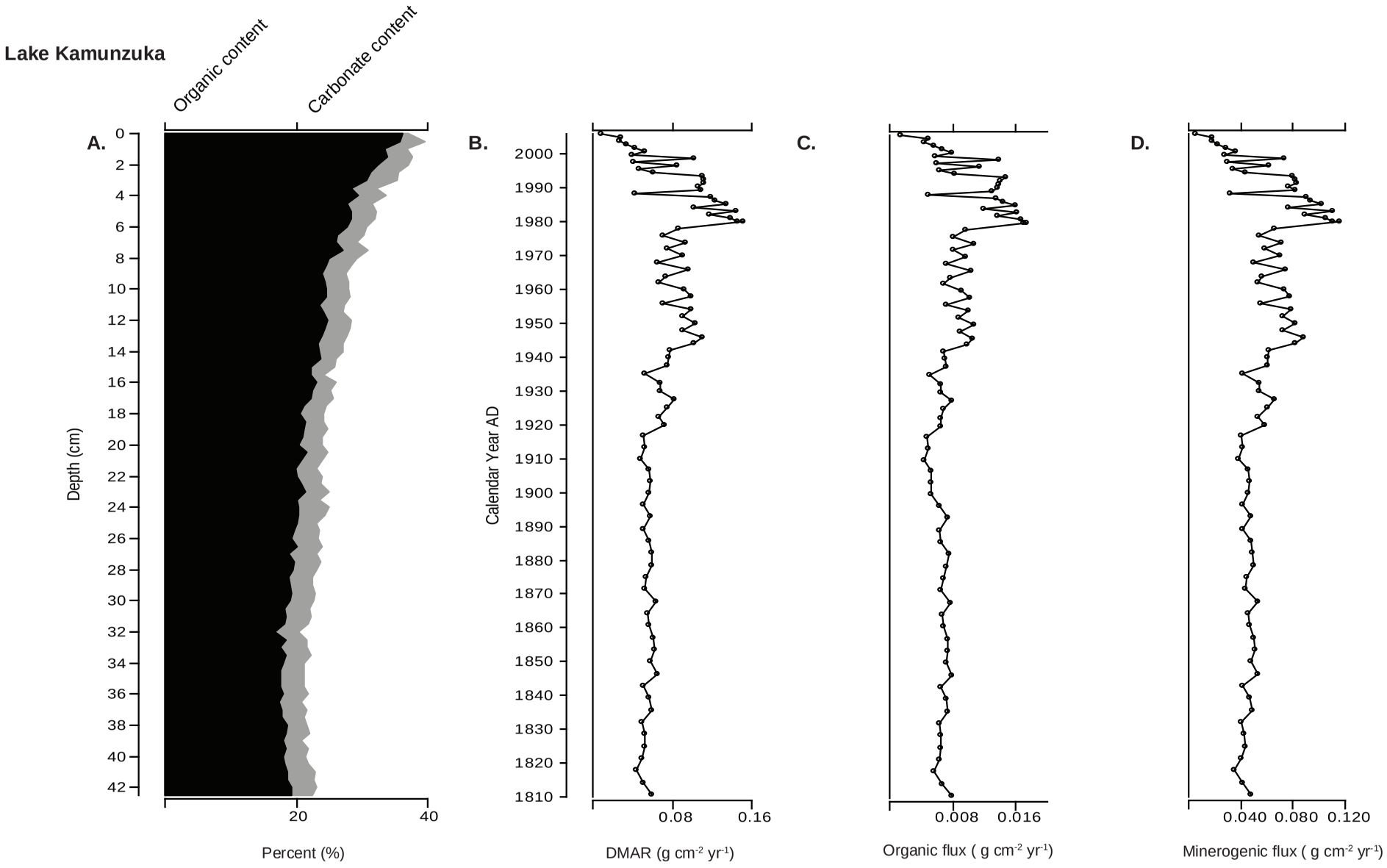

Figure 7.2 *Calculated flux data for Lake Kamunzuka.* **(A)** *Stacked organic and carbonate percentages versus core depth,* **(B)** *dry mass accumulation rate (DMAR) calculated using the dry bulk density and* ^{210}*Pb dates,* **(C)** *organic content displayed as flux (g cm*$^{-2}$ *yr*$^{-1}$*) and* **(D)** *minerogenic flux (g cm*$^{-2}$ *yr*$^{-1}$*). Graphs* **(B-D)** *are plotted against calendar year AD.*

Lake Kamunzuka

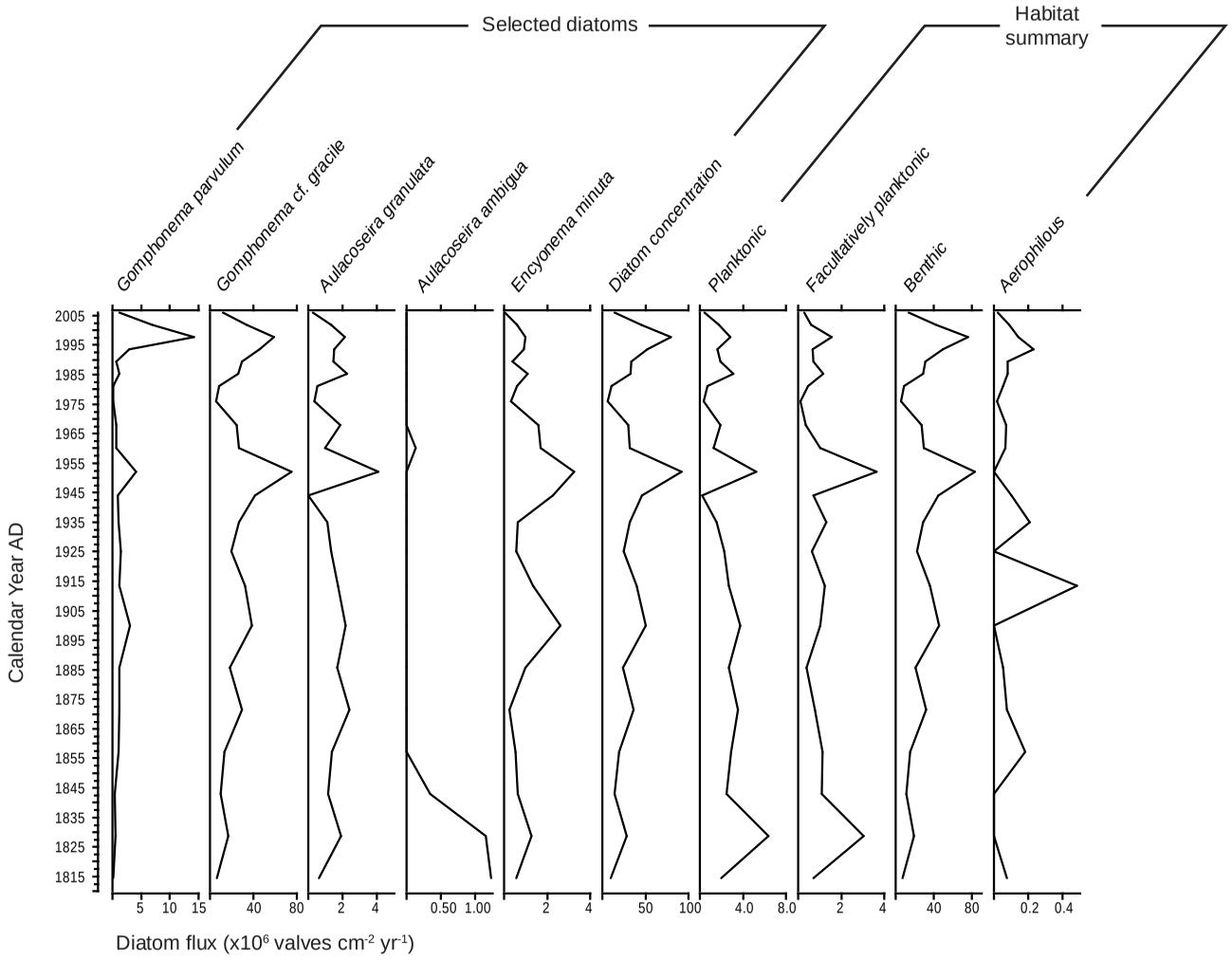

Figure 7.3 *Diatom flux for selected dominant taxa from Lake Kamunzuka displayed alongside the total diatom flux for each sample (left). The flux of diatoms within the habitat categories are also shown (right).*

(~5%) and indeed throughout the majority of the record. Diatom preservation is at its lowest in this basal zone (**F**-index of 0.7), but the diatoms are still remarkably well preserved. The preservation increases toward the top of this zone (**F**-index 0.9). Diatom concentrations are in the region of ~300-500 x 10^6 valves g^{-1}. Counts of testate amoeba are at their highest (1-6), with a peak at 40cm (AD 1830). The numbers of testate amoeba scales (testate amoebae: diatom ratio) decline towards the boundary of Km1 and Km2.

Zone Km2 (34-7 cm; AD 1880-1990) covers the longest period of all the zones. The presence of *G.* cf. *gracile* reaches its highest abundance in this zone and remains high (~80%) throughout. The presence of *G. parvulum*, *E. minuta*, *A. granulata* and *S. construens* are relatively constant, but at low abundances (generally <5%). In terms of the diatoms present, overall the zone appears to be relatively stable. The most noticeable change is the switch from the usual form of *F. tenera* to a deformed ('teratological') form of *F. tenera* (**Appendix E**, **Plate 2**) at the top of the zone, before this species and *S. construens* disappear from the record. Again, preservation is good in this zone (**F**-index ~0.9). Diatom concentrations tend to fluctuate, but are still high in the earlier part of this zone (300-1000 x 10^6 valves g^{-1}). Towards the top of the zone (12-14 cm; late 1970s early 1980s) the diatom concentration drops to the lowest values seen in the entire record (~90 x 10^6 valves g^{-1}). The second largest testate amoeba count (3) is recorded at 26 cm (1925). Testate amoeba scales are consistently present throughout Km2 and Km3 (7-0 cm; AD 1990-2006), but usually as just a single occurrence. The most prominent feature in the most recent zone is an increase in the abundance of *G. parvulum* (maximum 18%), coincident with a reduction in *G.* cf. *gracile* (70%). Other species that are consistently present in low numbers throughout the record (*E. minuta*, *A. granulata* and *S. construens*) decline in the uppermost samples. The diatom preservation in the most recent samples is excellent (**F**-index 0.95) and the diatom concentrations reach their highest values (*c.* 1000-1900 x 10^6 valves g^{-1}).

The diatom-inferred conductivity at Lake Kamunzuka remains extremely fresh throughout the 160 year record. The highest recorded value occurs in the earliest part of the record (zone Km1) and is centred on AD 1830 (45 µS cm^{-1}). The transition between zones Km1 and Km2 marks a drop in DI-conductivity (35 µS cm-1; AD 1870). After AD 1870 the reconstructed values begin to increase (to a maximum of 40 µS cm-1 at AD 1900). Values then begin to decline through the zone, where they reach a minimum at AD 1945 (35 µS cm^{-1}), before rising and peaking at AD 1990 (40 µS cm^{-1}). The reconstructed conductivity decreases towards the boundary with zone Km3. Conductivities peak during

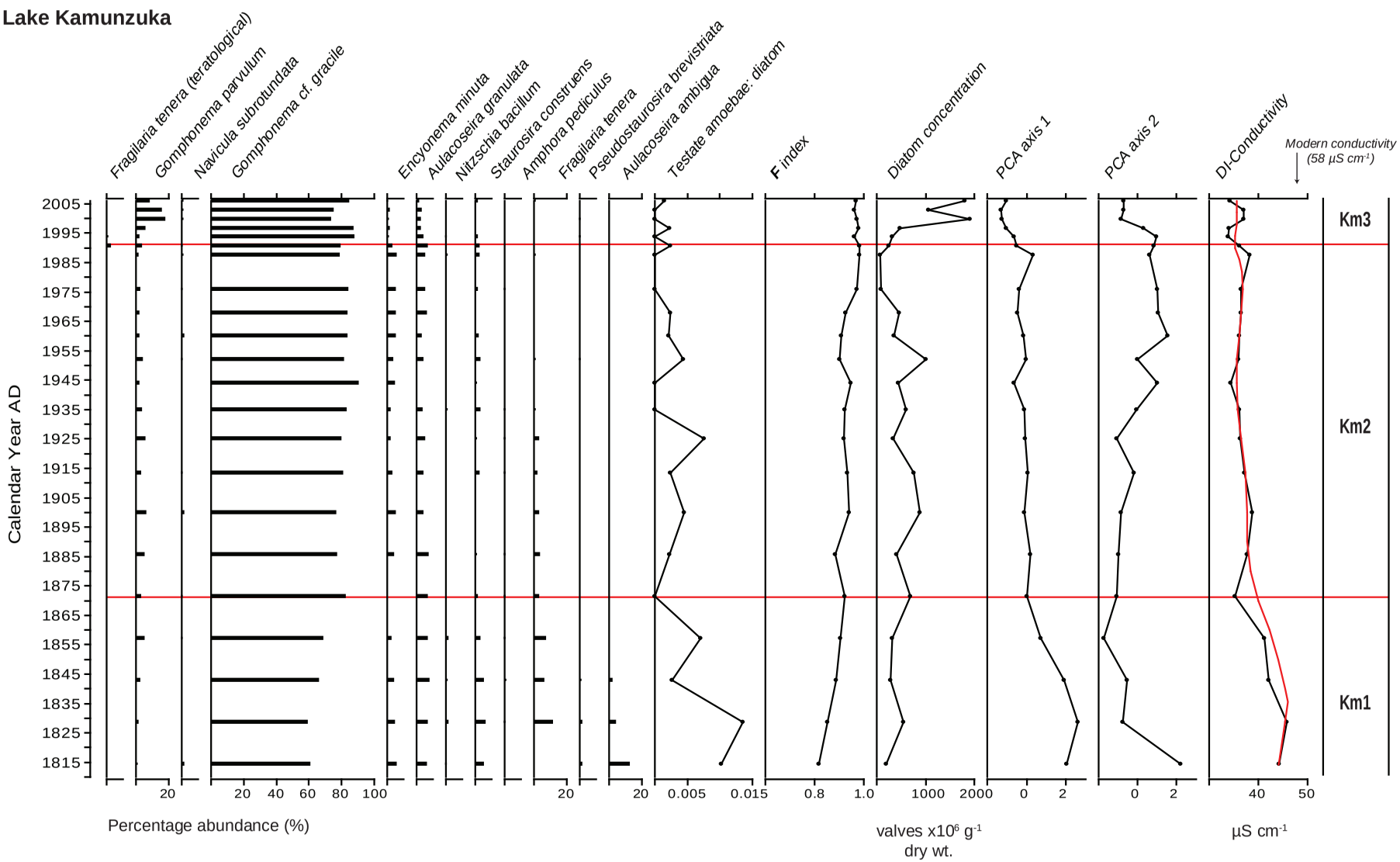

Figure 7.4 *Diatom stratigraphy from Lake Kamunzuka. All species > 5% in any one sample are displayed. The diatoms have been ordered according to their weighted average abundance in the core (ascending) and are split into assemblage zones Km1-3. The ratio of testate amoebae scales to diatoms is displayed alongside the diatom preservation index (**F** index), diatom concentrations and the axis 1 and axis 2 sample scores from Principal Components Analaysis (PCA; indirect ordination). Reconstructed conductivities are based on the crater lake transfer function (Combined_76; see **Chapter 5**), a smooth has been added to the reconstruction.*

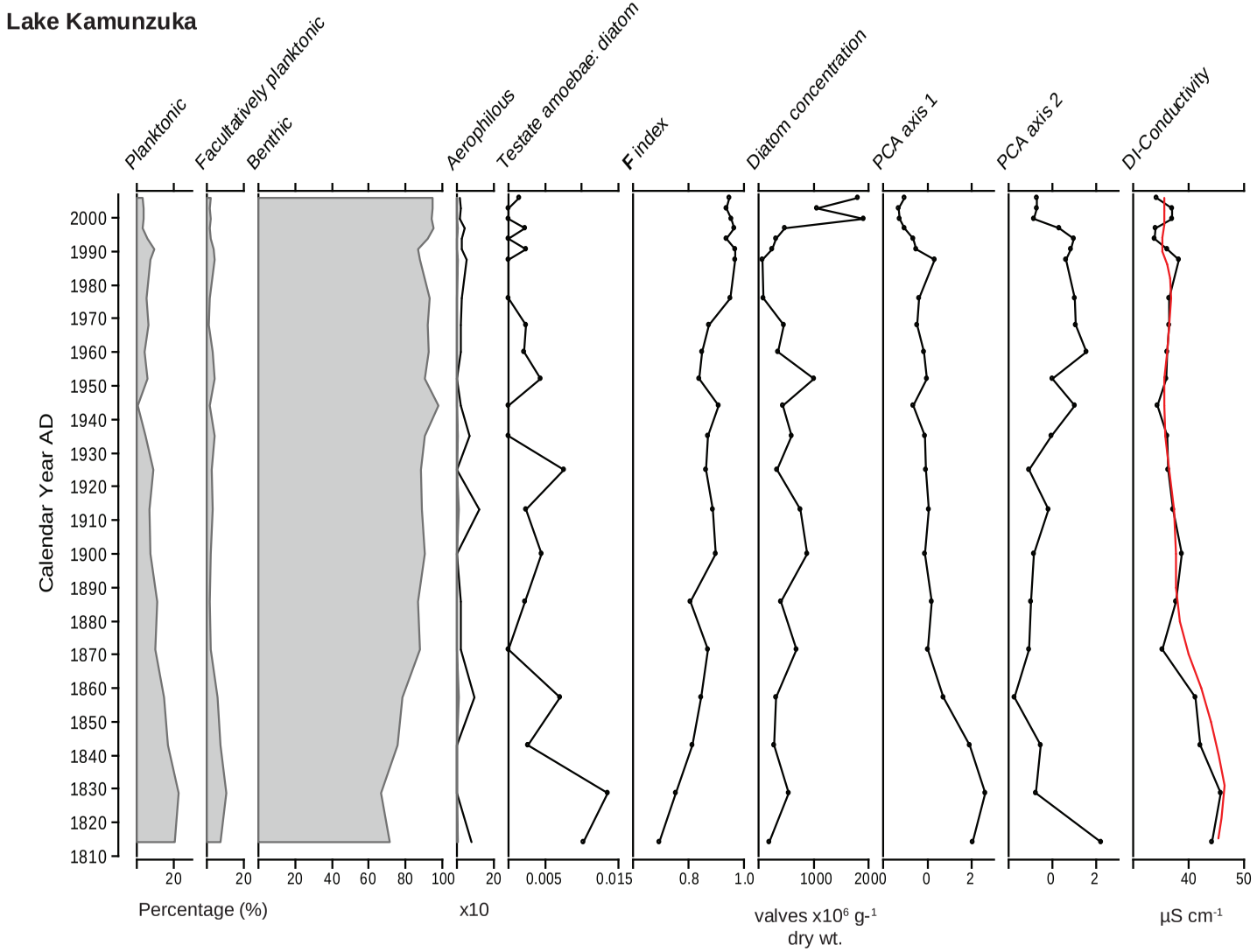

Figure 7.5 *Habitat summary of all diatom species from lake Kamunzuka (NB aerophilous taxa are displayed with an exaggeration multiplier of x10) displayed alongside the ratio of testate amoebae scales: diatom valves, dissolution index (**F** index), diatom concentration, sample scores from PCA axes 1 and 2 and diatom-inferred conductivity.*

the most recent zone (*c.* 40 µS cm^{-1}; *c.* AD 2000), before declining towards the reconstructed surface sample (35 µS cm-1; AD 2006), which is slightly lower than the actual recorded modern conductivity of 58 µS cm^{-1}.

Fossil data are very well covered by the crater lake conductivity model, with on average 93-100% of species abundance data included. Similarly, there are very good analogues for most levels, with average minimum dissimilarity coefficients of 51, and no samples >112.

7.2.4 Indirect ordination – Principal Components Analysis (PCA)

DCA on all taxa >0.5% abundance (43) revealed a gradient of 1.004 S.D. units; therefore a linear response model was appropriate for further analysis. A PCA plot of all the core samples and diatom species >5% are shown in Figure 7.6. Comparison to the broken stick model indicated that the four DCA axes were significant in explaining the variance in the diatom data (**Appendix B**), though axes 1 and 2 explained the majority of the variance in the dataset (59.3%); axes 3 and 4 explained only 18.4%. Eigenvalues for axes 1 and 2 are 0.373 and 0.22, respectively whereas those for axes 3 and 4 are only 0.108 and 0.076, and are not considered further (see **Appendix D** for CANOCO output).

The gradient represented by axis one appears to reflect the variation in the habitat preferences of the diatoms in the lake sediment sequences. The axis one sample scores are positively correlated to the abundance of planktonic species (r = 0.86) and negatively correlated to the abundance of benthic species (r = -0.76). These changes are predominantly driven by the abundances of *Gomphonema* cf. *gracile* (benthic) and the planktonic *Aulacoseira ambigua* and *A. granulata*.

The PCA ordination diagrams (Figure 7.6) show a split in the data (i and ii), with the bottom samples from the core (42-36 cm; AD 1810-1860) dominating the right side of the diagram and the upper samples (36-0 cm; AD 1860-2006) dominating the left side of the diagram (Figure 7.5). The samples from the lower parts of the core are mostly associated with planktonic species (*Aulacoseira* spp. and *Fragilaria tenera*); the uppermost samples are related to the periphytic/benthic species *Gomphonema* cf. *gracile* and *G. parvulum* and the planktonic *Fragilaria tenera* (in its 'teratological' form).

7.2.5 Interpretation of records from Lake Kamunzuka

This deep lake (*c.* 60 m) is dominated by the epiphytic *Gomphonema* cf. *gracile* (**Appendix E**, **Plate 4**). This species (along with *Aulacoseira granulata*) dominates both

Lake Kamunzuka

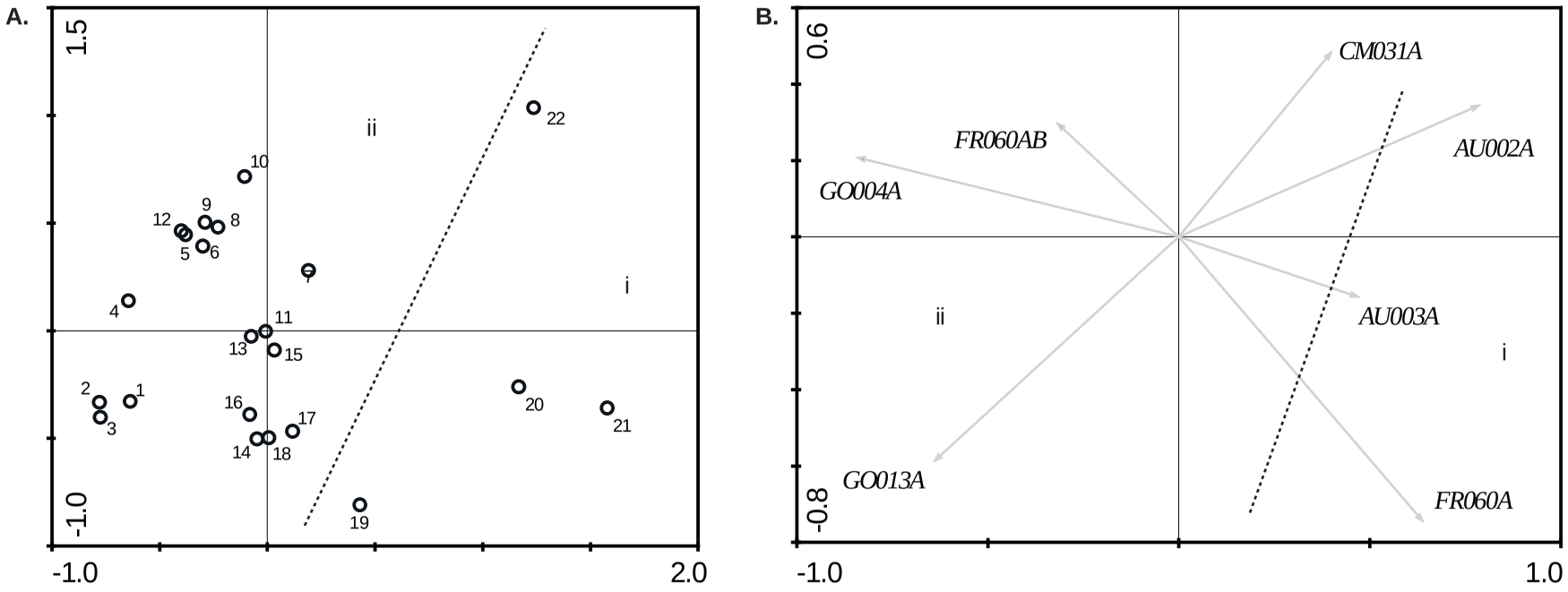

Figure 7.6 *Indirect ordination of diatom samples from Lake Kamunzuka. The Principal Components Analysis (PCA) of* **(A)** *samples (in depth, cm) and* **(B)** *species >5% are shown.*

the surface sediment samples and the phytoplankton net trawl, suggesting the deep, freshwater lake with high penetration of light (Secchi depth of 7.7 m) that occurs in the present, prevailed throughout the 150 year history of the lake sediment record (Kilham *et al*., 1986). *Gomphonema* cf. *gracile*, given the bathymetry of the lake (**Chapter 4,** Figure 4.1), most likely lives in the littoral area. Given the deep light penetration in this lake, the euphotic depth (the depth to which photosynthetic plants can survive) could be as deep as 20 m (2.5 times the Secchi depth; Cole, 1975). Therefore, there is potentially a large, oxygenated littoral area that could be colonised (the depth to anoxia in this lake was 37 m, 30th July 2006; **Chapter 4,** Table 4.4). If this diatom species is in fact a form of *Gomphonema* cf. *gracile*, then the species prefers a low nutrient content, evident in the contemporary setting of Kamunzuka (Patrick and Reimer, 1975). The persistent presence of *Gomphonema parvulum* in low quantities may attest to the low mineral content of this water (Gasse, 1986). However, recent studies show that during its life cycle, *G. gracile* can transform during asexual division into a morphology resembling *G. parvulum*. Therefore the presence of *G. parvulum* may just account for older specimens of *G. gracile* prior to sexual reproduction (E. Cox, NHM, *pers. comm*.).

The only minor perturbation that occurs in this lake is during the earliest phase of the record (*c.* AD 1830). There is a slight decrease in the relative abundance of *Gomphonema gracile* and a higher percentage of *Fragilaria tenera*, perhaps indicative of large inputs of very fresh or weakly acidic waters (van Dam *et al*., 1994; Wunsam, 1995; Wunsam *et al*., 1995; Hall and Smol, 1996; Kelly *et al*., 2005). The presence of *Aulacoseira granulata* throughout the record attests to the high silica and high light conditions in freshwater. For *Aulacoseira* species to occur there must be turbulence within the water column, to aid buoyancy and to keep the genus in suspension in the photic zone.

Worthy of note is the short lived period *c.* 1990 (boundary of Zone Km2 and Km3) where a teratological form of *Fragilaria tenera* exists, which may be indicative of increased heavy metal concentrations, perhaps as a result of catchment burning, or the inwash of volcanic catchment soils into the lake system (Cremer and Wagner, 2004).

There is coherence between the sedimentary data and the diatom data. It appears that the flux data and the diatom concentrations move in opposition; when organic and minerogenic flux is high, diatom concentrations tend to be low. The most obvious excursion, and relationship in the data occurs *c.* AD 1980-1995, where the organic and minerogenic flux records from Kamunzuka peak. This coincides with a large drop in the

concentrations of diatoms recorded in the sedimentary record. Following the peak in the flux data, the diatom concentrations reach their maximum.

It is likely that the increase in the flux of sedimentary material to the lake diluted the diatom concentrations. The subsequent increase in the diatom concentrations may be attributed to a diatom bloom caused by an increase in nutrient supply to the lake (as a result of the previous catchment in-wash).

7.3 Lake Nyungu

7.3.1 ^{210}Pb dating

The surface concentration at Nyungu is low (~390 Bq kg^{-1}). Though not an irregular record, Nyungu demonstrates a change of gradient at ~20 cm, most likely a result of a recent acceleration in the sedimentation rate (P.G. Appleby, *pers. comm.*). Equilibrium with the supporting ^{226}Ra occurs at around 25 cm and the highest ^{137}Cs concentration occurs in the 17.5-18.5 cm sample. This is in agreement with the position of 1963 as calculated using the CRS model, suggesting that this part of the core is from the early 1960s (P.G. Appleby, *pers. comm.*). Tentative radiometric dates were calculated using the CRS ^{210}Pb dating model (Appleby *et al*. 1978), and compared with the best estimate of the 1963 stratigraphic date suggested by the ^{137}Cs record. The age model for Lake Nyungu was constructed by the linear extrapolation between dated horizons (Figure 7.7).

7.3.2 Physical properties

The Nyungu sediments, prior to AD 1950, have a low organic content (LOI ~5%; Figure 7.8). After AD 1950, the sediments become organic-rich, with organic content generally at 30%, though the record of the last 50 years is punctuated by three low-organic events (where organic content falls to around *c.* 10%). The carbonate content of the sediment also mirrors the pattern of organic matter. Carbonate values in the earlier record (prior to AD 1950) are relatively stable at ~6%, but the carbonate content increases dramatically after this period to values of *c.* 15-30%. As would be expected, the minerogenic (non-carbonate residue) is high in the earlier part of the record (values *c.* 80%), and values decline after AD 1950 (50%). The observed troughs in the organic data are related to three peaks in the minerogenic fraction (centred on *c.* AD 1970, 1985 and 1995). The dry mass accumulation rate (DMAR) at Nyungu shows an interesting correlation with the minerogenic record. The DMAR is low prior to AD 1930 (21 cm), after which date the values double for a period of

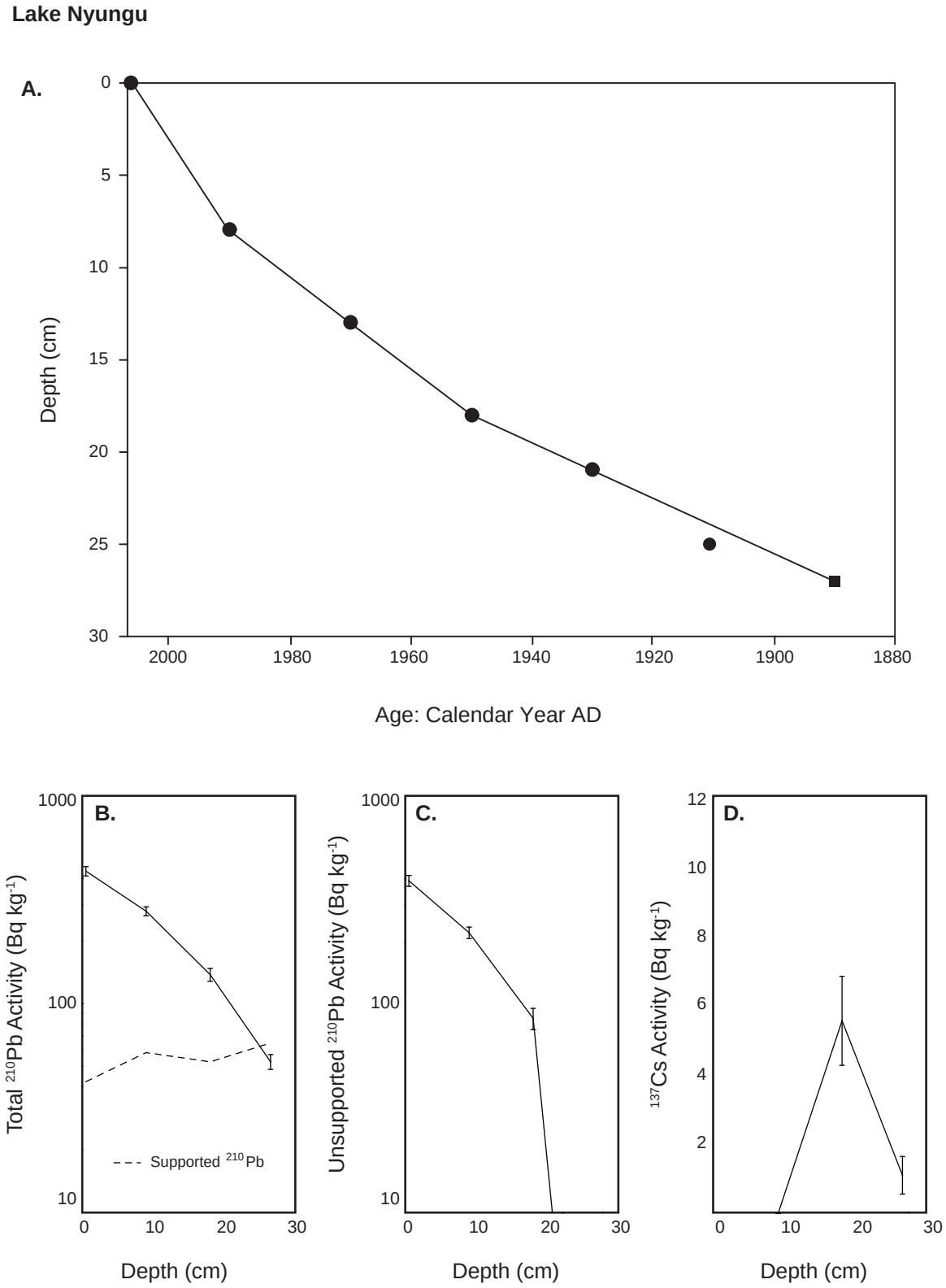

Figure 7.7 *^{210}Pb and ^{137}Cs data for Lake Nyungu.* **(A)** *^{210}Pb chronology for Nyungu (using linear extrapolation between the dated horizons). Filled circles represent actual dated horizons, the filled square is the base of the sequence, dated by linear extrapolation.* **(B-D)** *Fallout radionuclides in the Nyungu core showing* **(B)** *total and supported ^{210}Pb,* **(C)** *unsupported ^{210}Pb and* **(D)** *^{137}Cs concentrations versus depth.*

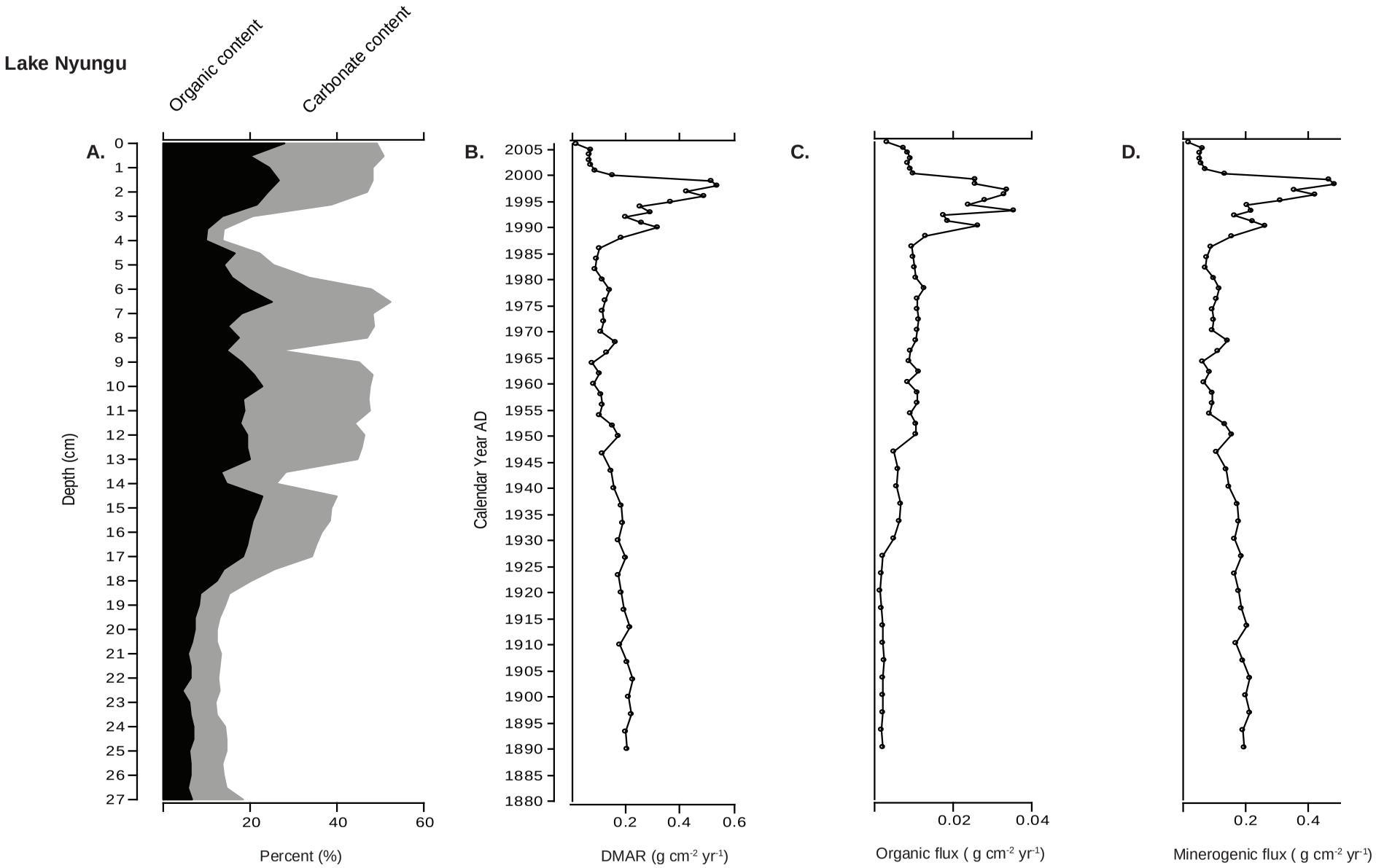

Figure 7.8 *Calculated flux data for Lake Nyungu.* **(A)** *Stacked organic and carbonate percentages versus core depth,* **(B)** *dry mass accumulation rate (DMAR) calculated using the dry bulk density and ^{210}Pb dates,* **(C)** *organic content displayed as flux (g cm^{-2} yr^{-1}) and* **(D)** *minerogenic flux (g cm^{-2} yr^{-1}). Graphs* **(B-D)** *are plotted against calendar year AD.*

c. 20 years. After *c.* 1950 (18 cm), the DMAR values are relatively stable until *c.* AD 1985 (9 cm), though one small peak is noted (13 cm; AD 1970). After 1985, there is a major excursion in the data, recognisable as a double peak in the DMAR, centered on AD 1990 (8 cm) and AD 2000 (*c.* 4 cm). These spikes are coincident with the peaks in the minerogenic record and the troughs in the organic and carbonate data.

The record of the dry mass accumulation, and hence the inferred organic and minerogenic fluxes at Nyungu can be divided in to distinct units, with the major change in DMAR occurring *c.* 1930. Prior to this date (between AD 1890 and 1930) the DMAR is high (0.2 g cm^2 yr^{-1}) showing a decreasing trend until *c.* AD 1945. Organic and minerogenic fluxes are low (*c.* 0.002 and 0.2 g cm^2 yr^{-1}, respectively) and stable. At 1945 the DMAR increases (0.17 g cm^2 yr^{-1}), as does the flux of the minerogenic matter. Following a peak in DMAR values in the early 1930s, DMAR drops to values *c.* 0.08 g cm^2 yr^{-1}. Further peaks in the DMAR record occur at *c.* 1970, 1990 and 2000, with the latter representing the largest excursion in the data (up to values of 0.53 g cm^2 yr^{-1}). The minerogenic flux follows a very similar pattern to the DMAR, with peaks in the data centered on AD 1970 (0.14 g cm^2 yr^{-1}), 1990 (0.26 g cm^2 yr^{-1}), *c.* 2000 (0.48.g cm^2 yr^{-1}). The organic flux at Nyungu bears some similarities to the DMAR record, however the peaks observed in the DMAR and minerogenic records prior to AD 1990 are less obvious in the organic record. A small peak in values occurs in the early 1930s, after which the flux of organic matter to the lake increases to *c.* 0.006 g cm^2 yr^{-1} and remains relatively stable until *c.* 1990 after which date values peak again (*c.* 0.02 g cm^2 yr^{-1}). Values remain high until the late 1990s, after which values decrease towards the present day.

The total diatom flux record from Lake Nyungu exhibits two distinct phases (Figure 7.9). Total diatom flux is generally low (< 40 x 10^6 valves cm^{-2} yr^{-1}) prior to AD 1950; although values are not as low as those recorded in Lakes Nyamogusingiri and Kyasanduka (<5 and <0.4 x 10^6 valves cm^{-2} yr^{-1}, respectively; **Chapter 6**, *sections 6.3.3* and *6.4.3*). There is a large increase in total diatom flux after AD 1950 to values up to a maximum of *c.* 310 x 10^6 valves cm^{-2} yr^{-1}. After AD 1965 total diatom flux declines towards the present (to values < 150 x 10^6 valves cm^{-2} yr^{-1}). The large increase in total diatom flux is driven primarily by the increase in the flux of *Gomphonema pumilum* and also *Diadesmis contenta*, *Hantzschia amphioxys* and *Encyonema muelleri* (*c.* 110, 8, 2.5 and 23 x 10^6 valves cm^{-2} yr^{-1}, respectively). The flux of these species declines towards the present, in most cases, relatively quickly (< 10 years) after the AD 1960 peak. More recently, peaks in the flux of benthic and aerophilous taxa (*c.* AD 1990 and 2000). The

Lake Nyungu

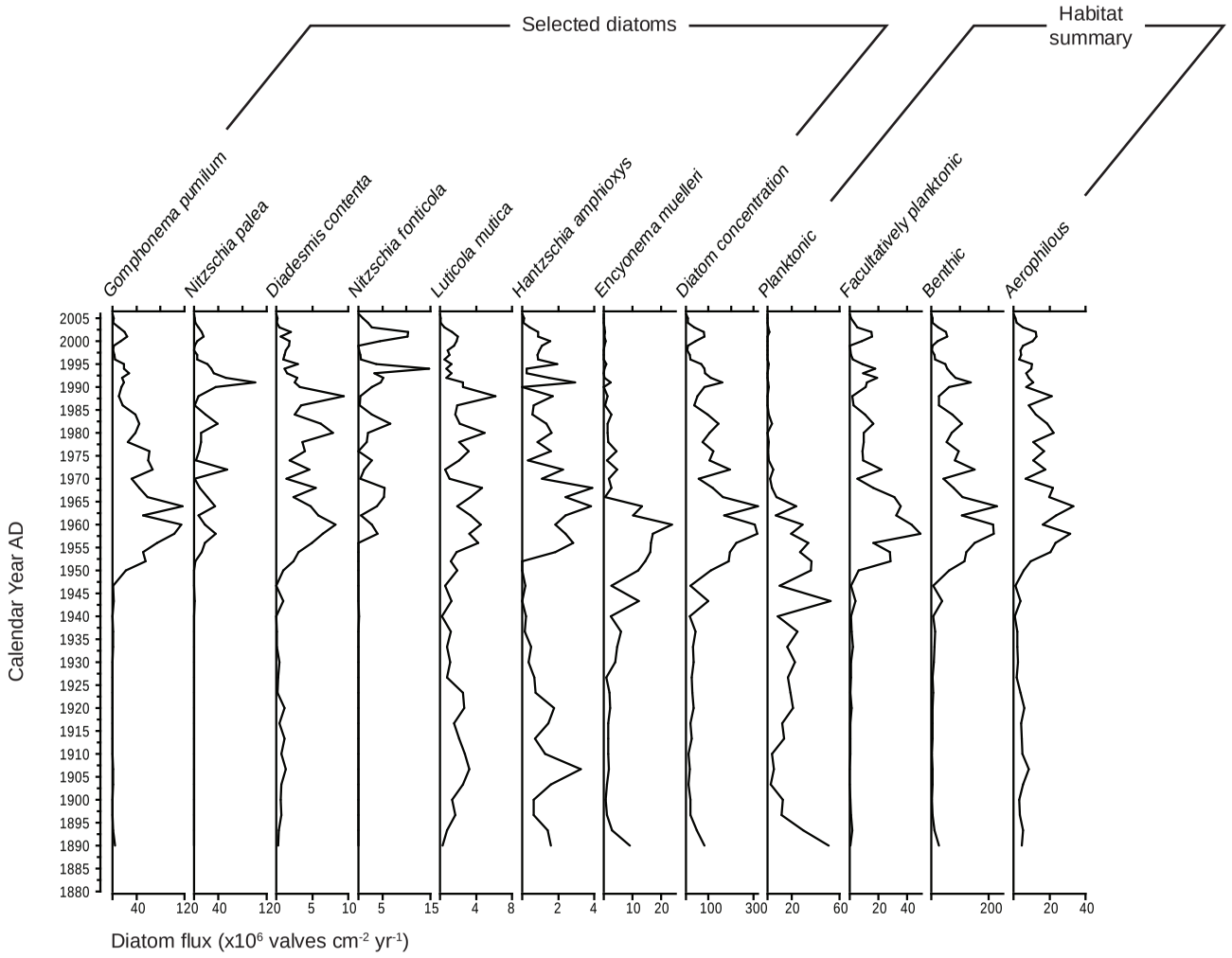

Figure 7.9 *Diatom flux for selected dominant taxa from Lake Nyungu displayed alongside the total diatom flux for each sample (left). The flux of diatoms within the habitat categories are also shown (right).*

peak *c.* AD 1990 is likely driven by the increase in the flux of *Nitzschia palea, Hantzschia amphioxys* and *Nitzschia fonticola,* and the latter peak (*c.* AD 2000) is driven by *N. fonticola, H. amphioxys* and *Luticola mutica*.

7.3.3 Diatom Analyses

The diatom record from Lake Nyungu is split into seven assemblage zones (Nu1-7; Figure 7.10). Samples were analysed at 0.5 cm intervals (55 samples) and 109 diatom species were identified. Habitat summaries are illustrated in Figure 7.11.

There are two distinct diatom assemblages in the Nyungu record. The earlier part of the core shows a record dominated by the species Nitzschia lancettula and a variety of benthic and epiphytic diatoms. At approximately AD 1950 (18 cm) the assemblage switches to one dominated by *Gomphonema pumilum* and *Nitzschia palea*.

Zone Nu1 (27-25 cm; AD 1890-1900) the earliest zone has an assemblage dominated by *Nitzschia lancettula* (60%). The littoral/benthic species *Amphora copulata, A. pediculus* and the epiphytic *Encyonema muelleri* are also present in this zone, though they do decrease in abundance towards the boundary with zone Ny2. Several aerophilous taxa (*Hantzschia amphyioxys, Luticola mutica* and *Diadesmis contenta*) are present in small quantities (~5%). Diatom preservation is good, but is comparatively low in this section of the core (**F**-index 0.6-0.8) and concentrations are extremely low (0.7-3 x 10^6 valves g^{-1}). A large number of testate amoeba scales were noted (>60), and the number increases from the bottom of the zone towards the boundary with Zone Nu2 (25-23.5 cm; AD 1900-1910). The main feature of the second zone is a large drop in the numbers of the planktonic *N. lancettula* (30%; values decrease by half in comparison to Ny1) at the beginning of the zone and a peak in the values of *H. amphioxys* (17%), *L. mutica* (22%) and *D. contenta* (7%). As in zone Ny1 *Amphora copulata, A. pediculus* and *Encyonema muelleri* are present in low quantities (<10%). The **F**-index in this zone is similar to that of Nu1 (*c.* 0.7) and once again the diatom concentrations are extremely low (0.5 x 10^6 valves g^{-1}). The testate amoeba: diatom ratio is this zone is high (*c.* 0.25) but tails off towards the top of the zone.

Zone Nu3 (23.5-17.5 cm; AD 1910-1950) is once again dominated by *N. lancettula,* which has its highest abundance in the record (*c.* 70%). After AD 1925 (21.5 cm) the values of *N. lancettula, H. amphioxys, L. mutica* and *D. contenta* appear to decline. This is coincident with a peak in the percentages of *A. copulata, A. pediculus* and *E. muelleri* as well as the appearance of *G. pumilum* (in very low percentages, *c.* 2%). The

preservation in this section of the core is still good (>0.6), but tends to fluctuate. Diatom concentrations are generally low and reflect the concentrations seen in the earlier zones, though the concentrations do increase towards the boundary with Nu4. Testate amoeba scales are present (counts >30). There are two small peaks in the testate amoeba: diatom ratio *c.* AD 1925 (22 cm) and *c.* AD 1930 (21 cm; 55 scales) before a small decline in numbers.

Zone Nu4 (17.5-8.5 cm; AD 1950-1990) marks the transition between the two distinct diatom assemblages. The former dominant species *N. lancettula* disappears relatively rapidly at the start of this zone and is replaced by an assemblage dominated by *Gomphonema pumilum* (~35%), *G. parvulum* (>5%), *Nitzschia palea* (>5%) and *N. amphibia* (>5%). There is also an appearance of *N. fonticola*, *N. bacata*, *Navicula cryptonella*, *Cymbella subalpina* and *Cocconeis placentula* v. *lineata*. *Amphora copulata*, *A. pediculus* and *Encyonema muelleri* decrease towards the top of this zone and *Luticola mutica* and *Diadesmis contenta* increase slightly, reaching their peak at the boundary with Nu5. The **F**-index fluctuates in this particular zone, with values oscillating backwards and forwards between *c.* 0.6 and 0.8. Diatom concentrations dramatically increase relative to the previous three zones. Again these values are highly variable (4-22 x 10^6 valves g^{-1}). The testate amoeba: diatom ratio starts off relatively low (*c.* 0.06), before increasing to maximum values (0.2-0.3) from AD 1970.

Nitzschia palea reaches its highest values in zone Nu5 (8.5-4 cm; AD 1990-2000), before gently declining towards the top of the zone. The peak in *N. palea* is followed by a peak in the values of the planktonic species *N. fonticola*. The high values of *N. palea* (AD 1990; 7.5 cm) are coincident with a reduction in *N. amphibia* and *Gomphonema pumilum*. *G. parvulum* maintain values of ~5% in this zone. *Amphora copulata* and *A. pediculus* disappear in this zone, and *E. muelleri* reduces to percentages of ~1%. *Nitzschia bacata* shows a small peak, which is coincident with the appearance and peak of the aerophythytic/benthic taxon *Amphora montana*. The preservation in this zone is higher than Nu4 (0.7-0.9) and diatom concentrations remain high (3-21 x 10^6 valves g^{-1}). The ratio of testate amoeba: diatoms declines from high (0.3) at the start of the zone, to low (0.13) towards boundary with Nu6.

Although Zone Nu6 (4-2 cm; AD 2000-2002) is a comparatively small zone, the excursion in the diatom data is a prominent feature in the upper section of the record. There is a sharp drop in the abundance of *Nitzschia palea* and *N. bacata* which is coincident with a small rise in *Gomphonema* cf. *gracile* and a spike in the taxa *Hantzschia*

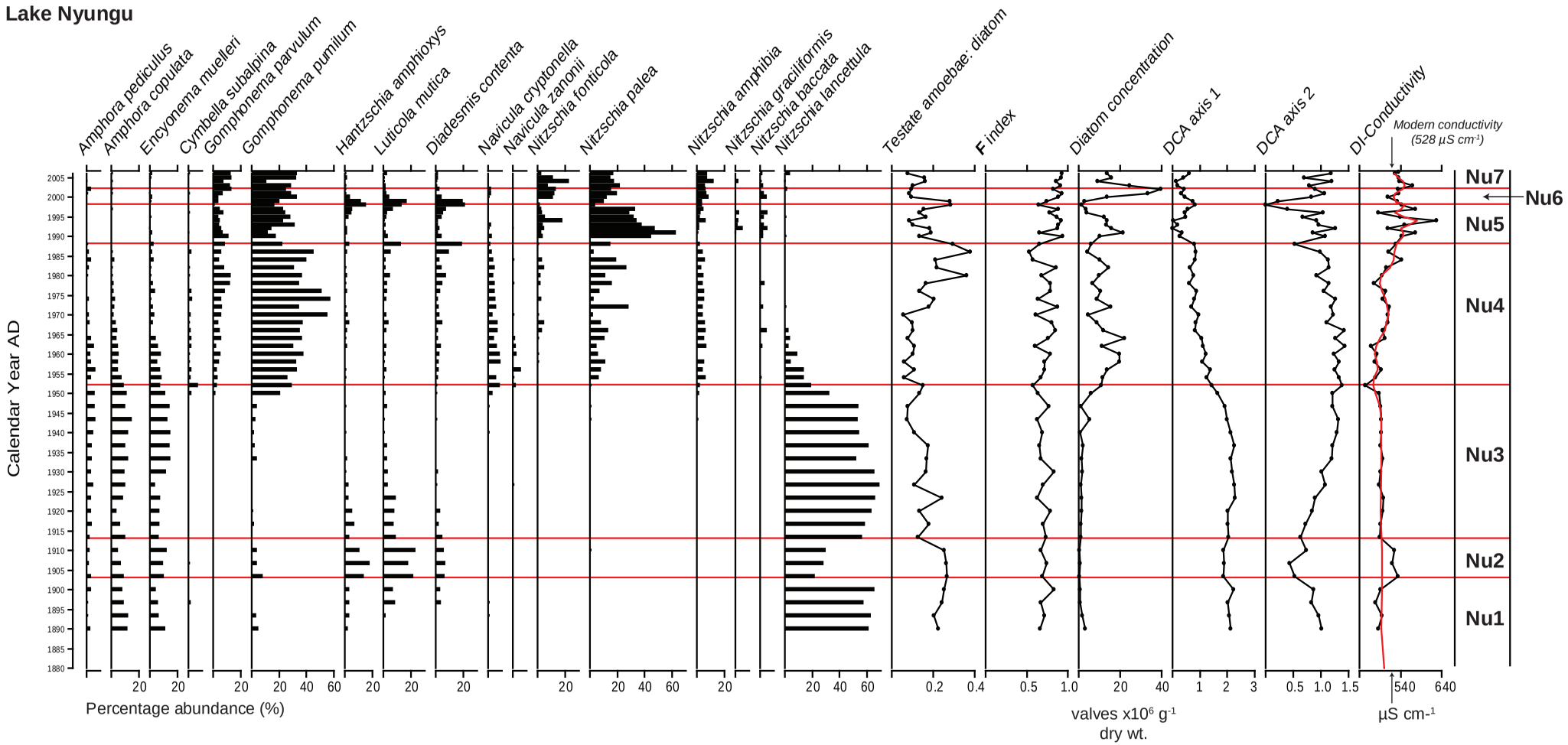

Figure 7.10 *Diatom stratigraphy from Lake Nyungu. All species > 5% in any one sample are displayed. The diatoms have been ordered according to their weighted average abundance in the core (ascending) and are split into assemblage zones Nu1-7. The ratio of testate amoebae scales to diatoms is displayed alongside the diatom preservation index (***F** *index), diatom concentrations and the axis 1 and axis 2 sample scores from Detrended Correspondence Analaysis (DCA; indirect ordination). Reconstructed conductivities are based on the crater lake transfer function (Combined_76; see* ***Chapter 5****), a smooth has been added to the reconstruction.*

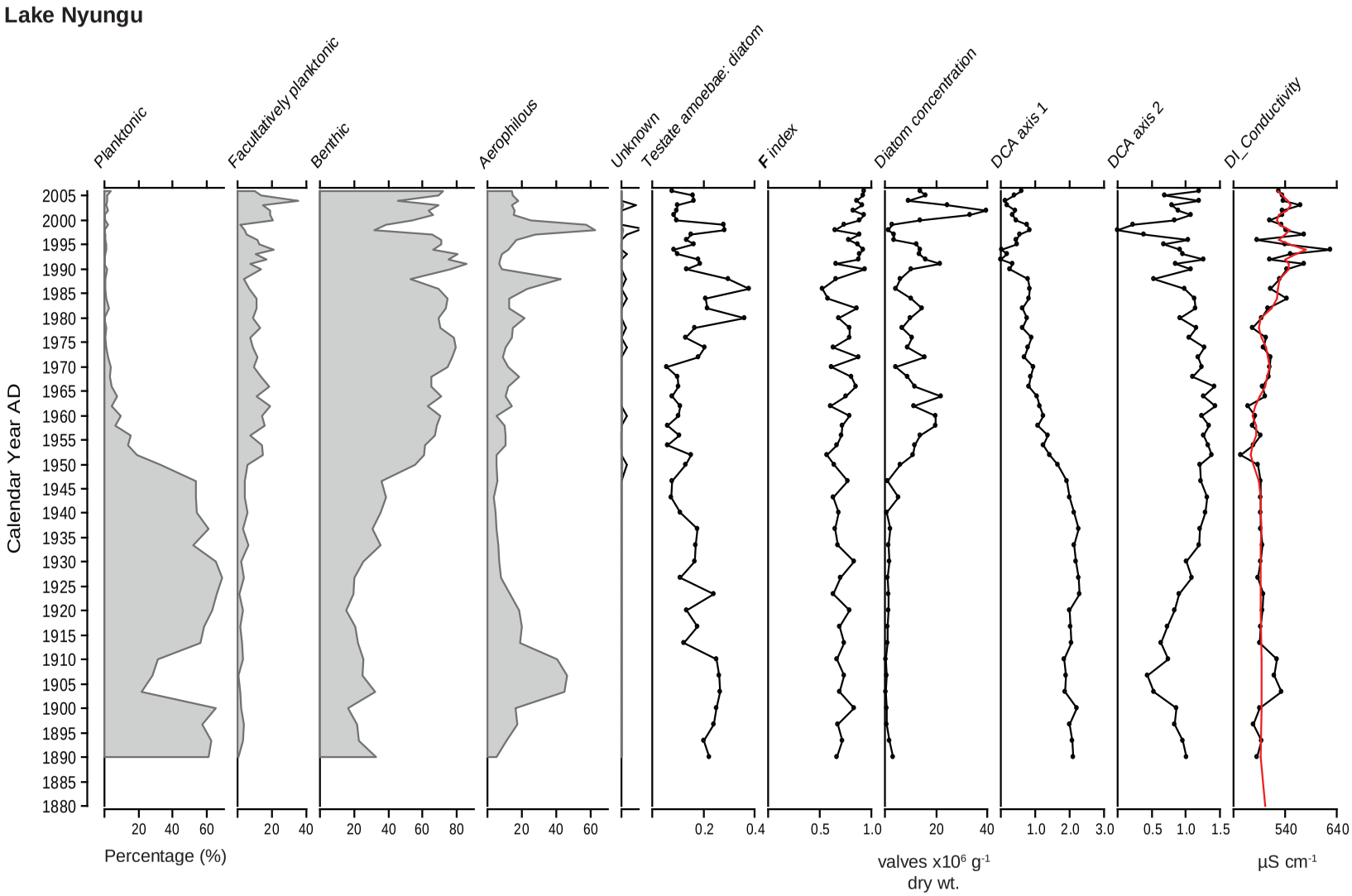

Figure 7.11 *Habitat summary of all diatom species from Lake Nyungu displayed alongside the ratio testate amoeba scales to diatoms, dissolution index (**F** index), diatom concentration, sample scores from DCA axes 1 and 2 and diatom-inferred conductivity.*

amphioxys, *Luticola mutica* and *Diadesmis contenta*. At this time, diatom preservation reduces (0.6) as does the diatom concentration (1.5 x 10^6 valves g^{-1}). There is also a peak in the number of testate amoeba scales recorded (ratio 0.3).

Zone Nu7 (2-0cm; AD 2002-2006), the uppermost assemblage consists of *Gomphonema pumilum*, *G. parvulum*, *Nitzschia palea*, *N. fonticola* and *N. amphibia*. There is a small reappearance of *N. lancettula* and the majority of benthic, epiphytic and aerophilous taxa which have been almost consistently present in the earlier record are absent from this zone (e.g. *Amphora copulata*, *A. pediculus*, *Encyonema muelleri*, *Hantzschia amphioxys*, *Luticola mutica* and *Diadesmis contenta*). The diatom preservation is excellent in these top samples (0.92) and diatom concentrations, although high (39 x 10^6 valves g^{-1}) at the boundary with Nu6, are particularly low towards the top of the record (9-15 x 10^6 valves g^{-1}). The number of testate amoeba scales decreases towards the present.

The diatom-inferred conductivity for Lake Nyungu shows some variation throughout its record, with an excursion in the data at *c.* AD 1900-1910 and large fluctuations occurring from AD 1950 to the present day. The earliest part of the record (zone Nu1; AD 1890-1900) indicates a freshwater lake with values not too dissimilar from the modern recorded conductivity at Lake Nyungu (Nu1 range: 475-530 µS cm^{-1}; modern value of 527 µS cm^{-1}). An excursion in the data, to a higher DI-conductivity, occurs at the transition between Nu1 and Nu2 (AD 1900). This period of higher conductivity lasts for *c.* 10 years, and exhibits conductivities of between 520 and 530 µS cm^{-1}. After AD 1900, and on the boundary of Nu2 and Nu3, reconstructed conductivity drops to *c.* 490 µS cm^{-1}. Throughout zone Nu3 (AD 1910-1950) the reconstructed conductivity is very stable (*c.* 490 µS cm^{-1}). Conductivity drops to its lowest recorded value just before the transition to zone Nu4 (450 µS cm^{-1}). Throughout zone Nu4, there is generally increasing trend in the reconstructed conductivity, though values do tend to fluctuate (range: 450-540 µS cm^{-1}), and there is a large dip in conductivity at AD 1975 (470 µS cm^{-1}); as highlighted by smooth applied to the reconstructed conductivity. The reconstructed conductivities fluctuate markedly in zone Nu5, with values between 485 and 630 µS cm^{-1} (the highest recorded value in this record). The smallest zone, Nu6, has a low reconstructed conductivity (*c.* 510 µS cm^{-1}; AD 2000), which increases to 570 µS cm^{-1} at the start of the most recent zone (Nu7), and then decreases towards the present day, where the modern reconstructed value (526 µS cm^{-1}) matches the measured conductivity (527 µS cm^{-1}).

Fossil data are very well covered by the crater lake conductivity model, with on average 97-100% of species abundance data included. Similarly, there are very good

analogues for most levels, with average minimum dissimilarity coefficients of 59, and no samples >103.

7.3.4 Indirect ordination – Detrended Correspondence Analysis (DCA)

DCA on all taxa >0.5% abundance (109) revealed a gradient of 2.290 S.D. units; therefore a unimodal response model was appropriate for further analysis. Correspondence Analysis (CA) indicated an arch in the data, thus DCA was deemed the most appropriate response model. A DCA plot of all the core samples and diatom species >5% are shown in Figure 7.12. Comparison to the broken stick model indicated that the four DCA axes were significant in explaining the variance in the diatom data (**Appendix B**), though axes 1 and 2 explained the majority of the variance in the dataset (36.4%). Eigenvalues for axes 1 and 2 are 0.341 and 0.077, respectively whereas those for axes 3 and 4 are only 0.04 and 0.03. The gradient represented by axis one appears to reflect the variation in the habitat preferences of the diatoms in the lake sediment sequences. The axis one sample scores are positively correlated to the abundance of planktonic species (r = 0.92) and negatively correlated to the abundance of benthic species (r = -0.82). These changes are predominantly driven by the abundances of *Gomphonema pumilum* (benthic) and the planktonic *Nitzschia lancettula*. Axis 2 appears to be negatively correlated with the presence of aerophilous taxa (r = -0.79*)*.

The DCA ordination diagrams (Figure 7.12) split the Nyungu core into three main zones: (i) the bottom samples (27-18.5 cm; AD 1890-1945); (ii) the middle core samples (18-9.5 cm; AD 1950-1985) and (iii) the upper core (9-0 cm; AD 1985-2006). The first group (i) is associated with the planktonic species *Nitzschia lancettula* and benthic species such as *Hantzschia amphioxys, Diadesmis contenta, Luticola mutica, Encyonema muelleri* and *Amphora copulata*. The second group (ii) is associated with *Gomphonema pumilum, G. parvulum* and *Nitzschia amphibia*. The division between the diatoms included in groups (ii) and (iii) is not overtly distinct, with many of the species overlapping (e.g. the *Gomphonema* spp.). However, a prominent feature of group (iii) is the dominance of benthic/facultatively planktonic *Nitzschia* species (*N. palea, N. fonticola* and *N. graciliformis*).

7.3.5 Interpretation of records from Lake Nyungu

The earliest phase (AD 1890-1950) generally suggests a period of deep, freshwater in Lake Nyungu. This deep water lake is characterised by the presence of *Nitzschia lancettula,* a

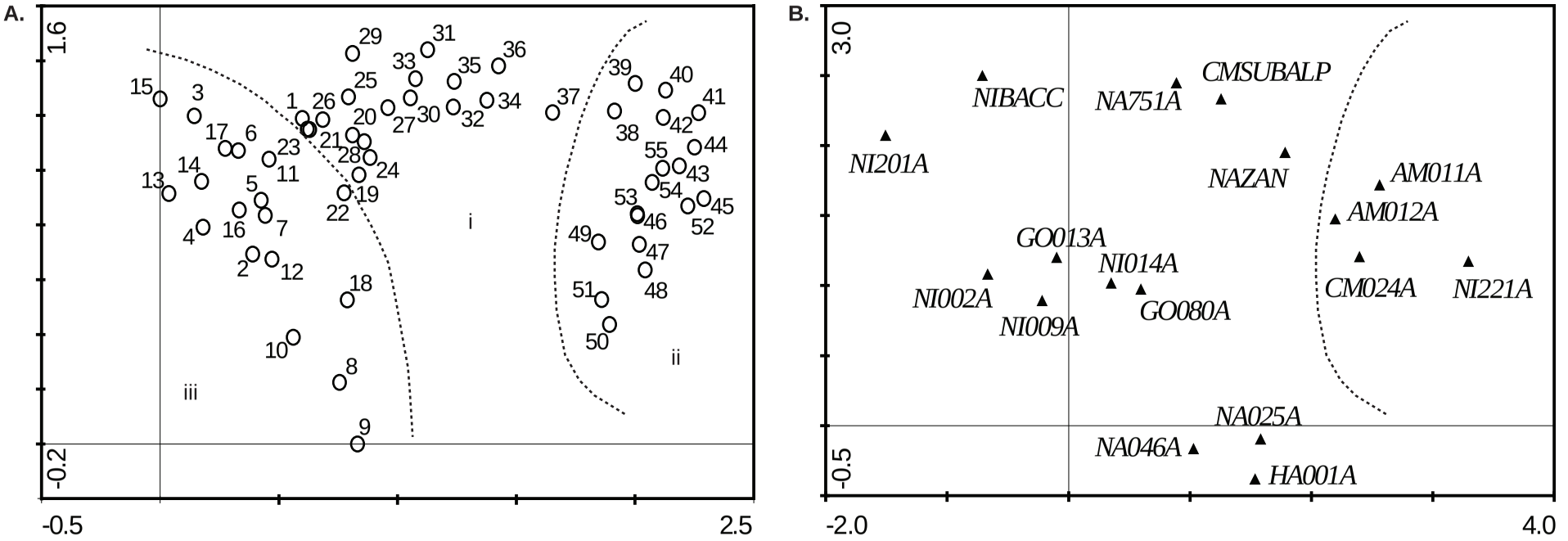

Figure 7.12 *Indirect ordination of diatom samples from Lake Nyungu. The Detrended Correspondence Analysis (DCA) of* **(A)** *samples (in depths, cm) and* **(B)** *species >5% are shown.*

species also present in Lake Victoria at times of inferred high-stands (Stager *et al*., 2005). During this period there is also evidence of well developed littoral vegetation around the lake shores, as suggested by the presence of *Encyonema muelleri* and the benthic *Amphora copulata*. The benthic/periphytic *Amphora pediculus* is also present. All of these species are indicative of low conductivity waters with a pH *c.* 8 (Gasse, 1986). This period is seemingly punctuated by a short-lived period of lower lake levels (*c.* AD 1910-1900). This lower lake level is denoted by a large drop in the abundance of *Nitzschia lancettula* and a rise in the abundance of aerophilous species (i.e. *Hantzschia amphioxys, Luticola mutica* and *Diadesmis contenta*).

A major switch in the diatom assemblage occurs at *c.* AD 1950. There is a sharp decline in the abundance of *Nitzschia lancettula*, alongside a reduction in the fresh water *Amphora copulata* and *Encyonema muelleri*; *N. lancettula* disappears from the record *c.* AD 1965. The reduction in the abundance of *E. muelleri*, may attest to the destabilisation of littoral vegetation. The original planktonic diatom assemblage is replaced by an assemblage dominated by benthic and periphytic species, most notably *Gomphonema pumilum*, although *Nitzschia palea* becomes increasingly important. The aerophilous species *H. amphioxys, L. mutica* and *D. contenta* are also consistently present throughout this zone. The presence of *Gomphonema pumilum* perhaps attests to lower oxygen content in the lake water than the earlier assemblage (Gasse, 1986). It may also be an indication of very little catchment disturbance or catchment stability in the middle part of the record (cf. Leira and Sabater, 2005), prior to the major peak in *Nitzschia lancettula* (*c.* AD 1990).

The increase and variation in the *Nitzschia palea* record from *c.* AD 1990 appears to be closely related to increases in the input of catchment sediments to the lake system (Sabater, 2000). *Nitzschia palea* is a polysaprobic species, thus a good indicator of waters with a heavy load of decomposed organic matter, with little or no free oxygen (Leland and Porter, 2000). In addition to this, *N. palea* is a nitrogen-heterotroph, requiring the presence of a nitrogen fixing host (e.g. cyanophytes such as microcystis; Cholnoky, 1968; Kilham *et al*., 1986). *Nitzschia palea* has the ability to harvest light energy in extremely turbid environments and is able to sustain a rapid population growth under such conditions (Leland *et al*., 2001), and is common in water bodies draining agricultural land (Leland and Porter, 2000) where it may be indicative of eutrophic/hyper-eutrophic conditions (van Dam *et al*., 1994). It is probable that this period in time marks the onset of catchment erosion, delivering sediments and nutrients to the lake and lowering the available oxygen content. If catchment inwash is the driver behind the observed changes, it is likely that the

induced turbid conditions caused the decline of the planktonic *Nitzschia lancettula*. Interestingly, the double peak in the sediment flux to the lake is also coincident with a double peak in the aerophilous taxa *Hantzschia amphioxys*, *Luticola mutica* and *Diadesmis contenta*.

The largest change in the diatom flora is coincident with a large increase in the sedimentary organic matter and precipitated carbonates; though the actual increase in the flux of organic and minerogenic sedimentary material predates these changes (flux begins to increase *c.* AD 1930). The shift in the organic content coincides with a change in the diatom flora from a planktonic dominated system (*Nitzschia lancettula*), to one dominated by benthic taxa (particularly *Gomphonema pumilum*) and an increase in the number of testate amoeba scales recorded. This change may be the result of lowering of lake levels or increased catchment in-wash causing more littoral diatoms to be washed into the lake basin. It is also worthy noting that the two largest peaks in the sedimentary flux data (*c.* AD 1990 and AD 2000) coincide with peaks in the number of aerophilous taxa recorded.

7.4 Lake Kako

7.4.1 ^{210}Pb dating

The record of ^{210}Pb fallout from Kako is not as good as other records in the area. Kako also lacks a subsurface peak in ^{137}Cs activity (Figure 7.13). Lake Kako has a very irregular ^{210}Pb record, although it has a similar surface activity (~382 Bq kg^{-1}) to Nyungu (~390 Bq kg^{-1}; P.G. Appleby, *pers. comm.*). Notably, there is a large reduction in concentrations at around 10 cm. Equilibrium with the supporting ^{226}Ra appears to occur at ~30 cm, though in view of the irregular record and high concentration at 22 cm it is impossible to say whether sediments at this depth date from the 19th century. The highest ^{137}Cs concentration occurs in the 21.5-22.5 cm sample; however there is no clear peak and it is therefore likely that all sediments above 23 cm are younger than 1960 (P.G. Appleby, *pers. comm.*). This is in turn supported by the ^{210}Pb dates which place 1963 at a depth of around 25 cm. Kako has the highest sedimentation rates of all lakes analysed. In the earlier part of the record sedimentation rates were ~0.1 g cm^{-2} yr^{-1}. Post-1970 the sedimentation rates increase to ~0.33-0.52 g cm^{-2} yr^{-1} (P.G. Appleby, *pers. comm.*). Tentative radiometric dates were calculated using the CRS ^{210}Pb dating model (Appleby *et al.* 1978), and compared with the best estimate of the 1963 stratigraphic date suggested by the ^{137}Cs record. The age model

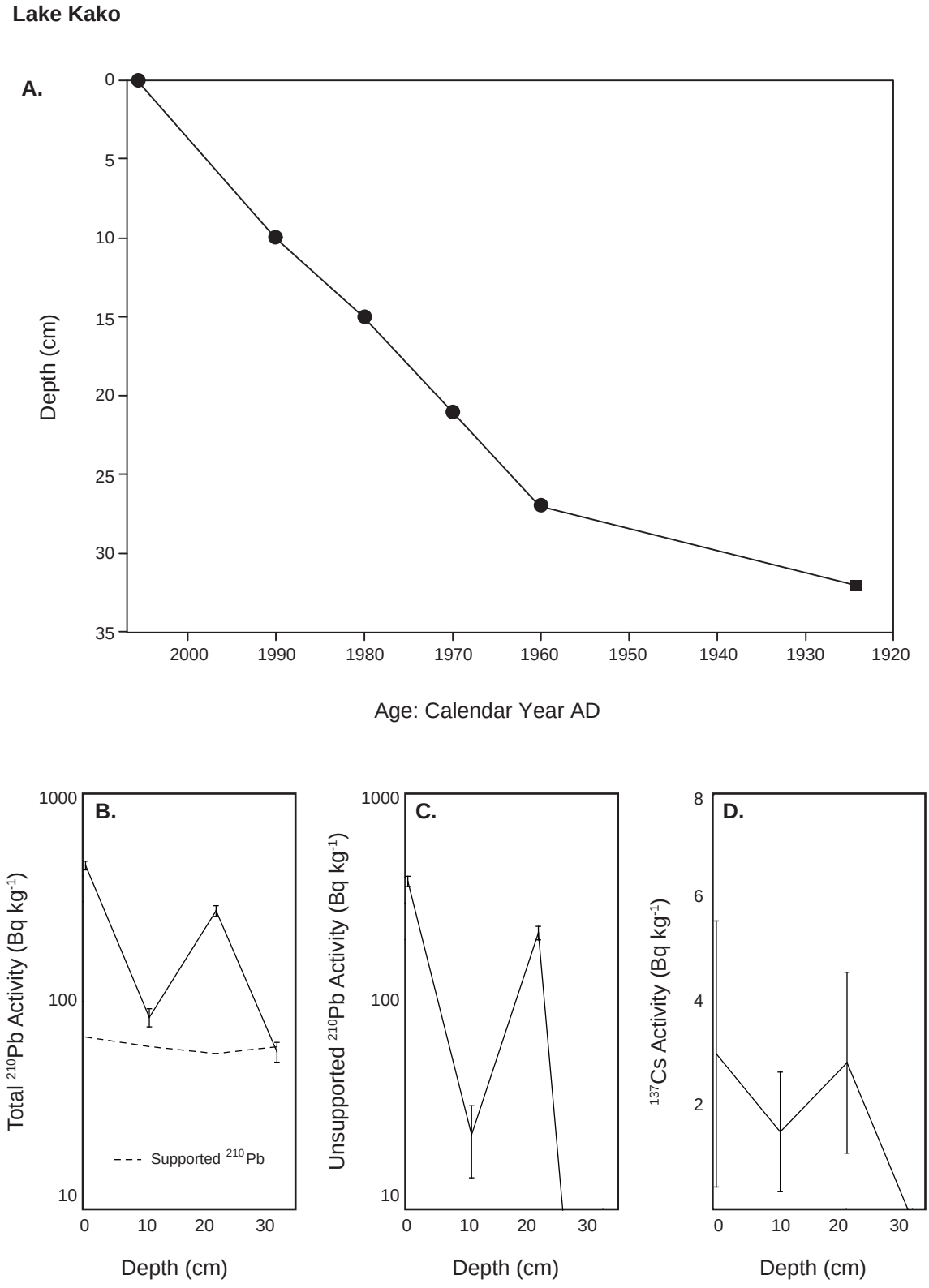

Figure 7.13 *^{210}Pb and ^{137}Cs data for Lake Kako.* **(A)** *^{210}Pb chronology for Kako (using linear extrapolation between the dated horizons). Filled circles represent actual dated horizons, the filled square is the base of the sequence, dated by linear extrapolation.* **(B-D)** *Fallout radionuclides in the Kako core showing* **(B)** *total and supported ^{210}Pb,* **(C)** *unsupported ^{210}Pb and* **(D)** *^{137}Cs concentrations versus depth.*

for Lake Kako was constructed by the linear extrapolation between dated horizons (Figure 7.13).

7.4.2 Physical properties

During the last 75 years covered by the Lake Kako sediments, the organic record has been relatively smooth and stable, with a general decreasing trend towards the present and no major excursions in the data (Figure 7.14). Prior to AD 1960, the organic content is in the region of 26%, and this decreases gradually over time to ~15% between AD 1965 and AD 1995. After 1995, there is a small dip in the organic content to ~8%, this event is short-lived (lasting <5 years). Following this brief period, values begin to rise to pre-1995 levels (*c.* 14%). In addition to the organic record, the carbonate data are extremely stable throughout the entire record with values of 2-3%, likewise the minerogenic residue is high and stable throughout the record (*c.* 70-80%), though a small peak in values (~88%) coincides with the small drop in the organic content. Conversely, the dry mass accumulation rate (DMAR) at Kako shows more variability over time. At the beginning of the record (32.5 cm; AD 1920), accumulation rates are low (0.05 g cm^2 yr^{-1}) and increase after AD 1955. The values continue to increase, reaching a peak in values at *c.* 15 cm (1980), the values remain high until the early 1980s when values decrease once more. The DMAR stabilises before increasing after AD 1990 (10 cm). A major excursion is evident at *c.* AD 1995 when the DMAR values reach their peak. Subsequently, DMAR values decline from AD 2000 (4 cm) to the present day.

Over its short time span (*c.* 75 years), the organic and minerogenic flux records from Kako show high variability and exhibit similar patterns. Prior to *c.* 27 cm (AD 1955) the organic an minerogenic flux is very stable, fluctuating around 0.08 g cm^2 $yr^{-1}$and 0.02 g cm^2 yr^{-1}). After AD 1960 there is a notable rise in the flux of both organic and minerogenic matter to the lake, which decreases at 15 cm (AD 1980). From AD 1980 the values decrease slightly before gently rising. A peak in the minerogenic flux is reached *c.* 1995 (6 cm), as is a peak in the organic flux, though the high organic flux values are reached slightly earlier than the peak in minerogenic material. A second smaller peak is seen in both the organic and minerogenic fluxes at *c.* 3 cm (AD 2000), after which the values all decline towards the present day.

The total diatom flux in the Lake Kako sediments steadily increases over time (Figure 7.15). The total diatom flux is low (< 20 x 10^6 valves cm^{-2} yr^{-1}) between AD 1950 and AD 1980 and increases towards the present with three peaks evident: AD 1985,

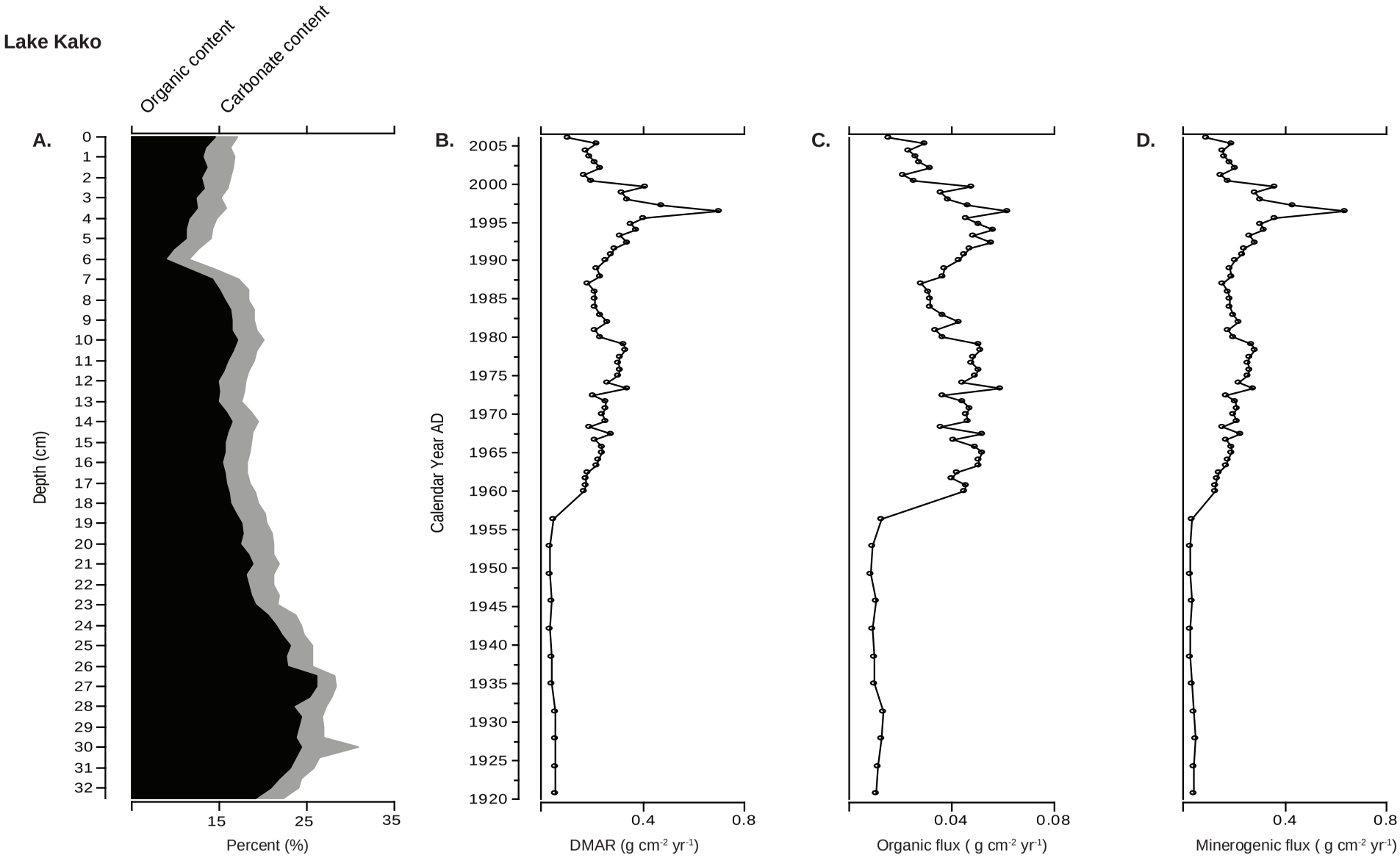

Figure 7.14 *Calculated flux data for Lake Kako.* **(A)** *Stacked organic and carbonate percentages versus core depth,* **(B)** *dry mass accumulation rate (DMAR) calculated using the dry bulk density and ^{210}Pb dates,* **(C)** *organic content displayed as flux (g cm^{-2} yr^{-1}) and* **(D)** *minerogenic flux (g cm^{-2} yr^{-1}). Graphs* **(B-D)** *are plotted against calendar year AD.*

Lake Kako

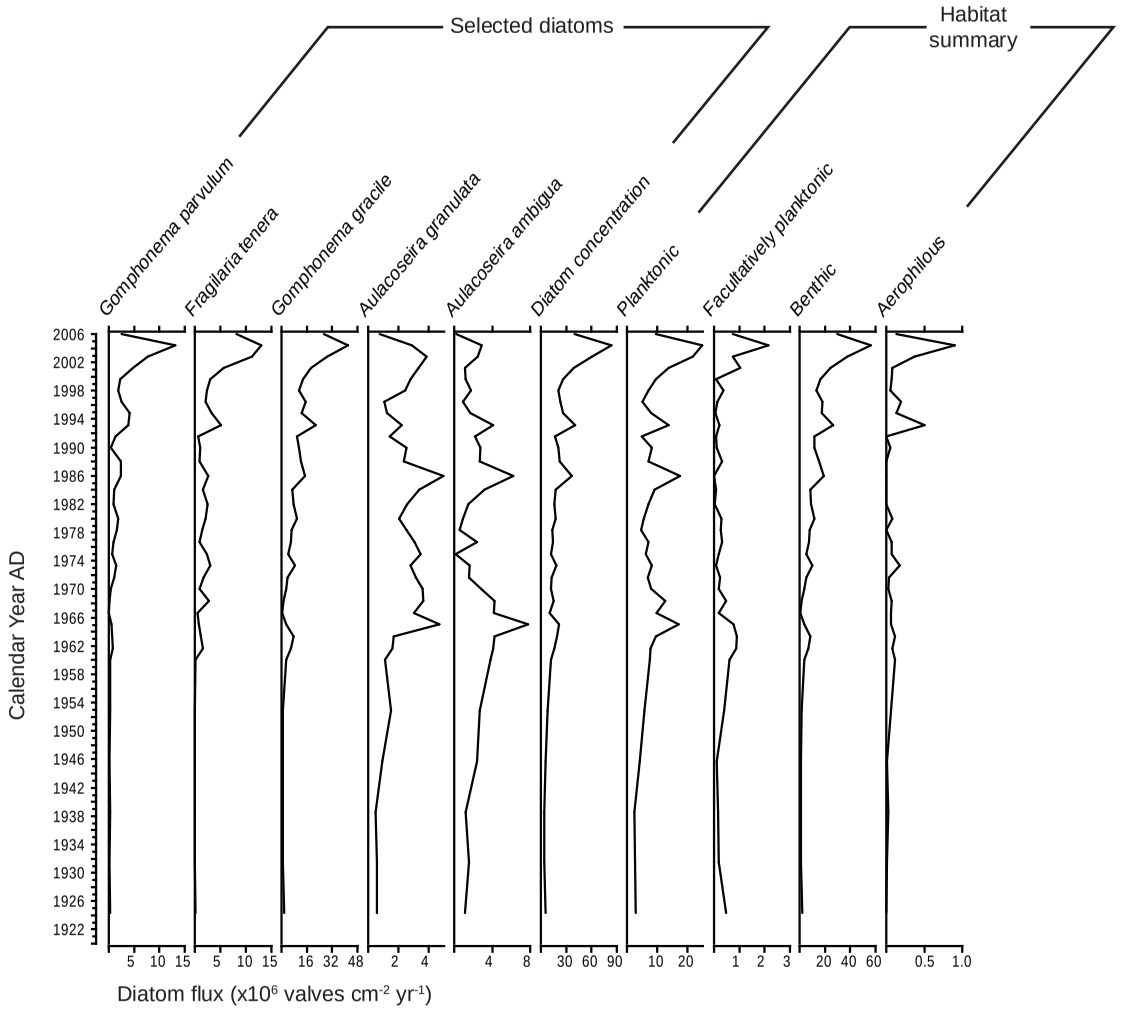

Figure 7.15 *Diatom flux for selected dominant taxa from Lake Kako displayed alongside the total diatom flux for each sample (left). The flux of diatoms within the habitat categories are also shown (right).*

AD 1990 and AD 2004 (*c.* 35, 40 and 80 x 10^6 valves cm^{-2} yr^{-1}, respectively). The earliest peak (AD 1985) is concomitant with a peak in the flux of planktonic taxa, driven by the abundance of the *Aulacoseira* species *A. ambigua* and *A. granulata* (*c.* 4 and 6 x 10^6 valves cm^{-2} yr^{-1}). The latter peaks are coincident with planktonic (*Fragilaria tenera*, *A. granulata* and *A. ambigua*) and benthic taxa (*Gomphonema* cf. *gracile*).

7.4.3 Diatom analyses

The diatom record from Lake Kako is shown in Figure 7.16 and habitat summaries in Figure 7.17. Thirty-three samples were analysed at 1 cm intervals and 70 species were recorded. The sediment record was divided into six assemblage zones (Kk1-6).

There are two distinct diatom assemblages apparent in the record from Kako. The earlier part of the record is an *Aulacoseira* dominated assemblage, at *c.* AD 1970 (21 cm) the assemblage switches to a one dominated by *Gomphonema*, *Fragilaria* and *Staurosira* spp. An interesting feature of this record is the apparent interaction between the epiphytic *G. gracile* and the pelagic *Aulacoseira* spp (*A. ambigua* and *A. granulata*), as one increases the other decreases in abundance. In addition to this, a similar pattern exists between *A. ambigua* and the number of testate amoeba scales recorded. The abundances of *A. granulata* also seem to co-vary with increases in the number of testate amoeba scales.

As with Lake Kamunzuka, in the *Gomphonema* dominated assemblage a form of *Gomphonema* cf. *gracile* is the dominant species, accounting for up to 60% of the total diatom counts in all samples since AD 1970. The diatom preservation within the core is generally good (**F**-index values between 0.7 and 0.95), though the values do fluctuate. The occurrence of testate amoeba scales in the Kako record is higher than Lake Kamunzuka, but again lower than at other sites.

Zone Kk1 (32-28 cm; AD 1920-1950). The earliest record indicates an assemblage increasingly dominated by various forms of *Aulacoseira ambigua* (20-40%) and *A. granulata* (10-20%), with a steady decrease in the abundance *Gomphonema* cf. *gracile* (30-13%). *G. parvulum* is continuously present with abundances of ~5%. *Staurosirella pinnata* v. *pinnata* and *Staurosira construens* v. *venter* are also present in this zone, but at very low abundances (~2%). Preservation is very high, and increases throughout the zone (**F**-index 0.87-0.97). Diatom concentrations are low (68-100 x 10^6 valves g^{-1}), but are average values for the entire record. The occurrence of testate amoeba scales is high (7) at the base of the sequence and the number recorded declines towards the top of the zone.

Zone Kk2 (28-25 cm; AD 1950-1960) sees a reverse of the trend seen in Zone Kk1. The abundance of *Gomphonema* cf. *gracile* starts to increase, and the relative abundances of *Aulacoseira ambigua* and *A. granulata* decline. *G. parvulum* is still present at low abundances, as in the previous zone. The appearance of *Fragilaria delicatissima* occurs towards the top of this zone (26 cm; AD 1960). Again preservation is good and diatom concentrations are similar to the previous zone. The number of testate amoeba scales recorded declines to around 1 per sample

The assemblage of zone Kk3 (25-21 cm; AD 1960-1970), is similar to that of Kk1, with the assemblage becoming increasingly dominated by *A. ambigua* and its varieties and *A. granulata* until AD 1965 (23 cm) when the abundance of these species starts to reduce. The percentage of *Gomphonema* cf. *gracile* falls dramatically in this zone, reaching its lowest percentage in the entire record (~ 3%). Preservation is exceptionally high (0.96) and diatom concentrations are low (50-90 x 10^6 valves g^{-1}) within this zone. The occurrence of testate amoeba scales also begins to increases through this zone, reaching a maximum in Zone Kk4 (21-12 cm; AD 1970-1985) at AD 1975. This peak in testate amoeba values (AD 1975) is coincident with a short-lived drop in many of the taxa (*A. ambigua*, *G.* cf. *gracile* and *F. tenera*) and a slight increase in *A. granulata*. This zone generally sees the waxing and waning of *Aulacoseira ambigua* and *A. granulata* and the simultaneous decreases and increases of *G.* cf. *gracile*. *Fragilaria tenera* becomes important during this period, reaching abundances of ~20%. Towards the top of this zone *G. gracile* is the dominating species, but its abundance is slightly lower as *A. ambigua* and *A. granulata* increase very slightly. Diatom preservation is relatively poor in this section of the core, however, in terms of its calculated **F**-index, the values are still high (*c.* 0.8). Diatom concentrations are also low, but are relatively stable at ~50 x 10^6 valves g^{-1}.

Zone Kk5 (12-8 cm; AD 1985-1990), the abundance of *G. gracile* remains high (~55%) throughout this zone, and *G. parvulum* is again consistently present. *Aulacoseira ambigua* and *A. granulata* are still present in this zone at abundances of *c.* 12%, and decline upwards into zone Kk6. *Fragilaria tenera* is still present but in lower quantities than the previous and proceeding zones (~5%) and a deformed ('bendy') version of *F. tenera* appears in this zone at *c.* AD 1990 (10 cm). Preservation is good (0.75-0.83) and the diatom concentration is *c.* 55 x 10^6 valves g^{-1}. Testate amoeba scale counts are low at the start of this zone (1) and increase towards the top (7).

Zone Kk6 (0-8 cm; AD 1990-2006) the most recent zone is dominated by the species of *G.* cf. *gracile* (*c.* 50%), *F. tenera* (*c.* 15%; >20% when amalgamated with its

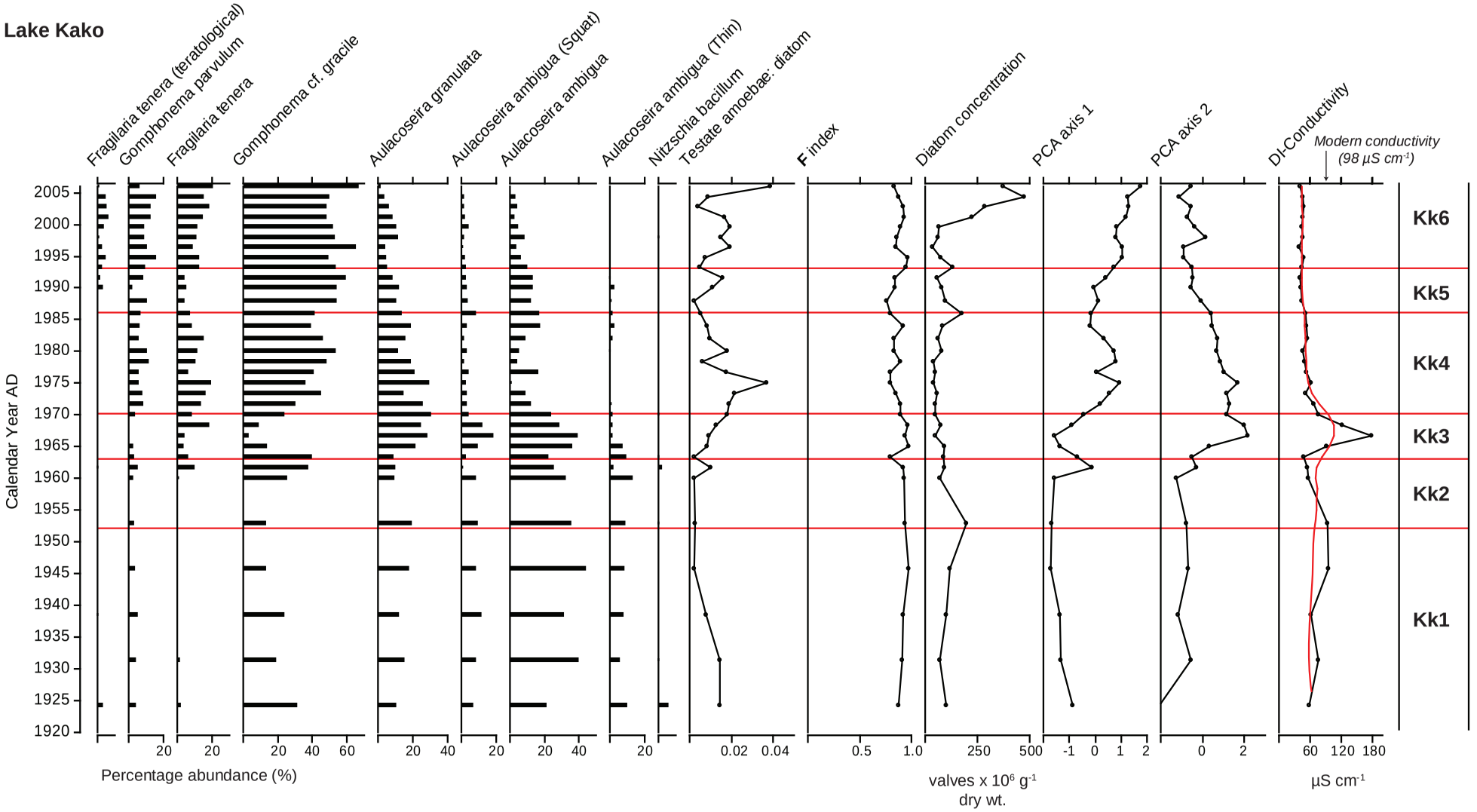

Figure 7.16 *Diatom stratigraphy from Lake Kako. All species > 5% in any one sample are displayed. The diatoms have been ordered according to their weighted average abundance in the core (ascending) and are split into assemblage zones Kk1-6. The ratio of testate amoebae scales to diatoms is displayed alongside the diatom preservation index (**F** index), diatom concentrations and the axis 1 and axis 2 sample scores from Principal Components Analaysis (PCA). Reconstructed conductivities are based on the crater lake transfer function (Combined_76; see **Chapter 5**), a smooth has been added to the reconstruction.*

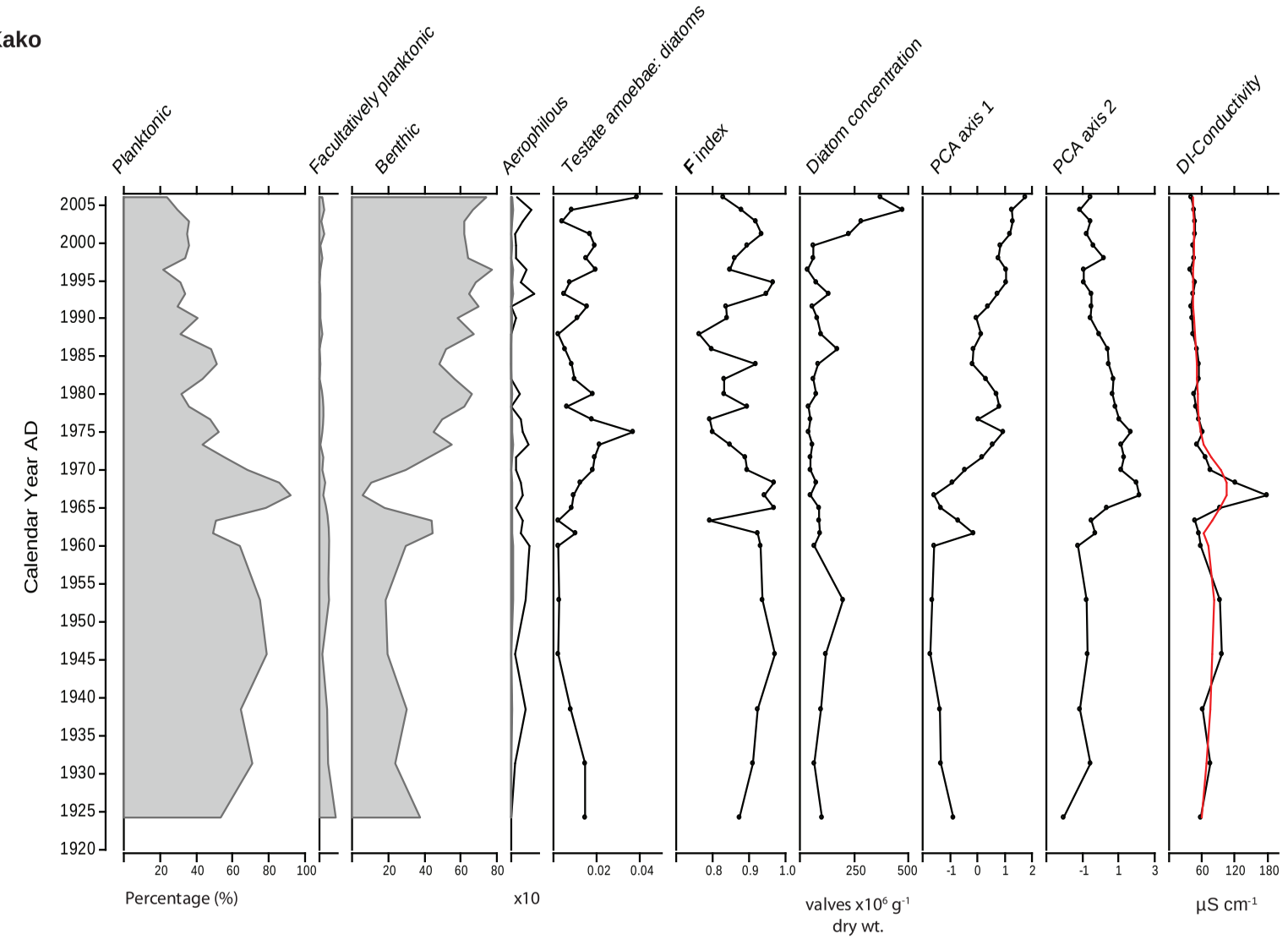

Figure 7.17 *Habitat summary of all diatom species from lake Kako (NB aerophilous taxa are displayed with an exaggeration multiplier of x10) displayed alongside the ratio of testate amoebae scales: diatom valves, dissolution index (**F** index), diatom concentration, sample scores from PCA axes 1 and 2 and diatom-inferred conductivity.*

deformed variety) and *G. parvulum* (*c.* 10%). The presence of *A. ambigua* and *A. granulata*, although fluctuating, is low (<10%) in comparison to previous zones. The diatom dissolution in this zone is low (**F**-index 0.8-0.9) and diatom concentrations range from 33 x 10^6 valves g^{-1} to almost 500 x 10^6 valves g^{-1} (the highest concentration values in the record). The number of testate amoeba recorded also increases in this zone, with occurrences of 8 per sample, and a maximum number of 23 recorded in the surface sediment (1-0 cm; 2006).

In the earliest part of the record (AD 1920-1950; Kk1), diatom-inferred conductivity fluctuates around the modern recorded conductivity at Lake Kako (60-100 µS cm^{-1}; modern conductivity is 98 µS cm^{-1}). The inferred conductivity decreases after 1950 (start of zone Kk2) to values <50 µS cm^{-1} and remains stable until *c.* AD 1960 (zone Kk3) when the conductivity dramatically increases to its highest reconstructed values. The reconstructed conductivity reaches a maximum of *c.* 180 µS cm^{-1} at AD 1965. After AD 1965 the diatom-inferred conductivity drops, reaching pre-1965 values of *c.* 65 µS cm^{-1} at AD 1970 (zone Kk4). The reconstructed conductivity remains stable throughout the remainder of the record (AD 1970-2006; zones Kk4-Kk6) at values of *c.* 40-50 µS cm^{-1}. The surface sediment is reconstructed at 40 µS cm^{-1}, half the value of the modern recorded conductivity.

Fossil data are relatively well covered by the crater lake conductivity model, with on average 78-98% of species abundance data included. Similarly, there are very good analogues for most levels, with average minimum dissimilarity coefficients of 34, and no samples >48.

7.4.4 Indirect ordination – Principal Components Analysis (PCA)

A PCA plot of all the core samples and diatom species >5% are shown in Figure 7.18. The eigenvalue for axis 1 is 0.532, whereas those for axes 2, 3 and 4 are only 0.142, 0.063 and 0.05, respectively. The first axis therefore captures around 53% of the variation in the diatom data set. The gradient represented by axis one appears to reflect the variation in the habitat preferences of the diatoms in the lake sediment sequences. The axis one sample scores are strongly positively correlated to the abundance of benthic species (r = 0.84) and strongly negatively correlated to the abundance of planktonic species (r = -0.87). These changes are predominantly driven by the abundances of *Gomphonema* cf. *gracile* (benthic) and the planktonic *Aulacoseira ambigua* and *A. granulata*.

The PCA ordination diagrams show a split in the data (i and ii on Figure 7.18), with the bottom samples from the core (32-21 cm; AD 1920-1970) dominating the left side of the diagram and the upper samples (21-0 cm; AD 1970-2006) dominating the right side of the diagram (Figure 7.18). The samples from the lower parts of the core are mostly associated with planktonic species (*Aulacoseira* spp. and *Nitzschia bacillum*); the uppermost samples are related to the periphytic/benthic species *Gomphonema* cf. *gracile* and *G. parvulum*, although the planktonic Fragilaria tenera (in both its normal and 'bendy' form) is also related to the uppermost samples.

7.4.5 Interpretation of records from Lake Kako

The earliest phase in Lake Kako (AD 1920-1965) is indicative of a well-mixed deep lake, becoming increasingly dominated by *Aulacoseira ambigua* and a thin, elongate form of *A. ambigua*. The high abundances of *Aulacoseira* suggests a system with a high availability of Si (Kilham and Kilham, 1975; Kilham *et al*., 1986) and nutrients (Barker *et al*., 2003). *Aulacoseira granulata* is also present continuously throughout the zone, indicating a well mixed lake. The continuous presence of the planktonic *Fragilaria tenera* throughout the majority of the record is indicative of low nutrient conditions (van Dam *et al*., 1994; Wunsam, 1995; Wunsam *et al*., 1995; Hall and Smol, 1996; Kelly *et al*., 2005). *Fragilaria tenera* is indicative of oligotrophic water, and often tolerant of mild pollution.

A form of *Gomphonema* cf. *gracile* (similar to that observed in Lake Kamunzuka; **Appendix E**, **Plate 4**) is also present in high abundances, attesting to the presence of submerged aquatic vegetation or shallow littoral areas in a very freshwater lake with, in the main, a very gently sloping catchment. This deep, clear, freshwater phase lasts for *c.* 40 years, before a rapid transition to more shallow, turbid waters causing a decline in *Aulacoseira ambigua* (AD 1965-1975) and an increase in *Aulacoseira granulata*. This transition is also marked by a sharp drop in the presence of the very freshwater species *G.* cf. *gracile* (AD 1965), after which this taxon steadily increases. The increasing abundance of *A. granulata* perhaps represents a short-lived period of lower lake levels, resulting in increased conductivity and turbidity. The disappearance of the very freshwater *G.* cf. *gracile* perhaps attests to this conductivity rise, or these changes may have caused a reduction in the available habitats for *G.* cf. *gracile* (e.g. lowered light levels may have prevented the growth of submerged aquatic vegetation). The taxon *Aulacoseira granulata* has low light requirements and is often indicative of eutrophic conditions, perhaps suggesting a period of increased nutrient inwash as a result of catchment disturbance.

Lake Kako

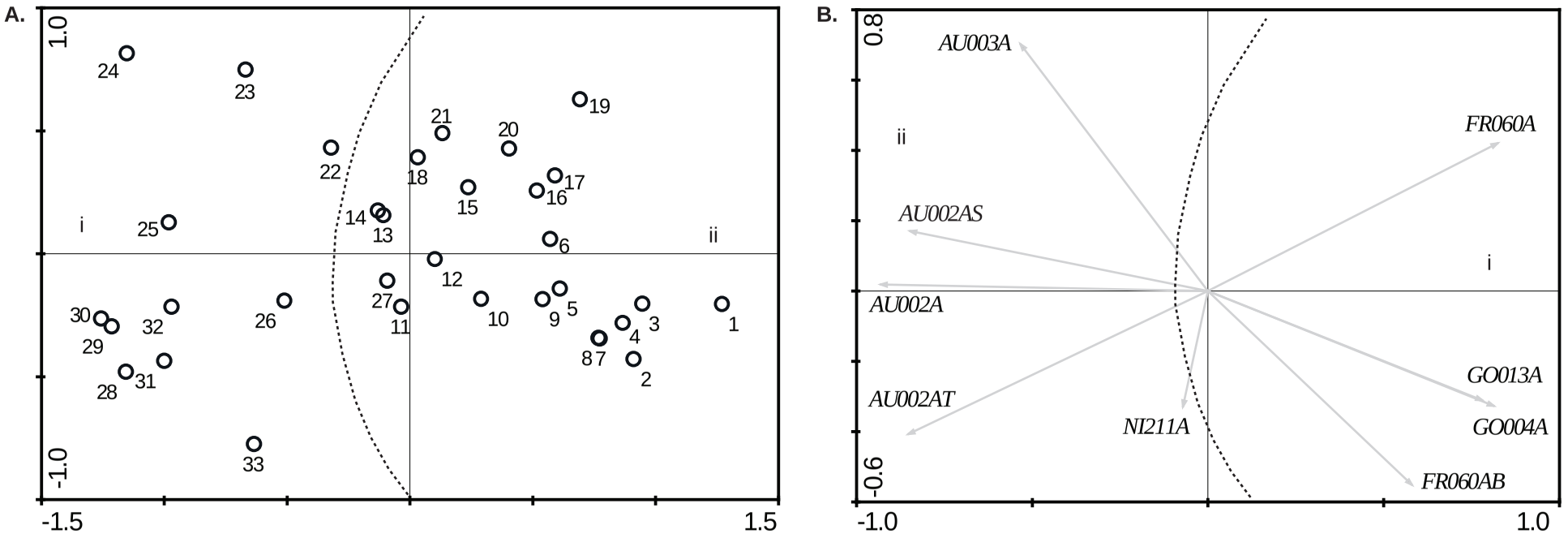

Figure 7.18 *Indirect ordination of diatom samples from Lake Kako. The Principal Components Analysis (PCA) of* **(A)** *samples (in depths, cm) and* **(B)** *species >5% are shown.*

Furthermore, *A. granulata* is generally a poor competitor for Si and requires high concentrations (Kilham *et al*, 1986), however, an increase in lake turbidity causing a reduction in *A. ambigua* (which requires high light conditions; Kilham *et al*., 1986), would allow *A. granulata* to become more competitive for Si and therefore the more dominant taxon. After *c.* AD 1975 *Aulacoseira granulata* declines, suggesting that the lake water is less turbid than the previous phase, allowing an increase in *A. ambigua* (AD 1975-1990). *Gomphonema* cf. *gracile* is the most dominant taxa in conjunction with a continuous presence of *G. parvulum* (abundances of *c.* 10%), almost certainly suggesting a return to fresher conditions.

All *Aulacoseira* species decline towards the present, though *A. granulata* does peak slightly *c.* AD 2000. In recent times *Gomphonema* cf. *gracile*, *G. parvulum* and *Fragilaria tenera* are the most dominant species, suggesting an extremely freshwater, oligotrophic lake, which is in accordance with the modern conductivity (98 $\mu S\ cm^{-1}$) and the calculated Carlson's TSI which places Kako as an oligo- to meso-trophic lake (see **Chapter 4**, Table 4.11). Interestingly, as in Lake Kamunzuka, during the last 10 years *Fragilaria tenera* is present in two morphotypes; the "normal shaped" type and a teratological ('abnormal shape') valve (**Appendix E**, **Plate 2**).

There appears to be an inverse relationship between the sedimentary flux to the lake and the diatom concentrations (perhaps as a result of dilution). Similarly there is a relationship between the abundance of aerophilous species noted in the core and the influx of sedimentary matter to the lake. This is particularly noticeable between AD 1980 and AD 1990 when organic and minerogenic matter entering the lake appears to decrease; aerophilous taxa also disappear from the record. These changes are also mirrored in the testate amoeba record. The largest shift in the diatom record occurs at *c.* AD 1965 when planktonic diatoms decrease and benthic diatoms increase, though there is no sedimentary evidence that accounts for this change. The 1960s was a particularly wet decade in Uganda (KNMI; Royal Netherlands Meteorological Institute, 2008), and the increase and subsequent decrease of planktonic species may be attributable to increasing lake levels, particularly given the dominance of *Aulacoseira ambigua* in the early part of the record. This peak in *Aulacoseira* is coincident with a decrease in the epiphytic *Gomphonema* cf. *gracile*, which may indicate a reduction in the area available for the growth of aquatic macrophytes, as a result of increasing lake level. In turn, the subsequent increase in the number of benthic species (post-AD 1965) may be related to a lowering of the lake level, increasing the area available for macrophyte growth and higher light attenuation around the

margins of the lake; this is certainly possible given the shallow gradient of the Kako catchment and basin.

7.5 Lake Mafura

7.5.1 ^{210}Pb dating

The ^{210}Pb record in the Mafura core is very similar to that of Lake Kamunzuka (Figure 7.19). There is a high surface concentration (~1700 Bq kg^{-1}) and a regular decline with depth, though the ^{210}Pb/^{226}Ra equilibrium is shallow (at ~25 cm) suggesting lower accumulation rates (P.G. Appleby, *pers. comm.*). The highest ^{137}Cs concentration occurs in the 8.5-9.5 cm sample. Since ^{210}Pb dates calculated using the CRS model place 1963 at a depth of 9-10 cm, sediments from around this depth almost certainly date from the early 1960s (P.G. Appleby, *pers. comm.*). Tentative radiometric dates were calculated using the CRS ^{210}Pb dating model (Appleby *et al*. 1978), and compared with the best estimate of the 1963 stratigraphic date suggested by the ^{137}Cs record.

7.5.2 Physical properties

Lake Mafura has an irregular organic content profile over the last 130 years. The sediment record is very organic-rich in places, reaching values of *c.* 60% (Figure 7.20). There are three large peaks in the organic data; these are centred on AD 1865 (~21 cm), AD 1940 (12 cm) and in the upper, most recent sediments (*c.* AD 2000; ~1 cm). Each peak is separated by a drop in the organic content (to values *c.* 10%), and these occur at AD 1890 (~17.5 cm) and AD 1980 (6 cm). The transition between these peaks and troughs is relatively smooth; they do not appear to be abrupt in any instance. Conversely, the carbonate record is relatively stable; the majority of the record has values of ~4%. There are a number of small excursions in the data, notably at AD 1830 (~26 cm) and AD 1880 (~18.5 cm). The minerogenic values also fluctuate throughout the record, though the values are not as variable as those in the organic record. The values in the earliest part of the record are high (>70%), and dip slightly at AD 1860, coincident with a peak in organic content. At *c.* AD 1890 minerogenic values decrease, reaching a minima at AD 1950 (LOI peak). The values increase to their highest at AD 1975 (~85%; coincides with a drop in the organic content), before decreasing towards the present day values (40%).

The dry mass accumulation rates (DMAR) at Mafura show several large excursions, occurring at 27 cm (AD 1820), *c.* 18 cm (AD 1885), *c.* 10 cm (AD 1960) and

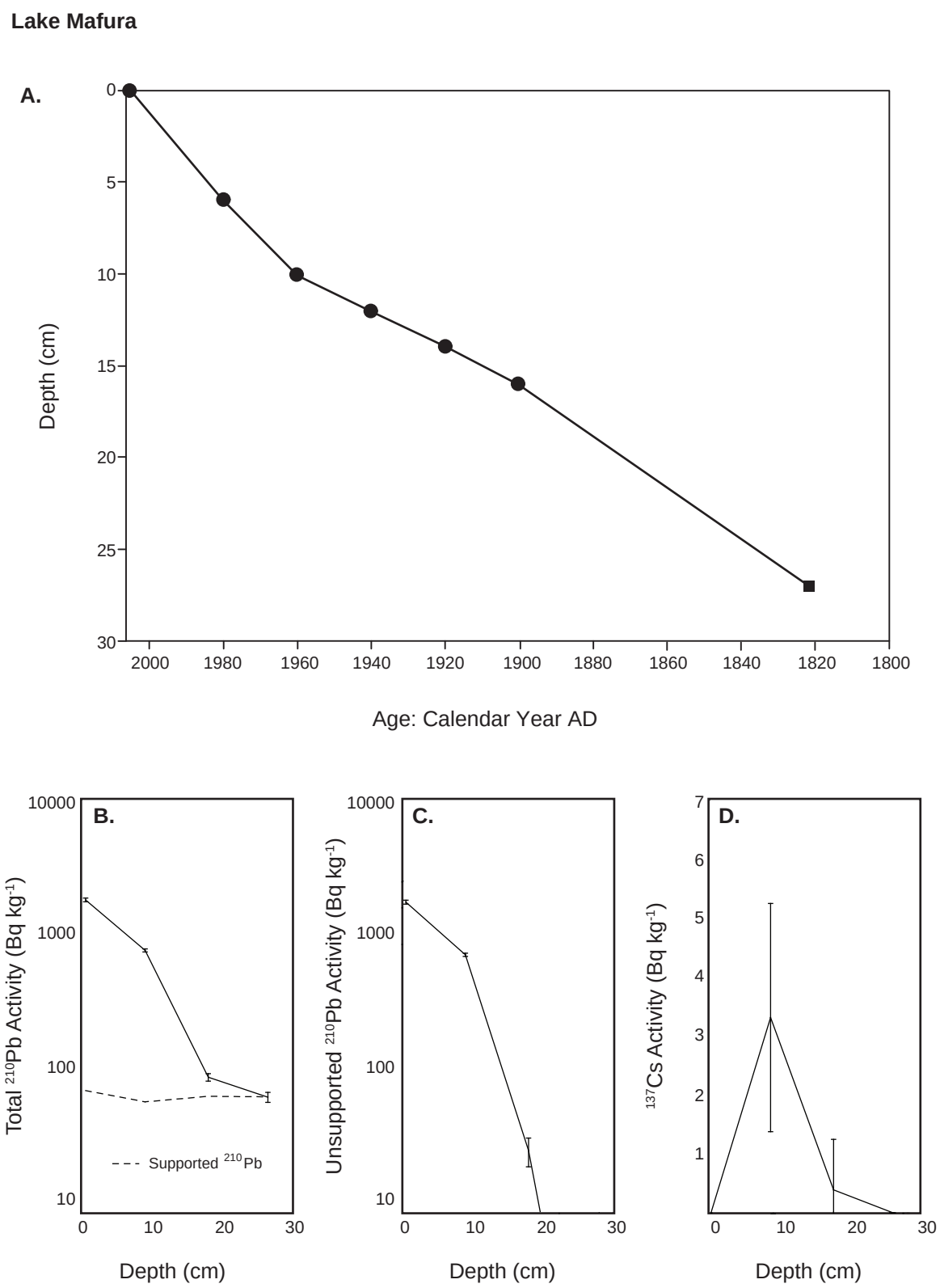

Figure 7.19 *^{210}Pb and ^{137}Cs data for Lake Mafura.* **(A)** *^{210}Pb chronology for Mafura (using linear extrapolation between the dated horizons). Filled circles represent actual dated horizons, the filled square is the base of the sequence, dated by linear extrapolation.* **(B-D)** *Fallout radionuclides in the Mafura core showing* **(B)** *total and supported ^{210}Pb,* **(C)** *unsupported ^{210}Pb and* **(D)** *^{137}Cs concentrations versus depth.*

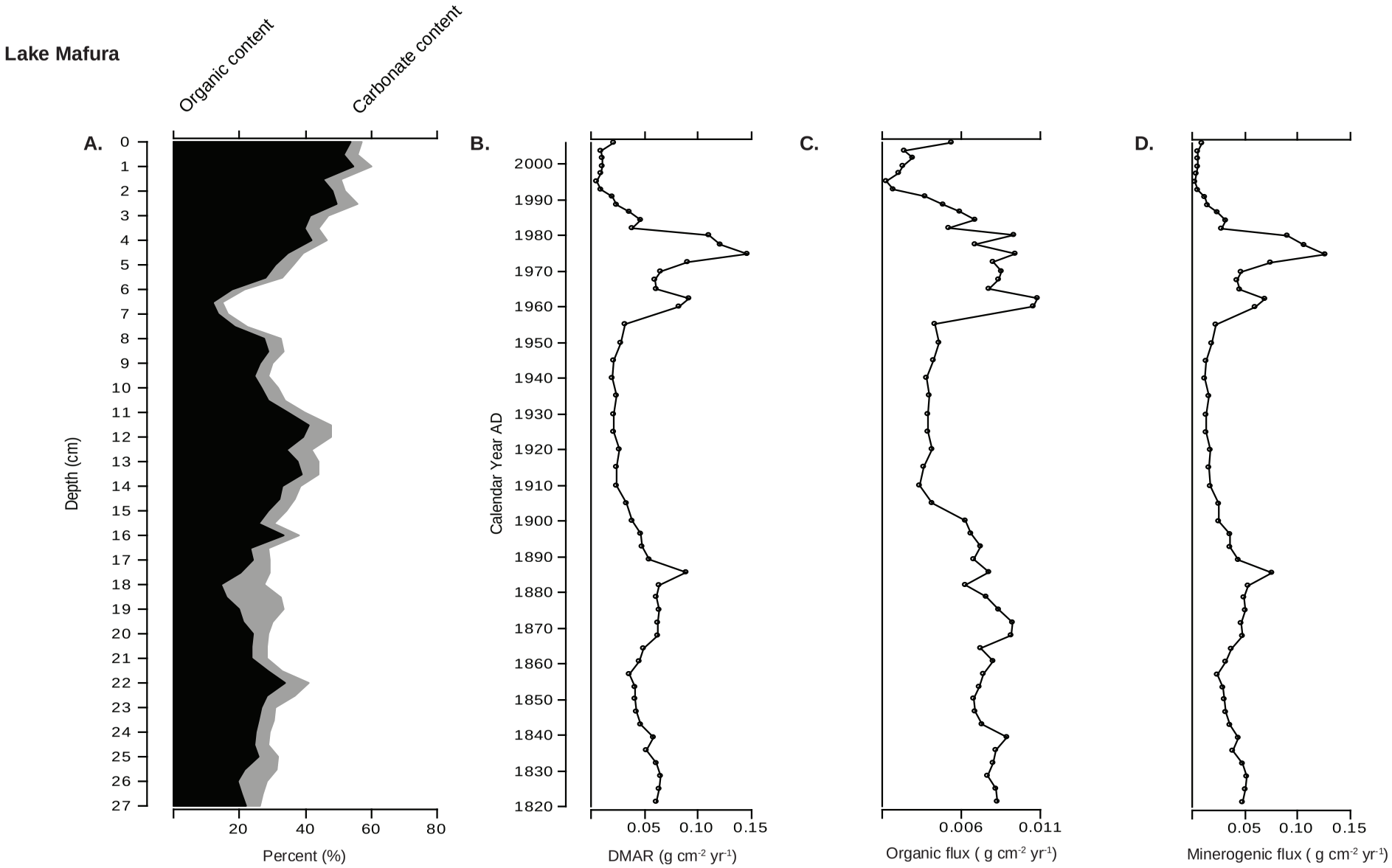

Figure 7.20 *Calculated flux data for Lake Mafura.* **(A)** *Stacked organic and carbonate percentages versus core depth,* **(B)** *dry mass accumulation rate (DMAR) calculated using the dry bulk density and* ^{210}*Pb dates,* **(C)** *organic content displayed as flux (g cm*$^{-2}$ *yr*$^{-1}$*) and* **(D)** *minerogenic flux (g cm*$^{-2}$ *yr*$^{-1}$*). Graphs* **(B-D)** *are plotted against calendar year AD.*

c. 7 cm (AD 1975). Between the peaks of AD 1885 and AD 1960, DMAR values are very low and following the peak of AD 1975, DMAR declines towards the present day.

The organic and minerogenic flux records from Lake Mafura show three excursions in the data. The earliest peak in the values appears to occur at the very start of the record (*c.* AD 1840). Following this peak, values drop (*c.* AD 1860) before rising to a second peak in the late 1800s (AD 1870-1880). Following the high values in the organic and minerogenic fluxes (0.009 and 0.07 g cm^2 yr^{-1}, respectively) both records show a decline to lower values (0.04 and 0.01 g cm^2 yr^{-1}; *c.* AD 1910). Values remain low until the early 1950s when the final excursion in the data occurs. The final excursion exhibits a double peak, the first occurring at *c.* AD 1960 and the second at *c.* AD 1975, before the values decline towards the present.

7.6 Lake Kigezi

7.6.1 ^{210}Pb dating

Kigezi has a relatively good ^{210}Pb record, though the surface concentration is quite low (~840 Bq kg^{-1}). There is a change of gradient at ~20 cm suggesting a recent acceleration in the sedimentation rate (P.G. Appleby, *pers. comm.*). This change also coincides with a shift from dense sediments below 20 cm to much lighter sediments above 12 cm. Equilibrium with the supporting ^{226}Ra occurs at around 30 cm. The highest ^{137}Cs concentration occurs at 10.5-11.5 cm sample. ^{210}Pb dates calculated using the CRS model place 1963 at a depth of 16-17 cm. Thus the early 1960s occurs somewhere between 11-17 cm (P.G. Appleby, *pers. comm.*). Tentative radiometric dates were calculated using the CRS ^{210}Pb dating model (Appleby *et al*. 1978), and compared with the best estimate of the 1963 stratigraphic date suggested by the ^{137}Cs record (Figure 7.21).

7.6.2 Physical properties

The organic, carbonate and minerogenic record from Lake Kigezi is generally stable throughout the record (Figure 7.22). The organic content fluctuates between 15-20% (though values do peak at ~30% in the most recent sediments), the carbonate fraction constitutes <10% and the minerogenic fraction is *c.* 80% throughout. There are a number of extremely small excursions in the organic data at *c.* AD 1940, AD 1970 and AD 1990 (22.5, 15 and 6 cm, respectively), but there are no major changes in the record. Conversely,

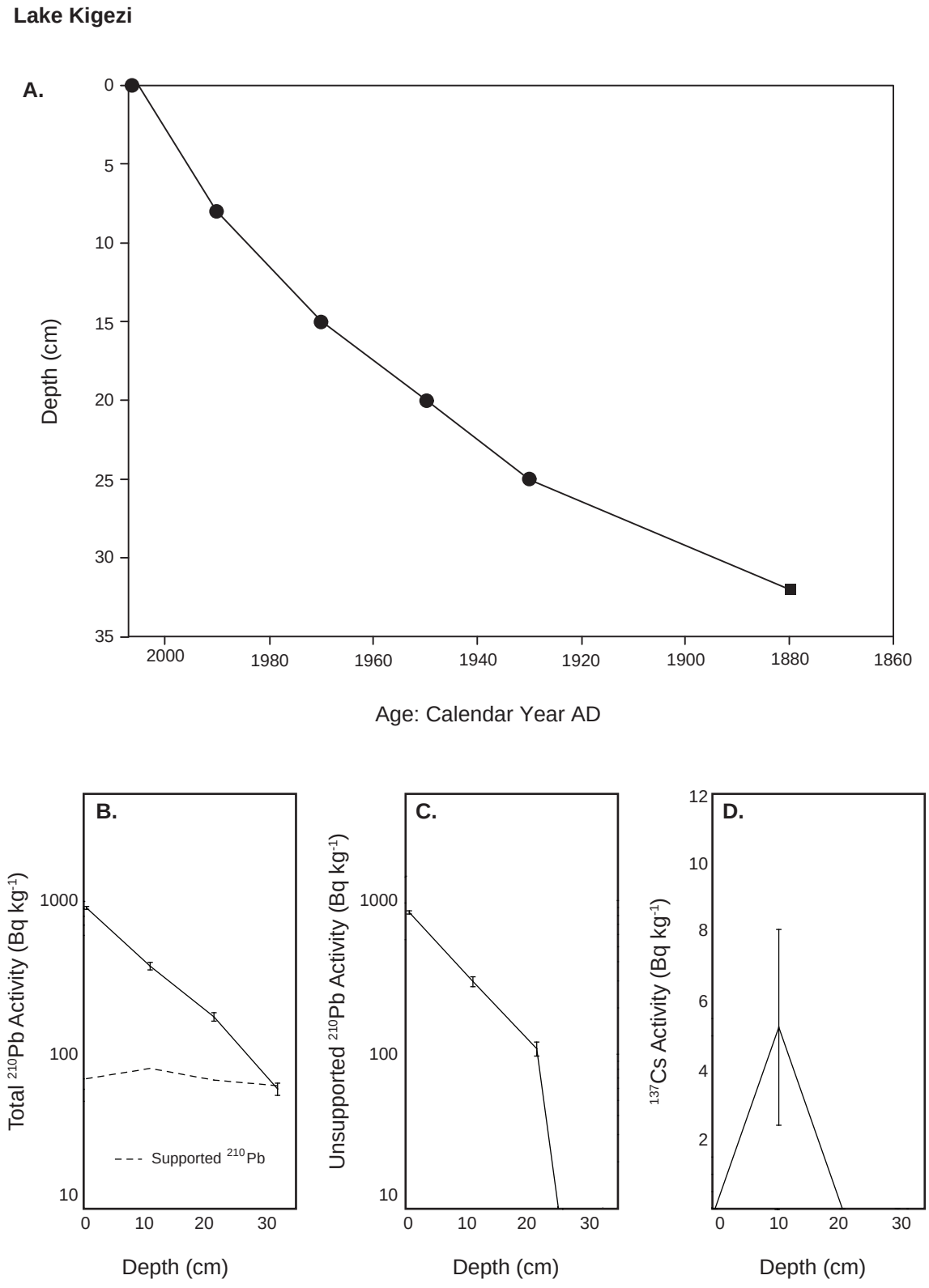

Figure 7.21 *^{210}Pb and ^{137}Cs data for Lake Kigezi.* **(A)** *^{210}Pb chronology for Kigezi (using linear extrapolation between the dated horizons). Filled circles represent actual dated horizons, the filled square is the base of the sequence, dated by linear extrapolation.* **(B-D)** *Fallout radionuclides in the Kigezi core showing* **(B)** *total and supported ^{210}Pb,* **(C)** *unsupported ^{210}Pb and* **(D)** *^{137}Cs concentrations versus depth.*

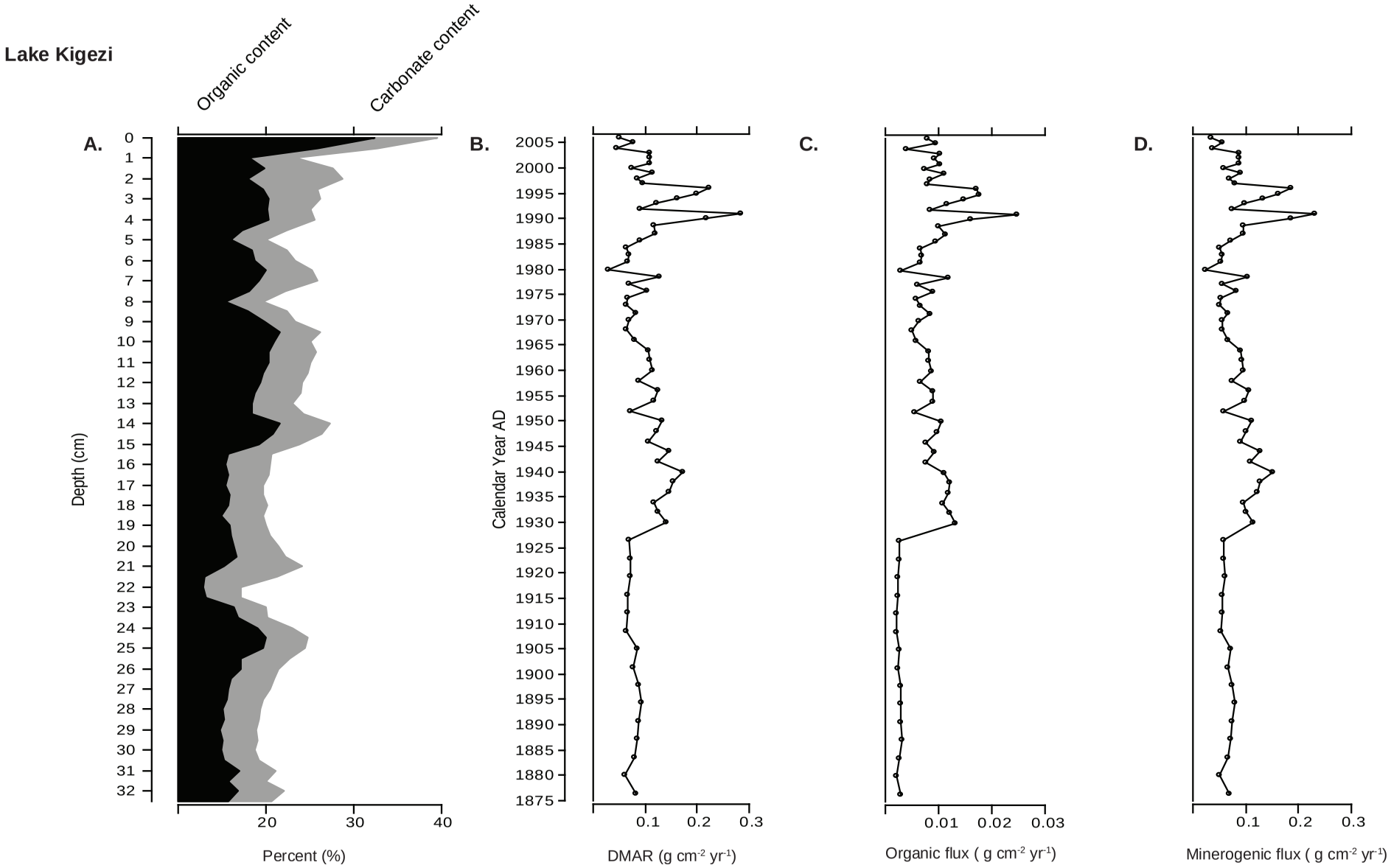

Figure 7.22 *Calculated flux data for Lake Kigezi.* **(A)** *Stacked organic and carbonate percentages versus core depth,* **(B)** *dry mass accumulation rate (DMAR) calculated using the dry bulk density and* ^{210}*Pb dates,* **(C)** *organic content displayed as flux (g cm*$^{-2}$ *yr*$^{-1}$*) and* **(D)** *minerogenic flux (g cm*$^{-2}$ *yr*$^{-1}$*). Graphs* **(B-D)** *are plotted against calendar year AD.*

the dry mass accumulation rates from Kigezi show a number of interesting changes. Prior to AD 1930 (25 cm), the DMAR is very stable, with very low values. After this point the DMAR increases and becomes more variable. From AD 1940, the values begin to slowly decline, before a double peak in the DMAR occurs at AD 1990 (7.5 cm) and AD 1995 (5 cm). DMAR decline towards the present day.

Whilst the organic and carbonate records from Kigezi exhibit two excursions in the data (at AD 1930-1940 and AD 1990), the flux records (organic and minerogenic) are noisy. From AD 1875 to AD 1925 the organic and minerogenic flux is low (*c.* 0.003 and 0.07 g cm^2 yr^{-1} respectively). After AD 1925 the organic sediment flux rises to 0.01 g cm^2 yr^{-1} and the minerogenic sediment flux to 0.12 g cm^2 yr^{-1}. Following the peak in the data, both records steadily decline until *c.* AD 1980, after which the values peak for the second time (organic flux 0.02 g cm^2 yr^{-1} and minerogenic flux ~0.2 g cm^2 yr^{-1}). These high values manifest a double peak. From AD 1995, the organic and minerogenic sediment flux declines towards the present.

7.7 Summary

- Five short (27 – 43 cm) sediment cores spanning the last *c.* 150 years were retrieved from lakes across a landscape (different catchment types from pristine to heavily impacted) in western Uganda.
- Multiproxy analyses (organic content, diatoms and calculation of flux data) were completed on three of the core sequences (Kamunzuka, Nyungu and Kako) and sediment data (organic content and flux data) exist for the remaining two cores (Mafura and Kigezi).
- Whilst all three lakes differ in their overall diatom species composition and their response to both external and internal factors, they do share some common features.
- The 'pristine' lake Kamunzuka reveals very little variation in its diatom assemblage since AD 1810. Conversely, 'impacted' Lakes Nyungu and Kako indicate a significant shift in the diatom data in the last *c.* 50 years, with a change in habitat from a planktonic to a benthic dominated system.
- These major changes in the diatom flora are coincident with an increase in the flux of sediment to the lake system.
- The sedimentary records from all five lakes demonstrate an increase in sediment flux to the lakes in the last 20-50 years. This similar response across all lakes suggests that a

regional driver is responsible for the observed recent changes in the record, perhaps related to the onset of human activity, overprinted on known regional climatic fluctuations.

- Prior to AD 1950 sediment flux to all lakes is low, yet changes still occur in the diatom assemblage data, perhaps suggesting two alternative drivers for the sediment sequences (e.g. climate driver pre-AD 1950 and human related drivers in the last 50 years).

Chapter 8

Discussion

8.1 Introduction

The results from the long cores (Lakes Nyamogusingiri and Kyasanduka) and short cores (Lakes Kamunzuka, Kako and Nyungu) presented in **Chapters 6** and **7** are now synthesised and discussed with reference to the original aims and specific research questions outlined in **Chapter 1**. Figure 8.1 highlights the schematic structure of the discussion chapter, beginning with the shorter-term records spanning the last 150 years before looking at the longer-term records spanning the last millennium. In all cases, the degree of regional and temporal coherence between the various palaeolimnological records is evaluated whilst considering these records within a wider context by comparison with other published palaeoclimatic and palaeoenvironmental records from western Uganda and Eastern Africa.

8.2 Coherence of signals between lakes

Climate and environmental (e.g. catchment) changes are external drivers of lake dynamics; however uniform changes in climate across a region can produce a variety of responses in lake ecosystems. This is primarily due to the way in which these different ecosystems filter these signals and alter their expression (Magnuson *et al*., 2004). Understanding the temporal coherence of lakes at various spatial scales will provide insight into the factors influencing lake dynamics.

Sediments from a range of lakes in the landscape provides an ideal set of temporal and spatial scales to study climate change and lake ecosystems (Magnuson *et al*., 2004). The ability to simultaneously understand time (such as long-term dynamics) and space (a number of lakes with differing characteristics across a landscape) is becoming increasingly important in (palaeo)limnological studies (cf. Magnuson *et al*. 2004). This is a particularly pertinent approach when realising that not all lakes respond to external (e.g. climate) forcing in a similar way. Whilst climate change has been shown in the broadest sense to manifest as general trends across regions and continents (and beyond), these are only really apparent and addressed in long-term (e.g. millennial) studies of lake sediments; the

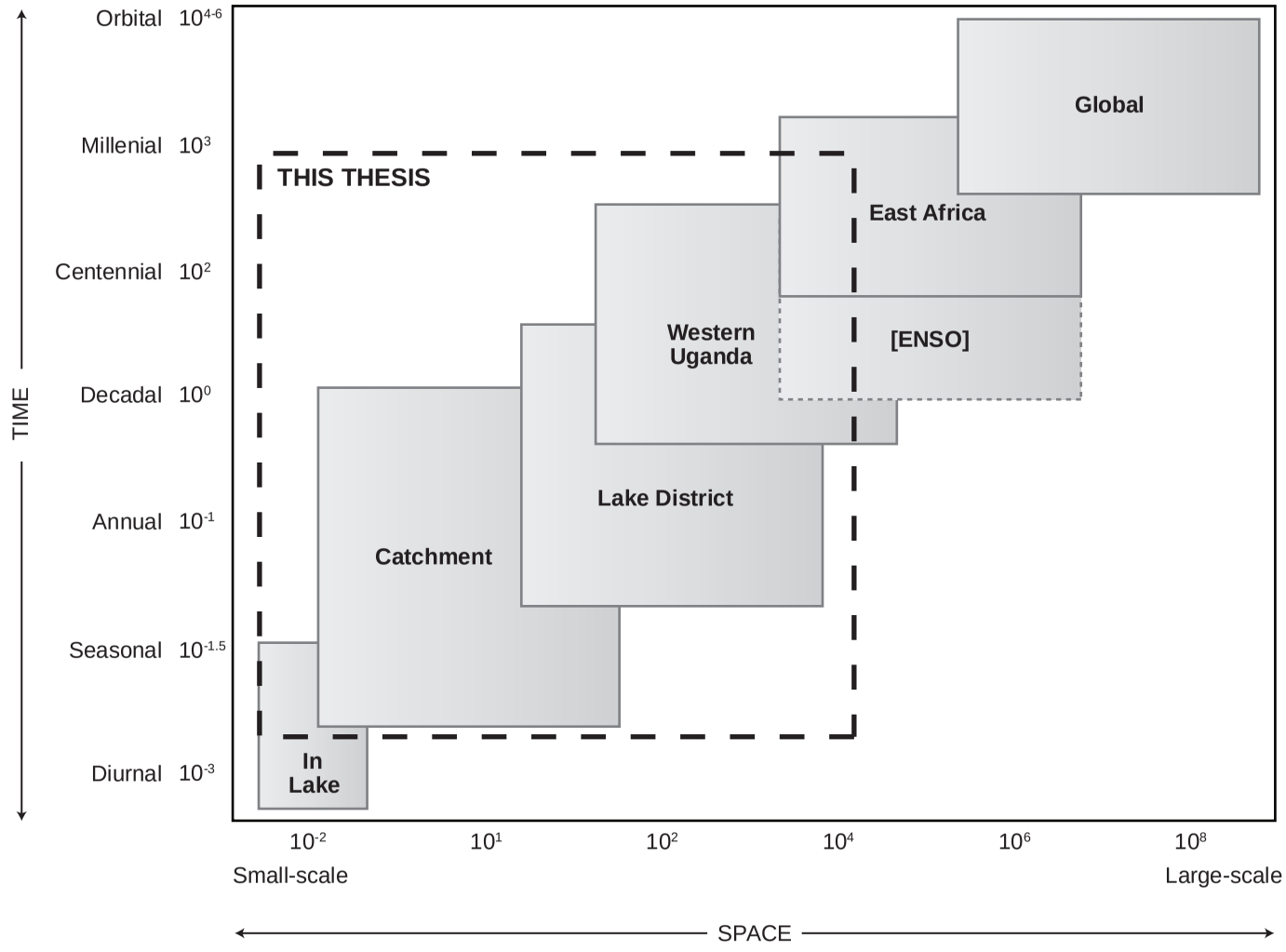

Figure 8.1 *Stommel diagram highlighting the various temporal and spatial scales on which environmental changes occur. This also forms the structure of the discussion chapter. The dashed box highlights periods covered by this thesis.*

dynamics controlling a lake's response can often be overlooked (cf. Magnuson *et al*., 2004). A notable exception to this generalisation has been the work on the effect of temperature changes on the ecology of Lake Tanganyika (Verburg *et al*., 2003; O'Reilly *et al*., 2003), with 20th century climate warming in conjunction with a reduction in the strength of the trade winds leading to a marked reduction in fish yields (Verburg *et al*., 2003; O'Reilly *et al*., 2003, Verschuren *et al*., 2003).

All of the lakes analysed in this study were located within a narrow belt (*c.* 7 km by 15 km) and thus in close proximity to each other. Two of the lakes, from which the longer cores were extracted, were immediate neighbours located to the west of the cluster on the rift valley floor (Lakes Kyasanduka and Nyamogusingiri, within the Queen Elizabeth National Park). The remaining five lakes (Kamunzuka, Nyungu, Kako, Kigezi and Mafura) were located on the moist shoulder of the rift valley system; four were located in an unprotected belt of land, subject to human activity (clearance for agriculture and plantations), the fifth lake was located in a forest reserve to the east (Kamunzuka). The location of these lakes within a region of similar geology and climate, suggests broad trends in climate and environmental changes would be expected to manifest as similar patterns within the various lake sedimentary records, with the lake ecosystems perhaps responding to similar drivers. It is likely that the altitude of the lake systems plays an important role, i.e. whether the lakes are located on the rift valley floor (Nyamogusingiri and Kyasanduka) or the moist shoulder of the rift valley (Lakes Kamunzuka, Kako, Nyungu, Mafura and Kigezi), especially in terms of the lake groundwater regime and rainfall. Lakes Nyamogusingiri and Kyasanduka receive *c*. 900-1300 mm yr^{-1}, the lakes on the shoulder receive a higher annual rainfall (*c*. 1300 mm yr^{-1}; Lock, 1967; see *section 2.7.1*).

The sedimentary records from all lakes highlight several differences in their functioning, which might be expected given the range of lake and catchment morphologies, size and most likely differing land use histories (cf. Magnuson *et al*., 2004; Ssemmanda *et al*., 2005; Ryves *et al*., submitted). However, despite this, there are several commonalities between the lakes in terms of the diatom assemblage zones. Most of the lakes differ in their diatom assemblages and response, yet independent zoning of the diagrams shows several significant and regionally important time zones (Figure 8.2 and 8.3).

The two long core (Kyasanduka and Nyamogusingiri) sequences show remarkably good correlation with regards to their zonation, with boundaries common to both cores

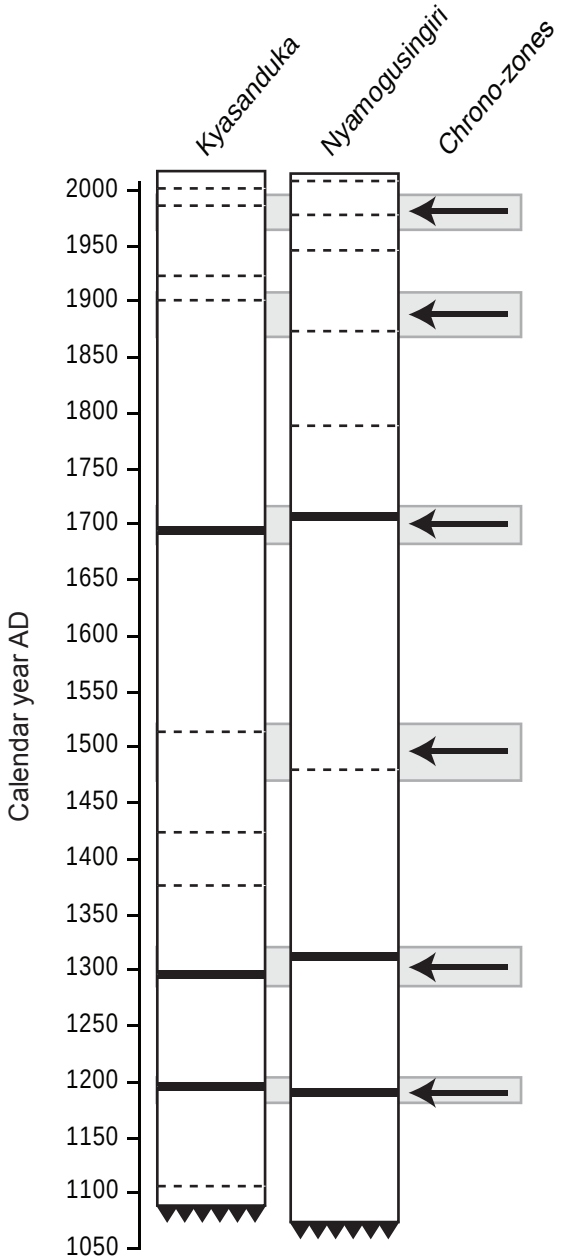

Figure 8.2 *Schematic diagram comparing the age of the statistically significant zones between the two long cores (dashed horizontal lines): Nyamogusingiri and Kyasanduka (AD 2007-AD 1050). Triangle lines indicate the base of the cores. Solid black lines indicate zones common between cores and arrows indicate chrono-zones. The arrows represent major zones that are considered similar within the errors of the dating method.*

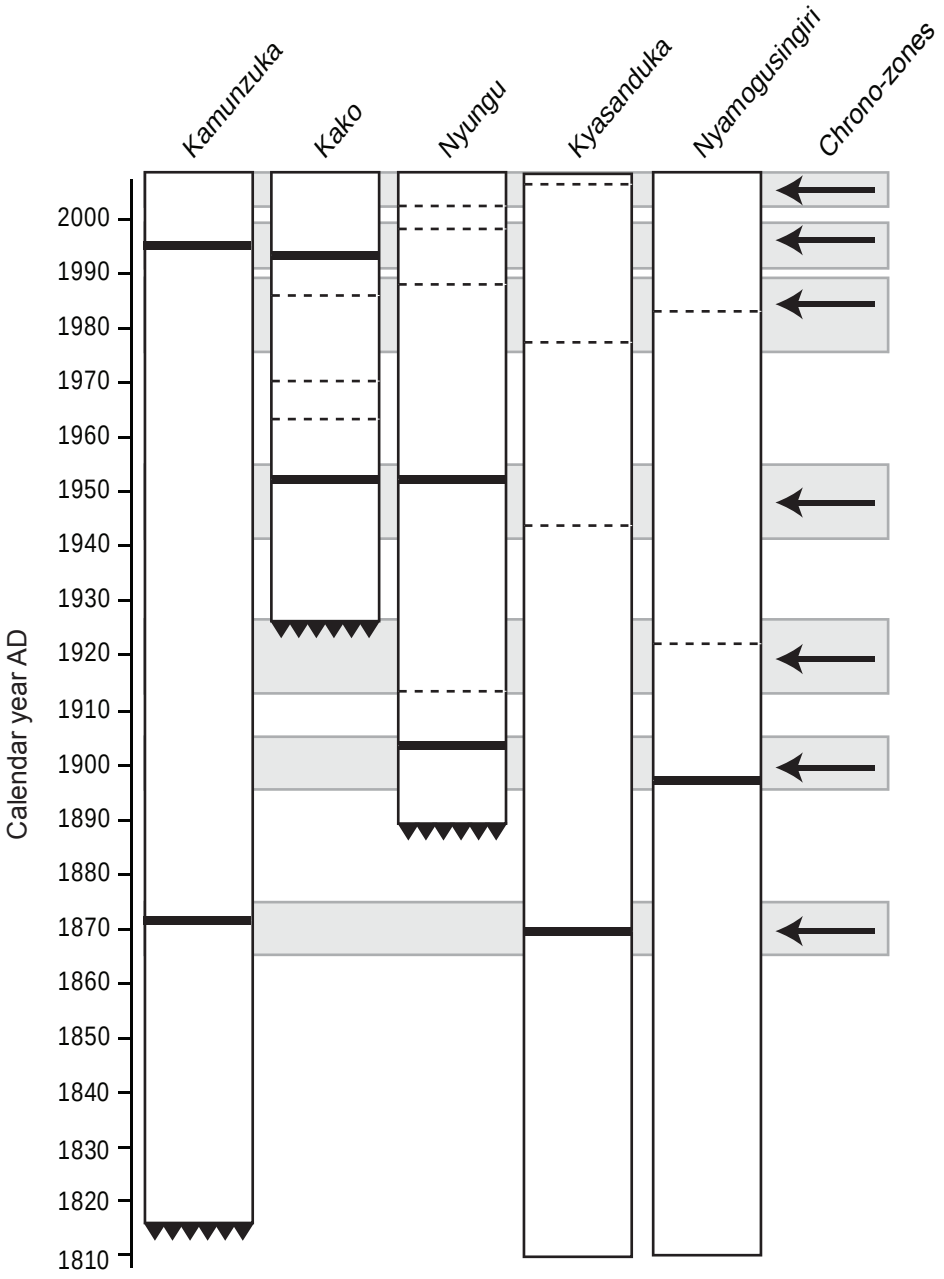

Figure 8.3 *Schematic diagram comparing the age of the statistically significant zones between the various short cores (dashed horizontal lines): Kamunzuka, Kako, Nyungu, Nyamogusingiri and Kyasanduka (AD 2007-AD 1850). Triangle lines indicate the base of the cores. Solid black lines indicate zones common between cores and arrows indicate chrono-zones. The arrows represent major zones that are considered similar within the errors of the dating method.*

(given potential errors in the core chronologies) occurring at *c.* AD 1200, AD 1300, AD 1500, AD 1700, AD 1900 and the late 20th century (*c.* AD 1990; Figure 8.2). Similarly, there is a relatively good agreement in the position of zone boundaries in the short cores spanning the last *c.* 150 years (Figure 8.3). Lake Kamunzuka shares a boundary with Kyasanduka *c.* AD 1870, and Nyungu shares the AD 1900 boundary with Nyamogusingiri. The record obtained from Lake Nyungu also terminates *c.* AD 1890. In the recent past, Lakes Kyasanduka, Nyungu and Kako show a change *c.* AD 1950 and AD 1980 and Lakes Kamunzuka, Kako and Nyungu show a change in the mid-1990s.

The reason for the variation in system responses to shared external forcing almost certainly arises from the complexity of lake ecosystems in their response to these drivers. For example, a model presented by Magnuson *et al.* (2004) suggests that lakes have several levels of filters that allow them to respond uniquely (Figure 8.4). A lake's response to external forcing is governed by factors such as its morphometry, chemistry, local hydrology (e.g. groundwater) and ecology. The model outlined by Magnuson *et al.* (2004) suggests that lakes may amplify, attenuate, delay or extend the climate signal (Figure 8.3).

Table 8.1 *Comparison of the limnological features of the 4 crater lakes in the cleared corridor.*

Lake	Altitude (m)	Max. depth (m)	Cond. ($\mu S\ cm^{-1}$)	Lake area (L; km^2)	Catchment area (CA; km^2)	CA:L
Mafura	1217	27.4	342	0.18	1.36	2.4 : 1
Nyungu	1190	25.2	528	0.17	1.83	10.8 : 1
Kigezi	1247	26	271	0.11	0.59	5.4 : 1
Kako	1375	29	98	0.2	0.48	7.6 : 1

With specific reference to the lakes used in this study, the morphometry and size of the lake basin is almost certainly one of the largest factors controlling the response of the lake ecosystem. Lake Kyasanduka has a very large, flat, shallow basin, with the majority of the catchment consisting of gentle slopes, except to the east where there is a section of high ground (*c.* 1500 m), sloping at quite a steep angle (*c.* 40°[1]) towards the lake. The littoral and benthic zone is extremely important throughout the sedimentary record, given the shallow nature of the lake basin. Similarly, the littoral zone is the most dominant habitat in Lake Kamunzuka, which again has a rather gently sloping catchment. However, in this

[1] Value obtained from a DEM of the catchment area, modelled using ArcGIS.

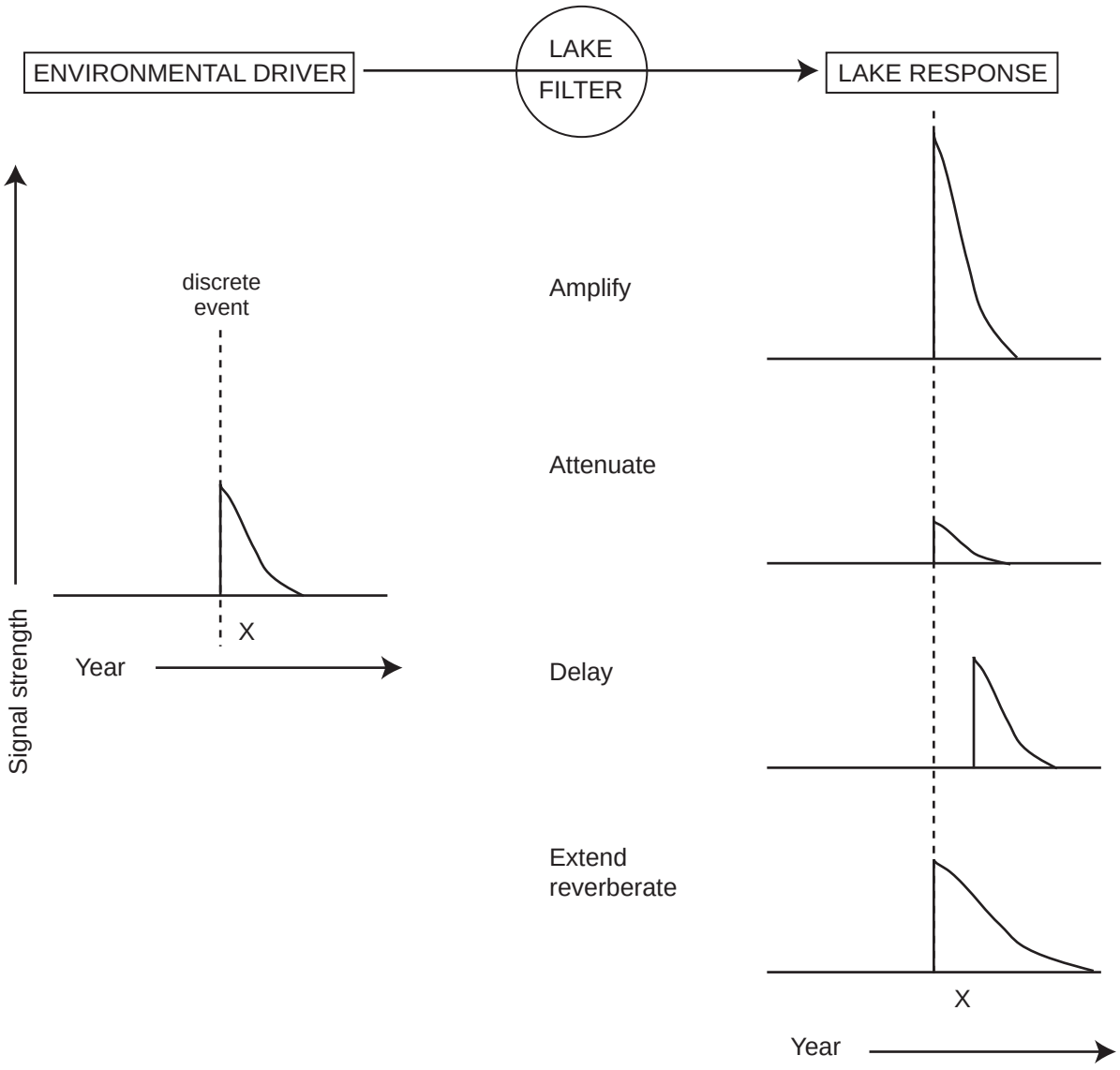

Figure 8.4 *Diagram illustrating possible responses of a lake system to an environmental driver (X; e.g. climatic perturbation, catchment disturbance etc). The various lake filters would modify the strength and timing of the lake response to that environmental driver. (Redrawn from Magnuson et al. [2004]).*

the crater. The role of groundwater is also likely to be important in the crater, allowing the constant removal of salts, keeping the water fresh, even during low stands (inferred from the diatom habitat summary).

Through the comparison of independent lake level reconstructions from diatom and other sedimentary records, changes common to each record provide strong evidence for regional-scale processes and drivers (e.g. rainfall variability). The use of a regional, multi-lake study therefore allows the identification of regional climate events, from local-scale, in-lake processes.

8.3 Lake level reconstructions

In outflow lake systems, past changes in climate may be reconstructed through the use of lake level changes; during periods of aridity, lake levels decrease, and if lake levels drop below the outflow threshold, there may also be a rise in salinity. Under wetter conditions, lake levels rise and will overflow (depending on the height of the outflow system). Whilst the potential climate signal recorded within freshwater, outflow lakes is often less sensitive compared to closed-basin (and saline) systems, studies on such systems have shown climate reconstructions are still possible (cf. work on Lake Victoria by Stager and colleagues).

In the sediment record, planktonic species, colonizing open water, are assumed to increase in abundance during periods of higher lakes levels, whilst benthic taxa will decrease, and *vice versa*. Ratios based on the abundance of planktonic versus benthic species can be successfully used to reconstruct lake level changes (Gasse *et al*., 1989, Barker *et al*, 1994; Stager *et al*., 2005; Stone and Fritz, 2004). It has been shown that this relationship of planktonic species and higher water levels can be complicated in the recent past due to human activity in lake catchments.

Relative lake levels for each of the core sequences were reconstructed using the diatom data. Reconstructions were based upon the known habitat preferences of the most dominant taxa. For example, in Nyamogusingiri, the presence of the fresh, deep water taxon *Nitzschia lancettula* was used as the main basis for lake level reconstruction. Similarly, *Aulacoseira* spp. (*A. ambigua* and *A. granulata*) were used as indicators of deeper water in Lake Kysanduka. The dominance of benthic species was used as an indicator of lower lake level. The general trends observed in the relative lake level curves broadly reflect the habitat summaries given in **Chapters 6** and **7** (Figures 6.9, 6.25, 7.5, 7.11 and 7.17).

Using the biological and physical indicators from the lake sedimentary archives (**Chapters 6** and **7**) observed changes in the inferred lake level changes are interpreted as climatically driven changes until the late nineteenth to early 20th century. There have been large fluctuations in lake levels during the last 1000 years, and some fluctuations during the last 150 years (Figure 8.5).

There is general agreement between the long-term lake level changes observed in Lakes Nyamogusingiri and Kyasanduka, even though the levels at Kyasanduka are much lower for the entire record (the lake could not have reached depths greater than *c.* 4 m in the past, accounting for the infilling of sediment over the last 1000 years and the presence of an outflow). Both lakes record extremely low levels at the beginning of their records (*c.* AD 1070), where a prolonged period of aridity persists for almost 100 years. This arid period is punctuated by a freshwater event in Lake Nyamogusingiri, centred on AD 1130, before returning once again to lower levels, though this second phase of lake level reduction in Lake Nyamogusingiri is not a severe as the first, with lower reconstructed conductivity during the latter phase compared to the early phase (which is controlled by the lower abundances of saline and benthic *Amphora coffeaeformis* during the second period of lower lake levels). These low lake levels at the beginning of the record coincide with the northern hemisphere's Medieval Warm Period (see *section 8.5* for a full discussion) and a well-documented period of aridity which affected most of East Africa at the start of the second millennium AD (Ricketts and Johnson, 1996; Verschuren *et al.*, 2000; Alin and Cohen, 2003; Verschuren, 2004; Russell and Johnson, 2005; Bessems, 2007; Ryves *et al.*, submitted). Whilst saline species are noted during this severe arid phase in Lake Nyamogusingiri, Lake Kyasanduka remains relatively fresh, with aerophilous, littoral and benthic species dominating the record and a high ratio of testate amoeba scales, illustrating the importance of marginal lake areas. Furthermore, groundwater is clearly an important influence on the lake ecosystem at Kyasanduka, allowing this lake to remain fresh and allowing continuous sedimentation during periods when other, deeper lakes in the region experienced much lower lake levels (cf. Bessems, 2007; Russell *et al.*, 2007; Bessems *et al.*, 2008).

High lake levels return to Nyamogusingiri in the early 13th century, during a wet phase mirrored in Lake Kyasanduka, with a peak *c.* AD 1200. These higher lake levels persist until the end of the 13th century, after which there is a return to lower lake levels.

deep lake (61 m) the littoral zone is sustained as a result of water clarity, allowing light penetration to almost 20 m (depth of the photic zone based on Secchi disk depth) and supporting a large benthic diatom community consisting primarily of the genus *Gomphonema*. The four lakes located within the "cleared corridor" are extremely similar in their altitude, size and depth (Table 8.1), but differ slightly in terms of their catchment size and therefore their catchment area: lake ratio (Table 8.1). All lakes having steep sided slopes and extensive human activity present within their catchments.

Lake Nyamogusingiri is somewhat different to the other lakes consisting as it consists of two sections: a deep (*c.* 13 m) crater (hereafter Lake Nyamogusingiri Crater) located to the west (where the sediment for this research was obtained), which is currently joined to a much larger (*c.* 3.5 km), flatter and shallow (*c.* 4 m) basin to the east. These two lakes are separated by a sill *c.* 1.2 m in depth; if the lake level were to fall by this depth, then the currently conjoined basins would operate as separate basins. In Lake Nyamogusingiri crater there is evidence of this in the past, with dead, submerged trees and stumps located several meters offshore and rooted at *c.* 2.5 m depth. The presence of these trees around, what is likely to be, a former shoreline attest to lake levels that were low enough, and for long enough, for vegetation to establish itself at the lake edge and it is therefore expected that the crater lake would have operated independently from the main basin. The opening and closing of the two basins has had an affect on the functioning of the Nyamogusingiri crater ecosystem and hence the fossil diatom assemblages contained within the sediments obtained. For the majority of its record, Lake Nyamogusingiri has remained relatively fresh aside from two extremely saline periods *c.* AD 1130 and AD 1950, which are the only conductivity changes inferred by the diatom transfer function and are denoted by the presence of saline taxa such as *Amphora coffeaeformis* (AD 1130) and *Thalassiosira rudolfi* (AD 1950). Despite little change in reconstructed conductivity at Nyamogusingiri, there are notable changes in diatom habitat (from benthic dominated to plankton dominated systems; see **Chapter 6**, Figure 6.9). It is likely that these two saline periods represent times when the crater lake was isolated from the main basin. With levels dropping > 1.2 m, this would also prevent any overland outflow which is currently evident in the crater at times of high levels. During these extreme low-stands, which likely represent periods of aridity linked to the Medieval Warm Period, the crater would have behaved as a closed lake system, experiencing evaporative enrichment, until rainfall caused levels to rise sufficiently to reconnect the two basins, thus allowing the exchange of salts from Nyamogusingiri crater to main the basin and via an outflow to the northwest of

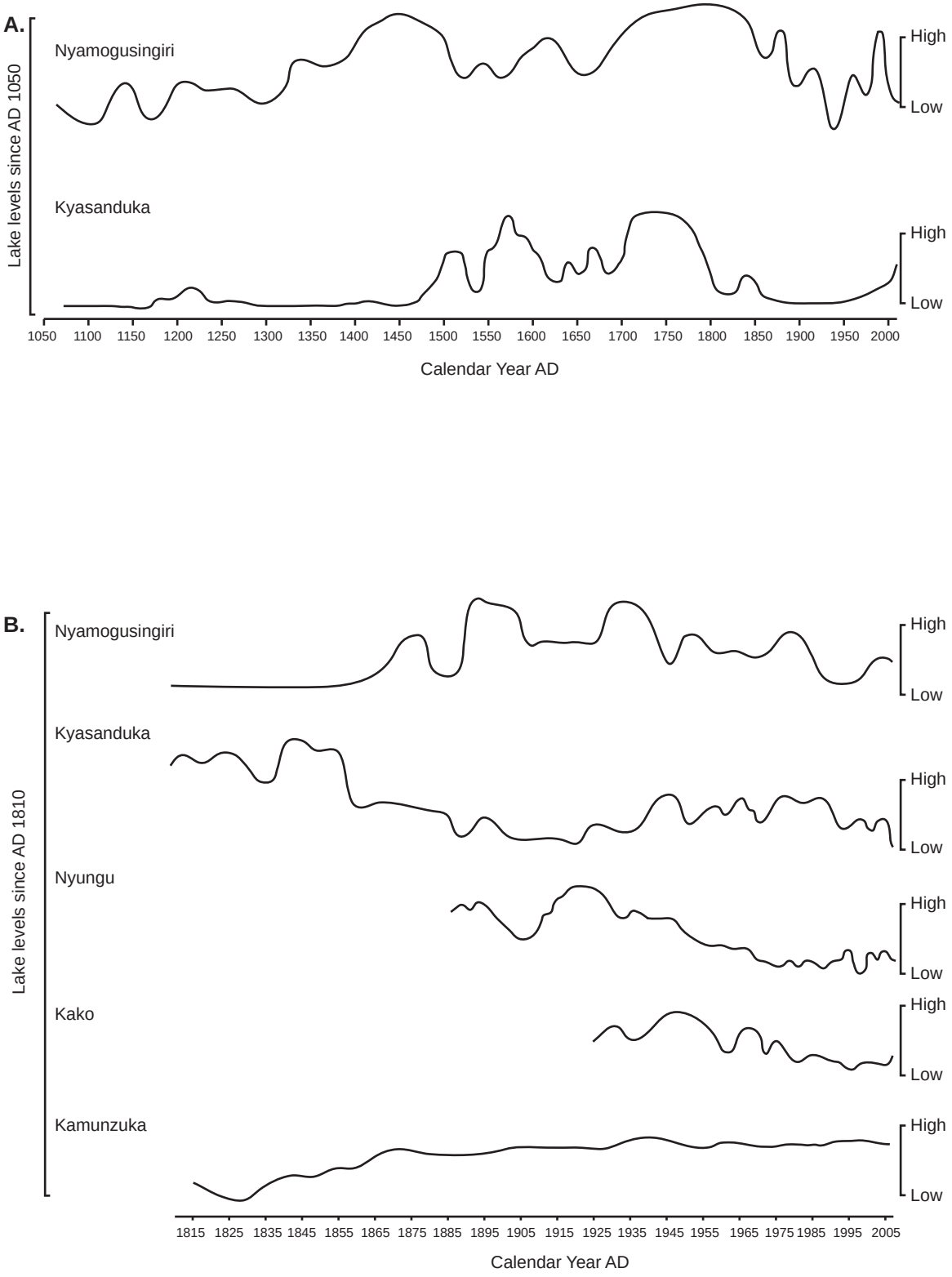

Figure 8.5 *Reconstructed lake levels from diatom data from five crater lakes in western Uganda.* **(A)** *Records of lake level fluctuations over the last 1000 years from lakes Nyamogusingiri and Kyasanduka,* **(B)** *lake level fluctuations over the last 150 years from lakes across a landscape gradient.*

Levels remain low at Kyasanduka until the mid 1400s, whilst Nyamogusingiri indicates a steady rise to higher levels, with a small peak at *c.* AD 1350 proceeded by a short-lived fall in levels centred on AD 1370, before reaching a peak at AD 1450. The increase in the level of the lake occurs slightly later at Kyasanduka (towards the end of the 15th century). Lake Kyasanduka appears to become more open at this time, with a significant reduction in littoral diatoms that previously dominated the record and an increase in *Aulacoseira ambigua*, indicative of more well-mixed, nutrient enriched, deeper, open water (Leira and Sabater, 2005; Stager *et al*., 1997; C. Sayer, *pers. comm*.).

Both records show a slight decrease in their lake levels around AD 1530, followed by a recovery of the levels culminating in a high-stand at Kyasanduka during the late 1500s and occurring slightly later at Nyamogusingiri (*c.* AD 1600). Lake levels decline in both records in the 1600s, after which lake levels rise after AD 1700 and remain high until *c.* AD 1800-1850.

The last 150-200 years presents a slightly more complicated record for the long cores, with a higher temporal resolution for the various proxies (annual), allowing finer scale changes in lake levels to be identified. However, in general, both lakes show a general decline in lake levels from *c.* AD 1850 onwards. All lakes appear to show a decreasing trend in lake level since the early 19th century towards the present. Nyamogusingiri and Kyasanduka record lower levels *c.* AD 1880. Whilst the record from Nyungu does not extend back quite this far, the core record terminates just after this date (*c.* AD 1890). When retrieving the core from Nyungu, it was not possible to penetrate the sedimentary sequence deeper than 27 cm (*c.* AD 1890) due to the presence of a compacted, clay layer. As a likely desiccation surface, this observation lends support to the onset of regional aridity during the 1880s.

Most lakes record a period of higher lake levels immediately after this inferred arid period (*c.* AD 1890) before declining once again to lower levels in the early 1900s (*c.* AD 1905). Lakes Kako and Nyungu show higher levels *c.* 1925, whilst Nyamogusingiri and Kyasanduka are lower, peaking slightly later at Nyamogusingiri (AD 1935) and Kyasanduka (AD 1945). Nyamogusingiri records a period of high conductivity and inferred lower levels *c.* AD 1940-AD 1950, when other lakes suggest slightly higher levels. Lake levels rose across East Africa *c.* AD 1965, following a particularly wet period at the beginning of the 1960s (1963 was one of the wettest years on record in Uganda) before declining *c.* AD 1970. Subtle rises in levels are recorded in Lakes Kako and Nyungu and a larger rise in Nyamogusingiri and Kyasanduka between AD 1975-1980. A period of aridity

is also inferred since the mid-1990s, with all lakes (Nyamogusingiri, Kyasanduka, Nyungu and Kako) showing a decrease in lake levels, generally remaining lower towards the present.

The record from Lake Kamunzuka does not appear to be a sensitive record of lake levels in response to regional short-lived periods of aridity. Kamunzuka does suggest a change in the diatom assemblage, suggesting lower lake levels during the early 1800s, before continually rising and becoming stable towards the present. This could be an artefact of the resolution of the record compared to the other lake systems in this study. However, the sediment record from this lake is dominated by the benthic *Gomphonema* cf. *gracile*, which today can live in depths of up to *c.* 20 m (see **Chapter 7**, *section 7.2.5*). The changes in the abundance of this *Gomphonema* species is most likely controlled by turbidity, which may be linked to lake levels changes, as lower lake levels would lead to increased mixing, which may increase the turbidity of the lake. The record is certainly buffered against the relatively minor climate fluctuations of the last *c.* 150 years, only responding to the inferred period of aridity around AD. 1830, which coincides with lower levels in the Lake Victoria basin (Nicholson, 1998a).

There is evidence of increasing human impacts over the last 150 years in this region of western Uganda, with changes in catchment vegetation due to the replacement of forest with agriculture (Ssemmanda *et al.*, 2005). Vegetation changes would affect catchment hydrology, i.e. some responses may be nutrient and/or turbidity driven, not necessarily as a result of climate changes (e.g. Battarbee, 2000; Becht and Harper, 2002; Verschuren *et al.*, 2002; Legesse *et al.*, 2003; Legesse *et al.*, 2004; Cohen *et al.*, 2005; Plater *et al.*, 2006).

8.4 Long term records of environmental change: the last 1000 years

Much of the palaeoenvironmental research from Uganda is based on sequences from peat or swamp deposits and the large lakes (e.g. Victoria). These records generally span longer time frames (Pleistocene and Holocene; Hamilton *et al.*, 1986; Morrison, 1968; Morrison and Hamilton, 1974; Taylor, 1990; Jolly *et al.*, 1997; Marchant *et al.*, 1997; Marchant and Taylor, 1998; Taylor *et al.*, 1999; Taylor and Robertshaw, 2001; Russell *et al.*, 2003; Beuning and Russell., 2004; Leiju *et al.*, 2005; Russell and Johnson, 2005). Recent research in Uganda has focused on the shorter-term, higher-resolution archives contained within the small crater lakes across western Uganda (e.g. Bessems, 2007; Russell *et al.*, 2007; Bessems *et al.*, 2008; Ryves *et al.*, submitted; this study) to try and understand the

regional complexity of the perturbations associated with climate anomalies, such as the Little Ice Age (LIA; Russell *et al*., 2007) and the Medieval Warm Period (MWP).

Within western Uganda, there is also an increasing attempt to try and understand socio-economic and environmental interactions. In the past, linking the archaeological research to environmental changes was limited due to the large spatial separation of sources of evidence, or the reliance on the larger lakes, (e.g., Lakes Victoria, Edward and Albert) which, although sensitive to major impacts, may smooth any regional complexity in climate and environmental change by integrating responses over large areas, and often over longer timescales (Fritz, 2008). A high-resolution record of environmental change does exist from a large lake in East Africa. The varved sediments of Lake Malawi provide information on decadal scale changes in productivity as a result of lake level fluctuations over the last 700 years (Johnson *et al*., 2001). However, records such as these are rare.

Selected proxy lake level records based on a variety of geochemical, sedimentological and biotic indices from across East Africa, together with inferred lake level curves from Lakes Nyamogusingiri and Kyasanduka (Figure 8.6) demonstrate some of the spatial and temporal similarities of records from across East Africa during the last millennium (accounting for problematic dating in individual records).

There is general agreement that, prior to AD 1100, the climate in Uganda showed a transition to drier conditions, which likely began earlier during the mid-Holocene (Gasse, 2002; Lejju *et al*., 2005). Lakes Nyamogusingiri and Kyasanduka confirm this period of aridity recorded across East Africa at the onset of the 2nd millennium (AD 1000-1200). The evidence for this arid phase is widespread elsewhere across East Africa, with records from Ethiopia (Lake Hayq, Lamb *et al*., 2007), Kenya (Naivasha, Verschuren *et al*., 2000) and from lakes within Uganda itself (Victoria, Stager *et al*., 2005; Edward, Russell and Johnson, 2005; Kitigata, Russell *et al*., 2007; Kasenda, Ssemmanda *et al*., 2005; Ryves *et al*., submitted). From AD 1000 to AD 1200, summer Nileometer readings were at a minimum, Lake Victoria levels were high and Naivasha levels were low. This variation in regional climate is coincident with the northern hemispheric phenomenon termed the 'Medieval Warm Period' (MWP; AD 1000-1200).

The low-stand of *c.* AD 1050 in lakes Nyamogusingiri and Kyasanduka persists until the late 13th century (Nyamogusingiri) and as late as AD 1450 in Kyasanduka. The diatom-inferred low-stand is supported by sedimentary evidence; the clays present at the base of both core sequences may represent deposits formed under periodically inundated or

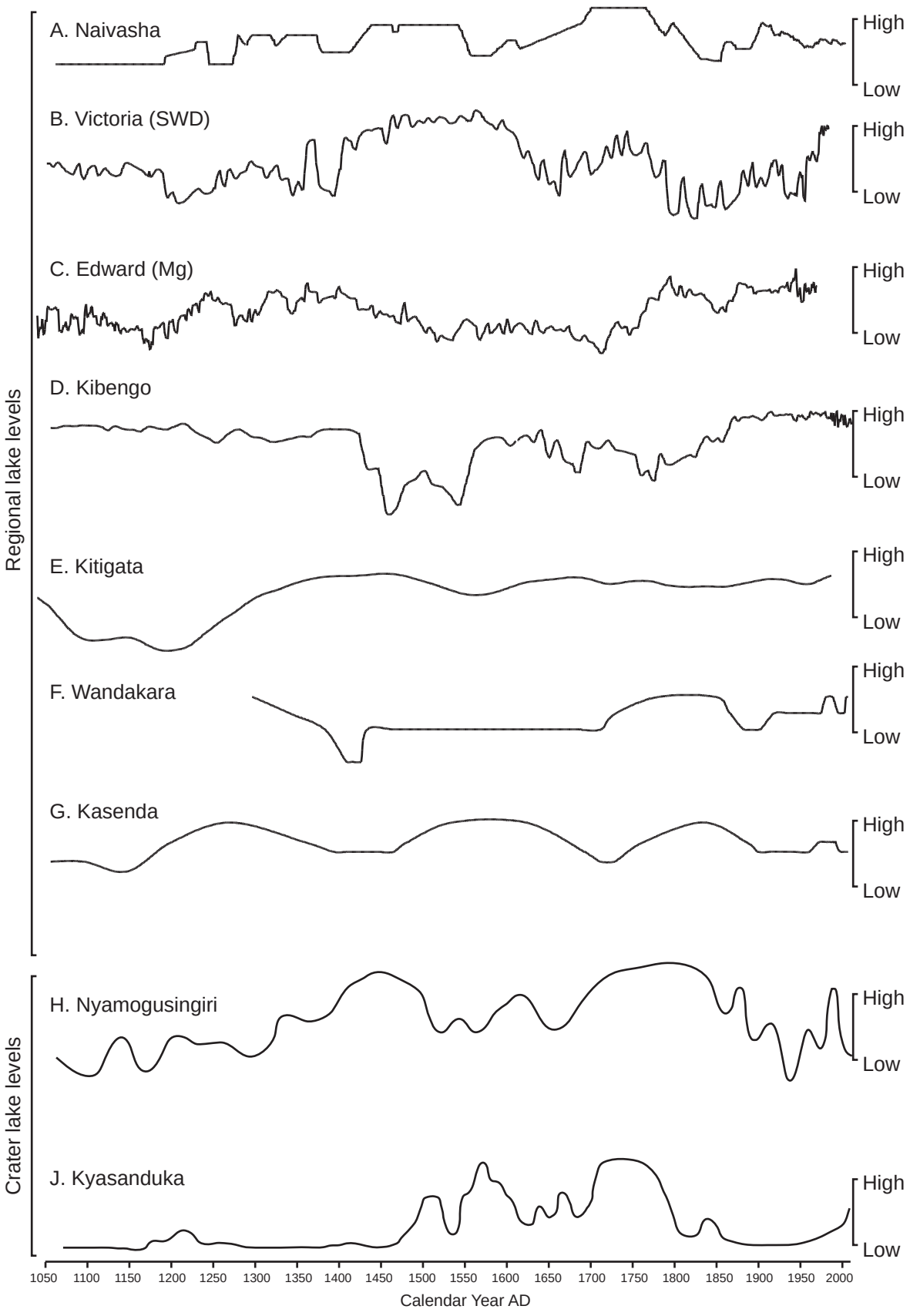

Figure 8.6 *Comparison of regional lake levels in East Africa* **(A-G)** *to the reconstructed lake levels from Nyamogusingiri and Kyasanduka* **(H-J)** *over the last 1000 years.*

shallow water conditions (cf. Leyden *et al*., 1998). Lake Naivasha provides evidence that this arid phase was punctuated by a freshwater event in the early 13th century (Verschuren *et al*., 2000). Within the errors of the core chronologies, both lakes record a shift to fresher (*Nitzschia lancettula*, Nyamogusingiri) and/or deeper, open water (*Aulacoseira ambigua*, Kyasanduka) conditions *c.* AD 1210, providing further evidence in East Africa for this freshwater phase that is also observed in Lakes Naivasha (Verschuren *et al*., 2001), Edward (Russell and Johnson, 2005) and Kasenda (Ryves *et al*., submitted) and suggesting that this could be the result of a regional climatic perturbation (Figure 8.6). Lake Nyamogusingiri also records a fresher event prior to this in the 12th century (*c.* AD 1140), although there is no evidence for a similar event at Kyasanduka. With some minor fluctuations, the wet phase beginning *c.* AD 1210 in Nyamogusingiri declines, culminating in a low-stand *c.* AD 1290. Kyasanduka remains low until the mid 15th century.

Human occupation at the Munsa archaeological site is documented during this period (AD 1000-1200) which is also coincident with the onset of deforestation and increased burning (Lejju *et al*., 2005). Further evidence for a drier climate is also apparent around the northern lake cluster of Ndale (Lake Kasenda; **Chapter 2**, Figure 2.5), with pollen data from Lake Kasenda suggesting the contraction of moist-deciduous forest and the expansion of grassland, concomitant with fire and increasing erosion (Ssemmanda *et al*., 2005) and Kabata Swamp (Taylor *et al*., 1999). The period around AD 1100 is also coincident with a phase of large-scale immigration to the region (Lejju *et al*., 2005)

All African records (Naivasha, Malawi, Turkana, Tanganyika, Victoria and Mount Kilimanjaro) suggest a return to much wetter conditions and higher lake levels from the end of the 13th century and into the 14th century (Verschuren, 2004). During this period, lake level at Tanganyika fell to their lowest levels and did not recover until the late 1800s. Similarly, Lake Chad was high *c.* AD 1100 and AD 1600, with lower levels during the 15-16th century when East African lake levels were high (Verschuren, 2004). These results suggest that the periodic, wetter conditions and therefore higher lake levels associated with the onset of the LIA are restricted to East Africa; with lake levels in West and South Africa showing lower lake levels at this time.

Lake level reconstructions from western Uganda, however, suggest a more arid climate. This aridity is also evident in the records from Nyamogusingiri and Kyasanduka. However, lake levels do fluctuate somewhat, with Lake Kyasanduka experiencing it some deepening during this period. This open water phase is likely a consequence of the

fluctuating climatic conditions associated with the Little Ice Age[2] (LIA; *c.* AD 1500-1800; Verschuren *et al*., 2000; Stager *et al*., 2005; Russell *et al*., 2007). At Lake Naivasha, the relatively wetter conditions were punctuated by three persistent arid phases and corresponding lower lake levels (AD 1380-1420; AD 1560-1620 and AD 1760-1840; Verschuren *et al*., 2000). Both Nyamogusingiri and Kyasanduka also record fluctuations in their lake levels with particularly low-stands occurring at AD 1380-1400, 1510-1580 and *c.* AD 1640-1680 in Nyamogusingiri and AD 1530 and AD 1610-1680 in Lake Kyasanduka. In the broadest sense, the fluctuations observed at Nyamogusingiri and Kyasanduka bear similarities to those inferred at Lake Naivasha, and appear opposite to changes observed further north in Lake Kasenda (Ryves *et al*., submitted; though this could be due to the much lower resolution at Lake Kasenda, with only 40 samples over the last 1200 years). However, lake levels overall appear to be lower in Nyamogusingiri and Kyasanduka during the main phase of the LIA (AD 1500-1800), compared to the higher recorded levels during the onset (late 15th century) and at the end of the LIA (c. AD 1750).

Lake Nyamogusingiri has high lake levels centred on *c.* AD 1450 and 1750 and at Kyasanduka higher levels or open, freshwater phases occur *c.* AD 1500, 1570, 1740. Inferred lake levels from larger lakes across East Africa at all these times are high (e.g. Verschuren *et al*., 2001; Stager *et al*., 2005). It has been suggested that these high levels occur in response to rising atmospheric $\delta^{14}C$ residual series (Stuiver and Brauzanias, 1989). $\delta^{14}C$ rose during the Wolf (AD 1280-1350), Spörer (AD 1416-1534) and Maunder sunspot minima (AD 1645-1715; Nesje and Dahl, 2000), which broadly correspond to the high levels at Nyamogusingiri and Kyasanduka. There is evidence from Lake Victoria that this relationship between sunspot minima and higher lake levels reversed during the late 19th and early 20th century (AD 1890-1927), coincident with the Dalton sunspot minimum (AD 1790-1820; Stager *et al*., 2005). This reversal caused low lake levels to occur coincident with the Dalton minimum. Lakes Nyamogusigiri and Kyasanduka both record lower lake levels broadly coincident with this period, with low-stands at AD 1850 [Nyamogusingiri] and AD 1810 [Kyasanduka], respectively.

Comparison of the records with reconstructed $\delta^{14}C$ production (a proxy for solar radiation; Figure 8.7) reveals that the observed aridity in the Nyamogusingiri and

[2] Whilst the MWP-LIA transition is suggested to have culminated c. 1400 (Maasch *et al*., 2005), there is no universally accepted or precise definition for the start of, or the duration of the LIA (Maasch *et al*., 2005), however, in East Africa, the main phase of the LIA is often denoted as ~AD 1500 to AD 1800.

Kyasanduka records during the MWP, and the three periods of drought during the 13-18th centuries, are broadly coeval with periods of high solar radiation, and intervening periods of increasing moisture balance coincide with phases of low solar radiation, suggesting that solar radiation contributes to decadal scale rainfall variability (Verschuren, 2004; Stager *et al*., 2005).

Whilst records from Lakes Tanganyika and Turkana are not of comparable temporal resolution to the data presented here, the general trends are consistent. The data from these lakes support the notion of a drier East Africa during the 11th and 12th century and relatively wet during the 13th-18th century (Verchuren *et al*., 2000). Similarly, the incomplete record from Lake Chilwa supports a likely high-stand during the period associated with the LIA (*c.* 1650-1760 in Chilwa; Verschuren *et al*., 2000).

Similar to other lake level inferences from western Uganda (Figure 8.6), levels are high at Nyamogusingiri and Kyasanduka *c.* AD 1690-AD 1800 (and until *c.* AD 1840 in Nyamogusingiri). Levels from Kasenda and Wandakara (north of Nyamogusingiri and Kyasanduka) and Edward provide evidence for increasing lake levels, whilst Victoria, Abiyata (Legesse *et al*., 2002), Naivasha and Kibengo are all at high-stands. It is likely that wet conditions *c.* AD 1750 were confined to a narrow belt along the equatorial region of East Africa. This is further supported by inferred drought at Lakes Malawi (Brown and Johnson, 2005) and Tanganyika (Cohen *et al*., 2005), further south, at the same time.

Despite the generally high levels in Kyasanduka and Nyamogusingiri during the 1700s, there is some evidence for the widely reported late 18th early 19th century drought in Lake Kyasanduka (Nicholson, 1995; 1998; Verschuren *et al*., 2000; Stager *et al*., 2005; Bessems *et al*., 2008; Figure 8.6). Nyamogusingiri documents a decline in lake level several years after Kyasanduka (*c.* AD 1840). It is possible that these two periods of lake level changes are a result of the same external driver; with Kyasanduka being the shallower lake system, an immediate response to climate forcing might be expected, whereas the deep lake Nyamogusingiri may be less sensitive to changes, thus displaying a delayed response to the same forcing mechanism (Figure 8.6). This widespread drought in western Uganda during the late 1700s may also be linked to the decline and abandonment of nucleated settlements to the east. The Late Iron Age was a period of time marked by nucleated Late Iron Age settlements based on cereal agriculture and herding (Sutton, 1998; Ssemmanda *et al*., 2005). These centres were abandoned by AD 1800, and settlements became dispersed with the reliance on pastoralism rather than agriculture (Ssemmanda *et*

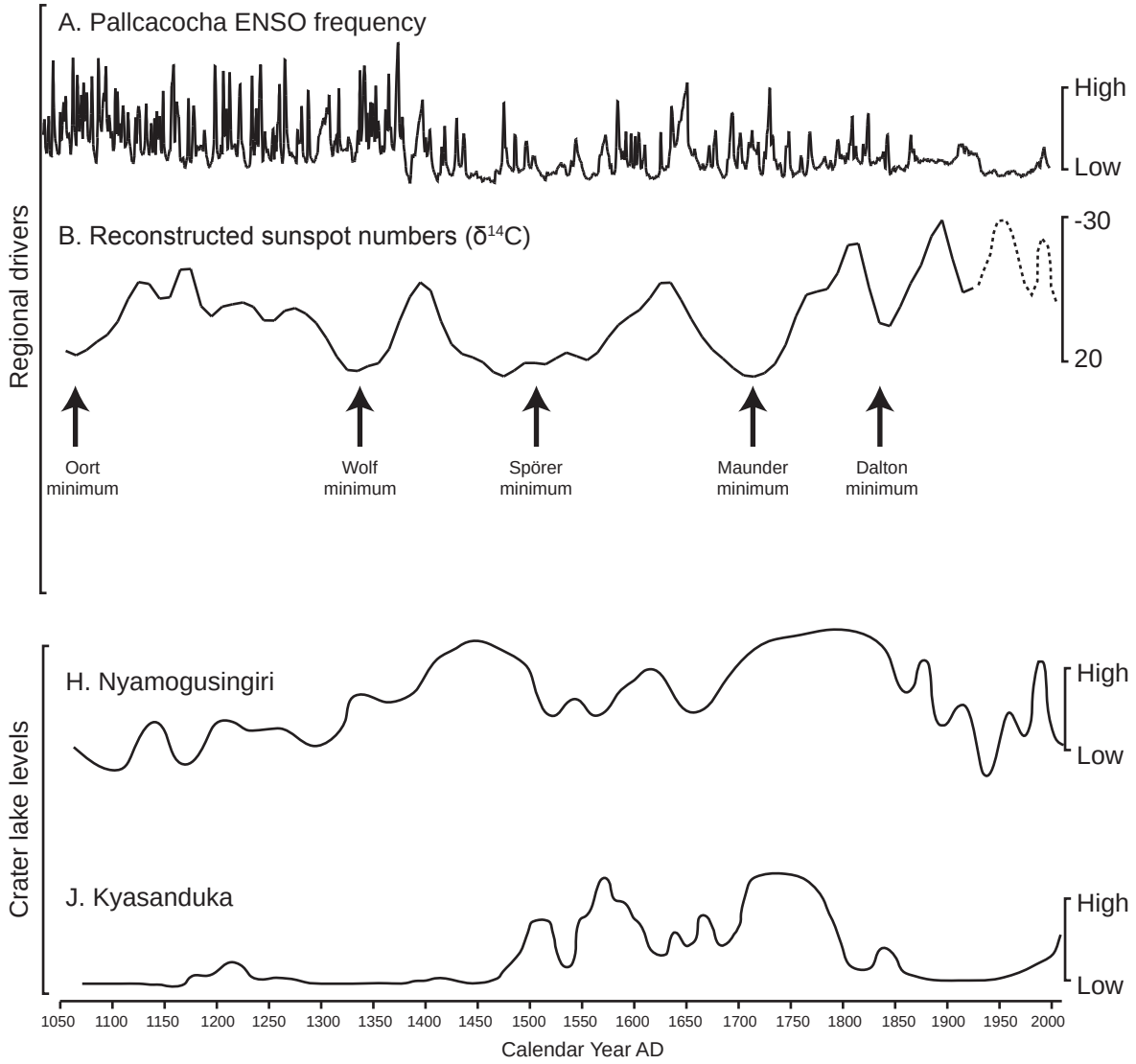

Figure 8.7 *Comparison of climate drivers* **(A-B; A** *Pallcacocha ENSO record [Moy et al., 2002] and* **B** *reconstructed sunspot numbers [Solanki et al., 2004]***)** *to reconstructed lake levels from Nyamogusingiri and Kyasanduka* **(C-D)**.

al., 2005). This prolonged late 18th century drought is suggested to continue into the early 19th century and has been linked to a drought recorded in the oral traditions of the inter-lacustrine region (Webster, 1979), though the reliability of such data is often questionable (Webster, 1979).

A return to wetter conditions since the early 1800s is seen in Kyasanduka (AD 1840) and Nyamogusingiri (AD 1860) as well as across east Africa (Lamb *et al*. 2007, Bessems *et al*. 2008; Ryves *et al*., submitted), and it is likely that this wet period, given the possible errors in the various chronologies, is simultaneous. From the late 19th century, written records and observations can supplement palaeolimnological data (Endfield *et al*., in press). There is documentary evidence of a dry period *c.* AD 1890s and also evidence of low lake levels in Lake Victoria (Nicholson, 1998). These low levels are also observed in lakes Nyamogusingiri and Kyasanduka as well as lakes Edward, Kasenda and Wandakara (Ryves *et al*., submitted) suggesting that this short-lived perturbation was in fact a regional event.

For the most recent phase of environmental change, a study of lake levels across Africa by Street (1980) showed similar trends exhibited in lakes Nyamogusingiri and Kyasanduka: a lake level decline AD 1890 followed by a peak. A long decline in lake level occurred culminating in a low-stand *c.* 1940-1950. The low-stand recorded in Lake Nyamogusingiri *c.* AD 1940, is interpreted as an extremely saline event, characterised by the presence of the saline taxon *Thalassiosira rudolfi*. The inferred conductivity also increases at this time, suggesting that the crater was cut-off from the main basin and operated as a closed-basin system. A high-stand occurred after the heavy rainfall of the early 1960s in Lake Nyamogusingiri, and causes a rise in levels in Lake Kyasanduka. Lower levels in Nyamogusingiri observed in recent decades are perhaps a response to ENSO cyclicity, as suggested by previous studies (Verschuren, 2004).

8.4.1 Drivers of environmental changes over the last 1000 years

Equatorial East Africa has a complex, regional patchwork of climate regimes, with a general eastward trend of increasing aridity. Over long timescales, there are multiple interacting drivers that appear to have a causal relationship with long-term trends in rainfall and lake levels. The causes of century- to millennial-scale climate variability in tropical Africa and the drivers of some of the significant climatic perturbations (e.g. MWP and LIA) are poorly understood (Russell and Johnson, 2005), however several climatic scenarios (hypotheses) have been suggested in the literature

It is now well established that the drought centred on AD 1150, coincident with the northern hemispheric Mediaeval Warm Period (MWP) affected much of East Africa (Verschuren *et al*., 2001; Verschuren, 2004; Russell and Johnson, 2005; Russell *et al*., 2007; this study). The arid conditions associated with the MWP are linked to a period of increased solar activity or changes in the North Atlantic thermohaline circulation (Broecker *et al*., 1999). A study by Ssemmanda *et al*. (2005) suggest wetter conditions prevailed in western Uganda during Mediaeval times, and given these findings contrast with other records, it was hypothesized that strong regional gradients must have existed across the East African plateau. Lakes to south of those studied by Ssemmanda *et al.* (2005; e.g. Lakes Victoria, Edward and Nyamogusingiri), show a decrease in lake levels *c*. AD 1150, with levels dropping from a short-lived high-stand just prior to AD 1150. It is possible both an east to west and north to south gradient may have existed at this time.

Unlike the relative simplicity and widespread aridity of the MWP, the manifestation of the LIA in East Africa appears to be much more complex, with increasing evidence for a climatic gradient during this time (Russell *et al*., 2007). Russell *et al*. (2007) suggest that AD 1500 marked the onset of arid conditions in western Uganda, which also coincide with shifts in settlement patterns (Robertshaw *et al*., 2004). The results from this study, go someway to corroborating the hypothesis of Russell *et al*. (2007) and suggest common anti-phasing between western sites (Kibengo, Kitigata, Edward, Tanganyika, Nyamogusingiri and Kyasanduka) and sites from eastern equatorial Africa (Naivasha, Victoria; Russell *et al*., 2007). This confirms the existence of an east-west gradient in which wet conditions in eastern equatorial East Africa were synchronous with arid conditions in western equatorial East Africa (Russell *et al*., 2007).

The patterns of climate variability across East Africa and their links to changes at higher latitudes is a question that remains to be fully resolved (Barker and Gasse, 2003; Brown and Johnson, 2005; Russell and Johnson, 2005a,b). It has been suggested that mechanisms controlling rainfall anomalies during the LIA are unlike those occurring during the last 100 years (Nicholson, 1986). The southward migration of the inter-tropical convergence zone (ITCZ) in response to cooling at higher latitudes is often cited as the main hypothesis for explaining the changes during the LIA (Baker *et al*., 2001; Haug *et al*., 2001; Brown and Johnson, 2005; Russell and Johnson, 2005a; Russell *et al*., 2007). However, changes in the Indian Ocean dipole (IOD; Marchant *et al*., 2006) coupled with El Niño-Southern Oscillation (ENSO) may be the cause of high rainfall anomalies (Nicholson *et al*., 1997). In addition to this lake level fluctuations in Lake Victoria have

long been linked to sunspots (Brooks, 2003; Stager *et al*., 2005), however the inconsistency of sun–rainfall associations (e.g. during the Dalton Minimum) questions this proposed relationship (Stager *et al*., 2005), unless sun-climate relationships in East Africa are subject to abrupt variability.

ENSO has been cited as an important controlling mechanism of inter-annual variability in East African rainfall on short timescales (2-6 years; Nicholson, 1996) and is often correlated with an increased intensity of rains during the latter part of the year (October-November; 'short rains'). However, whilst ENSO has been shown to be one of the primary determinants of such inter-annual variability in rainfall at low latitudes, its influence over Africa remains controversial (Nicholson and Kim, 1997). Rather than ENSO controlling moisture variability in East Africa, it is more plausible that the Atlantic and Indian oceans are influencing the movement of the ITCZ (Nicholson, 1996). Whilst ENSO is linked to rainfall fluctuations in East Africa, it is more likely that the changes in rainfall are a result of a response to SST fluctuations in the Atlantic and Indian Oceans, which occur in the context of ENSO (Nicholson, 1996). Similarly, Black et al (2003) demonstrated that extreme East African short rains are associated with large-scale SST anomalies in the Indian Ocean, and it is the relationship between El Niño and the IOD that explains the previously described association between El Niño and high East African rainfall. ENSO is most likely the teleconnection linking the northern hemispheric cooling to the migration of the ITCZ (Nicholson, 1996).

Russell and Johnson (2007) also suggest that it is ENSO which is the key factor linking high-latitude cooling, the ITCZ, and moisture gradients within Africa, and models suggest that increased insolation in the southern hemisphere and southward migration of the ITCZ are associated with more intense ENSO years (Haug *et al*., 2001; Moy *et al*., 2002). Russell and Johnson (2007) suggest that it is therefore possible that interactions between the ITCZ and the ENSO system during the Little Ice Age may have triggered a shift toward El Niño–like conditions, increasing rainfall in easternmost Africa, while southward ITCZ migration led to increased aridity in the west.

8.5 Cultural and environmental changes during the last 150 years

As part of this research, the general trends in the sediment flux data from a single core in each lake basin were reconstructed. These core data can provide an integrated record of sediment accumulation (Anderson, 1990a; 1990b). The accumulation of sediments in a lake basin is often highly heterogeneous, due to the variability of depositional processes

both spatially and temporally (Davis, 1976; Dearing *et al*., 1981; Davis and Ford; 1982; Anderson, 1990a; 1900b). Sediment distribution is affected by a number of factors including: topography, shelter and limnological processes that can be influenced by climate (e.g. the process of stratification; Anderson, 1990a). In many cases, accurate and precise chronologies are rare (especially when based on ^{14}C dates). In addition, the reconstruction of trends in the sediment data is more useful, especially when using accumulation rates from a single long core (Dearing, 1994).

A significant and large change in the diatom and sedimentary data is observed in all lakes after AD 1850 and throughout the twentieth century. In terms of the diatom records, in all lakes there is a declining trend in the number of planktonic species (**Chapters 6** and **7**, Figures 6.9, 6.25, 7.5, 7.11 and 7.17) and an increase in the abundance of diatoms with a preference for benthic habitat (or those that are facultatively planktonic). The sedimentary records all suggest an increase in the dry mass accumulation and hence an inferred increase in the amount of organic and minerogenic material being delivered to the lake system. Calculated minerogenic influx rates were compared to changes in the diatom assemblages and diatom valve flux rates from the five lakes studied. Coincident increases in benthic, periphytic and aerophilous taxa and sediment influx rates suggest a causal link between diatom response and catchment disturbance. Although in many instances sediment influx has decreased in the most recent period (late 1990s), the relative abundance of benthic and periphytic taxa remain high. This could be the result of the crossing of a threshold within the lakes, allowing them to remain in an alternative state, or more simply, not enough time has elapsed to allow the lakes to return to previous conditions. The re-occurrence of *Nitzschia lancettula* in Lake Nyamogusingiri may suggest some ecosystem recovery towards pre-AD 1870 conditions (**Chapter 6**, Figures 6.7 and 6.8).

All of the core analyses exhibit an increase in the sediment flux over successive time zones, reaching a maximum between AD 1930 and AD 1990, and all (but not in Kyasanduka) declining to a surface minimum. Although high, these accumulation rates can perhaps be considered estimates and whole basin fluxes (using multiple cores) would need to be calculated to understand the sediment fluxes to the lake and changes in sediment focusing over time (cf. Anderson, 1990b). However, the increases in sediment flux in most lakes manifest as a double peak (Figure 8.8). This is a signature seen in many other lakes around the world affected by human intervention; the occurrence of sediment pulses (e.g. Lakes Nyamogusingiri, Kako and Kigezi) may indicate substantial environmental impact during initial settlement stages, with the first peak related to the removal of catchment

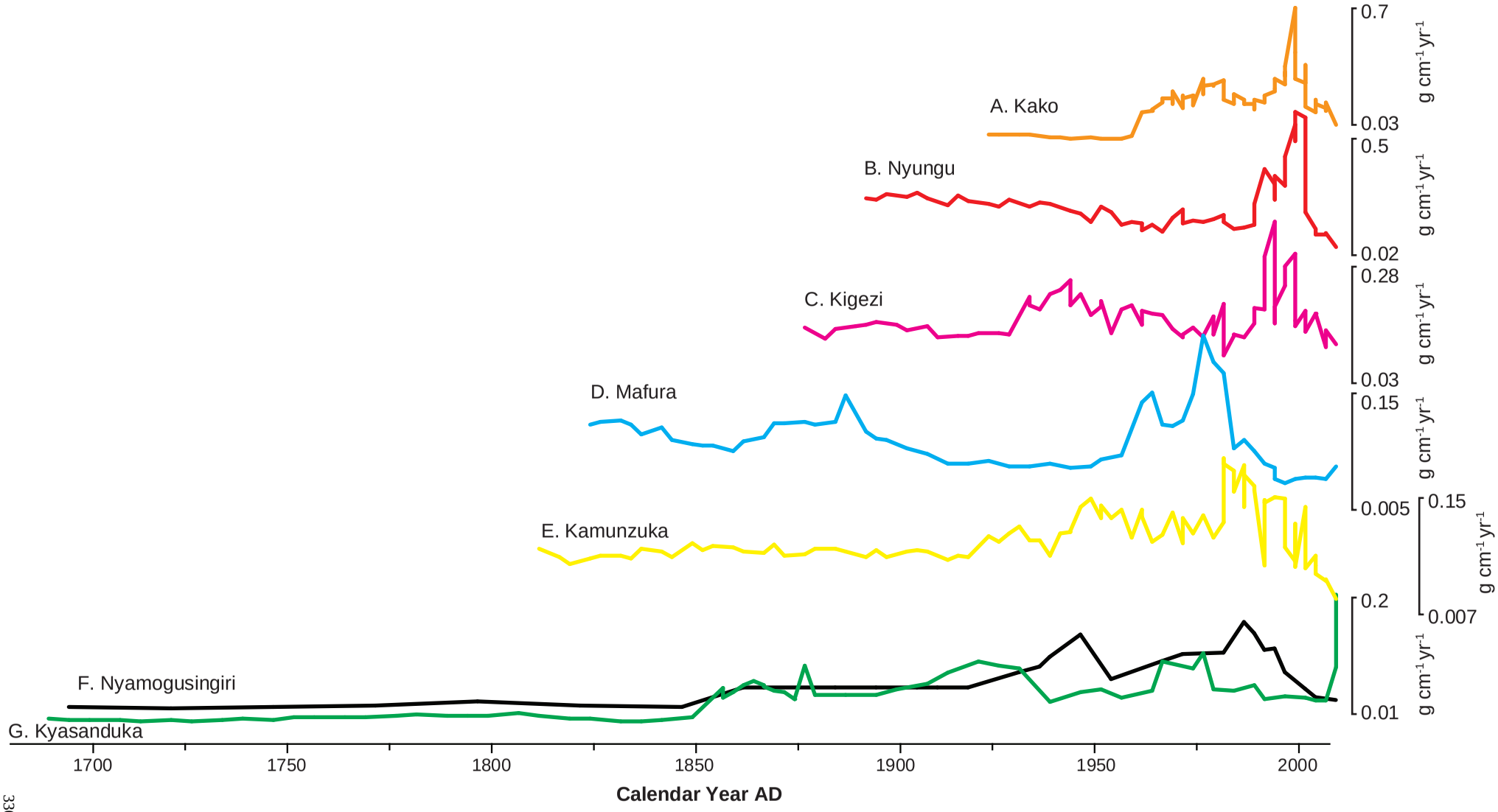

Figure 8.8 *Stacked dry mass accumulation rates for the 7 cores since AD 1700, illustrating the increase in the deposition of sediments in the lake basins over the last c. 50-75 years.*

vegetation, and the second related to the onset of agriculture (cf. Oldfield *et al*., 1980;Fisher *et al*., 2003; Anselmetti *et al*., 2007). Marchant *et al.* (1997) observed substantial wet-season erosion of sediments from forested hillsides around Mubwindi Swamp. The destabilisation of these slopes as a result of vegetation removal, either naturally (fire) or more recently as a result of anthropogenic clearance for agriculture, would lead to the exacerbation of this erosion, especially at times of enhanced precipitation (Marchant *et al*., 1997).

8.5.1 Drivers of environmental changes since AD 1850

The period of major change (AD 1850-present) coincides with the end of the Little Ice Age (LIA, *c.* AD 1800). Prior to this period, lake levels and sunspots in East Africa appear to co-vary (Stager *et al*., 2005); a pairing that seemingly breaks down at the end of the LIA but recovers in the latter 20th century (Figures 8.9 and 8.10). It has been proposed that the LIA was the result of the latest pulse of a 1500-year solar cycle (Mayewski *et al*., 1997; Bond *et al*., 2001). Stager *et al*. (2005) postulate that either the Dalton sunspot minimum marks the last of these 1500-year cycles, or that the sensitivity of lakes to solar (climate) forcing was modified as the African climate system restructured towards the end of the 18th century. It is possible that the breakdown of the relationship between sunspots and lake levels is due to the confounding effects of strong El Niño-Southern Oscillation (ENSO) events throughout the 20th century. These ENSO events are documented to have been 'inconsistent' throughout the 20th century (Nicholson and Yin, 2001; Conway, 2002). A high resolution study of Laguna Pallcacocha in Ecuador reveals fluctuations in ENSO activity over the last *c.* 12,000 years. The high resolution analyses suggest a decline in the frequency of ENSO events over the last 1200 years, with a further decline just prior to AD 1850 (Figure 8.7).

The breakdown of the sunspot-lake level correlations in Lake Victoria is also prominent between AD 1927 and AD 1968 (Stager *et al*., 2005). This period of time coincides with disruptions in climate systems outside of East Africa (Hoyt and Schatten, 1997) suggesting that changes were not only related to solar variability, but perhaps as a response to changes in Indian rainfall (Kumar *et al*., 1999) and the North Atlantic Oscillation index (Jones *et al*., 2001). AD 1927-1968 is a period that records some interesting changes in the sediment flux to the seven lakes analysed in this thesis (Figure 8.8), with many lakes experiencing an increase in the amount of organic and minerogenic material delivered to the lake (*c.* AD 1930), with a second phase of increased

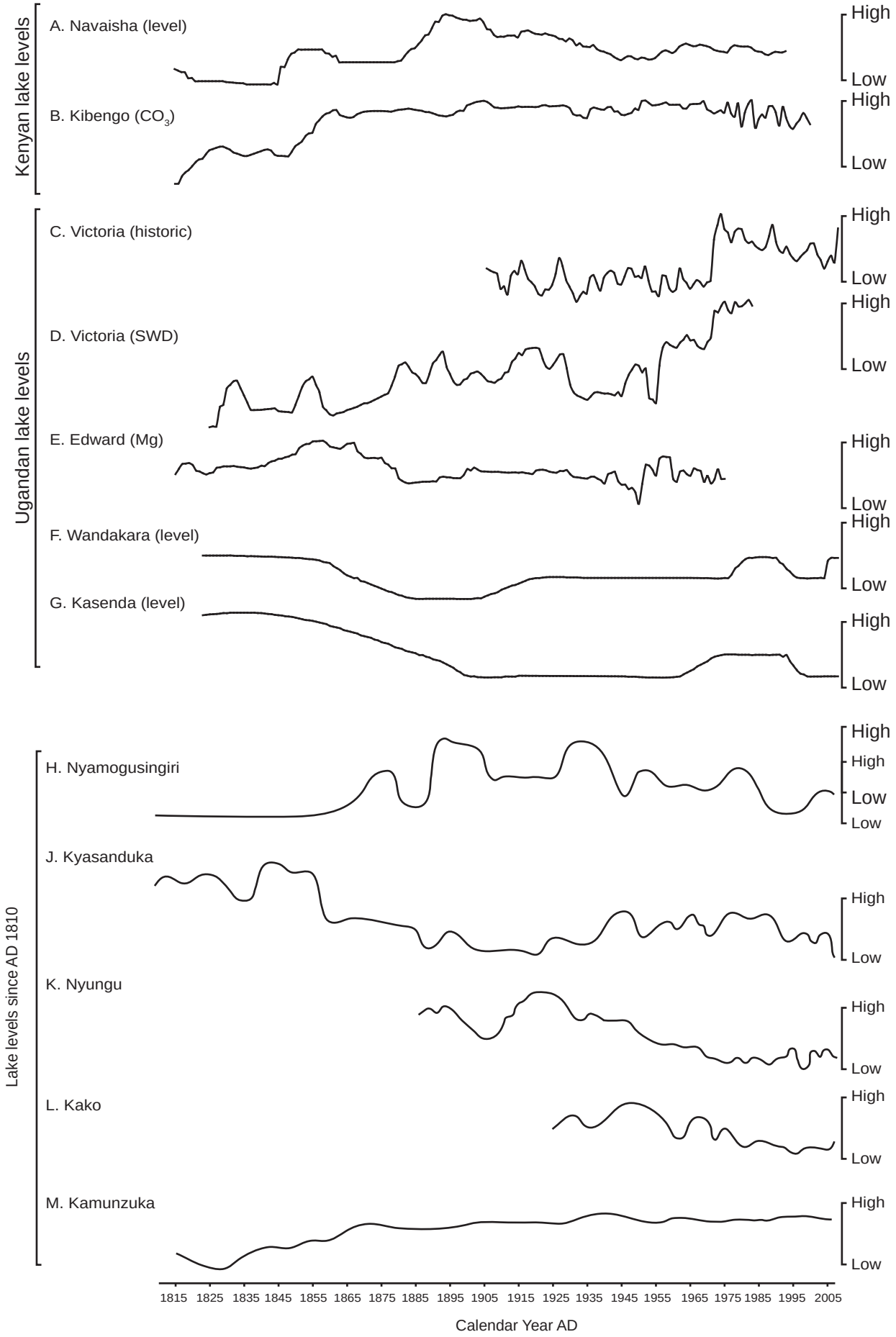

Figure 8.9 *Inferred crater lake levels* **(G-K)** *compared to published lake levels from Uganda and Kenya* **(A-F)** *since AD 1815.*

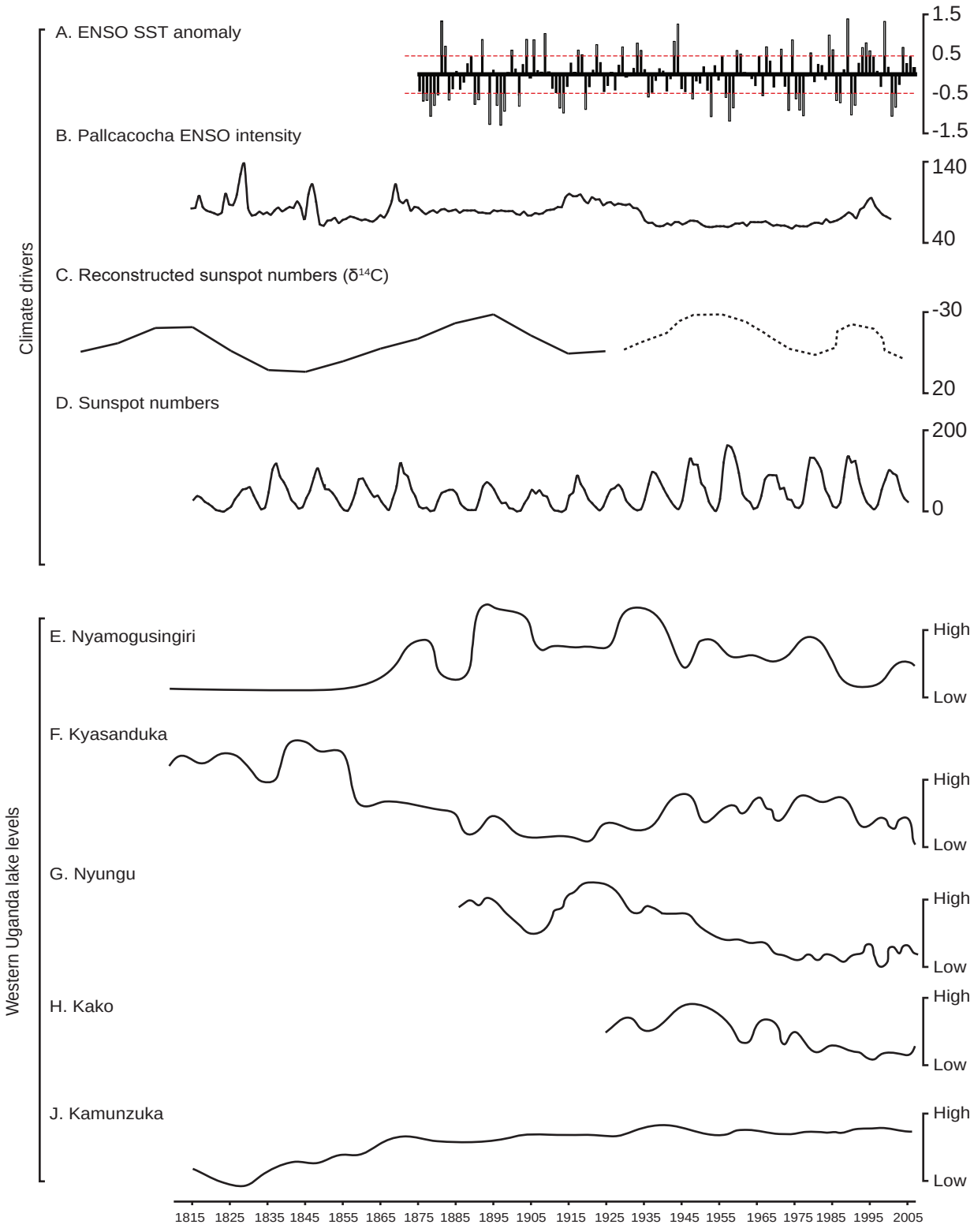

Figure 8.10 *Comparison of climate drivers* **(A-D***; A El Niño-Southern Oscillation [ENSO] displayed as SST anomalies [NOAA – http://www.cdc.noaa.gov/Pressure/Timeseries]*; **B** *Pallcacocha ENSO record [Moy et al., 2002];* **C** *reconstructed sunspot numbers [Solanki et al., 2004] and* **D** *recorded sunspot numbers [NOAA – http://www.cdc.noaa.gov/Pressure/Timeseries]*) *to reconstructed lake levels used in this study* **(E-J)** *since AD 1815.*

sediment delivery between AD 1960 and 1980. Whilst it is likely that some of these changes are, in part due to climate forcing, especially given increasing aridity in East Africa since the 1900s (Karlén *et al*., 1999), it is unlikely that climate alone is the only factor driving the observed large floral and sedimentary changes in the crater lakes of western Uganda.

The 20th century is also a period of time in which human activity impacts on the sediment archives of climate change. The removal of catchment vegetation for small-scale agriculture and plantations would have a large effect on the amount of sediments delivered to the lake. This increase in sediment delivery, observed in the sediment flux data discussed above, also appears to have a profound effect on the diatom flora in recent years, through the increasing nutrient input and/or an increase in lake turbidity. Whilst these changes in sedimentation rates are coincident with recent, prolonged aridity, the changes in the sediment flux of the last 100 years, is unprecedented in many of the records (Kyasanduka, Nyungu, Kako, Kigezi, Mafura and Kamunzuka). The only exception to this is Lake Nyamogusingiri where comparable changes in the sediment flux are seen in the earlier part of the record (*c.* AD 1100). However, all of the evidence suggests a significantly different environment was present at Nyamogusingiri *c.* 900 years BP; the system was dominated by terrestrial vegetation (based on interpretations of organic isotope analyses; **Chapter 6**, Figure 6.11) and the lake was very low, dominated by benthic, saline taxa. The sedimentary record has a soil/peaty-clay unit at the base of the core stratigraphy. Low water content (*c.* 50%) was measured in this unit, and this will have caused an apparent increase in the dry mass accumulation rates through this portion of the record. A further potential problem with the flux rates at Nyamogusingiri stems from the chronological control (AMS ^{14}C dates). Ages were linearly extrapolated between dated horizons, and in some cases this has caused an apparent increase in the accumulation rates. This problem is not apparent in Kyasanduka. Despite problems in the radiocarbon-dated core section of Nyamogusingiri, there is confidence in the dry mass accumulation in the sections of the cores dated by ^{210}Pb; especially given the number of samples dated and the consistency between the records.

It is likely that in many regions of the world, records spanning the last two centuries do not reflect natural sediment yields (cf. Dearing, 1994). A number of lake-based studies in a variety of landscapes have produced records of sediment flux over the last 200 years. This is a period of time that can be well dated by ^{210}Pb and is coincident

with the increasing pressures of human activity on the natural environment (cf. Dearing, 1994).

Catchment disturbance in western Uganda during the last two hundred years may be attributed to the exploitation of resources during the early colonial period and the influx of people to the west of Uganda following the onset of political instability (Taylor and Robertshaw, 2001). The impact of human activity on lake catchments over the last 200 years has been highlighted by a number of other studies outside Africa. For example, research on Frains Lake in Michigan, illustrated the erosional impact of catchment vegetation clearance from AD 1800 (Davis, 1976). The clearance of catchment woodland caused increases in erosion rates to almost 80-times the pre-settlement rates (Davis, 1976). However, there are few studies based on sediment flux from the tropics (Deevey *et al*., 1979; Dearing, 1994; Anselmetti *et al*., 2007), thus the results presented here are amongst the first data from tropical East Africa relating to sediment yields over the last 200 to 1000 years.

Exceptions to this generalisation are studies from Guatemala, where the rise and decline of the Mayan civilisation is clearly recorded in the sediment record (Deevey *et al*., 1979). Through the process of deforestation and agriculture, the Mayan civilisation caused the acceleration of topsoil erosion, leading to the increased sedimentation to lake basins and depleted soil nutrients (Deevey *et al*., 1979; Anselmetti *et al*., 2007). Similarly, studies of the cultural and climatic history of Lake Cobá within a Mayan city indicate an increase in the sediment influx to the lake, concomitant with a period of disturbance as a result of clearance for agriculture (Leyden *et al*., 1998). Whilst the palaeoecological record ties in with the well documented archaeological record, the climate signal from Lake Cobá has been muted by the persistent human disturbance, to such an extent that documented (historical) droughts cannot be reconstructed from the sedimentary record (Leyden *et al*., 1998).

In many of these lake records, the evidence for catchment disturbance occurs as an increase in the input of sediments to the lake system (Oldfield *et al*., 1980; Worsley and Oldfield, 1988). The disturbance in these lakes often falls into two discrete periods separated by a period of relatively low impact. In most cases, the first period of disturbance is related to initial forest clearance which increases sediment influx to lakes. The latter period of increased sedimentation rates is likely a result of an increase in the intensification of cultivation (Worsley and Oldfield, 1988; Deevey *et al*., 1979; Anselmetti *et al*., 2007).

These patterns are mirrored in the lake records analysed in this investigation (Figure 8.8) with peaks in AD 130 and 1960s-1980s.

The increase in the delivery of sediments to the lake systems is also likely to have caused an increase in the amount of nutrients delivered to the lake system. Increasing nutrients can lead to the deterioration of lake water quality, largely through eutrophication. Many lakes in the developing world are experiencing eutrophication, salinisation and pollution as a consequence of increasing human pressure, and problems with surface water quality is one of the twentieth century's largest and most widespread environmental problems (Smith, 1998; Dong *et al*., 2008).

Cultural eutrophication of lake waters occurs as result of human activity within the lake's catchment that increases the nutrient input to the aquatic ecosystem, which can in turn increase algal productivity and can lead to water quality issues and deep water anoxia (Smith, 1998; Ekdahl *et al*., 2004). Whilst many studies have shown that early societies have modified catchments (e.g. removal of vegetation for agricultural purposes) and therefore water chemistries of lakes in Europe (Fritz, 1989; Renberg *et al*., 1993; Bradshaw *et al*., 2005), tropical America (Deevey *et al*., 1979; Anselmetti *et al*., 2007) and North America (Ekdahl *et al*., 2004), the study of human impacts on lacustrine ecosystems and the onset of cultural eutrophication in East Africa, has been limited to the larger lakes, such as lake Victoria (Hecky, 1993; Verschuren *et al*., 2002) and Malawi (Hecky, 2000; Puchniak *et al*., 2005). The only exception to this is a comparative study of data over a 30-year span (1971-2000) at Lake Saaka, near Fort Portal, which suggested that eutrophication had occurred over the time period in question. Although this study was based on one dataset collected in 1971 (Melack, 1978) and compared to data collected during monthly monitoring between 1995 and 1998, it indicated that the lake had been undergoing cultural eutrophication since the 1970s. This eutrophication was attributed the enlargement of a prison farm and agricultural expansion on the flanks of the crater as well as the introduction of Nile perch in the 1970s which would have caused alterations to the food web, leading to the observed increase in trophic state (*Lates niloticus*; Goldschmidt *et al*., 1993; Crisman *et al*., 2001).

In the present study, the increases observed in organic accumulation rates and decreases in organic-matter C/N values (**Chapter 6**, Figures 6.5, 6.11, 6.21 and 6.27) are likely an indicator of increased photosynthetic algal activity stimulated by increased nutrient input (cf. Ekdahl *et al*., 2004). This change in the organic isotope record in conjunction with shifts to higher nutrient indicative taxa, such as *Cyclotella meneghiniana*

and *Nitzschia palea* (cf. Lakes Kyasanduka and Nyamogusingiri) are often signs of eutrophication (Dong *et al*., 2008). The results from this study bear similarities to those from other continents that show long lasting effects of deforestation for agriculture upon limnological systems that are currently protected (Deevey *et al*., 1979; Fritz, 1989; Renberg *et al*., 1993). It is likely that changes in catchment hydrology (both natural and/or anthropogenic) and the increase in nutrient inputs since the early 1900s has fundamentally, and perhaps permanently, modified the lake ecosystems under investigation. This in turn would alter the response of the individual lakes to ongoing climate changes in the region. Similar isotope studies in Uganda show enhanced phytoplankton production since AD 1950 and AD 1970 in Lakes Kanyanmukali and Chibwera (Bessems *et al*., 2008). Only the change in Kanyanmukali is attributed to anthropogenic eutrophication as subsistence agriculture occurs within the lake's catchment; conversely Chibwera's catchment is currently protected within the QENP and the possible onset of eutrophication is attributed to the pressure from grazing hippo (cf. Macintyre, 1975).

8.6 Potential drivers of changes in the crater lake records

8.6.1 Core trajectories

One approach for trying to unravel changes in the diatom records through time is to compare the diatom responses from the lake cores directly to the surface sediments and selected environmental variables used in the diatom training set (see **Chapter 5**). A canonical correspondence analysis (CCA) with forward selection was used to define which environmental variables influenced the diatom distributions and abundances in the modern calibration data set. The statistically significant environmental variables $p \leq 0.05$ (with Bonferroni adjustments) that were included were depth, conductivity and total nitrogen (see **Chapter 5** for more detail). The down-core diatom samples were then fitted as passive samples into the CCA ordination space (cf. Velle *et al*., 2005). Figure 8.11 shows the results of this ordination, illustrating the time-trajectories from five sediment cores (B, bottom; T, top) in an attempt to try and assess the long-term patterns in the development of the fossil assemblages with reference to the diatom–environmental relationships in the modern calibration set (see **Chapter 5**). This technique can help to identify which environmental variables have influenced the down-core diatom assemblages through time (Birks *et al*., 1990).

The results indicate that Lakes Nyungu and Nyamogusingiri have responded in a similar way over time, with the most recent samples being very closely related. Both lakes oscillate along the total nitrogen variable, with Nyamogusingiri also being influenced by changes in conductivity over time. Lakes Kako and Kamunzuka are clearly located at the fresher end of the conductivity scale throughout their record, with apparent fluctuations in depth and minor conductivity fluctuations occurring in the middle sections of their records. The apparent fluctuations in 'depth' at Lake Kako may also be linked to changes in the clarity/turbidity of the water column (**Chapter 7**, *section 7.4.5*). Lake Kyasanduka has by far the most complex record (Figure 8.11c) showing some major changes throughout its 1000 year record, encompassing changes in TN, depth and conductivity over time. The trajectories indicate a clear split in the data, with two groups apparent. Group 1 contains lakes Nyamogusingiri, Kyasanduka and Nyungu suggesting that all have responded similarly over time, and even though they present differences in their diatom assemblage data, these three lakes almost certainly are responding to similar drivers. Lakes Kamunzuka and Kako form group 2, again suggesting a similar driver controlling these two lakes, though given their separation from each other, does suggest some of the drivers are more significant in Lake Kako, with Kamunzuka being located close to the centroid (mean).

8.6.2 Redundancy Analysis

To investigate the environmental factors that might be driving changes in the aquatic environment a set of predictor (e.g. organic and minerogenic accumulation rates, sunspots, regional lake levels; Table 8.2) and response (diatom taxa) variables were created for the two time scales (1000 years and 150 years) for the 5 lakes with diatom data. Ordinations were carried out using CANOCO 4.5 (ter Braak and Šmilauer, 2002). DCA of the diatom data showed the gradient lengths to vary from 1.004 (Kamunzuka) to 1.76 (Kyasanduka). Where the gradient length was >1.5 standard deviations (Nyungu, Nyamogusingiri and Kyasanduka) a unimodal technique (CCA) was employed; where the standard deviation was <1.5 (Kamunzuka and Kako) a linear model (RDA) was used. For all lakes a CCA or RDA of the whole dataset, using sediment age as an explanatory variable with Monte Carlo permutation tests (n = 999 unrestricted permutations) showed that sediment age was significantly correlated with the diatom data (p <0.001). As a result, sediment age was included as a covariable in all subsequent ordinations to partial-out the variance resulting

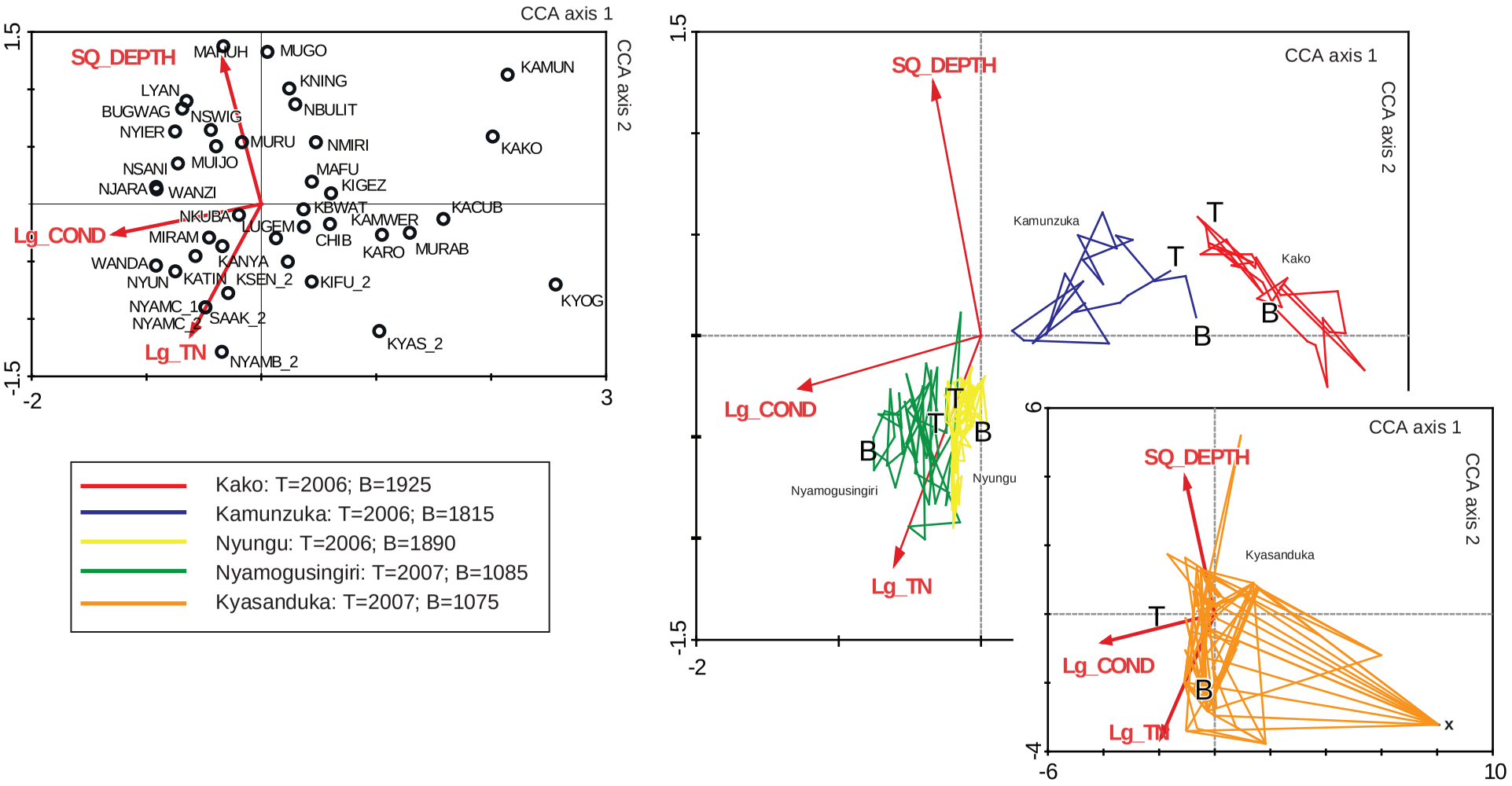

Figure 8.11 *Trajectories for the core samples.* **(A)** *CCA of surface-sediment diatom samples and the 3 forward-selected variables (see* **Chapter 5***).* **(B)** *Core trajectories. Core samples plotted as passive samples over the surface sediment CCA; (***C** *inset) Trajectory of Kyasanduka fossil diatom samples. The point marked* ***x*** *on Kyasanduka (***C** *inset) does not consist of one single point, rather it is made up of 6 points, all of which coincide with major switches in the diatom flora (and are coincident with some of the statistical zones).*

from the sediment age, thus making the variation explained by other variables easier to interpret (Odgaard, 1994).

For the longer core sequences (1000 years, Lake Nyamogusingiri and Kyasanduka), to try and explore changes in predictor and response correlations, the analyses of shorter time periods were made. It was not possible to split and analyse the core samples into groups related to the diatom zones calculated in **Chapters 6** and **7**, as many of the results were deemed insignificant, with a very small gradient, this was most likely due to the small sample sizes in some cases (*c*. 4 or 5). The cores were therefore split into groups of the same sample size (15 = Nyamogusingiri; 40 = Kyasanduka), whilst these samples are even spatially, it should be noted that they are temporally uneven (cf. Tables 8.10 and 8.11).

Distinct groups (7 for Nyamogusingiri and 5 for Kyasanduka) were analysed, overlaps were not used as has been used in other studies (cf. Bradshaw *et al*., 2005) due to the computational complexity of having to process between 130 and 240 samples. For each sample group, a DCA was applied to the diatom data to check the gradient length (which in most cases demonstrated a linear response), and then partial RDA (with sediment-age as a covariable) was applied to the predictor and response variables. Analyses used down-weighting of rare species and Bonferroni-adjusted forward selection to identify a subset of significant explanatory variables (see also **Chapter 5**, *section 5.5.3*). Monte Carlo permutation tests (n = 999 unrestricted permutations) were used to test the significance of the remaining variables.

CCA or RDA were carried out to assess: (i) which of the specific drivers were significant in explaining change in the fossil assemblages (e.g. sunspots, ENSO) and (ii) to explore whether the data shared any similarities with other proxy records of environmental change from across East Africa (e.g. similarities to other lake level records: e.g. Lakes Victoria and Kasenda). The analyses highlight some of the main drivers behind the changes observed in the different records. The inclusion of other proxy lake level data also helps to illustrate similarities between the various records. These similarities could be interpreted as either regional scale events (e.g. Medieval Warm Period) or perhaps that the similar lake records share a similar driver (e.g. if similar to Lake Victoria levels, the lake may be responding to solar forcing).

The results of CCA and RDA for the 150 year records are shown in Tables 8.3-8.7. Full core CCA for RDA for Nyamogusingiri and Kyasanduka are shown in Tables 8.8 and 8.9, and the results for RDA on subsets from Lakes Nyamogusingiri and Kyasanduka are

Table 8.2 *Environmental variables used in the RDA and CCA. The data were not transformed prior to analysis as all indicated a Gaussian distribution when tested in CALI.*

Variable	Code	Notes	Reference
Dry Mass Accumulation Rate	DMAR	Calculated flux data (g $cm^{-2}yr^{-1}$)	This study
Organic flux	ORGAN	Calculated flux data (g $cm^{-2}yr^{-1}$)	This study
Minerogenic flux	MINER	Calculated flux data (g $cm^{-2}yr^{-1}$)	This study
$\delta^{13}C$ – bulk organic isotopes	$\delta^{13}C$	‰ VPDB	This study
CN	CN	Atomic ratio	This study
Lake Victoria level	VIC_L	Expressed as % of shallow water diatoms (high % = low inferred lake level)	Stager et al. (2005)
Lake Kasenda level	KASEN	Quantified using a scale of 1-4 (1 = low, 4 = high)	Ryves et al. (submitted)
Lake Kitigata – magnetic susceptibility	KITI	High magnetic susceptibility = low lake levels	Russell et al. (2007)
Lake Kibengo - calcium carbonate content	KIBEN	High carbonate content = low lake levels	Russell et al. (2007)
Lake Naivasha level	NAIV		Verschuren et al. (2000)
Sunspot numbers – $\delta^{14}C$ reconstruction	$\delta^{14}C$		Stuiver and Becker (1993)
Pallcacocha ENSO frequency	PALLCAC		Moy et al. (2002)
Lake Wandakara level	WAND	Quantified using a scale of 1-4 (1 = low, 4 = high)	Ryves et al. (submitted)
El Niño Southern Oscillation - SST anomaly	ENSO		http://www.cdc.noaa.gov/Pressure/Timeseries
Indian Ocean Dipole – SST anomaly	IOD		Kaplan (1998)

presented in Tables 8.10 and 8.11. Whilst these samples are even in “space” (in terms of sample size), they represent uneven periods of time. These subsets were chosen as they permitted statistically significant (p <0.001) variables to be assessed. The highlighted variables (Tables 8.10 and 8.11) are those that were selected as being statistically significant in 'explaining' variation in the diatom data. In addition to this, the age range of samples in the subset and percentage of variation in the diatom data 'explained' by the selected variables are shown (cf. Bradshaw *et al.*, 2005).

RDA and CCA of the full core datasets of predictor and response variables gave statistically significant models (p <0.001) with between 2 (Kamunzuka) and 5 (Nyungu and Nyamogusingiri) independently significant variables explaining between 11% (Kyasanduka) and 30% (Nyamogusingiri) of the variation in the diatom data over the last 150 years (Tables 8.3-8.7). The results for full core CCA spanning the last 1000 years for Nyamogusingiri and Kyasanduka gave statistically significant models with 6 and 7 (respectively) independently significant variables explaining around 24% of the variation in both datasets (Tables 8.8 and 8.9).

The results from the CCAs of the subsets from Nyamogusingiri and Kyasanduka are presented in Tables 8.10 and 8.11. For each subset, DCA suggested that the diatom response was linear (axis 1 gradient length <1.5). Only those predictor variables that were significant in explaining diatom variance for each subset are shown and the total variance for each subset and the total variance explained is given for each subset. All subsets (7, Nyamogusingiri; 5 Kyasanduka) produced statistically significant models based on the selected variables ($P < 0.01$).

Canonical correspondence analyses of the predictor and response variables from the full cores spanning the last 150 and 1000 years suggest that different processes have influenced diatom assemblage through time and that change in the aquatic ecosystem has had different triggers. The periods represented overlap and so only major trends are discussed. Furthermore, correlations are scale-dependent: those demonstrated for diatoms and environmental variables at the century-millennial scale may not be the same as those observed at shorter timescales (Bradshaw and Anderson, 2003; Bradshaw, 2005). The correlations are complex and although not necessarily reflecting direct cause and effect relationships, suggest some general patterns in the response of the diatoms to impacts on the lake ecosystem. Where samples have high loadings with levels from other lake sequences (e.g. Wandakara and Kasenda), they tend to be linked to higher levels at

Table 8.3 *Results of RDA of the 2 forward selected (FS) environmental variables at Lake Kamunzuka. The unique variance explained by each variable is also given.*

FS Variable	Canonical eigenvalue	% variance	*p*-value
All (2)	0.294	29.4	0.001
ENSO	0.165	16.5	0.001
$\delta^{14}C$	0.117	11.7	0.014

Table 8.4 *Results of RDA of the 3 forward selected (FS) environmental variables at Lake Kako. The unique variance explained by each variable is also given.*

FS Variable	Canonical eigenvalue	% variance	*p*-value
All (3)	0.254	25.4	0.001
Kasenda	0.056	5.6	0.005
$\delta^{14}C$	0.052	5.2	0.006
Wandakara	0.048	4.8	0.019

Table 8.5 *Results of CCA of the 5 forward selected (FS) environmental variables at Lake Nyungu. The unique variance explained by each variable is also given.*

FS Variable	Canonical eigenvalue	% variance	*p*-value
All (5)	0.232	22.0	0.001
$\delta^{14}C$	0.056	5.3	0.001
Kitigata	0.032	3.0	0.001
Mineral	0.03	2.9	0.002
Wandakara	0.023	2.2	0.008
Kasenda	0.022	2.0	0.006

Table 8.6 *Results of CCA of the 5 forward selected (FS) environmental variables at Lake Nyamogusingiri (last 150 years). The unique variance explained by each variable is also given.*

FS Variable	Canonical eigenvalue	% variance	*p*-value
All (5)	0.384	30.5	0.001
$\delta^{14}C$	0.151	12.0	0.001
Organic	0.104	8.3	0.001
Kasenda	0.063	5.0	0.001
Wandakara	0.040	3.2	0.001
Naivasha	0.034	2.7	0.001

Table 8.7 *Results of CCA of the 3 forward selected (FS) environmental variables at Lake Kyasanduka (short core, last 150 years). The unique variance explained by each variable is also given.*

FS Variable	Canonical eigenvalue	% variance	*p*-value
All (3)	0.098	11.0	0.001
$\delta^{14}C$	0.032	3.6	0.001
Mineral	0.027	3.1	0.001
Wandakara	0.025	2.8	0.008

Table 8.8 *Results of CCA of the 6 forward selected (FS) environmental variables at Lake Nyamogusingiri (long core, last 1000 years). The unique variance explained by each variable is also given.*

FS Variable	Canonical eigenvalue	% variance	*p*-value
All (6)	0.394	23.9	0.001
Organic	0.071	6.8	0.001
Mineral	0.050	4.8	0.001
$\delta^{13}C$	0.041	4.0	0.001
$\delta^{14}C$	0.037	3.7	0.001
Kasenda	0.029	2.9	0.001
Kitigata	0.019	1.9	0.001

Table 8.9 *Results of CCA of the 7 forward selected (FS) environmental variables at Lake Kyasanduka (long core, last 1000 years). The unique variance explained by each variable is also given.*

FS Variable	Canonical eigenvalue	% variance	*p*-value
All (7)	0.433	24.6	0.001
Organic	0.094	8.7	0.001
CN	0.041	4.0	0.001
$\delta^{14}C$	0.032	3.2	0.001
Kitigata	0.023	2.3	0.001
Kasenda	0.021	2.1	0.001
Naivasha	0.018	1.8	0.001
$\delta^{13}C$	0.016	1.6	0.001

those sites, equally samples at the opposite ends of the vector are linked to lower inferred lakes levels. The reverse is true for $\delta^{14}C$, higher loadings suggest a lower number of sunspots (due to the inverse relationship between $\delta^{14}C$ and sunspot numbers). Where the records bear similarities to other records from across Uganda, it can perhaps be inferred that the lake level fluctuations are a regional signal and where records bear similarities the lake level from Naivasha, it is most likely an East African signal.

Many of the lakes, over the last 150 years and 1000 years, exhibit similar drivers that explain significant variation in the diatom data (Tables 8.3-8.11). All record suggest some link to $\delta^{14}C$ (a proxy for sunspot numbers), as well as similarities to other records (inferred lake levels) from western Uganda, suggesting some coherence of regional lake level fluctuations over the time period in question. Results from Nyamogusingiri also suggest a connection between the changes in Uganda and other areas of East Africa (Naivasha lake level identified as a significant driver). In the more recent past, the influx of minerogenic or organic matter appears to be important in explaining the variation in the diatom data.

The RDA results from the subsets of longer cores, suggest that in lower sections of Nyamogusingiri (AD 1085-1240) the flux of organic material and Lake Kasenda levels are significant predictor variables, explaining 18.9% of the total diatom variance, at this time, inferred lake levels at Nyamogusingiri and Kasenda are low (Table 8.12) and this time period coincides with the arid phase associated with the MWP. A section follows where the diatom data from Nyamogusingiri bear similarities to lake level at Kitigata and $\delta^{14}C$ (a proxy for sunspot numbers, Solanki *et al*., 2004; AD 1250-1480). During this period inferred lake levels from Nyamogusingiri and Kitigata are low and rise over the period, this period is also coincident with two sunspot minima and one maximum (the Wolf and Spörer minimum). The lake levels from Nyamogusingiri are high during the sunspot minima. Between AD 1495 and AD 1590 Lake Kasenda is a significant driver of diatom changes, though at this time lake levels in Nyamogusingiri are inferred to be generally lower than previous lake level, but does show a peak *c*. AD 1550 (coincident with high lake levels at Kasenda). $\delta^{14}C$ is also an important driver *c*. AD 1600-1875, a period of time coincident with the Maunder and Dalton sunspot minima. In the last 150 years (AD 1880-1935) changes in $\delta^{13}C_{org}$ predict changes in the diatom data, with $\delta^{13}C_{org}$ and C/N suggesting a shift towards increasing algal productivity. More recently, Nyamogusingiri bears similarities to lake levels from Kitigata (AD 1940-1980) and Kasenda (AD 1980-

2000; generally a period of increasing lake levels). The flux of organic matter over the last 20 years (AD 1980-2000) is important in explaining diatom variance.

Similar drivers, during similar time periods are also observed in the RDA of subsets from Lake Kyasanduka, with the flux of minerogenic material and (low) lake levels at Kasenda significant between AD 1070-1480 (coincident with MWP drought and explaining 15.1% of the variance in the diatom data). $\delta^{14}C$ and C/N are significant drivers AD 1480-1755, a period coincident with the Spörer and Maunder sunspot mimima and a sunspot maximum. The C/N during this period is indicative of decreasing terrestrial impact on the lake and the increasing importance of algal productivity. Lake levels from Kasenda and Kitigata explain significant variance between AD 1760 and 1900, a period of generally declining lake levels in Kyasanduka. Similar to Nyamogusingiri, in the most recent past (AD 1950-2000), sediment flux to the lake (minerogenic) is the most significant driver in explaining the diatom data.

Some minor differences can be observed between the full core CCA and the RDA of subsets from the two longer core sequences, with the full core sequences suggesting that additional variables are perhaps important (e.g. Nyamogusingiri, minerogenic flux; Kyasanduka $\delta^{13}C$ and Naivasha levels). The full core CCA tends to identify the general trends within the data, and interestingly suggests that some of the general patterns observed in Kyasanduka are comparable to some trends in the Lake Naivasha data, suggesting some of the responses observed in the diatom data from Kyasanduka may well be the result of climatic or environmental perturbations affecting East Africa.

Table 8.10 *Results of the moving window RDA on the samples from Lake Nyamogusingiri.*

Year AD	Organic	Kasenda	Kitigata	$\delta^{13}C_{org}$	$\delta^{14}C$	% explained
2000 - 1981	■	■				18.7
1979 - 1939			■			11.6
1937 - 1882				■		11.9
1877 - 1602					■	9.0
1594 - 1488		■				11.8
1480 - 1251			■		■	28.9
1243 - 1086	■	■				18.9

Table 8.11 *Results of the moving window RDA on the samples from Lake Kyasanduka.*

Year AD	Mineral	Kitigata	Kasenda	$\delta^{14}C$	C/N	% explained
2000 - 1952	■					10.9
1950 - 1900		■				7.4
1898 - 1761			■			7.3
1755 - 1487				■	■	23.3
1478 - 1074	■		■		■	15.1

The results do illustrate changes in drivers through time, and in many cases this can involve subtle changes. Both lakes indicate a general trend from a sequence driven by sedimentary fluxes (organic flux, Kyasanduka; minerogenic flux, Nyamogusingiri) *c.* AD 1000, to sections of the record driven by changes in $\delta^{14}C$ and showing similarities to lake levels from Kitigata, Kasenda (Nyamogusingiri), Naivasha and Kitigata (Kyasanduka). In the more recent past a shift to drivers relating to sedimentary proxies is also apparent. If there were more samples available, it would be interesting to run the RDA on subsets from the shorter cores in a similar manner to the longer core sequences to try and understand shifting drivers through time and to see if there is a regional coherence of drivers over the short term. This approach may also help us in some respects to try and understand the interaction of natural and anthropogenic drivers on lake ecosystem response.

This technique (RDA) allows a unique insight into the data that would not be apparent in the direct comparison of the crater lake (level) records to other published work. This is particularly true in the case of Kamunzuka, where there is very little change evident in the *Gomphonema* dominated record. However, multivariate investigations illustrate that even minor fluctuations in the diatom data may be significant (p <0.001) in response to external drivers. Furthermore, this study shows that the correlations are scale-dependent (cf. Bradshaw and Anderson, 2003; Bradshaw *et al*., 2005). For example, the correlations between diatoms and drivers at the sub-millennial scale are different to those observed at shorter timescales (Tables 8.6-8.9). The correlations alluded to are complex, and may not be the result of a 'cause and effect' relationship, yet they do reflect the general patterns of response of the diatom assemblages to various impacts on the lake ecosystem over time (cf. Bradshaw *et al*., 2005).

8.7 Summary

Reconstructions over the last 1000 years can be beset with problems associated with the dating of these sediments (the period between ^{210}Pb and ^{14}C) and problems with associated with ^{14}C dating, with the need to use terrestrial macrofossils (see section *8.8.2)* as well as the confounding impact of humans on the sediment climate record (Ssemmanda *et al*., 2005). There is an increasing need to improve the understanding of the history of human-environment interrelationships in tropical Africa (Taylor and Robertshaw, 2001), with one of the most pressing issues being the separation of 'natural' and 'anthropogenic' changes in the sedimentary record.

Taylor and Robertshaw (2001) provided an overview of evidence for human impacts within the interlacustrine region of East Africa, with specific reference to western Uganda. There are cases in Africa where, despite rich archaeological changes, human induced changes cannot be identified in the sedimentary record (e.g. Manga grasslands in Nigeria; Salzmann and Waller, 1998). It is often assumed that human disturbance within Africa is widespread and ecologically disruptive and where there is a lack of pollen evidence, human impact is often identified by evidence of burning and clearance (Taylor and Robertshaw, 2001). However, there is growing evidence that whilst there may be a long history of human impact in Africa, many early cultures most likely relied on shifting cultivations, making use of natural forest gaps (perhaps in some cases caused by the foraging by elephant; Laws *et al*., 1975). It is now also thought that some forms of agriculture actually promote the growth of forest (such as the cultivation of palm oil; Taylor and Robertshaw, 2001). It is therefore likely that many of the lake records, as suggested in this study, record only the occurrence of intensive, pervasive and permanent forms of human impact which occurs later in the sediment records and in African history (cf. Taylor and Robertshaw, 2001).

During the last 50-75 years in particular, human impact has increased and partially obscured the climate record within the sediments of Lakes Kyasanduka and Nyamogusingiri, and the high sedimentation rates can be confidently attributed to changes in land-use as a result of human activity within the lake catchment (cf. Lakes Kasenda and Wandakara, Ssemmanda *et al*., 2005). These findings may have implications for how Ugandan lakes can be better managed in the future (i.e. to reduce the effect of human influence on their systems), and how records of climate are to be monitored from these lakes from now on (i.e. to assess the response of lakes to future environmental changes).

8.8 Considerations

Having discussed the implications of results from lake studies, and placed findings into wider context, this section considers some of the further considerations and problems that were encountered during the study; namely those related to (i) diatom taxonomy and valve morphology, and (ii) radiocarbon dating of African lake sediments.

8.8.1 Diatom taxonomy and morphology

This section considers several issues that were highlighted during this research with regards to taxonomic problems and morphometric differences within certain diatom species.

8.8.1.1 Taxonomy

Diatom taxonomy is constantly being updated, with diatoms being classified into new genera (cf. Round *et al*., 1990). Initially, the diatom taxonomy for this thesis was reliant upon the regional key of Gasse (1986) and generic keys of Krammer and Lange-Bertalot (1988-1991), Germain (1981) and Patrick and Reimer (1966; 1975), all of which rely on older taxonomy (e.g. they do not utilise the new genera *Pseudostaurosira* [*Fragilaria*], *Diadesmis* and *Luticola* [*Navicula*]), and as a result older taxonomic names were initially in use. The use of the older names also allowed synonymy between the EDDI taxon codes used to identify the species in statistical packages and for the purposes of the transfer function (see **Chapter 5**). In an effort to 'modernise' the data collected in this study, where applicable all diatom names were updated and replaced with the new taxonomy, but in all instances the old taxon codes were retained (which in some cases may have led to the merging of diatom taxa). **Appendix A** highlights all species that were identified from all cores and surface sediments used in this study, and gives, where necessary the new synonym is used in this research. It also lists the taxon codes used for every species. In some instances, updating the names can cause apparent inconsistency with previous studies, especially as very little taxonomic work appears to have focused on diatoms of East Africa since the original works of Hustedt (1949) and Gasse (1986). Currently there is no taxonomic work in existence for the crater lakes in western Uganda, although some work is under way by C. Cocquyt (National Botanical Gardens, Belgium; *pers. comm*.).

8.8.1.2 Valve morphology

A particularly interesting issue that arose during this research, but which was not directly addressed, was the large variation in morphometry within certain diatom species (e.g. *Cyclotella meneghiniana* (Kützing), *Amphora copulata* (Schoeman & Archibald), *Nitzschia bacillum* (Hustedt) and *Fragilaria tenera* ([W. Smith] Lange-Bertalot). There were several differences occurring in the morphometry of the valves. The most obvious difference was an (a) apparent preference for larger or smaller valve sizes within some downcore samples, though it should be noted the variation did lie within the published range for the species (e.g. *Cyclotella meneghiniana* [Kützing] and *Amphora copulata* [Schoeman & Archibald]; see **Appendix E**, **Plate 1**); (b) within the modern surface samples, rather than the occurrence of large and small valve sizes, the species *Nitzschia bacillum* (Hustedt)appeared to differ subtly in morphometry between lakes, with ends becoming more protracted and the valve shape more rhomboid. In addition to this *Nitzschia bacillum* (Hustedt) seemed to form a continuum into the species denoted in this research as *Nitzschia confinis* (Hustedt), which formed the longer valves [15-40 μm] with protracted ends (see **Appendix E**, **Plate 5**); finally (*c*) teratological differences occurred in several fossil samples containing *Fragilaria tenera*, with deformities manifesting as a sigmoidal shaped bend in the central area.

The co-occurrence of both small and large valves of the same species was noted in many fossil samples and is most likely representative of a normal distribution of diatoms within their natural lifecycle. However, some samples were almost totally comprised of either the small or the large form of the valve. Population studies of fossil diatom sequences have shown that variation in frustule size and morphometry can be caused by several factors. For example, the size of diatoms within a population has been linked to environmental factors such as silicate and phosphate limitation (Lund, 1950; Tilman and Kilham, 1976), the rate of nitrate input into the cell (Parsons and Takeshi, 1973; Gaskin, 1979); grazing pressures (Kerr, 1974) and increasing productivity (Gaskin, 1979). If the supply of nutrients becomes limiting with increasing biomass, productivity may only be maintained with a reduction of mean population size (Gaskin, 1979). In ocean systems, size-dependent nutrient requirements select for smaller cells, and under low nutrient conditions small diatoms will dominate; larger diatoms are successful when nutrient availability is high (Finkel *et al*., 2005). Using this relationship it can perhaps be inferred that the size structure of fossil phytoplankton communities may be a biological indicator of the changes in the availability of nutrients in the euphotic zone (Finkel *et al*., 2005). With

regards to lake systems, studies have suggested that increases in salinity may prevent sexual reproduction in diatoms, by preventing the formation of auxospores, thereby reducing the size of diatom cells and resulting in a decline in population size (Clavero *et al*., 2001; Campagna, 2007). Work on Lake Tahoe has suggested shifts in the size of planktonic diatoms over centennial timescales (Smol *et al*., 2005) linked to changes in water column stability in response to changing climate. The study of the historical diatom communities of Lake Tahoe show that climate warming is a possible selection pressure on diatom cell size, with results particularly pertinent in the genus *Cyclotella* (Winder *et al*., 2008). Similarly studies regarding *Cyclotella meneghiniana* have suggested iron limitation (Lewandowsak and Kosakowska, 2004), nutrient limitation (Rosen and Lowe, 1984) and salinity (Tuchman *et al*., 1984) are amongst some of the factors affecting the growth of the species.

The variation in the morphology of *Nitzschia bacillum* and its observed continuum into *Nitzschia confinis* may perhaps be a result of subtle variations in lake water chemistry and other environmental pressures (e.g. lake depth, stratification or grazing pressures) and may also be linked to factors controlling the 'large' and 'small' cell sizes described above. The teratological forms noted in the fossil sediments of Lakes Kamunzuka and Kako are most likely a result of heavy metal contamination of the lake waters (cf. Cremer and Wagner, 2004), but analyses were not carried out for metal concentrations.

8.8.2 Radiocarbon dating of African lake sediments

Lake-based chronologies of hydrological and climate changes in Africa continue to rely upon a combination of ^{210}Pb and ^{14}C dating. However one of the most pertinent problems in the radiocarbon dating of East African lakes is the presence of a radiocarbon reservoir age associated with the dating of bulk material (cf. Beuning *et al*., 1997; Stager and Johnson, 2000; Russell *et al*., 2007). Terrestrial macrofossils tend to yield more reliable ages as the plants obtain their ^{14}C from atmospheric CO_2 (Verschuren, 2003). The dating of bulk sediments in some of the larger and smaller (crater) lakes in East Africa has proved problematic. In many instances, bulk sedimentary material may contain considerable ^{14}C from aquatic algae, which can overestimate the true age of the sediment. Aquatic algae derive their ^{14}C from the dissolved inorganic carbon (DIC) from the lake water, and in many closed-basin lakes, the long residence time can cause a reduction in the $^{14}C/^{12}C$ ratio relative to the atmosphere (Verschuren, 2003). For example, radiocarbon dated sediments from Lake Victoria suggest a 500-600 yr offset in core tops (Beuning *et al*., 1997; Stager

and Johnson, 2000). This offset was identified and corrected for using a combination of ^{210}Pb and ^{14}C dating of pre-1945 sediments as well as comparing dates from bulk organic matter and terrestrial plant macrofossils at intervals further back in time (Verschuren, 2003).

Terrestrial macrofossils can themselves produce problems with radiocarbon dating. For example, there may be significant delays in the burial of large terrestrial plant remains in offshore lake sediments due to the retention of these macrofossils in soils or nearshore sediments. Furthermore, wood remains can survive for many years (decades; even centuries) before being delivered to the burial site. In this study, the majority of rejected dates were either charcoal (charred wood) or large wood, which in the majority of cases appeared to produce erroneously older ages. The exclusion of these dates is on the basis that these large wood fragments (>5 mm) may have been resident in the catchment (e.g. trapped in littoral vegetation) for a long period before being washed into the lake. Furthermore, some of the charcoal may have been produced through the incomplete burning of older wood material, thus producing an older age in relatively young sediments.

The accepted dates were those where more brittle terrestrial plant material (e.g. leaf fragments) and smaller pieces of wood and charcoal (<250 μm). These more delicate plant fragments would likely be destroyed by prolonged aerial exposure. Furthermore, when such remains are found in offshore sediments, they most likely reflect direct deposition from the air (Verschuren, 2003).

Many recent studies of East African lake level fluctuations use polynomial regression curves to create a radiocarbon chronology (cf. Verschuren *et al*., 2000; Russell *et al*., 2007). However as these models minimise and smooth the variation in the sedimentation rates in the cores (Verschuren *et al*, 2000), they may not capture the true shape of the age-depth relationship caused by the changes in sediment-accumulation rate that usually accompany lake-level fluctuations, especially inferred low sedimentation during low-stands (cf. Verschuren, 2001) and true corrections of sediment accumulation rates may prove elusive (Verschuren, 2003). In addition to this, problems arise with inferring sediment flux.

The chronological integrity of the Kyasanduka and Nyamogusingiri crater lake sediments as archives of climate history is somewhat constrained by the analytical uncertainty associated with ^{14}C-based age determination and the additional uncertainty due to the occurrence of non-unique calendar ages (cf. Verschuren *et al*, 2000). The calculation of the calendar ages is particularly problematic during the last 1000 years due to the ‘de

Vries effect', which causes several plateaus as well as age reversals in the radiocarbon calibration curve (Figure 8.12). This results in multiple calibrated ages for single samples, many with almost equal probabilities (see **Chapter 6,** Tables 6.2 and 6.4). The 'de Vries effect' is a natural phenomenon often linked to variations in sunspot activity, which can cause problems with the precision of calibrated radiocarbon dates from AD 1450 to AD 1950 (Stuiver and Becker, 1993; Figure 8.12). There are two main perturbations ("de Vries effect") in the ^{14}C time scale during this period. The first is centred on 150 ^{14}C yr BP (a, on Figure 8.12), with a calibrated range interval of 285 years (AD 1665-1955 at two sigma error). The second is centred on 350 ^{14}C yr BP (b, on Figure 8.12, with a two sigma range of 200 years (AD 1450-1600; Stuiver and Becker, 1993). In some instances these perturbations can cause limitations when resolving the actual ages of the sediments.

Despite many of these inherent issues, the AMS ^{14}C dating of sediments from the two freshwater crater lakes (long cores) has demonstrated a continuous sediment record (which in itself can be unusual in East Africa, especially for shallow lakes such as Kyasanduka [cf. Verschuren, 2004]), as well as a good number of terrestrial macrofossils that were suitable for dating, thus eliminating the need to rely on bulk sediment dating, and the complicating factor of calculating and understanding of reservoir ages for each system.

Despite the fact that dating remains problematic for some periods for many records across East Africa during the last 1000 years (not least as this period spans the interval between ^{210}Pb dating methods and more secure ^{14}C dating), patterns in the spatial and temporal signature of climate change across equatorial East Africa in the last millennium are clearly evident.

8.8.3 Crater lake transfer function and the use of EDDI

For this research a new transfer function was developed for the crater lakes of western Uganda to infer past changes in conductivity as a result of climatic perturbations over the last 1000 years, despite the existence of a training set for the East African region in general. Exploration of the EDDI dataset and the application of the EDDI transfer function to reconstruct surface sediment conductivities and down core conductivity changes highlighted several issues with the application of this particular transfer function to the sediments from the crater lakes. All quantitative reconstructions using diatom data were carried out using the ERNIE (v.1.2) software package within EDDI.

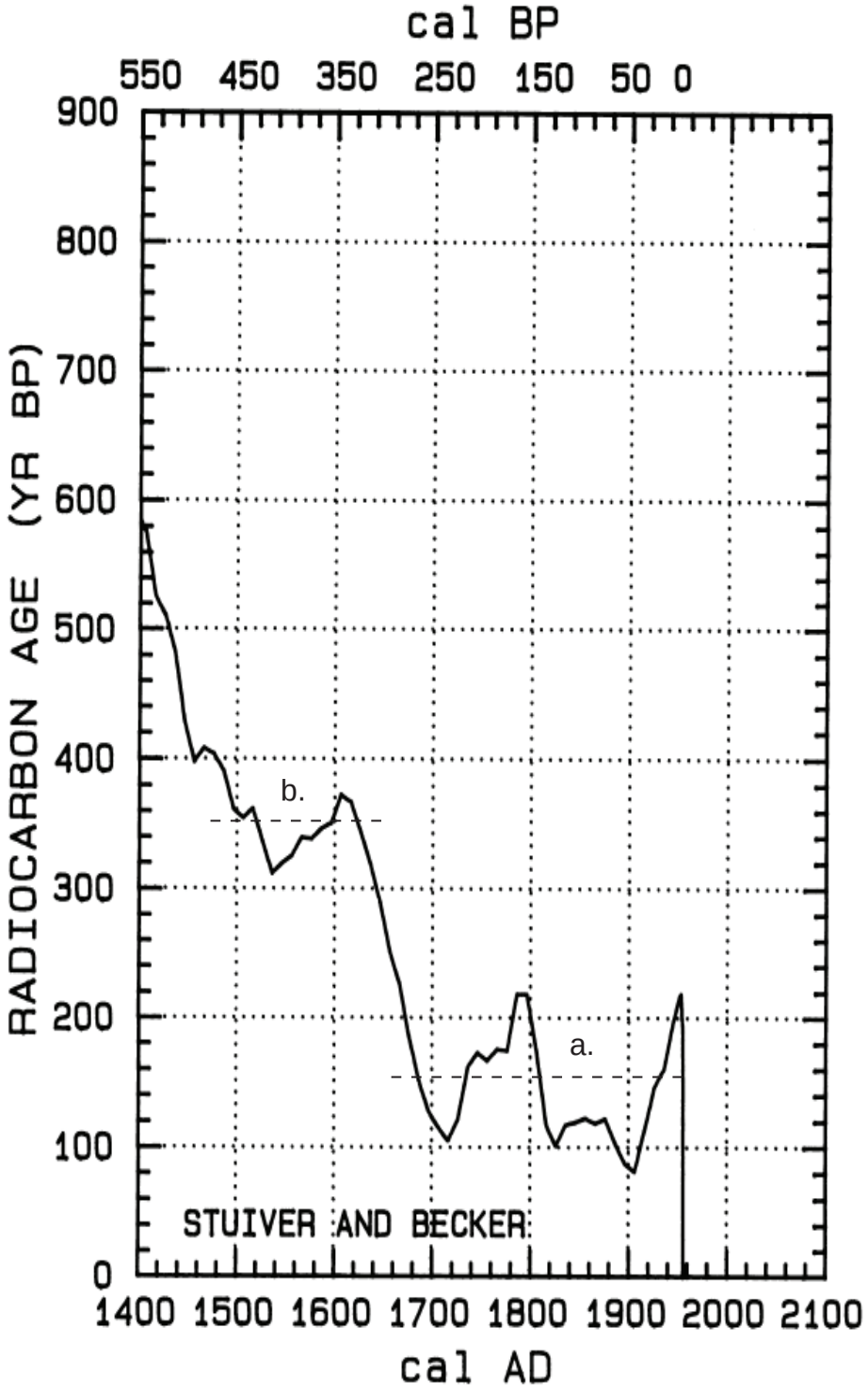

Figure 8.12 *Relationship between radiocarbon and calendar ages for the period AD 1400- AD 1900. This curve highlights the problematic 'de Vries' effect (***a** *and* **b***). The de Vries'effect causes 'time warps' throughout the Holocene. The fluctuations and uncertainties in the calibration curve causes discrete calibrated ages to broaden in range. Thus* ^{14}C *determinations have larger calibration ranges and are less precise (Taylor, 1997). Figure redrawn from Stuiver and Becker (1993).*

Analogue matching of surface sediment and fossil core samples used in this research with the full salinity dataset (n = 370 modern samples) within EDDI including samples from north and east Africa (Gasse *et al*. 1995), showed that the closest analogues in all cases were from the East African subset (n = 179). The East African conductivity model performs well when internally validated by jack-knifing (conductivity, East African dataset, n = 179, WA_{inv}: r^2_{jack} = 0.784, RMSEP = 0.41 log units); with an r^2_{jack} only slightly better than the crater lake training set (r^2_{jack} = 0.74), the crater lake training set had a lower RMSEP (0.256) than the East African training set.

The verification of the datasets using EDDI suggested that in most cases a good proportion of the diatom data would be included in the reconstruction (Table 8.12). The biggest problem occurred with the fresher water lakes Kamunzuka and Kako, where only 20% and 50% of the diatom data was included in the reconstructions, this was largely due to the presence of the unique form of *Gomphonema* f. *gracile* and *Fragilaria tenera*, which either do not occur in the EDDI training set, or were under-represented.

Based on the high percentages of diatom data that would be included (in most lakes) in the reconstructions, the East African transfer function was applied to all down-core sequences. The EDDI transfer function was then applied to the Combined_76 training set to see how well it could predict the modern surface conductivities of all lakes included in crater lake transfer function and to asses the differences in the optima of species in both the EDDI training set and the Combined_76 training set. The results of the EDDI reconstructions compared to those from the Combined_76 training set are shown in Figure 8.13. Aside from the reconstructions at Nyamogusingiri and Kako, which on first glance, EDDI appears to reconstruct similar trends in conductivity through time, all of the other lakes record rather large discrepancies in the trends over time. For example, Lake Kyasanduka is reconstructed as being fresh (*c*. 200 μS cm^{-1}) for almost the entire record, with a big change in conductivity occurring in the last 200 years, coincident with the increase in the abundance of *Nitzschia palea* and *Cyclotella meneghininana* in the core samples. Problems arise in the reconstructions at Kamunzuka as the dominating freshwater taxa *Gomphonema* f. *gracile* (*c*. 90% abundance in most core samples) does not appear in the training set. The reconstructions from Nyungu using the EDDI dataset are opposite to those reconstructed by the Combined_76 training set. In addition to the differences in reconstructed conductivity trends across the lakes, the values obtained in the EDDI reconstructions were, in most cases (except Kako and the early Kyasanduka record), far higher than those reconstructed in by Combined_76 model (Figure 8.13).

Table 8.12 *Comparison of the average percentage of diatom taxa included in the reconstructions using the Combined_76 and East Africa (EDDI) training set.*

Lake	Combined_76 (%)	East African (%)
Nyamogusingiri	98.7	96.3
Kyasanduka	99.0	90.9
Kamunzuka	99.5	20.8
Kako	90.8	50.5
Nyungu	99.6	96.7

To try and assess the differences between the two training sets, the EDDI East African transfer function was applied to the Combined_76 training set to see how well modern surface conductivities were reconstructed. A scatter plot of the measured surface conductivities and those reconstructed by the Combined _76 and EDDI models are shown in Figure 8.14. The plots show far more scatter in the data points using the EDDI transfer

Another factor affecting the use of the EDDI transfer function for reconstructing conductivity is the differences in the taxa included in the dataset. The lakes sampled for the EDDI training set are generally very large and very deep and therefore many of the samples consist of 'true' planktonic taxa. However it should be noted that in the sediments of the western Uganda crater lakes, many lakes have a very large benthic influence, which may influence the outcome of the transfer function, especially when they are indicative of fresher conditions, but are under-represented in the EDDI training set. The frequent dominance of non-planktonic diatoms in the sediments of these crater lake systems, may be more sensitive to changes in habitat availability than to fluctuations in conductivity, especially with the confounding influence of groundwater in many of these lakes that keep the lakes fresh, even during periods of severe aridity.

8.8.4 Multiproxy research

This research has produced sound evidence for environmental changes in western Uganda over the last 1000 years and shown that reliable inferences of regional changes can be made from these largely unexplored crater lakes. However, it has also highlighted some of the problems with using freshwater lakes as indicators of environmental changes. The freshwater lakes do provide a continuous record of environmental changes over the last

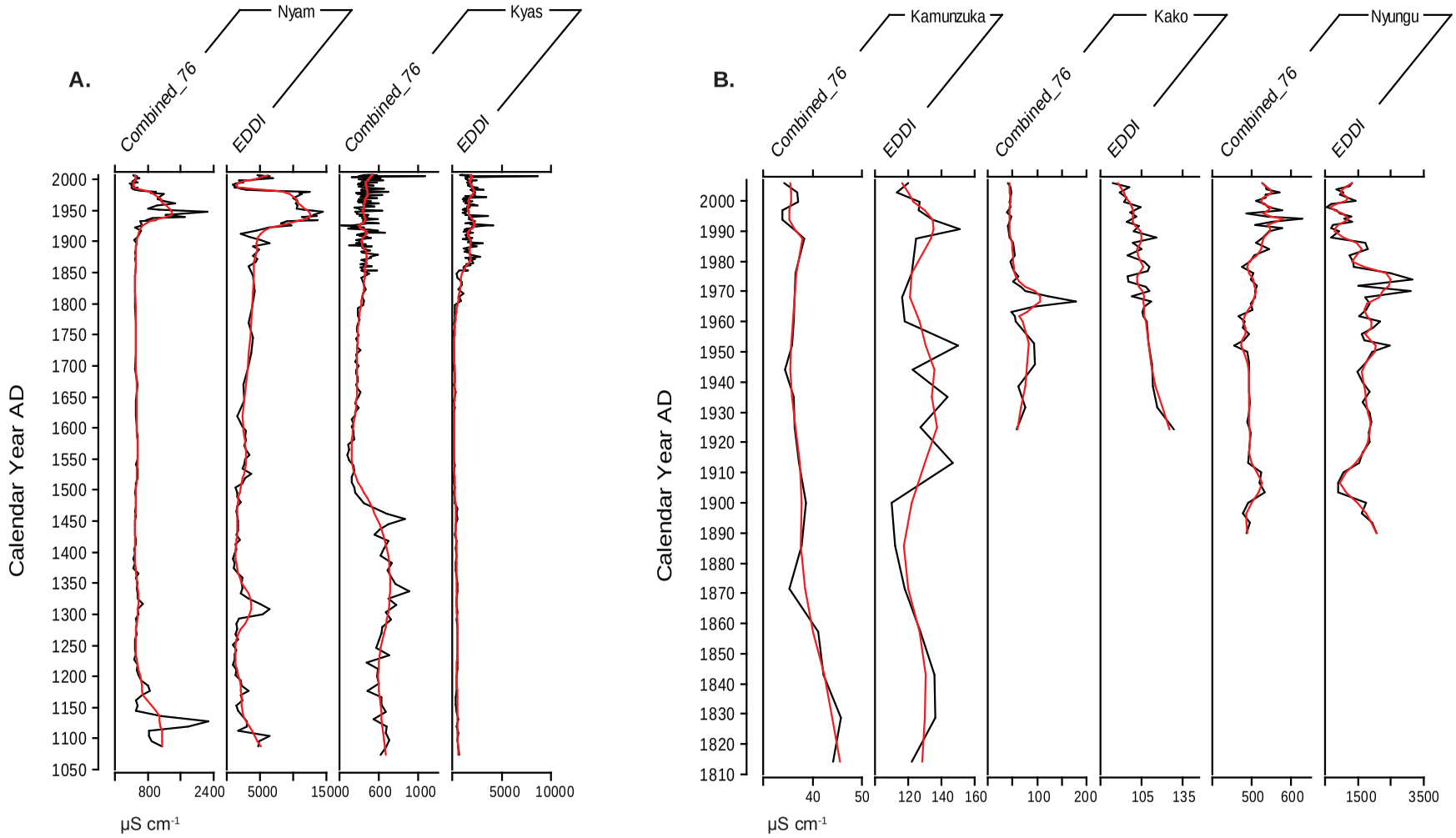

Figure 8.13 *Comparison of reconstructed conductivity (µS cm^{-1}) using the Combined_76 and EDDI (East African) training sets* **(A)** *long cores: Nyamogusingiri and Kyasanduka and* **(B)** *short cores: Kamunzuka, Kako and Nyungu. A lowess smoother has been applied to each reconstruction. NB the change of y-axis sacle between* **A** *and* **B**.

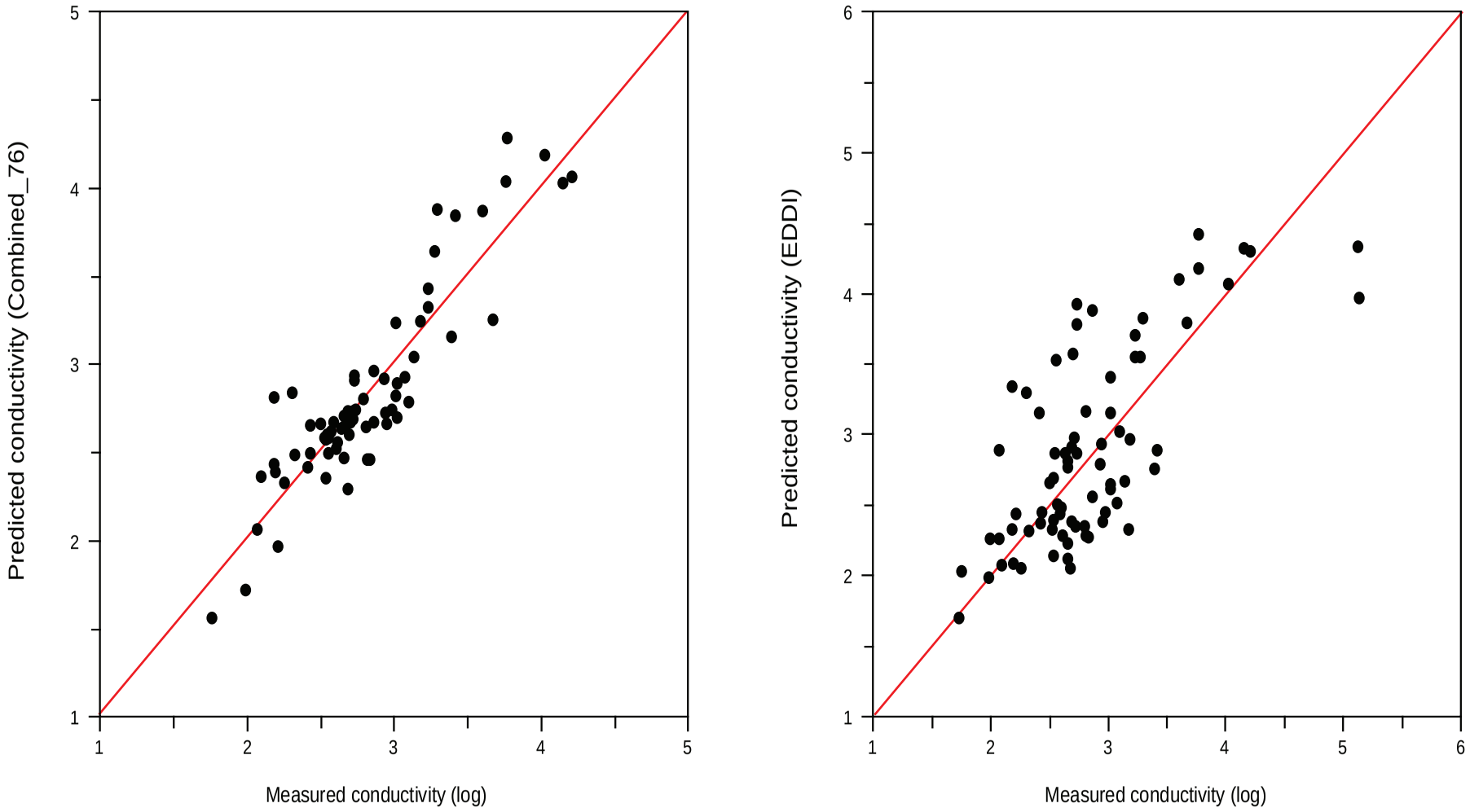

Figure 8.14 *Comparison of measured surface water conductivity of the Combined_76 dataset compared to* **(A)** *reconsonstructed conductivity using the Combined_76 training set and* **(B)** *reconstructed conductivity using the EDDI training set. A 1:1 line is shown in red on both diagrams.*

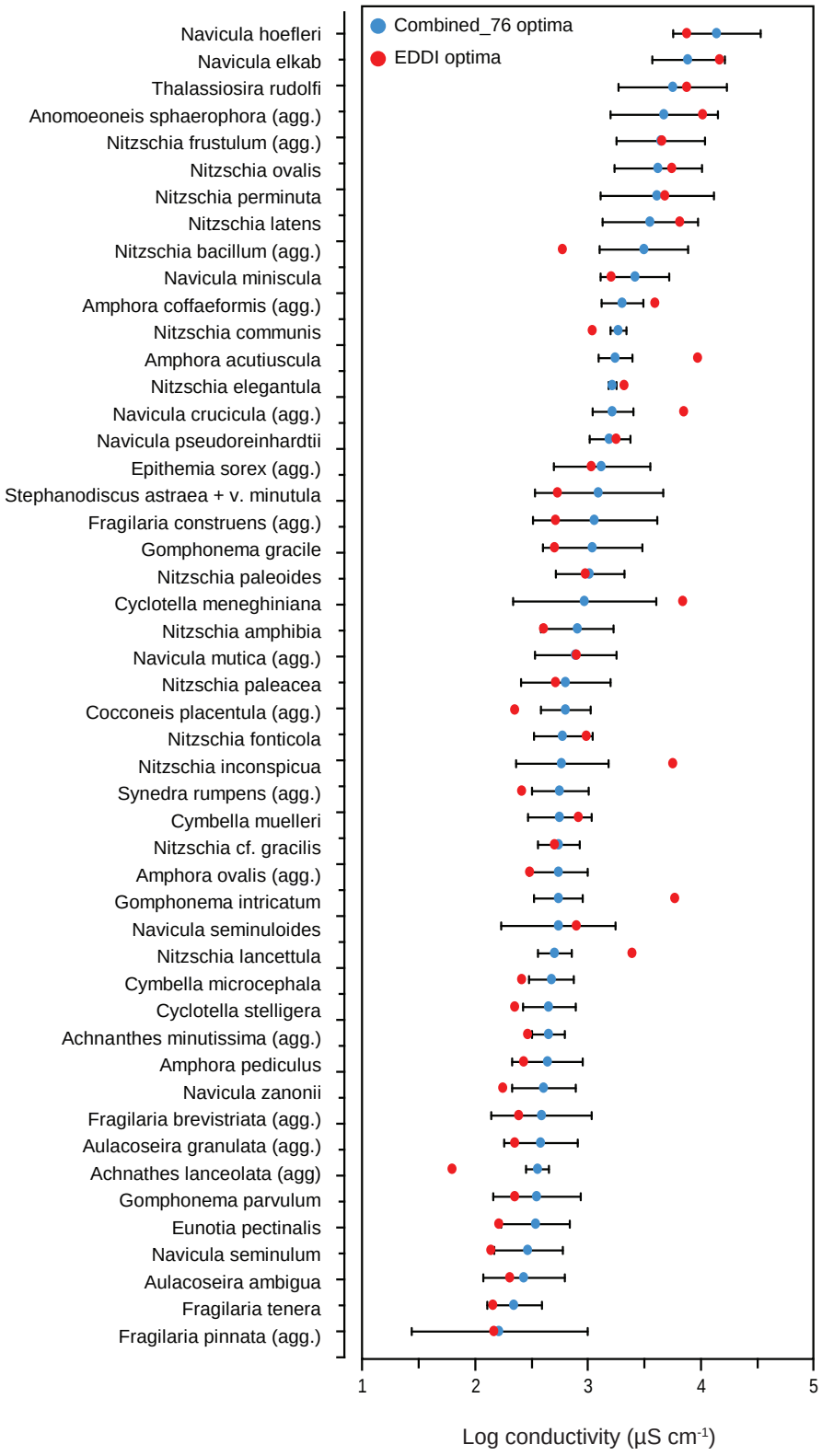

Figure 8.15 *Weighted average conductivity optima and tolerances for species >10% in any one sample from the Combined_76 dataset (blue circles) compared to the conductivity optima as estmiated using the EDDI transfer function for conductivity (East African dataset; red circles).*

1000 years, although to achieve this continuous archive, the sensitivity of the record is compromised. The lakes that are likely to contain some of the most interesting records are those that are prone to complete desiccation (cf. Verschuren, 2004). Similarly these sensitive lakes (usually the more saline lakes) are less likely to contain the biota (e.g. diatoms) required for detailed analyses either because of their salinity or issues concerning the preservation of valves within the sediment archive (cf. Barker, 1990).

This research does highlight the need for, and the value of, a multiproxy approach to reconstructing past climatic and environmental changes. The combination of diatom analyses, organic isotopes and sedimentary properties (e.g. organic content and flux data) in conjunction with statistical analyses has allowed environmental changes to be inferred via multiple lines of evidence. The use of a multi-site approach to this research has allowed climatic and environmental reconstruction in both space and time. In addition to this, the comparison and similarity of the records from the Ugandan crater lakes to published studies from other lakes in Uganda and across East Africa also validate the findings arising from this research, as well as highlighting aspects of the regional complexity during periods of major climatic perturbations (e.g. LIA).

In addition to the data collected for this research, pollen analysis is currently being completed for the two long cores (Nyamogusingiri and Kyasanduka; I. Ssemmanda, Makerere University, Uganda). The addition of this proxy record will enhance the data from the bulk organic isotope data and may also aid the interpretation of the increases in sediment flux to the lake in the recent past, to see whether it is related to catchment clearance, with pollen types that are perhaps indicative of human disturbance (e.g. higher fern spore accumulation rates; Ssemmanda *et al*., 2005). For future research, a whole ecosystem approach to reconstructing changes would provide an insight into lake functioning (e.g. chironomids, macrofossils, cladocerans along with the aforementioned proxies) and the responses of different biota to climate and environmental changes, especially as some proxies may be more sensitive than others. This type of approach, combining proxies with different response times can help to understand the reaction of biotic and abiotic systems to climate changes, and may allow the ‘understanding of community ecology under a changing climate’ (Ammann, 1989). Similarly the detection of common trends between independent proxies will only serve to make the reconstructions more credible (Lotter, 2003).

8.9 Future work

In the light of this research and the above discussion, some of the key areas that hold potential for further enquiry include:

(i) **Chronology**; one of the problems of understanding the climatic and environmental changes during the last 1000 years is the ability to date lake sediments with accuracy and precision. The dating of the most recent lake deposits (*c.* 150 years) using ^{210}Pb is now a standard technique often allowing the most recent sediments to be constrained with an error of only a few years. Similarly, the application of radiocarbon dating to recent sediments, such as undertaken on cores in this study, is becoming a much more widely employed technique. An issue raised during this research (and highlighted in other studies) is the problem of non-unique ages which commonly occur during a specific 500 year period (*c.* AD 1450-AD 1950; Stuiver and Becker, 1993) due to a phenomenon related to solar radiation (de Vries effect). This, in effect, can lead to a section of late Holocene records (*c.* 400 years) with large uncertainties in the absolute calibrated radiocarbon age. This problem occurs between the base of ^{210}Pb dating (*c.* AD 1850) and the beginning of the more reliable ^{14}C dating, prior to AD 1450, where the probability of obtaining a unique age is much higher. Unfortunately, this particular period is also one of interest for many researchers, as it is the period concomitant with the onset of the LIA. This period also encompasses the late 18th century drought recognized in several (but not all) lake sediment sequences across Africa (including lakes in this study) as well as coinciding with some of the large shifts identified in the archaeological record. Improved dating accuracy during the above periods would, undoubtedly, allow an improved correlation of drought sequences across the region.

During this research all of the radiocarbon dates were obtained from terrestrial macrofossils However, some of these samples occurred in extremely small quantities causing concern as to whether there would be enough carbon to date. In some cases, only charcoal was available, and in many instances they provided dates that were out of sequence (i.e. older) when compared to those obtained from leaf and wood fragments. Unfortunately radiocarbon dating of bulk samples does not provide the answer in the absence of sufficient macrofossils. Studies from the lakes of East Africa have shown that many of the lakes experience a problem with radiocarbon reservoir ages due to the long residence time of the water and carbon in these closed lake basins (Beuning *et al*., 1997; Stager and Johnson, 2000; Russell *et al*., 2007). It would be of interest to see whether the

sediments in more of the smaller lakes in western Uganda do suffer from ^{14}C reservoir ages, to rule out or validate the use of bulk sediments for dating in freshwater systems.

Recent studies on crater Lakes Kibengo (Russell *et al*., 2007), Wandakara and Katinda (Bessems, 2007) in western Uganda do suggest that radiocarbon reservoirs of between 200 (Kibengo) and 700 years (Wandakara). One reservoir age obtained by Bessems (2007) suggests a reservoir age of *c*. 1800 years in Wandakara, though it is more likely that this is a result of a contaminated sample. Given the existence of these ages in some of the crater lakes, it may be interesting to explore how the reservoir age differs down core (i.e. can a single age correction be applied to all core dates; cf. Russell *et al*., 2007; Bessems, 2007) as would a more accurate quantification of their offset (through the use of multiple dates from single horizons and using different sample types) would allow future researchers to make accurate adjustments for reservoir storage effects, and thus, improve their core chronologies.

To avoid the complication of radiocarbon reservoir ages and the scarcity of material suitable for dating (i.e. macrofossils) it is now possible to radiocarbon date pollen grains and organic sediment fractions (cf. research on Lake Baikal; Coleman *et al*. 1996; Horiuchi *et al*. 2000; Piotrowska *et al*., 2004). However, it is an extremely complicated procedure requiring the separation and chemical cleaning of the samples in order to obtain as pure a sample as possible (Piotrowska *et al*., 2004). Furthermore, the study by Piotrowska *et al.* (2004) showed an offset between the radiocarbon age and the expected surface age. Whilst suggested this may have been due to incomplete core recovery, other studies have suggested that dates obtained from pollen can be consistently older, perhaps as a result of specific properties of pollen grains (cf. Lake Gościąż; Kilian *et al*., 2002).

Perhaps a new avenue of research in situations such as these may be the employment of a different dating technique, which is beyond the scope of many palaeolimnological and palaeoecological studies. Recently, research into the luminescence dating of lake sediments has been explored in a few lake systems where there are problems with reservoir ages (cf. Lake Hoare, Antarctica, Berger and Doran, 2001), to test the accuracy of the technique compared to ^{14}C dating (cf. Lake El'gygytgyn, Siberia, Forman *et al*., 2007; Crummock Water, UK, Shen *et al*., 2008) and between depositional environments (Spencer *et al*., 2003). Research is also currently underway on the luminescence dating of sediments from Lake Malawi. In essence, luminescence dating has the potential to work just as well in lacustrine environments as it does in terrestrial depositional environments but is inevitably site specific and reliant on slow rates of

accretion for the very best results (thereby achieving good bleaching of old signals allowing lower dating errors [~2%] and confidence in the dates). An accurate chronology is essential for assessing causative links between proxy environmental indicators and broader climate drivers, such as solar insolation. Luminescence geochronology is emerging as an important approach for deciphering palaeolimnological records because it is one of the few techniques that can be applied to a variety of aquatic settings and potentially dating environmental events spanning as much as the past ca. 200 ka (e.g. Berger and Anderson 2000; Wolfe *et al*. 2000; Kaufman *et al*., 2001; Berger *et al*. 2004).

(ii) **Long-term monitoring**; much of the long-term monitoring in Uganda is directed towards the larger lakes (e.g. Lake Victoria) and an understanding of the consequences of human impact on the lake ecosystems, given the heavy reliance on these lake systems as a source of food, water and power by the countries surrounding the lake. However, very little attention has been paid to the smaller lakes of western Uganda which support large rural populations, and in some cases provides some of the only freshwater supply for some of the very remote villages.

A detailed modern limnological survey of 24 of the crater lakes across the four lake clusters in western Uganda supplemented by surface sediment samples for diatom analysis and corresponding water chemistry of an additional 40 sites has provided an update on some of the well known early limnological works of Talling, Kilham and Melack (presented in **Chapter 4**). One of the most striking issues with regards to Ugandan limnology is the lack of long-term monitoring, even on lakes within the country's national parks, with the exception of two published studies (a 3-year monitoring of Lake Saaka in the late 1990s [Crisman *et al*., 2001] and a long-term monitoring of Lake Nkugute with various measurements collected in visits spanning ten years, though not strictly continuous or seasonal sampling [Beadle, 1966]). In recent years, 15 lakes near the Kibale National Park (lakes in the north of the field study area, within the Fort Portal and Kasenda lake clusters, **Chapter 2**, Figures 2.1 and 2.5) are being monitored by researchers from McGill University (Lauren and Colin Chapman; *pers*. *comm*.), with the collection of basic limnological data from these lakes (e.g. maximum depth, temperature and conductivity of the surface waters). In some instances, monthly data exist for some of the lakes (e.g. Saaka [Crisman *et al*., 2001], and Nyierya [Kizito and Nauwerck, 1995). Data that exist cover the last 10 years (since *c*. 1997), although sampling is not always regular, and may not be ongoing for all lakes.

Consequently, very little is known about the seasonal and inter-annual functioning of many of the crater lakes in Uganda, especially in terms of lake stratification and whether this is seasonal or persistent. The data collected for this research were obtained during the dry season only (which is also similar for many other studies in the region), so the data are biased in favour of this season, allowing few conclusions to be drawn on the overall functioning of the lake system. With only sporadic samples through time on various lakes, it is also difficult, in many lakes, to define "base-line" (natural variablilty) conditions to understand how the lakes are responding to (a) long-term climatic changes, (b) seasonal changes in rainfall, (c) limnological changes coincident with the exploitation of the lakes as a water and fishery resource as well as the utilization of many of the lake catchments for agricultural activity and (d) tourism and development along shores of many lakes (e.g. safari lodges and camps on the shores of Lakes Nyamogusingiri, Muijongo, Nyamirima, Kasenda, Nyinambuga, Nyinambulita, Nkuruba, Kifuruka and Lyantonde). The long-term monitoring of these lake systems would allow a better understanding of how the lakes function today, and this may aid our understanding of how lakes function in the past, especially in terms of nutrient (re)cycling and the interpretation of diatoms and other biota (physical signals as proxies for climate and environmental change).

Furthermore, with mounting pressure on lakes outside of national parks and forest reserves, an understanding of the impact of human activity and recent climate trends and the resultant degradation of water quality is becomingly an increasingly important issue in the management of these vulnerable freshwater resources. Monitoring of lakes within and outside national parks, would perhaps provide the ideal opportunity to establish baseline conditions for lakes in near natural settings ('pristine' lakes protected in national parks and forest reserves) and improve understanding of how the various stressors are changing the limnological ecosystems in unprotected lakes. In the context of lake resource management and preservation, such studies may be important under predicted climate scenarios and increasing population pressures for the future (IPCC, 2007).

(iii) **Diatom taxonomy and ecology**; the original diatom flora for East Africa dates back to the early descriptions by Hustedt (1949) and more recently by Gasse (1986). For this research, this regional flora was supplemented by identification keys from Lake Tanganyika (Cocquyt, 1998) and the generic diatom keys of Germain (1981), Patrick and Reimer (1966; 1975) and Krammer and Lange-Bertalot (1988-1991). Whilst these floras proved extremely useful for the identification of many cosmopolitan and endemic taxa,

there were subtle differences noted in some of the species. The most interesting, and somewhat confusing group was that assigned to *Nitzschia fonticola*, *N. bacillum*, and *N. confinis*. *Nitzschia fonticola* in many floras covers a wide variety of morphologies and hence is a rather confusing species. After in depth discussion with Dr Christine Cocquyt (Ghent Botanical Gardens), many of the *Nitzschia fonticola* identified within the crater lake surface sediment training set were reassigned to *Nitzschia bacillum*. It appeared in the crater lake calibration set that there were various morphotypes of the species *N. bacillum*, which formed a continuum into what was ascribed to *Nitzschia confinis* (see **Appendix E, Plate 5**; see *section 8.8.1*). Morphometric differences were also noted in the species *Gomphonema gracile*. Additionally, it was apparent that many of these morphotypes were lake specific. Thus, it would be interesting to study the various morphotypes of these species, to see whether (a) these species are indeed related and (b) to try and ascertain the environmental conditions affecting or causing the variations in morphology as this may have implications for the use of diatoms as environmental indicators across the region. For example if diatom population sizes or variation in the morphology (cf. *Nitzschia bacillum*) were linked to a particular environmental gradient (such as silica depletion, depth or phosphate concentrations; see *section 8.8.1*), the changes in mean population size or morphology through time could also be used to infer past environmental changes.

In several of the lakes, teratological forms of *Fragilaria tenera* were observed in sediments of the last 10 years, and it is probable that the *Gomphonema* species that dominates the Lake Kamunzuka sediment record is a teratological form of *G. gracile* (**Appendix E**, **Plate 4**). It is widely accepted that heavy metal contamination is often the causal agent behind such deformities (Dickman, 1998; Stevenson and Bahls, 1999; Peres, 2000; Fore and Grafe, 2002) and it is accepted as the factor behind the deformities observed in the crater lake records, though further research on heavy metal concentrations within the sediments, lake water and diatom frustules would be required to support this suggestion. Only major (whole valve) deformations were observed in the crater lake records under light microscopy (LM). A recent study by Morin *et al*. (2008) suggests that subtle aberrations may occur in many species, which are not picked up under LM but would require detailed SEM analyses. Furthermore, a study of the live samples may also help to understand the abnormal forms of some diatom species, especially as toxin uptake (either natural [geology/volcanism] or as a result of pollution) can affect the diatoms not only at a species level, but also in terms of colony formation.

(iv) **Longer sediment records**; there is the potential for extracting longer records from the crater lakes of western Uganda. Given the technique employed for the extraction of cores during this study, it was not possible to obtain long core sequences, especially at many lakes (e.g. Kyasanduka, Nyamogusingiri and Nyungu) with the presence of clay/peat horizons preventing the penetration of the Russian corer to greater depths. It was also impossible to core lakes deeper than *c*. 20 m due to the bending of the core rods. The employment of an alternative coring technique, such as a piston core, would in future alleviate problems associated with 'hand' coring techniques and offers the potential to penetrate some of the stiffer sediment, thereby allowing the extraction of longer sediment sequences. The use of a Livingstone corer might allow the retrieval of cores from deeper lakes (>20 m) as the rods used for this corer tend to bend less than those used for a Russian and piston corer. To core some of the deeper lakes, the use of casing would needed, this would help to prevent the bending of the core rods in deeper water. However, this may lead to additional logistical problems associated with the transportation of more than 20 m of casing to and from the crater lakes.

At present, there is uncertainty in the age of crater formation in western Uganda and the absolute depths of sediments within these craters are currently unknown. The application of seismic techniques in Lake Victoria (Johnson *et al*., 2000) and Lake Tana (Lamb *et al*., 2007) have allowed the depth and subsurface stratigraphy of the sediments to be investigated, and in the case of the Tana record, have allowed the identification of numerous buried desiccation surfaces. Whilst geophysical studies may in some cases be expensive and on occasion logistically difficult, the potential of exploring the lake basins and the sediments contained therein would be a first for many of the Ugandan crater lakes and would undoubtedly provide a unique insight into sediment accumulation and sequences in these lakes.

Chapter 9

Conclusions

This thesis has presented independent and unequivocal high-resolution biological and sedimentological evidence of past climate and environmental changes (both natural and anthropogenic) in western Uganda over the last 1000 years using a single region, multi-lake approach.

The sedimentary archives from the Ugandan crater lakes provide high-resolution, annual to sub-decadal records of lake level fluctuations during the last 1000 years. All of the lakes demonstrate an individualistic response to external (e.g. climatic) drivers, in terms of their absolute diatom assemblages (although they do share some common species). However, given limnological variations in e.g. depth and salinity, reconstructed lake levels and independent statistical analyses (e.g. ZONE and direct and indirect ordination techniques) indicate a regional coherence within these sediment archives, with many of the lakes responding to the same drivers through time and at similar times (within the errors and limits of the dating techniques employed). As a result, it can be concluded that the sedimentary proxies from crater lakes can be used to make reliable inferences regarding regional changes in climate and environmental history. Furthermore, statistical analyses and the direct comparison of these archives to previous palaeolimnological work in Uganda and across East Africa suggest that the western Uganda crater lakes are indeed sensitive to climatic perturbations such as a major arid phase coincident with the northern hemispheric Mediaeval Warm Period (MWP; AD 1000-1200) and a drier Little Ice Age (main phase AD 1500-1600), though the latter is also characterised by fluctuating lake levels and a short-lived high-stand *c.* AD 1575-1600. The general trends support the hypothesis of an east to west (wet to dry) gradient across East Africa during the LIA, however, the relationship breaks down and is more complex towards the end of the LIA (c. AD 1700-1750) when the inferred changes in lake levels at Nyamogusingiri and Kyasanduka are synchronous with changes observed at Lakes Naivasha (Kenya) and Victoria and diverge from 'local' lake level records (from Edward, Kasenda and Wandakara).

These minor discrepancies may be attributable to: (i) chronological issues between sites, (ii) the regional complexity in major climatic perturbations in East Africa causing an

east to west rainfall gradient or (iii) the individual nature or buffering of a lake's response. For example, the deeper water lake Nyamogusingiri does not respond to the the well documented 18th century drought in East Africa, with a shift to lower lake levels occurring c. 50 years later. Conversely, Nyamogusingiri's shallow, neighbouring lake, Kyasanduka responds almost immediately to this climatic anomaly. This suggests that time-lags do occur in these lake systems and the response of the lake to climate change is dependent on the antecedent conditions of the lake, most likely as a result of regional groundwater hydrology. This study clearly highlights the importance of multiple lake studies. Whilst being representative of the lake ecosystem, single cores from individual lakes may not represent a regional signal, and neither might it represent a climate signal. Thus, with multi-lake studies, regional changes can be inferred by assessing a range of local (individual) responses, taking into account the limnological differences.

Records spanning the last 150 years, in conjunction with the two longer core sequences, demonstrate unprecedented levels of sediment influx occurring over the last 50-75 years. Many of the lakes show, that during this period, the major changes in the diatom assemblages are coincident with a large influx of sediment to the lake, most likely as a result of increased nutrient inputs due to increasing human impacts within the lake catchments. These changes also coincide with diatom habitat changes, from predominantly planktonic to benthic systems. These extremely high inputs of sediment are not solely a response to fluctuating climates over the last century as lake-level records from Victoria (Nicholson and Yin, 2001), Naivasha (Verschuren et al., 2000), Kasenda and Wandakara (Ryves et al., submitted) suggest a drier regional climate from 1900 to 1960. This is followed by a dramatic rise in the level of Lake Victoria following an intense period of rainfall associated with a severe ENSO event in 1963; lake level at Victoria has declined towards the present day. Given what is known from published pollen studies (e.g. Ssemmanda et al., 2005) and anecdotal evidence of agricultural development and rural populations in western Uganda during 20th century, it is likely that these changes are partly driven by human activity within most of the lake catchments. In 1994, Marchant and colleagues observed wet-season erosion of sediments from fully vegetated hillsides near Mubwindi Swamp (Marchant et al., 1997). The authors postulated that such erosion would be enhanced during periods of less dense vegetation cover and higher levels of rainfall (Marchant et al., 1997). It is likely that the onset of human activity and associated catchment disturbance during drier periods served to enhance erosion during the onset of a wet period in the early 1960s.

However, it does seem that this signal of human impact is imprinted over a background climatic record, with clear evidence of lake level fluctuations in the recent past that are comparable to documentary evidence (e.g. the high lake levels in the early 1960s [1963] associated with a severe ENSO event). This suggests that in tropical systems, where climate fluctuations are the principal driver of lake level fluctuations, human activity does not fully overprint the sediment-climate record, even in the relatively recent past.

The limnological survey of 24 crater lakes provided a much needed update on these important aquatic resources and limnological systems of western Uganda. The number of, and natural variation in these lakes provide a unique opportunity for comparative limnology. In the light of increasing human impacts on lakes outside of national parks (such as shore-side tourist developments and agriculture, causing sediment and nutrient loading), the monitoring of these systems is perhaps a pressing issue. Whilst future climate scenarios predict a reduced water stress in Eastern Africa in the next 50 years (IPCC, 2007), the monitoring and management of these lake systems is an important issue that needs to be addressed, especially with the increasing reliance of remote populations on these resources as a source of freshwater and fisheries. Even in the absence of climate change, increasing population trends and patterns of current water use indicate that African countries will exceed the limits of their 'economically usable, land-based water resources before 2025' (Ashton, 2002; IPCC, 2007).

The successful development of a crater lake transfer function for conductivity opens the opportunity to explore other variables that were not addressed in this study but which were shown to be important (TN and depth). It would be beneficial to apply this transfer function to other crater lakes in the region to assess the performance of the model, especially given that the 'open' crater lakes of Nyamogusingiri and Kyasanduka did not perhaps provide the ideal sites for the testing of the model. Salinity fluctuations in these particular lake systems appear to be muted, most likely due to the local importance of groundwater. Ideal sites for testing would be those with known (monitored) salinity for comparison (such as lakes further north, near Fort Portal where spot-samples and some short-term monitoring data exists in both published and unpublished sources [c.f. Beadle, 1966, Melack, 1978 and Chapman and Chapman, unpublished data]). Also, it would be preferable to test the model on lakes with a simpler hydrology (particularly where groundwater influence is less important) and sites where human impact today, and in the past has been kept to a minimum. There was a need for an updated transfer function to address changes in the Ugandan crater lakes as pre-existing transfer function often over-

estimated the conductivity optima of many species, causing erroneously high values in reconstructions. However, it was clear that some species in this transfer function were not well represented in the training set which prevented the identification of minor oscillations clearly evident in the lake records. In addition to this, the lakes sampled for the transfer function do show a continuous salinity gradient as observed in other conductivity training sets (e.g. Northern Great Plains, Fritz et al., 1993 and British Columbia, Wilson et al., 1996). The lakes in Uganda are either fresh (shoulder of the rift valley), or very saline (floor of the rift valley), and the training set perhaps bears similarities to the Spanish dataset of Reed (1998). This problem was overcome by the addition of extra sites of intermediate salinities from the EDDI East African training set. Whilst this undoubtedly improves the models performance, it may not be ecologically realistic if these systems are subject to abrupt transitions between fresh and saline. However it is likely that under a different climatic regime (e.g. LIA) that intermediate salinities may have been present in some of the Ugandan crater lakes.

Further investigation and future expansion of the dataset and long-term monitoring of key lakes types would be useful, with, for example, seasonal sampling of the lakes which could be used to address intra-annual and inter-annual variability and to aid our understanding of how this might be recorded in the lake-sediment archives.

References

Ahl, T. (1970). Principal features of the chemistry of L. Mälaren. In: Milway, C.P. (Ed.). *Eutrophication in large lakes and impoundments – OECD Uppsala symposium May 1968*: 169-195.

Alin, S.R., Cohen, A.S. (2003). Lake-level history of Lake Tanganyika, East Africa, for the past 2500 years based on ostracode-inferred water-depth reconstruction. *Palaeogeography, Palaeoclimatology, Palaeoecology* **199**: 31-49.

Almendinger, J.E. (1990). Groundwater control of closed-basin lake levels under steady-state conditions. *Journal of Hydrology* **112**: 293-318.

Anderson, N.J. (1986). Diatom biostratigraphy and comparative core correlation within a small lake basin. *Hydrobiologia* **143**: 105-112.

Anderson, N.J. (1990a). Variability of diatom concentrations and accumulation rates in sediments of a small lake basin. *Limnology and Oceanography* **35**: 497-508

Anderson, N.J. (1990b). Spatial pattern of recent sediment and diatom accumulation in a small, monomictic, eutrophic lake. *Journal of Paleolimnology* **3**: 143-160.

Anderson, N.J. (1993). Natural versus anthropogenic change in lakes: the role of the sediment record. *Trends in Ecology and Evolution* **8**: 356-361.

Anderson, N.J. (1995). Using the past to predict the future: lake sediments and the modelling of limnological disturbance. *Ecological Modelling* **78**: 149-172.

Anderson, N.J. (2000). Diatoms, temperature and climatic change. *European Journal of Phycology* **35**: 307-314.

Anderson, N.J., Battarbee, R.W. (1994). Aquatic community persistence and variability: A palaeolimnological perspective. In : P. S. Giller, Hildrew, A.G. Raffaell (eds) *Aquatic Ecology: Scale, Pattern and Processes*. London, Blackwell Scientific Publications.

Anselmetti, F.S., Hodell, D.A., Ariztegui, D., Brenner, M., Rosenmeier, M.F. (2007). Quantification of soil erosion rates related to ancient Maya deforestation. *Geology* **35**: 915-918.

Appleby, P.G. (2001). Chronostratigraphic techniques in recent sediments. In: Last, W.M. and Smol, J.P. (eds) *Tracking Environmental Change Using Lake Sediments Volume 1: Basin Analysis, Coring, and Chronological Techniques*. Kluwer Academic, pp171-203.

Appleby, P.G., Oldfield, F. (1978). The calculation of ^{210}Pb dates assuming a constant rate of supply of unsupported ^{210}Pb to the sediment. *Catena* **5**: 1-8.

Appleby, P.G., Nolan, P.J., Gifford, D.W., Godfrey, M.J., Oldfield, F., Anderson, N.J., Battarbee, R.W. (1986). ^{210}Pb dating by low background gamma counting. *Hydrobiologia* **141**: 21-27.

Appleby, PG., Richardson, N., Nolan, P.J. (1992). Self-absorption corrections for well-type germanium detectors. *Nuclear Instruments and Methods in Physics Research Section B* **71**: 228-233.

Arad, A., Morton, W.H. (1969). Mineral springs and saline lakes of the Western Rift Valley, Uganda. *Geochemica et Cosmochimica Acta* **33**: 1169-1181.
Atlas of Uganda (1962). Entebbe, Government Printer.

Bahati, G. (2003). Geochemical Exploration. Paper presented at the 2nd KENGEN Geothermal Conference, Nairobi, Kenya (7-9 April).

Bahati, G., Pang, Z., Armannsson, H., Isabirye, E.M., Kato, V. (2005). Hydrology and reservoir characteristics of three geothermal systems in western Uganda. *Geothermics* **34**: 568-591.

Baker, P.A., Seltzer, G.O., Fritz, S.C., Dunbar, R.B., Grove, M.J., Tapia, P.M., Cross, S.L., Rowe, H.D., Broda, J.P. (2001). The History of South American Tropical Precipitation for the Past 25,000 Years. *Science* **291**: 640-643.

Barker, D.S., Nixon, P.H. (1989). High-Ca, low-alkali carbonatite volcanism at Fort Portal, Uganda. *Contributions to Mineralogy and Petrology* **103**:166-177.

Barker, P. (1990). *Diatoms as palaeolimnological indicators: a reconstruction of Late Quaternary environments in two East African salt lakes*. Loughborough University of Technology. PhD.

Barker, P., Gasse, F. (2003). New evidence for a reduced water balance in East Africa during the Last Glacial Maximum: implication for model-data comparison. *Quaternary Science Reviews* **22**: 823-837.

Barker, P., Gasse, F., Roberts, N., Taieb, M. (1991). Taphonomy and diagenesis in diatom assemblages; a Late Pleistocene palaeoecological study from Lake Magadi, Kenya. *Hydrobiologia* **214**: 267-272.

Barker, P., Fontes, J-C., Gasse, F., and Durant, J-C. (1994). Experimental dissolution of diatom silica in concentrated salt solutions and implications for paleoenvironmental reconstruction. *Limnology and Oceanography* **39**: 99-110.

Barker, P., Telford, R., Merdaci, O., Williamson, D., Taieb, M., Vincens, A., Gibert E. (2000). The sensitivity of a Tanzanian crater lake to catastrophic tephra input and four millennia of climate change. *The Holocene* **10**: 303-310.

Barker, P., Street-Perrott, F.A., Leng, M.J., Greenwood, P.B., Swain, D.L., Perrott, R.A., Telford, R.J., Ficken, K.J. (2001). A 14,000-Year Oxygen Isotope Record from Diatom Silica in Two Alpine Lakes on Mt. Kenya. *Science*, **292**: 2307-2310.

Barker, P., Telford, R., Gasse, F., Florian, T. (2002). Late Pleistocene and Holocene palaeohydrology of Lake Rukwa, Tanzania, inferred from diatom analysis. *Palaeogeography, Palaeoclimatology, Palaeoecology* **187**: 295-305.

Barker, P., Williamson, D., Gasse, F., Gibert, E. (2003). Climatic and volcanic forcing revealed in a 50,000-year diatom record from Lake Massoko, Tanzania. *Quaternary Research*, **60**: 368-376.

Barker, P., Talbot, M., Street-Perrott, A., Marret, F., Scourse, J., Odada, E. (2004). Late Quaternary climatic variability in intertropical Africa. In: *Past climate variability through Europe and Africa*. Battarbee, R.W., Gasse, F., Stickley, C. Dordrecht, Springer, pp 117-38.

Battarbee, R.W. (1986). Diatom Analysis. In: Berglund, B.E. (Ed.). *Handbook of Holocene Palaeoecology and Palaeohydrology*. Chichester, John Wiley & Sons. pp 527-57.

Battarbee, R.W. (2000). Palaeolimnolgical approaches to climate change, with special regard to the biological record. *Quaternary Science Reviews* **19**: 107-204.

Battarbee, R.W., Kneen, M.J. (1982). The use of electronically counted microspheres in absolute diatom analysis. *Limnology and Oceanography* **27**: 184-188.

Battarbee, R., Charles, D.F., Dixit, S., Renberg, I. (1999). Diatoms as indicators of surface water acidity. In: Stoermer, E.F., and Smol, J.P., (Eds.). *The Diatoms: Applications for Environmental and Earth Sciences*. Cambridge University Press, Cambridge. pp. 85-127.

Battarbee, R., Jones, V.J., Flower, R.J., Cameron, N.G., Bennion, H., Carvalo, L., and Juggins, S. (2001). Diatoms. In: Smol, J.P., Birks, H.J.B., Last, W.M., (Eds.). *Tracking Environmental Change Using Lake Sediments. Volume 3: Terrestrial, Algal, and Siliceous Indicators*. Kluwer Academic Publishers, Dordrecht, The Netherlands. pp. 155-202.

Baxter, R.M., Prosser, M.V., Talling, J.F., Wood, R.B. (1965). Stratification in tropical African lakes at moderate altitudes (1500 to 2000 m). *Limnology and Oceanography* **10**: 510-520.

Beadle, L.C. (1932). The waters of some East African Lakes. *Journal of the Linnean Society (Zoology)* **38**: 157-211.

Beadle, L.C. (1936). The waters of some East African lakes in relation to their fauna and flora. *Journal of the Linnean Society of London (Zoology)* **38**: 157-211.

Beadle, L.C. (1966). Prolonged stratification and deoxygenation in Tropical Lakes. I. Crater Lake Nkugute, Uganda, compared with Lakes Bunyoni and Edward. *Limnology and Oceanography* **11**: 152-163.

Beadle, L.C. (1967). Circulation in tropical lakes in relation to productivity. *The Journal of Animal Ecology* **36**: 45-62.

Beadle, L.C. (1974). *The inland waters of tropical Africa: an introduction to tropical limnology*. First Edition. London, Longman.

Beadle, L.C. (1981). *The inland waters of tropical Africa :an introduction to tropical limnology*. Second Edition. London, Longman.

Becht, R., Harper, D.M. (2002). Towards an understanding of human impact upon the hydrology of Lake Naivasha, Kenya. *Hydrobiologia* **488**: 1-11.

Belokopytov, I.E. and Beresnevich, V.V. (1955). Giktorf's peat borers. Torf. Prom. **8**: 9–10.

Bennion, H. (1994). A diatom-phosphorus transfer function for shallow, eutrophic ponds in southeast England. *Hydrobiologia* **275/276**: 391-410.

Bennion, H., Juggins, S., Anderson, N.J. (1996). Predicting epilimnetic phosphorous concentrations using and improved diatom-based transfer function and its application to lake eutrophication management. *Environmental Science and Technology* **30**: 2004-2007.

Berger, G.W., Anderson, P.M. (2000). Extending the geochronometry of arctic lake cores beyond the radiocarbon limit by using thermoluminescence. *Journal of Geophysical Research* **105**: 15439-15455.

Berger, G.W., Doran, P. (2001). Luminescence-dating zeroing tests in the Taylor Valley (McMurdo Dry Valleys), Antarctica. *Journal of Paleolimnology* **25**: 519-529.

Berger, G.W., Melles, M., Banerjee, D., Murray, A.S., Raab, A. (2004). Luminescence chronology of nonglacial sediments in Changeable Lake, Russian High Arctic and implications for limited Eurasian ice-sheet extent during the LGM. *Journal of Quaternary Science* **19**: 513-523.

Bergonzini, L., Chalie, F., Gasse, F. (1997). Paleoevaporation and Paleoprecipitation in the Tanganyika Basin at 18,000 Years B.P. Inferred from Hydrologic and Vegetation Proxies. *Quaternary Research* **47**: 295-305.

Bessems, I. (2007*). Late-Holocene climate reconstruction in equatorial East Africa: sedimentology and stable-isotope geochemistry of lake deposits*. Unpublished PhD thesis. University of Ghent, Ghent, p. 194.

Bessems, I., Verschuren, D., Russell, J.M., Hus, J., Mees, F., Cumming B.F. (2008). Palaeolimnological evidence for widespread late 18th century drought across equatorial East Africa. *Palaeogeography, Palaeoclimatology, Palaeoecology* **259**: 107-120.

Beuning, K.R. M., Russell, J.M. (2004). Vegetation and sedimentation in the Lake Edward Basin, Uganda-Congo during the late Pleistocene and early Holocene. *Journal of Paleolimnology*, **32**: 1-18.

Beuning, K., Talbot, M.R., Kelts, K. (1997). A revised 30,000-year paleoclimatic and paleohydrologic history of Lake Albert, East Africa. *Palaeogeography, Palaeoclimatology, Palaeoecology* **136**: 259-279.

Birks, H.J.B. (1995). Quantitative palaeoenvironmental reconstructions. In: Maddy, D., and Brew, J.S. (Eds.). *Statistical Modelling of Quaternary Science Data*, Quaternary Research Association Technical Guide 5. Cambridge. pp. 161-254.

Birks, H.J.B. (1998). Numerical tools in paleolimnology - progress, potentialities, and problems. *Journal of Paleolimnology* **20:** 307-332.

Birks, H.J.B., Birks, H.H. (1980). *Quaternary Palaeoecology*. London, Edward Arnold.

Birks, H.J.B., Gordon, A.D. (1985). *Numerical methods in Quaternary Pollen Analysis*. Academic Press, London: 1-317.

Birks, H.H., Birks, H.J.B. (2003). Reconstructing Holocene climates from pollen and plant macrofossils. In: Mackay, A.W., Battarbee, R.W., Birks, H.J.B., Oldfield, F. (Eds.). *Global Change in the Holocene*. London, Arnold. pp 342-357.

Birks, H.J.B., Line, J.M., Juggins, S., Stevenson, A.C., ter Braak, C.J.F. (1990). Diatoms and pH reconstruction. *Philisophical Transactions of the Royal Society of London B* **327**: 263-278.

Bishop, W.W. (1969). *Pleistocene stratigraphy in Uganda*. Memoir No. X. Geological Survey of Uganda, Government printer.Use the "Insert Citation" button to add citations to this document.

Black, E., Slingo, J., Sperber, K.R. (2003). An observational study of the relationship between excessively strong short rains in coastal East Africa and Indian Ocean SST. *Monthly Weather Review* **131**: 74-94

Bond, G., Kromer, B., Beer, J., Muscheler, R., Evans, M.N., Showers, W., Hoffmann, S., Lotti-Bond, R., Hajdas, I., Bonani, G. (2001). Persistent solar influence on North Atlantic climate during the Holocene. *Science* **294**: 2130-2136.

Bonnefille, R., Riollet, G., Buchet, G., Icole, M., Lafont, R., Arnold, M. (1995). Glacial/interglacial record from tropical Africa, high resolution pollen and carbon data at Rusaka, Burundi. *Quaternary Science Reviews* **14**: 917-936.

Bootsma, H.A., Hecky, R.E. (1993). A comparative introduction to the biology and limnology of the African Great Lakes. *Journal of Great Lakes Research* **29**: 3-18.

Borcard, D., Legendre, P., Drapeau, P. (1992). Partialling out the spatial component of ecological variation. *Ecology* **73**: 1045-1055.

Boreham, S., Field, M.H., Gibbard, P.L. (1999). Middle Pleistocene interglacial sediments at Tye Green, Stanstead Airport, Essex, England. *Journal of Quaternary Science* **14**: 207-222.

Borman, F.H., Likens, G.E. (1970). The nutrient cycles of an ecosystem. *Scientific American* **223**: 92-101.

Bradley, R.S. (2000). 1000 years of climate change. *Science* **288**: 1353-1354.

Bradshaw, E.G., Anderson, N.J. (2001). Validation of a diatom–phosphorus calibration set for Sweden. *Freshwater Biology*, **46**: 1035-1048.

Bradshaw, E.G., Anderson, N.J. (2003). Environmental factors that control the abundance of Cyclostephanos dubius (Bacillariophyceae) in Danish lakes, from seasonal to century scale. *European Journal of Phycology* **38**: 265-76.

Bradshaw, E.G., Anderson, N.J., Jensen, J.P., Jeppesen, E. (2002). Phosphorus dynamics in Danish lakes and the implications for diatom ecology and palaeoecology. *Freshwater Biology* **47**: 1963-1975.

Bradshaw, E.G., Rasmussen, P., Odgaard, B.V. (2005). Mid- to late-Holocene land-use change and lake development at Dallund Sø, Denmark: synthesis of multiproxy data, linking land and lake. *The Holocene* **15**: 1152-1162.

Braille, L.W., Keller, G.R., Wendlandt, R.F., Morgan, P., Khan, M.A. (1995). The East African Rift System. In: Olsen, K.H. (Ed.) *Continental Rifts: Structure, Evolution.* Tectonics (CREST), Elsevier, Amsterdam. pp. 213–232.

Broecker, W.S., Sutherland, S., Peng, T.-H. (1999). A possible 20th-century slowdown of Southern Ocean deep water formation. *Science* **286**: 1132-1135.

Brooks, C.E.P. (1923). Variations in the levels of the central African lakes Victoria and Albert. *Geophysical Memoirs* **20**: 337-344.

Brown, E.T., Johnson, T.C. (2005). Coherence between tropical East Africa and South American records of the Little Ice Age. *Geochemistry, Geophysics, Geosystems* **6**: 1-11.

Butzer, K.W., Isaac, G.L., Richardson, J.L., Washbourn-Kamau, C. (1972). Radiocarbon dating of East African lake levels. *Science* **175**: 1069-1076.

Bwanika, G.N., Makanga, B., Kizito, Y., Chapman, L.J., Balirwa, J. (2004). Observations on the biology of Nile tilapia, Oreochromis niloticus, L., in two Ugandan Crater lakes. *African Journal of Ecology* **42**: 93–101.

Caljon, A.G., Cocquyt, C.Z. (1992). Diatoms from surface sediments of the northern part of Lake Tanganyika. *Hydrobiologia* **230**: 135-156.

Campagna, V.S. (2007). Limnology and biota of Lake Yindarlgooda – an inland salt lake in Western Australia under stress. Unpublished PhD thesis. Curin University of Technology, Australia. pp. 245

Campbell, P.G.C., Hansen, H.J., Dubrueuil, B., Nelson, W.O. (1992). Geochemistry of Quebec North Shore salmon rivers during snowmelt: organic acid pulse and aluminum mobilization. *Canadian Journal of Fisheries and Aquatic Sciences* **49**: 1938-1952.

Carlson, R.E. (1977). A trophic state index for lakes. *Limnology and Oceanography* **22**: 361-369.

Chalié, F., Gasse, F. (2002). Late Glacial-Holocene diatom record of water chemistry and lake level change from the tropical East African Rift Lake Abiyata (Ethiopia). *Palaeogeography, Palaeoclimatology, Palaeoecology* **187**: 259-283.

Chapman, L.J., Kramer, D.L. (1991). The consequences of flooding for the dispersal and fate of poeciliid fish in an intermittent tropical stream. *Oecologia* **87**: 299-306.

Chapman, L.J., Chapman, C.A., Crisman, T.L., Nordlie, F.G. (1998). Dissolved oxygen and thermal regimes of a Ugandan crater lake. *Hydrobiologia* **385**: 201-211.

Charles, D.F., Acker, F.W., Hart, D.D., Reimer, C.W., Cotter, P.B. (2006). Large-scale regional variation in diatom-water chemistry relationships: rivers of the eastern United States. *Hydrobiologia* **561**: 27-57.

Chivas, A.R., De Dekker, P., Cali, J.A., Chapman, A., Kiss, E., Shelly, J.M.G. (1993). Coupled stable isotope and trace element measurements of lacustrine carbonates as palaeoclimatic indicators. In: Swart, P.K., Lohmann, K.C., McKenzie, J.A. and Savin, S. (Eds.). Climate change in continental isotopic records, *Geophysical Monograph* **78**: 113-122.

Cholnoky, B.J. (1953). Studien zur Ökologie der Diatomeen cines eutrophen subtropischen Gewässers. Berichte der Deutschen Botanischen Gesellschaft **66**: 346-355.

Cholnoky, B.J. (1968). *Die Ökologie der Diatomeen in Binnengewassern*. J. Cramer, Braunschweig.

Cholnoky, B.J. (1970). *Bacillariophyceae from the Bangweulu Swamps*. Cercle Hydrobiologique de Bruxelles, Brussels.

Clavero, E., Garcia-Pichel, F., Grimalt, O., Hernandez-Marine, M. (2001). Behaviour of diatoms apparently adapted to salinity. The case of *Climaconeis scopuloroides* and *Amphora* aff. *Hyaline*. In: Elster, J, Seckbach, J., Vincent, W.F., Lhotsky, O. (Eds.). *Algae and extreme environments: Ecology and physiology*. Proceedings of the international conference. J.Cramer, Berlin. pp 453-463.

Cocquyt, C. (1998). *Diatoms from the Northern Basin of Lake Tanganyika*. Bibliotheca Diatomologica 39. Crammer, Berlin/Stuttgart.

Coetzee, J.A. (1967). Pollen analytical studies in east and southern Africa. *Palaeoecology of Africa* **3**: 1–146.

Cohen, A.S., Palacios-Fest, M.R., Msaky, E.S., Alin, S.R., McKee, B., O'Reilly, C.M., Dettman, D.L., Nkotagu, H., Lezzar, K.E. (2005). Paleolimnological investigations of anthropogenic environmental change in Lake Tanganyika: IX. Summary of paleorecords of environmental change and catchment deforestation at Lake Tanganyika and impacts on the Lake Tanganyika ecosystem. *Journal of Paleolimnology* **34**:125–145.

Cole, G.A. (1975). *Textbook of Limnology*. The C.V. Mosby Co. Saint Louis. p283.

Cole, J. (2003). Dishing the dirt on coral reefs. *Nature*, **421**: 705-706.

Cole, J., Dunbar, R., McClanahan, T., Muthiga, N. (2000). Tropical Pacific forcing of decadal SST variability in the Western Indian Ocean over the past two centuries. *Science*, **287**: 617-619.

Colman, S.M. (1996). Acoustic stratigraphy of Bear Lake, Utah-Idaho-Late Quaternary sedimentation patterns in a simple half-graben. *Sedimentary Geology* **185**: 113-125.

Coleman, S.M., Jones, G.A., Rubin, M., King, J.W., Peck, J.A., Orem, W.H. (1996). AMS radiocarbon analyses from Lake Baikal, Siberia: challenges of dating sediments from a large, oligotrophic lake. *Quaternary Science Reviews* **15**:669–84.

Conway, D. (2002). Extreme Rainfall Events and Lake Level Changes in East Africa: Recent Events and Historical Precedents. In: Odada, E.O., Olago, D.O. (eds). *The East African Great Lakes: Limnology, Palaeolimnology and Biodiversity*. Springer Netherlands. pp 63-92.

Cook, R.D., Weisberg, S. (1982). *Residuals and Influence in Regression*. Chapman and Hall, New York.

Craig, H. (1961). Isotopic variations in meteoric waters. *Science* **133**: 1833-1834.

Creer, K.M., Thouveny, N. (1996). The Euromaar project. *Quaternary Science Reviews* **15**: 99–245.

Cremer, H., Wagner, B. (2004). Planktonic diatom communities in High Arctic lakes (Store Koldewey, Northeast Greenland). *Canadian Journal of Botany* **82**: 1744-1757.

Crisman, T. L., Chapman, L.J., Chapman, C.A., Prenger, J. (2001). Cultural eutrophication of a Ugandan highland crater lake: a 25-year comparison of limnological parameters. *Verhandlungen Internationale Vereinigung für Limnologie* **27**: 3574-3578.

Crumpler, L.S., Aubele, J.C. (2001). Volcanoes in New Mexico: an abbreviated guide for non-specialists. In: Crumpler, L.S., Lucas, S.G. (Eds.) Volcanology in New Mexico, *Museum of Natural History and Science Bulletin* **18**: 5-15.

Cumming, B.J., Smol, J.P. (1993). Development of diatom-based models for paleoclimatic research from lakes in British Colombia (Canada). *Hydrobiologia* **269/270**: 179-196.

Cumming, B.F., Wilson, S.E., Hall, R.I., Smol, J.P. (1995). *Diatoms from British Columbia (Canada) Lakes and their Relationship to Salinity, Nutrients and Other Limnological Variables*. Bibliotheca Diatomologica: 31. Stuttgart, Germany. pp. 207.

Curtis, P.J., Adams, H.E. (1995). Dissolved organic-matter quantity and quality from fresh-water and saltwater lakes in east-central Alberta. *Biogeochemistry* **30**: 59–76.

Davies, S.J., Metcalfe, S.E., Caballero, M.E., Juggins, S. (2002). Developing diatom-based transfer functions for Central Mexican lakes. *Hydrobiologia* **467**: 199-213.

Davis, M.B. (1976). Erosion rates and land-use history in southern Michigan. *Environmental Conservation* **3**: 139–148.

Davis, M.B., Ford, M.S. (1982). Sediment focusing in Mirror Lake, New Hampshire. *Limnology and Oceanography* **27**: 137-150.

DeBusk Jr, G.H. (1998). A 37,500-year pollen record from Lake Malawi and implications for the biogeography of afromontane forests. *Journal of Biogeography* **25**: 479-500**.**

Dean, W.E. Jr. (1974). Determination of carbonate and organic matter in calcareous sediments and sedimentary rocks by loss on ignition: Comparison with other methods. *Journal of Sedimentary Petrology* **44**: 242–248.

Dearing, J.A. (1994). Reconstructing the history of soil erosion; In: Roberts, N. (Ed.). *The Changing Global Environment*. Blackwell, Oxford. p242-261.

Dearing, J.A., Elner, J.K., Happey-Wood, C.M. (1981). Recent sediment flux and erosional processes in a Welsh upland lake catchment based on magnetic susceptibility measurements. *Quaternary Research* **16**: 356-372.

Deevey, E.S., Rice, D.S., Rice, P.S., Vaughan, H.H., Brenner, M., Flannery, M.S. (1979) Mayan urbanism: impact on a tropical karst environment. *Science* **206**: 298–306.

deMenocal, P., Ortiz, J., Guilderson, T., Sarnthein, M. (2000). Coherent high- and low-latitude climate variability during the Holocene warm period. *Science*, 288: 2198-2202.

Dickman, M. (1998). Benthic marine diatom deformities associated with contaminated sediments in Hong Kong. *Environment International* **24**: 749–759.

Dixon, C.G., Morton, W.H. (1970). Thermal and mineral springs in Uganda. *Geothermics* **2**: 1035-1038.

Dong, X., Bennion,H., Battarbee,R., Yang,X., Yang,H., Liu,E. (2008). Tracking eutrophication in Taihu Lake using the diatom record: potential and problems. *Journal of Paleolimnology* **40**: 413-429.

Doyle, S. (2006). *Crisis & Decline in Bunyoro: Population & Environment in Western Uganda 1860-1955*. Ohio University Press, pp: 320.

Duigan, C.A., Birks, H.H. (1997). The late-glacial and early-Holocene palaeoecology of cladoceran microfossil assemblages at Kråkenes, western Norway, with a quantitative reconstruction of temperature changes. *Journal of Paleolimnology* **23**: 67-76.

Dunbar, R. B., Cole, J.E. (1999). Annual Records of Tropical Systems (ARTS). *Workshop Report, Series 99-1*, PAGES/CLIVAR Initiative: 73.

Ebinger, C.J. (1989). Tectonic development of the western branch of the East African rift system. *Geological Society of America Bulletin* **101**: 885–903.

Eby, G.N., Lloyd, F.E., Woolley, A.R., Stoppa, F., Weaver, S.D. (2003). Geochemistry and mantle source(s) for carbonatitic and potassic lavas, Western Branch of the East African Rift System, SW Uganda. *Geolines* **15**: 23–27.

Eggermont H., Verschuren, D. (2004a). Subfossil Chironomidae from East African low- and mid-elevation lakes. 1. Tanypodinae and Orthocladiinae. *Journal of Paleolimnology* **32**: 383-412.

Eggermont H., Heiri, O. Verschuren, D. (2006). Subfossil Chironomidae (Insecta: Diptera) as quantitative indicators for past salinity variation in African lakes. *Quaternary Science Reviews* **25**: 1966-1994.

Eggermont, H., Russell, J. M., Schetter, G., Vandamme, K., Verschuren, D. (2007). Physical and chemical limnology of alpine lakes and pools in the Rwenzori Mountains, Uganda-Congo. *Hydrobiologia* **592**: 151-173.

Ekdahl, E.J., Teranes, J.L., Guilderson, T.P., Turton, C.L., McAndrews, J.H., Wittkop, C.A., Stoermer, E.F. (2004). Prehistorical record of cultural eutrophication from Crawford Lake, Canada. *Geology* **32**: 745-748.

Endfield, G., Ryves, D.B., Mills, K., Berrang-Ford L (2009). "The gloomy forebodings of this dread disease": climate, environment and sleeping sickness in East Africa around the turn of the twentieth century. *Geographical Journal*.

Engstrom, D.R. (1987). Influence of vegetation and hydrology on the humus budgets of Labrador lakes. *Canadian Journal of Fisheries and Aquatic Sciences* **44**: 1306-1314.

European Diatom Database (EDDI). http://craticula.ncl.ac.uk/Eddi/ [accessed 20/08/08]

Fee, E.J., Hecky, R.E., Kasian, M.S.E., Cruikshank, D.R. (1996). Effects of lake size, water clarity, and climatic variability on mixing depths in Canadian Shield lakes. Limnology and Oceanography **41**: 912-920.

Fichtler, E., Trouet, V., Beeckman, H., Coppin, P., Worbes, M. (2004). Climatic signals in tree rings of Burkea africana and Pterocarpus angolensis from semi-arid forests in Namibia. *Trees*, **18**:442–451

Ficken, K.J., Li, B., Swain, D.L., Eglinton, G. (2000). An *n*-alkane proxy for the sedimentary input of submerged/floating freshwater aquatic macrophytes. *Organic Geochemistry* **31**: 745-749.

Ficken, K.J., Street-Perrot, F.A., Perrott, R.A., Swain, D.L., Olago, D.O., Eglinton, G. (1998). Glacial/interglacial variations in carbon cycling revealed by molecular and isotope stratigraphy of Lake Nkunga, Mt. Kenya, East Africa. *Organic Geochemistry* **29**: 1701-1719.

Ficken, K.J., Wooller, M.J., Swain, D.L., Street-Perrott, F.A., Eglinton, G. (2002). Reconstruction of a subalpine grass-dominated ecosystem, Lake Rutundu, Mount Kenya: a novel multi-proxy approach. *Palaeogeography, Palaeoclimatology, Palaeoecology* **177**: 137-149.

Filippi, M.L., Talbot, M.R. (2005). The palaeolimnology of northern Lake Malawi over the last 25 ka based upon the elemental and stable isotopic composition of sedimentary organic matter. *Quaternary Science Reviews* **24**: 1303-1328.

Finkel, Z.V., Katz, M.E., Wright, J.D., Shofield, O.M.E., Falkowski, P.G. (2005). Climatically driven macroevolutionary patterns in the size of marine diatoms over the Cenozoic. *PNAS* **102**: 8927-8932.

Fisher, C.T., Pollard, H.P., Israde-Alcántara, I., Garduño-Monroy, V.H., Banerjee, S.K. (2003). A re-examination of human-induced environmental change within the Lake Pátzcuaro Basin, Michoacán, Mexico. *PNAS* **8**: 4957-4962.

Fore, L.S., Grafe, C. (2002). Using diatoms to assess the biological consition of large rivers in Idaho (USA). *Freshwater Biology* **47**: 2015-2037.

Forman, S.L., Pierson, J., Gomez, J., Brigham-Grette, J., Nowaczyk, N.R., Melles, M. (2007). Luminesence geochronology for sediments from Lake El'gygytgyn, northeast Siberia, Russia: constraining the timing of palaeoenvironmental events for the past 200 ka. *Journal of palaeolimnology* **37**: 77-88.

Fritz, S.C. (1989). Lake development and limnological response to prehistoric and historic land-use in Diss, Norfolk, U.K. *Journal of Ecology* **77**: 182–202.

Fritz, S.C. (1990). Twentieth-Century salinity and water-level fluctuations in Devils Lake, North Dakota: Test of a diatom-based transfer function. *Limnology and Oceanography* **35**: 1771-1781.

Fritz S.C. (2008). Deciphering climatic history from lake sediments. *Journal of Paleolimnology* **39**: 5-16.

Fritz, S.C., Juggins, S., Battarbee, R.W., Engstrom, D.R. (1991). Reconstruction of past changes in salinity and climate using a diatom-based transfer function. *Nature* **352**: 706-708.

Fritz, S.C., Juggins, S., Battarbee, R.W. (1993). Diatom assemblages and ionic characterization of lakes of the Great Northern Plains, North America: a tool for reconstructing past salinity and climate fluctuations. *Canadian Journal of Fisheries and Aquatic Sciences* **50**: 1844-1856.

Fritz, S.C., Cumming, B.F., Gasse, F., and Laird, K. (1999). Diatoms as indicators of hydrologic and climate change in saline lakes. In: Stoermer, E.F., Smol, J.P. (Eds.). *The Diatoms: Applications for Environmental and Earth Sciences*. Cambridge University Press, Cambridge. pp. 41-72.

Fritz S.C. (2008). Deciphering climatic history from lake sediments. *Journal of Paleolimnology* **39**: 5-16.

Ganf, G.G. (1974a). Diurnal mixing and the vertical distribution of phytoplankton in a shallow equatorial lake (Lake George, Uganda). *The Journal of Ecology* **62**: 611-629.

Ganf, G.G. (1974b). Phytoplankton biomass and distribution in a shallow eutrophica lake (Lake George, Uganda). *Oecologia* **16**: 9-29.

Gaskin, D.E (1979). Change of particle size in diatom populations as a possible factor in pelagic marine ecosystem resilliance. *Tuatara* **24**: 23-39.

Gasse, F. (1986). *East African diatoms; Taxonomy, ecological distribution*. Bibliotheca Diatomologica 11. Crammer, Berlin/Stuttgart.

Gasse, F. (2000). Hydrological changes in the African tropics since the Last Glacial Maximum. *Quaternary Science Reviews* **19**: 189-211.

Gasse, F. (2002). Diatom-inferred salinity and carbonate oxygen isotopes in Holocene waterbodies of the western Sahara and Sahel (Africa). *Quaternary Science Reviews* **21**: 737-767.

Gasse, F. (2006). Climate and hydrological changes in tropical Africa during the past million years. *Comptes rendus Palevol*, **5**: 35-43.

Gasse, F., Tekaia, F. (1983). Transfer functions for estimating paleoecological conditions (pH) from East African diatoms. *Hydrobiologia* **103**: 85-90.

Gasse, F., Fontes, J-C. (1989). Palaeoenvironments and palaeohydrology of a tropical closed lake (Lake Asal, Djibouti) since 10,000 yr BP. *Palaeogeography, Palaeoclimatology, Palaeoecology* **69**: 67–102.

Gasse, F., van Campo, E. (1994). Abrupt post-glacial climate events in West Asia and North Africa monsoon domains. *Earth and Planetary Science Letters*, **126**: 435-456.

Gasse, F., Talling, J.F., Kilham, P. (1983). Diatom assemblages in East Africa: classification, distribution and ecology. *Review Hydrobiology Tropical* **116**: 3-34.

Gasse, F., Ledee, V., Massault, M., Fontes, J-C. (1989). Water level fluctuations of Lake Tanganyika in phase with oceanic changes during the last glaciation and deglaciation. *Nature* **342**: 57-59.

Gasse, F., Juggins, S., Ben Khelifa, L. (1995). Diatom-based transfer functions for inferring past hydrochemical characteristics of African lakes. *Palaeogeography, Palaeoclimatology, Palaeoecology* **117**: 31-54.

Gasse, F., Juggins, S., Khelifa, L.B. (1995). Diatom-based transfer functions for inferring past hydrochemical characteristics of African lakes. *Palaeogeography, Palaeoclimatology, Palaeoecology*, **117**: 31-54.

Gasse, F., Barker, P., Gell, P.A., Fritz, S.C., Chalie, F. (1997). Diatom-inferred salinity in palaeolakes: An indirect tracer of climate change. *Quaternary Science Reviews* **16**: 547-563.

Gasse, F., Barker, P., Johnson, T.C. (2002). A 24,000 yr diatom record from the northern basin of Lake Malawi. In: Odada, E.O., Olago, D.O. (Eds). *East African Great Lakes: Limnology, Paleolimnology and Biodiversity. Advances in Global Change Research*, Kluwer Academic, Dordrecht.

Gauch, H.G. (1982). *Multivariate Analysis in Community Structure*. Cambridge University Press, Cambridge.

Gell, P.A. (1998). Quantitative reconstructions of the Holocene palaeosalinity of paired crater lakes based on a diatom transfer function. *Palaeoclimates* **3**: 83–96.

Gergel, S.E., Turner, M.G., Kratz, T.K. (1999). Dissolved organic carbon as an indicator of the scale of watershed influence on lakes and rivers. *Ecological Applications* **9**: 1377-1390.

Germain, H. (1981). *Flore des diatomées. Eaux douces et saumâtres du Massif Armoricain et des contrées voisines d'Europe occidentale*. Boubée, Paris, France.

Goldschmidt, T., Witte, F., Wanink, J. (1993). Cascading Effects of the Introduced Nile Perch on the Detritivorous/Phytoplanktivorous Species in the Sublittoral Areas of Lake Victoria**.** *Conservation Biology* **7**: 686 - 700

Golterman, H.L. (1973). Natural phosphate sources in relation to phosphate budgets: a contribution to the understanding of eutrophication. *Water Research* **7**: 3-17.

Gorham, E. (1955). On the acidity and salinity of rain. *Geochemica et Cosmochim Acta* **7**: 231-239.

Grasshoff, K., Ehrhardt, M., Kremling, K. (1983). *Methods of seawater analysis*. Verlag Chemie, Weinheim.

Green, J. (1986). Zooplankton associations in some Ethiopian crater lakes. *Freshwater Biology* **16**: 495-499.

Gregory J.W. (1896). *The Great Rift Valley*. London.
Gunkel, G. (2000). Limnology of an equatorial high mountain lake in Ecuador, Lago San Pablo. *Limnologica* **30**: 113-120.

Hall, R.I., Smol, J.P. (1996). Paleolimnological assessment of long-term water-quality changes in south-central Ontario affected by cottage development and acidification. *Canadian Journal of Fisheries and Aquatic Sciences* **53**: 1-117.

Hamilton, A. (1972). The Quaternary history of African forests: its relevance to conservation. *African Journal of Ecology* **19**: 1-6.

Hamilton, A. (1982). *Environmental history of East Africa: A study of the Quaternary*. London, Academic Press.

Hamilton, A.C., Taylor, D., Vogel, J.C. (1986). Early forest clearances and environmental degradation in south-west Uganda. *Nature* **320**: 164–167.

Hammer U.T. (1986). Saline lake ecosystems of the world. In: Dumont, H.J. (Eds.) *Monographiae Biologicae*. Junk, Dordrecht. pp. 616.

Hassan, F.A. (1998) Climatic change, Nile floods and civilization. *Nature and Resources* **34**: 34-40

Hastenrath, S. (1981). The *glaciers of Equatorial East Africa*. Dordrecht, Reidel.

Hastenrath, S. (2001). Variations of East African climate during the past two centuries. *Climatic Change* **50**: 209-217.

Haug, G.H., Hughen, K.A., Sigman, D.M., Peterson, L.C., Röhl, U. (2001). Southward migration of the intertropical convergence zone through the Holocene. *Science* **293**: 1304-1307.

Hausmann, S., Lotter, A.F. (2001). Morphological variation within the diatom taxon *Cyclotella comensis* and its importance for quantitative temperature reconstructions. *Freshwater Biology* **46**: 1323-1333.

Hecky, R.E. (1971). *The palaeolimnology of the alkaline, saline lakes on the Mt. Meru lahar*. Ph.D. thesis, Duke University, Durham, N.C. pp 209.
Hecky, R.E. (1993). The eutrophication of Lake Victoria. *Verhandlungen Internationale Vereinigung für Limnologie* **25**: 39-48.

Hecky, R.E. (2000). A biogeochemical comparison of Lakes Superior and Malawi and the limnological consequences of an endless summer. *Aquatic Ecosystem Health and Management* **3**: 23-33.

Hecky, R.E., Kilham, P. (1973). Diatoms in alkaline, saline lakes: Ecology and geochemical implications. *Limnology and Oceanography* **18**: 53-71.

Hecky, R.E., Fee, E.J. (1981). Primary production and rates of algal growth in Lake Tanganyika. *Limnology and Oceanography* **26**: 532-547.

Hecky, R. E., Bugenyi, F.W.B. (1992). Hydrology and chemistry of the African great Lakes. *Mitteilungen der Internatinalen Vereinigung für Limnologie* **23**: 45-54.

Heiri, O., Lotter, A.F., Lemcke, G. (2001). Loss on ignition as a method for estimating organic and carbonate content in sediments: reproducibility and comparability of results. *Journal of Paleolimnology* **25**: 101-110.

Hill, M.O., Gauch, H.G. (1980). Detrended correspondence analysis: An improved ordination technique. *Plant Ecology* **42**: 47-58.

Hillaire-Marcel, C., Aucour, A-M., Bonnefille, R., Riollet, G., Vincens, A., Williamson, D. (1989). ^{13}C/Palynological evidence of differential residence times of organic carbon prior to its sedimentation in East African Rift lakes and peat bogs. *Quaternary Science Reviews* **8**: 207–212.

Holmes, A. (1965*) Principles of physical geology*. Nelson, London.

Holmgren, K., Karlen, W., Lauritzen, S., Lee-Thorp, J., Partridge, T., Piketh, S., Repinski, P., Stevenson, C., Svanered, O., Tyson, P (1999). A 3000-year high-resolution stalagmite record of palaeoclimate for North-Eastern South Africa. *The Holocene* **9**: 271-278.

Horiuchi, K., Minoura, K., Hoshino, K., Oda, T., Nakamura, T., Kawai, T. (2000). Palaeoenvironmental history of Lake Baikal during the last 23000 years. *Palaeogeography, Palaeoclimatology, Palaeoecology* **157**: 95–108.

Hoyt, D.V., Schatten, K.H. (1997). *The Role of the Sun in Climate Change*. Oxford. University Press. pp 279

Huang, Y., Street-Perrott, F.A., Eglinton, G. (1995). Molecular and carbon isotope stratigraphy of a glacial/interglacial sediment sequence from a tropical freshwater lake: Sacred Lake, Mt. Kenya. In: Grimalt, J.O., Dorronsoro, C. (Eds). *Organic Geochemistry: Developments and Applications to Energy, Climate, Environment and Human History*. Pergamon Press, Oxford, pp. 826-829.

Huisman, J., Olff, H., Fresco, L.F.M. (1993). A hierarchical set of models for species response analysis. *Journal of Vegetation Science* **4**: 37–46.

Hurst, H. E., Black, R.P. (1943-1949). *The Nile Basin: Vol VI-VIII*. Cairo, Government Press.

Hurst, H. E., Phillips, P. (1933-1946). *The Nile Basin: Vol I-V*. Cairo, Government Press.

Hustedt, F. (1949). Süßwaser-Diatomeen aus dem Albert-National park in Belgisch-Kongo. Exploratie van het Nationaal Albert.

Hutchison, G.E. (1957). *A treatise on limnology*.John wiley & Sons, New York. Pp. 1015.

Hutchinson, G.E., Löffler, J. (1956). The thermal classification of lakes. *Proceedings of the Natural Academic Sciences* **42**: 84–86.

Intergovernmental Panel on Climate Change. (2007). *Climate Change 2007: Fourth Assessment Report*. Cambridge University Press.

Jenkin, P.M. (1936). Reports on the Percy Sladden Expedition to some rift valley lakes in Kenya in 1929. VII. Summary of the ecological results with special reference to the alkaline lakes. *Annals and Magazine of Natural History* **10**: 133-181.

John, R., Ezekiel, M., Philbert, C., Andrew, A. (2008). Schistosomiasis transmission at high altitude crater lakes in Western Uganda. *BMC Infectious Diseases* **8**: 110.

Johnson, T.C. (1996). Sedimentary processes and signals of past climate change in the large lakes of the African Rift Valley. In: Johnson, T.C., Odada, E.O. (Eds). *The Limnology, Climatology and Paleoclimatology of the East African Lakes*. Amsterdam, Gordon and Breach.

Johnson, T.C., Kelts, K., Odada, E. (2000). The Holocene history of Lake Victoria. *Ambio* **29**: 2-11.

Johnson, T.C., Barry, S.L., Chan, Y., Wilkinson, P. (2001). Decadal record of climate variability spanning the past 700 yr in the southern tropics of East Africa. *Geology* **29**: 83-86.

Jolly, D., Taylor, D., Marchant, R., Hamilton, A., Bonnefille, R., Buchet, G., Riollet, G. (1997). Vegetation dynamics in central Africa since 18,000 yr BP: pollen records from the interlacustrine highlands of Burundi, Rwanda and western Uganda. *Journal of Biogeography* **24**: 495-512.

Jones, V., Juggins, S. (1995). The construction of a diatom-based chlorophyll a transfer function and its application at three lakes on Signy Island (maritime Antarctic) subject to differing degrees of nutrient enrichment. *Freshwater Biology* **34**: 433-445.

Jones, P. D., Osborn, T.J., Briffa, K.R. (2001). The evolution of climate over the last millinium. *Science* **292**: 662–667.

Jowsey, P.C. (1966). An improved peat sampler. *New Phytologist* **65**: 245-248.

Juggins S. (2001). The European Diatom Database User Guide: Version 1.0. University of Newcastle, Newcastle upon Tyne, 72 pp.

Juggins, S. (2002). *ZONE: a DOS program for the zonation (constrained clustering) of palaeoecological data*. Newcastle University.

Juggins, S. (2003). *C2, user Guide; Software for Ecological and Palaeoecological Data Analysis and Visualisation*. University of Newcastle, Newcastle upon Tyne, United Kingdom. pp. 66.

Juggins S., ter Braak C.J.F. (1997). *CALIBRATE – A Computer Program for Species – Environmental Calibration by [Weighted-Averaging] Partial Least Squares Regression (0.81)*. University of Newcastle, England.

Karlén, W., Fastook, J., Holmgren, K., Malmstrom, M., Matthews, J.A., Odada, E., Risberg, J., Rosqvist, G., Sandgren, P., Shemesh, A., Westerberg, L-O. (1999). Glacier fluctuations on Mount Kenya since ~6000 Cal. Years BP: Implications for Holocene climatic change in Africa. *Ambio* **28**: 409-418.

Kalff, J. (1983). Phosphorus limitation in some tropical African lakes. *Hydrobiologia* **100**: 101-112.

Kalff, J. (2003). *Limnology*. Prentice Hall Inc. New Jersey

Kalff, J., Watson, S. (1986). Phytoplankton and its dynamics in two tropical lakes: a tropical and temperate zone comparison. *Hydrobiologia* **138**: 161-176.

Kalyebara, R., Nkuba, J.M., Byabachwezi, M.S.R., Kikulwe, E.M., Edmeades, S. (2007). Overview of the Banana Economy in the Lake Victoria Regions of Uganda and Tanzania. In: Smale, M., Tushemereirwe, W.K. (Eds.) *An Economic Assessment of Banana Genetic Improvement and Innovation in the Lake Victoria Region of Uganda and Tanzania*. International Food Policy Research Institute, Research Report No. 155: 25-36.

Kaufman, D.K., Manley, W.F., Forman, S.L., Layer, P.W. (2001). The last interglacial to glacial transition, Togiak Bay, southwestern Alaska. *Quaternary Research* **55**:190–202.

Kelly, M.G., Bennion, H., Cox, E.J., Goldsmith, B., Jamieson, J., Juggins, S., Mann, D.G., Telford, R.J. (2005). Common freshwater diatoms of Britain and Ireland: an interactive key. Environment Agency, Bristol.

Kerr, S.R. (1974). Theory of Size Distribution in Ecological Communities. *Journal of Fisheries Research Board of Canada* **31**:1859-1862.

Kidoido, M.M., Kasenge, V., Mbowa, S., Tenywa, J.S., Nyende, P. (2002). Socioeconomic factors associated with finger millet production in eastern Uganda. *African Crop Science Journal* **10**: 111-120.

Kilham, P. (1971). *Biogeochemistry of African lakes and rivers*. Ph.D. thesis, Duke University, Durham, N.C. pp 199.

Kilham, P. (1971). A hypothesis concerning silica and the freshwater planktonic diatoms. *Limnology and Oceanography* **16**: 10-18.

Kilham, S.S., Kilham, P. (1975). *Melosira granulata* (Ehr.) Ralfs: Morphology and ecology of a cosmopolitan freshwater diatom. *Verhandlungen Internationale Vereinigung für Limnologie* **19**: 2716-2121.
Kilham, P., Kilham, S.S. (1990). Endless summer: internal loading processes dominate nutrient cycling in tropical lakes. *Freshwater Biology* **23**: 379-389.

Kilham, P., Kilham, S.S., Hecky, R.E. (1986). Hypothesized resource relationships among African planktonic diatoms. *Limnology and Oceanography* **31**: 1169-1181.

Kilian, M.R., van der Plicht, J., van Geel, B., Goslar, T. (2002). Problematic 14C-AMS dates of pollen concentrates from Lake Gościąż (Poland). *Quaternary International* **88**: 21–6.

Kingston, J.C., Birks, H.J.B., Uutala, A.J., Cumming, B.F., Smol, J.P. (1992). Assessing the trends in fishery resources and lake water aluminium from palaeolimnological analyses of siliceous algae. *Canadian Journal of Fisheries and Aquatic Sciences* **49**: 127–138.

Kizito, Y.S., Nauwerck, A. (1995). Temporal and vertical distribution of planktonic rotifers in a meromictic crater lake, Lake Nyahirya (western Uganda). *Hydrobiologia* **313-314**: 303-312.

Kizito, Y.S., Nauwerck, A., Chapman, L.J., Koste, W. (1993). A limnological survey of western Uganda crater lakes. *Limnologica* **23**: 335-347.

Kling, G.W. (1988). Comparative transparency, depth of mixing, and stability of stratification in lakes of Cameroon, West Africa. *Limnology and Oceanography* **33**: 27-40.

Kling, G.W., Clark, M.A., Wagner, G.N., Compton, H.R., Humphrey, A.M., Devine, J.D., Evans, W.C., Lockwood, J.P., Tuttle, M.L., Koenigsberg, E.J. (1987). The 1986 Lake Nyos disaster in Cameroon, West Africa. *Science* **236**: 169-175.

Korhola, A., Weckstrom, J., Holmstrom, L., Erasto, P. (2000). A quantitative Holocene climatic record from diatoms in Northern Fennoscandia. *Quaternary Research* **54**: 284-294.

Krammer, K., Lange-Bertalot, H. (1986). *Bacillariophyceae. 1. Teil. Naviculaceae*. Süßwasserflora von Mitteleuropa, Band 2/1. Stuttgart.

Krammer, K., Lange-Bertalot, H. (1988). B*acillariophyceae. 2. Teil. Bacillariaceae, Epithemiaceae, Surirellaceae*. Süßwasserflora von Mitteleuropa, Band 2/2. Stuttgart.

Krammer, K., Lange-Bertalot, H. (1991a). *Bacillariophyceae. 3. Teil. Centrales, Fragilariaceae, Eunotiaceae*. Süßwasserflora von Mitteleuropa, Band 2/3. Stuttgart.

Krammer, K., Lange-Bertalot, H. (1991b). *Bacillariophyceae. 4. Teil. Achnanthaceae, kritsche erganzungen zu Navicula (Lineolatae) und Gomphonema Gesamliteraturverzeichnis*. Süßwasserflora von Mitteleuropa, Band 2/4. Stuttgart.

Krider, P.R. (1998). Paleoclimatic significance of Late Quaternary lacustrine and alluvial stratigraphy, Animas Valley, New Mexico. *Quaternary Research* **50**: 283-289.

Kumar, K., Soman, M.K., Rupa Kumar, K. (1995). Seasonal forecasting of Indian summer monsoon rainfall: A review. *Weather* **50**: 449–466.
Lærdal, T., Talbot, M.R. (2002). Basin neotectonics of Lakes Edward and George, East African Rift. *Palaeogeography, Palaeoclimatology, Palaeoecology* **187**: 213-232.

Laird, K.R., Fritz, S.C., Grimm, E.C., Mueller, P.G. (1996). Century-scale paleoclimatic reconstruction from Moon Lake, a closed-basin lake in the northern Great Plains. *Limnology and Oceanography* **41**: 890-902.

Lamb, A. L., Leng, M.J., Lamb, H.F., Mohammed, M.U. (2000). A 9000-year oxygen and carbon isotope record of hydrological change in a small Ethiopian crater lake. *The Holocene* **10**: 167-177.

Lamb, A.L., Leng, M.J., Umer, M., Lamb, H.F. (2004). Holocene climate and vegetation change in the Main Ethiopian Rift Valley, inferred by the composition (C/N & $\delta^{13}C$) of lacustrine organic matter. *Quaternary Science Reviews* **23**: 881-891.

Lamb, H.F., Gasse, F., Benkaddour, A., Elhamouti, N., Vanderkaars, S., Perkins, W.T., Pearce, N.J., Roberts, C.N. (1995). Relation between Century-Scale Holocene Arid Intervals in Tropical and Temperate Zones. *Nature* **373**: 134-137.

Lamb, H.F., Bates, C.R., Coombes, P.V., Marshall, M.H., Umer, M., Davies, S.J., Dejen, E. (2007). Late Pleistocene desiccation of Lake Tana, source of the Blue Nile. *Quaternary Science Reviews* **26**: 287-299.

Langdale-Brown, I., Osmaston, H.A., Wilson, J.G. (1964). *The Vegetation of Uganda and Its Bearing on Land-Use*. Entebbe: Government of Uganda.

Lange-Bertalot, H. (1979). Pollution tolerance of diatoms as a criterion for water quality estimation. *Nova Hedwigia* **64**: 285-305.

Lauritzen, S-E., Lundberg, J. (1999) Speleothems and climate: a special issue of The Holocene: Editorial. *The Holocene* **9**: 643-647.
Laws, R.M., Parker, I.S.C., Johnstone, R.C.B. (1975). *Elephants and their habitats*. Clarendon Press, Oxford.

Lees, J.A., Flower, R.J., Ryves, D.B., Vologina, D., Sturm, M. (1998). Identifying sedimentation patterns in Lake Baikal using whole core and surface scanning magnetic susceptibility. *Journal of Paleolimnology* **20**: 187-202.

Legesse, D., Vallet-Coulomb, C., Gasse, F. (2003). Hydrological response of a catchment to climate and land use changes in Tropical Africa: case study South Central Ethiopia. *Journal of Hydrology* **275**: 67-85.

Legesse, D., Vallet-Coulomb, C., Gasse, F. (2004). Analysis of the hydrological response of a tropical terminal lake, Lake Abiyata (Main Ethiopian Rift Valley) to changes in climate and human activities. *Hydrological Processes* **18**: 487-504.

Leira, M., Sabater, S. (2005). Diatom assemblages distribution in Catalan rivers, NE Spain, in relation to chemical and physiographical factors. *Water Research* **39**: 73-82.

Lejju, B.J., Taylor, D., Robertshaw, P. (2005). Late-Holocene environmental variability at Munsa archaeological site, Uganda: a multicore, multiproxy approach. *The Holocene* **15**: 1044-1061.

Leland, H.V., Porter, S.D. (2000). Distribution of benthic algae I the upper Illinois River basin in relation to geology and land use. *Freshwater Biology* **44**: 279-301.

Leland, H.V., Brown, L.R., Mueller, D.K. (2001). Distribution of algae in the San Joaquin River, California, in relation to nutrient supply, salinity and other environmental factors. *Freshwater Biology* **46**: 1139-1167.

Leng, M.J., Marshall, J.D. (2004). Palaeoclimate interpretation of stable isotope data from lake sediment archives. *Quaternary Science Reviews* **23**: 811-831.

Leng, M.J., Lamb A.L., Heaton T.H.E., Marshall J.D., Wolfe B.B., Jones M.D, Holmes J.A. and Arrowsmith C. (2005). Isotopes in lake sediments. In: Leng M. J. (Ed.). *Isotopes in Palaeoenvironmental Research*. Springer, Dordrecht, The Netherlands.

Leong, L.S., Tanner, P.A. (1999). Comparison of Methods for Determination of Organic Carbon in Marine Sediment. *Marine Pollution Bulletin* **38**: 875-879.

Leps, J., Šmilauer, P. (2003). Multivariate Analysis of Ecological data using CANOCO. Cambridge University Press, Cambridge.

Lewandowska, J. Kosakowska, A. (2004). Effect of iron limitation on cells of the diatom *Cyclotella meneghiniana* Kützing. *Oceanologia* **46**: 269-287.

Lewis Jr., W.M. (1973). The thermal regime of Lake Lanao (Philippines) and its theoretical implications for tropical lakes. *Limnology and Oceanography* **18**: 200-217.

Lewis Jr., W.M. (1983). Temperature, heat, and mixing in Lake Valencia, Venezuela. *Limnology and Oceanography* **28**: 273-286.

Lewis Jr, W.M. (l984). A five-year record of the thermal and mixing properties of a tropical lake (Lake Valencia, Venezuela). *Archiv für Hydrobiologie* **99**: 340-346.

Lewis Jr., W. M. (1987). Tropical Limnology. *Annual Review of Ecology and Systematics* **18**: 159-184.

Leyden, B.W, Brenner, M., Dahlin, B.H. (1998). Cultural and climatic history of Cobá, a lowland Maya city in Quintana Roo, Mexico. *Quaternary Research* **49**: 111-122.

Lister, G.S., Kelts., K., Zao, C.K., Yu, J.K., Niessen, K. (1991). Lake Qinghai, China: closed basin lake levels and the oxygen isotope record for ostracoda since the Late Pleistocene. *Palaeogeography, Palaeoclimatology, Palaeoecology* **84**: 141–62.

Livingstone, D. (1967). Postglacial Vegetation of the Ruwenzori Mountains in Equatorial Africa. *Ecological Monographs* **37**: 25-52.

Livingstone, D.A., Melack, J.M. (1984). Some lakes of subsaharan Africa. In: Taub, F.B. (Ed.) *Lake and Reservoir Ecosystems*. Elsevier, Amsterdam.

Lock, J.M. (1967). *Vegetation in relation to grazing and soils in Queen Elizabeth National Park.* PhD Dissertation, Cambridge University, Cambridge, UK.

Lotter, A.F. (1998). The recent eutrophication of Baldeggersee (Switzerland) as assessed by fossil diatom assemblages. *The Holocene* **8**: 395-405.

Lotter, A.F. (2003). Multi-proxy Climatic Reconstructions. In: Mackay, A., Battarbee, R., Birks, J., Oldfield, F. (eds). *Global Change in the Holocene*. Hodder Arnold, New York.

Lund, J.W.G. (1950). Studies on *Asterionella formosa* Hass. II: Nutrient depletion and the spring maximum. *Journal of Ecology* **38**: 1-35.

MacIntyre, S. (1975). Orthophosphate concentrations in Kenyan lakes. *American Society of Limnology and Oceanography, 39th Annual meeting, Abstract.*

MacIntyre, S., Melack, J.M. (1982). Meromixis in an equatorial African soda lake. *Limnology and Oceanography* **27**: 595–609.

Mackay, A.W., Jones, V.J., Battarbee, R.W. (2003). Approaches to Holocene climate reconstruction using diatoms. In: Mackay, A.W., Battarbee, R.W., Birks, H.J.B., Oldfield, F. (Eds). *Global Change in the Holocene*. London, Arnold.

Magnuson, J.J., Benson, B.J., Kratz, T.K. (2004). Patterns of coherent dynamics within and between lake districts at local to intercontinental scales. *Boreal Environmental Research* **9**: 359-369.

Manly, B.F.J. (1992). *Randomization and Monte Carlo Methods in Biology*. Chapman and Hall, London. pp. 281.

Marchant, R., Taylor, D. (1998). Dynamics of montane forest in central Africa during the late Holocene: a pollen-based record from western Uganda. *The Holocene* **8**: 375-381.

Marchant, R., Taylor, D., Hamilton, A. (1997). Late Pleistocene and Holocene history at Mubwindi Swamp, Southwest Uganda. *Quaternary Research* **47**: 316-328.

Marchant, R., Mumbi, C., Behera, S., Yamagata, T. (2006). The Indian Ocean dipole – the unsung driver of climatic variability in East Africa. *African Journal of Ecology* **45**: 4-16.

Mathers, S.J. (1994). Industrial mineral potential of Uganda. In: Mathers, S.J., Notholt, A.J.G. (Eds). *Industrial Minerals in Developing Countries*. AGID Geosciences in International Development **18**: 144-166.

Mayewski, P.A., Meeker, L.D., Twickler, M.S., Whitlow, S.I., Yang, Q., Prentice, M. (1997). Major features and forcing of high latitude northern hemisphere atmospheric circulation over the last 110,000 years. Journal of Geophysical Research **102**: 26345-26,366.

Melack, J.M. (1978). Morphometric, physical and chemical features of the volcanic crater lakes of western Uganda. *Archive für Hydrobiologie* **84**: 430-453.

Melack, J. M. (1979). Photosynthesis and growth of Spirulina platensis (Cyanophyta) in an equatorial lake (Lake Simbi, Kenya). *Limnology and Oceanography* **24**: 753-760.

Melack, J. M., Kilham, P. (1972). Lake Mahega; A mesothermic, sulphato-chloride lake in Western Uganda. *African Journal of hydrobiology and fisheries* **2**: 141-150.

Melack, J. M., Kilham, P. (1974). Photosynthetic rates of phytoplankton in East African alkaline, saline lakes. *Limnology and Oceanography* **19**: 743-755.

Meyers, P.A., Ishiwatari, R. (1993). Lacustrine organic geochemistry: an overview of indicators of organic matter sources and diagenesis in lake sediments. *Organic Geochemistry* **20**: 867-900.

Meyers, P.A., Lallier-Vergès, E. (1999). Lacustrine records of changes in Late Quaternary continental environments and climates: an overview of sedimentary organic matter indicators. *Journal of Paleolimnology* **21**: 345-372.

Meyers, P.A., Teranes, J.L. (2001). Sediment organic matter. In: Last, W.M., Smol, J.P. (Eds). *Tracking Environmental Changes using Lake Sediments – Volume 2: Physical and Chemical Techniques*. Dordrecht, Kluwer Press.

Mitrovic, S.M., Chessman, B.C., Davie, A, Avery, E.L., Ryan, N. (2008). Development of blooms of *Cyclotella meneghiniana* and *Nitzschia* spp. (Bacillariophyceae) in a shallow river and estimation of effective suppression fows. *Hydrobiologia* **596**: 173-185.

Morin, S., Coste, M., Hamilton, P.B. (2008). Scanning electron microscopy observations of deformities in small pennate diatoms exposed to high cadmium concentrations. *Journal of Phycology* **44**: 1512-1518.

Morrison, M.E.S. (1968). Vegetation and climate in the uplands of South-Western Uganda during the later Pleistocene period: I. Muchoya Swap, Kigezi District. *Journal of Ecology* **56**: 363-384.

Morrison, M.E.S., Hamilton, A.C. (1974). Vegetation and climate in the uplands of south-western Uganda during the later Pleistocene period: ii. Forest clearance and other

vegetational changes in the Rukiga Highlands during the past 8000 years. *The Journal of Ecology* **62**: 1-31.

Morley, C.K., Wescott, W.A. (1999). Sedimentary environments and geometry of sedimentary bodies determined from subsurface studies in East Africa. In: Morley, C.K. (Ed.), *GeoScience of Rift Systems – Evolution of East Africa.* AAPG Studies in Geology, No. 44. pp. 211–231.

Moss, B., Moss, J. (1969). Aspects of the limnology of an endorheic African lake (L. Chilwa, Malawi). *Ecology* **50**: 109-118.

Moy, C.M., Seltzer, G., Rodbell, D.T., Anderson, D.M. (2002). Variability of El Niño/Southern Oscillation activity at millennial timescales during the Holocene epoch. *Nature* **404**: 162–165.

Musisi, J. (1991). *The Neogene geology of the Lake George-Edward basin, Uganda*. Ph.D. thesis. Vrije Universiteit, Brussels.

Nalewajko, C., Marin, L. (1969). Extra-cellular production in relation to growth of four planktonic algae and of phytoplankton populations from Lake Ontario. *Canadian Journal of Botany* **47**: 405-413.

Nesje, A.,Dahl, S.O. (2000). *Glaciers and Environmental Change.* Arnold, London.

Newman, F.C. (1976). Temperature steps in Lake Kivu: A bottom heated saline lake. *Journal of. Physical Oceanography* **6**: 157–163.

Nicholson, S.E. (1986). The spatial coherence of African rainfall anomalies: interhemispheric teleconnections. *Journal of Climatology and Applied Meteorology* **25**: 13651-13681.

Nicholson, S.E. (1995). Variability of African rainfall on interannual and decadal time scales. In: Climate Research committee (Eds.). *Natural Climate Variability on Decade-to-Century Time Scales*. National Academy Press, Washington. pp 32-43.

Nicholson, S.E. (1996). Environmental change within the historical period. In: Adams W.M., Goudie A.S., Orme A.R. (Eds.) *The physical geography of Africa*. Oxford University Press, Oxford. pp 60–87.

Nicholson, S.E. (1998a). Historical fluctuations of Lake Victoria and other lakes in the Northern Rift Valley of East Africa. In: Lehman, J.T. *Environmental Change and Response in East African Lakes*. Netherlands, Kluwer Academic Publishers, pp 7-36.

Nicholson, S.E. (1998b). Fluctuations of Rift Valley lakes Malawi and Chilwa during historical times: A synthesis of geological, aracheological and historical information. In: Lehman, J.T. *Environmental Change and Response in East African Lakes*. Netherlands, Kluwer Academic Publishers, pp 207-232.

Nicholson, S.E. (2000). The nature of rainfall variability over Africa on time scales of decades to millenia. *Global and Planetary Change* **26**: 137-158.

Nicholson, S.E. (2001a). Rainfall Conditions in Equatorial East Africa during the Nineteenth Century as Inferred from the Record of Lake Victoria. *Climatic Change* **48**: 387-398.

Nicholson, S.E. (2001b). Climatic and environmental change in Africa during the last two centuries. *Climate Research* **17**: 123-144.

Nicholson, S.E. (2001c). A semi-quantitative, regional precipitation data set for studying African climates of the nineteenth century, Part I. Overview of the data set. *Climatic Change* **50**: 317-353.

Nicholson, S.E., Kim, J. (1997). The relationship of the El Niño-Southern Oscillation to African rainfall. *International Journal of Climatology* **17**: 117-135.

Nicholson, S.E., Kim, J., Ba, M.B. (1997). The mean surface water balance over Africa and its interannual variability. *Journal of Climate* **10**: 2981-3002.

Nixon, P.H., Hornung, G. (1973). The carbonatite lavas and tuffs near Fort Portal, Western Uganda. *Overseas Geological and Mineral Research* **41**: 168-179.

Nordt, L.C., Boutton, T.W., Jacob, J.S., Mandel, R.D. (2002). C_4 plant productivity and climate-CO_2 variations in South-Central Texas during the Late Quaternary. *Quaternary Research* **58**: 182–1188.

O'Leary, M.H. (1988). Carbon isotopes in photosynthesis. *Bioscience* **38**: 328–336.

O'Reilly, C.M., Alin, S.R., Plisnier, P-D., Cohen, A.S., McKee, B.A. (2003). Climate change decreases aquatic ecosystem productivity of Lake Tanganyika, Africa. *Nature* **424**: 766-768.

Ogutu-Ohwayo, R. (1990). The reduction in fish species diversity in Lakes Victoria and Kyoga (East Africa) following human exploitation and introduction of non-native fishes. *Journal of Fish Biology* **37**: 207-208.

Oksanen, J., Minchin, P.R. (2002). Continuum theory revisited: what shape are species responses along ecological gradients? *Ecological Modelling* **157**: 119-129.

Olago, D.O. (1995). *Late Quaternary lake sediments of Mount Kenya, Kenya*. Unpublished D.Phil thesis, Oxford University.

Olago, D.O., Odada, E.O. (2004). Palaeo-research in Africa: relevance to sustainable environmental management and significance for the future. In: Battarbee, R.W., Gasse, F., Stickley, C. (Eds.). *Past Climate Variability through Europe and Africa*. Kluwer Academic Publishers, Dordrecht, The Netherlands.

Olago, D.O., Odada, E.O., Street-Perrott, F.A., Perrott, R.A., Ivanovich, M., Harkness, D.D. (2000). Long-term temporal characteristics of palaeomonsoon dynamics in equatorial Africa. *Global and Planetary Change* **26**: 159–171.

Oldfield, F., Appleby, P.G., Thompson, R. (1980). Palaeoecological studies of three lakes in the Highlands of Papua New Guinea. I. The chronology of sedimentation. *Ecology* **68**: 457-477.

Oldfield, F., Appleby, P.G., Thompson, R. (1980). Palaeoecological studies of lakes in the highlands of Papua New Guinea: I. The chronology of sedimentation. *The Journal of Ecology* **68**: 457-477.

Otim-Nape, G.W., Bua, A., Ssemakula, G., Acola, G., Baguma, Y., Ogwal, S., Van der Grift, R. (2005). Cassava development in Uganda. In: Otim-Nape, G.W., Bua, A. (Eds.). *A review of cassava in Africa with country case studies on Nigeria, Ghana, the United Republic of Tanzania, Uganda and Benin*. Proceedings of the validation forum on the global cassava development strategy. pp 357.

Overpeck J., Hughen K., Hardy D., Bradley, R., Case, R., Douglas, M., Finney, B., Gajewski, K., Jacoby, G., Jenning, A., Lamoureux, S., Lasca, A., MacDonald, G., Moore, J., Retelle, M., Smith, S., Wolfe, A., Zielinski, G. (1997) Arctic environmental change of the last four centuries. *Science* **278**: 1251–1256.

Owen, R.B. Crossley, R. (1992). Spatial and temporal distribution of diatoms in sediments of Lake Malawi, Central Africa, and ecological implications. *Journal of Paleolimnology* **7**: 55-71.

Palmer, M.W. (1993). Putting things in even better order: the advantages of canonical correspondence analysis. *Ecology* **74**: 2215-30.

Parsons, T. R., Takahashi, M. (1973). *Biological Oceanographic Processes*. Pergamon Press, Oxford. pp 186.

Patrick, R. (1948). Factors affecting the distribution of diatoms. *Botanical Review* **14**, 473 524.

Patrick, R., Reimer, C.W. (1966). *The diatoms of the United States*. Vol. 1. Monographs of the Academy of Natural Sciences of Philadelphia, Number 13.

Patrick, R., Reimer, C.W. (1975). *The diatoms of the United States*. Vol. 2, Part 1. Monographs of the Academy of Natural Sciences of Philadelphia, Number 13.

Peres, F. (2000). Mise en e´vidence des effets toxiques des me´taux lourds sur les diatome´es par l'e´tude des formes te´ratoge`nes. In Peres-Weerts, F. (Ed.). *Rapport d'e´tude*. Agence de l'Eau Artois Picardie, Boulogne sur Gesse, France. pp. 1–24.

Pfeiffer, M., Dullo, W.-C. (2006). Monsoon-induced cooling of the western equatorial Indian Ocean as recorded in coral oxygen isotope records from the Seychelles covering the period of 1840–1994 AD. *Quaternary Science Reviews* **25**: 993–1009.

Pienitz, P., Smol, J.P., Birks, H.J.B. (1995). Assessment of freshwater diatoms as quantitative indicators of past climatic change in the Yukon and Northwest Territories, Canada. *Journal of Paleolimnology* **13**: 21–49.

Pilskaln, C.H., Johnson, T.C. (1991). Seasonal signals in Lake Malawi sediments. *Limnology and Oceanography* **36:** 544-557.

Piotrowska, N., Bluszcz, A., Demske, D., Granoszewski, W., Heumann, G. (2004). Extraction and AMS radiocarbon dating of pollen from Lake Baikal sediments. *Radiocarbon* **46**: 181-187.

Plater, A.J., Boyle, J.F., Mayers, C., Turner, S.D., Stroud, R.W. (2006). Climate and human impacy on lowland lake sedimentation in Central Coastal California: the record from c. 650 AD to the present. *Regional Environmental Change* **6**: 71-85.

Prosser, M.V., Wood, R.B., Baxter, R.M. (1968). The Bishoftu crater lakes: a bathymetric and chemical study. *Archive für Hydrobiologie* **65**: 309-324.

Psenner, R., Schmidt, R. (1992). Climate-driven pH control of remote alpine lakes and effects of acid deposition. *Nature* **356**: 781-783.

Puchniak, M.K., Hall, R.I., Hecky, R.E. (2005). Sediment records of recent cultural eutrophication in Lake Malawi/Nyasa, East Africa. *EOS Transactions, AGU* **86**. Fall Meeting Supplement. Abstract PP21A-1549.

Rabe-Hesketh, S., Everitt, B. (2004). *A handbook of statistical analyses using Stata*. Chapman and Hall.

Racca, J.M.J., Prarie, Y.T. (2004). Apparent and real bias in numerical transfer functions in palaeolimnology. *Journal of Paleolimnology* **31**: 117-124.

Racca, J.M., Gregory-Eaves, I., Pienitz, R., Prairie, Y.T. (2004). Tailoring palaeolimnological diatom-based transfer functions. *Canadian Journal of Fisheries and Aquatic Sciences* **61**: 2440-2454.

Reed, J.M. (1998). A diatom-conductivity transfer function for Spanish salt lakes. *Journal of Paleolimnology* **19**: 399-416.

Reimer, P.J., Baillie, M.G.L., Bard, E., Bayliss, A., Beck, J.W., Bertrand, C.J.H., Blackwell, P.G., Buck, C.E., Burr, G.S., Cutler, K.B., Damon, P.E., Edwards, R.L., Fairbanks, R.G., Friedrich, M., Guilderson, T.P., Hogg, A.G., Hughen, K.A., Kromer, B., McCormac, F.G., Manning, S.W., Ramsey, C.B., Reimer, R.W., Remmele, S., Southon, J.R., Stuiver, M., Talamo, S., Taylor, F.W., van der Plicht, J., Weyhenmeyer, C.E. (2004). IntCal04 Terrestrial radiocarbon age calibration, 26 – 0 ka BP. *Radiocarbon* **46**: 1029-1058.

Renberg, I. (1990). A procedure for preparing large sets of diatom slides from sediment cores. *Journal of Paleolimnology* **4**: 87-90.

Renberg, I. (1991). The HON-Kajak sediment corer. *Journal of Paleolimnology* **6**: 167-70.

Renberg, I., Korsman, T., Birks, H.J.B. (1993). Prehsitoric increases in the pH of acid-sensitive Swedish lakes caused by land-use changes. *Nature* **362**: 824-827.

Richardson, J.L. (1968). Diatoms and lake typlogy in East and Central Africa. *International Revue gesamten Hydrobiologie* **53**: 299-338.

Ricketts, R.D., Johnson, T.C. (1996). Climate change in the Turkana basin as deduced from a 4000 year long [delta]O18 record. *Earth and Planetary Science Letters* **142**: 7-17.

Robertshaw, P., Taylor, D. (2000). Climate change and the rise of poltical complexity in western Uganda. *Journal of African History* **41**: 1-28.

Robertshaw, P., Taylor, D., Doyle, S., Marchant, R. (2004). Famine, climate and crisis in Western Uganda. In: Battarbee, R.W., Gasse, F., Stickley, C.E. *Past climate variability through Europe and Africa*. Dordrecht, Springer, pp: 638.

Rosen, B.H., Lowe, R.L. (1984). Physiological and ultrastructural responses of *Cyclotella meneghiniana* (Bacillariophyta) to light intensity and nutrient limitation. *Journal of Phycology* **20**: 173-183.

Rosén, P., Dåbakk, E., Renberg, I., Nilsson, M., Hall, R. (2000). Near-infrared spectrometry (NIRS): a new tool for inferring past climatic changes from lake sediments. *The Holocene* **10**: 161-166.

Rosendahl, B.R. (1987). Architecture of Continental Rifts with Special Reference to East Africa. *Annual Review of Earth and Planetary Sciences* **15**: 445-503.

Roubiex, V., Lancelot, C. (2008). Effect of salinity on growth, cell size and silification of an euryhaline freshwater diatom: *Cyclotella meneghiniana* Kütz. *Transitional Waters Bulletin* **1**: 31-38.

Round, F.E., Crawford, R.M., Mann, D.G. (1990). *The diatoms. Biology and morphology of the genera*. Cambridge University Press, Cambridge. pp 747.

Russell, J.M., Johnson, T.C. (2005b) Late Holocene climate change in the North Atlantic and Equatorial Africa: millennial scale ITCZ migration. *Geophysical Research Letters* **32**: doi: 10.1029/2005GL023295.

Russell, J.M., Johnson, T.C. (2005a). A high-resolution geochemical record from lake Edward, Uganda Congo and the timing and causes of tropical African drought during the late Holocene. *Quaternary Science Reviews* **24**: 1375-1389.

Russell, J.M., Johnson, T.C. (2006a). The water balance and stable isotope hydrology of Lake Edward, Uganda-Congo. *Journal of Great Lakes Research* **32**: 77-90.

Russell, J.M., Johnson, T.C. (2006b). Late Holocene climate change in the North Atlantic and equatorial Africa: Millenial-scale ITCZ migration. *Geophysical Research Letters* **32**: 1-4.

Russell, J.M., Johnson, T.C. (2007). Little Ice Age drough in equatorial Africa: Intertropical Convergence Zone migrations and El Nino-Southern Oscillation variability. *Geological Society of America* **35**: 21-24.

Russell, J.M., Johnson, T.C., Kelts, K.R., Laerdal, T., Talbot, M.R. (2003). An 11,000 year lithostratigraphic and paleohydrologic record from equatorial Africa: Lake Edward Uganda-Congo. *Palaeogeography, Palaeoclimatology, Palaeoecology* **193**: 25- 49.

Russell, J.M., Eggermont, H., Verschuren, D. (2007). Spatial complexity during the Little Ice Age in tropical East Africa: sedimentary records from contrasting crater lake basins in western Uganda. *The Holocene* **17**: 183-193.

Ruttner, F. (1931). Hydrographische und hydrochemische Beobachtungen auf Java, Sumatra, and Bali. *Archive für Hydrobiologie* **8**: 197–454.

Ruttner, F. (1932). Bericht über ältere, bisher unveröffentlichte bakteriologische Untersuchungen an den Lunzer Seen. *International Revue gesamten Hydrobiologie* **26**: 438-443.

Ruttner, F. (1937). Stabilität and Umschichtung in tropischen und temperierten Seen. *Archive für Hydrobiologie* **15**: 178-186.

Ryves, D.B., McGowan, S., Anderson, N.J. (2002). Development and evaluation of a diatom-conductivity model from lakes in West Greenland. *Freshwater Biology* **47**: 995-1014.

Ryves, D.B., Juggins, S., Fritz, S.C., Battarbee, R.W**.** (2001) Experimental diatom dissolution and the quantification of microfossil preservation in sediments. *Palaeogeography, Palaeoclimatology, Palaeoecology* **172**: 99-113.

Ryves, D.B., Amsinck, S.L., Anderson, N.J., Appleby, P.G., Clarke, A.L., Jeppesen, E., Landkildehus, F. (2004) Reconstructing the salinity and environment of the Limfjord and Vejlerne Nature Reserve, Denmark, using a diatom model for brackish lakes and fjords, *Canadian Journal of Fisheries and Aquatic Sciences* **61**: 1988-2006.

Ryves, D., Battarbee, R.W., Juggins, S., Fritz, S.C., Anderson, N.J. (2006). Physical and chemical predictors of diatom dissolution in freshwater and saline lake sediments of North America and West Greenland. *Limnology and Oceanography* **51**: 1355-1368.

Ryves, D.B., Battarbee, R.W., Fritz, S.C. (2009). The dilemma of disappearing diatoms: Incorporating diatom dissolution into palaeoenvironmental modelling and reconstruction. *Quaternary Science Reviews* **28**: 120-136.

Ryves, D.B., Mills, K., Bennike, O., Brodersen, K.P., Lambe, A.L., Leng, M., Russell, J.M., Ssemmanda, I. (in review). Testing the coherence of paired lakes to environmental change: a late Holocene multiproxy palaeolimnological study from two crater lakes in western Uganda. *Quaternary Science Reviews*.

Sabater, S. (2000). Diatom communities as indicators of environmental stress in the Guadiamar River, S-W Spain, following a major mine tailings spill. *Journal of Applied Phycology* **12**: 113-124.

Sanford, W.E., Wood, W.W. (1991). Brine Evolution and Mineral Deposition in Hydrologically Open Evaporite Basins. *American Journal of Science* **291**: 687-710.

Salzmann, U., Waller, M. (1998). The Holocene vegetational history of the Nigerian Sahel based on multiple pollen profiles. *Review of Palaeobotany and Palynology* **100**: 38-72.

Sarmento, H., Isumbisho, M., Descy, J.P. (2006). Phytoplankton ecology of Lake Kivu (eastern Africa). *Journal of Plankton Research* **28**: 815-829.

Schlüter, T. (1993). Comparison of the mineral composition of the lakes of the East African Rift system (Gregory Rift and Western Rift). In: Thorweihe, U, Schandelmeier, H. (Eds.) *Geoscientific Research in Northeast Africa*. Balkema Rotterdam, Canberra. pp. 657-662.

Schlüter, T. (2006). *Geological Atlas of Africa*. New York, Springer-Verlag.

Schmincke, H.U., Brey, G., Staudigel, H. (1974). Craters of phreatomagmatic origin on Gran Canaria, Canary Islands. *Naturwissenschaften* **61**: 125.

Schofield, P.J., Chapman, L.J. (2000). Hypoxia tolerance of introduced Nile Perch: Implications for survival of indigenous fishes in the Lake Victoria Basin. *African Zoology* **35**: 35-42.

Shaw, A. B., (1964). *Time in Stratigraphy*. McGraw-Hill, N.Y.

Shen, Z., Bloemendal, J., Mauz, B., Chiverrell, R.C., Dearing, J.A., Lang, A., Liu, Q. (2008). Holocene environmental reconstruction of sediment-source linkages at Crummock Water, English Lake District, based on magnetic measurements. *The Holocene* **18**: 129-140.

Simkin, T., Siebert, L. (2002-). Global Volcanism FAQs. Smithsonian Institution, Global Volcanism Program Digital Information Series, GVP-5 (http://www.volcano.si.edu/faq/). June 2008.

Smith, V.H. (1998). Cultural eutrophication of inland, estuarine and coastal waters. In: Pace, M.L., Groffman, P.M. (Eds). *Successes, limitations and frontiers in ecosystem science*. Springer, New York. p7–49.

Smol, J.P., Wolfe, A.P., Birks, H.J.B., Douglas, M.S.V., Jones, V.J, Korhola, A., Pienitz, R., Rühland, K., Sorvari, S., Antoniades, D., Brooks, S.J., Fallu, M-A., Hughes, M., Keatley, B.E., Laing, T.E., Michelutti, N., Nazarova, L., Nyman, M., Paterson, A.M., Perren, B., Quinlan, R., Rautio, M., Saulnier-Talbot, É, Siitonen, S., Solovieva, N., Weckström, J. (2005). Climate-driven regime shifts in the biological communities of arctic lakes. *PNAS* **102**, 4397–4402.

Snowball, I., Sandgren, P. (1996). Lake sediment studies of Holocene glacial activity in the Kårsa valley, northern Sweden: contrasts in interpretation. *The Holocene* **6**: 367-372.

Sobek, S., Tranvik, L.J., Prairie, Y., Kortelainen, P., Cole, J.J. (2007). Patterns and regulation of dissolved organic carbon: An analysis of 7500 widely distributed lakes. *Limnology and Oceanography* **52**: 1208-1219.

Speijer, P., Kajumba, C., Tushemereirwe, W.K. (1999). Dissemination and adaptation of a banana clean planting material technology in Uganda. *InfoMusa* **8**: 11–13.

Spencer, J.Q., Sanerson, D.C.W., Deckers, K., Sommerville, A.A. (2003). Assessing mixed does distributions in young sediments identified using small aliquots and a simple two-step SAR procedure: the *F*-statistic as a diagnostic tool. *Radiation Measurements* **37**: 425-431.

Ssemmanda I., Ryves D.B., Bennike O., Appleby P.G. 2005. Vegetation history in west Uganda during the last 1200 years: a sediment-based reconstruction from two crater lakes. *The Holocene* **15**: 119-132.

Stager, J.C. (1984). The diatom record of Lake Victoria (East Africa): The last 17,000 years. In: Mann, D.G. (Ed). *Proceedings of the Seventh International Diatom Symposium*. Strauss and Cramer, Koenigstein.

Stager, J.C., Johnson, T.C. (2000). A 12,400 14C yr offshore diatom record from east central Lake Victoria, East Africa. *Journal of Paleolimnology* **23**, 373–383.

Stager, J.C., Johnson T.C. (2002). A 12,400 14c yr Offshore Diatom Record From East Central Lake Victoria, East Africa. *Journal of Paleolimnology* **23**: 373-383.

Stager, J.C., Cumming, B.F., Meeker, L. (1997). A high-resolution 11,400-yr diatom record from Lake Victoria, East Africa. *Quaternary Research* **47**: 81-89.

Stager, J.C., Mayewski, P.A., Meeker, L.D. (2002). Cooling cycles, Heinrich event 1, and the dessication of Lake Victoria. *Palaeogeography, Palaeoclimatology, Palaeoecology* **183**: 169-178.

Stager, J.C., Cumming, B.F., Meeker, L.D. (2003). A 10,000-year high-resolution diatom record from Pilkington Bay, Lake Victoria, East Africa. *Quaternary Research* **59**: 172-181.

Stager, J. C., Ryves, D., Cumming, B.F., Meeker, L.D., Beer, J. (2005). Solar variability and the levels of Lake Victoria, East Africa, during the last millennium. *Journal of Paleolimnology* **33**: 243-251.

Stager, J.C., Ruzmaikin, A., Conway, D., Verburg, P., Mason, P.J. (2007). Sunspots, El Nino, and the levels of Lake Victoria, East Africa. *Journal of Geophysical Research* **112**: D15106.

Stoermer, E.F., Smol, J.P. (1999). Applications and uses of diatoms: prologue. In: Stoermer, E.F., Smol, J.P. (Eds). *The Diatoms: Applications for the Environmental and Earth Sciences*. Cambridge University Press.

Street, F.A. (1980). The relative importance of climate and local hydrogeological factors in influencing lake-level fluctuations, *Palaeoecology of Africa* **12**: 137–158.

Street-Perrot, A., Harrison, S. (1985). *Lake levels and climate reconstruction. Paleoclimatic Analysis and Modeling*. A. D. Hecht. Chichester, John Wiley.

Street-Perrot, F.A., Ficken, K.J., Huand, Y., Eglinton, G. (2004). Late Quaternary changes in carbon cycling on Mt. Kenya, East Africa: an overview of the $\delta^{13}C$ record in lacustrine organic matter. *Quaternary Science Reviews* **23**: 861-879.

Street-Perrot, F.A., Barker, P.A., Leng, M.J., Sloane, H.J., Woollller, M.J., Ficken, K.J., Swain, D.L. (2008). Towards an understanding of late Quaternary variations in the continental biogeochemical cycle of silicon: multi-isotope and sediment-flux data for Lake Rutundu, Mt Kenya, East Africa, since 38 ka BP. *Journal of Quaternary Science* **23**: 375-387.

Stevenson, R.J., Bahls, L. (1999). Periphyton protocols EPA 841-B-99-002. In: Barbour, M.T., Gerritsen, J., Snyder, B.D., Stribling, J.B. (Eds.). *Rapid Bioassessment Protocols for Use in Streams and Wadeable Rivers: Periphyton, Benthic Macroinvertebrates and Fish.* U.S. Environmental Protection Agency; Office of Water, Washington. pp 326.

Stone, J.R., Fritz, S.C. (2004). Three-dimensional modelling of lacustrine diatom habitat areas: improving paleolimnological interpretation of planktic: benthic ratios. *Limnology and Oceanography* **49**: 1540-1548.

Stuiver, M., Brauzanias, T.F. (1989). Atmospheric ^{14}C and century-scale solar oscillations. *Nature* **338**: 405-408.

Stuiver, M., Becker, B. (1993). High-precision decadal calibration of the radiocarbon timescale, AD 1950-6000 BC. *Radiocarbon* **35**: 35-65.

Stuiver, M., Reimer, P. J. (1993) Extended ^{14}C database and revised CALIB radiocarbon calibration program. *Radiocarbon* **35**: 215-230.

Stuiver, M., Reimer, P.J., Bard, E., Beck, J.W., Burr, G.S., Hughen, K.A., Kromer, B., McCormac, G., van der Plicht, J. and Spurk, M. (1998). INTCAL98 radiocarbon age calibration, 24,000-0 cal BP. *Radiocarbon* **40**: 1041-83.

Sullivan, T. J., Driscoll, C.T., Gherini, S.A., Munson, R.K., Cook, R.B., Charles, D.F., Yatsko, C.P. (1989). Influence of aqueous aluminum and organic acids on measurement of acid neutralizing capacity in surface waters. *Nature* **338**: 408-410.

Talbot, M.R., Livingston, D.A. (1989). Hydrogen index and carbon isotopes of lacustrine organic matter as lake-level indicators. *Palaeogeography, Palaeoclimatology, Palaeoecology* **70**: 121–137.

Talbot, M.R., Lærdal, T. (2000). The late Pleistocene-Holocene palaeolimnology of Lake Victoria, East Africa, based upon elemental and isotopic analyses of sedimentary organic matter. *Journal of Paleolimnology*, **23**: 141-164.

Talling, J.F. (1963). Origin of stratification in an African Rift lake. *Limnology and Oceanography* **8**: 68-78.

Talling, J.F. (1966). The annual cycle of stratification and phytoplankton growth in Lake Victoria (East Africa). *Internationale Revue der gesamten Hydrobiologie* **51**: 545-621.

Talling, J.F. (1969). The incidence of vertical mixing, and some biological and chemical consequences, in tropical African lakes. *Verhandlungen Internationale Vereinigung für Limnologie* **17**: 998–1012.

Talling, J.F. (1986). The seasonality of phytoplankton in African Lakes. *Hydrobiologia* **138**: 139-160.

Talling, J.F., Talling, I.B. (1965). The chemical composition of African Lake waters. *International Revue gesamten Hydrobiologie* **50**: 421-463.

Talling, J.F., Lemoalle, J. (1998). *Ecological dynamics of tropical inland waters*. Cambridge University Press.

Taylor, D. (1990). Late Quaternary pollen diagrams from two Ugandan mires: evidence for environmental change in the Rukiga Highlands of southwest Uganda. *Palaeogeography, Palaeoclimatology, Palaeoecology* **80**: 283-300.

Taylor, D., Marchant, R. (1995). Human-impact in southwest Uganda: long term records from the Rukiga Highlands, Kigezi. *Azania* **30**: 283-295.

Taylor, D., Robertshaw, P. (2001). Sedimentary sequences in western Uganda as records of human environmental impacts. *Palaeoecology of Africa* **27**: 63-76.
Taylor, D., Marchant, R., Robertshaw, P. (1999). Late glacial-Holocene history of lowland rain forest in central Africa: a record from Kabata Swamp, Ndale volcanic field, Uganda. *Journal of Ecology* **87**, 303-315.

Taylor, D., Robersthaw, P., Marchant, R.A. (2000). Environmental change and political-economic upheaval in precolonial western Uganda. *The Holocene* **10**: 527-536.

Taylor, R.E. (1997). Radiocarbon dating. In:Taylor, R.E., Aitken, M.J. (Eds.) *Chronometric Dating in Archaeology*. Springer.

Taylor, R.G**.**, Majugu, A., Okonga, J., Tindimugaya, C., Todd, M., Mileham, L. (2005). Hydrological and climatological implications of rapid glacial recession in the Rwenzori Mountains of East Africa. European Geophysical Union General Assembly 2005 (Vienna, Austria), EGU05-A-08487.

Taylor, R.G., Mileham, L., Tindimugaya, C., Majugu, A., Nakileza, R., Muwanga, A. (2006). Recent deglaciation in the Rwenzori Mountains of East Africa due to rising air temperatures. *Geophysical Research Letters* **33**: L10402.

Telford, R.J., Lamb, H.F. (1999). Groundwater-Mediated Response to Holocene Climatic Change Recorded by the Diatom Stratigraphy of an Ethiopian Crater Lake. *Quaternary Research* **52**: 63-75.

ter Braak, C.J.F. (1986). Canonical correspondence analysis: a new eigenvector technique for multivariate direct gradient analysis. *Ecology* **67**: 1167-1179.

ter Braak, C.J.F. (1987). *CANOCO - a FORTRAN programme for canonical community ordination by [partial] [detrended] [canonical] correspondence analysis, principle*

components analysis and redundancy analysis. Agricultural Mathematics Group, Wageningen.

ter Braak, C.J.F. (1988). Partial canonical correspondence analysis. In: (Ed. Bock, H.H.). *Classification and related methods of data analysis*. Amsterdam: North-Holland. pp. 551-558.

ter Braak, C.J.F. (1995). Non-linear methods for multivariate statistical calibration and their use in palaeoecology: a comparison of inverse (k-nearest neighbours, partial least squares and weighted averaging partial least squares) and classical approaches. *Chemometrics and Intelligent Laboratory Systems* **28**, 165-180.

ter Braak, C.J.F., Barendregt, L.G. (1986). Weighted averaging of species indicator values: its efficiency in environmental calibration. *Methematical Biosciences* **78**: 57-72.

ter Braak, C.J.F., Looman, C.W.N. (1986). Weighed averaging logistic regression and the Gaussian response model. *Vegetatio* **65**: 3-11.

ter Braak, C.J.F., Prentice, I.C. (1988). A theory of gradient analysis. *Advances in Ecological Research* **18**: 271–317.

ter Braak, C.J.F., van Dam, H. (1989). Inferring pH from diatoms: a comparison of old and new calibration methods. *Hydrobiologia* **178**: 209-223.

ter Braak, C.J.F., Juggins, S. (1993). Weighted averaging partial least squares regression (WA-PLS): an improved method for reconstructing environmental variables from species assemblages. *Hydrobiologia* **269/270**: 485-502.

ter Braak, C.J.F., Šmilauer, P. (1998). *CANOCO Reference Manual and User's guide to CANOCO for Windows: Software for Canonical Community Ordination (version 4.0).* Microcomputer Power. Ithaca, New York, USA. pp 352.

ter Braak, C.J.F., Šmilauer, P. (2002). *CANOCO reference manual and CanoDraw for Windows user's guide: software for canonical community ordination (version 4.5).* Microcomputer Power, Ithaca, New York: 1-352.

Thompson, L. G., Mosley-Thompson, E., Davis, M.E., Henderson, K.A., Brecher, H.H., Zagorodnov, V.S., Mashiotta, T.A., Lin, P-N., Mikhalenko, V.N., Hardy, D.R., Beer, J. (2002). Kilimanjaro Ice Core Records: Evidence of Holocene Climate Change in Tropical Africa. *Science* **298**: 589-593.

Thompson, L. G., Davis, M.E., Mosley-Thompson, E., Lin, P-N., Henderson, K.A., Mashiotta, T.A. (2005). Tropical ice core records: evidence for asynchronous glaciation on Milankovitch timescales. *Journal of Quaternary Science* **20**: 723-733.

Thornton, J. (1987). Aspects of eutrophication management in tropical/sub-tropical regions. *Journal of the limnological society of South Africa* **13**: 25-43.

Tiercelin, J.-J., Lezzar, K.E. (2002). A 300 million years history of rift lakes in Central and East Africa: an updated broad review. In: Odada, E.O., Olago, D.O. (Eds.) *The East*

African Great Lakes: Limnology, Palaeolimnology and Biodiversity. Advances in Global Change Research, Kluwer Academic Publishers. pp. 3–60.

Tilman, D., Kilham, S.S. (1976). Phosphate and silicate growth and uptake kinetics of the diatoms *Asterionella formosa* and *Cyclotella meneghiniana* in batch and semicontinuous culture. *Journal of Phycology* **12**: 375-383.

Tuchman, M.L., Theriot, E., Stoermer, E.F. (1984). Effects of low level salinity concentrations on the growth of *Cyclotella meneghinianana* Kütz (Bacillariophyta). *Archiv für Protistenkunde* **128**: 319-326.

Tuchman, N.C., Schollett, M.A., Rier, S.T., Geddes, P. (2006). Differential heterotrophic utilization of organic compounds by diatoms and bacteria under light and dark conditions. *Hydrobiologia* **561**: 167-1..

Tyson, R.V. (1995). *Sedimentary Organic Matter: organic facies and palynofacies*. Chapman and Hall, London.

Van Dam, H., Mertens, A., Sinkeldam, J. (1994). A coded checklist and ecological indicator values of freshwater diatoms from the Netherlands. *Netherlands Journal of Aquatic Ecology* **28**: 117-133

Velle, G., Brooks, S.J., Birks, H.J.B., Willassen, E. (2005). Chironomids as a tool for inferring Holocene climate: an assessment based in six sites in southern Scandinavia. *Quaternary Science Reviews* **24**: 1429-1462.

Verburg, P., Hecky, R.E., Kling, H. (2003). Ecological Consequences of a Century of Warming in Lake Tanganyika. *Science* **301**: 505-507.

Verschuren, D. (1994). Sensitivity of tropical-African aquatic invertebrates to short-term trends in lake level and salinity: a paleolimnological test at Lake Oloidien, Kenya. *Journal of Paleolimnology* **10**: 253-263.

Verschuren, D. (1997). Taxonomy and ecology of subfossil Chironomidae (Insecta, Diptera) from Rift Valley lakes in central Kenya. *Archive fur Hydrobiologia*, **4**: 467-512.

Verschuren, D. (1999a). Influence of depth and mixing regime on sedimentation in a fluctuating tropical soda lake. *Limnology and Oceanography* **44**: 1103-1113.

Verschuren, D. (2001). Reconstructing fluctuations of a shallow East African lake during the past 1800 years from sediment stratigraphy in a submerged crater basin. *Journal of Paleolimnology* **25**: 297-311.

Verschuren, D. (2002). Climate reconstruction from African lake sediments. *Unpublished ESF Holivar Workshop Report*. Lammi, Finland.

Verschuren, D. (2003). Lake-based climate reconstruction in Africa: progress and challenges. *Hydrobiologia* **500**: 315-330.

Verschuren, D. (2004). Decadal and century-scale climate variability in tropical Africa during the past 2000 years. In: Battarbee, R.W., Gasse, F., Stickley, C. (Eds). *Past climate variability through Europe and Africa*. Dordrecht, Springer.

Verschuren, D., Tibby, J., Leavitt, P.R., Roberst, N. (1999). The environmental history of a climate sensitive lake in the former 'White Highlands' of central Kenya. *Ambio* **28**: 494-501.

Verschuren, D., Laird, K.R., Cumming, B.F. (2000a) Rainfall and drought in equatorial east Africa during the past 1,100 years. *Nature* **403**, 410-414.

Verschuren, D., Johnson, T.C., Kling, H.J., Edgington, D.N., Leavitt, P.R., Brown, E.T., Talbot, M.R. and Hecky, R.E. (2002). History and timing of human impact on Lake Victoria, East Africa. *Proceedings of the Royal Society of London (B)* **269**: 289-294.

Vincens, A., Ssemmanda, I., Roux, M., Jolly, D. (1997). Study of the modern pollen rain in Western Uganda witha numerical approach. *Review of Palaeobotany and Palynology* **96**: 145-168.

Vinogradov, V.I., Krasnov, A.A., Kuleshov, V.N., Sulerzhitskiy, L.D. (1978). $^{13}C/^{12}C$, $^{18}O/^{16}O$, and ^{14}C concentrations in the carbonatites of the Kalyango Volcano (East Africa). *Izv Akad Nauk SSSR Ser Geol* **6**: 33–41.

Webster, J.B. (1979). *Chronology, Migration and Drought in Interlacustrine Africa*. African Publishing Co.

Wetzel, R.G. (1975). *Limnology*. Academic Press.

Wetzel, R.G. (1990). Clean water: a fading resource. In: Ilmavirta, V., Jones, R.I. (Eds.). *The dynamics and use of lacustrine systems*. Developmental Hydrobiology. Junk Publishers.

Wetzel, R.G. (1992). Clean water: a fading resource. *Hydrobiologia* **243/244**: 21-30.

Williams, M.A.J., Dunkerley, D.L., De Dekker, P., Kershaw, A.P., Stokes, T. (1993). *Quaternary environments*. London: Edward Arnold.

Wilson S.E., Cumming B.F., Smol J.P. (1996) Assessing the reliability of salinity inference models from diatom assemblages: an examination of a 219-lake data set from western North America. *Canadian Journal of Fisheries and Aquatic Sciences* **53**: 1580–1594.

Winder, M., Reuter, J.E., Schladow, S.G. (in press). Lake warming favours small-sized planktonic diatom species. *Proceedings of the Royal Society B.* doi: 10.1098/rspb.2008.1200.

Wolfe, A.P., Fréchette, B., Richard, P.J.H., Miller, G.H., Forman, S.L. (2000). Paleoecological Assessment of a >90,000-year record from Fog Lake, Baffin Island, Arctic Canada. *Quaternary Science Reviews* **19**: 1677-1699.

Wood, R.B., Talling, J.F. (1988). Chemical and algal relationships in a salinity series of Ethiopian inland waters. *Hydrobiologia* **158**: 29–67.

Wolin, J.A., Duthie, H.C. (1999). Diatoms as indicators of water level change in freshwater lakes. In: Stoermer, E.F., Smol, J.P., (Eds.). *The Diatoms: Applications for Environmental and Earth Sciences*. Cambridge University Press, Cambridge. pp. 183-202.

Wood, R.B., Prosser, M.V., Baxter, R.M. (1976). The seasonal pattern of thermal characteristics of four of the Bishoftu crater lakes, Ethiopia. *Freshwater Biology* **6**: 519-530.

Worsley, A.T., Oldfield, F. (1988). Palaeoecological studies of three lakes in the Highlands of Papua New Guinea. II. Vegetational history over the last 1600 years. *The Journal of Ecology* **76**: 1-18.

Worthington, E.B. (1931). Cambridge Expeditions to the East African lakes. *Nature* **127**: 337-338.

Worthington, S., Worthington, E.B. (1933). *Inland waters of Africa*. MacMillan.

Wright, S.W., Jeffrey, S.W., Mantoura, R.F.C., Llewellyn, C.A., Bjørnland, T., Repeta, D., Welschmeyer, N. (1991). Improved HPLC method for the analysis of chlorophylls and carotenoids from marine phytoplankton. *Marine Ecology Progress Series* **77**: 183 196.

Wright, S.W., Wright, J.W., Jeffrey, S.W. (1997). High resolution system for chlorophylls and carotenoids of marine phytoplankton. In: Jeffrey, S.W., Mantoura, R.F.C., Wright, S.W. (Eds.). *Phytoplankton pigments in oceanography: a guide to advanced methods*. SCOR-UNESCO, Paris.

Wunsam, S. (1995). Diatomeen (Bacillariophyceae) als Bioindikatoren in Alpenseed – Trans-ferfunktionen zwischen Diatomeen und Umweltvariablen. Universität Wien. p147.

Wunsam, S., Schmidt, R., Klee, R. (1995). *Cyclotella*-taxa (Bacillariophyceae) in lakes of the Alpine region and their relationship to environmental variables. *Aquatic Sciences – Research across Boundaries* **57**: 360-386.

Appendix A: Diatom synonyms

A list of all diatom species (and their authorities) identified during this research. When necessary the generic revision of species names and authorities are given. A list of species codes, as listed by EDDI and AMPHORA are also given. Where codes did not exist, a code comprising of 6-8 characters was derived using letters from the species name. These codes were used in all analyses as a means of identifying the diatom taxa.

Species names	*Authority*	*Revised species names (where applicable)*	*Authority*	*Code*
Achnanthes bahusiensis	(Grunow) Lange-Bertalot			AC164A
Achnanthes biasolettiana	(Kützing) Grunow	*Achnanthidium pyrenaicum*	(Hustedt) Kobayasi	AC037B
Achnanthes brevipes v. *intermedia*	(Kützing) Cleve			AC058C
Achnanthes buccola	Cholnoky			AC180A
Achnanthes cf. *thermalis*	(Rabenhorst) Schönfeldt			AC160A
Achnanthes chlidanos	Hohn & Hellermann	*Psammothidium chlidanos*	Lange-Bertalot	AC166A
Achnanthes coarctata	(Brebisson) Grunow			AC033A
Achnanthes curtissima	Carter			AC060A
Achnanthes delicatula	Kützing	*Planothidium delicatulum*	Round & Bukhtiyarova	AC016B
Achnanthes didyma	Hustedt	*Psammothidium didymium*	Bukhtiyarova & Round	AC039A
Achnanthes distincta	Messikommer	*Planothidium distinctum*	Lange-Bertalot	AC155A
Achnanthes exigua	Grunow	*Achnanthidium exiguum*	Czarnecki	AC008A
Achnanthes exigua v. *elliptica*	Hustedt			AC008D
Achnanthes helvetica	Hustedt	*Psammothidium helveticum*	Bukhtiyarova & Round	AC163A
Achnanthes holsatica	Hustedt	*Platessa holsatica*	Lange-Bertalot	AC117A
Achnanthes hungarica	(Grunow) Grunow	*Lemnicola hungarica*	Round & Basson	AC032A
Achnanthes laevis	Oestrup			AC083A
Achnanthes lanceolata	(Brébisson) Grunow	*Planothidium lanceolatum*	Round & Bukhtiyarova	AC001A
Achnanthes lanceolata v. *rostrata*	Hustedt	*Planothdium rostatum*	Round & Bukhtiyarova.	AC001B
Achnanthes minutissima v. *gracillima*	Meister			ACMINGR
Achnanthes minutissima v. *macrocephala*	Hustedt	*Achnanthidium macrocephalum*	Round & Bukhtiyarova	ACMMAC
Achnanthes minutissima v. *minutissima*	Kützing	*Acnanthidium minutissimum*	Czarnecki	AC013A
Achnanthes minutissima v. *scotica*	(Carter) Lange-Bertalot			ACMINSC
Achnanthes montana	Krasske	*Platessa montana*	Lange-Bertalot	AC098A
Achnanthes rupestoides	Hohn			AC175A

Species names	*Authority*	*Revised species names (where applicable)*	*Authority*	*Code*
Achnanthes ventralis	(Krasske) Lange-Bertalot	*Psammothidium ventralis*	Bukhtiyarova & Round	AC161A
Amphipleura pellucida	(Kützing) Kützing			AP001A
Amphora coffeaeformis	Agardh			AM006A
Amphora libyca	Ehrenberg	*Amphora copulata*	Schoeman. & Archibald	AM011A
Amphora montana	Krasske			AM084A
Amphora normanii	Rabenhorst			AM005A
Amphora ovalis	Kützing			AM001A
Amphora pediculus	(Kützing) Grun			AM012A
Amphora subcapitata	(kisselev) Hustedt			AM127A
Amphora submontana	Hustedt			AMSMON
Amphora tanganyike	Caljon			AMTANG
Amphora veneta	Kützing			AM004A
Anomoeoneis brachysira	(Brébisson.) Cleve	*Brachysira brebissonii*	Ross	AN008A
Anomoeoneis fragment				AN9999
Anomoeoneis sphaerophora	(Kützing) Pfitzer			AN009A
Anomoeoneis sphaerophora v. *sculpta*	(Ehrenberg) O. Müller			AN009B
Asterionella formosa	Hassall			AS001A
Aulacoseira ambigua	(Grunow) Simonsen			AU002A
Aulacoseira ambigua (Squat)				AU002AS
Aulacoseira ambigua (Thin)				AU002AT
Aulacoseira distans	(Ehrenberg) Simonsen			AU005A
Aulacoseira granulata	(Ehrenberg) Simonsen			AU003A
Aulacoseira granulata v. *angutissima*	(O. Müller) Simonsen			AU003B
Aulacoseira italica	(Ehrenberg) Simonsen			AU001A
Aulacoseira spp.				AU9999
Bacillaria paradoxa	Gmelin			BA001A
Caloneis bacillum	(Grunow) Mereschkowsky			CA002A
Caloneis molaris	(Grunow) Krammer			CA048A
Caloneis silicula	(Ehrenberg) Cleve			CA003A
Caloneis spp.				CA9999
Caloneis tenuis	(Gregory) Krammer			CA018A

Species names	*Authority*	*Revised species names (where applicable)*	*Authority*	*Code*
Caloneis undulata	(Gregory) Krammer			CAUNDU
Capartogramma cf. *karstenii*	(Zanon) Ross			CPKARS
Capertogramma spp.				CP9999
Cocconeis fragment				CO9999
Cocconeis neodiminuta	Krammer			CO066A
Cocconeis pediculus	Ehrenberg			CO005A
Cocconeis placentula v. *euglypta*	(Ehrenberg) Cleve			CO001B
Cocconeis placentula v. *klinoraphis*	Geitler			CO001D
Cocconeis placentula v. *lineata*	(Ehrenberg) Cleve			CO001C
Cocconeis placentula v. *placentula*	Ehrenberg			CO001A
Cocconeis thumensis	Mayer	*Cocconeis neothumensis*	Krammer	CO009A
Cyclostephanos tholiformis	Stoermer, Hakansson & Theriot			CC003A
Cyclostephanus dubius	(Fricke) Round			CC001A
Cyclotella comensis	Grunow			CY010A
Cyclotella comta	(Ehrenberg) Kützing	*Puncticulata comta*	Håkansson	CY001A
Cyclotella glomerata	Bachmannmann	*Discotella glomerata*	Houck & Klee	CY007A
Cyclotella meneghiniana	Kützing			CY003A
Cyclotella ocellata	Pantocsek			CY009A
Cyclotella pseudostelligera	Hustedt	*Discotella pseudostelligera*	Houk & Klee	CY002A
Cyclotella stelligera	Cleve & Grunow	*Discotella stelligera*	Houk & Klee	CY004A
Cyclotella stelligeroides	Hustedt	*Discotella stelligeroides*	Houk & Klee	CY045A
Cymatopleura fragment				CL9999
Cymatopleura solea	(Brébisson.) W. Smith			CL001A
Cymbella (Coarse and fat)				CM9999
Cymbella affinis	Kützing			CM022A
Cymbella alpina	Grunow	*Encyonema alpinum*	Mann	CM060A
Cymbella caespitosa	Kützing	*Encyonema caespitosum*	Brun	CM070A
Cymbella cf. *cesatii*	(Rabenhorst) Grunow	*Encyonopsis cesatii*	Krammer	CM015A
Cymbella cf. *gracilis*	(Rabenhorst) Cleve			CM018A
Cymbella cistula	(Ehrenberg) Kirchner			CM006A
Cymbella delicatissima	Hustedt			CMDELI

Species names	*Authority*	*Revised species names (where applicable)*	*Authority*	*Code*
Cymbella delicatula	Kützing			CM038A
Cymbella descripta	(Hustedt) Krammer & Lange-Bertalot	*Encyonopsis descripta*	Krammer	CM052A
Cymbella fonticola	Hustedt			CMFONT
Cymbella leptoceros	(Ehrenberg) Grunow			CM027A
Cymbella mesiana	Cholnoky	*Encyonema mesiana*	Mann	CM057A
Cymbella microcephala	Grunow	*Encyonopsis microcephala*	Krammer	CM004A
Cymbella minuta	Hilse ex Rabenhorst	*Encyonema minutum*	Mann	CM031A
Cymbella muelleri	Hustedt	*Encyonema muelleri*	Mann	CM024A
Cymbella pusilla	Grunow			CM023A
Cymbella silesiaca	Bleisch	*Encyonema silesiacum*	Mann	CM013A
Cymbella spp.				CM9999
Cymbella subalpina	Hustedt	*Encyonema subalpinum*	Mann	CMSUBALP
Cymbella tumidula	Grunow			CM109A
Cymbella turgidula	Grunow			CM110A
Cymbella ventricosa	Kützing			CM001A
Denticula tenuis	Kützing			DE001A
Diatoma vulgare	Bory	*Diatoma vulgaris*	Bory	DTVULG
Diploneis fragment				DP9999
Diploneis ovalis	(Hilse) Cleve			DP001A
Diploneis pseudovalis	Hustedt			DP053A
Diploneis species - small				DPSMALL
Epithemia adnata	(Kützing) Brébisson.			EP007A
Epithemia sorex	Kützing			EP001A
Eunotia (Side)				EU9999
Eunotia arcus	Ehrenberg			EU013A
Eunotia bilunaris v. *mucaphila*	Lange-Bertalot & Nörpel			EU070B
Eunotia cf. *incisa*	Gregory			EU047A
Eunotia curvata	(Kützing) Lagerstedt			EU049A
Eunotia flexuosa	(Brébisson) Rabenhorst			EU017A
Eunotia formica	Ehrenberg			EU018A
Eunotia fragment				EU9999

Species names	*Authority*	*Revised species names (where applicable)*	*Authority*	*Code*
Eunotia glacialis	Meister			EU024A
Eunotia minor	(Kützing) Grunow			EU110A
Eunotia monodon	Ehrenberg			EU008A
Eunotia paludosa	Grunow			EU040A
Eunotia pectinalis	(Kützing) Rabenhorst			EU002A
Eunotia praerupta	Ehrenberg			EU003A
Eunotia soleirolli	(Kützing) Rabenhorst			EU111A
Eunotia spp. *bumpy*				EUBUMP
Eunotia subaequalis	Hustedt			EUSUBA
Eunotia tchirchiana	O. Müller			EUTCHI
Fragilaria africana	Hustedt	*Staurosira africana*	Williams & Round	FRAFRI
Fragilaria alpestris	Krasske			FR073A
Fragilaria arcus	(Ehrenberg) Cleve	*Hannaea arcus*	Patrick	FRARC
Fragilaria biceps	(Kützing) Lange-Bertalot			FRBICEP
Fragilaria bidens	Heiberg	*Synedra ulna* v. *biceps*	Lange-Bertalot	FR026A
Fragilaria brevistriata	Grunow	*Pseudostaurosira brevistriata*	Williams & Round	FR006A
Fragilaria brevistriata v. *trigona*	Lange-Bertalot			FRBTRI
Fragilaria capucina	Desmazières			FR009A
Fragilaria capucina v. *amphicephala*	(Grunow) Lange-Bertalot			FR009L
Fragilaria capucina v. *gracilis*	(oestrup) Hustedt			FR009H
Fragilaria capucina v. *radians*	(Rabenhorst) Rabenhorst			FRCRAD
Fragilaria capucina v. *rumpens*	(Kützing) Lange-Bertalot			FR009G
Fragilaria capucina v. *vaucherie*	(Kützing) Lange-Bertalot	*Fragilaria vaucheriae*	Peterson	FRCVAU
Fragilaria cf. *heidenii*	Østrup			FR016A
Fragilaria cf. *nitzschioides*	Grunow			FR042A
Fragilaria construens	(Ehrenberg) Grunow	*Staurosira construens*	Williams & Round	FR002A
Fragilaria construens f. exigua	(W.Smith) Hustedt			FR002D
Fragilaria construens v. *venter*	Ehrenberg	*Staurosira construens* v. *venter*	Williams & Round	FR002C
Fragilaria crotonensis	Kitton			FR008A
Fragilaria fasciculata	(Agardh) Lange-Bertalot	*Tabularia fasciculata*	Williams & Round	FR057A
Fragilaria microrhombus	Cholnoky	*Navicula microrhombus*	(Cholnoky) Schoeman & Archibald	NAMICR

Species names	*Authority*	*Revised species names (where applicable)*	*Authority*	*Code*
Fragilaria nana	Steemann-Nielson			FRNANA
Fragilaria pinnata	Ehrenberg	*Staurosirella pinnata*	Williams & Round	FR001A
Fragilaria robusta	(Fusey) Manguin	*Pseudostaurosira robusta*	Williams & Round	FR063A
Fragilaria tenera	(W.Smith) Lange-Bertalot			FR060A
Fragilaria tenera (Bendy)				FR060AB
Fragilaria vaucherie	(Kützing) Boye-Peterson			FR007A
Frus/Nav fragment				FR9999
Frustulia fragment				FU9999
Frustulia rhomboides	(Ehrenberg) De Toni			FU002A
Frustulia rhomboides v. *viridula*	(Brebisson) Cleve	*Frustulia erifuga*	Lange-Bertalot & Krammer	FU002F
Gomphocymbella beccari	(Grunow) Forti			GOCMBEC
Gomphonema (Side)				GO9999
Gomphonema affine	Kützing			GO020A
Gomphonema augur	Ehrenberg			GO019A
Gomphonema clevei	Fricke			GO024A
Gomphonema gracile	Ehrenberg			GO004A
Gomphonema helveticum	Brun			GO042A
Gomphonema insigne	Gregory			GO043A
Gomphonema intricatum	Grunow	*Gomphonema dichotomum*	Kützing	GO014A
Gomphonema lanceolatum	Ehrenberg	*Gomphonema grunowii*	Patrick	GO017A
Gomphonema minutum	(Agardh) Agardh			GO050A
Gomphonema olivaceum	(Lyngbye) Kützing	*Gomphoneis olivaceum*	Dawson ex Ross & Simms	GO001A
Gomphonema parvulum	(Kützing) Grunow			GO013A
Gomphonema productum	(Grunow) Lange-Bertalot			GO083A
Gomphonema pumilum	Grunow			GO080A
Gomphonema truncatum	Ehrenberg			GO023A
Gomphonitzschia ungeri	Grunow			GONIUNG
Hantzschia amphioxys	Ehrenberg (Grunow)			HA001A
Hantzschia amphioxys fragment				HA9999
Hantzschia elongata	(Hantzsch) Grunow			HA002A
Hantzschia virgata	(Roper) Grunow			HA009E

Species names	*Authority*	*Revised species names (where applicable)*	*Authority*	*Code*
Mastagloia elliptica	(Aardh) Cleve			MA002C
Mastagloia elliptica v. *dansei*	(Thwaites) Cleve			MA002B
Melosira moniliformis	(O. Müller) Agardh			ME035A
Meridion circulare	(Greville) Agardh			MR001A
Navicula (Coarse)				NACOARS
Navicula aboensis	Hustedt			NA012A
Navicula absoluta	Hustedt			NA161A
Navicula accomoda	Hustedt	*Craticula accomoda*	Mann	NA096A
Navicula angusta	Grunow			NA037A
Navicula arvensis	Hustedt			NA038A
Navicula barbarica	Hustedt			NABARB
Navicula bryophila	Peterson			NA045A
Navicula cancellata	Donkin			NA268A
Navicula capitata var. hungarica	(Grunow) Ross			NA066B
Navicula capitoradiata	Germain			NA745A
Navicula cari	Ehrenberg			NA051A
Navicula cf. *molestiformis*	Hustedt	*Craticula* cf. *molestiformis*	Lange-Bertalot	NA124A
Navicula cf. *utermoehlii*	Hustedt			NA144A
Navicula cincta	(Ehrenberg) Ralfs			NA021A
Navicula clementiodes	Hustedt	*Placoneis clementiodes*	Cox	NA281A
Navicula clementis	Grunow	*Placoneis clementis*	Cox	NA050A
Navicula confervacea	Kützing	*Diadesmis confervacea*	Grunow	NA118A
Navicula contenta	Grunow	*Diadesmis contenta*	Mann	NA046A
Navicula cryptocephala	Kützing			NA007A
Navicula cryptocephala v. *veneta*	(Kützing) Grunow			NA007B
Navicula cryptonella	Lang-Bertalot			NA751A
Navicula cuspidata	Kützing	*Craticula cuspidata*	Mann	NA056A
Navicula descussis	Östrup	*Geissleria descussis*	Lange-Bertalot & Metzeltin	NA317A
Navicula egregaria	Hustedt	*Fallacia egregaria*	Mann	NA776A
Navicula elginensis	Gregory	*Placoneis elginensis*	Cox	NA057A
Navicula elkab	O. Müller	*Craticula elkab*	Mann	NA730A
Navicula erifuga	Lange-Bertalot			NA173A

Species names	*Authority*	*Revised species names (where applicable)*	*Authority*	*Code*
Navicula gallica	(W. Smith) Lagerst	*Diadesmis gallica*	W. Smith	NA389A
Navicula gastrum	(Ehrenberg) Kützing	*Placoneis gastrum*	Mereschkowsky	NA065A
Navicula gawaniensis	Gasse			NAGAWA
Navicula halophila	(Grunow) Cleve	*Craticula halophila*	Mann	NA022A
Navicula halophila v. *robusta*	Hustedt			NAHROB
Navicula harderii	Hustedt			NA415A
Navicula hoefleri	Cholnoky			NA040A
Navicula kotschyi	Grunow			NA465A
Navicula laevissima	Kützing	*Sellaphora laevissima*	Mann	NA102A
Navicula lanceolata	(Agardh) Ehrenberg			NA009A
Navicula lapidosa	Krasske			NA152A
Navicula menisculus	Schumann			NA030A
Navicula minima	Grunow			NA042A
Navicula miniscula	Grunow	*Adlafia miniscula*	Lange-Bertalot	NA122A
Navicula minisculoides	Hustedt	*Craticula minisculoides*	Lange-Bertalot	NA512A
Navicula modica	Hustedt			NA123A
Navicula monoculata	Hustedt	*Fallacia monoculata*	Mann	NA739A
Navicula mutica	Kützing	*Luticola mutica*	Mann	NA025A
Navicula nivalis	Ehrenberg	*Luticola nivalis*	Mann	NA529A
Navicula obsoleta	Hustedt			NA737A
Navicula phyllepta	Kützing			NA058A
Navicula platensis	(Frenguelli) Cholnoky			NAPLAT
Navicula pseudonivalis	Bock			NAPNIV
Navicula pseudoscutiformis	Hustedt	*Cavinula pseudocutiformis*	Mann & Stickle	NA013A
Navicula pseudoventralis	Hustedt			NA590A
Navicula pupula	Kützing	*Sellaphora pupula*	Mereschkowsky	NA014A
Navicula pupula v. *nyassensis*	(O. Müller) Lange-Bertalot			NAPNYA
Navicula pygmaea	Kützing	*Fallacia pygmaea*	Stickle & Mann	NA010A
Navicula radiosa	Kützing			NA003A
Navicula rhyncocephala	Kützing			NA008A
Navicula salincola	Hustedt	*Navicula incertata*	Hustedt	NA614A

Species names	*Authority*	*Revised species names (where applicable)*	*Authority*	*Code*
Navicula schadei	Krasske			NA110A
Navicula schoenfeldii	Hustedt			NA128A
Navicula schroeteri	Meister			NA764A
Navicula seminuloides	Hustedt			NA129A
Navicula seminulum	Grunow	*Sellaphora seminulum*	Mann	NA005A
Navicula subminuscula	Manguin			NA134A
Navicula submuralis	Hustedt			NA166A
Navicula subrhycocephala	Hustedt			NA743A
Navicula subrotundata	Hustedt			NA114A
Navicula subtilissima	Cleve	*Kobayasiella subtillisima*	Lange-Bertalot	NA033A
Navicula tenella	Brebisson			NA674A
Navicula tenelloides	Hustedt			NA675A
Navicula trivalis	Laneg-Bertalot			NA063A
Navicula vaucherie	Peterson			NA132A
Navicula veneta	Kützing			NA054A
Navicula ventralis	Krasske			NA017A
Navicula viridula				NA027A
Navicula viridula v. *rostellata*	(Kützing) Ehrenberg	*Navicula rostellata*	Kützing	NA027F
Navicula zanonii	Hustedt			NAZAN
Neidium affine	(Ehrenberg) Cleve			NE003A
Neidium affine v. *amphirhynchus*	Hustedt			NE003C
Neidium desestriatum	(Østrup) Krammer			NE013A
Neidium dubium	(Ehrenberg) Cleve			NE007A
Neidium hercynicum	A. Mayer			NE020A
Neidium iridis	(Ehrenberg) Cleve			NE001A
Neidium minutissimum	Krasske			NE030A
Neidium type?				NE9999
Nitzschia acicullariodes	Archibald			NI057A
Nitzschia acicularis	(Kützing) W. Smith			NI042A
Nitzschia aequalis	Hustedt			NIAEQU
Nitzschia alpina	Hustedt			NI202A

Species names	*Authority*	*Revised species names (where applicable)*	*Authority*	*Code*
Nitzschia amphibia	Grunow			NI014A
Nitzschia amphibia (L)	Grunow			NI014AL
Nitzschia angustiforminata	Lange-Bertalot			NI192A
Nitzschia bacata	Hustedt			NIBACC
Nitzschia bacillum	Hustedt			NI211A
Nitzschia calida	Grunow	*Tryblionella calida*	Mann	NI076A
Nitzschia cf. *vermicularis*	(Kützing) Hantzsch			NI049A
Nitzschia comutata	Grunow			NI011A
Nitzschia confinis	Hustedt			NI082A
Nitzschia constricta	(Kützing) Ralfs	*Tryblionella apiculata*	Gregory	NI083A
Nitzschia dissipata	(Kützing) Grunow			NI015A
Nitzschia filiformis	(W. Smith) Van Heurck			NI098A
Nitzschia fonticola	(Grunow) Gasse 1986			NI002A
Nitzschia frustulum	(Kützing) Grunow			NI008A
Nitzschia graciliformis	Lange-Bertalot and Simonsen			NI201A
Nitzschia inconspicua	Grunow			NI043A
Nitzschia intermedia	Hantzsch			NI044A
Nitzschia lacuum	Lange-Bertalot			NI198A
Nitzschia lancettula	O. Müller			NI221A
Nitzschia latens	Hustedt			NILATEN
Nitzschia latens v. *etoshensis*	Cholnoky			NIETOS
Nitzschia leibetruthii	Rabenhorst			NI203A
Nitzschia linearis	W. Smith			NI031A
Nitzschia obsoleta	Hustedt			NIOBSO
Nitzschia obtusa	W. Smith			NI036A
Nitzschia palea	(Kützing) W. Smith			NI009A
Nitzschia perminuta	(Grunow) M. Peragallo			NI193A
Nitzschia pusilla	Grunow			NI152A
Nitzschia recta	Hantzsch			NI025A
Nitzschia reversa	W. Smith			NI157A
Nitzschia rostellata	Hustedt			NIROST
Nitzschia sigma	(Kützing) W. Smith			NI006A

Species names	*Authority*	*Revised species names (where applicable)*	*Authority*	*Code*
Nitzschia sigmoidea	(Nitzsch) W. Smith			NI046A
Nitzschia sinuata	(Thwaites?) Grunow			NI164A
Nitzschia spp.				NI9999
Nitzschia subrostrata	Hustedt			NISUBRO
Nitzschia umbonata	(Ehrenberg) Lange-Bertalot			NI184A
Nitzschia valdecostata	Lange-Bertalot & Simonsen			NI038A
Nitzschia wuellerstorffii	Lange-Bertalot			NI214A
Orthoseira roeseana	(Rabenhorst) O'Meara			OS005A
Pinnularia acrosphaeria	Rabenhorst			PI031A
Pinnularia appendicula	(Aardh) Cleve			PIAPPEN
Pinnularia biceps	Gregory			PI018A
Pinnularia borealis v. *rectangularis*	Carlson			PI012D
Pinnularia braunii	(Grunow) Cleve			PI170A
Pinnularia cf. *lapponica*	Hustedt			PI125A
Pinnularia cf. *streptoraphe*	Cleve			PI159A
Pinnularia gibba	(Ehrenberg) W. Smith			PI001A
Pinnularia gibba v. *sancta*	Grunow			PIGSANC
Pinnularia interrupta	W. Smith			PI004A
Pinnularia microstauron	(Ehrenberg) Cleve			PI011A
Pinnularia obscura	Krasske			PI139A
Pinnularia spp.				PI9999
Pinnularia stomatophora	(Grunow) Cleve			PI024A
Pinnularia subcapitata	Gregory			PI022A
Pinnularia subrostrata	(A. Cleve)(Cleve-Euler			PI161A
Pleurosigma cf. *salinarum*	Grunow			PL050A
Rhabdonema spp.				RB9999
Rhizosolenia cf. *eriensis*	H. L. Smith			RZ011A
Rhoicosphenia curvata	(Kützing) Grunow Ex Rabenhorst	*Rhoicosphenia abbreviate*	Lange-Bertalot	RC001A
Rhopalodia acuminata	Krammer			RH010A
Rhopalodia cf. *Brébissonii*	Krammer			RH009A
Rhopalodia fragment				RH9999
Rhopalodia gibba	(Ehrenberg) O. Müller			RH001A

Species names	*Authority*	*Revised species names (where applicable)*	*Authority*	*Code*
Rhopalodia gibberula	(Ehrenberg) O. Müller			RH003A
Rhopalodia gracilis	O. Müller			RHGRAC
Rhopalodia hirundiformis	O. Müller			RHHIRUN
Rhopalodia rhopala	(Ehrenberg) Hustedt			RHRHOP
Stauroneis anceps	Ehrenberg			SA001A
Stauroneis obtusa	Agardh			SA058A
Stauroneis phoenicenteron	(Nitzsch) Ehrenberg			SA006A
Stauroneis producta	Grunow			SA008A
Stauroneis pseudosubobtusoides				SAPSEUD
Stephandodiscus astrea	(Ehrenberg) Grunow			ST003A
Stephanodiscus damasii	Hustedt	*Cyclostephanos damasii*	Stoermer & Håkansson	STDAMAS
Stephanodiscus hantzschii	Grunow			ST001A
Stephanodiscus spp.				ST9999
Surirella biseriata	Brébisson			SU004A
Surirella Brébissonii	Krammer & Lange-Bertalot			SU073A
Surirella cf. *heidenii*	Hustedt			SUHEID
Surirella constricta	Schumann			SU030A
Surirella engleri	O. Müller			SUENGL
Surirella fasciculata	O. Müller			SUFASC
Surirella fragment				SUFRAG
Surirella ovalis	Brébisson			SU003A
Synedra acus v. *radians*	Kützing			SY003B
Synedra nyansae	G. S. West			SYNYAN
Synedra rumpens	Kützing			SY002A
Synedra rumpens v. *fragilaroides*	Grunow	*Fragilaria capucina* v. *fragilariodes*	Ludwig & Flores	SY002C
Synedra rumpens v. *radians*	Kützing			SYRMRAD
Synedra ulna	(Nitzsch) Ehrenberg			SY001A
Synedra ulna v. *acus*	Kützing			SYUACUS
Thalassiosira rudolfi	(Bachmann) Hasle			TH003A
Thalassiosira spp.				TH9999
Unknown				UN9999

Species names	*Authority*	*Revised species names (where applicable)*	*Authority*	*Code*
Unknown *Achnanthes*				AC9999
Unknown *Amphora (montana)*				AM9999
Unknown *Cyclostephanus*				CS9999
Unknown *Epithemia*				EP9999
Unknown *Gomphonema*				G09999
Unknown *Navicula*				NA9999
Unknown *Nitzschia*				NI9999
Unknown *Surirella*				SU9999

Appendix B: Broken stick

Results (graphs) of broken stick analyses from all chapters (arranged by chapter).

CHAPTER 5

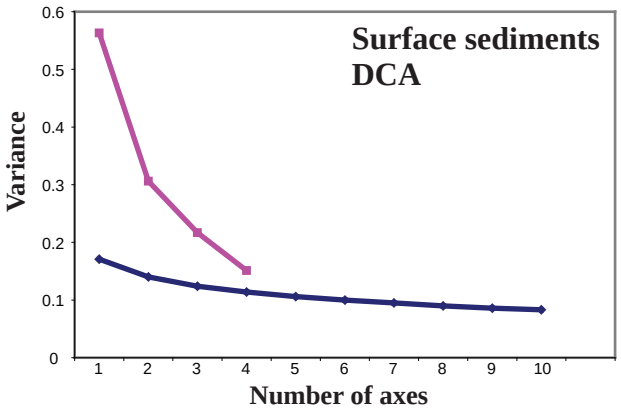

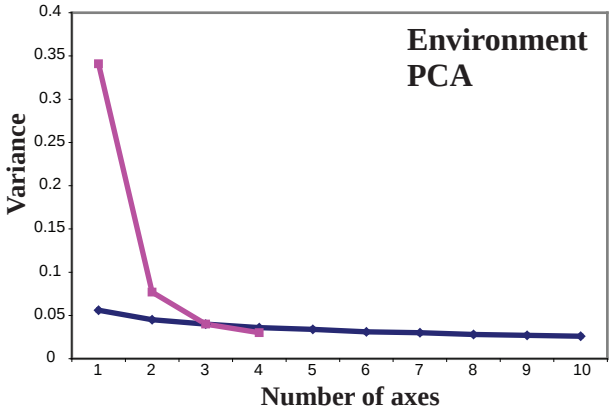

CHAPTER 6

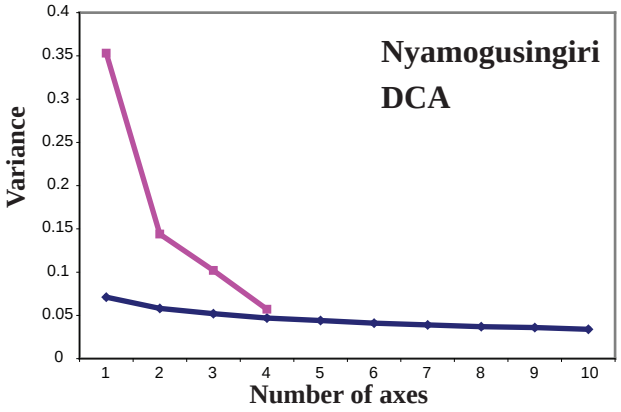

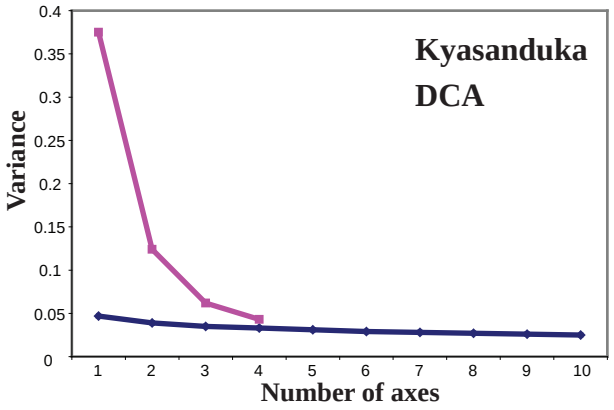

CHAPTER 7

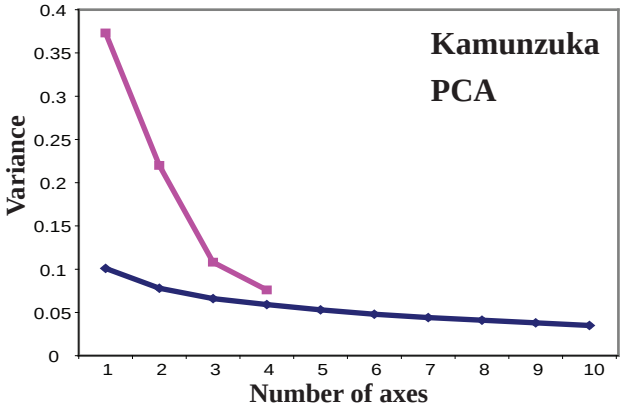

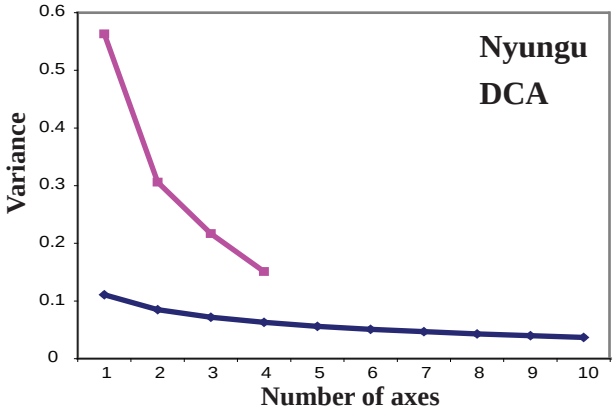

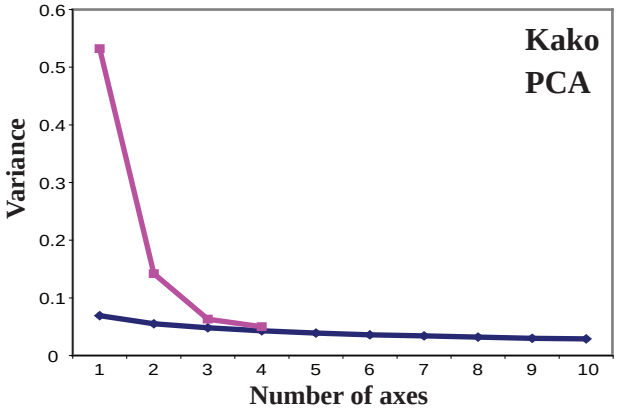

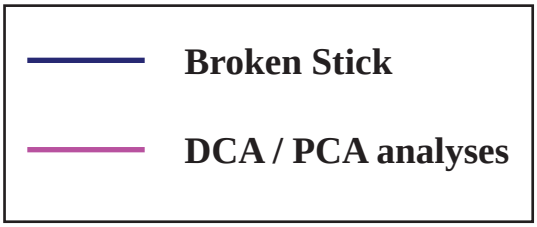

Appendix C: Chapter 6, additional data

Results of ^{210}Pb and ^{137}Cs dating of sediments from Lakes Nyamogusingiri (Tables C1 and C2) and Kyasanduka (Tables C4 and C5). Tables C3 and C6 show the results of Detrended Correspondence Analysis (DCA) of the diatom data from Lakes Nyamogusingiri and Kyasanduka respectively.

Table C1 *^{210}Pb dated horizons from Lake Nyamogusingiri.*

Depth (cm)	g cm^{-1}	Chronology			Sedimentation Rate		
		Year AD	Age yr	±	g cm^{-2} yr^{-1}	cm yr^{-1}	± (%)
0.0	0.00	2007	0	0			
0.5	0.01	2006	1	1	0.028	0.63	9.9
2.5	0.11	2003	4	1	0.031	0.67	10.3
4.5	0.22	2000	7	2	0.042	0.67	12.1
8.5	0.53	1994	13	2	0.064	0.75	13.3
10.5	0.72	1992	15	2	0.094	0.80	16.9
12.5	0.94	1989	18	2	0.092	0.80	17.6
14.5	1.20	1987	20	3	0.113	0.80	20.6
16.5	1.51	1984	23	3	0.127	0.57	18.8
18.5	1.93	1980	27	4	0.089	0.42	21.4
21.5	2.65	1972	35	6	0.086	0.35	25.4
24.5	3.38	1963	44	8	0.077	0.30	34.2
27.5	4.08	1952	55	9	0.054	0.32	45.9
30.5	4.73	1944	63	9	0.112	0.45	59.9
33.5	5.27	1939	68	9	0.084	0.48	52.9
35.5	5.65	1934	73	9	0.070	0.36	47.6
37.5	6.06	1928	79	9	0.064	0.29	25.4
39.5	6.48	1920	87.0	9	0.044	0.23	31.3
41.5	6.92	1910	97.0	10	0.044	0.20	31.3
43.5	7.35	1900	106.9	11	0.044	0.20	31.3
45.5	7.77	1890	116.7	12	0.044	0.20	31.3
47.5	8.21	1880	126.7	14	0.044	0.19	31.3
49.5	8.70	1869	137.9	17	0.044	0.18	31.3
51.5	9.19	1858	149.3	18	0.044	0.18	31.3

Table C2 *Fallout radionuclide concentrations from the Nyamogusingiri sediment core.*

Depth		^{210}Pb						^{137}Cs	
		Total		Unsupported		Supported			
Cm	g cm^{-1}	Bg kg^{-1}	±	Bg kg^{-1}	±	Bg kg^{-1}	±	Bg kg^{-1}	±
0.5	0.01	641.7	28.0	562.2	28.6	79.5	5.9	2.3	4.6
2.5	0.11	530.3	20.3	471.1	20.7	59.2	4.2	3.3	2.6
4.5	0.22	383.0	19.9	314.0	20.4	69.1	4.5	1.2	2.3
8.5	0.53	236.2	8.6	169.4	8.9	66.8	2.1	7.7	1.2
10.5	0.72	160.7	11.1	107.0	11.4	53.7	2.6	8.0	1.4
12.5	0.94	174.0	10.4	102.2	10.8	71.8	2.7	10.0	1.4
14.5	1.20	143.4	10.3	77.0	10.6	66.4	2.7	11.8	1.7
16.5	1.51	133.5	5.3	62.8	5.5	70.7	1.5	11.0	1.0
18.5	1.93	136.1	8.3	79.6	8.4	56.5	1.7	8.6	1.1
21.5	2.65	129.8	5.1	63.6	5.2	66.2	1.3	15.2	0.8
24.5	3.38	122.7	6.9	53.4	7.2	69.3	1.8	14.6	1.1
27.5	4.08	112.1	6.1	54.8	6.2	57.3	1.4	6.6	0.8
30.5	4.73	87.2	7.3	22.6	7.6	64.5	1.9	3.8	1.2
33.5	5.27	82.7	7.0	28.7	7.2	53.9	1.7	4.1	1.1
35.5	5.65	110.5	9.3	34.0	9.7	76.5	2.6	0.0	0.0
37.5	6.06	108.3	7.5	35.4	7.8	72.9	2.0	0.0	0.0
39.5	6.48	113.5	8.1	44.6	8.3	68.9	2.1	0.3	1.2
41.5	6.92	76.1	5.9	17.6	6.1	58.5	1.6	0.7	0.9
43.5	7.35	99.0	7.6	27.9	7.8	71.1	2.0	0.0	0.0
45.5	7.77	84.3	9.4	15.0	9.7	69.3	2.4	0.0	0.0
47.5	8.21	103.4	6.6	34.2	6.9	69.2	1.7	0.0	0.0
49.5	8.70	85.9	8.3	3.4	8.6	82.5	2.1	0.0	0.0
51.5	9.19	88.3	6.5	10.9	6.8	77.4	2.0	0.0	0.0

Figure C3 *Results of Detrended Correspondence Analysis (DCA) on the diatom data from Lake Nyamogusingiri.*

	Axis 1	Axis 2	Axis 3	Axis 4
Eigenvalues	0.353	0.142	0.105	0.056
Cumulative % variance	20.3	28.5	34.5	37.7
Length of DCA gradient	*2.722*			
Total inertia	*1.74*			

Table C4 *^{210}Pb dated horizons from Lake Kyasanduka.*

Depth (cm)	g cm^{-1}	Chronology			Sedimentation Rate		
		Year AD	Age yr	±	g cm^{-2} yr^{-1}	cm yr^{-1}	± (%)
0.0	0.00	2007					
0.5	0.00	2007	0	2	0.173	2.83	18.9
2.5	0.04	2007	0	2	0.103	2.83	11.2
4.5	0.09	2006	1	2	0.061	1.83	8.4
8.5	0.21	2004	3	2	0.040	1.36	7.9
11.5	0.31	2001	6	2	0.040	1.19	8.4
14.5	0.41	1999	9	2	0.043	1.14	9.1
17.5	0.51	1996	11	2	0.046	1.09	9.8
23.5	0.81	1990	17	2	0.042	0.90	12.0
26.5	0.99	1986	21	3	0.059	0.75	14.6
29.5	1.21	1982	25	3	0.053	0.67	15.1
32.5	1.46	1977	30	4	0.055	0.75	17.8
35.5	1.74	1974	33	4	0.100	1.00	20.4
38.5	1.99	1971	36	5	0.081	1.00	21.8
44.5	2.48	1965	42	6	0.089	0.96	32.7
48.5	2.80	1961	46	8	0.053	0.80	16.3
52.5	3.10	1955	52	8	0.044	0.66	9.0
55.5	3.34	1950	57	8	0.054	0.64	10.0
59.5	3.66	1944	63	9	0.051	0.60	9.6
64.5	4.06	1935	72	9	0.039	0.60	10.3
68.5	4.37	1929	78	10	0.080	0.94	14.7
74.5	4.82	1924	84	10	0.085	0.97	20.2
80.5	5.28	1918	89	10	0.090	1.00	25.6
86.5	5.76	1912	96	11	0.076	0.88	23.3
92.5	6.24	1905	102	11	0.061	0.77	21.0
96.5	6.59	1898	109	11	0.054	0.67	20.6
100.5	6.95	1892	115	12	0.047	0.57	20.1
104.5	7.29	1885	122	14	0.047	0.53	27.1
108.5	7.64	1877	130	16	0.047	0.49	34.1

Table C5 *Fallout radionuclide concentrations from the Kyasanduka sediment core.*

Depth		^{210}Pb						^{137}Cs	
		Total		Unsupported		Supported			
Cm	g cm^{-1}	Bg kg^{-1}	±	Bg kg^{-1}	±	Bg kg^{-1}	±	Bg kg^{-1}	±
0.5	0.00	246.5	35.4	202.8	35.6	43.7	3.5	0.0	0.0
2.5	0.04	385.0	29.5	340.3	30.1	44.7	5.9	3.2	4.0
4.5	0.09	605.1	25.3	562.3	25.7	42.8	4.9	4.6	3.1
8.5	0.21	845.7	16.3	804.1	17.0	41.5	4.9	4.0	1.8
11.5	0.31	773.9	14.4	731.2	14.6	42.8	2.2	2.5	1.7
17.5	0.51	598.1	13.6	553.7	13.9	44.4	2.7	3.5	1.7
23.5	0.81	525.1	13.1	487.5	13.3	37.7	2.6	6.2	1.4
26.5	0.99	353.3	20.1	306.1	20.5	47.2	3.8	1.7	2.4
29.5	1.21	348.0	11.0	303.6	11.2	44.4	2.3	7.6	1.4
32.5	1.46	295.2	13.5	252.5	13.7	42.6	2.7	9.7	1.8
35.5	1.74	169.9	8.9	124.4	9.1	45.4	2.0	11.8	1.5
38.5	1.99	188.6	9.5	140.5	9.8	48.1	2.3	13.8	1.5
44.5	2.48	152.5	22.2	107.1	23.0	45.4	6.2	13.7	4.2
48.5	2.80	310.5	40.1	265.0	41.7	45.5	11.3	19.2	7.2
52.5	3.10	490.7	33.5	442.8	34.3	47.9	7.2	15.2	5.6
55.5	3.34	351.6	25.6	307.3	26.3	44.3	5.9	5.2	3.7
59.5	3.66	324.2	19.7	270.2	20.3	54.0	4.7	7.6	3.0
64.5	4.06	320.4	18.1	267.6	18.5	52.8	3.8	10.0	3.1
68.5	4.37	155.8	12.7	110.0	13.2	45.8	3.5	9.4	2.7
80.5	5.28	113.8	16.2	69.4	16.7	44.4	4.0	0.0	0.0
92.5	6.24	107.6	11.9	68.3	12.3	39.3	3.2	0.0	0.0
100.5	6.95	114.4	9.8	74.4	10.1	39.9	2.4	0.0	0.0
108.5	7.64	119.4	11.1	81.8	11.4	37.6	2.5	0.7	1.7
116.5	8.48	55.3	7.5	8.3	7.8	47.0	2.2	0.0	0.0
124.5	9.49	26.6	6.0	0.3	6.2	26.3	1.6	0.0	0.0

Figure C6 *Results of Detrended Correspondence Analysis (DCA) on the diatom data from Lake Kyasanduka.*

	Axis 1	Axis 2	Axis 3	Axis 4
Eigenvalues	0.375	0.124	0.063	0.043
Cumulative % variance	21.1	28.3	31.8	34.3
Length of DCA gradient	*2.569*			
Total inertia	*1.764*			

Appendix D: Chapter 7, additional data

Results of ^{210}Pb and ^{137}Cs dating of sediments from Lakes Kamunzuka (Tables D1 and D2), Nyungu (Tables D4 and D5), Kako (Tables D7 and D8), Mafura (Tables D10 and D11) and Kigezi (Tables D12 and D13). Tables D3, D6 and D9 show the results of Correspondence Analyses (CA) and Detrended Correspondence Analysis (DCA) of the diatom data from Lakes Kamunzuka (CA), Nyungu (DCA) and Kako (CA) respectively.

Table D1 *^{210}Pb dated horizons from Lake Kamunzuka.*

Year AD	Depth (cm)	Sedimentation rate	
		g cm^{-2} y^{-1}	cm y^{-1}
2006	0.0		
1980	13	0.049	0.39
1960	18	0.043	0.32
1940	23	0.034	0.23
1920	27	0.025	0.16
1900	30	0.023	0.14

Table D2 *Fallout radionuclide concentrations from the Kamunzuka core.*

Depth		^{210}Pb						^{137}Cs	
		Total		Unsupported		Supported			
Cm	g cm^{-1}	Bg kg^{-1}	±	Bg kg^{-1}	±	Bg kg^{-1}	±	Bg kg^{-1}	±
0.5	0.0	1783.9	51.9	1729.7	52.4	54.1	7.3	7.5	6.2
14.5	1.3	639.0	20.0	586.6	20.3	52.4	3.8	13.6	2.4
28.0	3.6	228.9	13.2	188.0	13.5	40.9	2.8	0.8	1.9
42.0	5.9	50.3	5.9	7.3	6.1	43.0	1.5	0.0	0.0

Table D3 *Results of Principal Components Analysis (PCA) on the diatom data from Lake Kamunzuka.*

	Axis 1	Axis 2	Axis 3	Axis 4
Eigenvalues	0.373	0.220	0.108	0.076
Cumulative % variance	37.3	59.3	70.1	77.7
Length of DCA gradient	*1.004*			
Total variance	*1*			

Table D4 *^{210}Pb dated horizons from Lake Nyungu.*

Year AD	Depth (cm)	Sedimentation rate	
		g cm^{-2} y^{-1}	cm y^{-1}
2006	0		
1990	8	0.080	0.35
1970	13	0.072	0.25
1950	18	0.062	0.15
1930	~21		

Table D5 *Fallout radionuclide concentrations from the Nyungu core.*

Depth		^{210}Pb						^{137}Cs	
		Total		Unsupported		Supported			
cm	g cm^{-1}	Bg kg^{-1}	±	Bg kg^{-1}	±	Bg kg^{-1}	±	Bg kg^{-1}	±
0.5	0.0	433.1	22.8	390.8	23.3	42.3	4.9	0.0	0.0
9.0	1.5	278.4	13.5	220.0	13.9	58.4	3.1	0.0	0.0
18.0	4.2	138.1	9.8	85.4	10.0	52.7	2.4	5.5	1.3
26.5	8.7	55.1	5.3	-9.8	5.4	64.9	1.2	1.1	0.5

Table D6 *Results of Detrended Correspondence Analysis (DCA) on the diatom data from Lake Nyungu.*

	Axis 1	Axis 2	Axis 3	Axis 4
Eigenvalues	0.341	0.077	0.040	0.030
Cumulative % variance	29.7	36.4	39.9	42.6
Length of DCA gradient	*2.29*			
Total inertia	*1.148*			

Table D7 *^{210}Pb dated horizons from Lake Kako.*

Year AD	Depth (cm)	Sedimentation rate	
		g cm^{-2} y^{-1}	cm y^{-1}
2006	0		
1990	10	0.52	2.6
1980	15	0.33	1.7
1970	21	0.10	0.4
1960	27		

Table D8 *Fallout radionuclide concentrations from the Kako core.*

Depth		^{210}Pb						^{137}Cs	
		Total		Unsupported		Supported			
cm	g cm^{-1}	Bg kg^{-1}	±	Bg kg^{-1}	±	Bg kg^{-1}	±	Bg kg^{-1}	±
0.5	0.1	448.8	21.3	381.7	21.8	67.1	4.5	3.0	2.6
11.0	2.0	83.4	8.4	23.0	8.7	60.4	2.4	1.5	1.2
22.0	4.3	271.5	15.9	215.7	16.2	55.9	3.0	2.8	1.7
32.0	6.2	57.0	6.2	-3.3	6.5	60.3	1.9	0.0	0.0

Figure D9 *Results of Principal Components Analysis (PCA) on the diatom data from Lake Kako.*

	Axis 1	Axis 2	Axis 3	Axis 4
Eigenvalues	0.532	0.142	0.063	0.050
Cumulative % variance	53.2	67.4	73.7	78.6
Length of DCA gradient	*1.453*			
Total variance	*1*			

Table D10 *^{210}Pb dated horizons from Lake Mafura.*

Year AD	Depth (cm)	Sedimentation rate	
		g cm^{-2} y^{-1}	cm y^{-1}
2006	0		
1980	6	0.023	0.17
1960	10	0.023	0.12
1940	12	0.027	0.13
1920	14	0.031	0.14
1900	16	0.036	0.14

Table D11 *Fallout radionuclide concentrations from the Kigezi core.*

Depth		^{210}Pb						^{137}Cs	
		Total		Unsupported		Supported			
Cm	g cm^{-1}	Bg kg^{-1}	±	Bg kg^{-1}	±	Bg kg^{-1}	±	Bg kg^{-1}	±
0.5	0.0	906.7	19.8	836.4	20.0	70.3	3.2	0.0	0.0
11.0	0.9	379.3	21.3	297.4	21.9	81.9	5.2	5.3	2.8
21.5	2.7	177.4	11.1	108.7	11.4	68.7	2.5	0.0	0.0
32.0	5.3	60.2	5.5	-3.1	5.8	63.3	1.7	0.0	0.0

Table D12 *^{210}Pb dated horizons from Lake Kigezi.*

Year AD	Depth (cm)	Sedimentation rate	
		g cm^{-2} y^{-1}	cm y^{-1}
2006	0		
1990	8	0.023	0.41
1970	15	0.023	0.32
1950	20	0.027	0.22
1930	25		

Table D13 *Fallout radionuclide concentrations from the Mafura core.*

Depth		^{210}Pb						^{137}Cs	
		Total		Unsupported		Supported			
Cm	g cm^{-1}	Bg kg^{-1}	±	Bg kg^{-1}	±	Bg kg^{-1}	±	Bg kg^{-1}	±
0.5	0.0	1764.2	55.9	1699.2	56.8	64.9	9.8	0.0	0.0
9.0	0.9	736.3	18.5	682.8	18.7	53.5	2.8	3.3	1.9
18.0	3.1	81.8	5.3	23.0	5.6	58.8	1.7	0.4	0.9
26.5	5.5	58.0	5.0	-0.4	5.2	58.4	1.4	0.0	0.0

Appendix E: Diatom plates

Key species and unusual morphologies of diatoms identified during this research

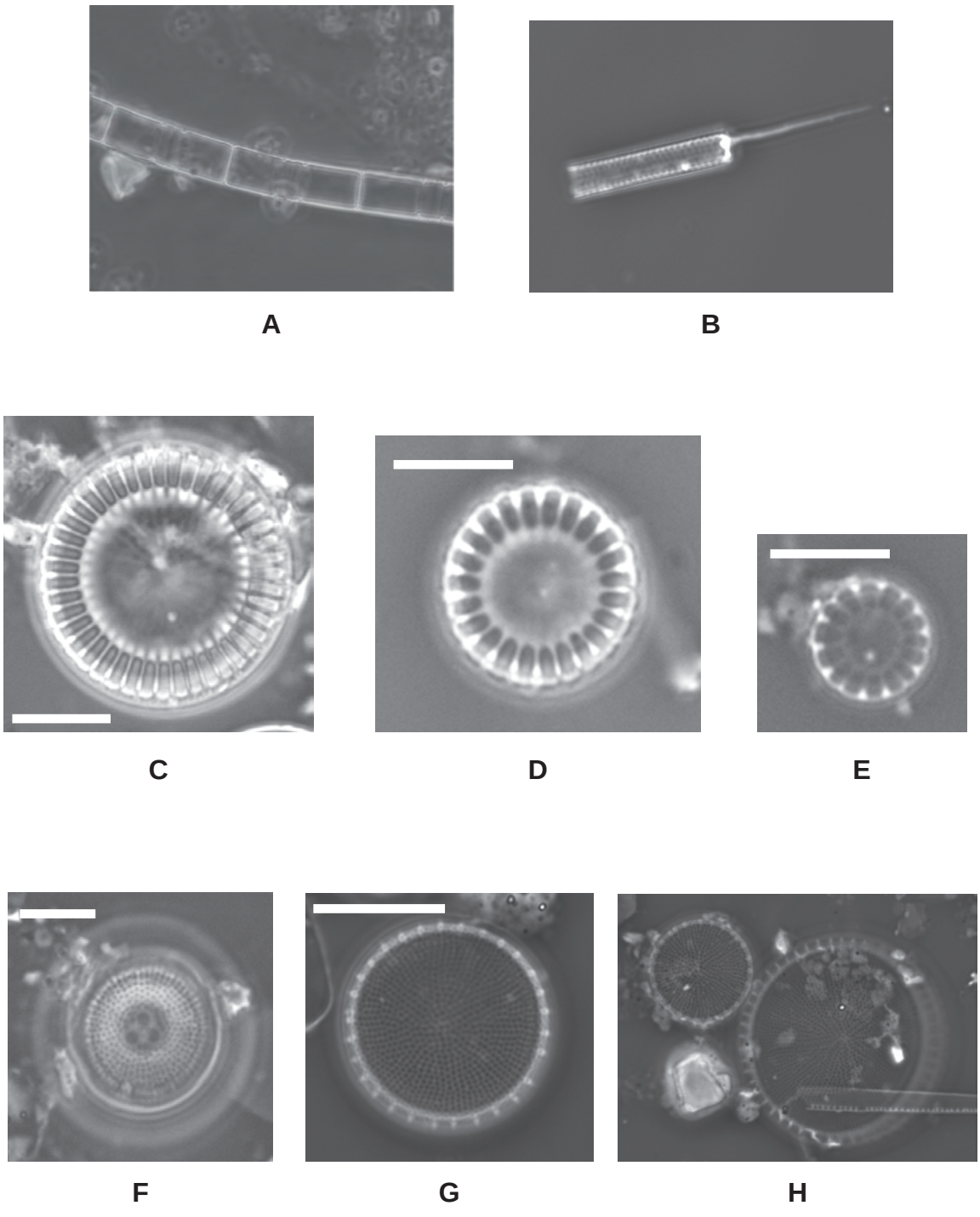

PLATE 1: Scale bar where shown is 10 µm. **(A)** *Aulacoseira ambigua* (Grunow) Simonsen; **(B)** *Aulacoseira granulata* (Ehrenberg) Simonsen; **(C)** *Cyclotella menghiniana* Kützing (large); **(D)** *Cyclotella meneghiniana* Kützing (medium); **(E)** *Cyclotella meneghiniana* Kützing (small); **(F)** *Orthoseira roeseana* Rabenhorst O'Meara; **(G)** *Thalassiosira rudolfi* (Bachmann) Hasle; **(H)** *Thalassiosira rudolfi* (Bachmann) Hasle (comparison of large and medium size valves).

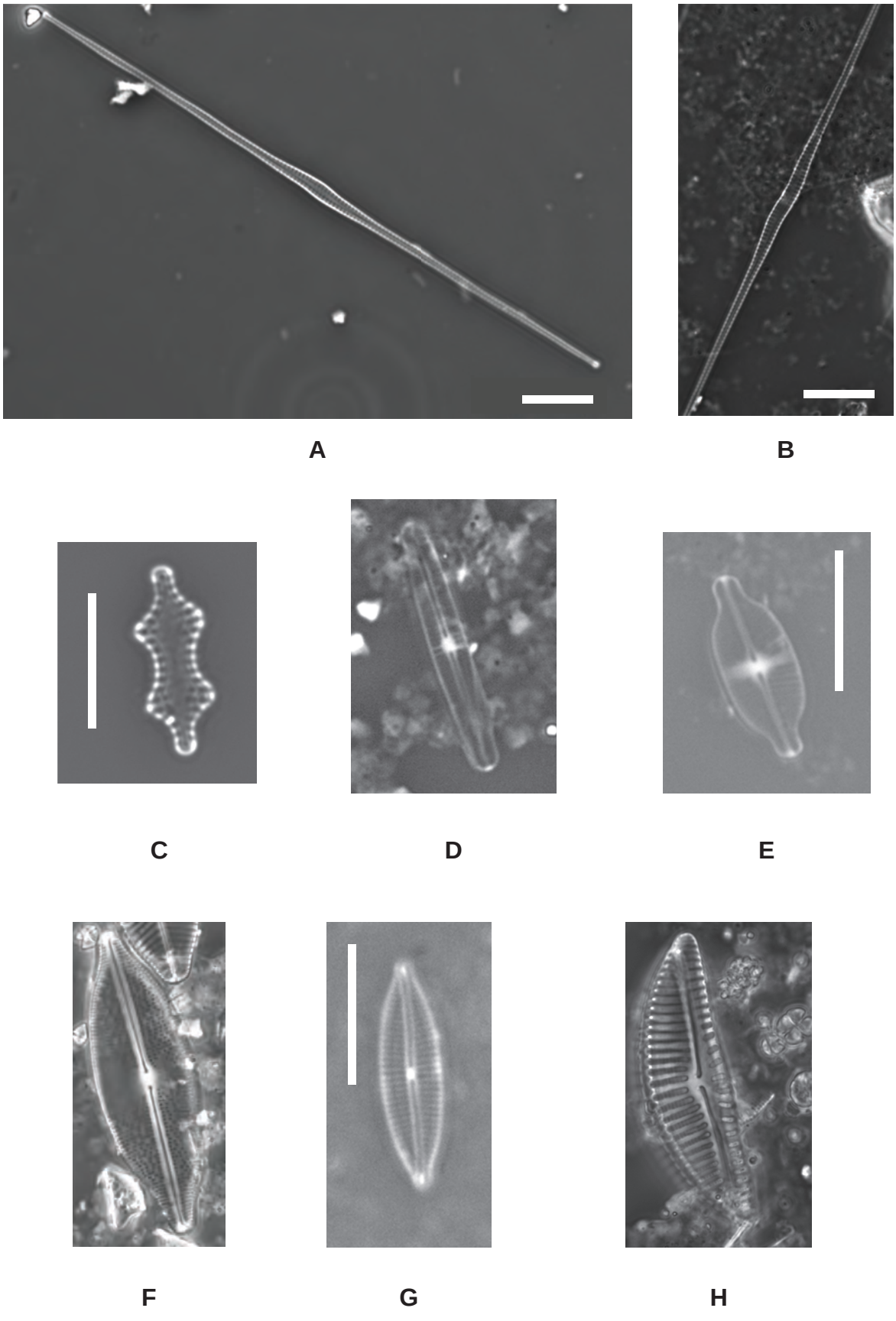

PLATE 2: Scale bar where shown is 10 µm. **(A)** *Fragilaria tenera* (W.Smith) Lange-Bertalot (normal); **(B)** *Fragilaria tenera* (W. Smith) Lange-Bertalot (teratological form); **(C)** *Pseudostaurosira robusta* Williams & Round; **(D)** *Achnanthidium minutissimum* Czarnecki; **(E)** *Planothidium lanceolatum* Round & Bukhtiyarova; **(F)** *Anomoeoneis sphaerophora* (Kützing) Pfitzer; **(G)** *Encyonopsis microcephala* Krammer; **(H)** *Encyonopsis muelleri* Mann.

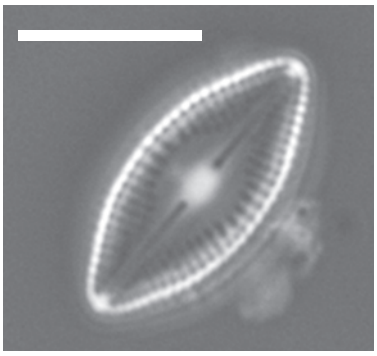

A

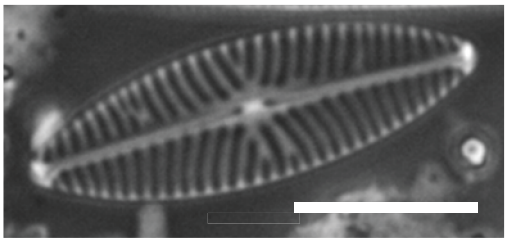

B

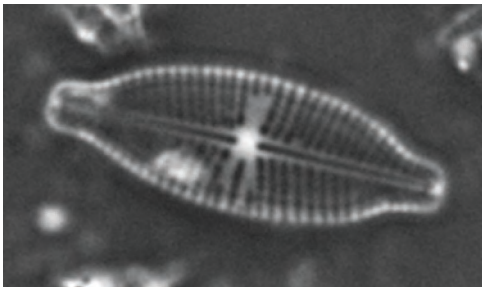

C

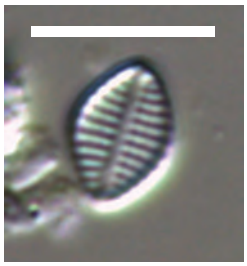

D

E

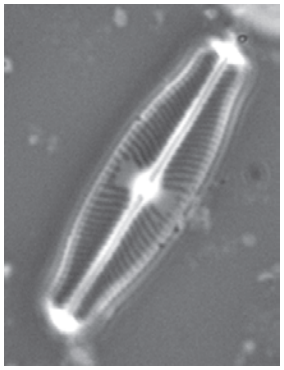

F

PLATE 3: Scale bar where shown is 10 μm. **(A)** *Diadesmis confervacea* Grunow; **(B)** *Navicula cryptonella* Lange-Bertalot; **(C)** *Navicula kotschyi* Grunow; **(D)** *Navicula microrhombus* (Cholnoky) Schoeman & Archibald; **(E)** *Navicula platensis* (Frenguelli) Cholnoky; **(F)** *Sellaphora pupula* (Kützing) Mereschkowsky.

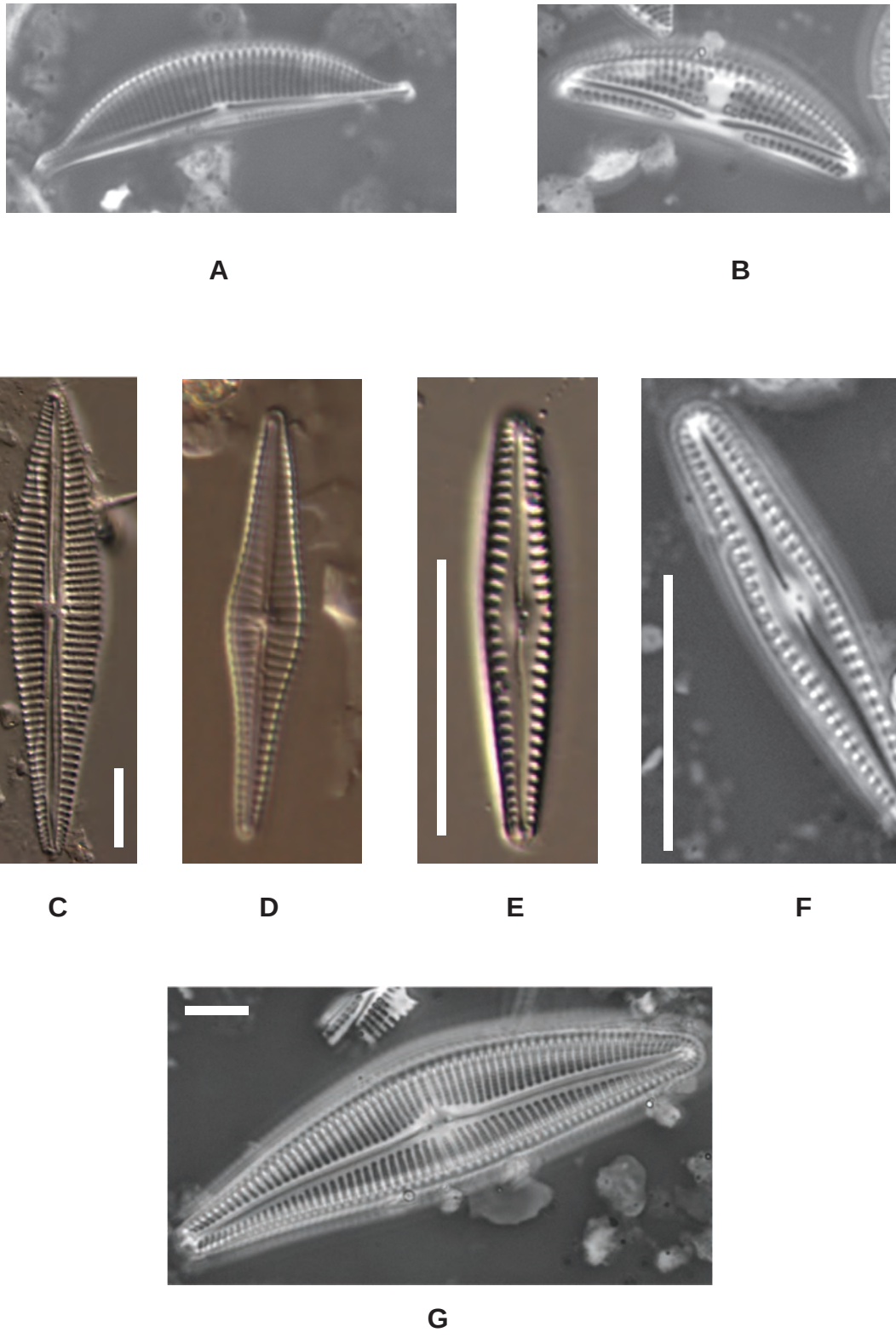

PLATE 4: Scale bar where shown is 10 μm. **(A)** *Amphora coffeaeformis* Agardh; **(B)** *Amphora copulata* Schoeman & Archibald; **(C)** *Gomphonema gracile* Ehrenberg; **(D)** *Gomphonema* cf. *gracile* Ehrenberg (teratological form?); **(E)** *Gomphonema pumilum* Grunow; **(F)** *Gomphonema pumilum* Grunow; **(G)** *Gomphocymbella beccari* (Grunow) Forti.

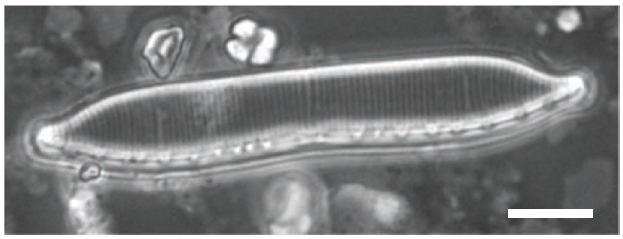

A

B

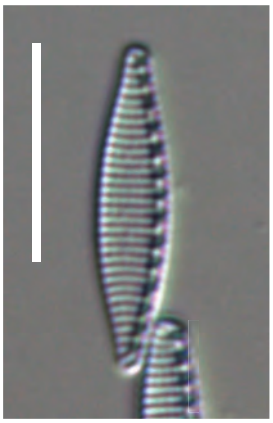

C

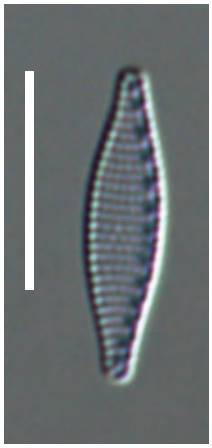

D

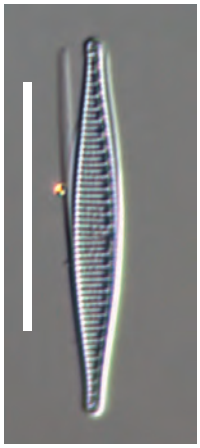

E

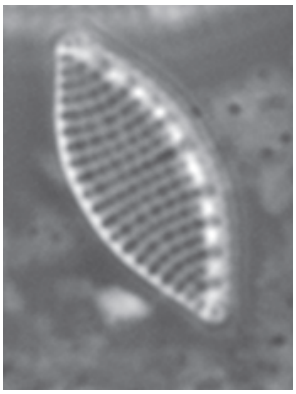

F

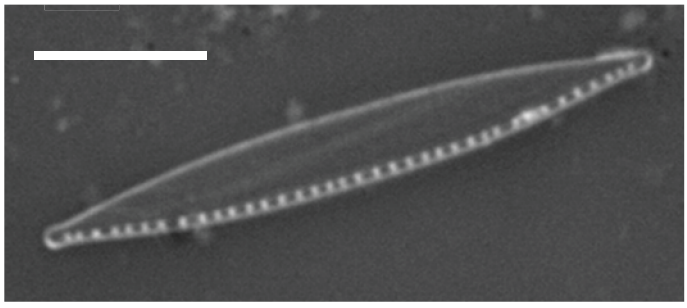

G

PLATE 5: Scale bar where shown is 10 μm. **(A)** *Hantzschia amphioxys (*Ehrenberg) Grunow; **(B)** *Nitzschia confinis* Hustedt; **(C)** *Nitzschia bacillum* (aff. *fonticola?*) Hustedt; **(D)** *Nitzschia bacillum* (aff. *fonticola?*) Hustedt; **(E)** *Nitzschia bacillum* (aff. *fonticola?*) Hustedt; **(F)** *Nitzschia lancettula* Müller; **(G)** *Nitzschia palea* (Kützing) W. Smith.